468

ЖУРНАЛ
ЭКСПЕРИМЕНТАЛЬНОЙ И ТЕОРЕТИЧЕСКОЙ
ФИЗИКИ
АКАДЕМИЯ НАУК СССР

SOVIET PHYSICS

JETP

VOLUME 37 (10) NUMBER 1

A Translation

of the

Journal of Experimental and Theoretical Physics

of the

Academy of Sciences of the USSR

Volume 37

JANUARY, 1960

Published by the

AMERICAN INSTITUTE OF PHYSICS
INCORPORATED

SOVIET PHYSICS
JETP

A translation of the Journal of Experimental and Theoretical Physics of the USSR.

A publication of the

AMERICAN INSTITUTE OF PHYSICS

Governing Board

RALPH A. SAWYER, *Chairman*
WALTER S. BAIRD
JESSE W. BEAMS
RAYMOND T. BIRGE
R. H. BOLT
HARVEY BROOKS
J. W. BUCHTA
J. H. DILLON
VERNET E. EATON
HERBERT A. ERF
IRVINE C. GARDNER
S. A. GOUDSMIT
WINSTON E. KOCK
R. BRUCE LINDSAY
WALTER C. MICHELS
G. E. PAKE
R. RONALD PALMER
JOSEPH B. PLATT
H. D. SMYTH
JOHN STRONG
GEORGE E. UHLENBECK

Officers and Staff

ELMER HUTCHISSON
Director
HENRY A. BARTON
Associate Director
WALLACE WATERFALL
Secretary and Treasurer
EDWARD P. TOBER
Manager, Production and Distribution
THEODORE VORBURGER
Advertising Manager
RUTH F. BRYANS
Publication Manager
KATHRYN SETZE
Assistant Treasurer
ALICE MASTROPIETRO
Circulation Manager
EUGENE H. KONE
Director of Public Relations
WILLIAM C. KELLY
Director of Educational Projects
EMILY WOLF
Office Manager

American Institute of Physics Advisory Board on Russian Translations

ROBERT T. BEYER, *Chairman*
J. GEORGE ADASHKO, FREEMAN DYSON, DWIGHT GRAY, MORTON HAMERMESH, HAROLD F. WEAVER

Editor of SOVIET PHYSICS—JETP

J. GEORGE ADASHKO, 25 WEST 81ST ST., NEW YORK 24, NEW YORK

SOVIET PHYSICS—JETP is a monthly journal published by the American Institute of Physics and contains a complete translation of the JOURNAL OF EXPERIMENTAL AND THEORETICAL PHYSICS of the U.S.S.R. Academy of Sciences.

This translating and publishing project was undertaken by the institute in the conviction that dissemination of the results of researches everywhere in the world is invaluable to the advancement of science. The NATIONAL SCIENCE FOUNDATION of the United States has encouraged the project initially and is supporting it in large part by a grant.

The American Institute of Physics and its translators propose to translate faithfully all the material appearing in the original articles. The views expressed in the translations are therefore those of the original authors, and not those of the translators nor of the American Institute of Physics.

Volume 1 of SOVIET PHYSICS—JETP corresponds to Russian Volume 28 (1955). Two volumes are published annually, each of six issues. Each volume contains the translation of one volume of the JOURNAL OF EXPERIMENTAL AND THEORETICAL PHYSICS.

Beginning with Vol. 9 (36), the transliteration of the names of Russian authors follows British Standard 2979, which is being adopted in 1959 by a large number of scientific journals in the United States. The Library of Congress transliteration is followed in the earlier volumes.

Subscription Prices

Per Year (12 issues)

General:	
United States and Canada	$75.00
Elsewhere	79.00
Libraries of non-profit degree-granting Institutions:	
United States and Canada	$35.00
Elsewhere	39.00
Back Numbers	$ 8.00

Subscriptions should be addressed to the American Institute of Physics, 335 East 45th Street, New York 17, New York.

SOVIET PHYSICS, JETP is published monthly by the American Institute of Physics, Inc. Second Class postage paid at Ann Arbor, Michigan.

Copyright by American Institute of Physics 1960

SOVIET PHYSICS

JETP

A translation of the Journal of Experimental and Theoretical Physics of the USSR.

SOVIET PHYSICS JETP VOL. 37 (10), NO. 1, pp. 1-233 JANUARY, 1960

ANGULAR DISTRIBUTION OF SHOWER PARTICLES IN STARS PRODUCED BY HIGH-ENERGY PARTICLES

L. A. SAN'KO, Zh. S. TAKIBAEV, Ts. I. SHAKHOVA, and L. Ya. BALATS

Nuclear Physics Institute, Academy of Sciences, Kazakh S.S.R.

Submitted to JETP editor November 14, 1958

J. Exptl. Theoret. Phys. (U.S.S.R.) **37**, 3-10 (July, 1959)

An analysis is carried out of the angular distribution of a unique star consisting of 20 + 15 + 59p, and probably produced by a proton of energy > 1000 Bev. The angular distribution of shower particles is characterized by two maxima and is explained by the anisotropic angular distribution and a power-law energy spectrum of the produced particles in the c.m.s. The presence of a large number of strongly ionized particles indicates that the Heitler-Terreaux theory does not give a correct description of π meson production. The angular distribution of 11 other showers with the same characteristic anisotropy is also investigated.

INTRODUCTION

In the scanning of an emulsion stack exposed to cosmic radiation at the latitude of Moscow at an altitude of ~ 30 km, an event was recorded, a shower 35 + 59p, in which a proton interacted with an emulsion nucleus. A general picture of this is given in Fig. 1. Half of all shower particles are found within a cone with the opening angle $\theta_{1/2} = 1°39'$, and the mean geometrical angle θ_g, calculated according to the formula

$$\ln\tan\theta_g = \frac{1}{n_s}\sum_{i=1}^{n_s}\ln\tan\theta_i$$

(where n_s is the number of charged particles in the shower), equals $2°42'$.

Assuming a symmetrical emission of particles in c.m.s. and their mono-energetic distribution, we obtain for the energy γ_c of the nucleon, in the c.m.s., $\gamma_c(\theta_{1/2}) = 34.7$ and $\gamma_c(\theta_g) = 21.2$. The length of the tunnel l, punched by the incident nucleon in the target nucleus,[1] in units of the nucleonic diameter d, is $l/d = 8$. Consequently, the interaction involved a heavy emulsion nucleus, as confirmed also by the presence of a large number of black and grey tracks $N_h = 35$.

Taking into account the collision with a tunnel containing approximately 8 nucleons, the energy of the incident nucleon is equal[2] to $E = 19 \times 10^3$ Bev. An estimate of the energy of the primary particle, taking into account the energy spectrum of the shower (secondary) particles and the energy spectrum of the shower-producing (primary) particles, was carried out similarly to that in reference 3. If the spectrum of shower-producing particles is $\sim E^{-2.7}$, and the spectrum of shower particles is $\sim E_0^{-2}$, then

$$\ln(2\gamma_c^2) = \bar{x} + \ln B^2 - 2.7\,\sigma^2/n_s,$$

where

$$\bar{x} = \frac{1}{n_s}\sum_{i=1}^{n_s}\ln\frac{2}{\tan^2\theta_i}, \qquad B = 0.6, \qquad \sigma^2 = \frac{1}{n_s}\sum_{i=1}^{n_s}(x_i - \bar{x})^2.$$

Hence, $\gamma_c = 8.6$, and the energy is $E = 1280$ Bev.

In the estimate of the energy it is necessary to take into account the fluctuations in the backward-

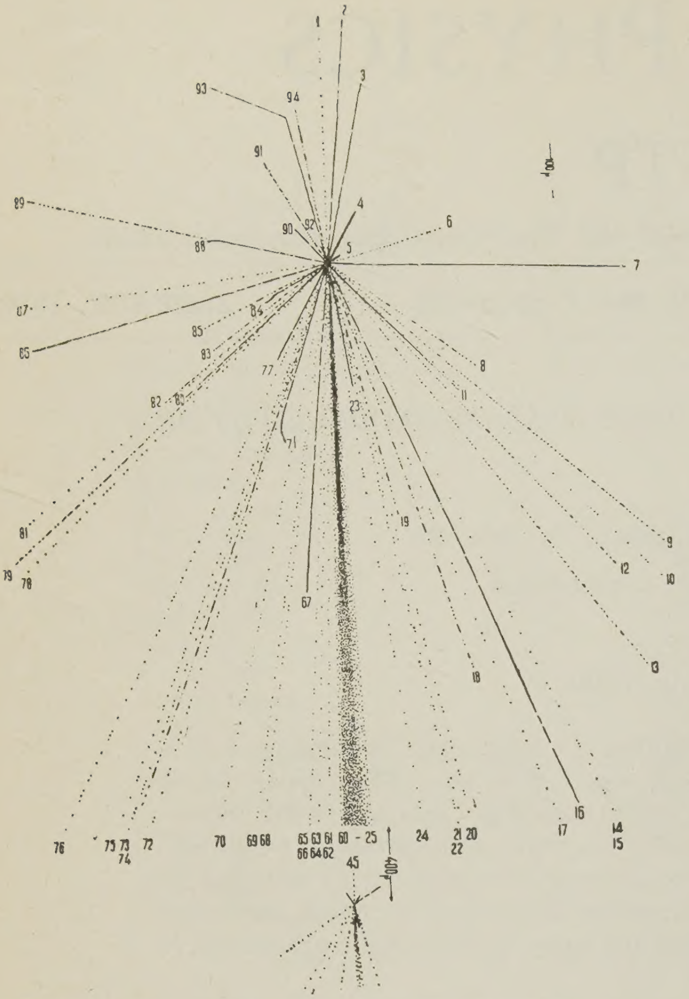

FIG. 1. Microgram of the shower 20 + 15 + 59p and of the secondary interaction 4 + 8 (p or π) produced by a charged particle with energy E = 23.5 Bev.

forward distribution of the particles in c.m.s., and also the fluctuations in the angular distribution. The errors in the energy, due to fluctuations in the distribution of particles in c.m.s., are as a rule larger than the errors due to fluctuations of the angular distribution. Accordingly, we take into account only the errors ΔE due to the first factor. If the shower particles are anisotropically distributed in the c.m.s., $N(\theta^*) \sim \cos^2\theta^*$, then the fraction of particles f emitted in the angle θ_f^* is equal to

$$f = \int_0^{\theta_f^*} \sin\theta^* N(\theta^*)\,d\theta^* \Big/ \int_0^{\pi} \sin\theta^* N(\theta^*)\,d\theta^* = (1 - \cos^3\theta_f^*)/2.$$

If we take into account the fluctuations in the forward-backward distribution, then $n_s/2 + \sqrt{n_s/2}$ of the particles are contained in the angle θ_1^*, and $n_s/2 - \sqrt{n_s/2}$ are contained in the angle θ_2^*. The angles θ_1^* and θ_2^* can be found from the relation

$$f = {}^1\!/_2(1 - \cos^3\theta_f^*) = {}^1\!/_2 \pm \sqrt{1/2n_s}.$$

The corresponding angles in the laboratory system, $\theta_{\min}$ and $\theta_{\max}$, give the possible deviations from $\theta_{1/2}$ and are given by the formula:

$$\tan\theta_{\substack{min\\max}} = \sin\theta_f^* / \gamma_c(1 + \cos\theta_f^*).$$

The angles $\theta_{\min}$ and $\theta_{\max}$, calculated for various forms of the angular distribution in the c.m.s. (isotropy, $\sim\cos^2\theta^*$, $\sim\cos^4\theta^*$), are given in Table I.

TABLE I

	$\theta_{1/2}$	θ_{max}	θ_{min}	γ_c^{max}	γ_c^{min}
Experiment	1°39′	6°01′	0°54′	63.7	9.7
Isotropic distribution	1°39′	1°59′	1°29′	38.6	28.8
$\sim\cos^2\theta^*$	1°39′	3°09′	0°52′	66.2	18.2
$\sim\cos^4\theta^*$	1°39′	4°01′	0°46′	74.7	14.2

Experimentally, allowance for the redistribution of particles in the c.m.s. system reduces to a determination of the angles $\theta_{\min}$ and $\theta_{\max}$, which contain $n_s/2 \pm \sqrt{n_s/2}$ particles in the laboratory system. The values of the angles $\theta_{\min}$ and $\theta_{\max}$ for the shower 35 + 59p are also given in Table I.

It can be seen from the comparison that the experimental data agree satisfactorily with theoretical data for an anisotropic distribution; the higher the degree of anisotropy, the better the agreement. Such a conclusion confirms our assumption about the character of the anisotropy ($\sim\cos^{2n}\theta^*$) of the analyzed 35 + 59p shower.

The energy determined, taking the fluctuations into account, is equal to

$$E = \left(19.2\,{}^{\pm 50.7}_{-14.0}\right)\cdot 10^3 \text{ Bev}.$$

For such a large energy of the primary particle the star should contain, according to Heitler and Terreaux,[4] a small number of heavily ionizing particles (3 or 4), since the energy of the excitation of the nucleus would be small in this case. However, the analyzed shower contains $N_h = 35$. Hence it follows that the theory of Heitler and Terreaux cannot explain the experimental results.

ANGULAR DISTRIBUTION OF SHOWER PARTICLES OF THE STAR 35 + 59p

The differential angular distribution of shower particles of the star 35 + 59p is given in Fig. 2. It has two different maxima for the narrow and for the diffused cones. If we assume[5] that in the case of a collision between a nucleon and a nucleus

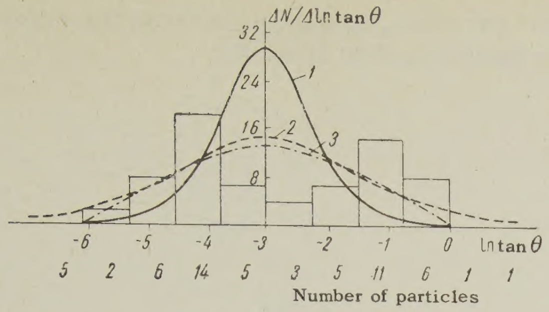

FIG. 2. Histogram of the angular distribution of shower particles of the star in the laboratory system. Curve 1 – isotropic distribution in the c.m.s.; curve 2 – angular distribution according to Heisenberg; curve 3 – according to Landau.

the angular distribution does not differ essentially from the angular distribution of mesons produced in a nucleon-nucleon collision, then, as can be seen from Fig. 2, the theories of Heisenberg[6] and Landau[7] do not explain the observed angular distribution [the probability of a fit is $P(\chi^2) < 0.01$].

The possibility of explaining each maximum of the histogram by an isotropic angular distribution of the produced particles (Fig. 3, curve 2) in a certain coordinate system [$P(\chi^2) \sim 0.75$] makes it possible to use the Takagi model for the production of secondary particles.[8] According to that model, the mesons are produced not at the moment of collision but considerably later. After a collision in the c.m.s. the nucleons are strongly excited and move away from the center of collisions, each conserving its initial energy but having a smaller momentum and, consequently, a larger mass. If we neglect the angular momentum, the angular distribution of produced mesons will be isotropic in a system of coordinates where the excited nucleon is at rest. The emission of mesons by each nucleon follows the statistical theory of Fermi.[9] Thus, in the c.m.s., two sources of mesons are present, and the angular distribution of the produced meson is anisotropic.

It can be assumed that the observed two maxima of the differential angular distribution of Fig. 3 are the results of emission of mesons by two independent centers moving in different directions in c.m.s. These centers are fully equivalent: 30 particles are contained in a narrow angle, while 29 are contained in the diffused one. If the coordinate systems fixed on the emitting centers move in the laboratory system with velocities v_1 and v_2, and the velocity of c.m.s. is v_c, then the centers move in the c.m.s. with velocities $\bar{v}_1$ and $\bar{v}_2$, which can be found from the transformation formula

$$\bar{v}_1 = \frac{v_1 - v_c}{1 - v_1 v_c / c^2}, \qquad \bar{v}_2 = \frac{v_c - v_2}{1 - v_c v_2 / c^2},$$

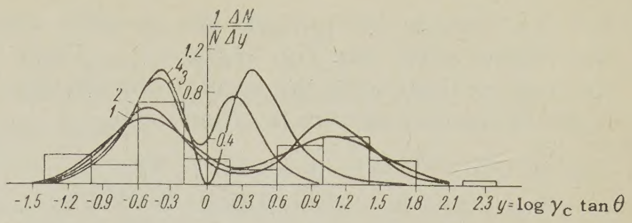

FIG. 3. Differential angular distribution of shower particles in the laboratory system. Curves 1 and 2 – Gaussian and isotropic distributions in the c.m.s., calculated for each maximum separately; curves 3 and 4 – for anisotropy $\cos^2\theta^*$ in the c.m.s. taking into account the energy spectrum of the produced particles, and assuming them to be monoenergetic, respectively.

where

$$v_1 = \sqrt{\gamma_1^2 - 1}/\gamma_1, \qquad v_2 = \sqrt{\gamma_2^2 - 1}/\gamma_2,$$
$$v_c = \sqrt{\gamma_c^2 - 1}/\gamma_c.$$

Here γ_1 and γ_2 are the energies of the emitting centers in the laboratory system. These are determined from the angular distribution of the narrow and wide cones separately. From these formulae we find, in the c.m.s. $\bar{\gamma}_1 = 2.85$ and $\bar{\gamma}_2 = 2.95$; we can assume that $\bar{\gamma}_1 = \bar{\gamma}_2 \equiv \bar{\gamma}$.

We plotted the angular distribution in the c.m.s. for different values of $\bar{\gamma}$ (1.5 and 2.5) and compared them with the experimental histogram constructed under the assumption $\beta_c = \beta_\pi^*$. Both curves are different from the histogram; consequently, the model shown above does not describe the observed meson distribution in the c.m.s. even for $\beta_c = \beta_\pi^*$. If we calculate $\bar{\gamma}$, γ_c', and the inelasticity factor k, as was done in reference 10, then the obtained values $\bar{\gamma} = 3.02$ and $\gamma_c' = \sqrt{\gamma_1 \gamma_2} = 21.52$ differ very little from our values of $\bar{\gamma}_1$, $\bar{\gamma}_2$, and γ_c, and the inelasticity factor $k = 1.5 n_s E_\pi \bar{\gamma}/2\gamma_c' \approx 3$ for $E_\pi = 0.5$ Bev is substantially larger than unity, which has no physical meaning.

For a full analysis of the star under consideration, from the point of view of the Takagi model, we calculated the excited masses of the colliding particles. Applying the energy and momentum conservation laws to a nucleon-nucleon collision, we obtained $M_1/M_2 = M_1^*/M_2^* \approx 1$ for the ratio of the excited masses in the laboratory system and in the c.m.s. For a collision of a nucleon and a nucleus, the ratio is greatly different from unity: $M_n/M_{\text{tunnel}} = 0.09$. After such a detailed analysis, we came to the conclusion that the Takagi model does not explain all features of the observed showers.

Next, to ascertain the shape of the true angular distribution of the mesons, each maximum of the histogram was approximated by a Gaussian curve with a distribution dispersion of shower particles

$\sigma_1 = 0.39$ for the narrow cone and $\sigma_2 = 0.44$ for the diffused cone (see Fig. 3, curve 1). Then, the function describing the angular distribution in the laboratory system is of the form

$$N(y) = 0.55\,(1.03 \exp\{-(y+0.52)^2/0.30\} + 0.90 \exp\{-(y-1.08)^2/0.39\}),$$

where $y = \log \gamma_c \tan \theta$.

To determine the character of the anisotropy it will be necessary to find a function of the angular distribution $N(\theta^*)$ in the c.m.s., using the formulae for transformation of the angles. In view of the complicated computations involved, the analytic form of this function was not found even for $\beta_c = \beta_\pi^*$; a graphical analysis shows that the form of the anisotropy of such a shower does not agree with the anisotropy predicted according to the Takagi model.

An investigation of the angular distribution of the shower 35 + 59p was next carried out in the laboratory system under the assumption of an anisotropy of the type $\sim \cos^{2n} \theta^*$ in the c.m.s. The curve corresponding to the anisotropy $\cos^2 \theta^*$ in the c.m.s. has two symmetric maxima in the laboratory system and is strongly different from the observed angular distribution (see Fig. 3, curve 4). Account of the energy spectrum of the shower particles and of an anisotropy of the type $\cos^{2n} \theta^*$ yields a curve with two different maxima, which is closer to the true angular distribution (Fig. 3, curve 3). With increasing degree of anisotropy, and with an energy spectrum proportional to E_0^{-2}, the asymmetry in the position of the maxima increases (the maxima move away and decrease). Thus, taking into the account the power-law energy spectrum and the anisotropy of the angular distribution in the c.m.s. provides a possibility of explaining the angular distribution of shower particles in the laboratory system.

For a complete description of the shower, we give the integral angular distribution of the shower particles, taking into account the errors of the measurements (Fig. 4).

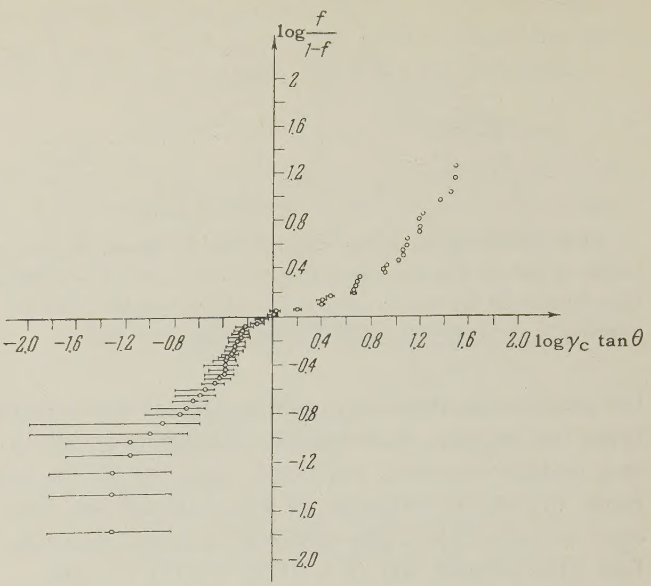

FIG. 4. Integral angular distribution of shower particles of the star 35 + 59 p.

DIFFERENTIAL ANGULAR DISTRIBUTION OF SHOWER PARTICLES IN SHOWERS WITH PRIMARY ENERGY E > 100 Bev

If a sharp division of particles into narrow and diffuse cones is observed in the shower, then the histogram of the differential angular distribution always has two maxima. The positions of the maxima and of the minimum in the shower differ and depend on the energy of the primary particle and, apparently, also on other features of each shower. Showers with such distributions are observed among the stars produced by nucleons with energies > 100 Bev (Table II). Table II lists data on 12 showers (N_g and N_b, are the numbers of grey and black tracks respectively): the summary histogram of their angular distribution is given in Fig. 5. This figure shows also the curve of the

TABLE II

No.	$N_b + N_g + n_s$	θ_g	$\gamma_c\,(\theta_g)$	$\theta_{1/2}$	$\gamma_c\,(\theta_{1/2})$	l/d	$E \cdot 10^3$, Bev
1	0+0+20p	0°50′	68.5	0°41′	83.8	1	13
2	7+2+27p	9°39′	5.9	7°00′	8.1	8	0.9
3	19+4+38p	10°52′	5.2	10°22′	5.5	13	0.4
4	16+3+39p	7°17′	7.8	8°21′	6.8	12	0.7
5	7+2+18p	4°40′	12.1	3°30′	16.3	4	1.9
6	11+5+39p	8°43′	6.5	13°41′	4.1	16	0.2
7	4+3+24p	10°14′	5.5	5°03′	11.3	6	1.4
8	3+1+23p	6°02′	9.5	5°13′	10.9	6	1.3
9	3+2+27p	4°00′	14.3	3°04′	18.7	5	3.2
10	20+15+59p	2°42′	21.2	1°39′	34.7	8.5	19
11	2+2+36p	3°41′	15.5	6°28′	8.8	9	1.2
12	10+3+23p	5°06′	11.2	5°07′	11.2	6	1.4

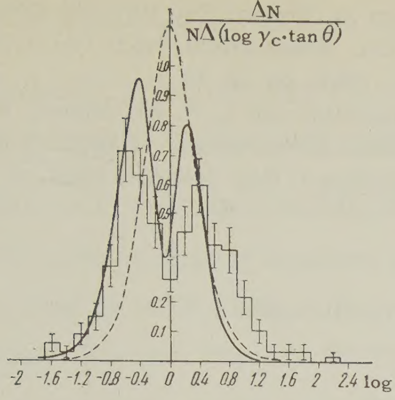

FIG. 5. Total histogram of the angular distribution of shower particles of 12 showers with E > 100 Bev. The dotted curve corresponds to an isotropic distribution in the c.m.s.; the solid curve – to a distribution $\cos^2\theta^*$ and to the energy spectrum of shower particles.

differential distribution, calculated under the condition that the energy spectrum of the produced mesons is proportional to E_0^{-2}, and that the distribution in the c.m.s. is anisotropic, proportional to $\cos^2\theta^*$. This curve describes satisfactorily the experimental histogram.

ANGULAR DISTRIBUTION OF BLACK AND GREY TRACKS OF THE STAR 35 + 59p

As has been stated above, the interaction involved a heavy nucleus of the emulsion (Ag, Br). If we assume that the incident proton traversed the diameter of the nucleus, then according to the theory of Heitler and Terreaux[4] the excitation energy U ~ 150 Mev, and the observed number of heavily ionizing particles should be equal to 3 or 4.

However, in the star analyzed, the number of black tracks is $N_b = 20$ and the experimentally estimated lower limit of the excitation energy is ~ 350 Mev, which is considerably greater than the value predicted by the Heitler-Terreaux theory. According to the evaporation theory (U = 800 Mev, see reference 11), the emission of particles from an excited nucleus should be isotropic. This has not been observed for the black tracks of the star 35 + 59p; the ratio of the number of particles going in the forward direction to the number of particles in the backward direction equals 1.5. We have tried to explain the deviation from isotropy by assuming that a velocity is imparted to the target nucleus, owing to the transfer of a large momentum to it from the primary particle. This velocity is found to be equal to v/c = 0.02 under the assumption that the evaporated particles are protons. For such a velocity of the nucleus, the excess of evaporated protons in the lower hemisphere equals $0.2/E_p^{1/2} = 0.07$. The experimentally observed excess is much larger than this value.

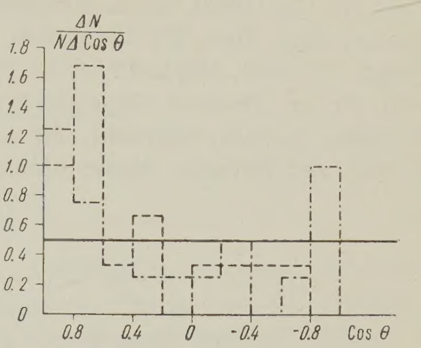

FIG. 6. Differential angular distribution of the grey (dotted) and black (dashed) tracks of the star 35 + 59 p. The straight line corresponds to an isotropic distribution.

Thus, the velocity imparted to the target nucleons (even if we assume that multiply-charged particles are among the evaporated ones) does not explain the observed anisotropy of the black tracks. This is confirmed by the fact that the correlation coefficient[12] of black and grey tracks equals K = 0.43 ± 0.29.

The differential angular distribution of the grey tracks is anisotropic. The ratio of the number of tracks going in the forward direction to those going in the backward direction equals 2.75. The following mechanism is proposed for the production of grey tracks: the incident nucleon interacts with a tunnel filled with nuclear matter, inside of which the mechanism of multiple-particle production is effective. The particles which get outside the tunnel emit additional nucleons in passing through the nucleus. These recoil nucleons we establish as the grey tracks.

---

[1] San'ko, Takibaev, and Shakhova, J. Exptl. Theoret. Phys. (U.S.S.R.) **35**, 574 (1958), Soviet Physics JETP **8**, 396 (1959).

[2] Takibaev, Usik, and Antonova, Dokl. Akad. Nauk SSSR **111**, 341 (1956), Soviet Phys. "Doklady" **1**, 666 (1957).

[3] Zh. S. Takibaev, J. Exptl. Theoret. Phys. (U.S.S.R.) **35**, 277 (1958), Soviet Phys. JETP **8**, 191 (1959).

[4] W. Heitler and C. H. Terreaux, Proc. Phys. Soc. **66**, 929 (1953).

[5] S. Z. Belen'kiĭ and L. D. Landau, Usp. Fiz. Nauk **56**, 309 (1955).

[6] W. Heisenberg, Kosmische Strahlung, Springer-Verlag Berlin-Goettingen, 1953, p. 563-564.

[7] L. D. Landau, Izv. Akad. Nauk SSSR, Ser. Fiz. **17**, 51 (1953).

[8] E. L. Feĭnberg and D. S. Chernavskiĭ, Dokl. Akad. Nauk SSSR **81**, 795 (1951), S. Takagi, Progr. Theoret. Phys. **7**, 123 (1952), W. L. Kraushaar and L. I. Marks, Phys. Rev. **93**, 326 (1954). Z. Koba, Progr. Theoret. Phys. **17**, 288 (1957).

[9] E. Fermi, Progr. Theoret. Phys. **5**, 570 (1950).

[10] Giok, Coghen, Gierula, Holynski, Jurak, Miesowicz, Saniewska, and Pernegr, Nuovo cimento **8**, 166 (1958).

[11] Progress in Cosmic Ray Physics (North Holland Publishing Co., Amsterdam 1952) Vol. 1, Russ. Transl. IIL, 1954, pp. 36-47.

[12] I. G. Venetskiĭ and G. S. Kil'dishev, Пособие по математической статистике (Handbook of Mathematical Statistics), GSI, Moscow 1956, p. 146.

Translated by H. Kasha
1

SOVIET PHYSICS JETP VOLUME 37 (10), NUMBER 1 JANUARY, 1960

PHOTOPRODUCTION OF NEUTRAL π MESONS ON HYDROGEN BY γ QUANTA WITH ENERGY BETWEEN THE THRESHOLD AND 240 Mev

R. G. VASIL'KOV, B. B. GOVORKOV, and V. I. GOL'DANSKIĬ

P. N. Lebedev Physics Institute, Academy of Sciences, U.S.S.R.

Submitted to JETP editor January 23, 1959

J. Exptl. Theoret. Phys. (U.S.S.R.) **37**, 11-22 (July, 1959)

The angular distribution of neutral π mesons produced on hydrogen by γ quanta with energy between the threshold and 240 Mev have been investigated. The energy dependence of photoproduction was studied employing the method of a multichannel analysis of the data of the monitor and of the counters recording single decay γ quanta during an expanded synchrotron pulse. The angular distribution of the π^0 mesons in the c.m.s. has the form given by Eq. (2), which signifies that the photoproduction of neutral π mesons occurs not only in the P but also in the S state. The experimental data on the contribution of the S state are in agreement with the results of the calculations based on Watson's[16] and Feld's[22] theories and makes it possible to estimate the contribution of the direct π^0 meson photoproduction processes and the "intranucleon charge exchange" of π^+ mesons in the S state.

1. INTRODUCTION

THE photoproduction of π^0 mesons on protons has recently been subject to a series of investigations[1-6] because of its importance for the theory of the meson-nucleon interaction. However, the majority of sufficiently accurate measurements[4-6] were carried out for an energy of primary γ quanta higher than 260 Mev, far from the threshold of π^0-meson photoproduction (145 Mev). In the cited experiments, it was found that the main contribution to the total cross section σ_p of the reaction

$$\gamma + p \rightarrow \pi^0 + p \qquad (1)$$

is due to the process associated with the production of an intermediate isobaric (excited) nucleonic state $^3/_3$, $^3/_2{}^+$ with total and isotopic spins $^3/_2$ and positive parity. The isobaric state $^3/_2$, $^3/_2$ corresponds to the production of the meson in the form of a P wave and principally to M1 absorption of γ quanta in the photoproduction. The angular distribution of π^0 mesons should then be described by the two-term formula $d\sigma/d\Omega = 2 + 3\sin^2\theta$, as has been found in reference 4.

In the energy range close to the meson photoproduction threshold, relatively accurate measurements were carried out essentially in one experiment only, that of Koester and Mills.[2] In this experiment, the total cross sections σ_p of process (1) were measured, and it was found that, near the threshold (up to the energy of ~ 180 Mev), σ_p varies as $\tilde{q}^3$, where $\tilde{q}$ is the c.m.s. momentum of the π^0 meson. An analysis of the obtained data based on the theory of Chew and Low[7] confirmed the important role of the ($^3/_2$, $^3/_2{}^+$) state in reaction (1) also in this energy range. Koester and Mills also obtained information regarding the asymmetry in the S state of the angular distribution of π mesons with respect to the direction of 90° due to the photoproduction of π^0 mesons at energies close to the threshold.

A rather strong production of mesons in the S state takes place in the photoproduction of charged π mesons, owing to a straight E1 interaction of γ quanta with the meson cloud. Although an electromagnetic interaction of γ quanta with the π^0p system should also take place (as was indicated by Fermi[8]), it is still markedly weaker than for π^+n and π^-p systems, since, in the first case, the classical radius of the charge carrier, the proton, amounts to $\mu/M \sim 0.15$ of the corresponding value for $\pi^\pm$ mesons. The contribution of photoproduction in the S state for π^0 mesons is therefore much weaker than for $\pi^\pm$ mesons. In the case of the π^0 meson, the bulk of photoproduction in the S state is due not to the straight process of π^0 production but to the production of $\pi^\pm$ mesons with subsequent internal charge exchange.

The effect of π^0 production in the S state should be especially clearly observed in angular distributions near the production threshold. The presence of a small S wave in the production of π^0 mesons should lead to an asymmetry of angular distributions due to the interference between the S wave and the predominating P wave, so that the angular distribution for energies close to the threshold should be described by a three-term formula

$$d\sigma/d\Omega = A + B\cos\theta + C\cos^2\theta, \tag{2}$$

in which the coefficients A, B, and C are determined by the contribution of the different variants (E1, M1, and E2) of the absorption of γ quanta. It is the purpose of the present work to establish the energy dependence of the coefficient A, B, and C near the photoproduction threshold of π^0 mesons, which will make possible to draw a series of conclusions about the mechanism of photoproduction in this energy range.

2. METHOD OF OBSERVATION OF π^0 MESONS

In principle, five methods of observation of the process (1) are possible:

1) Detection of single γ quanta from π^0 meson decay.

2) Detection of single recoil protons.

3) Detection of coincidences of one of the decay γ quanta and the recoil proton.

4) Detection of coincidences of the two decay γ quanta.

5) Detection of coincidences of the two decay γ quanta and the recoil proton.

The small cross section for process (1) for energies close to the π^0 photoproduction threshold, and also the small magnitude of the energy of recoil protons, have determined the choice of the first of the methods listed above for this work. If the cross section for the photoproduction of π^0 mesons in the c.m.s. for a given energy of the primary quantum is given by formula (2) (see Appendix), then the counting rate of γ quanta at an angle θ_γ in the laboratory system (l.s.) per single proton and unit intensity of the incident flux of primary photons is given by the equation

$$N(\theta_\gamma) = \int\limits_{E_{min}}^{E_{max}} N(\theta_\gamma, E_\gamma)\,\eta(E_\gamma)\,dE_\gamma$$

$$= a(\theta_\gamma)A + b(\theta_\gamma)B + c(\theta_\gamma)C, \tag{3}$$

where E_γ is the energy of the decay γ quantum in the l.s.;

$$E_{min} = (1-\widetilde{\beta})\frac{\widetilde{\varepsilon}}{2\gamma_c(1-\beta_c\cos\theta_\gamma)},$$

$$E_{max} = (1+\widetilde{\beta})\frac{\widetilde{\varepsilon}}{2\gamma_c(1-\beta_c\cos\theta_\gamma)};$$

$\eta(E_\gamma)$ is the efficiency of detection of γ quanta with energy E_γ:

$$N(\theta_\gamma, E_\gamma) = \frac{2}{\widetilde{q}\gamma_c(1-\beta_c\cos\theta_\gamma)}\left\{A + B\left(\frac{\cos\theta_\gamma - \beta_c}{1-\beta_c\cos\theta_\gamma}\right)\right.$$
$$\times\left[\frac{1}{\widetilde{\beta}} - \frac{\mu^2}{2\widetilde{q}\gamma_c(1-\beta_c\cos\theta_\gamma)E_\gamma}\right] + C\left\{\frac{\sin^2\theta_\gamma}{2\gamma_c^2(1-\beta_c\cos\theta_\gamma)}\right.$$
$$+\frac{3}{2}\left[\frac{1}{\widetilde{\beta}} - \frac{\mu^2}{2\widetilde{q}\gamma_c(1-\beta_c\cos\theta_\gamma)E_\gamma}\right]^2$$
$$\left.\left.\times\left[\left(\frac{\cos\theta_\gamma-\beta_c}{1-\beta_c\cos\theta_\gamma}\right)^2 - \frac{1}{3}\right]\right\}\right\}; \tag{4}$$

$\beta_c = h\nu/(h\nu + M)$ is the velocity of the c.m.s. in the l.s., and

$$\widetilde{\varepsilon} = (2Mh\nu + \mu^2)/2(2Mh\nu + M^2)^{1/2},$$
$$\widetilde{q} = (\widetilde{\varepsilon}^2 - \mu^2)^{1/2},\quad \widetilde{\beta} = \widetilde{\varepsilon}/\widetilde{q}$$

are the energy, momentum, and velocity of the π^0 meson in the c.m.s. respectively.

Thus, the measured counting rate of single photons from π^0 decay can be correlated with the angular coefficients of Eq. (3).

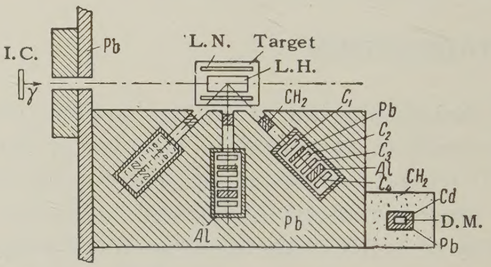

FIG. 1. Schematic diagram of the array. L. H. – Liquid hydrogen, L. N. – liquid nitrogen, I. C. – ionization chamber, D. M. – differential monitor, C_1, C_2, C_3, C_4 – scintillation counters.

3. METHOD OF MEASUREMENT

The experiments were carried out using the 265-Mev synchrotron of the Physics Institute of the U.S.S.R. Academy of Sciences, using the array shown in Fig. 1. Single γ quanta from the decay of π^0 mesons were detected by two telescopes consisting of four scintillation counters (of the type described earlier[9]). The telescopes were set up simultaneously at the angles 90° and 135° or 45° and 90° in the l.s. The length of the synchrotron pulses was stretched to 3000 μsec by a gradual lowering of the amplitude of the accelerating high-frequency voltage, and, during that time, the value of the magnetic field around the position of the synchrotron target was considerably varied, correspondingly changing the maximum energy of the bremsstrahlung spectrum. During each such stretched synchrotron pulse, detector pulses due to the decay γ quanta were fed, as described by us in reference 10, to five channels of a time analyzer, set and checked according to the intensity of the magnetic field through the use of this method. We determined in each measurement the yield of the decay γ quanta for five maximum bremsstrahlung energies simultaneously at both angles.

Apart from the counts of the telescopes that detected the decay γ quanta, the counts of the differential monitor (a single scintillation counter placed in the field of the scattered γ quanta) were fed to a multichannel analyzer. The measurements were carried out for seven maximum bremsstrahlung energy values in various channels, 130, 150, 170, 190, 210, 230, and 250 Mev.

The quantity measured in the experiments was the ratio of the observed numbers of decay γ quanta and the number of counts of the differential monitor for three angles of 45°, 90°, and 135° at the energies given above. To obtain from these data the energy dependence of the decay γ quanta yield at any of the angles, the dependence of the counting rate of the differential monitors per unit photon flux on the maximum bremsstrahlung energy was taken into account. The dependence of the monitor counting rate on the maximum bremsstrahlung energy and on the pulse intensity was determined with a good (~ 1%) statistical accuracy in special experiments discussed in reference 10, which is specially devoted to the present experimental method. The corrections for this dependence are the same for measurements at any angle, and in practice do not influence the measured angular distribution of the decay γ quanta.

To obtain the angular distributions of decay γ quanta from the experimental ratios of their counting rates at various angles, a correction was introduced for these angles for the difference of the product of the effective target volume by the acceptance solid angle of the telescope. This difference was assessed by comparing the counting rate of decay γ quanta during the irradiation of a polysterene "point" source and of a continuous foamed polystyrene target having the dimensions of the hydrogen target. To obtain absolute values of the volume, a correction was applied for the difference of the mean flux of the γ quanta on the surface of the target and on the "point" source. The correction for the not 100%-efficient detection of the anticoincidences by the γ telescope amounted to a fraction of one percent. Also of the same order magnitude were the corrections due to the delayed detection by the differential monitor of the slow neutrons. Both these corrections were neglected in view of their small magnitude.

The liquid hydrogen used in the experiments was contained in a hydrogen target of foamed polystyrene PS-4 (cooled by nitrogen) of cylindrical shape, 12 cm in diameter and 30 cm long. The γ quanta beam from the cyclotron, 6 cm in diameter, was incident upon the base of the cylinder. The background counting rate (from an empty target) amounted, on the average, to 30% (at 45°), 8% (at 90°), and 4% (at 135°) of the counting rate in the main experiments.

The absolute flux of γ quanta incident on the target was determined from the activation of specially calibrated graphite detectors in the $C^{12}(\gamma n)C^{11}$ reaction.

4. RESULTS OF THE EXPERIMENTS

The curves of the energy dependence of the relative yield of decay γ quanta at the angles of 45°, 90°, and 135°, with all the above-mentioned corrections made, are shown in Fig. 2.

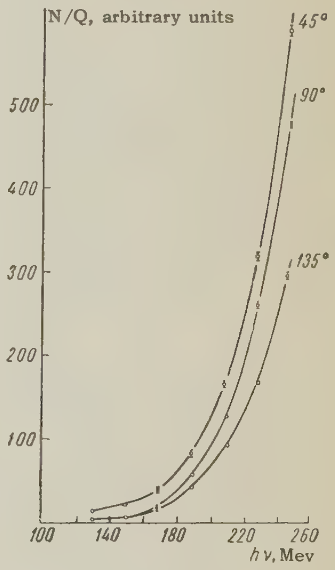

FIG. 2. Energy dependence of gamma yield of π^0-meson decay for 45°, 90°, and 135° in the l.s.

The cross sections for emission of decay γ quanta in the l.s. were obtained from these curves by means of the photon difference method, and were then compared with the values of $N(\theta_\gamma)$ calculated according to Eq. (4), for the determination of the coefficients A, B, and C in Eq. (2). As has been shown by a special analysis, even a rather strong variation of the form of the energy dependence of the detection efficiency of the telescope, $\eta(E_\gamma)$ influences $N(\theta_\gamma)$ very little at various angles for a given energy of the primary γ quanta. In the calculations, we used an efficiency curve for a telescope similar to the one used in the present experiment, as given in reference 1.

$$\eta(E_\gamma) = \alpha\left[1 - \exp\left\{-\left(\frac{E_\gamma - E_{\mathrm{thr}}}{4.3}\right)\right\}\right],$$

where, in our experiment, $E_{\mathrm{thr}} = 35$ Mev.

The absolute value of α ($\alpha = 0.13$) was obtained by comparing the yield of γ quanta from the elastic γp scattering for $h\nu = 130$ Mev, observed at 90°, with a calculated value based on the formula of Powell,[11] which was confirmed by a series of experiments. At present, additional experiments are being carried out to determine the absolute efficiency of detection of γ quanta of various energies by our telescope. The preliminary results of these experiments are in agreement with the calculations. The values of the coefficients $a(\theta_\gamma)$, $b(\theta_\gamma)$, and $c(\theta_\gamma)$ in Eq. (3), calculated for the form of $\eta(E_\gamma)$ given above for various photon energies, are shown in Fig. 3.

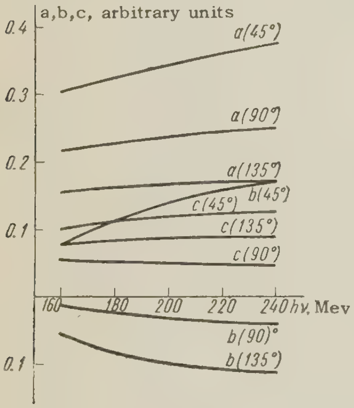

FIG. 3. Dependence of the coefficients $a(\theta_\gamma)$, $b(\theta_\gamma)$, and $c(\theta_\gamma)$ in Eq. (3) on the photon energy.

The obtained values of the coefficients A, B, and C, of the angular distribution, and also the values of the total cross section σ_p of process (1), are given in Table I.

The dependence of the coefficients on the energy of the quanta is shown in Fig. 4. Values of the coefficients obtained in other experiments[3-4] are also given for comparison.

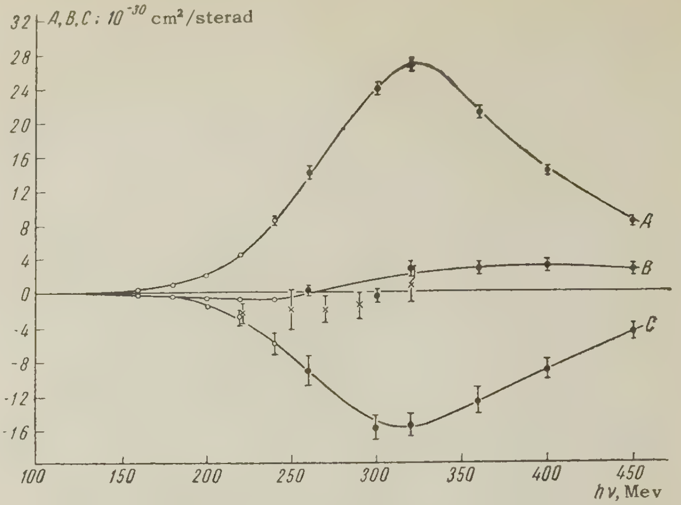

FIG. 4. Coefficients of the angular distribution of π^0 mesons (A, B, and C). ○ – our data, ● – data of reference 4, × – data of reference 3.

The energy dependence of the total cross section of the photoproduction of π^0 mesons on protons, as obtained from the data of our experiments and from those given in the literature,[2-4] is shown in Fig. 5. It can be seen that the total cross sections obtained in this experiment are in a good agreement with earlier published data. With respect to the data on angular distribution, there is no point in comparing them with the results of previous articles, since the only previously available data on the an-

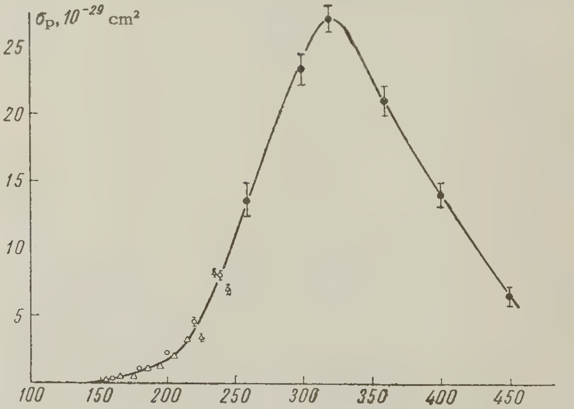

FIG. 5. Energy dependence of total cross sections for the photoproduction of π^0 mesons on protons: ○ – our data, ● – data of reference 4, Δ – data of reference 2.

TABLE I. The measured coefficients A, B, and C (in units of 10^{-30} cm²/sterad) and σ_p (in units of 10^{-29} cm²)

hν, Mev	A	B	C	σ_p
160	0.28±0.03	0.13±0.03	0.09±0.12	0.31±0.06
180	0.95±0.02	0.39±0.06	0.5 ±0.1	0.98±0.04
200	2.10±0.05	0.56±0.07	1.3 ±0.2	2.08±0.08
220	4.5 ±0.1	0.7 ±0.1	2.9 ±0.4	4.5 ±0.2
240	8.4 ±0.2	0.9 ±0.2	6.0 ±0.6	8.1 ±0.3

gular distribution of π^0 mesons in this energy range were obtained with a much lower accuracy.

The data of the present experiment for higher energies, as well as those of McDonald, Peterson, and Corson,[4] are represented in Fig. 6.

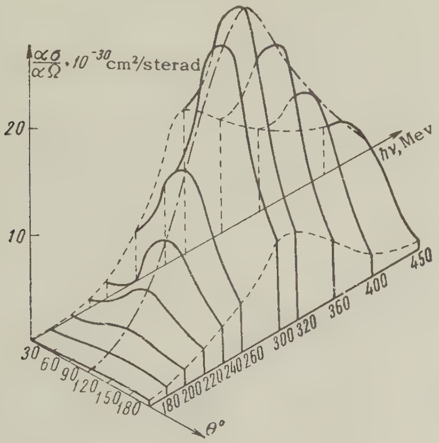

FIG. 6. The form of the angular distribution of π^0 mesons for the reaction $\gamma + p \rightarrow \pi^0 + p$ for γ-quanta energy from 160 to 450 Mev.

5. DISCUSSION OF RESULTS

By way of comparison of the obtained data on the energy dependence and the absolute values of coefficients A, B, and C with the corresponding data for π^+ mesons,[12–15] and to take into account the data available in the literature on the photoproduction of π^0 mesons at higher energies,[4–6] a certain phenomenological analysis was carried out by the method of Watson.[16] The basis of such an analysis is the expression of the cross section of the meson-photon production through the matrix elements of electric and magnetic multipole transitions obtained from general angular momentum and parity conservation considerations. In addition, in such an analysis one uses the assumption of the presence of an "amplified" contribution of the isobaric state $(^3/_3, {^3/_2}^+)$ in the photoproduction of mesons.

In the compilation of the photoproduction of π^+ and π^- mesons near the threshold, we compared the values of the coefficients of angular distributions for various energies of primary γ quanta, corresponding to identical momenta $\tilde{q}$ of produced mesons in the c.m.s. We thus introduced a correction for the difference of the masses of the π^+ and π^0 mesons (based on the fact that the photoproduction cross section is much less dependent on $\tilde{q}$ than on the energy of the primary γ quanta. The results of such a phenomenological analysis are given in Table II.

The parameters in Table II have the following meanings[16]: A_S is the contribution of the S wave to the cross section of photoproduction of π^+ mesons, A_{X_0} is the contribution of the "amplified" P wave that does not interfere with the S wave, A_{K_0} is the contribution of the "amplified" P wave interfering with the S wave, A_{Δ_1} is the contribution of the "non-amplified" P wave not interfering with the S wave, and A_{P^+} is the contribution of the P state to the isotropic part (A^+) of the angular distribution of the photoproduction of π^+ mesons. The values of these parameters were then used for the calculation of the ratio of the coefficients B/A of the angular distribution of π^0 mesons.

According to reference 16, the coefficient B can be expressed by the formula

$$B = -{}^4/_3 (A_S A_{K_0})^{1/2} \{[\cos(\alpha_{33} - \alpha_3) - \cos(\alpha_{33} - \alpha_1)]$$
$$+ (r + \sqrt{2}\, r_0) [\cos(\alpha_{33} - \alpha_3) + {}^1/_2 \cos(\alpha_{33} - \alpha_1)]$$
$$- (r + \sqrt{2}\, r_0)(3/8A_{K_0}) [A_{K_1} + 4A_{\Delta_3}]\}. \tag{5}$$

The quantities A_{K_1} and A_{Δ_3} are small, and we can therefore neglect the last term in Eq. (5). In that energy range where α_1 and α_3 are also small, Eq. (5) reduces to

TABLE II. Results of a phenomenological analysis of the photoproduction of π^0 and π^+ mesons (parameters A given in units of 10^{-30} cm²/sterad)

$h\nu$, Mev	A_S	A_{K_0}	A_{P+}	A_{X_0}	$A_{\Delta 1}$ with α_{33}
160	4.6 ±2.4	0.09±0.10	0.4±2.3	0.3±2.5	0.3±0.8
180	5.8 ±0.8	0.22±0.06	1.5±0.6	0.8±0.8	0.7±0.4
200	7.4 ±1.2	0.39±0.07	2.3±1.1	1.6±1.3	1.2±0.7
220	8.0 ±1.1	0.8 ±0.2	5.0±1.0	3.0±1.2	1.8±0.7
240	8.9 ±1.1	1.2 ±0.3	7.2±1.0	4.9±1.1	2.0±0.6
260	7.1 ±1.4	2.4 ±0.9	9.9±1.3	7.3±1.4	1.9±0.8
300	7.25±1.3	4.0 ±0.8	11.7±1.2	10.8±1.3	—0.2±0.8
320	5.8 ±1.3	5.5 ±0.7	12.6±1.2	11.7±1.3	—0.5±0.7
360	5.4 ±1.2	4.1 ±0.8	8.6±1.1	8.8±1.2	—1.3±0.7
400	4.9 ±1.1	2.5 ±0.6	3.8±1.0	5.4±1.1	—2.2±0.6
450	4.5 ±1.0	1.7 ±0.4	1.1±0.9	3.8±1.0	—2 ±0.6

$$B = -{}^4/_3 (A_S A_{K_0})^{1/2} [(\alpha_3 - \alpha_1) \sin \alpha_{33} + {}^3/_2 (r + \sqrt{2}\, r_0) \cos \alpha_{33}]. \qquad (6)$$

The first term in the square brackets in Eq. (6), which contains the scattering phases, can be interpreted as being connected with the production of π^0 mesons in the S state due to "charge exchange" scattering of π^+ mesons in the nucleon field, and the second term is connected with the direct production of π^+ mesons in the S state, due to the photoelectric effect caused by the presence of an electrical dipole moment in the final state.

On the basis of Eq. (6) we can first determine the sum $(r + \sqrt{2}\, r_0)$ for that energy of primary γ quanta for which B (or the ratio B/A) vanishes (i.e., the contributions of the "direct" and the "charge-exchange" photoproduction of π^0 mesons in the S state are equal to each other). It is evident that the following equation is satisfied for that energy:

$$\tan \alpha_{33} = -{}^3/_2 (r + \sqrt{2}\, r_0) / (\alpha_3 - \alpha_1). \qquad (7)$$

As can be seen from the data on the ratio B/A obtained in this work as well as in the experiment of McDonald, Peterson, and Corson,[4] (see Fig. 7), B vanishes for a primary γ-quanta energy of 260^{+20}_{-10} Mev, which corresponds to $(r + \sqrt{2}\, r_0) = 0.140^{+0.080}_{-0.020}$, if we assume Orear's values[17] of the phases of α_3 and of α_1 and Bruekner's values[18] of α_{33}. It should be noted that, using the values of B/A obtained in the work of Goldschmidt-Clermont, Osborn, and Scott,[3] for γ quanta of energy close to threshold we obtain, for $B/A = 0$, an energy of about 300 Mev; hence, $(r + \sqrt{2}\, r_0) = 0.45$.

From the dispersion relations[19] one can conclude that $r_0 = 0$ and $r = \mu/M = 0.144$ near the meson photoproduction threshold. In addition, the values r and r_0 should, as has been shown by Baldin,[20] be constant in a wide energy range. Thus, the value of $(r + \sqrt{2}\, r_0)_{B=0} = 0.14$ obtained above is in good agreement with the prediction of the field theory. It should be noted that the parameter r is directly related to the threshold ratio of the cross sections of photoproduction of π^- and π^+ mesons on nucleons, $(\sigma_-/\sigma_+)_{\text{thr}} = (1 + r)$. Evidently, according to our data $(\sigma_-/\sigma_+)_{\text{thr}} = 1.30^{+0.19}_{-0.05}$, while the old data[3] yield $(\sigma_-/\sigma_+)_{\text{thr}} \approx 2.1$. The given value of $(\sigma_-/\sigma_+)_{\text{thr}}$ is in agreement with the value obtained in the experiments of the Adamovich group.[21] Assuming that $(r + \sqrt{2}\, r_0) = \mu/M =$ const, we calculated the curve of the dependence of the ratio B/A on the energy of γ quanta up to 450 Mev, shown in Fig. 7. It is evident that all the collected experimental data are well described by this curve.

In Fig. 7 are also shown two curves of B/A calculated by Feld[22] on the basis of the semi-phenomenological "atomic" nucleon model. Feld calculated the photoproduction of π^0 mesons in the S state by perturbation theory, but applied a small correction to take into account the final mass of the nucleon and the possibility of a "charge exchange" scattering of π^+ mesons in the nucleon field. In the final expressions for the cross section only the contributions of transition amplitudes leading to the excited isobaric state and to the photoproduction of π^0 mesons in S state were taken into account. The angular distribution of π^0 mesons in the c.m.s. is then obtained in the following form

$$\frac{1}{\sigma_0} \frac{d\sigma}{d\Omega}(\theta) = A_0 + B_0 \times \left[1 - \frac{\tilde{\beta}^2 \sin^2 \theta}{2(1 - \tilde{\beta} \cos \theta)}\right] \cos \theta + C_0 \cos^2 \theta, \qquad (8)$$

where $\sigma_0 \approx 25\tilde{q}$ microbarn/sterad. The value in Eq. (8) is proportional to the sum $(\xi_r \cos \alpha_{33} + \xi_i \sin \alpha_{33})$, where ξ_r and ξ_i are respectively the real and imaginary parts of the electrical dipole amplitude of π-meson photoproduction. The factor in the square brackets of the second term in Eq. (8) is due to the role of the higher multipoles in the photoproduction of $\pi^\pm$ mesons (retarded effects).

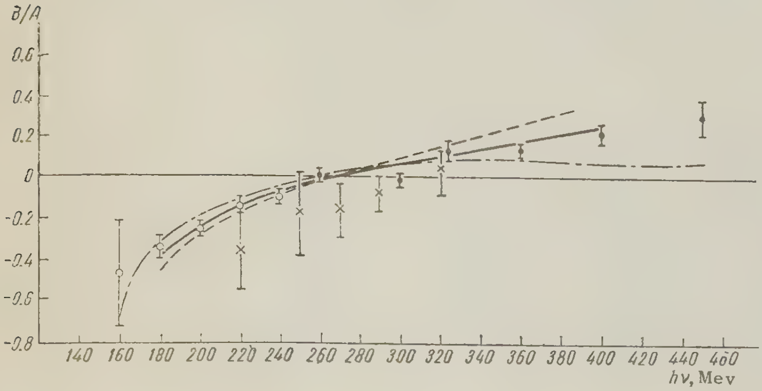

FIG. 7. Ratio of the coefficients B/A. Experimental data: ○ – our data, ● – data according to reference 4, × – data of reference 3; dash-dot line – calculated according to the method of Watson,[16] solid and dotted lines – according to the theory of Feld,[22] taking into account and neglecting the "retardation" effects respectively.

After averaging over the angles of the factor due to "retarding," Feld obtained the relations of the coefficients of the usual three-term development in the form

$$\frac{B}{A} = \frac{B_0}{A_0}\left[1 - \frac{\tilde{\beta}^2}{4\,(1 - \tilde{\beta}^2/2)}\right], \tag{9}$$

$$\frac{C}{A} = \frac{C_0}{A_0} - \frac{B_0}{A_0}\,\frac{\tilde{\beta}^3}{4\,(1 - \tilde{\beta}^2/2)}. \tag{10}$$

As can be seen from Fig. 7, our experimental data are in excellent agreement with the theoretical curves [solid curve corresponds to B/A, dotted line to B_0/A_0 obtained from Eq. (9)], which testifies in favor of the applicability of perturbation theory to calculations of the photoproduction of mesons in the S state near the threshold. The ratio of the real part (direct photoproduction) to the imaginary part (charge-exchange production) of the photoproduction amplitude of π^0 mesons in the S state in the energy range under consideration is close to unity $\xi_r/\xi_i \approx -0.8/\tilde{q}$.

In Fig. 8 we present experimental results, and calculated curves for the ratio C/A according to Feld's theory. For a pure M1 transition, C/A = −0.6. However, as has been mentioned in reference 22, the presence of a small electric-quadrupole contribution (E2) leads to a considerable variation of this ratio. The effects of "retardation" affect this ratio very little up to 300 Mev. As can be seen from Fig. 8, the experimental accuracy of all results obtained is still insufficient to reach a conclusion about the contribution of E2 absorption to meson-photon production. At present, a comparison of the obtained data with the predictions of dispersion relations[19] is being carried out. The results of this analysis will be published in the future.

The authors consider it their pleasant obligation to thank V. V. Pavlovskaya, O. A. Karpukhin, and A. V. Kutsenko, and also I. A. Erofeev for great help in the experimental part of the work, and to A. M. Baldin for valuable advice in the discussion of the obtained results. The authors are very grateful to the technical staff of the 265-Mev synchrotron of the Physics Institute of Academy of Sciences, U.S.S.R.

APPENDIX

KINEMATIC DISCUSSION OF THE REGISTRATION OF PROCESS (1) FROM THE OBSERVATION OF A SINGLE DECAY PHOTON

We shall write the angular distribution of the π^0 mesons in the photoproduction c.m.s. in the form $F(\theta_\pi, E_\pi)\,dE_\pi$. The number of mesons emitted as a result of reaction (1) at the angle θ_π with energy E_π into solid angle $d\Omega_\pi$ is equal to

$$F\,(\theta_\pi, E_\pi)dE_\pi \sin\theta_\pi\, d\theta_\pi\, d\varphi_\pi. \tag{11}$$

If the decay $\pi^0 \rightarrow 2\gamma$ is isotropic in the rest system of the π^0 mesons, the number of decay γ quanta emitted into the solid angle $d\Omega_\gamma$ at the angle θ_γ to the direction of the mesons in the laboratory system is given by

$$F\,(\theta_\pi, E_\pi)dE_\pi \sin\theta_\pi\, d\theta_\pi\, d\varphi_\pi\, \frac{1}{2\pi}\, \frac{1 - \tilde{\beta}^2}{1 - \tilde{\beta}\cos\theta_\pi} \sin\theta_n\, d\theta_n\, d\varphi. \tag{12}$$

The angles are identified in Fig. 9.

Taking into account that γ quanta emitted within the solid angle $d\Omega_\gamma$ can be produced by π^0 mesons going on the surface of a cone with opening angle θ_γ, depending on the energy of the π^0 mesons, we should integrate the expression (12) over the angle φ and the meson energy E_π. Since the energy of the π^0 mesons in the c.m.s. of photoproduction for a given energy of the primary γ quantum $(h\nu)$ should be expressed by a δ function, therefore we obtain by integrating (12)

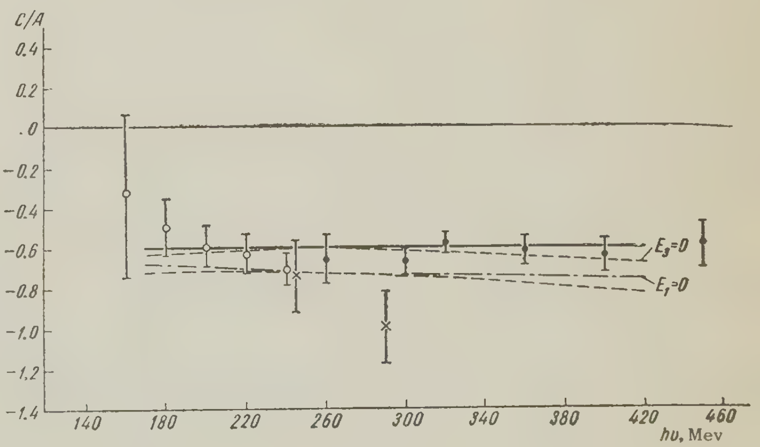

FIG. 8. Ratio of coefficients C/A. ○ – our data, × – data of reference 3, ● – data of reference 4; the upper solid curve corresponds to C/A = – 0.6; lower curves – obtained from the theory of Feld.

$$W(E_\gamma, \theta_\gamma) = \frac{1}{\pi} \int_0^{2\pi} F(\theta_\pi) \frac{d\varphi}{\sqrt{E_\pi^2 - \mu^2}}. \qquad (13)$$

The formulae for the transformation from the π^0 meson rest system to the c.m.s. of photoproduction readily relate the angle θ_γ with the energy of the π^0 mesons and the decay γ quantum:

$$\cos\theta_\gamma = (E_\pi - \mu^2/2E_\gamma)/\sqrt{E_\pi^2 - \mu^2}. \qquad (14)$$

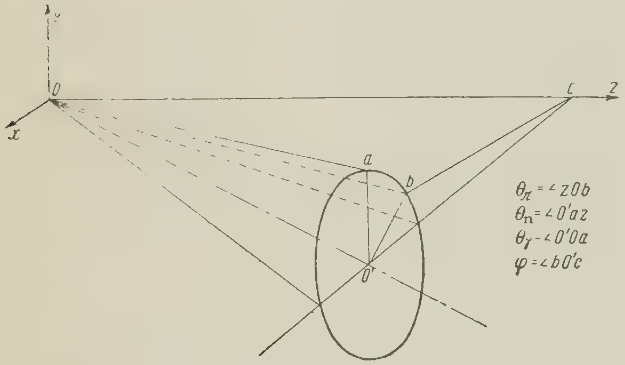

FIG. 9

On the other hand, it is easy to obtain from Fig. 9 the following relation between the angles

$$\cos\theta_\pi = \cos\theta_\gamma \cos\theta_n + \sin\theta_\gamma \sin\theta_n \cos\varphi. \qquad (15)$$

Going now over to the laboratory system of coordinates, we obtain Eq. (4).

---

[1] G. Cocconi and A. Silverman, Phys. Rev. **88**, 1230 (1952).

[2] L. Koester and F. Mills, Phys. Rev. **105**, 1900 (1957).

[3] Goldschmidt-Clermont, Osborn, and Scott, Phys. Rev. **97**, 188 (1955).

[4] McDonald, Peterson, and Corson, Phys. Rev. **107**, 577 (1957).

[5] D. Oakley and R. Walker, Phys. Rev. **97**, 1283 (1955).

[6] Walker, Oakley, and Tollestrup, Phys. Rev. **97**, 1279 (1955).

[7] G. Chew and F. Low, Phys. Rev. **101**, 1570 (1956).

[8] E. Fermi, Elementary Particles, Yale University Press, New Haven, 1951.

[9] Govorkov, Gol'danskiĭ, Karpukhin, Kutsenko, and Pavlovskaya, Dokl. Akad. Nauk SSSR **111**, 988 (1956), Soviet Phys. "Doklady" **1**, 735 (1957).

[10] Vasil'kov, Govorkov, and Kutsenko, Приборы и техника эксперимента (Instruments and Measurement Engg.), in press.

[11] J. Powell, Phys. Rev. **75**, 32 (1949).

[12] Beneventano, Stoppini, Tau, and Bernardini, CERN Symposium on High-Energy Accelerators and Pion Physics, Geneva, 1956, page 259.

[13] Walker, Teasdale, Peterson, and Vette, Phys. Rev. **99**, 210 (1955).

[14] Tollestrup, Keck, and Worlock, Phys. Rev. **99**, 220 (1955).

[15] Jenkins, Luck, Palfrey, and Wilson, Phys. Rev. **95**, 179 (1945).

[16] Watson, Keck, Tollestrup, and Walker, Phys. Rev. **101**, 1159 (1956).

[17] J. Orear, Phys. Rev. **96**, 176 (1954); **100**, 288 (1955).

[18] K. Brueckner, Phys. Rev. **87**, 1026 (1952).

[19] Chew, Goldberger, Low, and Nambu, Phys. Rev. **106**, 1344 (1957).

[20] A. M. Baldin, Nuovo cimento **8**, 569 (1958).

[21] Adamovich, Kuz'micheva, Larionova, and Kharlamov, J. Exptl. Theoret. Phys. (U.S.S.R.) **35**, 27 (1958), Soviet Phys. JETP **8**, 21 (1959).

[22] B. Feld, Annals of Phys. **4**, 189 (1958).

Translated by H. Kasha
2

SOVIET PHYSICS JETP VOLUME 37(10), NUMBER 1 JANUARY, 1960

RADIATIVE RECOMBINATION IN GERMANIUM CRYSTALS BOMBARDED BY FAST ELECTRONS

V. S. VAVILOV, A. A. GIPPIUS, M. M. GORSHKOV, and B. D. KOPYLOVSKIĬ

P. N. Lebedev Physics Institute, Academy of Sciences, U.S.S.R.

Submitted to JETP editor January 29, 1959

J. Exptl. Theoret. Phys. (U.S.S.R.) **37**, 23-26 (July, 1959)

Data are presented on the infrared spectrum accompanying the recombination of electrons and holes in germanium single crystals. It is shown that with increasing concentration of Frenkel defects caused by fast-electron bombardment the relative intensity of the emission band with a peak at 2.35 μ also increases.

INVESTIGATION of the emission spectrum accompanying electron-hole recombination in semiconductor single crystals with diamond structure - germanium and silicon - has provided new information concerning their band structure,[1] energy levels of impurities and dislocations[2,3] and phonon spectrum (lattice vibrations).[4] It may be expected that when carrier recombination occurs through capture by defects produced by fast-particle, especially electron, bombardment,[5] it will be accompanied by infrared emission, whose spectrum will provide a means of determining defect energy levels. We know of no published data on recombination emission from germanium containing defects produced in this manner. In the present work, which was performed for the purpose of obtaining such data, the crystal samples were Weierstrass spheres[6] with 4 mm radius; these were used in order to increase the emission yield, which is usually severely limited by total internal reflection. All samples were made of germanium with n-type conductivity $\rho = 10$ ohm-cm and carrier lifetime $\tau_0 = 220\ \mu$sec.

The results to be presented were obtained from three samples which differed as follows: In sample No. 1 emission was excited by hole injection from an alloyed indium junction, and in samples Nos. 2 and 3 from a pressure contact with indium. Sample No. 3 was irradiated with fast (0.7 Mev) electrons directed against its flat back surface, against the center of which the contact was then pressed. The active acceptor level concentration of defects produced by the bombardment was calculated to be about 5×10^{13} cm^{-3} near the surface, with decrease to zero at a depth of about 0.3 mm. It can be assumed in first approximation that the concentration of bombardment-produced recombination centers equals the concentration of active acceptor levels.

In experiments performed at T = 78°K the back surface of the sample was in direct contact with liquid nitrogen. Spectra were recorded by means of a quartz-prism spectrograph and dry-ice-cooled PbS photoconductive cell, from which signals were fed to a narrow-band amplifier, synchronous detector and EPP-09 recorder.

The spectra of all samples contain a band (Fig. 1) with 1.85 μ (0.67 ev) maximum at room temperature and 1.67 μ (0.74 ev) at 78°K, which was attributed[1] to the intrinsic emission of germanium crystals produced by inter-band transitions of electrons with the cooperation of lattice vibrations. The shift of the long-wave edge of this band is in good agreement with the width change of the forbidden germanium band. From our data the temperature coefficient β is 3.2×10^{-4} ev/deg, which is close to the result obtained by Haynes and Burstein.[1,7]

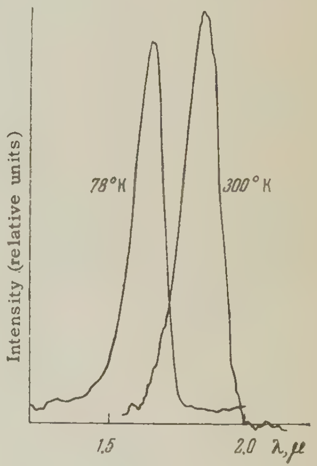

FIG. 1. Intrinsic germanium bands at 300° and 78° K.

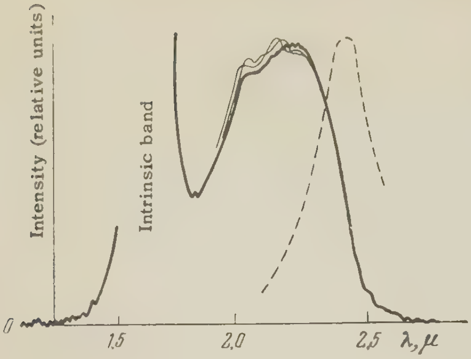

FIG. 2. Extrinsic and intrinsic spectra of germanium sample with alloyed indium junction at 78° K. The maximum of the intrinsic band lies far outside of the figure. Three successively recorded curves are given, and are compared with the spectrum observed by Newman (dashed line).[3]

All samples also yielded a weaker band from 2 to 2.5 μ, which is shown for sample No. 1 by the continuous curves in Fig. 2. Newman[3] and Benoit[8] have observed a band in this region, which Newman attributed to radiative recombination at dislocations because deformed germanium crystals were used in his experiments. The shape and position of the band that we observed at 78°K differ essentially from the spectra given by Newman, which are represented by the dashed curve in Fig. 2. We obtained curve a with spectrograph slits ($\Delta\lambda = 0.175\ \mu$) whose narrowness was limited by photoresistor noise. This broad band is observed in the region where germanium is transparent and there is reason to believe that it consists of a few narrower bands corresponding to impurity or dislocation levels; however, its structure could not be resolved.

The extrinsic spectrum of sample No. 2 at T = 78°K is shown in Fig. 3. The peak is located near 2.35 μ (0.53 ev), and the asymmetry of the curve suggests the existence of additional unresolved peaks.

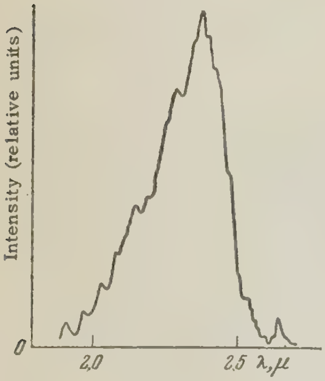

FIG. 3. Extrinsic emission spectrum of n-type germanium sample with neither alloyed indium nor electron bombardment; T = 78° K.

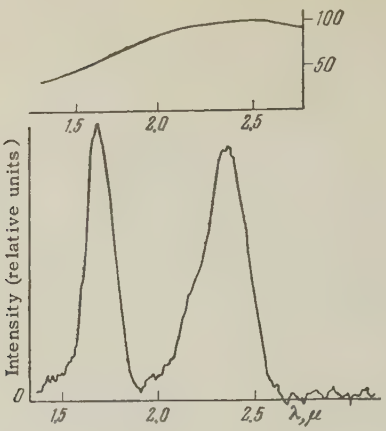

FIG. 4. Spectrum of n-type germanium at T = 78°K after irradiation by 0.7-Mev electrons at room temperature. The sensitivity curve of the PbS photoconductive cell is shown above.

Fig. 4 shows the spectrum of sample No. 3, which was not subjected to alloying with the indium and was irradiated by 0.7-Mev electrons, which strongly attenuated the intrinsic band. For an injection current of 100 μa the signal-noise ratio at the amplifier output for the intrinsic peak was 50 for sample No. 2 and unity for sample No. 3. The intensity of the extrinsic emission was of the same order for both samples.

If electron bombardment had not produced additional levels at which radiative recombination takes place, but only reduced the carrier lifetime (a well-known effect), the intensity of extrinsic radiation, proportional in first approximation to the carrier excess and therefore (for constant injection) to the lifetime ($\Delta p = G\tau$), should be reduced just as strongly. This is not observed, and it is therefore reasonable to assume that radiative recombination takes place at bombardment-produced levels, which evidently belong to Frenkel defects. The energy of these emitted photons is close to the extrinsic spectrum of unbombarded germanium (sample No. 2).

The nature of the centers that cause the extrinsic band of an unbombarded sample has not been established, but it may be assumed that the original material possesses a large number of structural defects or dislocations. The observed emission band may be associated with a level located 0.53 ev from one band of energy levels and therefore 0.22 ev from the other band. A conclusive answer will require experiments with germanium crystals containing a very small initial number of defects and dislocations.

According to existing ideas concerning the nature of recombination radiation, in the case of a large departure from equilibrium concentrations of electrons and holes (strong excitation) their direct recombination, which results in intrinsic radiation, is a bimolecular process; with a carrier lifetime which is independent of excitation the intrinsic band intensity should be proportional to the square of the carrier concentration. In our experiments on samples with an alloyed contact the emission intensity B near the intrinsic peak and the injection current J were related as $B \sim J^m$, where the exponent m is close to 1.7.

The experimental dependence of emission intensity on injection current can be used to give only very approximate results, as it is well known that the recombination rate in germanium usually changes with the injected carrier density. However, according to the statistics of Schockley and Read[9] the lifetime may be constant at large injection levels. Our experiments, with an injection current density above 10 amp/cm^2, may have reached a region where the lifetime is only slightly dependent on the injection level.

It must be pointed out that the intensity of the principal emission peak is a direct measure of carrier lifetime and that intensity measurements can therefore be used to obtain data on the rates of surface and volume recombination.

For the extrinsic band the recombination process obeys first-order kinetics and we may expect a linear dependence between the intensity B and excess concentration, with unchanged lifetime. In our experiments, for the extrinsic band with small injection currents the linear dependence of B on J gradually became sublinear. This can be accounted for by a shorter lifetime as well as by the fact that with increased injection recombination occurs in a larger region, while the concentration of recombination centers decreases with distance from the p-n junction.

The authors wish to thank the following: B. M. Vul for his interest, M. V. Fock and M. N. Alentsev for criticism and valuable suggestions, and L. N. Silonov for assistance with the adjustment of the electronic recording circuit.

---

[1] J. R. Haynes, Phys. Rev. **98**, 1866 (1953).

[2] J. R. Haynes and W. C. Westphal, Phys. Rev. **101**, 1676 (1956).

[3] R. Newman, Phys. Rev. **105**, 1715 (1957).

[4] J. R. Haynes, International Conference on Semiconductors, Rochester, 1958; Phys. and Chem. Solids **8**, 394 (1959).

[5] Vavilov, Smirnov, Galkin, Spitsyn and Patskevich, J. Tech. Phys. (U.S.S.R.) **26**, 1865 (1956), Soviet Phys. "Technical Physics" **1**, 1805 (1956); L. S. Smirnov and V. S. Vavilov, J. Tech. Phys. (U.S.S.R.) **27**, 427 (1957), Soviet Phys. "Technical Physics" **2**, 387 (1957).

[6] P. Aigrain, Physica **20**, 1010 (1954).

[7] E. Burstein and P. Egli, Advances in Electronics and Electron Physics VII, Academic Press, New York, 1955, pp. 1-84.

[8] C. Benoit la Guillaume, International Conference on Semiconductors, Rochester, 1958; Phys. and Chem. Solids **8**, 150 (1959).

[9] W. Shockley and W. T. Read, Phys. Rev. **87**, 835 (1952).

Translated by I. Emin
3

SOVIET PHYSICS JETP VOLUME 37(10), NUMBER 1 JANUARY, 1960

MAGNETIC TRAP WITH FIELD INCREASING TOWARD PERIPHERY

S. YU. LUK'YANOV and I. M. PODGORNYĬ

Submitted to JETP editor, February 1, 1959

J. Exptl. Theoret. Phys. (U.S.S.R.) **37**, 27—32 (July, 1959)

Results are given for the investigation of a plasma formed by an electron beam in a trap characterized by a magnetic field which increases toward the periphery.

OF the many magnetic traps used to contain hot plasmas special interest attaches to systems in which the magnetic field increases toward the periphery. It follows from theoretical considerations,[1,2] that in systems of this kind it should be possible to satisfy the requirements for producing stable equilibrium in the plasma, i.e. the plasma is trapped in a space surrounded by a magnetic "barrier."

In attempting to build a thermonuclear reactor of the trap type one invariably encounters the difficult problem of how the trap is to be filled with high-temperature plasma. In principle, a high-temperature plasma can be produced in the trap by heating a cold plasma in the trap itself or by injecting fast particles into the trap. In traps with a magnetic field which increases toward the periphery, formed by a system of solenoids connected in opposition, it would appear that fast particles can be injected by a method which was proposed recently,[3] in which plasmas are accelerated by electrodynamic methods. Consider the motion of a plasma through a region surrounded by a magnetic barrier (Fig. 1). For a given shape and orientation with respect to the magnetic field H_1 which bounds the trap, the plasma will move into the system if the following condition is satisfied:

$$W \gg H_1^2\tau/8\pi. \tag{1}$$

Here W is the kinetic energy of the directed motion of the plasma and τ is the volume which it occupies after moving into the system. If the plasma expands by virtue of thermal motions or if part of the energy of the ordered motion is converted into heat as a result of collisions after the plasma enters the region of lower magnetic field H_2, the plasma particles become trapped.

Particles can escape from a trap of this kind by diffusion across the magnetic field lines or by entering regions of the magnetic barrier in which the magnetic force lines run into the walls of the container. In the geometry being considered here the force lines run into the sidewalls of the system in circles and the slits through which the particles escape are ring shaped. For short-term processes the width of these slits is given by the expression[2]

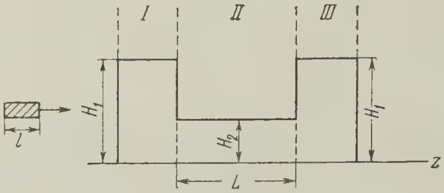

FIG. 1. Penetration of a plasma through a magnetic barrier.

$$\delta_1 = 4\rho_e, \tag{2}$$

where ρ_e is the radius of curvature of a plasma electron in the magnetic field. More precisely, Eq. (2) gives the width of the slit immediately after the production of the plasma inside the trap in a space free from magnetic field. The escape of plasma through the slit obtains by virtue of the thermal velocity of the ions.

If there are collisions the width of the slit increases in time in accordance with the relation for ambipolar diffusion. Hence it would be expected that in the stationary state the width of the slit would increase without limit. This conclusion, however, is not valid. Diffusion broadening stops at that value of δ_1 for which a plasma particle has a greater chance of escaping through the slit after several reflections from the magnetic wall than experiencing a collision with another particle. At low pressures this value of δ_1 can be smaller than $4\rho_e$ and the width of the slit can be the same in pulsed or continuous operation. At higher pressures the diffusion broadening becomes appreciable and the limiting slit width can be estimated by equating the path length of the particle in the trap

$$\lambda_1 = 4V/S = 4V/a\delta_1 \tag{3}$$

and the path length between collisions

$$\lambda_2 = 1/n\sigma \tag{4}$$

(in these formulas V is the volume of the trap, S and a are the area and length of the slit, n is the number of particles per cubic centimeter, and σ is the collision cross section).

The foregoing applies to the case in which the plasma is produced in a space free from magnetic field. If, however, the plasma is produced in a region which is filled with field, for example by means of a beam of fast electrons emitted from the surface of a heated cathode, we must add to δ_1 the width due to the dimensions of the injector. Under conditions of low pressure and strong magnetic field the thermionic electrons ionize the gas, forming a plasma mainly along the lines of the magnetic field. Under these conditions the fractional effective width of the slit due to the dimensions of the cathode and the configuration of the magnetic field is determined by the simple relation

$$\delta_2 = H_0 r^2 / 2 H_m R. \tag{5}$$

Here H_0 and H_m are the magnetic fields in the cathode region and slit region respectively, r is the radius of the cathode and R is the radius of the circular slit ($a = 2\pi R$). In the general case the effective width of the slit can be estimated from the relation

$$\delta = \sqrt{\delta_1^2 + \delta_2^2}. \tag{6}$$

In addition to the circular slits, in the trap being considered here there are two curved slits at the ends of the system close to the axis of symmetry. The radii of these slits are also determined by δ_1 and δ_2. It is easy to see that a large area for the circular slits makes their role decisive in the escape of particles.

In the present paper we describe experiments carried out to study the behavior of a plasma formed by an electron beam injected along the axis of the trap. The experimental parameters were not optimum but were determined by the available experimental apparatus. The vacuum chamber was a cylinder of stainless steel 100 cm long and 21 cm in diameter with ports at the flanges. Mounted in the ports were electron sources which made it possible to obtain an electron beam current of 0.5 amps with an injection voltage up to 1 kv. The vacuum chamber was located inside the system of coils which produced the magnetic field. Each coil consisted of 30 turns of copper tubing cooled by circulating water. The peak current through each coil was 350 amp. The coils could be connected in different ways so that it was possible to obtain the magnetic field configuration desired for a given experiment. An iron jacket was used to reduce the reluctance of the magnetic circuit. The system was evacuated through a side port by means of an oil diffusion pump. In those cases in which the experiment was carried out with hydrogen the gas was admitted to the system through a palladium valve.

The current to the wall was measured by probes which could be moved along the outside chamber. In certain cases the devices for moving the probes were provided with thermocouples with which the temperature could be measured. The direction of motion of the charged particles was studied by means of an oriented probe which was located in the median plane of the chamber. This probe was made from a hollow metal tube which contained a current detector. There was a small aperture in the outer tube so that it was possible to detect particles which entered within a known solid angle.

The radiation spectrum of the hydrogen plasma in the trap exhibited distinct molecular bands. The existence of these bands indicates that the electron temperature in the plasma was not greater than several electron volts.

The first experiments were undertaken to determine the nature of longitudinal current distribution to the wall (parallel to the z axis) as a function of the gas pressure in the chamber. When these experiments were completed the coils were connected in opposition. In Fig. 2 is shown the absolute magnitude of the magnetic field strength along the axis of the system. The current in each coil was 300 amp; this current is typical for the series of experiments considered here.

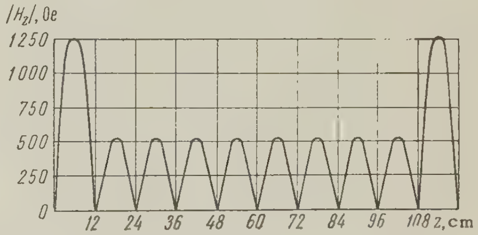

FIG. 2. Magnetic field distribution along the axis of a system; H_z is the magnetic field at the axis of the chamber.

It was shown by means of direct experiments that the charged particles escaped to the wall only through the circular slits in the magnetic field. In Fig. 3 is shown the variation of electron current to a probe kept at the potential of the wall while moved along the chamber; during these measurements the hydrogen pressure p_0 was maintained at 5×10^{-5} mm Hg. The clearly defined maxima in the current are opposite each circular magnetic slit; the intensity of these maxima falls off rapidly with slit number, i.e., with increasing distance from the source (the second source was not used in this experiment). A similar pattern is obtained

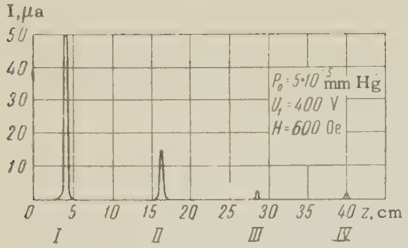

FIG. 3. Variation of current to the lateral probe as function of probe position.

if one studies the temperature distribution along the wall by means of a thermocouple which can be displaced along the z axis.

When the pressure changes the distribution of current between the slits also changes. Thus, when the chamber pressure is between 2 and 5×10^{-6} mm Hg and only one source is used almost all the charged particles escape through the circular slit closest to the source. However, when the pressure is increased the current at the first circular slit is reduced while the flow of particles through the successive slits is increased. In Fig. 4 is shown the variation of current through different slits as a function of the hydrogen pressure in the chamber. A characteristic feature of these curves is the marked dependence of current on pressure for slits located far from the injector. On the other hand the slit located closest to the electron beam exhibits a weak reduction as the chamber pressure is increased. Thus, with increasing pressure there is a clear-cut tendency toward the equalization of currents through the slits; this is a direct evidence of the increasing importance of collisions in the plasma.

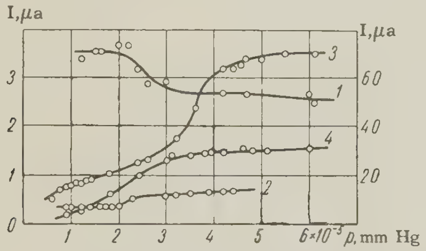

FIG. 4. The current through magnetic slits as a function of hydrogen pressure in the chamber. The number for each curve corresponds to the slit number. The scale at the right refers to Curves 1 and 2; the scale at the left corresponds to Curves 3 and 4.

Experiments carried out with the oriented probe indicated a small anisotropy in the current. However the asymmetry in the angular distribution was much smaller than what would be expected in the presence of a directed flow of electrons.

In the remaining experiments all the coils located on one side of the median plane were connected to produce a magnetic field in one direction while the coils on the other side were connected to produce a field in the opposite direction. This connection configuration made it possible to obtain a field up to approximately 1500 oersteds in the single lateral slit of the trap. With this field configuration the halfwidth of the slit was measured as a function of magnetic field at a fixed gas pressure. The measurements were carried out by means of a movable probe in front of the walls; this probe was a tungsten wire 0.5 mm in diameter and 30 mm long. The probe could be moved along the chamber as shown in Fig. 5. To obtain the distribution curve for the current through the slit, the current vs. probe position curve was differentiated graphically.

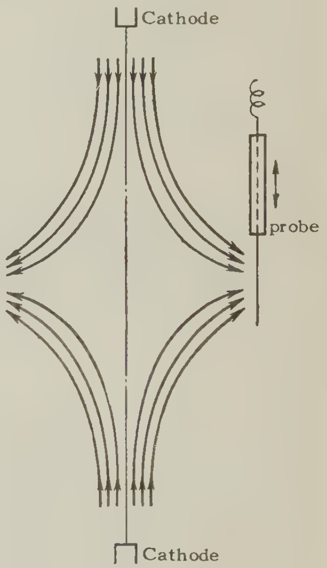

FIG. 5. Arrangement of the probe in the system.

In Fig. 6 are shown experimental curves for the dependence of effective slit width on magnetic field for several values of the energy in the primary electron beam U_1. The hydrogen pressure in the chamber p_0 was kept constant in these measurements (approximately 2×10^{-5} mm Hg).

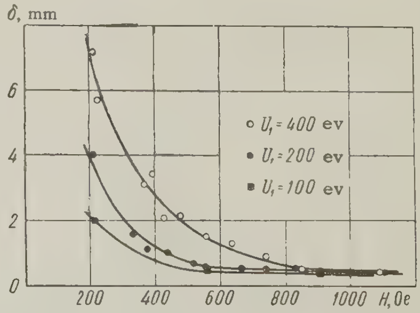

FIG. 6. The effective width of the magnetic slit δ as a function of field strength in the slit.

As is apparent from the figure, at strong magnetic fields (H > 800 oersteds) the effective width of the slit is independent of magnetic field and the energy of the primary electrons and is approximately 0.4 mm. We may note, however, that the value of δ remains constant even when the hydrogen pressure is increased to 5×10^{-4} mm Hg. At weak magnetic fields there is a rapid broadening of the slit which becomes especially pronounced at high primary electron energies.

We now propose an explanation for the observed behavior of $\delta = f(H)$. An estimate of δ_1 on the basis of Eqs. (3) and (4) indicates that this quantity is not greater than 0.1 mm in the pressure region of interest. Since there is essentially no change in the width of the slit as the pressure is increased by a factor of 10, apparently diffusion broadening need not be taken into account. The independence of δ on magnetic field at strong magnetic fields is direct evidence that the contribution of the $4\rho_e$ term to δ is not important. For reasonable values of the plasma electron energies (approximately 1 ev) $4\rho_e$ is less than 0.1 mm with $H = 1000$ oersteds and is correspondingly reduced at larger values of H. Thus it may be assumed that the measured values of the halfwidth in the curve for the electron current to the probe correspond to the electron-optical imaging of the surface of the cathode at the walls of the chamber. With $H_1 \approx H_2$, $r = 8.5$ mm and $R = 100$ mm, according to Eq. (5) δ_2 is 0.35 mm, in agreement with the experimental values of δ.

To explain the rise in the $\delta = f(H)$ curves at small values of H we must take account of the fact that the conditions for adiabatic invariance no longer hold when the Larmor radius of the primary electrons becomes comparable with the radius of curvature of the magnetic lines of force. Under these conditions the primary electrons "escape" from the lines of force and enter the "zero-field" region. Later, after a number of collisions with the magnetic walls these electrons again enter the strong-field region close to the slit, but have now acquired considerable transverse velocities. If the fraction of these electrons in the total current to the probe is significant (weak fields and high energies of the primary electrons tend to favor this condition) the effective width of the slit is again determined by the quantity $4\rho'_e$, where ρ'_e is the Larmor radius of electrons with high transverse energy. Qualitatively the experimental data are in good agreement with this picture.

In conclusion we may note that as the pressure in the chamber is increased to approximately 3×10^{-3} mm Hg the effective width of the slit in the strong field region increases. It is assumed that this effect is due to diffusion broadening.

The authors wish to take this opportunity to thank L. A. Artsimovich, R. Z. Sagdeev, and O. B. Firsov for interesting discussions and V. N. Sumarokov for help in carrying out the experiments.

---

[1] S. I. Braginskiĭ and B. B. Kadomtsev, Физика плазмы и проблема управляемых термоядерных реакций (Plasma Physics and the Problem of a Controlled Thermonuclear Reaction) Vol. III, U.S.S.R. Acad. Sci. Press, 1958, p. 300.

[2] O. B. Firsov, Физика плазмы и проблема управляемых термоядерных реакций (Plasma Physics and the Problem of a Controlled Thermonuclear Reaction) Vol. III, U.S.S.R. Acad. Sci. Press, 1958, P. 327.

[3] Artsimovich, Luk'yanov, Podgornyĭ, and Chuvatin, J. Exptl. Theoret. Phys. (U.S.S.R.) **33**, 3 (1957), Soviet Phys. JETP **6**, 1 (1958).

Translated by H. Lashinsky
4

SOVIET PHYSICS JETP VOLUME 37(10), NUMBER 1 JANUARY, 1960

PHASE DIAGRAM FOR LIQUID He^3-He^4 *SOLUTIONS*

K. N. ZINOV'EVA and V. P. PESHKOV

Institute for Physical Problems, Academy of Sciences, U.S.S.R.

Submitted to JETP editor February 3, 1959

J. Exptl. Theoret. Phys. (U.S.S.R.) **37**, 33-37 (July, 1959)

It is established that the critical point for phase separation in He^3-He^4 mixtures occurs at $T = 0.88°K$ and $x = 64\%$ He^3 molar concentration. At the point $T = 0.67°K$ and $x = 82\%$, the λ line intersects the phase separation curve. Above this temperature both phases are superfluid, while below, the He^3-rich phase is nonsuperfluid.

INTRODUCTION

EXPERIMENTS on the visual observation of separated He^3-He^4 mixtures[1] have shown that the boundary between the phases is clearly visible to the eye. The critical temperature at which a liquid of given concentration separates into phases may readily be deduced from the moment of appearance of the boundary. The critical point for phase separation in a He^3-He^4 solution having a concentration $He^3/(He^3 + He^4) = 51.1\%$ has already been determined by this method. The value of T^{cr} found for this concentration agreed to within the limits of error with the measurements of Walters and Fairbank.[2]

On the basis of a preliminary investigation into the character of the flow of the separated liquid, the suggestion was advanced in reference 1 that both phases were superfluid. It was essential that this hypothesis be confirmed by more direct observations. As we have previously noted,[1] the measurements of the λ line in solutions having high He^3 concentrations carried out by Daunt and Heer[3] indicate, rather, that the upper phase is in the normal state. These measurements, however, do not appear to be reliable. The data of Esel'son, Bereznyak and Kaganov,[4] as well as the data of Ptukha[5] and a number of other authors, were obtained with solutions having concentrations not exceeding 40%; thus the form of the λ line for concentrations above 40% has been in need of clarification.

In the present work we have set ourselves the task of investigating the temperature dependence of the λ transition curve simultaneously with the solution phase separation diagram. Direct determination of the temperature dependence of the λ line and the phase separation curve for solutions in the high-concentration region make it possible to reach a conclusion regarding the state of the liquid in the upper phase. In this work all measurements were performed using the visual method of observation.

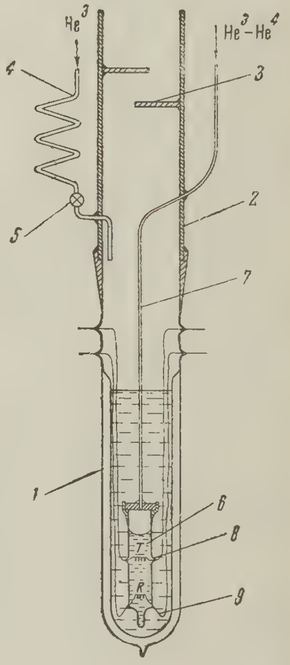

FIG. 1. Apparatus for measurements on the phase diagram of liquid He^3-He^4 solutions.

EXPERIMENTAL APPARATUS AND TECHNIQUE

The measurements were conducted with an apparatus whose interior is illustrated schematically in Fig. 1. A small transparent Dewar 1 filled with liquid He^3, 8 mm in diameter and 100 mm long, was placed within a double Dewar containing liquid He^4. A low temperature was produced within the small Dewar by pumping on the He^3 vapor with a mercury diffusion pump. The pumping was carried out through a 15-mm copper tube 2, joined farther up to one of steel. A copper screen 3 was fixed into the tube 2, in thermal contact with the liquid He^4, in order to reduce the heat transfer from above. The output side of the diffusion pump was connected to a coil 4, immersed in the helium bath, in which the He^3 vapor was re-condensed. Liquid He^3, cooled in the coil to bath temperature, ~1°K, was transferred into the inner Dewar as required through a bellows valve 5.

Within the He^3 Dewar there was submerged a glass capsule 6, 3.5 mm in diameter and 20-mm long, into which the He^3-He^4 mixture was condensed through a copper seal and a steel capillary 7. In order to increase the accuracy of determination of the moment at which phase separation occurred, the capsule was terminated at its lower end with a capillary extension 5 to 6 mm long and 0.5 mm in diameter.

A resistance thermometer 8 of 30-μ phosphor bronze and a heater 9 of constantan wire were sealed into the capsule containing the mixture. The temperature of the mixture was measured with the thermometer 8, which had previously been calibrated against the He^3 vapor pressure with the capsule unsealed. The vapor pressure was measured with a MacLeod gage. For determination of the temperature we employed the scale of Sydoriak and Roberts.[6]

The measurements were carried out in the following manner. The previously prepared mixture was condensed into the capsule at a temperature known to be above the λ point. The level of the liquid mixture was always kept below the copper-glass seal. Simultaneously with the initiation of pumping on the He^3 vapor, a small current was passed through the heater 9, causing the mixture to boil. Illumination was provided by a daylight lamp. When the meniscus of the solution was observed through a cathetometer, bubbles of gas were clearly visible, rising through the liquid to the surface. The boiling of the solution stopped immediately as the temperature reached the λ point. The meniscus, at the λ point, became quiet and immobile. We recorded the temperature at which the boiling of the solution suddenly ceased at the λ transition point. In order to repeat the λ point observation during a single experiment, it was necessary each time to stir the solution carefully, since radiation of heat within the superfluid phase led to a nonuniform volume distribution of concentrations. Stirring was accomplished by boiling the mixture above the λ point.

A determination of the solution phase separation temperature was made together with the λ point determination during one and the same experiment. To accomplish this, the power supply to the heater was shut off, and, as the temperature was reduced smoothly, the moment of appearance of the interphase boundary was recorded. The interphase boundary appeared within the capsule from below or above, accordingly as the concentration of the mixture was greater or less than 64% (the concentration corresponding to the peak of the phase separation diagram). Only for concentrations close to 64% did the boundary appear, practically instantaneously, in the central part of the capsule. The critical phase-separation temperature for each concentration was determined from a series of repeated observations of the appearance and disappearance of the boundary, as the system was cooled and heated slightly. For cooling and heating under quasi-stationary conditions, the appearance and disappearance of the boundary occurred at the same temperature. The results of individual measurements, both during the course of a single experiment and from experiment to experiment, agree well with one another. We should note that for all concentrations the reproducibility of the critical points for phase separation of the solutions was appreciably better than that of the λ points.

We recorded the phase separation diagram for the solutions in the absence of a thermal current. Control experiments showed, however, that the dissipation of a small amount of power in the heater caused only an insignificant shift in the critical phase separation temperature.

We were able to obtain the λ point and phase separation temperature for a mixture of one concentration during the course of a single experiment. Each individual experiment was carried out with a new mixture, prepared from the preceding one by the addition of He^4. The mixture was condensed into the capsule through a miniature charcoal trap, containing 1 g of charcoal cooled to liquid nitrogen temperature.

RESULTS OF THE MEASUREMENTS

The results of the measurements of the λ line and the phase separation diagram for He^3 - He^4 solutions are presented in Fig. 2. The two sets of

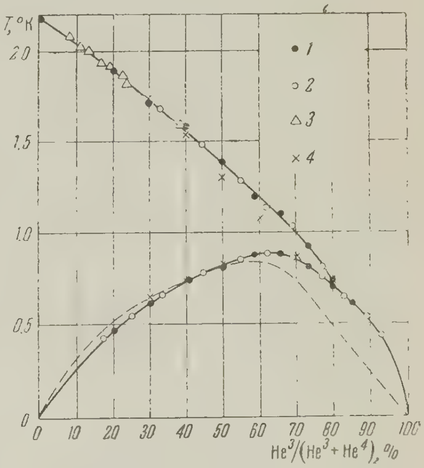

FIG. 2. Phase diagram for liquid He^3 - He^4 mixtures. 1, 2 – present work (apparatus 1 and 2); 3 – data of Esel'son, Bereznyak, and Kaganov;[4] 4 – data of Roberts and Sydoriak;[7] dashed curve – from the data of Walters and Fairbank.[3]

points represented by the closed and open circles correspond to measurements made using two different systems having different diameters for the capillary 7 and different dimensions for the capsule 6 (Fig. 1). In view of the fact that the concentration of a solution might be altered due to enrichment of the vapor in the lighter isotope, we attempted to keep to a minimum the volume occupied by the gaseous phase. In the second apparatus (open circles), the volume of the capsule was increased slightly, while the volume of the gaseous phase was reduced by more than four times, as compared with the first system. Calculation showed, however, that the mass of the vapor did not exceed 2% of the total condensed mass under the least favorable conditions, and that, as a consequence, there must have been virtually no variation in the liquid concentration due to enrichment of the vapor in He^3. It is clearly evident from the figure that the two sets of results do, in fact, agree with each other.

The phase separation diagram for the solutions, as can easily be seen, conforms in its general features to the results of the measurements of Walters and Fairbank,[2] represented in Fig. 2 by the dashed curve. According to our data, however, the maximum and the right-hand branch lie considerably higher. At the conclusion of the present work we were informed of the measurements of Roberts and Sydoriak.[7] Their data on the measurement of the phase separation diagram for solutions with concentrations from 30 to 80%, represented in Fig. 2 by the crosses, lie quite well on our curve.

In Fig. 2, the results of the measurements of the λ line are represented by the closed and open circles on the upper curve. For comparison, the data of Esel'son, Bereznyak, and Kaganov[4] obtained by a different method for solutions with concentrations less than 40%, are indicated by triangles. It is evident that our results agree well with their data. As regards the values of Roberts and Sydoriak (crosses), their λ temperatures in the concentration region above 40% lie appreciably lower than the λ points obtained by us. The discrepancy is evidently to be explained by experimental errors in the work of these authors.[7] We note that the values for the λ temperatures obtained by us are well represented for all concentrations by the empirical formula proposed by Kerr.[8]

$$T_{\lambda s} = T_{\lambda 4}\, x_4^{2/3},$$

where $T_{\lambda s}$ is the solution λ temperature, $T_{\lambda 4}$ is the λ temperature for pure He^4, and x_4 is the concentration of He^4 in the solution.

Values for the λ points and critical phase separation temperatures for mixtures of various concentrations obtained with the two different systems are given in the table. The phase separation temperatures are determined to an accuracy of ± 0.02°K.

Apparatus No. 1			Apparatus No. 2		
x, %	T^{cr}, °K	T_λ, °K	x, %	T^{cr}, °K	T_λ, °K
84.99	0.61	—	93.22	0.44	—
79.84	0.71	0.73	88.90	0.55	—
73.17	0.81	0.92	83.11	0.65	—
66.06	0.88	1.10	77.14	0.75	—
58.78	0.87	1.19	69.23	0.86	1.03
50.08	0.82	1.38	61.93	0.88	1.13
40.34	0.74	1.58	54.85	0.85	1.28
30.28	0.61	1.71	44.76	0.78	1.48
20.37	0.46	1.89	33.35	0.66	1.68
0	—	2.17	24.85	0.54	—
			17.2	0.42	—

From Fig. 2 it can quite clearly be seen that the λ line intersects the solution phase separation curve a substantial distance to the right of its maximum, which corresponds to a temperature $T^{cr}_{max} = 0.88 \pm 0.01$°K and a molar concentration $x = 64 \pm 1\%$. The point of intersection of the λ line with the phase separation curve has, according to our measurements, the coordinates $T^{cr}_{\lambda} = 0.67 \pm 0.02$°K and $x = 81 \pm 1\%$.

In addition to direct measurements of the λ line and the phase separation curve, we performed experiments which further confirmed the superfluidity of the upper phase near T^{cr}_{max}. The first experiment was as follows: a beaker, open at the top, 8 mm long and 1 mm inside diameter, was suspended within the capsule 6 (Fig. 1). The isotope mixture was condensed into the capsule at $T = 0.5$°K in such a way that only the upper phase was introduced into the beaker, while the liquid level was stopped 1 mm above its top. We then elevated the temperature by such an amount that the boundary outside the beaker rose upward, but did not reach the top of the beaker. As the temperature was raised, a boundary appeared at the bottom of the beaker and rose upward. If the upper phase had not been superfluid, the transfer within the beaker by diffusion of a quantity of He^4 sufficient for the appearance of the lower phase would have required tens of hours, while in our case the entire process was completed within ten minutes.

In a second experiment analogous to the first, the beaker, which had a blackened spot, was again completely submerged in the liquid and filled with the upper phase alone; when it was illuminated with a directed light beam, a boundary appeared immediately at the bottom, bearing witness to the filling of the beaker with He^4 by superflow from the upper phase outside the beaker.

A third experiment, testifying graphically to the occurrence of a λ transition in the upper phase, consisted of the following: a quantity of a He^3-He^4 mixture of initial concentration 63.1% was condensed into the capsule 6 at a temperature $\lesssim 0.5$°K, such that the heater was situated in the vicinity of the phase separation boundary in the mixture, lying principally in the upper phase. The volume ratio of the lower and upper phases in this case was ~ 1:2, and the meniscus of the mixture was somewhat lower than the thermometer. The temperature of the liquid was determined approximately with the thermometer, in the vapor region, as well as from the vapor pressure of the He^3 surrounding the capsule. (The difference between the true temperature of the liquid and the thermometer temperature did not exceed 0.01-0.02°K, as was established by observation above the mixture phase separation point.) Upon passage of a current $I = 1$ ma through the heater, $R = 10\Omega$, at a temperature $T \lesssim 0.5$°K, the upper phase boiled vigorously while the lower remained immobile, as could be clearly observed through the cathetometer telescope. As the temperature was raised farther, there came a moment at which the boiling of the upper phase with the heater turned on ceased instantaneously, becoming just as quiet and stationary as the lower phase. The λ transition temperature for the upper phase found in these observations agreed to within the limits of accuracy of the experiment with the value we had found previously, $T_\lambda^{cr} = 0.67 \pm 0.02$°K.

The experiments just described thus leave no doubt that the He^3-rich phase undergoes a λ transition. Above the λ transition temperature the upper phase is superfluid, just as the lower is. Below the transition temperature the He^3-rich phase becomes normal.

With the object of verifying the data on phase separation in He^3-He^4 solutions, we performed control experiments with a mixture of initial concentration $x_0 = 63.1\%$. In these experiments the dependence of the volumes of the upper and lower phases of the solution upon temperature was measured. Using the well-known "lever rule," as written for a presumed linear dependence of the solution density upon concentration:

$$(x_2 - x_0) V_2 = (x_0 - x_1) V_1,$$

where x_1 and x_2 are the He^3 concentrations in the upper and lower phases, whose volumes are, respectively, V_1 and V_2, it is possible from the temperature dependences of V_1 and V_2 and the initial concentration x_0 to compute one branch of the curve when the other branch is given, i.e., $x_1(T)$ for a curve $x_2(T)$. (The assumption of a linear dependence of density upon concentration is made on the basis of the measurements of Ptukha,[5] extrapolated to lower temperatures.) This check showed that to within the accuracy of the measurements of the volumes V_1 and V_2 (~ 2%), the "lever rule" yields the same curve as the direct measurements.

In conclusion, the authors express their gratitude to Academician P. L. Kapitza for his unfailing interest and attention to the problem, and to N. I. Yakovleva, who aided in the measurements and in the assembly of the apparatus.

---

[1] V. P. Peshkov and K. N. Zinov'eva, J. Exptl. Theoret. Phys. (U.S.S.R.) **32**, 1256 (1957), Soviet Phys. JETP **5**, 1024 (1957).

[2] G. K. Walters and W. M. Fairbank, Phys. Rev. **103**, 262 (1956).

[3] J. G. Daunt and C. V. Heer, Phys. Rev. **79**, 46 (1950).

[4] Esel'son, Bereznyak and Kaganov, Dokl. Akad. Nauk SSSR **111**, 568 (1956); Soviet Phys. "Doklady" **1**, 683 (1956).

[5] T. P. Ptukha, J. Exptl. Theoret. Phys. (U.S.S.R.) **34**, 33 (1958); Soviet Phys. JETP **34**, 22 (1958).

[6] S. G. Sydoriak and T. R. Roberts, Phys. Rev. **106**, 175 (1957).

[7] T. R. Roberts and S. G. Sydoriak, Proc. Fifth Internat. Conf. on Low Temp. Physics and Chemistry, Univ. of Wisconsin, 1958, p. 170 (preprint).

[8] E. C. Kerr, Proc. Fifth Internat. Conf. on Low Temp. Physics and Chemistry, Univ. of Wisconsin, 1958, p. 158.

Translated by S. D. Elliott
5

SOVIET PHYSICS JETP VOLUME 37(10), NUMBER 1 JANUARY, 1960

ANGULAR DISTRIBUTION OF FISSION FRAGMENTS IN FISSION INDUCED BY HEAVY IONS

V. A. DRUIN, Yu. V. LOBANOV* and S. M. POLIKANOV*

Submitted to JETP editor February 9, 1959

J. Exptl. Theoret. Phys. (U.S.S.R.) **37**, 38-40 (July, 1959)

The ratio of the yield of fission fragments emitted at angles of 135 and 90° was measured in the fission of gold nuclei induced by carbon and oxygen ions and also in the fission of U^{238} by carbon ions. Measurements were made of the ranges of the fission fragments from the same two reactions. Experimental values of the coefficient of anisotropy of the fission fragments are compared with theoretical values obtained on the basis of statistical theory.

1. INTRODUCTION

THE angular distribution of fission fragments is determined by the relation between the predominant orientation of the spin of the compound nucleus and the direction of fission. For a given total angular momentum the angular distribution depends on the magnitude of the component of the total angular momentum along the direction of fission.[1,2]

In experiments carried out in recent years an anisotropy of the angular distribution of fission fragments was observed in the case of fission of nuclei induced by neutrons,[3,4] protons,[5-7] α-particles,[8] C^{12} nuclei,[9] and γ quanta.[10] It was found that in the case of fission induced by nucleons the fission fragments are emitted primarily along the beam of particles giving rise to fission, whereas in the case of photofission they are emitted at right angles to the beam of γ quanta. This difference is due to the different orientation of the spin of the compound nucleus. The degree of anisotropy depends primarily on the magnitude of the angular momentum introduced by the bombarding particle.

In the present experiments, which are a continuation of the work in reference,[9] we have measured the anisotropy of the distribution of fission fragments in the case of fission induced by C^{12} and O^{16} ions. In this case the compound nuclei produced have larger values of angular momentum than when light particles are used, and this may lead to considerable anisotropy in the angular distribution of fission fragments.

The experimental results are presented below.

2. EXPERIMENTAL TECHNIQUE

The measurements were carried out using the internal beam of the 150-cm cyclotron of the U.S.S.R. Academy of Sciences. The energy of the accelerated particles at the largest radius amounted to 78 and 100 Mev for the C^{12} and O^{16} ions, respectively. The fission fragments were recorded by the activation method by means of a simple arrangement which is shown schematically in Fig. 1. The fission fragments were collected on aluminum foils situated at angles of 90 and 135° with respect to the direction of the beam. The relative yield of fission fragments at a given angle was determined by means of the intensity of β-radiation arising as a result of the decay of the fission fragments. The β particles were recorded by means of an MST-17 end-window counter. Since thick ($\sim 10\,\mu$) films of gold and natural uranium were used for targets, the aluminum collectors received fission fragments from a layer of fissionable material equal to the range of the fission fragments in the given substance. On taking this into account, the degree of angular anisotropy may be expressed in terms of the experimentally observed activation of the collectors by means of the following relation:

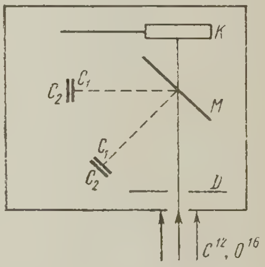

FIG. 1. Schematic diagram of the experiment. K – collector, M – target, D – diaphragm, C_1 – collector I, C_2 – collector II.

$$N(135°)/N(90°) = (A_{135°}\,\sigma_1\,R_{90°}/A_{90°}\,\sigma_2\,R_{135°})\cos 45°,$$

where $A_{135°}/A_{90°}$ is the ratio of the β activities of the collectors situated at corresponding angles, $R_{90°}$ and $R_{135°}$ are the ranges of the fission fragments at angles of 90 and 135°, σ_1 and σ_2 are the average fission cross sections in the layer of the fissionable substance from which the fission

---

*Joint Institute for Nuclear Research Institute Staff.

Reaction	Particle energy, Mev	$\frac{A_{135°}}{A_{90°}}$	$\frac{N(135°)}{N(90°)}$	$\frac{F(141°)}{F(102°)}$	$R_{135°}$, μ Al	$R_{90°}$, μ Al
Au (C^{12}, f)	66	1.03±0.06	0.92±0.08	1.00±0.09	10.1±0.7	10.9±0.9
	78	1.48±0.04	1.20±0.06	1.34±0.07		
	111*			1.62		
Au (O^{16}, f)	85	1.05±0.05	0.99±0.06	1.08±0.07	9.6±0.8	10.9±0.9
	100	1.23±0.05	1.09±0.06	1.23±0.07		
U^{238} (C^{12}, f)	78	1.18±0.05	1.05±0.06	1.11±0.06	11.1±0.7	11.2±0.8

*Data due to Reynolds (private communication).

fragments are collected by foils situated respectively at angles of 90 and 135°.

In order to calculate the coefficient of anisotropy it is necessary to know the ranges of the fission fragments and the dependence of the fission cross section on the energy. The ranges of the fission fragments were determined in separate experiments, when the thickness of the collectors I was less than the range of the fission fragments (2, 5, 8, and 10 μ). The ratio of the β activities of the first and the second collector is related to the range of the fission fragments in the following manner:

$$R = d(1 + A_2\sigma' / A_1\sigma''),$$

where d is the thickness of collector I, σ′, σ″ are the average fission cross sections in the layer of the fissionable material, the fission fragments from which are collected on foils II and I respectively.

The energy dependence of the fission cross section was measured in terms of the activation of the collector at various ion energies.

Chemical separation of individual fission fragments was not carried out. However, the fact that the ratio of the activities of the collectors at angles of 135 and 90° practically did not vary with time points to the small dependence of the angular anisotropy on the mass ratio of the fission fragments.

3. EXPERIMENTAL RESULTS AND DISCUSSION

As a result of the experiments which were carried out we have obtained data on the degree of angular anisotropy of fission fragments produced in the fission of gold by carbon and oxygen ions and in the fission of U^{238} by carbon ions. The experiments with gold were carried out at two different ion energies.

The experimental results are presented in the table. In this table in column 5 we have given the values of the coefficient of anisotropy in the center of mass system at corresponding angles. The errors shown are determined principally by geometric factors (dimensions of the ion beam, the accuracy of the placement of the collector with respect to the β counter, etc.) and by the statistical accuracy of measurement.

The coefficients of anisotropy obtained by us were compared with theoretical values obtained on the basis of the statistical theory.[2] From Fig. 2 it is seen that at a compound nucleus temperature of 1.0 to 2.0 Mev the rotational constant

$$B = \frac{\hbar^2}{2J_{\text{eff}}} \quad \left(\frac{1}{J_{\text{eff}}} = \frac{1}{J_{\parallel}} - \frac{1}{J_{\perp}}\right)$$

($J_{\parallel}$ is the moment of inertia of the compound nucleus with respect to the symmetry axis, $J_{\perp}$ is the moment of inertia of the compound nucleus with respect to an axis perpendicular to the symmetry axis) does not exceed 4 kev. This enables us to conclude that the moment of inertia of the compound nucleus at the saddle point is close to the moment of inertia of a solid.

On assuming that fission is fundamentally symmetric we can estimate the kinetic energy of the fission fragments on the basis of the experimentally observed values of their ranges. In this case the kinetic energy of the fission frag-

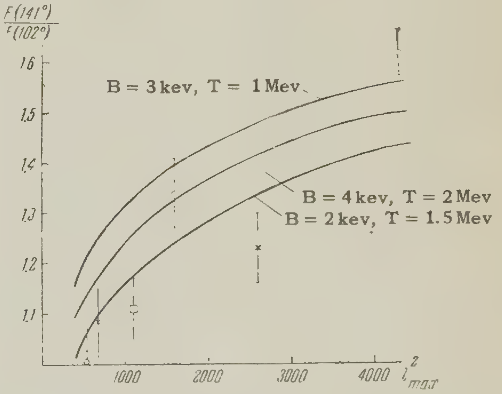

FIG. 2. Dependence of the ratio of the yield of fission fragments at angles of 141 and 120° (center of mass system) on the maximum angular momentum of the compound nucleus $l^2_{\max}$. The curves have been calculated by means of the formulas of reference 2. Experimental values: ○ – for the reaction Au(C^{12}, f), × – for Au(O^{16}, f), □ – for U^{238} (C^{12}, f).

ments is equal to ~ 110 Mev for the reactions Au (C^{12}, f), Au (O^{16}, f) and ~ 140 Mev for the reactions U^{238} (C^{12}, f).

In conclusion we consider it our pleasant duty to express our gratitude to Professor G. N. Flerov for directing the present work, and also to V. M. Strutinskiĭ and to G. A. Pik-Pichak for discussion of results.

---

[1] A. Bohr, Proc. Int. Conf. on Peaceful Uses of Atomic Energy, Geneva, 1955, report No. 911.

[2] V. M. Strutinskiĭ, Атомная энергия (Atomic Energy) **6**, 508 (1957).

[3] J. E. Brolley and W. C. Dickinson, Phys. Rev. **94**, 640 (1954).

[4] Brolley, Dickinson, and Henkel, Phys. Rev. **99**, 159 (1955).

[5] Lozhkin, Perfilov, and Shamov, J. Exptl. Theoret. Phys. (U.S.S.R.) **29**, 292 (1955), Soviet Phys. JETP **2**, 116 (1956).

[6] Cohen, Ferrell-Bryan, Combe, and Hullings, Phys. Rev. **98**, 685 (1955).

[7] J. W. Meadows, Phys. Rev. **110**, 1109 (1958).

[8] I. Halpern, Proc. All-Union Conf. on Nuclear Reactions at Low and Medium Energies, Moscow, 1957.

[9] V. A. Druin and S. M. Polikanov, Proc. All-Union Conf. on Nuclear Reactions at Low and Medium Energies, Moscow, 1957.

[10] E. J. Winhold and I. Halpern, Phys. Rev. **103**, 970 (1955).

Translated by G. Volkoff
6

SOVIET PHYSICS JETP VOLUME 37(10), NUMBER 1 JANUARY, 1960

FISSION OF Th^{232} *INDUCED BY THERMAL NEUTRONS*

E. I. KORNEEV, V. S. SKOBKIN, and G. N. FLEROV

Submitted to JETP editor February 9, 1959

J. Exptl. Theoret. Phys. (U.S.S.R.) **37**, 41-45 (July, 1959)

It is shown that the fission effect which occurs when thorium is irradiated with slow neutrons is in fact due to the fission of Th^{232} by thermal neutrons. The fission cross section is (0.06 ± 0.02) mbn. The results obtained are compared with available experimental data on the fission of even-even nuclei by thermal neutrons.

THE study of the fission of heavy nuclei from energy states lying below the fission barrier has made a considerable contribution both to the understanding of the fission process itself and also to the improvement in our understanding of the structure of atomic nuclei. At the present time investigations with a sufficiently great degree of detail have been carried out only with respect to fission from the ground state or spontaneous fission. A large number of experimental and theoretical papers have been published on the subject, and the most important regularities of spontaneous fission have consequently been established.

In addition to spontaneous fission (fission from states lying 5 or 6 Mev below the barrier) it is also of considerable interest to study fission at excitation energies near the barrier (approximately 1 Mev or less below the activation energy); such energy states are usually produced by the capture of slow neutrons by the so called "nonfissionable" nuclei. In such nuclei the energy of the added neutron is lower than the activation energy, i.e., the energy of excitation for which the lifetime with respect to fission is equal to the lifetime with respect to γ emission. An experimental determination of the probability of nuclear fission at such excitation energies will apparently allow us to obtain interesting information with respect to the shape of the fission barrier.

Some experimental results[1-3] in this direction have been obtained only comparatively recently. This is due to the specific difficulties of the experiment associated with the small values of the cross section. Principally, the results refer to thermal neutron fission; in the majority of cases only upper limits on the cross sections have been obtained. The value $2 \times 10^{-28}\mathrm{cm}^2$ was obtained for the upper limit on the thermal neutron fission cross section of Th^{232}.

The first indication that in all likelihood the observed phenomenon is fission of thorium by thermal neutrons is contained in reference 4. The object of the present work was to obtain more definite data on the fission of Th^{232} by thermal neutrons. Since the fission cross section of Th^{232} was expected to be very small (in any case $< 2 \times 10^{-28}\mathrm{cm}^2$), we have paid particular attention in our experiments to the elimination of possible background fission effects. This background may be due, for example, to the presence in thorium of fissionable impurities, to fission by fast neutrons and by γ-quanta with energies above the fission threshold (if such are emitted by the neutron source), or possibly to the hard γ radiation arising in the capture of thermal neutrons. Even preliminary experiments showed that the thermal column of a reactor could not be used as a source of thermal neutrons, because of the considerable intensity of fast neutrons and of hard γ radiation. In this respect, a photo neutron source is free from the above deficiencies. In our experiments we have used a photo neutron source ($\mathrm{Sb}^{124} + \mathrm{Be}$). The main part of the neutrons from such a source has an energy of ≈ 24 kev; approximately 7% of the intensity is due to neutrons of energy near 400 kev.

Evidently the only fissionable impurity (under the action of thermal neutrons) in thorium may be natural uranium, or more exactly the isotope U^{235}. Uranium concentrations of $\sim 10^{-6}$ are already dangerous. The thorium was purified by sorption of the uranium in an ion-exchange column (the method is described in detail in reference 4). The concentration of uranium in the thorium we used amounted to less than 10^{-7}.

A diagram of the experiment is shown in Fig. 1. The neutron source consisted of a beryllium cylinder of 90-mm diameter and 80-mm length; along the axis of the cylinder there was an opening into which the γ-emitter (Sb^{124}) was inserted in the form of a sphere of 19-mm diameter. The activity of the γ emitter amounted to ≈ 6 Curies. The intensity of the photo-neutron source was $10^8\ \mathrm{sec}^{-1}$.

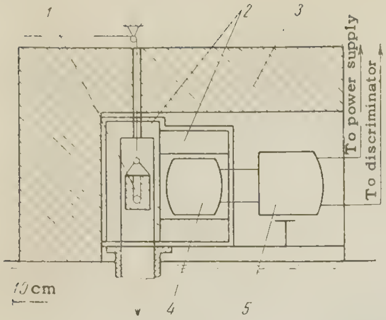

FIG. 1. Schematic experimental arrangement. 1) source, 2) paraffin, 3) shield (lead), 4) chamber, 5) amplifier.

The source was lifted by remote control from its container and placed into a paraffin cavity. The chamber was surrounded by a paraffin layer of 6-cm thickness. The paraffin blocks were surrounded on the outside by a lead screen 25 — 15 cm thick.

We used a multilayered ionization chamber (18-cm diameter, 15-cm height) to record the fission. Thorium in the form of the oxide ThO_2 was deposited on aluminum plates of total area ≈ 2300 cm^2. The total amount of actively utilized material was 2.5 g. The chamber was filled with industrially pure argon at a pressure of 1 atmos. Pulses from the chamber were applied to an amplifier and from there to a recording device with an amplitude discriminator. The amplitude of pulses from the fission fragments at the output of the amplifier amounted to several tens of volts.

To estimate the flux of thermal neutrons, we made use of a similar chamber containing 2.4 mg of natural uranium.

Upon irradiation of the thorium by thermal neutrons, a definite fission effect was observed (see table). To estimate the thermal-neutron fission we initially utilized a cadmium absorber (0.4-mm thick). The counting rate when the chamber was surrounded by cadmium amounted to approximately one half the counting rate without the absorber. Fission in the presence of the cadmium absorber could be ascribed both to neutrons of energy above the absorption limit in cadmium, and possibly also to the hard capture γ radiation from cadmium. Subsequent experiments showed the fission observed in the case of a cadmium absorber due principally to the γ radiation produced in the cadmium. The chamber was surrounded by a thick (≈ 0.6 g/cm^2) boron absorber, and by more cadmium above that. The boron layer effectively absorbed neutrons of a wider energy spectrum than cadmium. The counting rate was reduced by a factor of ~ 20 when the chamber containing the thorium was surrounded by boron. However, fission in the case of two absorbers (cadmium outside and boron inside) corresponded approximately to that in the case of cadmium alone. Therefore, the cadmium absorber (owing to the production of hard γ-radiation accompanying neutron capture) cannot be utilized to separate out the effect due to thermal neutrons. In subsequent work, a boron absorber was used for this purpose.

Experimental conditions	Absorber	Fission effect: Chamber with thorium (counts/hr)	Fission effect: Chamber with uranium (counts/hr)
Source and chamber in paraffin (chamber with copper walls)	–	122 ± 5	99 ± 3
	Cd	60 ± 5	5 ± 0.3
	B (600 mg/cm^2)	6 ± 1	2 ± 0.2
	Cd + B (600 mg/cm^2)	60 ± 8	–
Source and chamber in paraffin surrounded by boron – 100 mg/cm^2 (aluminum chamber)	–	123 ± 5	98 ± 3
	B (600 mg/cm^2)	27 ± 2	5 ± 0.2
Source and chamber in paraffin, additional piece of Be inside paraffin cavity.	–	121 ± 5	101 ± 3
Without paraffin.	B (600 mg/cm^2)	15 ± 3	

The essential role played by photofission in the experiments involving cadmium required the performance of a number of control experiments to estimate the photofission due to the capture γ radiation produced in the materials of the chamber and the shielding. For this purpose we compared thorium fission in two chambers containing the same amount of thorium: a heavy one (copper walls, thick aluminum plates), and a light one (thin aluminum walls, thin plates). The yield of hard capture γ radiation with $E_\gamma > 5.4$ Mev in the case of the light chamber ought to be approximately 20 times lower than for the heavy one. A comparison showed that fission due to the capture γ radiation arising in the materials of the chamber was insignificant. Further, it was shown that γ rays arising in the lead shield due to neutron capture also played an insignificant role. The observed fission effect did not change when the paraffin was surrounded on the outside by a layer of boron (100 mg/cm^2 B_4C). The results of these experiments are also presented in the table.

We have also estimated the possibility of the fission of thorium by fast neutrons, arising in beryllium through capture γ radiation (the cross section for the fission of Th^{232} by fast neutrons is ≈ 10^{-25}cm^2). However, the contribution due to fast neutron fission is apparently very small. When an additional piece of beryllium of approximately the same size as was used in the photoneutron source was introduced into the paraffin cavity, no increase in the number of fissions was observed.

Thus, the foregoing control experiments show that fission due to various side effects makes a very insignificant contribution to the observed effect. The negligibly small content of uranium in thorium ($< 10^{-7}$) excludes the possible explanation of the effect by means of uranium fission (U^{235}). Therefore, the only acceptable explanation is apparently the fission of Th^{232} by thermal neutrons. To estimate the fission of thorium by thermal neutrons, we made use of a thin (100 $mg/cm^2 B_4C$) boron absorber in the form of a layer of boron carbide held together by zapon lacquer. The counting rate of a standard (uranium) chamber with such an absorber was reduced by a factor of 20. As can be seen from the table, the effect due to the thermal neutron fission of thorium amounted to 96 fissions/hour.

Thus, it may be considered established that thorium (Th^{232}) undergoes fission by thermal neutrons. The fission cross section in this case amounts to $(0.06 + 0.02)$ mbn.

The results obtained by us (see Fig. 2) on the fission of Th^{232} may be compared with the available experimental data on the fission of even-even nuclei by thermal neutrons. Figure 2 shows the ratio of the fission cross section to the cross section for the formation of the compound nucleus σ_f/σ_c which is proportional to the probability of fission as a function of the difference $B_n - E_a$, where B_n is the neutron binding energy and E_a is the activation energy; σ_c for thermal neutrons is close to the value for the radiation capture cross section. The calculated threshold values are taken from the work of Vandenbosch and Seaborg.[5] The available experimental data are far from complete (in fact, only upper limits on fission cross sections are available); nevertheless it is apparently possible to speak of the existence of a definite dependence of the probability of fission on excitation energy, namely that the probability of fission decreases exponentially with an increase in $B_n - E_a$. This agrees with the expression provided by theory for the quantum mechanical barrier penetration factor $G \sim \exp\{-\Delta E/\epsilon\}$.[6] For purposes of comparison we have drawn an exponential curve through the point we obtained for fission of Th^{232}, taking the value of the coefficient ϵ in the exponent from theory ($\epsilon = 100$ kev).

Interesting results were recently obtained by Lamphere,[7] who measured the excitation curve for the fission of U^{238} (solid curve in Fig. 2) upon irradiation with neutrons of energy below threshold down to 400 kev. Although these results, strictly speaking, are not completely comparable with the data on the fission of even-even nuclei by thermal neutrons (we here are dealing with the fission of one nucleus at different excitation energies), generally speaking they do not contradict the regularity noted above. The excitation curve has exponential segments with the slope corresponding to $\epsilon \approx 100$ kev. However, the over-all picture is complicated by the presence of horizontal segments which appear near levels corresponding to inelastic scattering.

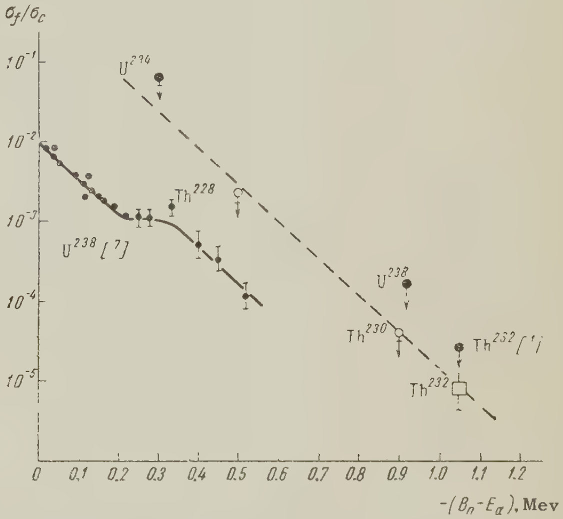

FIG. 2. Thermal neutron fission of even-even nuclei. □ – result of present work; ● – threshold determined experimentally, ○ – threshold calculated; arrow indicates that the value is known to be too high ($\sigma_f <$), crossed arrow indicates upper limit ($\sigma_f \leq$).

The probability of fission is apparently determined not so much by the excitation energy as by the difference between the excitation energy and the activation energy, irrespective of whether only the excitation energy varies, as in the case of a single nucleus, or whether E_a also varies for different nuclei. Thus, it would be interesting to accumulate further experimental data on the fission of even-even nuclei by thermal neutrons. There is also no doubt that the difficulties of carrying out an experiment on the fission by thermal neutrons are considerably less than in the case of fission by neutrons of other energies. In particular, it is of interest to determine the cross sections for thermal neutron fission of the uranium isotopes U^{234} and U^{236} for which fission thresholds have been obtained experimentally.

[1] Neutron Cross Sections, US AEC, 1955.

[2] R. L. Macklin and J. H. Lykins, J. Chem. Phys. **19**, 844 (1951).

[3] Ghiorso, Osborne, and Magnusson, The Transuranium Elements, New York, **14B**, 22 – 26, 1949.

[4] Flerov, Klochkov, Skobkin, and Terent'ev, Dokl. Akad. Nauk SSSR **118**, 69 (1958), Soviet Phys. "Doklady" **3**, 79 (1958).

[5] R. Vandenbosch and G. T. Seaborg, Phys. Rev. **110**, 507 (1958).

[6] V. G. Nosov, J. Exptl. Theoret. Phys. (U.S.S.R.) **31**, 335 (1956), Soviet Phys. JETP **4**, 263 (1957).

[7] L. Granberg and J. S. Levin, Phys. Rev. **109**, 2063 (1958).

Translated by G. Volkoff
7

SOVIET PHYSICS JETP VOLUME 37 (10), NUMBER 1 JANUARY, 1960

MEASUREMENT OF THE POLARIZATION OF DEUTERONS IN THE REACTION $p + p \rightarrow d + \pi^+$ AT PROTON ENERGIES OF 670 Mev

Yu. K. AKIMOV, K. S. MARISH, O. V. SAVCHENKO, and L. M. SOROKO

Joint Institute for Nuclear Research

Submitted to JETP editor February 17, 1959

J. Exptl. Theoret. Phys. (U.S.S.R.) **37**, 46-53 (July, 1959)

The spin polarization of deuterons from the reaction $p + p \rightarrow d + \pi^+$ was measured for proton energies of 670 Mev at three angles, 121°, 140° 30′, and 162°, in the center-of-mass system. The nonresonance p transition ${}^1S_0 \rightarrow {}^3S_1p_0$ was found. The contribution of this transition to the total cross section is about 1%. The measured angular dependence of the spin polarization does not contradict the assumption that the transition amplitudes from the initial two-proton states ${}^3F_2$ and ${}^3F_3$ are equal to zero.

1. INTRODUCTION

THE investigation of the polarization states of deuterons in the reactions

$$p + p \rightarrow d + \pi^+ \qquad (1)$$

is an integral part of the group of experiments connected with the elementary process of the formation of mesons in nucleon-nucleon collisions. In Tripp's experiment[1] the deuteron polarization was measured for proton energies of 340 Mev. His results made it possible to complete the determination of the phenomenological parameters that characterize reaction (1) in the Rosenfeld[2] and also the Gell-Mann and Watson[3] schemes. It was shown that the "resonance" transition ${}^1D_2 \rightarrow {}^3S_1p_2$ is dominant in this energy region, in comparison with the "nonresonance" transition ${}^1S_0 \rightarrow {}^3S_1p_0$. Besides this the Tripp experiment was able to give the ratio between the phase shifts for elastic p-p scattering in the ${}^1S_0$, ${}^1D_2$, and ${}^3P_1$ states and the complex phases of the transition amplitudes in reaction (1). The calculation of this ratio, as is well known, reduces the ambiguity in choosing from a group of phase shifts for 310-Mev p-p scattering.[4]

The results of reaction (1) studied in a polarized proton beam at energies of 536, 616, and 654 Mev[5] established that, beginning at proton energies of 450 Mev, the emission of particles in reaction (1) is observed, not only in s and p states, but also in d states. The results of these experiments and also of experiments with unpolarized beams[6,7] are consistent with the assumption that the d-transition amplitudes for ${}^3F_2 \rightarrow {}^3S_1d_2$ and ${}^3F_3 \rightarrow {}^3S_1d_3$ are equal to zero.

The purpose of the present experiment, besides obtaining supplementary information on reaction (1), was to examine the foregoing assumption and also to improve the estimates of partial cross sections for the examined process at proton energies of 670 Mev.

2. EXPERIMENTAL SETUP

In measuring the deuteron polarization state in reaction (1) we used the approximation method developed by Tripp[1], allowing us to determine the spin polarization of the deuteron.

It is well known that in the general case the polarization state of the deuteron beam is given by the average values of the following spin tensors[8]

$$T_{00} = 1, \quad T_{11} = -(\sqrt{3}/2)(S_x + iS_y), \quad T_{10} = \sqrt{3/2}\, S_z;$$

$$T_{22} = (\sqrt{3}/2)(S_x + iS_y)^2,$$

$$T_{21} = -(\sqrt{3}/2)\left[(S_x + iS_y) S_z + S_z (S_x + iS_y)\right],$$

$$T_{20} = \sqrt{1/2}\,(3S_z^2 - 2). \qquad (2)$$

For a fully unpolarized deuteron beam, the average values of all the spin tensors, with the exception of $\langle T_{00} \rangle$, go to zero. If the deuterons are scattered by some nucleus, then a deuteron polarization is produced. The angular distribution of the polarized deuterons from the second target is given by the relation

$$I = I_0 \left[1 + \alpha + e \cos \Phi + B \cos 2\Phi\right], \qquad (3)$$

where Φ is the azimuthal angle, determined by the relation $\mathbf{n}_1 \cdot \mathbf{n}_2 = n_1 n_2 \cos \Phi$, $\mathbf{n}$ is the normal to the scattering plane, and I_0 is the differential scattering cross section for unpolarized deuterons on the second target. As in the proton case, the deuteron spin after the first scattering lies along the vector $\mathbf{n}_1$, so that

$$\langle S_x\rangle = \langle S_z\rangle = 0, \quad \langle T_{11}\rangle = -i\frac{\sqrt{3}}{2}\langle S_y\rangle.$$

From (3) it is evident that an experiment on the double scattering of deuterons is characterized by three functions in the polar angle θ (not counting I_0):

1) the change in the differential scattering cross section, given by $\alpha = \langle T_{20}\rangle_1\langle T_{20}\rangle_2$;

2) the azimuthal asymmetry term $\sim\cos\Phi$ with the coefficient $e = 2[-\langle T_{21}\rangle_1\langle T_{21}\rangle_2 + i\langle T_{11}\rangle_1 i\langle T_{11}\rangle_2]$;

3) the other azimuthal asymmetry term, $\sim\cos 2\Phi$, with the coefficient

$$B = 2\langle T_{22}\rangle_1\langle T_{22}\rangle_2.$$

The investigation of the dual scattering of deuterons by carbon nuclei was carried out for energies from 94 to 157 Mev.[9] Here only one of the three possible effects showed up, the azimuthal asymmetry $\sim\cos\Phi$. The quadrupole deuteron polarization components $\langle T_{20}\rangle$ and $\langle T_{22}\rangle$ turned out to be equal to zero within the limits of experimental error. This result materially limits the possibilities of observing the deuteron quadrupole polarization, which also appear in other processes, in particular in reaction (1). The coefficient e is determined by both the vector and the tensor character of the deuteron polarization, but the calculations of Stapp[10] show that $\langle T_{21}\rangle$ from carbon is about zero at the same time as $\langle T_{20}\rangle$ and $\langle T_{22}\rangle$, or more exactly, $\langle T_{21}\rangle < 0.15\langle T_{11}\rangle$.

Thus, if we take $\langle T_{21}\rangle = 0$, the double scattering of deuterons from carbon is described by the relation

$$I = I_0[1 + 2i\langle T_{11}\rangle_1 i\langle T_{11}\rangle_2\cos\Phi]. \qquad (4)$$

If s, p, and d states of the emitted particles are taken into account in reaction (1), the deuteron vector polarization from an unpolarized beam of protons is described by the form[11]

$$i\langle T_{11}\rangle_{d\pi^+} = \frac{{}^1/_4\sqrt{{}^3/_2}\sin\theta^*\cos\theta^* e^{i\varphi}(\nu_0 + \nu_2\cos^2\theta^*)}{\gamma_0 + \gamma_2\cos^2\theta^*}, \qquad (5)$$

where θ^* and φ are the angles of emission of the deuterons in the center-of-mass system. The denominator of this expression is equal to the cross section for (1) for an unpolarized proton beam. The coefficients ν_0 and ν_2 are expressed in the following way by amplitudes of the transitions considered:

$$\begin{aligned}\nu_0 = {} & \tfrac{3}{4}\sqrt{5}\,|c_{p_0}|\,|c_{p_2}|\sin(c_{p_0}, c_{p_2})\\ & + |c_{d_1}|\left\{\tfrac{3}{2}\sqrt{\tfrac{5}{2}}\,|c_{d_2}|\sin(c_{d_1}, c_{d_2}) - \tfrac{\sqrt{15}}{2}\,|c_{d_3}|\sin(c_{d_1}, c_{d_3})\right\}\\ & + |c_{d_4}|\left\{\tfrac{25}{8}\sqrt{\tfrac{21}{2}}\,|c_{d_1}|\sin(c_{d_1}, c_{d_4}) - \tfrac{3}{8}\sqrt{\tfrac{105}{2}}\,|c_{d_2}|\sin(c_{d_2}, c_{d_4})\right.\\ & \left. - \tfrac{3}{8}\sqrt{35}\,|c_{d_3}|\sin(c_{d_3}, c_{d_4})\right\} + |c_s|\left\{\tfrac{9}{4}\,|c_{d_1}|\sin(c_s, c_{d_1})\right.\\ & + \tfrac{3}{4}\sqrt{5}\,|c_{d_2}|\sin(c_s, c_{d_2}) - \tfrac{1}{2}\sqrt{\tfrac{15}{2}}\,|c_{d_3}|\sin(c_s, c_{d_3})\\ & \left. + \sqrt{21}\,|c_{d_4}|\sin(c_s, c_{d_4})\right\},\\ \nu_2 = {} & \tfrac{15}{2}\sqrt{7}\,|c_{d_4}|\left\{-3\sqrt{\tfrac{3}{2}}\,|c_{d_1}|\sin(c_{d_1}, c_{d_4})\right.\\ & \left. - \sqrt{\tfrac{15}{2}}\,|c_{d_2}|\sin(c_{d_2}, c_{d_4}) + \sqrt{5}\,|c_{d_3}|\sin(c_{d_3}, c_{d_4})\right\}. \qquad (6)\end{aligned}$$

From (5) it is evident that, in contradistinction to Tripp's experiments, carried out only for one angle ($\theta_d^* = 115$ c.m.s.), the measurements for 670-Mev protons must be done at several angles so that the values of the coefficients ν_0 and ν_2 can be separately determined.

Since we had no data on deuteron scattering from carbon at all the necessary energies, the conditions of the experiment had to be chosen such that the energies of the deuterons from reaction (1) did not go significantly beyond the limits of the investigated energy interval. This requirement was fulfilled for deuteron emission angles greater than 90° in the center-of-mass system.

3. CONDITIONS OF THE EXPERIMENT

The experiment was carried out on a beam of protons with an average energy of 670 Mev and a total intensity of about 5×10^{10} protons/sec. The experimental scheme is shown in Fig. 1. The proton beam emerging from the accelerator was deflected magnetically, focused by quadrupole lenses, and directed onto the first target, in which the reaction $p + p \rightarrow d + \pi^+$ took place. The deuterons and the other secondary particles formed by the interaction of the protons in the primary target were segregated with two collimators and directed toward the center of the deflecting electromagnet, in which the charged particles underwent magnetic analysis. For the choice of the angle and direction of the deflecting in the magnetic field, we used the results of other experiments done under analogous conditions.[12] The deuterons and the other secondary particles were focused by shims set for momenta p = 900 Mev/c and finally were picked out by the collimator in the shielding wall. The secondary target was placed in the laboratory space directly behind the wall. The whole alignment was checked before each run. The ac-

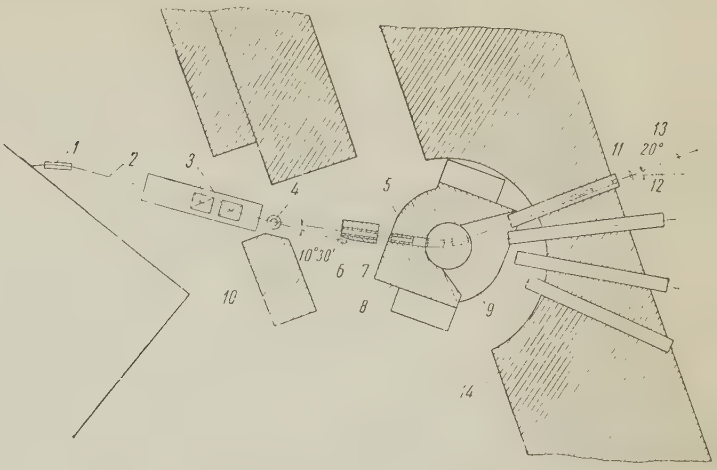

FIG. 1. Experimental setup: 1 – deflectors, 2 – unpolarized proton beam, 3 – 80 mm magnetic lenses, 4 – liquid hydrogen target, 5 – lead shielding, 6 – monitor, 7 – trajectory of particles with momenta 900 Mev/c, 8 – deflecting electromagnet, 9 – focusing shims, 10 – concrete shielding, 11 – carbon target, 12 – deuteron telescope, 13 – removable counter, 14 – shielding wall.

curacy of the alignment was ±1 mm.

The intensity of the proton beam was controlled by an ionization chamber whose current was provided by the δ electrons produced from the walls and electrodes by the action of the proton beam.

4. COUNTING APPARATUS

The telescope which recorded the deuterons elastically scattered by carbon nuclei consisted of five scintillation counters arranged as in the block diagram, Fig. 2. Counters 1, 2, and 4 registered on coincidences, counter 5 on anticoincidences. Pulses from the spectrometric counter 3, which had to act on the amplitude discriminator, passed through a high-speed filter circuit.[13] The pulse from the coincidence circuit acted as a "deciding" signal. If there was no "deciding" signal, the pulses from the spectrometric counter suppressed themselves. The "deciding" signal, destroying the "suppression" signal from the first anticoincidence circuit to the second, let the pulse from the spectrometric counter get to the amplitude discrimanator. After discrimination, pulses were formed by a Kipp oscillator and then impinged on a scaler circuit through a phase inverter and cathode follower. Simultaneously with this, pulses from the coincidence circuit went to another scaler.

5. RESULTS AND EVALUATION

The asymmetry values for the scattering of polarized deuterons, formed on carbon nuclei in the reaction $p + p \rightarrow d + \pi^+$, were measured at angles of 5°30′, 10°22′, and 12°47′. The emission of deuterons at these angles in the laboratory system corresponds to deuteron emission angles of 162°, 140°30′, and 121° in the center-of-mass system.

Figure 3 shows the results of the measurements of the quantity $i\langle T_{11}\rangle_{d\pi^+}$ for the three calculated angles. To determine $i\langle T_{11}\rangle_{d\pi^+}$ from the observed asymmetry e, we used the relation between the scattering asymmetry of deuterons from the second target and the average values of the spin

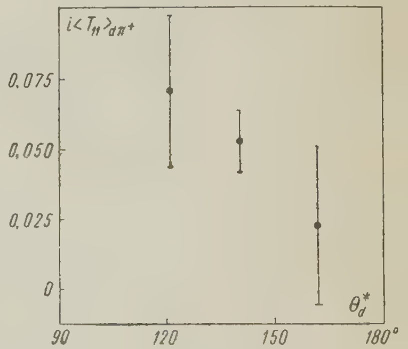

FIG. 3. Measured values of $i\langle T_{11}\rangle_{d\pi^+}$.

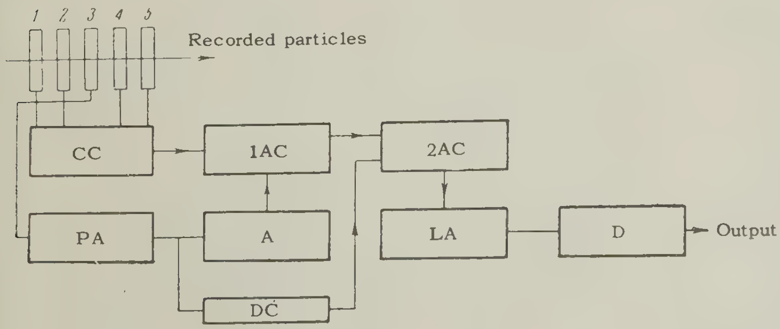

FIG. 2. Block diagram of the counter and discriminator arrangement: CC – coincidence circuit, 1AC – first anticoincidence circuit, 2AC – second anticoincidence circuit, PA – preamplifier, A – amplifier, LA – linear amplifier, D – discriminator, DC – delay circuit, 5 – anticoincidence counter, 3 – spectrometric counter.

tensors in the following approximate form:

$$e = 2i \langle T_{11} \rangle_{d\pi^+} \cdot i \langle T_{11} \rangle_{dC}. \tag{7}$$

Since the quantity $i \langle T_{11} \rangle_{dC}$ at the angle $\theta_d^{lab} = 20°$ is equal to 0.50 for energies from 125 to 156 Mev,[9] $i \langle T_{11} \rangle = e$. Analyzing the experimental data we effected the transition to the function

$$N(\theta_d^*) = \nu_0 + \nu_2 \cos^2 \theta_d^*$$

$$= i \langle T_{11}(\theta_d^*) \rangle_{d\pi^+} \frac{\gamma_0 + \gamma_2 \cos^2 \theta_d^*}{{}^1/_4 \sqrt{{}^3/_2} \sin \theta_d^* \cos \theta_d^* e^{i\varphi}}, \tag{8}$$

where (θ_d^*, φ) are the c.m. deuteron emission angles. Under the conditions of all three runs, $\varphi = 0°$. We used average values[5] for the values of γ_0 and γ_2. The values of $N(\theta_d^*)$ are given in Fig. 4.

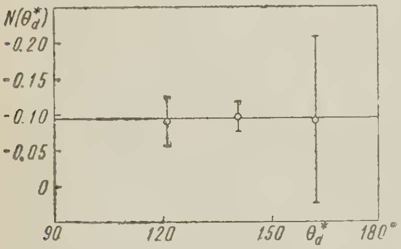

FIG. 4. Measured values of $N(\theta_d^*)$. Solid line – approximating function of the form: $-0.095 - 0.002 \cos^2 \theta_d^*$.

The coefficients ν_0 and ν_2 were determined by the method of orthogonal polynomials for a system of weighted points[14] and were equal to

$$\nu_0 = -(9.5 \pm 2.6) \cdot 10^{-2}, \qquad \nu_2 = -(0.2 \pm 3.6) \cdot 10^{-2}, \tag{9}$$

where the correlated error $\delta\nu_0 \delta\nu_2 = -6.7 \times 10^{-4}$. The choice of a solution with two coefficients of expansion was made on the basis both of the χ^2 criterion and of the insignificant[14] difference in the estimates of S_1^2 and S_{22}^2.

Since $\nu_2 \approx 0$, it follows from (6) that either $|c_{d_4}| = 0$ or

$$-3\sqrt{\tfrac{3}{2}}\,|c_{d_1}| \sin(c_{d_1}, c_{d_4}) - \sqrt{\tfrac{15}{2}}\,|c_{d_2}| \sin(c_{d_2}, c_{d_4})$$

$$+ \sqrt{5}\,|c_{d_3}| \sin(c_{d_3}, c_{d_4}) = 0.$$

For direct conclusions about the d-transition amplitudes, these two possible relations alone are not enough. However, the observed value of ν_2 is consistent with the assumption that the transition probabilities ${}^3F_2 \rightarrow {}^3S_1d_2$ and ${}^3F_3 \rightarrow {}^3S_1d_3$ are equal to zero and that these transitions can be completely neglected. This assumption corresponds to the first assumption above, $|c_{d_4}| = 0$.

Knowledge of the coefficient ν_0 lets us set up a quantitative relation with the amplitudes c_{p_0} and c_{p_2} if we suppose that the basic transition in the reaction $p + p \rightarrow d + \pi^+$ is ${}^1D_2 \rightarrow {}^3S_1p_2$ and that the amplitudes of all the rest of the transitions are significantly less in absolute value. In this case all the terms except the first in the expression for ν_0 can be dropped, and then

$$\nu_0 = \tfrac{3}{4}\sqrt{5}\,|c_{p_0}|\,|c_{p_2}| \sin(c_{p_0}, c_{p_2}). \tag{10}$$

Since the value of $|c_{p_2}|$ under the same assumption is equal to 0.56, if we use the data of Meshcheryakov and Neganov[6] on the total cross sections we get

$$c_{p_0} \sin(c_{p_0}, c_{p_2}) = -0.102.$$

From the angular distribution data used in the estimate of the coefficients γ_0 and γ_2, we find

$$c_{p_0} \cos(c_{p_0}, c_{p_2}) = 0.0465.$$

This approximation of the last quantity may have to be corrected slightly if we estimate the probability of an s-state of the particles in the reaction $p + p \rightarrow d + \pi^+$ (${}^3P_1 \rightarrow {}^3S_1s_1$ transition), using the results of the phenomenological analysis of Gell-Mann and Watson[3] and extrapolating these data to 670 Mev. This estimate of the s-state contribution to the total cross section of the reaction gives a result of about 8%, and this is evidently not an underestimate. Neganov's data[15] on the magnitude of the s-state matrix element corresponding to this contribution (equal to 4% of the total cross section) agree with our result. Consequently, we get

$$c_{p_0} \cos(c_{p_0}, c_{p_2}) = 0.074 \pm 0.04,$$

$$c_{p_0} \sin(c_{p_0}, c_{p_2}) = -0.102 \pm 0.027,$$

$$|c_{p_0}| = 0.126 \pm 0.032, \qquad \angle(c_{p_0}, c_{p_2}) = -54°. \tag{11}$$

Figure 5 shows the plane of the complex variable c_p and the value found for the amplitude $c_{p_0}^{670}$. For comparison, the amplitude $c_{p_2}^{670}$ and also the ampli-

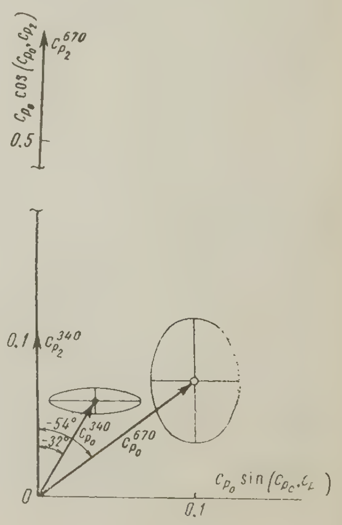

FIG. 5. Transition amplitudes c_{p_0} and c_{p_2} in the complex c_p plane: ● – according to reference 1, ○ – present work.

tudes c_{p_0} and c_{p_2} for a proton energy of 340 Mev are shown:[1]

$$c_{p_0}\cos(c_{p_0}, c_{p_2}) = 0.061 \pm 0.008,$$

$$c_{p_0}\sin(c_{p_0}, c_{p_2}) = -0.0383 \pm 0.0296, \quad |c_{p_0}| = 0.072,$$

$$|c_{p_2}| = 0.102, \quad \angle(c_{p_0}, c_{p_2}) = -32^\circ. \tag{12}$$

Using these data, we determine the contribution of the nonresonance transition $^1S_0 \rightarrow {}^3S_1p_0$ to the total cross section for the reaction $p + p \rightarrow d + \pi^+$ at 670 Mev, or

$$\sigma(^1S_0 \rightarrow {}^3S_1p_0)/\sigma_t \approx \sigma(^1S_0 \rightarrow {}^3S_1p_0)/\sigma(^1D_2 \rightarrow {}^3S_1p_2)$$

$$= |c_{p_0}|^2/5|c_{p_2}|^2 = \left(1.0 {+0.6 \atop -0.45}\right) \cdot 10^{-2}.$$

6. NOTE ON THE APPROXIMATION METHOD OF MEASURING THE DEUTERON VECTOR POLARIZATION

As mentioned above, the basis of the approximation method of measuring the deuteron spin polarization is the vanishing of the spin tensor $\langle T_{21}(20^\circ)\rangle_{dC}$ for double scattering of about 150 Mev deuterons from carbon nuclei. However, experimentally this is not yet proved, so that it is necessary to indicate those possible deviations of this quantity from zero, which would not materially distort the results obtained here.

Let us compare for this purpose the average values of the spin tensors $\langle T_{11}\rangle$ and $\langle T_{21}\rangle$ in the reaction $p + p \rightarrow d + \pi^+$. Using explicit expressions,[11] we get

$$|\langle T_{11}\rangle|_{d\pi+}/|\langle T_{21}\rangle|_{d\pi+}$$

$$= \tfrac{1}{4}\sqrt{\tfrac{3}{2}}\sin\theta\cos\theta\,\nu_0 / \tfrac{1}{8}\sqrt{\tfrac{3}{2}}\sin\theta\cos\theta\,\rho_0 = 2\nu_0/\rho_0.$$

Further

$$\nu_0 = \tfrac{3}{4}\sqrt{5}\,|c_{p_2}|\,|c_{p_0}|\sin(c_{p_0}, c_{p_2});$$

$$\rho_0 = -5|c_{p_2}|^2 + \sqrt{\tfrac{5}{2}}\,|c_{p_2}|\,|c_{p_0}|\cos(c_{p_0}, c_{p_2}) \approx -5|c_{p_2}|^2,$$

$$|\langle T_{11}\rangle|_{d\pi+}/|\langle T_{21}\rangle|_{d\pi+} = 3|c_{p_0}|\sin(c_{p_0}, c_{p_2})/2\sqrt{5}\,|c_{p_2}|.$$

Since for 670 Mev $|c_{p_0}|\sin(c_{p_0}, c_{p_2}) \sim 0.1$, and $|c_{p_2}| = 0.56$, we have

$$|\langle T_{11}\rangle|_{d\pi+}/|\langle T_{21}\rangle|_{d\pi+} = 0.12.$$

Thus, owing to the very large value of $\langle T_{21}\rangle_{d\pi^+}$ the values of $\langle T_{21}\rangle_{dC}(20^\circ)$ must be contained within the limits

$$\langle T_{21}\rangle_{dC} \ll 0.12\langle T_{11}\rangle_{dC}.$$

If this condition is not fulfilled, it is necessary to introduce a correction into the analysis of the results obtained.

For Tripp's experiment at 340 Mev

$$|c_{p_0}|\sin(c_{p_0}, c_{p_2}) \sim 0.038, \quad |c_{p_2}| = 0.102,$$

$$|\langle T_{11}\rangle|_{d\pi+}/|\langle T_{21}\rangle|_{d\pi+} = 0.25.$$

At this energy the limits are somewhat widened:

$$\langle T_{21}\rangle_{dC} \ll 0.25\langle T_{11}\rangle_{dC}.$$

The assumption of the smallness of the quantity $\langle T_{21}\rangle_{dC}$ at $\theta_d^{lab} = 20^\circ$ requires an experimental examination, and this will provide a problem for future experiments.

7. CONCLUSIONS

1. The measured values of the spin polarization of deuterons in the reaction $p + p \rightarrow d + \pi^+$ together with the data on the angular distribution from this reaction on an unpolarized proton beam allow us to determine the amplitude for the transition $^1S_0 \rightarrow {}^3S_1p_0$. The contribution of this transition to the total cross section is equal to

$$\left(1.0 {+0{,}6 \atop -0{,}45}\right) \cdot 10^{-2}\,\sigma_{\text{tot}}\,(p + p \rightarrow d + \pi^+).$$

2. The transition amplitude $^1S_0 \rightarrow {}^3S_1p_0$ increases somewhat (~ 1.7) as the energy goes from 340 to 670 Mev, and its complex phase relative to the transition $^1D_2 \rightarrow {}^3S_1p_2$ changes roughly by 20°.

3. The measured angular dependence of the magnitude of the deuteron polarization does not contradict the assumption that the amplitudes of the transitions $^3F_2 \rightarrow {}^3S_1d_2$ and $^3F_3 \rightarrow {}^3S_1d_3$ are equal to zero.

The authors want to express their thanks to V. I. Komarov for his part in the measurements, and also to L. I. Lapidus, M. G. Meshcheryakov and R. M. Ryndin for discussions.

---

[1] R. D. Tripp, Phys. Rev. **102**, 862 (1956).

[2] A. H. Rosenfeld, Phys. Rev. **96**, 139 (1954).

[3] M. Gell-Mann and K. Watson, Annual Reviews of Nuclear Science **4**, 219 (1954).

[4] Chamberlain, Segre, Tripp, Wiegand, and Ypsilantis, Phys. Rev. **105**, 288 (1957).

[5] Akimov, Savchenko, and Soroko, J. Exptl. Theoret. Phys. (U.S.S.R.) **35**, 89 (1958), Soviet Phys. JETP **8**, 64 (1959).

[6] M. G. Meshcheryakov and B. S. Neganov, Dokl. Akad. Nauk (U.S.S.R.) **100**, 677 (1955).

[7] B. S. Neganov and L. B. Parfenov, J. Exptl. Theoret. Phys. (U.S.S.R.) **34**, 767 (1958), Soviet Phys. JETP **7**, 528 (1958).

[8] W. Lakin, Phys. Rev. **98**, 139 (1955).

[9] Baldwin, Chamberlain, Segre, Tripp, Wiegand, and Ypsilantis, Phys. Rev. **103**, 1502 (1956).

[10] H. P. Stapp, UCRL-3098, Berkeley (1955).

[11] L. M. Soroko, Polarization Effects in the Reaction $p + p \rightarrow d + \pi^+$ with Account of the s, p, and d States of the π^+ Meson, Preprint, R-186, Joint Inst. for Nuc. Res., 1958.

[12] Mescheryakov, Neganov, Vzorov, Zrelov, and Shabudin, Dokl. Akad. Nauk (U.S.S.R.) **109**, 499 (1956), Soviet Phys. "Doklady" **1**, 447 (1956).

[13] Yu. K. Akimov, Приборы и техника эксперимента (Instrum. and Meas. Engg.) **2**, 116 (1957).

[14] N. P. Klepikov and S. N. Sokolov, Analysis of Spectral Data by the Maximum Likelihood Method, Preprint, R-235, Joint Inst. for Nuc. Res., 1958.

[15] B. S. Neganov, Thesis, Joint Inst. for Nuc. Res., 1958.

Translated by W. Ramsay
8

SOVIET PHYSICS JETP VOLUME 37(10), NUMBER 1 JANUARY, 1960

(d, t) REACTIONS ON Li^6, Li^7, *AND* Be^9 *NUCLEI*

N. A. VLASOV and A. A. OGLOBLIN

Submitted to JETP editor February 27, 1959

J. Exptl. Theoret. Phys. (U.S.S.R.) **37**, 54-61 (July, 1959)

The spectra of tritons emitted at various angles in the (d, t) reactions on Li^6, Li^7, and Be^9 have been studied for 20-Mev deuterons. The probability of formation of excited states in the final nucleus decreases sharply with increasing excitation energy. Angular distributions have been obtained for triton groups corresponding to the formation of Li^5 in the ground state, Li^6 in the ground and in the first two excited states, and Be^8 in the ground and in the first excited state. The angular distributions are in good agreement with those computed from the Butler formula for (d, t) reactions, but the radius increases with the level energy.

INTRODUCTION

DEUTERON reactions are widely used in nuclear spectrometry in connection with the possibility established by Butler[1] of determining characteristics of nuclear levels from the angular distributions of the reaction products. By now a large amount of data have been accumulated concerning the (d, p) and (d, n) stripping reactions.

The inverse pickup reactions — (p, d), (n, d), (d, t), etc., have been studied much less extensively, although they allow one to obtain the same kind of spectrometric data as do the stripping reactions. The few available experimental results[2,3] confirm the agreement of the angular distributions in pickup reactions with Butler's theory. However, with respect to the probability of excitation of various levels of the final nucleus, the pickup reactions must differ significantly from the stripping reactions. In a stripping reaction, the nucleon from the deuteron is captured with the greatest probability into a single particle level of the nucleus, whereas the probability of excitation of other levels associated with a readjustment of the nucleus itself is small. In pickup reactions from a target nucleus in the ground state, one of its nucleons is removed. If in this case the probability of readjustment of the remaining nucleus is also small, then one should expect that in pickup reactions the greatest probability corresponds to the excitation of hole levels whose structure is compatible with the ground state of the target nucleus.

Consequently, a study of pickup reactions might give rise to the possibility of picking out a specific class of nuclear levels which is different from that observed in stripping reactions, and it is from this point of view that such a study is apparently of greatest interest.

The experimental study of pickup reactions presents certain difficulties, since these reactions in the majority of cases have a negative value of Q, and the particles produced in these reactions have to be recorded in the presence of a strong background of high-energy primary particles. Therefore until now pickup reactions have not been studied sufficiently well. The available data refer only to one or two lowest states of the final nucleus.[2,3] The probability of excitation over a wide energy range has not been investigated.

The method of studying nuclear reactions accompanied by the formation of tritium which has been developed in our laboratory[4] enables us to investigate one type of pickup reactions — the (d, t) reaction — under conditions in which we are entirely free from the background of other particles. The study of the spectra and of the angular distributions of tritons at a deuteron energy of approximately 20 Mev enables us to investigate the probability of excitation of levels of final nuclei over a wide energy range from 0 to 15 or 20 Mev. In this paper we present the first results of such an investigation concerning the (d, t) reaction on Li^6, Li^7, and Be^9.

Deuterons were accelerated to an energy of 20 Mev by means of a cyclotron. The tritons produced in a thin target were caught by stacks of aluminum foil situated at a distance of 15 cm from the target at different angles in the range 7 — 150°. After irradiation tritium was extracted from the foils by means of heating and was introduced into a Geiger counter. A measurement of the tritium activity contained in each individual foil enabled us to determine the distribution of tritons with respect to range at different angles.

For the calculation of angular distributions we used Butler's formula modified by Newns[5] for the case of the (d, t) reactions. The triton form factor was taken from French's article:[6]

$$G^2(k) = 113/(1+2.4k^2)^2 \quad \text{for } k \leqslant 0.7.$$

In evaluating this factor, French utilized the triton wave function proposed by Irving.[7]

THE $Li^7(d, t)Li^6$ REACTION

The target of 2.5 or 3 mg/cm^2 thickness was prepared from natural metallic lithium by sputtering onto a zapon film (~ 0.01 mg/cm^2). The transfer of the target from the sputtering apparatus into the apparatus where the irradiation occurred took place without interrupting the vacuum. In order to obtain the absolute value of the cross section we used a target of LiF sputtered onto an aluminum foil.

Figure 1 shows the triton spectrum obtained at an angle of 7°. Spectra obtained at other angles have approximately the same form. Three triton groups may be clearly seen corresponding to the formation of Li^6 in the ground and the first two excited states (2.19 and 3.58 Mev), and also a continuous triton spectrum. The levels with energies of 4.5 and 5.3 Mev are much less clearly pronounced. Since the shape of the continuous spectrum in this range of triton energies is not known, it is not possible to estimate in any reliable fashion the magnitude of the cross section for the formation of Li^6 in these states. No levels of Li^6 with a higher excitation energy were observed at any angle. The upper limit on the cross section for their formation is equal to 1.5 mbn/sterad at small angles.

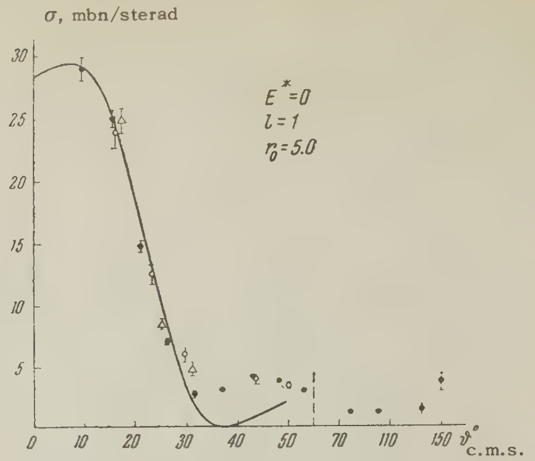

FIG. 2. The angular distribution of tritons in the $Li^7(d, t)Li^6$ reaction with the formation of Li^6 in its ground state ($E^* = 0$; $l = 1$, $r_0 = 5.0$). Dots, circles, and triangles indicate results of different irradiations. The solid curve has been calculated on the basis of Butler's theory.

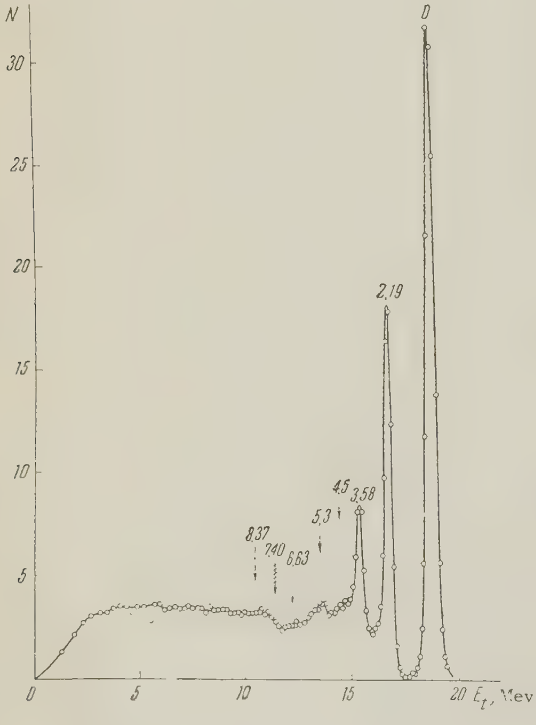

FIG. 1. The triton spectrum in the $Li^7(d, t)Li^6$ reaction at an angle of 7°. Arrows indicate the known levels[8] of Li^6. The hatched arrow corresponds to a broad level.

The observed continuous triton spectrum is formed, apparently, as a result of the decay of residual excited nuclei in the reactions

$$Li^7(d, n)Be^{8*} \to Li^5 + t \quad \text{or} \quad Li^7(d, d')Li^{7*} \to He^4 + t.$$

Figures 2 and 3 give angular distributions for three triton groups which agree well with those calculated on the basis of Butler's theory (solid curves). In all three cases the value of the angular momentum transferred is $l = 1$, which agrees

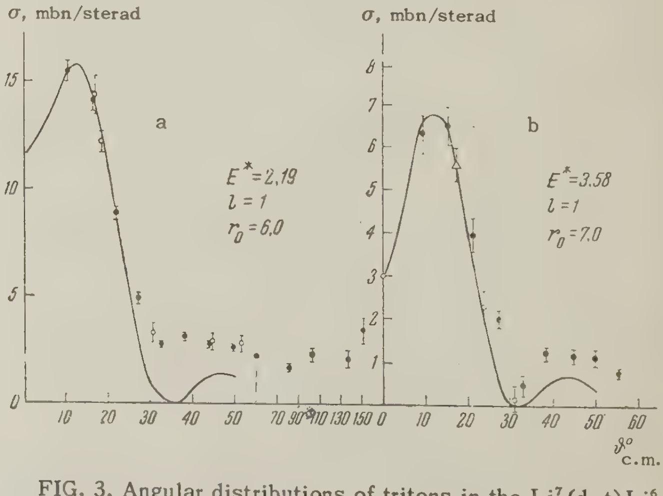

FIG. 3. Angular distributions of tritons in the $Li^7(d, t)Li^6$ reaction with the formation of Li^6: a) in the first, b) in the second excited states. Dots, circles, and triangles indicate results of different irradiations. The solid curves have been calculated on the basis of Butler's theory.

Residual nucleus	Level energy, Mev	σ_{max} in c.m.s., mbn/sterad	$r_0 \times 10^{-13}$ cm	l	θ^2 from present work	θ^2 from other work
Li^5	0	52.3 (9.5°)	5.5	1	0.24	0.05[1]
Li^6	0	29.0 (9.5°)	5.0	1	0.11	0.11[2] 0.05[3]
	2.19	15.5 (10°)	6.0	1	0.061	0.061[2] 0.035[3]
	3.58	6.5 (16°)	7.0	1	0.083	0.055[4]
	5.3					0.017[4]
	other levels in interval 5.5—15 Mev	<1.5				
Be^8	0	17.9 (9.5°)	4.0	1	0.086	0.024[3]
	2.9	19.8 (9.5°)	5.0	1	0.082	
	4.2	~1 (15°)				
	4.9	~0.7 (15°)				
	5.3	~0.5 (15°)				
	6.0	~0.3 (9,5°)				
	other levels in interval 5.5—17 Mev	<0,1				
	17	~0.2 (18°)				

[1] From the reaction He^4 (d, p) He^5 at E_d = 14 Mev.[11]
[2] From the reaction Li^7 (d, t) Li^6 at E_d = 14.3 Mev.[3]
[3] From the reaction (p, d) at E_p = 18 Mev.[2]
[4] From the reaction Li^7 (d, He^3) He^6.[3]

with the well-known[8] level scheme for Li^6. The values of the radius r_0 adopted in calculating the curves, and also the values of the reduced widths obtained from the magnitude of the maximum cross section are given in the table.

THE Li^6 (d, t) Li^5 REACTION

The target was prepared in the form of a foil of 4 mg/cm^2 thickness from enriched metallic lithium (Li^6 content — 90%) by rolling in oil. Before being set up for irradiation the target was washed in CCl_4. The absolute value of the cross section was obtained on the basis of measurements with a target of natural LiF.

Figure 4 gives the triton spectrum obtained at an angle of 6.5°. One can clearly see the broad triton group which corresponds to the formation of the Li^5 nucleus in its ground state. The width of this level is equal to 1.3 ± 0.2 Mev. In the measured spectra one may also easily see two groups of tritons originating in the (d, t) reaction in the 10% admixture of Li^7 and corresponding to the formation of Li^6 in the ground and the first excited states. If the peak corresponding to the level of the Li^5 nucleus of energy ~ 2 Mev [the possibility of whose existence was indicated by our experiments[4] with the Li^7 (p, t) Li^5 reaction] does exist, then at all angles it is masked by the triton group corresponding to the ground state of Li^6.

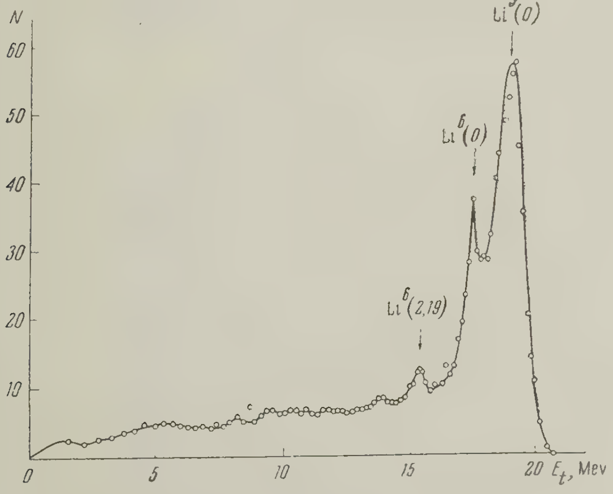

FIG. 4. The triton spectrum in the Li^6(d, t)Li^5 reaction at 6.5°.

The observed continuous triton spectrum may be formed in different ways, for example, as a result of the reaction

$$Li^6\,(d,\,p)\,Li^{7*} \rightarrow He^4 + t.$$

The angular distribution of the tritons from the Li^6 (d, t) Li^5 reaction with the formation of Li^5 in the ground state is shown in Fig. 5. The solid curve is calculated on the basis of Butler's theory with l = 1 and r_0 = 5.5.

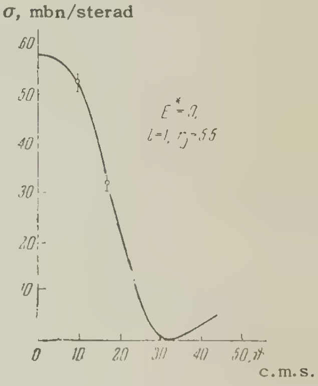

FIG. 5. The angular distribution of tritons in the Li^6(d,t) Li^5 reaction with the formation of Li^5 in the ground state. The solid curve was calculated on the basis of Butler's theory.

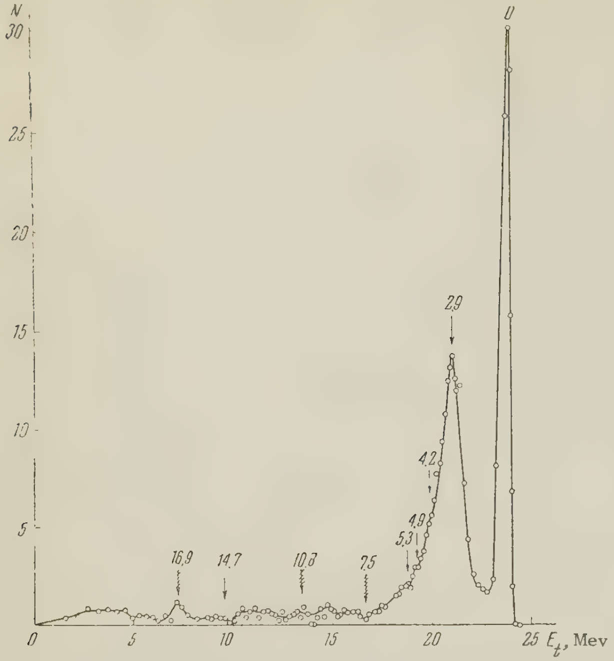

FIG. 6. The triton spectrum in the Be^9(d, t)Be^8 reaction at at 11.5°. Arrows show the known levels[8] of Be^8.

THE Be^9(d, t)Be^8 REACTION

A beryllium foil of 4-mg/cm^2 thickness prepared by means of electrolysis from molten BeF_2 salt[9] served as the target. In order to remove fluorine impurities the foil was heated in vacuo at a temperature of approximately 1000° C.

Figure 6 shows the triton spectrum obtained at an angle of 11.5°. The spectra obtained at other angles are of the same nature. Arrows show the positions of the Be^8 levels known from other work.[8] In addition to the ground state of Be^8, the 2.9-Mev level is also strongly excited. According to our measurements, the width of this level amounts to 1.35 ± 0.15 Mev. Possibily there is also an indication of levels of energies 4.2, 4.9, 5.4, and 6.0 Mev. The peaks which correspond to these values of excitation energy of Be^8 were observed at several angles; however they are of very low intensity. The high lying levels of Be^8, just as in the case of the Li^7(d, t)Li^6 reaction, are practically not observed. The only exception is the level which has an energy of approximately 17 Mev which is apparently excited by the removal of one of the strongly bound neutrons. This level is observed fairly clearly at several angles. It is of interest to note[10] that in the Be^9(p, d)Be^8 reaction at a proton energy of 95 Mev, the formation of Be^8 in this state occurs with a higher probability than in the ground and the first excited states.

Figure 7 shows angular distributions of tritons in the Be^9(d, t)Be^8 reaction for transitions to the ground and the first excited states of Be^8. In both cases the transferred orbital angular momentum is $l = 1$, which is in agreement with the known values of the spin and parity of the corresponding states of Be^9 and Be^8.

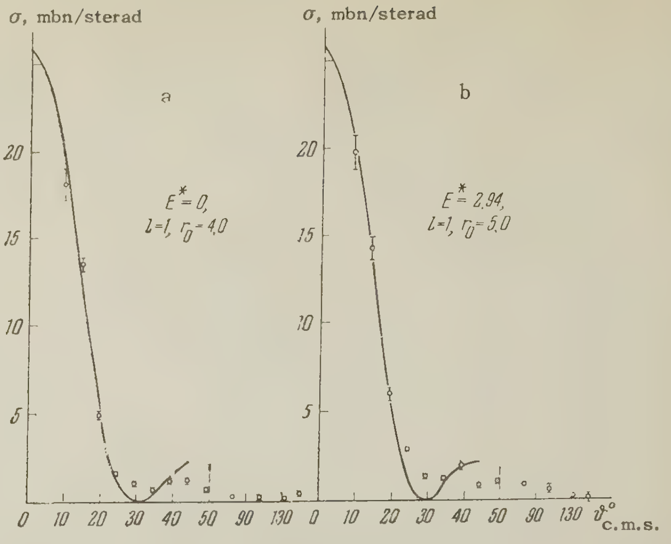

FIG. 7. Angular distributions of tritons in the Be^9(d, t)Be^8 reaction with the formation of Be^8: a) in the ground, b) in the first excited states. The solid curves were calculated on the basis of Butler's theory.

The observed continuous triton spectrum is formed apparently as a result of the reaction Be^9(d, α)$Li^{7*} \rightarrow He^4 + t$. The total cross section for the formation of the tritons in the continuous spectrum amounts to 50 mbn.

The principal results of this work are summarized in the table. The reduced widths θ^2 are given in dimensionless Wigner units ($\theta^2 = 3\mu n\gamma^2/2\hbar^2$). In the last column of the table we have given the reduced widths obtained in other papers for comparison.

The experimental error in the measurements of the absolute values of the cross sections in the present work amounts to ± 20%.

DISCUSSION OF RESULTS

The measured angular distributions of the monoenergetic triton groups agree satisfactorily with those calculated on the basis of Butler's theory which allows us, as in the case of stripping reactions, to determine the spins and the parities of the corresponding levels. This has already been demonstrated in previous work on (d, t) reactions.[3,5,12] All the characteristics of the Li^5, Li^6, Be^8 levels obtained by us agree with those known from other work.

However, it should be noted that the most suitable value of the radius r_0 (see table) increases monotonically as the level energy increases. The

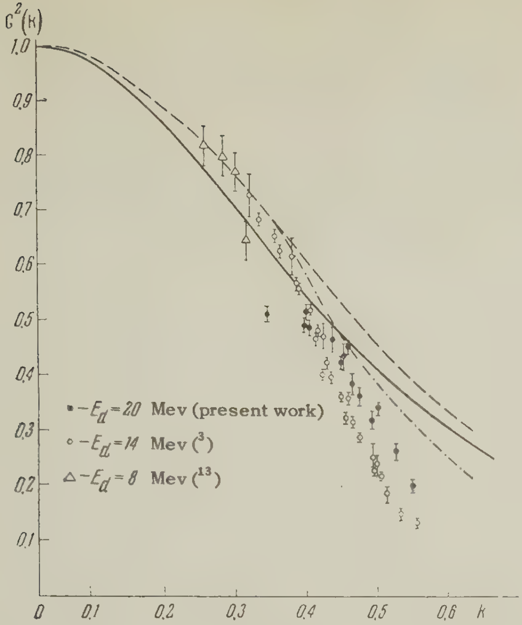

FIG. 8. Neutron momentum distribution in the triton obtained from the angular distributions of the tritons in the Li^7(d, t)Li^6 reaction. The value of the nuclear radius was chosen equal to 5.5×10^{-13} cm. The curves represent the calculated momentum distributions with approximations being made to the triton wave-function: solid line – by means of the Irving function (French[6]); dotted line – by means of the Irving function (Newns[5]); dash-dotted line – by means of the Gauss function (Newns[5]).

same tendency of an increase in r_0 was observed in the (d, t) and (d, He^3) reactions on Li^7 at an energy of 14.4 Mev.[3] It is difficult to assume that the nuclear radius actually varies so strongly from level to level, particularly since this is not observed in the (d, p) and (p, d) reactions. It appears more natural to assume that the use of the simplest approximations for the triton wave function does not give the correct expression for the triton form factor.

Figure 8 shows the momentum distribution in the triton obtained from the angular distributions of the Li^7(d, t)Li^6 reaction on the assumption that the nuclear radius r_0 has the same value in all the lower states and is equal to 5.5×10^{-13} cm. In addition to the data from the present work, we have also made use of the angular distribution of the tritons from the Li^7(d, t)Li^6 reaction obtained at energies of $E_d = 14.4$ Mev,[3] and $E_d = 8$ Mev.[13] The relative values of the form factor obtained from the angular distributions of the different groups were matched at the overlapping intervals. It can be seen from Fig. 8 that the triton form factor obtained in this fashion falls off at large values of neutron momentum considerably more rapidly than the form factor obtained from the Irving or the Gauss functions.

The determination of the triton form factor from the angular distributions in the Be^9(d, t)Be^8 reaction does not give a clear result, since it is difficult to choose some one definite value for the interaction radius r_0 because of its dependence on the energy in the pickup reactions in Be^9.

As may be seen from the table, the reduced widths obtained from the (d, t) reactions are larger than those obtained from the (p, d) reactions in the same nuclei. The reduced width for the Li^6(d, t)Li^5 reaction also turns out to be considerably larger than the reduced width for the definitely single-particle reaction He^4(d, p)He^5. Apparently this also shows the necessity of obtaining a more accurate triton wave function.

The most significant feature of the measured triton spectra is the strong dependence of the intensity of the individual groups on the excitation energy of the corresponding levels of the residual nucleus. The probability of excitation is high only for the ground and for one or two lower excited states. The probability of excitation for higher lying states over the whole rather wide energy range that has been investigated turns out to be smaller by one or perhaps even by two orders of magnitude. The preliminary data obtained by us in the case of the F^{19}(d, t)F^{18} reaction also confirm this behavior.

Such a strong dependence cannot be explained by an increase in the transferred angular momentum *l*. Thus, for example, in the Be^9(d, t)Be^8 reaction several of the higher lying levels of Be^8 could be excited by transferring the same angular momentum $l = 1$, as in the case of the lower levels, while the cross section for their excitation is less by a factor of more than 10. As is well-known, in stripping reactions the energy range for strongly excited levels is considerably wider. This confirms the hypothesis stated at the beginning of this paper on the essential difference between pickup reactions and stripping reactions with respect to the probability of excitation of different states of the final nucleus, and this has great significance for the classification of nuclear levels and for the investigation of their structure.

The authors express their gratitude to S. P. Kalinin for his interest in their work, to the members of the cyclotron group directed by Yu. M. Pustovoĭt for carrying out the irradiations, and to A. I. Baz' and D. P. Grechukhin for a discussion of results.

---

[1] S. T. Butler, Proc. Phys. Soc. A208, 559 (1951).

[2] K. G. Standing, Phys. Rev. **101**, 152, 158 (1956).

[3] Levine, Bender, and McGruer, Phys. Rev. **97**, 1249 (1955).

[4] N. A. Vlasov and A. A. Ogloblin, Paper delivered at the Moscow Conference on Nuclear Reactions, 1957.

[5] H. C. Newns, Proc. Phys. Soc. **A65**, 916 (1952).

[6] A. P. French, Phys. Rev. **107**, 1655 (1957).

[7] J. Irving, Phil. Mag. **42**, 338 (1951).

[8] F. Ajzenberg and T. Lauritsen, Revs. Modern Phys. **27**, 77 (1955).

[9] M. C. Henderson, Phys. Rev. **56**, 207 (1935).

[10] W. Selove, Phys. Rev. **101**, 231 (1956).

[11] E. Warburton and J. N. McGruer, Phys. Rev. **105**, 639 (1957).

[12] A. Werner, Nucl. Phys. **1**, 9 (1956).

[13] J. R. Holt and T. N. Marsham, Proc. Phys. Soc. **A66**, 1032 (1953).

Translated by G. Volkoff
9

SOVIET PHYSICS JETP VOLUME 37(10), NUMBER 1 JANUARY, 1960

ON THE ANALYTIC PROPERTIES OF VERTEX PARTS IN QUANTUM FIELD THEORY

L. D. LANDAU

Institute of Physical Problems, Academy of Sciences, U.S.S.R.

Submitted to JETP editor February 19, 1959; resubmitted April 7, 1959

J. Exptl. Theoret. Phys. (U.S.S.R.) 37, 62-70 (July, 1959)

A general method is developed, on the basis of the diagram technique, for finding the singularities of quantities involved in quantum field theory.

In recent years many papers have been devoted to the so-called dispersion relations. As is well-known, these relations are expressions of analytic properties of quantities involved in quantum field theory. Therefore the main problem is that of the location of the singularities of the quantities in question. As has recently been discovered,[1, 2] the most effective method for studying the location and character of the singularities of vertex parts is the direct examination of diagrams. It is often supposed that a treatment by means of diagrams is not sufficiently convincing, since it would seem to be associated with the use of perturbation theory, unlike other methods that would seem to be more rigorous. Actually this belief is based on a misunderstanding. Since a rigorous theory using a Hamiltonian makes the interaction zero, the only completely rigorous dispersion relation in this theory is 0 = 0. In setting ourselves the problem of studying the analytic properties of the quantities of quantum field theory, we, in fact, go beyond the framework of the existing theory. In this connection the assumption is automatically made that there exists a theory not making the interaction zero, and not using ψ-operators and Hamiltonians, but retaining the diagram technique. Therefore the use of the diagram technique in the derivation of dispersion relations is actually the only consistent method, since if we renounce the diagram technique, the very statement of the problem loses its meaning.

The diagram method is by no means equivalent to perturbation theory, since in it one treats as particles all particles that are stable from the point of view of the strong interactions, independently of whether they are "simple" or "complex." In fact, in such a treatment the first steps are made toward the construction of a new diagram technique that will be a generalization of the old one. This technique must be the basis of the future theory. Of course, the applicability of the diagram technique in such a form in the future theory is itself a hypothesis, and the testing of the results so obtained will also be a test of the hypothesis itself.

Unfortunately, the expressions obtained from the consideration of the more complicated diagrams become very lengthy, and this makes their study difficult. It can be shown, however, that such a study can be carried through in general form, and that it is much simplified by a suitable graphical representation.

An arbitrary diagram represents a certain integral

$$\int \frac{B d^4k d^4l \ldots}{A_1 A_2 A_3 \ldots}, \tag{1}$$

where

$$A_i = m_i^2 - q_i^2, \tag{2}$$

q_i is a certain four-momentum, corresponding to a given line in the diagram; m_i is the mass of the corresponding particle and B is a certain polynomial in the vectors q_i. According to the well-known method of Feynman, we can write

$$\frac{1}{A_1 A_2 \ldots A_n} = (n-1)! \int_0^1 \ldots \int_0^1 \frac{d\alpha_1 d\alpha_2 \ldots d\alpha_n \cdot \delta(\alpha_1 + \alpha_2 + \ldots + \alpha_n - 1)}{(\alpha_1 A_1 + \alpha_2 A_2 + \ldots + \alpha_n A_n)^n}. \tag{3}$$

The expression $\alpha_1 A_1 + \alpha_2 A_2 + \ldots$ in the denominato is a polynomial of the second degree in the variable of integration k, l, ... By a transformation of the variables of integration, we can always eliminate from this polynomial the terms linear in k, l, ... ; when this has been done we get

$$\alpha_1 A_1 + \alpha_2 A_2 + \ldots = \varphi + K(k', l', \ldots). \tag{4}$$

Here K is a homogeneous quadratic form in the ne variables of integration with coefficients depending only on the parameters α_i, and φ is an inhomogeneous quadratic form in the vectors p_i that characterize the external lines of the diagram in question.

Let us confine ourselves to the case of real values of both the squares and also the scalar products of the vectors p_i. It is easily verified that for positive values of φ the integral over k, l, ... is a real quantity (in the case of spinor functions, a self-adjoint spinor), since the substitutions $k_4 \rightarrow i\kappa$ and $l_4 \rightarrow i\lambda$ make the quadratic form K positive definite (in virtue of the fact that all the α_i are positive). Therefore, if $\varphi > 0$ for all values of the α_i, the vertex part is real; conversely, if for some values of the α_i the form φ is negative, the vertex part becomes complex. The nearest singularity of the vertex part is obviously located at the values of the p_i for which φ vanishes for definite values of all the quantities α_i and is positive for all other values of the α_i; in other words, singularities correspond to the vanishing of the minimum value of φ, regarded as a function of the α_i. If we are to discuss the singularities in the complex region, then we must consider an arbitrary extremum of the function φ. We note that since φ is a homogeneous function of the first degree in the variables α_i, in finding the conditions for the existence of an extremum equal to zero we can omit the condition $\Sigma\alpha_i = 1$.

Let us denote the quantity $\alpha_1 A_1 + \alpha_2 A_2 + \dots$ by the letter f. Since K is a quadratic form in the variables k', l', ... , it is clear that φ is the value of the function f under the subsidiary conditions

$$\partial f / \partial k' = \partial f / \partial l' = \dots = 0,$$

or, since k differs from k′ by a constant vector, these conditions can be written in the form

$$\partial f / \partial k = \partial f / \partial l = \dots = 0. \tag{5}$$

In finding the conditions for a minimum we must take into account the fact that the quantities α_i are positive. From this it follows that for each quantity α_i we must have either the condition $\partial\varphi/\partial\alpha_i = 0$ or the condition $\alpha_i = 0$. In the latter case it is obvious that for the nearest singularity $\partial\varphi/\partial\alpha_i > 0$. Furthermore we have by definition

$$\frac{\partial\varphi}{\partial\alpha_i} = \frac{\partial f}{\partial\alpha_i} + \frac{\partial f}{\partial k}\frac{\partial k}{\partial\alpha_i} + \frac{\partial f}{\partial l}\frac{\partial l}{\partial\alpha_i} + \dots$$

Since, according to Eq. (5), all the $\partial f/\partial k$ are equal to zero, it follows that the condition $\partial\varphi/\partial\alpha_i = 0$ is equivalent to the condition $\partial f/\partial\alpha_i = 0$, i.e., by the definition of f,

$$A_i = 0. \tag{6}$$

Thus the singularity of the vertex part can be obtained by solving simultaneously the conditions $A_i = 0$ (or $\alpha_i = 0$) under the subsidiary conditions

$$\sum_i \alpha_i \frac{\partial A_i}{\partial k} = \sum_i \alpha_i \frac{\partial A_i}{\partial l} \quad \dots = 0. \tag{7}$$

Here it is essential that these equations must have solutions with positive α_i.

Thus regarding each line of a Feynman diagram, it can be declared that it either satisfies the condition $q_i^2 = m_i^2$, or else drops out of the treatment altogether (when $\alpha_i = 0$). In the latter case, the singularity in question can be ascribed not to the given diagram, but to the diagram in which the i-th line is absent, i.e., the vertices it connects are merged. Therefore in the analysis of the singularities of diagrams, it suffices to confine ourselves to the case in which all $\alpha_i \neq 0$.

It is easy to see that condition (7) can be written in the form $\Sigma\alpha_i q_i = 0$, where the summation is taken not over all the lines of the Feynman diagram, but over any set of lines forming a closed contour, with the directions of the vectors q_i corresponding to a direction of passage around the contour. The positive nature of the coefficients means that if one thinks of the vectors q_i as directions of forces, the possibility of satisfying Eq. (7) implies the possibility of choosing the magnitudes of these forces so that they are in equilibrium.

By means of this method one can analyze the singularities that occur with comparative ease. Let us begin with an examination of diagrams for the Green's function. In this case, all the vectors q determined from the equations that have been stated are obviously parallel to the vector p.

Let us consider the diagram of Fig. 1. Writing the formula $\Sigma\alpha_i q_i = 0$ for the contour formed by any pair of lines, and recalling that the quantities α_i are positive, we come to the conclusion that all of the vectors q_i have the same sense relative to the vertex of the diagram. Using the fact that the lengths of the vectors are equal to the corresponding masses, we get without difficulty the obvious result $p^2 = (\Sigma m_i)^2$ for the singularities. We note that in the case of Green's functions, it is superfluous to consider any other type of diagram, for example, such as that shown in Fig. 2. In fact, the number of equations for the determination of the quantities α_i is equal to the number of independent contours in the diagram, so that in the example shown it is two. At the same time, the total number of quantities α_i in this example is five; it is clear from this that one of them can be set equal to zero, and the result is that the diagram reduces to one of the diagrams of the type already considered. We note that all of these arguments are also equally applicable to diagrams of the type shown in Fig. 3, where the role of the momen-

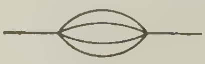
FIG. 1

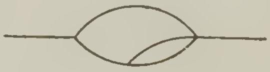
FIG. 2

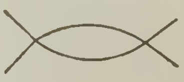
FIG. 3

tum is played by the corresponding sum of momenta.

Let us now go on to the vertex part with three external lines. Since, by the conservation laws, these three lines represent three vectors lying in one plane, and the vectors k, l ... are determined from Eqs. (6) and (7), it is clear that these latter vectors lie in the same plane. Thus in this case the problem reduces to the consideration of a plane system of vectors.

Let us consider first the simplest example, which has been analyzed in detail by Karplus, Sommerfield, and Wichmann[3] (Fig. 4). It is easy to see that the relation between the vectors is represented by the scheme shown in Fig. 5. The condition (7) obviously requires that the point 0 lie inside the triangle. The tacit assumption here is that all the vectors have the properties of Euclidean (not pseudo-Euclidean) vectors; this is easily shown for the nearest singularities.

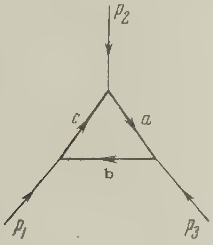

FIG. 4

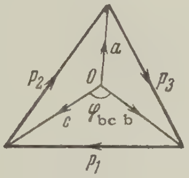

FIG. 5

To begin with, we show how to formulate analytically the relations that are expressed graphically by diagrammatic schemes. First, let us consider the scheme of Fig. 5, which corresponds to the diagram of Fig. 4. If we introduce the unit vectors $n_a = q_a/m_a$, $n_b = q_b/m_b$, $n_c = q_c/m_c$, the condition (7) can be written in the form

$$\beta_a n_a + \beta_b n_b + \beta_c n_c = 0,$$

where $\beta_i = \alpha_i m_i$ are obviously also positive quantities. Projecting these equations successively on the vectors n_a, n_b, n_c and introducing the notations $(n_a n_b) = \mu_c = \cos\varphi_{ab}$, etc., we get the three equations

$$\beta_a + \beta_b\mu_c + \beta_c\mu_b = 0, \qquad \beta_a\mu_c + \beta_b + \beta_c\mu_a = 0,$$
$$\beta_a\mu_b + \beta_b\mu_a + \beta_c = 0. \tag{9}$$

Equating the determinant of this system to zero gives the equation

$$1 + 2\mu_a\mu_b\mu_c = \mu_a^2 + \mu_b^2 + \mu_c^2, \tag{10}$$

which determines the position of the singularity, under the simultaneous condition that all the β's are positive, if we use the fact that μ_a, μ_b, μ_c are connected with p_1^2, p_2^2, p_3^2 by the formulas

$$\mu_a = \frac{m_b^2 + m_c^2 - p_1^2}{2m_b m_c}, \qquad \mu_b = \frac{m_a^2 + m_c^2 - p_2^2}{2m_a m_c},$$
$$\mu_c = \frac{m_a^2 + m_b^2 - p_3^2}{2m_a m_b}. \tag{11}$$

Returning to the question of the properties of the vectors for the nearest singularity, let us consider any angle, say φ_{bc}. According to Eq. (11), μ_a is a real quantity. It is larger than -1 since otherwise we would have $p^2 > (m_b + m_c)^2$; that is, we would have gone beyond the singularity defined by the diagram of Fig. 6, which is obtained from the diagram under consideration by the liquidation of one of the lines. At the same time we see from Eq. (9) that at least two of the three cosines must be negative. But a negative cosine larger than -1 always corresponds to a real angle. Therefore two of the three angles are certainly real, and since their sum is 2π, the third is also real. Thus Fig. 5, which was mentioned in reference 2, completely solves the problem.

FIG. 6

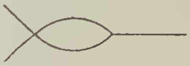

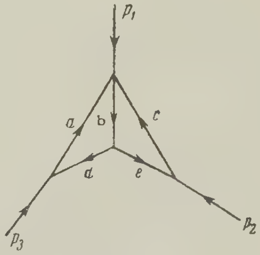

FIG. 7

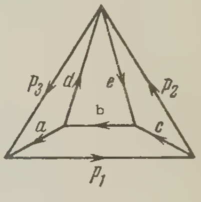

FIG. 8

Let us now go on to more complicated diagrams. Let us consider, for example, the diagram shown in Fig. 7. The corresponding scheme is shown in Fig. 8. The construction of such a scheme is very simple, if we use the fact that to each point of the Feynman diagram there corresponds a polygon in the scheme, with its number of sides equal to the number of lines that come together at the point, and to each polygon of the Feynman diagram there corresponds a point in the drawing of the scheme. The condition (7) requires the corresponding location of the vectors a, b, and d on one side, and b, c, and e on the other. It is not hard to write the analytical expression of this scheme. The triangle bde, as all the parts of the drawing, is real, since the diagram involves only stable particles, and therefore the mass of each of the particles in b, d, e is less than the sum of the other two.

In cases in which one or more of the coefficients

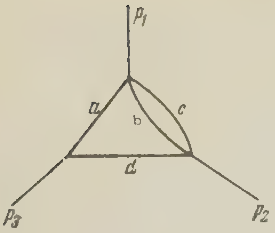

FIG. 9

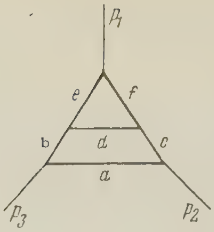

FIG. 10

$\alpha_i = 0$, the diagram is simplified. For example, if $\alpha_c = 0$, the diagram of Fig. 7 becomes the diagram of Fig. 9, analogous to Fig. 4.

Going on to more complicated Feynman diagrams, one often finds that the case with all $\alpha_i \neq 0$ is impossible. Let us examine, for example, the diagram shown in Fig. 10. In this case the number of vector equations for α_i is two; that is, in view of the plane character of the vectors we have four equations, but the number of quantities α_i is six, and therefore one of them can be set equal to zero. The same argument applies to diagrams of the type shown in Fig. 11.

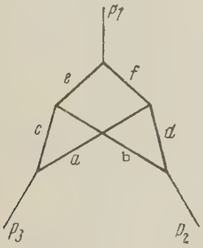

FIG. 11

It is easy to see how the results found here are changed when we concern ourselves with things beyond the nearest singularity, i. e., with the appearance of complex quantities and of singularities in quantities that are already complex. If a singularity is not the nearest one, then, generally speaking, we cannot assume that all of the angles are real, as we have done earlier for the nearest singularities.

Let us first consider the scheme of Fig. 5, corresponding to the diagram of Fig. 4. In the "Euclidean" case, with all the angles real, all the μ_i lie between −1 and + 1. In the general case, a study of Eq. (10) shows that the corresponding surface in the space of μ_a, μ_b, μ_c consists of four parts, that intersect each other in three points: $\mu_a = 1$, $\mu_b = -1$, $\mu_c = -1$, and the points obtained by interchange of the indices a, b, c. One of these surfaces is a curved triangle bounded by the straight lines joining the three points. This triangle corresponds to the "Euclidean" case. The three other surfaces go to infinity, each beginning at the corresponding point of intersection. On each of these surfaces one of the μ's is positive and larger than unity, and the two others are negative and in absolute value also larger than unity. As has already been pointed out, these surfaces always correspond to singular points that are not the nearest.

It is easy to see that in the diagrams under consideration, the non-Euclidean case is possible only in the diagram of Fig. 4. For example, in the scheme of Fig. 8, corresponding to the diagram of Fig. 7, the role of the vectors a, b, c is played by the vectors a, b, d on the one side, and by b, c, e on the other. As has already been shown, however, the angles in the triangle made up of the vectors b, d, e are necessarily real. Otherwise one of the particles b, d, e would be unstable. At the same time, as has just been shown, in the non-Euclidean case all the cosines must have absolute values larger than unity, and consequently all the angles must be complex.

Let us now discuss Feynman diagrams with four external lines. In this case, we obviously have to consider schemes that lie not in a plane but in space, and naturally this complicates the problem. The most important such diagrams are those with physical external lines, i. e., those in which the squares of the momenta in question are equal to the squares of the masses of the particles. The simplest singularities are associated with diagrams of the type of Fig. 12. Here the middle line can correspond either to one particle or to several particles. The singularities of such a diagram obviously correspond to

$$(p_1 + p_2)^2 = m_a^2,$$

where m_a is the sum of the masses of these particles. The one-particle case gives an isolated pole. The two-particle case is the boundary of the complex region.

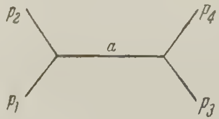

FIG. 12

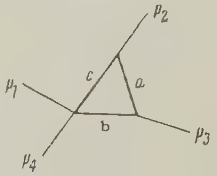

FIG. 13

Figure 13 corresponds entirely to Fig. 4 in its properties, and therefore requires no further analysis.

To Fig. 14 there corresponds the scheme of Fig. 15, where four of the six edges of the tetrahedron are determined by the lengths of the corresponding

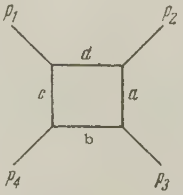

FIG. 14

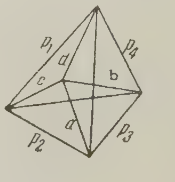

FIG. 15

external lines, and the other two are equal to $p_1 + p_2$ and $p_2 + p_3$, respectively. (We note that this sort of graphical construction for this diagram occurs in the work of Karplus et al.[3]) Here, too, a detailed analysis shows that for the case of the nearest singularity, all of the angles are real, and the condition that the coefficients α are positive corresponds to the condition that the central point lie inside the tetrahedron. (The situation corresponding to the singularities in the complex region is more complicated, and we shall not discuss it.) As in the analysis of the diagrams with three external lines, it is convenient to introduce four unit vectors in the directions of the vectors a, b, c, d and find an equation connecting the cosines of the angles between them. It turns out that instead of Eq. (10) we get an equation of the fourth degree. We note the following curious fact. If we consider diagrams with four physical external lines, then as can be seen from the scheme of Fig. 5, for the diagram of Fig. 13 the following condition must be satisfied: the sum of the angle between the sides a and b in the triangle abp_3 and that between the sides a and c in the triangle acp_2, both of which are fixed by the masses of corresponding particles, must be larger than π. The analogous condition for the diagram of Fig. 14 is obviously that the sum of four angles in the triangles corresponding to the four vertices must exceed 2π. From this it follows directly that a necessary, though of course not sufficient, condition for the existence of "nontrivial" nearest singularities is the presence of an obtuse angle in at least one of the triangles, and for this it is in turn necessary that for the virtual decay of at least one of the particles an inequality of the type

$$m_2^2 > m_a^2 + m_c^2.$$

must hold. This relation obviously cannot be satisfied for either mesons or nucleons. Therefore, the nearest singularities for the scattering of these particles by each other correspond to the diagram of Fig. 12. We emphasize, however, that this does not apply to singularities in the complex region.

Let us now examine the nature of the singularities that are obtained. For this purpose we return to the basic formula (1), writing it in the form

$$\int (\varphi + K)^{-n} B d^4k' d^4l' \ldots d\alpha_1 d\alpha_2 \ldots \delta(\alpha_1 + \ldots + \alpha_n - 1).$$

Expanding φ in powers of $\alpha_i' = \alpha_i - \alpha_{0i}$, where the α_{0i} correspond to the minimum value of φ, we can write this integral in the form

$$\int (\varphi_0 + Q)^{-n} B d^4k' d^4l' \ldots d\alpha_1' d\alpha_2' \ldots \delta(\alpha_1' + \ldots + \alpha_n'), \quad (12)$$

where φ_0 is the minimum value of φ, which is equal to zero at the singularity itself (for prescribed values of the vectors for the external lines), and Q is a quadratic function both in the variables k', l', ... and in the variables α_i'. To find the character of the singularity, it suffices to confine ourselves to the values of B at $k' = l' = \ldots = 0$. If the degree of the numerator with respect to the variables of integration is lower than the degree of the expression Q^n, the integral (12) converges for large values of these variables; in other words, its value is determined by values of the variables corresponding to $Q \sim \varphi_0$; i.e., the integration occurs over small values of the variables, for which the expression (12) has sufficient accuracy. It is obvious that in this case the expression (12) can be written in the form

$$\text{const} \cdot \varphi_0^{m/2-n}, \quad (13)$$

where m is the number of integrations. If $m \geqslant 2n$, the integral (12) diverges at high values, and these arguments do not apply. In order to determine the character of the singularity in this case, it is simplest to differentiate the expression (12) with respect to φ_0 as many times as necessary to make the degree of the denominator larger than that of the numerator. After this, we can use the resulting formula, which now has to be integrated the same number of times. The constants that appear in the integrations obviously give integral powers of φ_0, which have no singularity at $\varphi_0 = 0$. Accordingly we again get the result (13), except in cases in which $m/2 - n$ is zero or a positive integer. In this case instead of (13) one obviously gets

$$\text{const} \cdot \varphi_0^{m/2-n} \ln \varphi_0.$$

We note that although we speak here of a minimum, these results are equally applicable to any extremum of φ.

The quantity n is the number of internal lines in the Feynman diagram; the number of vectors k over which one integrates is equal to the number ν of independent contours that make up the diagram in question. Accordingly,

$$m = 4\nu + n - 1.$$

It follows from this that the character of the singularity is given by the expression

$$\varphi_0^{2\nu-(n+1)/2},$$

or if $2\nu - (n+1)/2$ is zero or a positive integer, by the expression

$$\varphi_0^{2\nu-(n+1)/2} \ln \varphi_0.$$

The quantity φ_0 is obviously proportional to the distance of the point in question from the hypersurface in the space of p_i^2, $(p_i p_k)$, ... on which the singular points are located. In counting the number of contours we must include also the "diangles" that occur when several particles go along a single line. For example, in the diagram of Fig. 9, $\nu = 2$, and, since $n = 4$, the singularity has the character $\varphi_0^{3/2}$.

We note that instead of the number of independent contours, one can use the more convenient number of vertices. In fact, the number of independent contours, i.e., the number of independent integrations, is equal to the number of lines minus the number of subsidiary conditions. This last number is equal to one less than the number of vertices, since the δ-function goes over into the final result. Thus we have

$$\nu = n - v + 1$$

(where v is the number of vertices),* and the degree of the singularity can be written in the form $(3/2)(n+1) - 2v$.

Let us formulate briefly the general rules for finding the singularities. One considers various diagrams with the given external lines. In the construction of such diagrams an arbitrary number of lines can meet at a vertex, subject of course to the conservation laws (for example, an odd number of π-meson lines cannot meet at a point). All particles stable under the strong interactions can occur as lines. After drawing a diagram one studies the scheme constructed according to the principle of replacing polygons in the diagram by vertices in the scheme, from each of which there emerges a corresponding number of straight line-segments. The lengths of all the internal lines in the scheme are equal to the corresponding masses. At the essential intersections in the scheme (those that arise from polygons in the diagram), the conditions $\Sigma\alpha_i q_i = 0$ must hold, where the q_i are the vectors emerging from a given intersection, and all of the α_i are positive. Nearest singularities correspond to schemes in Euclidean space.

In the application of these results to the scattering amplitude, a number of circumstances must be kept in mind. We shall consider the scattering amplitude as a function of one variable x (this can be, for example, the total energy or the momentum transfer), regarding all other variables as given. As is well-known, the integrals considered here define functions whose values in the upper and lower half-planes are connected by the relation $f(x^*) = f^*(x)$; in other words, above and below the axis we are dealing with essentially different functions, which are by no means analytic continuations of each other, and at real values of x we have, in general, a discontinuity. The scattering amplitude, which is obtained by using the Feynman rules for passage around poles, in general has the form $a(x + i\delta) + b(x - i\delta)$ (δ is infinitely small). The analytic properties considered earlier refer to the function $a(x + i\delta)$, continued into the upper half-plane of the variable x, and to the function $b(x - i\delta)$, continued into the lower half-plane. The behavior of the analytic continuation of the function $a(x + i\delta)$ into the lower half-plane, and that of the continuation of the function $b(x - i\delta)$ into the upper half-plane, are by no means evident from the foregoing discussion.

In the "foreign" half-plane the function a or b can have any singularities, located in any way, and they, in general, cannot be determined from any general considerations. For example, as is well-known, in addition to the singularity associated with the formation of a deuteron, the proton-neutron scattering amplitude has a singularity associated with the so-called virtual state of this system, which does not correspond to any real particle, and which indeed lies in the "foreign" half-plane of the total energy of the system. Another example is the well-known resonance in the scattering of π-mesons by nucleons, which also corresponds to a singularity in the "foreign" half-plane, and obviously at a complex value of the total energy of the system. It is clear that such singularities in principle cannot be predicted from general considerations, but can be obtained only from a theory that gives concrete expressions for the scattering amplitude.

The problem is greatly simplified in cases in which there is a region of values of x for which the amplitude in question is real. Then in the complex plane we have two segments of the real axis, and it is easy to see that the function $a(x + i\delta)$ has only the right-hand segment, and the function $b(x - i\delta)$ only the left-hand segment. If instead of the scattering amplitude we consider the quantity $a + b^*$, for which we have only to change the sign of the imaginary part of the amplitude on the left-hand segment, we get a function that has no singularities in the upper half-plane, and which leads to the usual dispersion relations.

In conclusion I would like to thank L. B. Okun', A. P. Rudik, and Ya. A. Smorodinskiĭ for many helpful comments.

---

*My attention was called to this fact by L. Okun' and A. Rudik.

[1] Y. Nambu, Nuovo cimento, **6**, 1064 (1957).

[2] Karplus, Sommerfield, and Wichmann, Phys. Rev. **111**, 1187 (1958).

[3] Karplus, Sommerfield, and Wichmann, preprint.

Translated by W. H. Furry
10

SOVIET PHYSICS JETP VOLUME 37 (10), NUMBER 1 JANUARY, 1960

ULTRASONIC ABSORPTION IN METALS IN A MAGNETIC FIELD. I.

V. L. GUREVICH

Institute of Semiconductors, Academy of Sciences, U.S.S.R.

Submitted to JETP editor December 16, 1958

J. Exptl. Theoret. Phys. (U.S.S.R.) **37**, 71-82 (July, 1959)

Ultrasonic absorption in metals at low temperatures and in a strong magnetic field (Larmor frequency of conduction electrons much higher than the collision frequency) is studied theoretically. A case is considered of an arbitrary law of energy dispersion of the electrons and of an arbitrary orientation of the field **H** relative to the axes of the crystal and the direction of sound propagation. It is found that the sound absorption coefficient Γ can experience two types of periodic variation with respect to 1/H: oscillations and increments (changes of a given sign which commence periodically). An expression is obtained for the periodic part of Γ for an arbitrary form of the collision operator. It is established that the experimental investigation of the increments permits the determination of the Gaussian curvature of the Fermi surface at all its elliptic points; a study of the oscillations permits the complete reconstruction of the Fermi surface if it possesses a center of symmetry.

AN interesting effect has been established in the experiments of Bommel[1] and of Morse, Bohm, and Gavenda[2] — the oscillation of the ultrasonic absorption coefficient Γ in a metal upon variation in the magnitude of the magnetic field H. It was noted in Pippard's work[3] that the period of the oscillation is determined by the relation between the dimensions of the orbit of the electrons in the magnetic field and the sound wavelength. Starting from this representation, the authors of reference 2 estimated the mean limiting Fermi momentum for the substance studied (copper).

The theory of ultrasonic absorption in metals in the absence of a magnetic field was set up in the researches of Akhiezer,[4] and Akhiezer, Kaganov, and Lyubarskiĭ.[5] The aim of the present research was to discover what information can be obtained, relative to the shape of the Fermi surface in a metal, by studying the periodic part of the function Γ(H) for different orientations of the field **H** relative to the sound propagation vector **k**, and also to give order-of-magnitude estimates of the absorption coefficient Γ.*

It is also of interest to determine the asymptotic behavior of the coefficient Γ in strong magnetic fields, when the dimensions of the orbit of the electrons are much smaller than the sound wavelength, and the dependence of Γ (H) has a monotonic character. Here many different possibilities are encountered, and this question deserves special consideration.

1. The coefficient Γ can undergo periodic changes of two types: oscillations and periodic increments. The latter can exist only in the case in which the time average value of the velocity of the electron $\tilde{\mathbf{v}}$ in the direction of the sound wave is, generally speaking, different from zero. The distribution function of the electrons moving in the field of the sound wave, $F = F_0 + f$, where F_0 is the equilibrium distribution, f is a nonequilibrium addition of the form $f_0 \cos(\omega t - \mathbf{k}\cdot\mathbf{r})$. We shall see below that the absorption coefficient is determined by the quantity f_0^2. Obviously, f_0^2 is a maximum for those electrons which, after the time $T = 2\pi/\Omega$ of a revolution in the magnetic field, fall in the planes of equal phase of the sound wave. In this case, the frequency of variation of the sound-wave field, which acts on the electron in its motion,* is shown to be equal to the frequency Ω of rotation of the electron in the magnetic field H. For such electrons, the condition

$$\tilde{\alpha} = \mathbf{k}\tilde{\mathbf{v}}/\Omega = n \qquad (1.1)$$

must be satisfied (n is an integer or zero). The frequency $\Omega = eH/m^*c$, (where e is the electron charge and m* the effective mass of the electron

---

*The ultrasonic absorption in a metal for certain cases of mutual orientation of the vectors **k** and **H** and for an isotropic quadratic energy dispersion law for the electrons has been studied by Steinberg.[6]

*Consideration of the motion of the electron in the static field of the sound wave, which lies at the basis of these qualitative considerations, is valid inasmuch as the velocity of sound $w \ll v$.

in the given trajectory) was introduced by I. M. Lifshitz, Azbel' and Kaganov.[7] The quantities $\tilde{v}$ and m^* are functions of the quantities that are conserved in the presence of a magnetic field, namely the energy ϵ_0 and the projection of the quasi-momentum $\mathbf{p}$ in the direction of the field (the z axis).

In the absorption of sound, those electrons play a role for which the energy ϵ_0 is close to the value of the chemical potential μ_0. However, the dependence on p_z is very important. Because of it, for a given H, the condition (1.1) can be satisfied only for certain values of p_z. These values include, first, the solutions of the equation $\mathbf{k}\cdot\tilde{\mathbf{v}} = 0$ (if the Fermi surface is closed, this equation obviously always possesses at least one solution). Equation (1.1) is satisfied for $n = 0$ by these p_z for any value of the field, and if the field H (and also the frequency Ω) is sufficiently large, then (1.1) can have no other solutions.

If we decrease the field, then (1.1) ought to have a solution also at $n = \pm 1$ for H less than a certain H_1. A new group of electrons appears, whose distribution function differs markedly from the equilibrium distribution. Therefore, as the field H goes through the value H_1, the absorption coefficient Γ ought to increase. Further changes of this type in the coefficient Γ should occur when the field assumes the values $H_n = H_1/|n|$. Evidently, these considerations on the presence of periodic changes in the coefficient Γ apply, generally speaking, only to the case of a closed trajectory in the quasi-momentum space,[7] when the motion of the electron in the magnetic field is periodic. In the present paper we consider only this case.

The changes mentioned earlier can be of two types, depending on for which p_z (1.1) is first satisfied. The first type is connected with $|p_z|$ equal to p_z^0, the extremal values of $|p_z|$ on the Fermi surface. We shall see below that the corresponding changes are sufficiently smooth — sharp jumps take place in the derivatives of the coefficient Γ with respect to the magnetic field. By measuring the field H_1, it is possible to find the product $v_z^0 m^* = K^{-1/2}$, i.e., to determine the Gaussian curvature K of the Fermi surface at its elliptic point, to which the normal is directed along p_z. If the Fermi surface is nonconvex, then there can be several such points, to each of which, generally speaking, there corresponds a value of H_1. If the Fermi surface is open in the direction of H, then the increments of the first type ought to be absent.

Increments of the second type, as we shall see below, represent sharp jumps. They are associated with such values of p_z for which the function $\tilde{\alpha}(p_z)$ has extrema, i.e., $d\tilde{\alpha}/dp_z = 0$. If the Fermi surface is an ellipsoid, then it is easy to see that this derivative does not vanish (it is equal to a constant). Therefore, the presence of jumps testifies to a sharp departure in the shape of the Fermi surface from ellipsoidal.

Clearly, these increments exist if the electron does not experience collisions within the period of rotation in the magnetic field. More precisely, for this result it is necessary that the inequality

$$\Omega t_0/2\pi \gg 1, \tag{1.2}$$

be satisfied, where $1/t_0$ is the collision frequency of the conduction electrons. We shall assume below that (1.2) holds. The frequency of the ultrasound can also be such that $\omega t_0 < 1$, and in our research just this limiting case was considered.

2. The oscillations of the coefficient Γ take place, generally speaking, for any relative orientation of the vectors $\mathbf{k}$ and $\mathbf{H}$. But it is easiest to observe them when these vectors are perpendicular, since the periodic increments are then absent. In fact, in this case $\tilde{\alpha} = 0$, inasmuch as $\tilde{v}_x = \tilde{v}_y = 0$ (the trajectories in the quasimomentum space are closed); we therefore consider the case in which $\mathbf{k} \perp \mathbf{H}$.

The trajectory of the electron at different points intersects the plane $\mathbf{k}\cdot\mathbf{r} = \text{const}$ at different angles. In particular, there are at least two points on it, and possibly more, in which the tangent to it lies in the plane $\mathbf{k}\cdot\mathbf{r} = \text{const}$. In it, the velocity component of the electron in the direction of the change of the field of the sound wave is equal to zero, and the electron spends more time close to the plane of equal phase, where such points lie, than to the other planes. Therefore, the quantity f_0^2 is determined fundamentally by the value of the field at these points, since the effect of the rapidly changing field on f_0^2 outside their immediate vicinity is shown to be very small. The latter confirmation is valid to a greater degree the larger the number of waves contained between these points becomes, since the effect on f_0^2 of the rapidly oscillating field between them becomes smaller.

Let us consider two such points — 1 and 2. The quantity f_0^2 reaches a relative extremum for a definite difference in the phase of the field of the sound wave at the given points. For a change in the constant magnetic field H, this difference returns to the previous value, when the number of sound waves between the points

$$a = (2\pi)^{-1} \int_{t_1}^{t_2} \mathrm{k}v\,dt = A/2\pi \tag{2.1}$$

changes by an integer ($t_2 - t_1$ is the time of motion of the electron from point 1 to point 2). In this case f_0^2 again passes through an extremum each time.

Let us compute the integral (2.1). Let the vector **k** be directed along the ξ axis. The equations of motion of the electron in the magnetic field have the form

$$dp_\xi/dt = -(eH/c)\,v_\eta, \qquad dp_\eta/dt = (eH/c)\,v_\xi. \tag{2.2}$$

Then

$$A = (ck/eH)\,(p_\eta^{(2)} - p_\eta^{(1)}), \tag{2.3}$$

where $p_\eta^{(1)}$ and $p_\eta^{(2)}$ are the values of the projections of the quasimomentum on the η axis at points 1 and 2. Consequently, if $A \gg 1$, f_0^2 oscillates as a function of $1/H$ with period $\Delta(H^{-1}) = 2\pi e/ck \times |p_\eta^{(2)} - p_\eta^{(1)}|$. The period depends on p_z; therefore in the total experimentally-observed effect there will exist only oscillations corresponding to the distinct values of p_z, namely values for which $\Delta H^{-1}(p_z)$ has an extremum. If the plane $p_z = 0$ intersects the Fermi surface or surfaces, these values will necessarily include value $p_z = 0$. This follows from the fact that the Fermi surfaces either possess radial symmetry or occur in pairs that possess radial symmetry with respect to each other.

3. In the simplest case, when the Fermi surface has a center of symmetry, it is possible to point to an extraordinarily simple method which permits us to establish the surface from the period of oscillation of the coefficient Γ. This method can be shown to be suitable for experimenters, since it is connected in principle with the use of only a single specimen, the surface of which does not need careful treatment for the given purposes.

The method for establishing the Fermi surface lies in the following. Leaving the orientation of the field **H** unchanged relative to the crystallographic axes, we measure the periods of oscillation of $\Gamma(\mathbf{H})$ for various directions of the vector **k** in the plane perpendicular to **H**. We assume initially that the oscillations are connected only with $p_z = 0$. Then, if the vector **k** is directed along the ξ axis we can determine the ordinates $p_\eta^{(i)}$ of the points at which the line $l(\mathbf{H})$ of intersection of the surface $\epsilon_0(\mathbf{p}) = \mu_0$ with the plane $p_z = \text{const}$ is parallel to the ξ axis. We draw the straight lines $p_\eta = p_\eta^{(i)}$ in the given plane, lines on which these points lie. Repeating such a procedure for different directions of the vector $\mathbf{k} \perp \mathbf{H}$, we obtain a family of lines in the plane $p_z = 0$. Evidently, the envelope of this family is indeed the line $l(\mathbf{H})$. Changing the direction of **H**, we can determine the form of all possible central sections of the Fermi surface and thus establish it completely. We note that by determining the curve $l(\mathbf{H})$ for a given direction of **H**, we can simultaneously establish a control on the validity of the determination of the line $l(\mathbf{H})$ for other orientations of the field. The possibility of such a control permits us to ascertain what oscillations correspond to $p_z = 0$, what (if there are any) correspond to other values of p_z, and also to determine whether the Fermi surface has a center of symmetry. The determination of the Gaussian curvature of this surface from the increments of the first type can serve as an additional means of control.

We note that if we succeed by experiment in obtaining a sufficiently strong inequality $A \gg 1$, then the use of films in place of bulk specimens can facilitate considerably the interpretation of the experimental data.

4. We now turn to the quantitative solution of the problem. Following Akhiezer,[4] we shall consider that in the field of a sound wave with $u_i = u_{i0} \exp[i(\omega t - \mathbf{k}\cdot\mathbf{r})]$ (u_i are the components of the displacement vector) the energy of the electron $\epsilon_0(\mathbf{p})$ is increased by an amount

$$\varepsilon' = \lambda_{ik} u_{ik}, \tag{4.1}$$

proportional to the strain tensor u_{ik}. The distribution function of the conduction electrons $F = F_0[(\epsilon - \mu)/T] + f$ represents the sum of the equilibrium Fermi function (μ = chemical potential at the given point of the metal) and the nonequilibrium addition $f = -\chi \partial F_0/\partial\epsilon$. It can be shown that $\mu = \mu_0 + \mu'$, where μ_0 is the chemical potential in the undeformed metal,

$$\mu' = \bar{\lambda}_{ik} u_{ik} + u_{ii} N_0 h^3/2 \oint (d\Sigma/v) \tag{4.2}$$

is a contribution which is determined both by the change in the energy of the electrons (the first component) and also by the change in their equilibrium density (second part) under the action of the deformation. Here N_0 is the density of electrons in the undeformed metal, the bar indicates averaging over the Fermi surface ($d\Sigma$ is an element of this surface, and v is the velocity of the electrons on it):

$$\varphi \qquad \oint \varphi\,(d\Sigma\;v)'\;\oint (d\Sigma/v).$$

As shown in references 4 and 5, the temperature change in the field of the sound wave can be neglected in the kinetic equations.

The kinetic equation for the electrons in a magnetic field in the form assumed by I. M. Lifshitz, Azbel', and Kaganov[7] which is applicable to the present case, has the form

$$i\omega\chi + \Omega\partial\chi/\partial\tau - i\mathbf{vk}\chi + \hat{W}\chi = \Lambda\dot{u} - e\mathscr{E}_\nu v_\nu \equiv Q. \qquad (4.3)$$

Here $\tau = \Omega t$ is a dimensionless variable proportional to the time of motion of the electron in the magnetic field:

$$m^* = (2\pi)^{-1}\,\partial S/\partial\varepsilon,$$

where S is the area of the intersection of the surface $\epsilon_0(\mathbf{p}) = \text{const}$ with the plane $p_z = \text{const}$, and $\hat{W}$ is the collision operator. χ should be a periodic function of τ with period 2π. The right side of (4.3) is computed in reference 5:

$$\Lambda_{ik} = \lambda_{ik} - \bar{\lambda}_{ik} - \left[N_0 h^3/2 \oint (d\Sigma/v)\right]\delta_{ik};$$

the tensor notation in the expression $\Lambda_{ik}\dot{u}_{ik}$ is omitted here and below. Further,

$$\mathscr{E}_\nu = E'_\nu + [\dot{\mathbf{u}}\times\mathbf{H}]_\nu/c, \qquad \mathbf{E}' = \mathbf{E} + \nabla\mu'/e, \qquad (4.4)$$

the field $\mathbf{E}$ is determined from the Maxwell equations

$$\operatorname{curl}\mathbf{E} = -(i\omega/c)\,\mathbf{H}', \quad \operatorname{curl}\mathbf{H}' = (4\pi/c)\,\mathbf{j}, \qquad (4.5)$$

$$\operatorname{div}\mathbf{E} = -(8\pi e/h^3)\,\bar{\chi}\oint (d\Sigma/v), \qquad (4.6)$$

whereas the field $\mathbf{G} = \dot{\mathbf{u}} \times \mathbf{H}/c$ arises because of the motion of the conductor in the magnetic field.

For good conductors, as noted in reference 5, (4.6) reduces to the equation

$$\bar{\chi} = 0, \qquad (4.7)$$

i.e., to the condition of the vanishing of the volume density of charge. Two other equations for the components of $\mathbf{E}$ are obtained by substituting the expression for the components of the current density into (4.5):

$$j_\beta = -(2e/h^3)\int v_\beta\chi\,(d\Sigma/v),$$

where β denotes η or ζ.

The coefficient of sound absorption is

$$\Gamma = \sigma/2wE_{\text{so}}, \qquad (4.8)$$

where $\sigma = T\dot{S}$, $\dot{S}$ is the rate of change of the entropy density, which is determined by the electronic collisions, E_{so} is the energy density of the sound wave, and w is the sound velocity.

Making use of the expression for the entropy density of a Fermi gas

$$S = -2h^{-3}\int [F\ln F + (1-F)\ln(1-F)]\,d^3\mathbf{p},$$

it is not difficult to show that

$$\sigma = h^{-3}\int |\chi\hat{W}\chi|\,d\Sigma/v. \qquad (4.9)$$

In a number of interesting cases it is found possible to introduce the relaxation time, i.e., to assume that the collision operator is

$$\hat{W} = 1/t_0(\mathbf{p}). \qquad (4.10)$$

Postponing the investigation of this question to Sec. 7, we now find a periodic solution (in τ) of (4.3) with account of (4.10). It is advantageous to write it down with the help of an operator R which acts on periodic functions of τ (with period 2π) in the following fashion:

$$\hat{R}\psi = \Omega^{-1}\int_{-\infty}^{\tau}\exp\left[\int_{\tau}^{\tau'}(-i\alpha+\gamma)\,d\tau''\right]\psi(\tau')\,d\tau' = \Omega^{-1}\int_{\tau}^{\tau+2\pi}\exp\left[\int_{\tau}^{\tau'}(-i\alpha+\gamma)\,d\tau''\right]\psi(\tau')\,d\tau'/[\exp[2\pi(-i\tilde{\alpha}+\tilde{\gamma})]-1]$$

$$\equiv \hat{r}\psi/[\exp[2\pi(-i\tilde{\alpha}+\tilde{\gamma})]-1], \qquad (4.11)$$

where $\alpha = \mathbf{k}\cdot\mathbf{v}/\Omega$, $\gamma = 1/\Omega t_0$; the sign ~ over a letter indicates averaging over the period 2π. The solution of Eq. (4.3) is

$$\chi(\tau) = \hat{R}Q. \qquad (4.12)$$

We assume that $\omega t_0 \ll 1$. We further recall that, in accord with (1.2), $2\pi\gamma \ll 1$.

We now determine the components of the vector $\mathscr{E}_\nu$. It follows from (4.7) that

$$\mathscr{E}_\xi = \mathscr{E}_{0\xi} + \sum_\beta a_\beta\mathscr{E}_\beta, \qquad (4.13)$$

where

$$\mathscr{E}_{0\xi} = \overline{R\Lambda\dot{u}}/e\overline{Rv_\xi}, \qquad a_\beta = -\overline{Rv_\beta}/\overline{Rv_\xi}. \qquad (4.14)$$

Substituting the expression for j_β into (4.5), we arrive at the following equations:

$$E_\beta = E_{0\beta} + \sum_\nu b_{\beta\nu}\mathscr{E}_\nu, \qquad (4.15)$$

where

$$E_{0\beta} = (8\pi iew^2/\omega c^2h^3)\int v_\beta R\Lambda\dot{u}\,d\Sigma/v,$$

$$b_{\beta\nu} = -(8\pi ie^2w^2/\omega c^2h^3)\int v_\beta Rv_\nu\,d\Sigma/v. \qquad (4.16)$$

Their solution is

$$\mathscr{E}_\beta = \sum_{\beta'}(1-d)^{-1}_{\beta\beta'}(\mathscr{E}_{0\beta'} + G_{\beta'}), \qquad (4.17)$$

where

$$d_{\beta\beta'} = b_{\beta\beta'} + b_{\beta\xi}a_{\beta'}, \qquad \mathscr{E}_{0\beta} = E_{0\beta} + b_{\beta\xi}\mathscr{E}_{0\xi} \qquad (4.18)$$

We are interested in the case of large relaxation times ($t_0 \gtrsim 10^{-11}$ sec) and ultrasonic frequencies of the order of $10^8 - 10^9$ sec^{-1}. Under these conditions, it is usually true that $|d_{\beta\beta'}| \gg 1$. For example, for the case in which $\mathbf{H} \perp \mathbf{k}$ and $|\alpha| \gg 1$, it is possible to obtain the estimate

$$|d_{\beta\beta'}| \sim 4\pi\sigma_0 w^2/\omega c^2 \alpha, \tag{4.19}$$

the validity of which will be demonstrated in what follows. Here σ_0 is the conductivity of the metal in the absence of a magnetic field. Assuming $\sigma_0 \sim 10^{20}$ sec^{-1}, $\omega \sim 10^9$ sec^{-1}, $\alpha \sim 10$, we obtain $|d_{\beta\beta'}| \sim 10$. Such estimates are easily obtained in other cases. If the inequality $|d_{\beta\beta'}| \gg 1$ holds, then

$$\mathscr{E}_\beta = -\sum_{\beta'} d^{-1}_{\beta\beta'} (\mathscr{E}_{0\beta'} + G_{\beta'}). \tag{4.20}$$

This case is of fundamental interest to us. However, for very high ultrasonic frequencies, there is an opposite limiting case $|d_{\beta\beta'}| \ll 1$. Then

$$\mathscr{E}_\beta = \mathscr{E}_{0\beta} + G_\beta. \tag{4.21}$$

Evidently, the field $\mathbf{G}$ associated with the motion of the conductor in the magnetic field differs from zero only if the directions of the vectors $\mathbf{u}$ and $\mathbf{H}$ do not coincide, and its presence can affect the form of the coefficient Γ only if it is not directed along $\mathbf{k}$. It is of interest to compare the order of magnitude of $\Lambda\dot{u}$ and $e\mathbf{v}(1-d)^{-1}\mathbf{G}$ which enter into the right-hand side of the kinetic equation. For example, in the case in which the estimate (4.19) is valid, their ratio is of the order of $4\pi\sigma_0 w^2/\omega c^2 \ll 1$, and the right-hand side of the kinetic equation can be represented with sufficient accuracy in the form

$$Q = \Lambda\dot{u} - e\mathbf{E}'\mathbf{v}. \tag{4.22}$$

Inasmuch as we are interested in the case of not too strong magnetic fields, in which the dimensions of the electronic orbit are greater than or of the order of the acoustic wavelength, we shall assume in what follows that the right side of the kinetic equation has the form (4.22). We emphasize, however, that the field $\mathbf{G}$ can be shown to be important in the determination of the absorption coefficient in the case of a sufficiently strong magnetic field when $A \ll 1$.

On the other hand, components containing E_β on the right side of the kinetic equation are small in comparison with the term Λu, roughly speaking, when $|d_{\beta\beta'}| \ll 1$. In the most interesting case, $|d_{\beta\beta'}| \ll 1$, the terms are generally comparable, and it is necessary to take them all into account in the determination of the absorption coefficient.

5. We begin with the determination of the coefficient Γ when the vectors $\mathbf{k}$ and $\mathbf{H}$ are mutually perpendicular. If $|\alpha| \gg 1$ for most values of τ, then the integral $\hat{r}\Lambda\dot{u}$ can easily be computed by the method of stationary phase, and is equal to

$$\hat{r}\Lambda u = \Omega^{-1} e^{iA(\tau)} [\Lambda_1 \sqrt{2\pi/\alpha_1'}\, e^{-i(A_1+\pi/4)} + \Lambda_2 \sqrt{2\pi/|\alpha_2'|}\, e^{-i(A_2-\pi/4)}]\, \dot{u}, \tag{5.1}$$

$$A(\tau) = (ck/eH)[p_\eta(\tau) - p_\eta(0)] = \int_0^\tau \alpha d\tau'. \tag{5.2}$$

The prime here denotes differentiation with respect to τ; the indices 1 and 2 indicate that the values of the function are taken at points of stationary phase, where $\mathbf{k}\cdot\mathbf{v}(\tau) = 0$. In this case, it is assumed that $\alpha_1' > 0$, $\alpha_2' < 0$. For simplicity, we have assumed that such points are two in number; however, the contribution can easily be generalized to a case in which there are more than two.

In the calculation of the integral (5.1), we have taken into account only the first component on the right side of (4.4), because, if $|d_{\beta\beta'}| \gg 1$, $\gamma \ll 1$, then the contribution from it is larger than from the second component. This is readily verified by computing the quantities entering into (4.20) and making use of the integration formula (5.1). In this fashion it is easy to obtain also the estimate (4.19).

The integrand in (4.9) is

$$t_0^{-1}|\chi|^2 = (2\pi)^{-1} t_0 [|\Lambda_1\dot{u}|^2/\alpha_1' + |\Lambda_2\dot{u}|^2/|\alpha_2'| - 2(\Lambda_1\dot{u}^*)(\Lambda_2\dot{u}) \sin A/\sqrt{|\alpha_1'\alpha_2'|}], \tag{5.3}$$

where $A = A_2 - A_1$. It is clear that σ represents the sum of the part of σ_0 which depends smoothly on H and the oscillating component $\Delta\sigma$.

Substituting (5.3) into (4.9) and taking into account the identity $d\Sigma/v = m^* d\tau\, dp_z$, it is possible to represent the expression for σ_0 in the following form:

$$\sigma_0 = h^{-3} \int \Omega t_0 \delta(\mathbf{kv}) |\Lambda\dot{u}|^2 d\Sigma/v \sim N_0\mu_0\Omega t_0 \omega^3 \mathbf{u}_0^2 / vw. \tag{5.4}$$

For the calculation of $\Delta\sigma$ it is again necessary to make use of the method of steepest descents:

$$\Delta\sigma = -\frac{2eH}{ckh^3} \int t_0 (\Lambda_1\dot{u}^*)(\Lambda_2\dot{u}) \sin A\, |v'_{\xi 1} v'_{\xi 2}|^{-1/2} dp_z = \sigma' \sin\left[\frac{ck}{eH}(p^0_{\eta 2} - p^0_{\eta 1}) \pm \frac{\pi}{4}\right], \tag{5.5}$$

where

$$\sigma' \sim \sigma_0 (\Omega w/\omega v)^{1/2}. \tag{5.6}$$

The superscript 0 denotes that the corresponding quantities are taken at the saddle point where the first derivative vanishes:

$$d(p_{n2} - p_{n1})/dp_z = 0, \qquad (5.7)$$

and the sign of the phase in (5.5) coincides with the sign of the second derivative at this point.* If there are other values of p_z near $p_z = 0$ for which (5.7) holds, $\Delta\sigma$ is the sum of the several components of type (5.5).

Let us estimate the absorption coefficient Γ. Substituting (5.4) in (4.9) and taking it into account that $E_{so} = \rho\omega^2 u_0^2/2$ (ρ = density of the crystal) and $\Lambda_{ik} \sim \mu_0$, we find that the nonoscillating part is

$$\Gamma_0 \sim N_0\mu_0\Omega t_0\omega / \rho v w^2. \qquad (5.8)$$

It is proportional to the magnetic field and the ultrasonic frequency. If we investigate the dependence of Γ_0 on the frequency at a given maximum or minimum, i.e., for a fixed value of $\alpha = \omega v/\Omega w$, then we find that the coefficient Γ_0 is proportional to the square of the frequency. According to (5.6),† $\Delta\Gamma \sim \Gamma_0\sqrt{\Omega w/\omega v}$.

6. We now turn to the investigation of the increment of the coefficient Γ. To estimate the relative value of the effect, we determine the absorption coefficient in such a field H that for most electrons, the quantity $|\tilde{\alpha}|$ is close to unity but is always less than it.

We again consider a case in which (4.22) is valid with sufficient accuracy. It is easy to verify that the important region in the integral (4.9) is that close to $p_z = 0$ and to the other p_z (if they exist) which cause $\tilde{\alpha}$ to vanish. For simplicity, we assume that the value $p_z = 0$ is alone in this relation. We expand $\tilde{\alpha}$ near it up to the linear term $\tilde{\alpha} = \tilde{\alpha}' p_z$, and integrate over infinite limits, obtaining

$$\sigma = \frac{1}{2\pi h^3}\int \frac{m^*}{\Omega^2 t_0}\frac{|\widetilde{rQ}|^2 dp_z}{\tilde{\alpha}'^2 p_z^2 + \gamma^2} = \frac{m^*|\widetilde{rQ}|^2}{2h^3 \mathbf{k}(\partial\tilde{\mathbf{v}}/\partial p_z)} \qquad (6.1)$$

(the values of all the quantities are taken at $p_z = 0$). Then

$$\Gamma_0 \sim N_0\mu_0\omega / \rho v w^2. \qquad (6.2)$$

This estimate remains valid even when $\tilde{\alpha}(p_z) = 0$ has several solutions.

If $2\pi\gamma \ll 1$, then the derivative $d\Gamma/dH$ must undergo a sharp jump near $H = H_1$. Under such conditions, near $H = H_n \equiv H_1/|n|$, the higher-order derivatives of the coefficient of absorption with respect to the magnetic field ought to undergo jumps. In practice, it is easiest to discover jumps in the first derivative [a discontinuity in the function $\Gamma(H)$], and we shall consider in detail the case $|n| = 1$. To estimate the value of the jump, we determine the increment experienced by the coefficient Γ when the field reaches the value H_1. We write

$$v_i(\tau) = \tilde{v}_i + \Delta v_i(\tau).$$

It is not difficult to show (see, for example, reference 9) that near $p_z = p_z^0$ on the Fermi surface, $\Delta v_i(\tau)$ generally has the form

$$\Delta v_i(\tau) = \eta_i v_z^0 \sqrt{|\Delta p_z/p_z^0|}\cos(\tau + \varphi_i) + \cdots, \qquad (6.3)$$

where $\Delta p_z = p_z - p_z^0$. The next term of the expansion is linear in $|\Delta p_z/p_z^0|$, and may already contain the cosine of twice the angle, etc. Similarly, $\Lambda = \tilde{\Lambda} + \Delta\Lambda$, wherein $\Delta\Lambda$ close to p_z^0 is determined by an expansion of the type (6.3).

If $|\Delta\alpha| < 1$, χ has the order of $|\Lambda/\Omega\alpha|$ and is a smooth function of p_z for all p_z except those for which $\tilde{\alpha}(p_{zn}) = n$. For $p_z = p_{zn}$, χ has a sharp maximum [the width is of the order of $\gamma/(\partial\tilde{\alpha}/\partial p_z)_n$]. The presence of such maxima points up the character of the dependence of $\Gamma(H)$. Let us determine the form of the function χ close to such a maximum. Let $|p_{zn} - p_z^0| \ll p_z^0$. Then

$$p_{zn} - p_z^0 = (n - \alpha^0)/(\partial\tilde{\alpha}/\partial p_z)^0 \qquad (6.4)$$

(the superscript 0 means that the corresponding quantities are evaluated at $p_z = p_z^0$). Close to $p_z = p_{zn}$, we have

$$\chi(\tau) = \int_{\tau}^{\tau+2\pi} \exp\left[\int_{\tau}^{\tau'}(-in - i\Delta\alpha - i\delta\tilde{\alpha} + \tilde{\gamma})\,d\tau''\right] \times (Q^0 + \Delta Q + \delta\tilde{Q})\,d\tau' / 2\pi\Omega(-i\delta\tilde{\alpha} + \tilde{\gamma}). \qquad (6.5)$$

Here,

$$\delta\tilde{\alpha} = (\partial\tilde{\alpha}/\partial p_z)^0 (p_{zn} - p_z),$$

while $\delta\tilde{Q}$ is determined in similar fashion. If $|\Delta\alpha| \ll 1$, we can expand the exponent in (6.5) in powers of $-i\Delta\alpha$. In this case, a sharp maximum is absent from the zero-order term in $\sqrt{|\Delta p_z/p_z^0|}$. In computing the terms of higher order in $\sqrt{|\Delta p_z/p_z^0|}$, we neglect $\tilde{\gamma}$ in the exponent in (6.5).

Is is seen that when $|n| = 1$, the term of first order actually has a maximum for $p_z = p_{z1}$. However, if $|n| > 1$, this term vanishes for $p_z = p_{zn}$ because of the orthogonality of the trigonometric functions. Therefore, when $|n| = 2$, sharp maxima can exist only for terms beginning with the second order, etc. We now consider in detail the case $|n| = 1$. We see that if $|p_{z1} - p_z^0| \ll p_z^0$, then $|\chi|^2/t_0$, the integrand of (4.9), can be represented in the form of a sum of two components. One of them is a smooth function of p_z close to p_z^0. The second, is very small in the range of integration in (4.9) if the difference $H - H_1$ is of one sign, and has a sharp maximum as a function of p_z in this interval if the difference $H - H_1$ is of another sign. Close to $p_z = p_{z1}$, it has the form

---

*If the line $l(H)$ is not convex, cases for which $\alpha(\tau_i) = \alpha'(\tau_i) = 0$ are possible for certain directions of the vector $\mathbf{k} \perp \mathbf{H}$. The expression for the periods of the corresponding oscillations remains in these cases as before, but the phase and the dependence of the amplitude on the field change slightly.

†We note that a much weaker inequality than (1.2), $\Omega t_0 \gtrsim 1$, is actually necessary for the existence of the oscillation. If $\Omega t_0 \sim 1$, the periods of oscillation are determined by (5.5) as before.

$$b\,|p_z - p_{z1}|\,/\,(\delta\tilde{\alpha}^2 + \tilde{\gamma}^2). \tag{6.6}$$

The integral of the first component is a smooth function of H. Equation (6.1) represents an estimate of its contribution to the absorption coefficient Γ. The contribution from the second component is essentially different from zero only for a definite sign of the difference $H - H_1$. In the given case it also represents the increment in the coefficient Γ. In order to determine it, it suffices to integrate (6.6). As a result we get

$$\delta_1\Gamma = \pm\Gamma_1\,|H_1 - H|\,/\,H_1, \tag{6.7}$$

where

$$\Gamma_1 \sim N_0\mu_0\omega\,/\,\rho v w^2. \tag{6.8}$$

Equation (6.7) gives the dependence on the field in the interval $\gamma \ll |H_1 - H|/H_1 \ll 1$ with sufficient accuracy. It differs from zero only for $H > H_1$ or for $H < H_1$, depending whether the derivative $\mathbf{k}\cdot(\partial\tilde{\mathbf{v}}/\partial p_z)^0$ is negative or positive, respectively. For an increase of the field the sign of (6.7) is opposite to the sign of this derivative. We see that $d\Gamma/dH$ experiences sharp jumps close to $H = H_1$; if the field changes by an amount of the order γH_1, this derivative changes by an amount of the order Γ/H_1. It is clear that if $|n| = 2$, $\delta_2\Gamma \sim (H_2 - H)^2/H_2^2$, and the second derivative $d^2\Gamma/dH^2$ can have a sharp jump close to $H = H_2$, etc.

The graph [constructed for one of the cases in which the vectors **k** and **H** are parallel, $\epsilon_0 = \mathbf{p}^2/2m^*$, $2\pi\gamma(H_1) = 0.1$] permits us to visualize the form of the function $\Gamma(H^{-1})$. The dashed lines on the graph extrapolate the dependence $\Gamma(H^{-1})$ under the assumption that the derivatives of the absorption coefficient with respect to the field do not experience sharp discontinuities at the corresponding points.

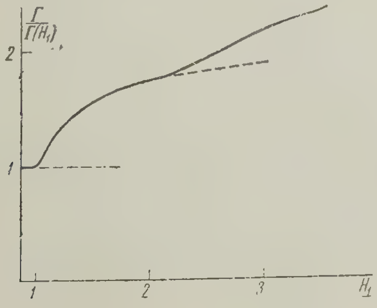

In this same way, it is not difficult to estimate the increment of the second type. For example, for $|n| = 1$, $|\Delta\alpha| \lesssim 1$, it is equal in order of magnitude to

$$\delta\Gamma \sim N_0\mu_0 t_0^{1/2}\Delta v^2\omega^{3/2}\,/\,\rho v^{5/2}w^{5/2}. \tag{6.9}$$

The coefficient Γ experiences this increment if the field changes by an amount of the order γH_1, i.e., it has the character of a sharp jump. Upon a subsequent change in the field in the same direction, the value of p_{z1} will depart from the extremum point of the function $\tilde{\alpha}(p_z)$, which, generally speaking, ought to lead to a decrease in the absorption coefficient.

In this case discontinuities can occur also for $|n| > 1$.

We have considered two basic types of increment. If the Fermi surface has a complicated structure (for example, if it is self-intersecting), then, in addition to those described, there can be other types.

7. In conclusion we turn our attention to the possibility of introducing a relaxation time. The collision operator has the form

$$\hat{W}f = f(\zeta)\int M(\zeta, \zeta')m^{*\prime}d\varepsilon' dp_z' d\tau' - \int N(\zeta, \zeta')f(\zeta')m^{*\prime}d\varepsilon' dp_z' d\tau', \tag{7.1}$$

where ζ denotes the set of variables ϵ, p_z, and τ. It is evident that the relaxation time can be introduced in all cases when $|\alpha| \gg 1$. Then $f(\epsilon, p_z, \tau)$ represents a rapidly oscillating function of τ, the second term in (7.1) is much less than the first, and

$$\hat{W} = t_0^{-1} = \int M(\zeta, \zeta')\,m^{*\prime}d\varepsilon' dp_z' d\tau'. \tag{7.2}$$

Thus, we can conclude the presence of an oscillation of the coefficient Γ for an arbitrary character of the collision.

It is useful to note one other case, in which a relaxation time exists. It can also be introduced if, for certain p_z, $|\chi|$ has a sharp maximum that exceeds markedly the average value of this function, and the coefficient Γ or its increment are determined fundamentally by the behavior of the function χ close to this maximum. Such is the case when the expression (6.1) is valid for increments of both the first and the second type. Then again the first term in (7.1) is much larger than the second, which contains the average of the function χ. The situation here is somewhat reminiscent, as shown by Azbel' and Kaner,[11] of the anomalous skin effect. There, too, the possibility of the introduction of a relaxation time is brought about by the presence of a maximum of the distribution function of the electrons whose velocities are almost parallel to the surface of the metal.

In the remaining cases, the assumption on the collision operator of the form (4.10) permits us to estimate the order of magnitude of the absorption coefficient.

In conclusion, the author thanks Academician L. D. Landau for a discussion of the work and for a number of valuable suggestions.

---

[1] H. Bömmel, Phys. Rev. **100**, 758 (1955).

[2] Morse, Bohm, and Gavenda, Phys. Rev. **109**, 1394 (1958).

[3] A. B. Pippard, Phil. Mag. **2**, 1147 (1957).

[4] A. I. Akhiezer, J. Exptl. Theoret. Phys. (U.S.S.R.) **8**, 1330 (1938).

[5] Akhiezer, Kaganov, and Lyubarskiĭ, J. Exptl. Theoret. Phys. (U.S.S.R.) **32**, 837 (1957), Soviet Phys. JETP **5**, 685 (1957).

[6] M. S. Steinberg, Phys. Rev. **109**, 1486; **110**, 772 (1958).

[7] Lifshitz, Azbel', and Kaganov, J. Exptl. Theoret. Phys. (U.S.S.R.) **31**, 63 (1956); Soviet Phys. JETP **4**, 41 (1957).

[8] L. D. Landau and E. M. Lifshitz, Механика сплошных сред, (Mechanics of Continuous Media), Gostekhizdat 1954.

[9] V. L. Gurevich, J. Exptl. Theoret. Phys. (U.S.S.R.) **35**, 668 (1958), Soviet Phys. JETP **8**, 464 (1959).

[10] A. H. Wilson, Theory of Metals, Cambridge, 1954.

[11] M. Ya. Azbel' and É. A. Kaner, J. Exptl. Theoret. Phys. (U.S.S.R.) **32**, 896 (1957), Soviet Phys. JETP **5**, 730 (1957).

Translated by R. T. Beyer
11

$$f(r) = \left[1 + \exp\frac{r - R_0}{d}\right]^{-1}, \qquad d = \frac{\Delta R}{4.4}.$$

The particle-nucleus interaction energy is first represented in the K′ coordinate system and then transformed to the K system. Limiting ourselves to inelastic scattering with the nucleus making a transition from its ground state to an excited state with spin 2^+ and assuming that only $\alpha_{\lambda\mu}$ with $\lambda = 2$ differs from zero, we have

$$V_1 = -V_0 r\frac{\partial f(r)}{\partial r}\sum_{\mu}\alpha_\mu Y_{2\mu}(\Theta, \Phi), \tag{1.2}$$

where

$$\alpha_\mu = \sum_{\nu} a_\nu D^{(2)}_{\mu\nu}(\theta_i). \tag{1.3}$$

In (1.2) and (1.3) a_ν are the coordinates of a nuclear deformation in the K′ system [$a_0 = \beta\cos\gamma$, $a_2 = a_{-2} = (\beta/\sqrt{2})\sin\gamma$, $a_1 = a_{-1} = 0$], α_μ are nuclear deformation coordinates in the K system and $D^{(2)}_{\mu\nu}$ is the transformation matrix of second order spherical harmonics. Since $a_2 = a_{-2} = 0$ for an axially symmetrical nucleus, (1.2) can be rewritten as follows:

$$V_1 = -V_0 r\frac{\partial f(r)}{\partial r}\beta\cos\gamma\sum_{\mu}\sqrt{\frac{4\pi}{5}}Y_{2\mu}(\theta, \varphi)Y_{2\mu}(\Theta, \Phi). \tag{1.4}$$

If the quasi-classical condition $kR \gg 1$ is satisfied, particle motion in the nuclear field $Z_1Z_2e^2/r + V_0(r)$ can be described by means of classical mechanics, assuming $\mathbf{r} = \mathbf{r}(t)$. Assuming, furthermore, that the energy $\Delta E = E_f - E_i$ transferred to the nucleus in a collision is small compared with the collision energy E ($\Delta E < E$), we may neglect the change in the character of particle motion as energy is imparted to the nucleus. In other words, we shall assume that in inelastic scattering the trajectory of a charged particle is indistinguishable from that of an elastically scattered particle.

We know[7] that when $kR_0 \gg 1$ and $\eta = Z_1Z_2e^2/\hbar v \gg 1$, Coulomb scattering plays the principal role for scattering angles $\vartheta \leq 2\eta/kR_0$, while diffraction scattering occurs for $\vartheta > 2\eta/kR_0$. In the scattering of α particles (as well as of C^{12}, N^{14} and other ions) by heavy nuclei at angles $\vartheta > 2\eta/kR_0$ the angular distribution of elastically scattered particles does not possess the diffraction maxima and minima which appear, for example, in the scattering of α particles by light nuclei, but is characterized by an exponential reduction of the cross section as the scattering angle increases. This property of the angular distribution has been explained by the optical-model theory of elastic α-particle scattering[8] as well as by a number of quasi-classical theories.[9,10] Porter[10] accounts for the non-Rutherfordian differential cross section for elastic scattering by assuming that the decreased absolute value of the elastic scattering cross section is due to the fact that α particles are knocked out of the beam upon traversing a nucleus. It is also assumed that the Coulomb trajectory of the particles is not changed because of $V_0(r)$. The differential cross section for elastic scattering is then given by

$$\sigma(\vartheta)_{\mathbf{elast}} = \sigma(\vartheta)_{\mathbf{Ruth}}\exp\left\{-2R_0\Pi_0 h\left(\frac{D}{R_0}, \frac{\Delta R}{R_0}\right)\right\},$$

$$D(\vartheta) = \frac{Z_1Z_2e^2}{2E}\left(1 + \frac{1}{\sin(\vartheta/2)}\right), \tag{1.5}$$

where Π_0 is the absorption coefficient for particles passing through the center of the nucleus and $h(D/R_0, \Delta R/R_0)$ is a tabulated function.[10] If the nucleus has a sharply defined boundary we have

$$h(D/R_0, \Delta R/R_0)_{\Delta R=0} = \sqrt{1 - (D/R_0)^2}. \tag{1.6}$$

We shall use the collision-parameter method to determine inelastic scattering cross sections. When all conditions mentioned above are satisfied the differential cross section for inelastic scattering is

$$\sigma(\vartheta)_{\mathbf{inelast}} = \sigma(\vartheta)_{\mathbf{elast}} P(\vartheta), \tag{1.7}$$

where P is the probability of nuclear transition from the ground state to the final state. Nuclear excitation results from the time-dependent action of the incident particle's electromagnetic field and from the time-dependent interaction of the particle with the noncentral part of the potential (1.1). Assuming, furthermore, that the combined effect of the fields is small and can be treated as a first approximation, we have

$$P = \sum_{M_f}|b_{if} + b^c_{if}|^2, \tag{1.8}$$

where

$$b_{if} = \frac{1}{i\hbar}\int_{-\infty}^{\infty} e^{i\omega t}\langle f|V_1(\mathbf{r}(t), \theta_i)|i\rangle\, dt, \tag{1.9}$$

$\omega = \Delta E/\hbar$, M_f is the projection of the nuclear spin in the final state on the Z axis and b^c_{if} is a transition amplitude for Coulomb excitation.[6]

In calculating nuclear transition amplitudes b_{if} resulting from nuclear forces we first consider the excitation of rotational states in even-even nuclei. This becomes the problem of scattering on a nucleus with fixed orientation, that is, we determine the transition amplitude b_{if} which is dependent on the orientation and then average this amplitude over all orientations.

The wave functions of the deformed nucleus in the ground and excited states are[4]

$$\Psi_i \approx Y_{00}(\theta, \varphi)\varphi_i(\beta, \gamma), \qquad \Psi_f \approx Y_{IM}(\theta, \varphi)\varphi_f(\beta, \gamma), \quad (1.10)$$

where $\varphi_i(\beta, \gamma)$ and $\varphi_f(\beta, \gamma)$ represent the surface vibrations of a nucleus with axial symmetry.

Substituting (1.4) and (1.10) into (1.9), we obtain the following expression for the amplitude of a nuclear transition from state i to state f:

$$b_{if} = -(V_0\beta / i\hbar\sqrt{5})\sum_\mu S_{2\mu}, \quad (1.11)$$

where

$$S_{2\mu} = \int_{-\infty}^{\infty} e^{i\omega t} Y_{2\mu}(\Theta, \Phi)\frac{\partial f(r)}{\partial r}\,dt, \quad (1.12)$$

$$\overline{\beta} = \langle\varphi_f(\beta, \gamma)\,|\,\beta\cos\gamma\,|\,\varphi_i(\beta, \gamma)\rangle. \quad (1.13)$$

We shall now consider the excitation of vibrational states in even-even nuclei. In this case α_μ can be associated with creation and annihilation operators of excitation quanta (phonons)[4] with spin $\lambda = 2$ and spin projection μ on the fixed Z axis:

$$\alpha_\mu = \sqrt{\hbar\omega / 2C_2}\,[q_\mu + (-1)^\mu q_\mu^*] \quad (1.14)$$

where q_μ^* is a phonon-creation operator and q_μ is an annihilation operator. The wave functions of the ground state and first excited state will then be $\Psi_i = \Psi_{00}^0$ (in the absence of phonons) and $\Psi_f = \Psi_{2\mu}^1$ (for one phonon with spin 2 and its projection μ). Calculating the matrix elements of the operators q_μ and q_μ^*, which are then substituted into (1.9), we obtain

$$b_{if} = -(V_0 / i\hbar)\sqrt{\hbar\omega /2C_2}\sum_\mu S_{2\mu}, \quad (1.15)$$

where $S_{2\mu}$ is defined by (1.12).

2. CALCULATION OF EXCITATION PROBABILITY

For the purpose of calculating the excitation probability we write the equation of motion of a charged particle in the parametric form

$$r = a(\varepsilon\cosh w - 1), \quad x = a(\cosh w + 1),$$

$$y = a\sqrt{\varepsilon^2 - 1}\sinh w, \quad t = (a / v)(\varepsilon\sinh w + w), \quad (2.1)$$

where $a = Z_1Z_2e^2/\mu v^2$ and ϵ is the orbital eccentricity. Since $\mathbf{r} = (r, \Theta, \Phi) = (r, \pi/2, \Phi)$ in the K coordinate system, we have

$$Y_{2\mu}(\Theta, \Phi) = \left(\frac{x + iy}{r}\right)^\mu Y_{2\mu}\left(\frac{\pi}{2}, 0\right). \quad (2.2)$$

After (2.1) and (2.2) are inserted in (1.12), the excitation probability of collective levels of even-even nuclei is obtained from (1.11) and (1.8):

$$P = \frac{9A}{25}\left(\frac{R}{a}\right)^4 \eta^2 \sum_\mu \left| Y_{2\mu}\left(\frac{\pi}{2}, 0\right)\right|^2 \Big| I_{2\mu}(\vartheta, \xi) - \frac{5}{6}\frac{kR_0}{\eta}\left(\frac{V_0}{E}\right)\left(\frac{a}{R}\right)^2 \frac{a^2}{R_0 d} \times I_{2\mu}(\vartheta, \xi, a, R_0, d)\Big|^2, \quad \text{if } d \neq 0, \quad (2.3)$$

$$P = \frac{9A}{25}\left(\frac{R}{a}\right)^4 \eta^2 \sum_\mu \left| Y_{2\mu}\left(\frac{\pi}{2}, 0\right)\right|^2 \Big| I_{2\mu}(\vartheta, \xi) - \frac{5}{6}\frac{kR_0}{\eta}\left(\frac{V_0}{E}\right)\left(\frac{a}{R}\right)^2 K_{2\mu}(\vartheta, \xi, a, R_0)\Big|^2, \quad \text{if } d = 0, \quad (2.4)$$

where $A = \overline{\beta}^2/5$ for the excitation of rotational states and $A = \Delta E/2C_2$ for the excitation of vibrational states; R is the nuclear radius ($R = 1.2 \times 10^{-13}$ cm); $\epsilon = 1/\sin(\vartheta/2)$; $I_{2\mu}(\vartheta, \xi)$ are the classical orbital integrals for E2 Coulomb excitation, which were tabulated in reference 6:

$$I_{2\mu}(\vartheta, \xi, a, R_0, d) = \int_{-\infty}^{\infty} e^{i\xi(\varepsilon\sinh w + w)} \frac{(\cosh w + \varepsilon + i\sqrt{\varepsilon^2 - 1}\sinh w)^\mu}{(\varepsilon\cosh w + 1)^{\mu - 2}} \times g(\vartheta, a, R_0, d, w)\,dw, \quad (2.5)$$

$$\begin{aligned} K_{2\mu}(\vartheta, \xi, a, R_0) &= a\int_{-\infty}^{\infty} e^{i\xi(\varepsilon\sinh w + w)} \frac{(\cosh w + \varepsilon + i\sqrt{\varepsilon^2 - 1}\sinh w)^\mu}{(\varepsilon\cosh w + 1)^{\mu - 1}} \times \delta[a(\varepsilon\cosh w + 1) - R_0]\,dw \\ &= \frac{e^{i\xi(\varepsilon\sinh\Lambda + \Lambda)}}{\varepsilon\sinh\Lambda}\left\{\frac{(\cosh\Lambda + \varepsilon + i\sqrt{\varepsilon^2 - 1}\sinh\Lambda)^\mu}{(\varepsilon\cosh\Lambda + 1)^{\mu - 1}} - \frac{(\cosh\Lambda + \varepsilon - i\sqrt{\varepsilon^2 - 1}\sinh\Lambda)^\mu}{(\varepsilon\cosh\Lambda + 1)^{\mu - 1}}\right\}, \end{aligned} \quad (2.6)$$

where

$$g(\vartheta, a, R_0, d, w) = \exp\left[\frac{a(\varepsilon\cosh w + 1) - R_0}{d}\right] \times \left[1 + \exp\frac{a(\varepsilon\cosh w + 1) - R_0}{d}\right]^{-2}, \quad (2.7)$$

$$\Lambda = \ln\left[\frac{1}{\varepsilon}\left(\frac{R_0}{a} - 1\right) + \sqrt{\frac{1}{\varepsilon^2}\left(\frac{R_0}{a} - 1\right)^2 - 1}\right]. \quad (2.8)$$

In calculating (2.3) and (2.4) we have used

$$b_{if}^c = (3/5i)A(R / a)^2\eta Y_{2\mu}(\pi / 2, 0)I_{2\mu}(\vartheta, \xi), \quad (2.9)$$

which is easily obtained by writing Eq. (2Γ, 7) of reference 6 in our notation.

To calculate the fuctions $I_{2\mu}(\vartheta, \xi, a, R_0, d)$ in (2.3) we must calculate the following integrals:

$$I_{22}(\vartheta, \xi, a, R_0, d) = I_1(\vartheta, \xi, a, R_0, d) - I_2(\vartheta, \xi, a, R_0, d), \quad (2.10)$$

$$I_{20}(\vartheta, \xi, a, R_0, d) = I_0(\vartheta, \xi, a, R_0, d), \quad (2.11)$$

$$I_{2-2}(\vartheta, \xi, a, R_0, d) = I_1(\vartheta, \xi, a, R_0, d) + I_2(\vartheta, \xi, a, R_0, d), \quad (2.12)$$

$$I_1(\vartheta, \xi, a, R_0, d)$$

$$= 2\int_0^\infty [(\cosh w + \varepsilon)^2 - (\varepsilon^2 - 1)\sinh^2 w]\, g(\vartheta, a, R_0, d, w)$$

$$\times \cos[\xi(\sinh w + w)]\, dw, \tag{2.13}$$

$$I_2(\vartheta, \xi, a, R_0, d)$$

$$= 4\sqrt{\varepsilon^2 - 1}\int_0^\infty (\sinh w)(\cosh w + \varepsilon)\, g(\vartheta, a, R_0, d, w)$$

$$\times \sin[\xi(\sinh w + w)]\, dw, \tag{2.14}$$

$$I_0(\vartheta, \xi, a, R_0, d) = 2\int_0^\infty (\varepsilon \cosh w + 1)^2 g(\vartheta, a, R_0, d, w)$$

$$\times \cos[\xi(\sinh w + w)]\, dw. \tag{2.15}$$

The function $g(\vartheta, a, R_0, d, w)$ is defined by (2.7). The imaginary parts of the integrals in (2.5) vanish because the imaginary parts of the integrands are odd. Since $g(\vartheta, a, R_0, d, w)$ decreases rapidly as the parameter w increases, it is usually sufficient for the calculation of I_0, I_1, and I_2 to perform a numerical integration from 0 to 2 — 2.5.

3. CONDITIONS FOR THE SEMICLASSICAL METHOD

For calculating the excitation probability of collective nuclear levels it was assumed that the combined effect of the electric and nuclear fields is small and can be regarded as a time-dependent perturbation. To determine the conditions for the validity of this hypothesis we require that the excitation probability P be smaller than unity for any scattering angle ϑ. When the incident particle energy exceeds the Coulomb barrier height we have $|b_{if}| > |b_{if}^c|$, with opposite signs for the two quantities. Therefore in analyzing the validity conditions we neglect b_{if}^c and obtain the following expression for the probability:

$$P \approx A(kR_0)^2\left(\frac{V_0}{E}\right)^2 \begin{cases} I(\vartheta, \xi, a, R_0, d), & d \neq 0 \\ K(\vartheta, \xi, a, R_0), & d = 0, \end{cases} \tag{3.1}$$

where

$$I(\vartheta, \xi, a, R_0, d) = \tfrac{1}{4}\left(\frac{a}{d}\right)^2\left(\frac{a}{R_0}\right)^2 \sum_\mu \left|Y_{2\mu}\left(\frac{\pi}{2}, 0\right)\right|^2$$

$$\cdot \left|I_{2\mu}(\vartheta, \xi, a, R_0, d)\right|^2, \tag{3.2}$$

$$K(\vartheta, \xi, a, R_0)$$

$$= \tfrac{1}{4}\sum_\mu \left|Y_{2\mu}\left(\frac{\pi}{2}, 0\right)\right|^2 |K_{2\mu}(\vartheta, \xi, a, R_0)|^2. \tag{3.3}$$

The highest value of this probability is obtained at scattering angles ϑ determined by the relation $D(\vartheta) = a(1+\epsilon) = R_0$. Considering that for these scattering angles the absolute values of $I(\vartheta, \xi, a, R_0, d)$ (Fig. 1) and $K(\vartheta, \xi, a, R_0)$ are of the order of unity, we have

$$P < 1, \quad \text{if} \quad A(kR_0)^2(V_0/E)^2 < 1. \tag{3.4}$$

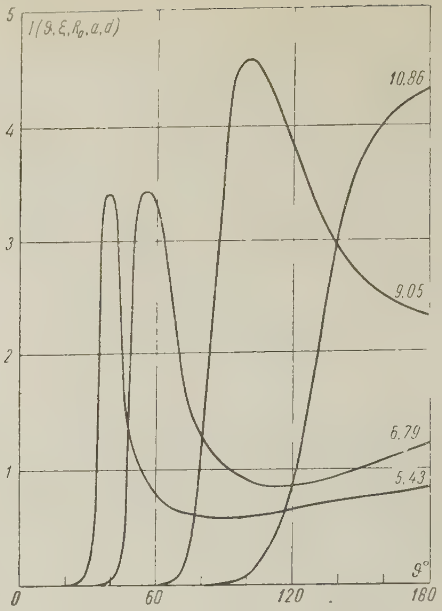

FIG. 1. $I(\vartheta, \xi, R_0, a, d)$ as a function of the scattering angle for $\xi = 0$ and $R_0/d = 22$. The ratio a/d is indicated on each curve.

Experiments on the elastic scattering of α particles by heavy nuclei indicate $V_0 \approx 30 - 40$ Mev. When the incident α-particle energy is within this range (3.4) reduces to $\bar{\beta}^2(kR_0)^2 < 1$ or $(\Delta E/2C_2)(kR_0)^2 < 1$. We know[11,12] that the collective states of axially symmetrical even-even nuclei are of two types — excitations which are and which are not accompanied by considerable change of the nuclear quadrupole moment. Transitions of the first type occur between states with $\gamma = 0$; for these transitions we have

$$\bar{\beta} = \langle \varphi_f(\beta, \gamma) \,|\, \beta\cos\gamma \,|\, \varphi_i(\beta, \gamma)\rangle \approx \beta.$$

A transition from the ground level (with $\gamma = 0$) to an excited level with $\gamma = \pi$ occurs with a change of both the sign and absolute value of $\bar{\beta}$; $\bar{\beta} \ll \beta$ for the absolute value. Transitions of the second type occur in almost spherical nuclei and do not play an important part in markedly nonspherical nuclei when the energy change is small. Davydov and Filippov[12] have indicated a large number of even-even nuclei whose second excited states with spin 2^+ may be assigned to this second type. The experimental data now available[13] indicate that $\bar{\beta}$ for these transitions is smaller than β by a factor of 10 or more.

It is easily calculated that when α particles with 20 — 50 Mev are scattered by heavy nuclei $kR_0 \sim 20$, which is reduced to 10 for deuteron scattering. For the excitation of the first nuclear rotational levels we therefore have $\bar{\beta}(kR_0) \approx \beta kR_0 \approx (0.1 - 0.3)\, 20 > 1$ and the condition for applying perturbation theory to inelastic scattering is not fulfilled. For the excitation of second levels with spin 2^+ (excitations of the second type) we have $\bar{\beta}(kR_0) \ll \beta(kR_0) < 1$.

A similar conclusion is reached by analyzing the requirement that the product $(\Delta E/2C_2)(kR_0)^2$ be small compared with unity. For the excitation of the first levels of even-even nuclei with spin 2^+, C_2 (the surface tension parameter) lies between 15 Mev and 100 Mev for most nuclei,[6] whereas $C_2 \sim 2000 - 2000$ Mev for the second levels[13]. In other words, for the excitation of first vibrational levels of even-even nuclei $P > 1$, but $P < 1$ for the excitation of second levels. The semiclassical method can therefore be used to analyze experimental data on inelastic scattering of charged particles accompanied by the excitation of second levels with spin 2^+ in even-even nuclei.

4. INELASTIC SCATTERING CROSS SECTION

The expressions obtained for the excitation probability of vibrational and rotational nuclear levels enable us to put the formulas for the differential inelastic scattering cross section into final form:

$$\sigma(\vartheta) = 9\cdot 10^{-2} A\eta_i^2 a^2 \left(\frac{R}{a}\right)^4 \sin^{-4}\frac{\vartheta}{2} \exp\left\{-2R_0\Pi_0 h\left(\frac{D}{R_0}, \frac{\Delta R}{R_0}\right)\right\}$$

$$\times \sum_{\mu} \left| Y_{2\mu}\left(\frac{\pi}{2}, 0\right)\right|^2 \left| I_{2\mu}(\vartheta, \xi) - \frac{5}{6}\frac{kR_0}{\eta}\left(\frac{V_0}{E}\right)\left(\frac{a}{R}\right)^2 \frac{a^2}{R_0 d} I_{2\mu}(\vartheta, \xi, a, R_0, d)\right|^2, \qquad (4.1)$$

if $d \neq 0$, and

$$\sigma(\vartheta) = 9\cdot 10^{-2} A\eta_i^2 a^2 \left(\frac{R}{a}\right)^4 \sin^{-4}\frac{\vartheta}{2}$$

$$\times \exp\{-2R_0\Pi_0 \sqrt{1-(D/R_0)^2}\} \sum_{\mu} \left| Y_{2\mu}\left(\frac{\pi}{2}, 0\right)\right|^2 \left| I_{2\mu}(\vartheta, \xi) - \frac{5}{6}\frac{kR_0}{\eta}\left(\frac{V_0}{E}\right)\left(\frac{a}{R}\right)^2 K_{2\mu}(\vartheta, \xi, a, R_0)\right|^2, \qquad (4.2)$$

if $d = 0$.

Equations (3.10) and (4.1) have been used to calculate the excitation probability of a second level with spin 2^+ in Th^{232}_{90} ($\Delta E = 0.790$ Mev) by α particles with the energies 25, 30, 40, and 50 Mev and the corresponding angular and energy distributions.

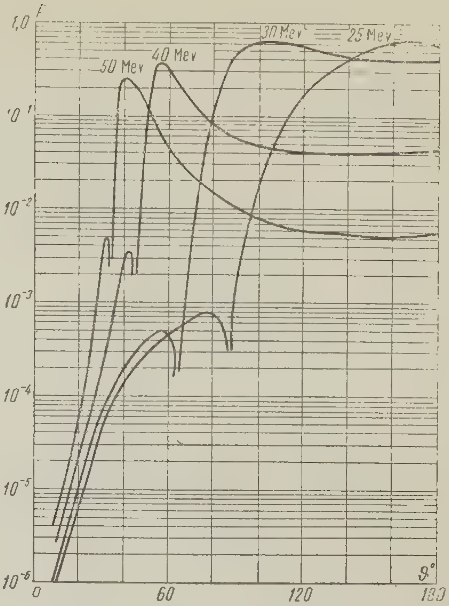

FIG. 2. Excitation probability of a second level with spin 2^+ in Th^{232} ($\Delta E = 0.790$ Mev) as a function of scattering angle for a few values of incident α-particle energy.

Figure 2 gives $P(\vartheta)$ curves for different energies, Fig. 3 gives angular distributions for inelastically scattered α particles and Fig. 4 gives the total cross section as a function of energy. In calculating the differential cross sections the parameters of $T = \exp\{-2R_0\Pi_0 h(D/R_0, \Delta R/R_0)\}$, which takes into account the degree of attenuation of the α-particle beam, were selected in agreement with Porter:[10] $R_0 = 10.5 \times 10^{-13}$ cm, $\Delta R = 2.1 \times 10^{-13}$ cm and $\Pi_0 = 3.5$. The depth V_0 of the potential well was 40 Mev[8] and $C_2 = 2960$ Mev.[13]

It is apparent from Figs. 3 and 4 that the angular dependence of the inelastic scattering cross section possesses a single maximum, whose half-width decreases as the incident-particle energy rises. The absolute value of the differential cross

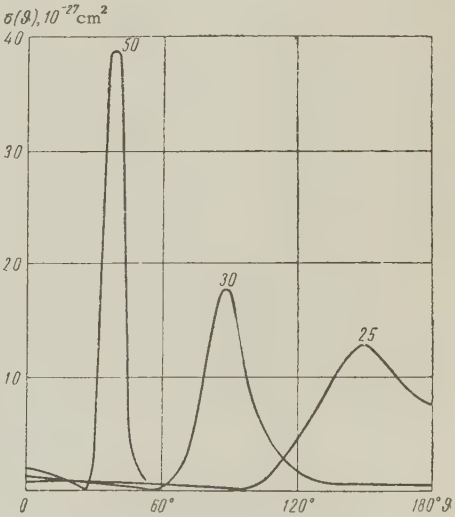

FIG. 3. Angular distributions of α particles scattered inelastically on Th^{232} ($\Delta E = 0.790$ Mev). Numbers on the curves indicate the energies of the incident α particles in Mev.

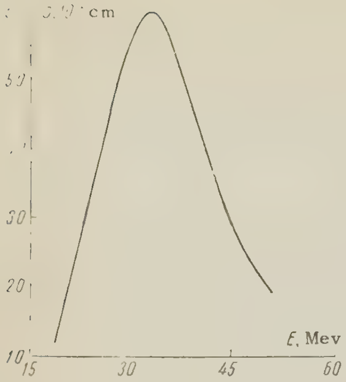

FIG. 4. Energy dependence of total cross section for inelastic scattering of α-particles on Th^{232}.

section maximum for inelastic scattering increases with the energy. The total cross section increases with energy up to a maximum at some E_m and then decreases. With increasing energy α particles remain in the vicinity of a nucleus for a shorter time; also, fewer α particles remain unabsorbed by the nucleus and can be scattered inelastically.

When the energy ΔE transferred during collision is such that the parameter ξ differs from 0 the general character of all curves is conserved. The maxima of the $\sigma(\vartheta)$ curves are shifted toward larger angles, the absolute value of the cross section is reduced and E_m, for which the total cross section reaches its maximum, is shifted toward higher energies.

In conclusion the author wishes to thank S. S. Vasil'ev for his interest, A. S. Davydov, S. I. Drozdov, V. G. Neudachin and K. A. Ter-Martirosyan for discussions, as well as G. S. Tyurikov for assistance with the numerical calculations.

[1] S. I. Drozdov, J. Exptl. Theoret. Phys. (U.S.S.R.) **34**, 1288 (1958), Soviet Phys. JETP **7**, 889 (1958).

[2] S. I. Drozdov, J. Exptl. Theoret. Phys. (U.S.S.R.) **28**, 734 (1955), Soviet Phys. JETP **1**, 591 (1955); Атомная энергия (Atomic Energy) **2**, 501 (1957).

[3] E. V. Inopin, J. Exptl. Theoret. Phys. (U.S.S.R.) **31**, 901 (1956), Soviet Phys. JETP **4**, 764 (1957).

[4] A. Bohr, Kgl. Danske Videnskab. Selskab, Mat.-fys Medd. **26**, 14 (1952).

[5] K. A. Ter-Martirosyan, J. Exptl. Theoret. Phys. (U.S.S.R.) **22**, 284 (1952).

[6] Alder, Bohr, Huus, Mottelson, and Winter, Revs. Modern Phys. **28**, 432 (1956).

[7] A. I. Akhiezer and I. Ya. Pomeranchuk, Usp. Fiz. Nauk **65**, 593 (1958).

[8] G. Igo and R. M. Thaler, Phys. Rev. **106**, 126 (1957).

[9] Kerlee, Blair, and Farwell, Phys. Rev. **107**, 1343 (1957).

[10] C. E. Porter, Phys. Rev. **99**, 1400 (1955).

[11] A. S. Davydov and G. F. Filippov, J. Exptl. Theoret. Phys. (U.S.S.R.) **32**, 945 (1957), Soviet Phys. JETP **5**, 773 (1957).

[12] A. S. Davydov and G. F. Filippov, J. Exptl. Theoret. Phys. (U.S.S.R.) **33**, 723 (1957), Soviet Phys. JETP **6**, 555 (1958).

[13] F. K. McGowan and P. H. Stelson, Bull. Am. Phys. Soc. Ser. II, **2**, 207 (1957).

Translated by I. Emin
12

SOVIET PHYSICS JETP VOLUME 37 (10), NUMBER 1 JANUARY, 1960

STABILITY OF A HOLLOW GAS CONDUCTOR IN A MAGNETIC FIELD

L. M. KOVRIZHNYKH

P. N. Lebedev Physics Institute, Academy of Sciences, U.S.S.R.

Submitted to JETP editor December 25, 1958

J. Exptl. Theoret. Phys. (U.S.S.R.) **37**, 92-94 (July, 1959)

Stability conditions are obtained for a hollow gaseous conductor located in a longitudinal magnetic field.

THE author has shown earlier[1] that if a conductor carrying a return current is placed on the axis of a discharge chamber then, under certain conditions, the discharge will be localized within a narrow region inside the chamber and will form a hollow thin walled cylinder separated from the walls. It seems that in this case the conditions required to stabilize the discharge ought to be less rigid. We therefore investigate in the present paper the question of the stability of such a plasma layer with respect to small oscillations.

We consider a hollow plasma cylinder of internal radius r_2 and external radius r_3 situated in a region bounded by two coaxial perfectly conducting cylinders of radii r_1 $(r_1 < r_2)$ and r_4 $(r_4 > r_3)$. The initial system of equations consists of the magnetohydrodynamic equations for a perfectly conducting fluid, Maxwell's equations for the field, and boundary conditions on the surfaces of discontinuity (see, for example, reference 2).

We assume that in equilibrium the plasma pressure p_0 is balanced by magnetic forces set up by currents flowing in the surface of the plasma, that the velocity is equal to zero, that the plasma is uniform with respect to φ and z, and that the field components H_φ^0 and H_z^0 differ from zero. We shall assume that within the plasma $H_\varphi^0 = 0$, while H_z^0 is everywhere uniform, i.e.,

$$H_z^0 = \begin{cases} H_{z1}^0 \\ H_{z2}^0, \\ H_{z3}^0 \end{cases} \qquad H_\varphi^0 = \begin{cases} 2I_1/cr & \text{for } r_1 < r < r_2 \\ 0 & \text{for } r_2 < r < r_3 \\ 2I_3/cr & \text{for } r_3 < r < r_4 \end{cases} \tag{1}$$

with

$$H_{z1}^{02} + H_{\varphi 1}^{02} = H_{z3}^{02} + H_{\varphi 3}^{02} = H_{z2}^{02} + 8\pi p_0, \tag{2}$$

where

$$H_{\varphi 1}^0 = 2I_1/cr_2, \qquad H_{\varphi 3}^0 = 2I_3/cr_3.$$

By assuming that the deviations from the equilibrium state are small and by solving the equations of motion by the standard method (see, for example, reference 2), we obtain a dispersion relation for the frequency spectrum of the system:*

$$\begin{aligned}\Delta(\Omega^2, k) = &-\alpha_{11}\{\alpha_{11}[I_m(\zeta r_3)K_m(\zeta r_2) - I_m(\zeta r_2)K_m(\zeta r_3)] \\ &+ (\alpha_{12}/\zeta r_2)[I_m'(\zeta r_2)K_m(\zeta r_3) - I_m(\zeta r_3)K_m(\zeta r_2)]\} \\ &+ (\alpha_{22}/\zeta r_3)\{\alpha_{11}[I_m'(\zeta r_3)K_m(\zeta r_2) - I_m(\zeta r_2)K_m'(\zeta r_3)] \\ &+ (\alpha_{12}/\zeta r_2)[I_m'(\zeta r_2)K_m'(\zeta r_3) \\ &- I_m'(\zeta r_3)K_m'(\zeta r_2)]\} = 0,\end{aligned} \tag{3}$$

where

$$\alpha_{12} = h_{\varphi 1}^2 + (\varepsilon_{1m}/kr_2)[mh_{\varphi 1} + kr_2 h_{z1}]^2,$$

$$\alpha_{22} = h_{\varphi 3}^2 - (\varepsilon_{2m}/kr_3)[mh_{\varphi 3} + kr_3 h_{z3}]^2,$$

$$\varepsilon_{1m} = \frac{I_m(kr_2)K_m'(kr_1) - I_m'(kr_1)K_m(kr_2)}{I_m'(kr_2)K_m'(kr_1) - I_m'(kr_1)K_m'(kr_2)},$$

$$\varepsilon_{2m} = \frac{I_m(kr_3)K_m'(kr_4) - I_m'(kr_4)K_m(kr_3)}{I_m'(kr_4)K_m'(kr_3) - I_m'(kr_3)K_m'(kr_4)},$$

$$\alpha_{11} = 1 - \frac{4\pi\gamma p_0}{H_{z2}^{02}}\frac{\Omega^2}{k^2 - \Omega^2}, \qquad \zeta^2 = \frac{(\Omega^2 - k^2)(\Omega^2 - q^2k^2)}{q^2k^2 - (1+q^2)\Omega^2},$$

$$q^2 = H_{z2}^{02}/4\pi\gamma p_0, \qquad h_{\varphi,z} = H_{\varphi,z}^0/H_{z2}^0,$$

$$\Omega^2 = \rho_0\omega^2/\gamma p_0. \tag{3'}$$

Primes indicate differentiation with respect to the argument; I_m and K_m the modified Bessel functions of order m.

We obtain the stability criterion from the condition that the dispersion relation have no solutions, $\Omega^2 < 0$. It has the form

$$\begin{aligned}\alpha_{22}(k) < kr_3\{&[I_m(kr_3)K_m(kr_2) - I_m(kr_2)K_m'(kr_3)] \\ &+ (\alpha_{12}/kr_2)[I_m'(kr_2)K_m(kr_3) \\ &- I_m(kr_3)K_m'(kr_2)]\}\{[I_m'(kr_3)K_m(kr_2) \\ &- I_m(kr_2)K_m'(kr_3)] + (\alpha_{12}/kr_2)[I_m(kr_2)K_m'(kr_3) \\ &- I_m'(kr_3)K_m'(kr_2)]\}^{-1}.\end{aligned} \tag{4}$$

Indeed, in this case, as Ω^2 varies from 0 to

---

*We assume, as usual, that all the quantities are proportional to $\exp(i\omega t + ikz + im\varphi)$.

$-\infty$, $\Delta(\Omega^2, k)$ is always less than zero, and, consequently, Eq. (3) does not have any roots $\Omega^2 < 0$.

It is easily seen that when $H^0_{z2} = 0$ the inequality (4) agrees exactly with the stability criterion obtained for a solid cylindrical conductor,[3,4] i.e., the stability criteria are not relaxed without a "frozen-in" longitudinal field. We also note that when $h^2_{\varphi 3} = 0$ the condition (4) is fulfilled for all m and k, i.e., absolute stability exists.

Without going into a detailed investigation of the stability criterion obtained above, we consider only the stability conditions for the two most dangerous forms of perturbation, with $m = 0$ and $m = 1$. In carrying this out we assume that the outer metal wall is absent; i.e., we shall set $r_4 = \infty$ in the expression for ϵ_{2m}.

1) $m = 0$. As k varies from 0 to ∞ the right-hand side of the inequality (4) increases, whereas the left-hand side decreases. Consequently equilibrium will be stable when

$$H^{02}_{z2} > \frac{1}{2} H^{02}_{\varphi 3} (\delta_2^2 - 1) \frac{H^{02}_{\varphi 1} + 2\delta_1^2 H^{02}_{z1} / (\delta_1^2 - 1)}{\delta_2^2 [H^{02}_{\varphi 1} + 2\delta_1^2 H^{02}_{z1} / (\delta_1^2 - 1)] - H^{02}_{\varphi 3}}, \quad (5)$$

where $\delta_1 = r_2/r_1$; $\delta_2 = r_3/r_2$. When $H^0_{z1} = H^0_{z3} = 0$ relation (5) coincides with the stability criterion obtained for a solid cylinder.

2) $m = 1$. In this case the stability condition depends on the magnitude of h_{z3}. In the case $kr_3 \ll 1$ it has the form

$$H^{02}_{z2} > \frac{\delta_2^2 - 1}{\delta_2^2 + 1} H^{02}_{\varphi 3} \ln \frac{1}{kr_3}, \quad (6)$$

if $h_{z3} = 0$, and

$$|H^0_{z2}| > \frac{|H^0_{\varphi 3}|}{kr_3} \frac{2|h_{z3}|(\delta_2^2 - 1)}{h^2_{z3}(\delta_2^2 - 1) + (\delta_2^2 + 1)}, \quad (6')$$

if $h_{z3} \gg kr_3$.

It follows from the foregoing that when $\delta_2 \rightarrow 1$ the stabilizing field in the case of a hollow cylindrical conductor is less than the field required for the stabilization of a solid conductor by a factor $\sim (\delta_2^2 - 1)^{-1/2}$ (when $h_{z3} = 0$) and by a factor $\sim (\delta_2^2 - 1)^{-1}$ (when $h_{z3} \neq 0$).

---

[1] L. M. Kovrizhnykh, Атомная энергия (Atomic Energy) **5**, 648 (1956).

[2] M. Kruskal and M. Schwarzschild, Proc. Roy. Soc. **A223**, 348 (1954).

[3] V. D. Shafranov, Атомная энергия (Atomic Energy) **5**, 38 (1956).

[4] R. I. Taylor, Proc. Phys. Soc. **B70**, 31, 1049 (1957).

Translated by G. Volkoff
13

SOVIET PHYSICS JETP VOLUME 37 (10), NUMBER 1 JANUARY, 1960

RESONANCE CHARGE EXCHANGE OF DOUBLY CHARGED IONS IN SLOW COLLISIONS

I. K. FETISOV and O. B. FIRSOV

Submitted to JETP editor December 29, 1958

J. Exptl. Theoret. Phys. (U.S.S.R.) **37**, 95-97, (July, 1959)

The cross section for resonance charge exchange of doubly charged ions has been computed in the adiabatic approximation. A comparison is made between the experimental and theoretical charge exchange cross sections for doubly charged positive A, Kr, Xe, and Ne ions.

ONE-ELECTRON resonance charge exchange has been considered by many authors.[1-6] In the present paper we calculate the cross section for two-electron resonance charge exchange in the adiabatic approximation.

It has been shown earlier[7] that in the adiabatic approximation the cross section for charge exchange of an ion with an atom is

$$\sigma = \tfrac{1}{2}\pi R_0^2, \tag{1}$$

where R_0 is determined by the condition

$$\int_0^\infty \frac{E_a(R) - E_s(R)}{\hbar v}\, dx = k \approx \frac{1}{\pi}. \tag{2}$$

Here $x^2 = R^2 - R_0^2$; R is the distance between the nuclei in the ion and the atom; R_0 is the collision parameter; E_a is the energy of the electrons for the anti-symmetric wave function; E_s is the energy of the electrons for the symmetric wave function. Thus, the problem reduces to the calculation of the splitting of the electron levels as the nuclei approach each other.

We shall assume that for internuclear distances which are not too small it is possible to compute $E_a - E_s$ approximately, taking for He^{++}:

$$\psi_{s,a} \simeq [\varphi_A(r_1, r_2) \pm \varphi_B(s_1, s_2)] / \sqrt{2}, \tag{3}$$

as is done for the molecular hydrogen ion (the upper and lower signs refer respectively to ψ_s and ψ_a). Here φ_A and φ_B are the helium wave functions for electrons in the ground state when the electrons are attached to nucleus A or nucleus B; r is the distance of the electron from nucleus A, s is the distance from nucleus B. In this approximation the energy of the electrons is given by the expression

$$E_{s,a} = \frac{\int (\varphi_A \pm \varphi_B) H (\varphi_A \pm \varphi_B)\, d\tau_1\, d\tau_2}{\int (\varphi_A \pm \varphi_B)^2\, d\tau_1\, d\tau_2}$$

$$E - \frac{4e^2 \left[\int r_1^{-1} \varphi_B^2\, d\tau_1\, d\tau_2 \pm \int r_1^{-1} \varphi_A \varphi_B\, d\tau_1\, d\tau_2\right]}{1 \pm \int \varphi_A \varphi_B\, d\tau_1\, d\tau_2} \tag{4}$$

For large internuclear distances $\int r_1^{-1} \varphi_B^2 d\tau_1 d\tau_2 \sim 1/R$ and the remaining integrals are exponentially small. Hence,

$$E_a - E_s \approx \frac{8e^2}{R} \left(R \int \frac{\varphi_A \varphi_B}{r_1}\, d\tau_1\, d\tau_2 - \int \varphi_A \varphi_B\, d\tau_1\, d\tau_2 \right). \tag{5}$$

The function φ is taken as the simple helium function

$$C \exp[-\alpha(r_1 + r_2)], \qquad \alpha = a_0^{-1} \sqrt{(E_1 + E_2)/2E_0},$$

where $E_1 + E_2$ is the total energy of the electrons in the atom, E_0 is the energy of the electron in the hydrogen atom and a_0 is the Bohr radius. The value of α for the helium atom is $1.71\, a_0^{-1}$, which corresponds to the minimum energy for the chosen wave function and also corresponds to the asymptotic region for a wave function having the mean binding energy [large r (or s)].

The analysis given here applies for relative velocities which satisfy the inequality $v \ll (\alpha e^2/\hbar)\, a_0$.

The results of the calculations are shown in Fig. 1; along the abscissa is plotted the relative velocity of the nuclei and along the ordinate axis is plotted $\alpha^2\sigma$, where σ is the cross section for two-electron charge exchange. On this same curve are plotted the measured experimental cross sections for two-electron charge exchange in the noble gases A, Ne, Kr, Xe.[8,9] Since one-electron charge exchange can occur in two-electron charge exchange

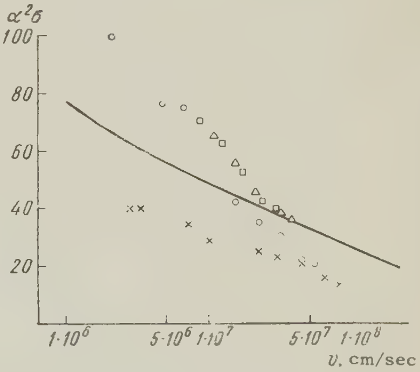

FIG. 1. ×) Ne; o) A; △) Kr; □) Xe.

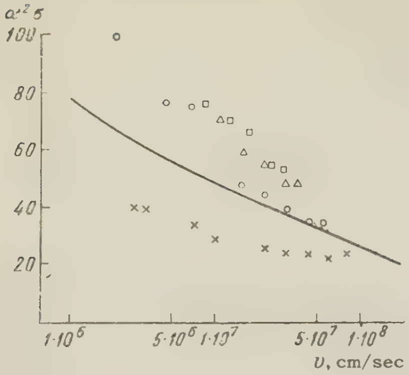

FIG. 2. ×) Ne; ○) A; △) Kr; □) Xe.

and in elastic scattering, and since this factor has not been taken into account in computing the cross section, the theoretical curve really corresponds to $\sigma_{20} + \frac{1}{2}\sigma_{21}$, where σ_{20} is the cross section for two-electron charge exchange and σ_{21} the cross section for one-electron charge exchange. A comparison of the experimental curves with the theory for this case is given in Fig. 2.

The theory given by Gurnee and Magee[9] for resonance charge exchange is similar to the present one but is less "rigorous." They make comparisons with some very old experimental results.[10,11] These authors assume $\psi = c \exp\{-\alpha(r_1 + r_2)\}/r^n$ and obtain $\alpha_{\mathrm{Ne}} = 1.4$, $n = 1$; $\alpha_{\mathrm{A}} = 1.3$, $n = 3$. As a result the cross sections obtained by Gurnee and Magee for Ne and A are larger than ours by approximately a factor of 2. The present results show better agreement with experiment.

---

[1] Yu. N. Demkov, Уч. зап. ЛГУ (Scientific Notes, Leningrad State University) **146**, 74 (1952).

[2] D. R. Bates and A. Dalgarno, Proc. Phys. Soc., **A65**, 919 (1952).

[3] A. Dalgarno and H. N. Jadov, Proc. Phys. Soc., **A66**, 173 (1953).

[4] J. D. Jackson, Can. J. Phys. **32**, 60 (1954).

[5] B. M. Bransden, Dalgarno and King, Proc. Phys. Soc. **A67**, 1075 (1954).

[6] B. L. Moiseiwitsch, Proc. Phys. Soc. **A69**, 653 (1956).

[7] O. B. Firsov, J. Exptl. Theoret. Phys. (U.S.S.R.) **21**, 1001 (1951).

[8] I. P. Flaks and E. S. Solov'ev, J. Tech. Phys. (U.S.S.R.) **28**, 599 (1958), Soviet Phys. "Technical Physics" **3**, 564 (1958).

[9] E. F. Gurnee and J. L. Magee, J. Chem. Phys. **26**, 1237 (1957).

[10] F. Wolf, Ann. Physik, **29**, 33 (1937).

[11] F. Wolf, Ann. Physik, **34**, 341 (1938).

Translated by H. Lashinsky
14

SOVIET PHYSICS JETP VOLUME 37 (10), NUMBER 1 JANUARY, 1960

THE ULTRAVIOLET ASYMPTOTIC VALUE FOR THE INTERACTION OF K MESONS WITH BARYONS

J. WRZECIONKO

Joint Institute for Nuclear Research

Submitted to JETP editor January 3, 1959

J. Exptl. Theoret. Phys. (U.S.S.R.) 37, 98-104 (July, 1959)

The ultraviolet asymptotic value for the interaction of K mesons with baryons is studied for different kinds of relative baryon parity under the assumption of weak coupling.

1. INTRODUCTION

THE investigation of ultraviolet asymptotic values in quantum field theory can be carried out either by solving the Dyson integral equations for boson and fermion Green's functions together with a specific equation for the source particle,[1,2] or by the method of the renormalization group.[3,4] The weak coupling hypothesis is used in both cases. Moreover, these investigations are limited to the examination of one fermion field with a specific boson field (quantum electrodynamics or meson theory). It seems to us more logical to consider all possible (renormalizable) interactions in the study of the ultraviolet asymptotic value.

As an example we look at the ultraviolet asymptotic value for the interaction of K mesons with baryons (customarily called the theory of medium strong interactions). For this we take into consideration the interaction constants for K mesons with all baryons. The use of the weak-coupling hypothesis in meson theory is not well founded. But there is sufficiently strong proof that the K-baryon interaction constants are significantly less than the π-meson constant $(g_K^2/4\pi \ll g_\pi^2/4\pi)$.[5,6] It can be shown that there exists a reasonable, physical momentum interval in which the weak coupling assumption is legitimate. Special attention is given to the ultraviolet asymptotic value for different kinds of relative baryon parity.

2. THE RENORMALIZATION GROUP IN THE THEORY OF MEDIUM STRONG INTERACTIONS

Assuming charge independence for the interaction of K mesons with baryons, we write the Lagrangian of the system in the form

$$L = L_{\text{coup}} + L_{\text{int}},$$

$$L_{\text{int}} = g_1 \overline{N}_1 \Gamma_1^0 \Lambda K + g_2 N_1 \overline{\Gamma_2^0} \boldsymbol{\tau} \underline{\Sigma} K + g_3 \overline{N}_2 \Gamma_3^0 \Lambda K + g_4 N_2 \overline{\Gamma_4^0 \boldsymbol{\tau} \Sigma K} + h(\overline{K}K)(\overline{K}K) + \text{Herm. conj.} \qquad (1)$$

where

$$N_1 = \begin{pmatrix} p \\ n \end{pmatrix}, \quad N_2 = \begin{pmatrix} \Xi^0 \\ \Xi^- \end{pmatrix}, \quad K = \begin{pmatrix} K^+ \\ K^0 \end{pmatrix},$$

$$\Lambda = \Lambda^0, \quad \Sigma \quad \begin{pmatrix} \Sigma^+ \\ \Sigma^0 \\ \Sigma^- \end{pmatrix},$$

$$\Gamma_i^0 = 1, \ \gamma_5 \quad (i = 1, \ldots, 4), \quad \gamma_5 = -\gamma_5.$$

The choice of 1 or γ_5 depends on the relative parity of the baryons. We represent the fermion Green's function in the form

$$G_B(p) = (S_B(p^2)\hat{p} + S'_B(p^2) m_B)(p^2 - m_B^2)^{-1}. \qquad (2a)$$

The index B on S and m means the baryons (N_1, N_2, Λ, Σ). We write the K-meson Green's function and the source particles as

$$D_K(p) = S_K(p^2)/(p^2 - m_K^2); \qquad (2b)$$

$$\Gamma_i = \Gamma_i^0 G_i, \quad G_i = G_i(p^2, q^2, (p-q)^2), \quad i = 1, \ldots, 4;$$
$$\Box = \Box(p'^2, q'^2, p^2, q^2, (p'-q)^2, (p+q)^2). \qquad (2c)$$

The source $\Box$ corresponds to the diagrams with four incoming K-meson lines.

For brevity, we do not write out the renormalization group. There is the following system of invariant charges:

$$\sigma_1 = S_{N_1} S_\Lambda S_K G_1^2 g_1^2, \quad \sigma_2 = S_{N_1} S_\Sigma S_K G_2^2 g_2^2,$$
$$\sigma_3 = S_{N_2} S_\Lambda S_K G_3^2 g_3^2,$$
$$\sigma_4 = S_{N_2} S_\Sigma S_K G_4^2 g_4^2, \quad \rho = S_K^2 \Box h. \qquad (3)$$

The Lie equations for the invariant charges (3) are given in Appendix 1. We have written down these equations for the ultraviolet asymptotic case.

Let us look at a simpler problem. We notice that the system (A1) is invariant under the change $\sigma_1 \rightarrow \sigma_3$, $\sigma_3 \rightarrow \sigma_1$, $\sigma_2 \rightarrow \sigma_4$, $\sigma_4 \rightarrow \sigma_2$. This circumstance allows us to transform this system into a simpler one. Let $g_1 = g_3$, $g_3 = g_4$ in the Lagrangian (1). Polkinghorne employed such a Lagrangian.[7] Neglecting the mass differences between the baryons, which is fully justified in the ultraviolet asymptotic case, we get

$$\sigma_1 = \sigma_3, \qquad \sigma_2 = \sigma_4, \tag{4}$$

and the system (A1) leads to a system of three equations

$$d\sigma_i / dx = \sigma_i \sum_{j=1}^{2} \beta_i^j(\varepsilon)\,\sigma_j + \varkappa_1 \sigma_i \rho^2 \qquad (i = 1, 2);$$

$$d\rho / dx = 3F_0\,[\sigma_1^2 + \sigma_1\sigma_2(2+\varepsilon) + 9\sigma_2^2]$$

$$+ 2F_1\,[\sigma_1 + 3\sigma_2]\,\rho + F_2\rho^2, \tag{5}$$

where

$$\beta_i^j(\varepsilon) = \frac{1}{32\pi^2}\begin{pmatrix} 5 & 3 + 12(1-\varepsilon) \\ 1 + 4(1-\varepsilon) & 7 \end{pmatrix},$$

$x = \ln(p^2/\lambda^2)$, λ the normalization momentum.

The scalar functions S, G_i, and ☐ are determined by the equation

$$\frac{\partial}{\partial x}\ln S(x, g_1^2, g_2^2, h) = \frac{\partial}{\partial \xi} S^0(\xi, \sigma_1, \sigma_2, \rho)\big|_{\xi=1}; \tag{6}$$

S^0 is obtained with the aid of perturbation theory. The parameter ϵ takes on the two values ±1. The choice of + or − depends on the type of relative parity of the baryons. We denote by I_{AB} the parity of baryon A relative to baryon B, then

$$\begin{aligned} \varepsilon = +1, \quad & \text{if } I_{\Lambda N_1} = I_{\Sigma N_1} = I_{\Lambda N_2} = I_{\Sigma N_2} = \pm 1, \\ & \text{or } I_{\Lambda N_1} = I_{\Sigma N_1} = -I_{\Lambda N_2} = -I_{\Sigma N_2} = \pm 1, \\ & \text{or } -I_{\Lambda N_1} = I_{\Sigma N_1} = -I_{\Lambda N_2} = I_{\Sigma N_2} = \pm 1; \\ \varepsilon = -1, \quad & \text{if } -I_{\Lambda N_1} = I_{\Sigma N_1} = I_{\Lambda N_2} = -I_{\Sigma N_2} = \pm 1. \end{aligned} \tag{7}$$

3. INVESTIGATION OF THE ULTRAVIOLET ASYMPTOTIC VALUE

We shall not take into account K-K meson scattering processes. Then in the version given by (4), the Lie equations have the form

$$d\sigma_1 / dx = \beta_1^1\sigma_1^1 + \beta_1^2(\varepsilon)\,\sigma_1\sigma_2,$$

$$d\sigma_2 / dx = \beta_2^1(\varepsilon)\,\sigma_1\sigma_2 + \beta_2^2\sigma_2^2. \tag{8}$$

We examine two cases.

A. $\epsilon = -1$. From Eq. (8) we get a formula determining the dependence of σ_1 on σ_2. In the (σ_1, σ_2) plane we have the family of integral curves shown in Fig. 1. The straight line $\sigma_1 = 5\sigma_2$ is stationary, so that it is sufficient to solve Eq. (8) for this value. We get

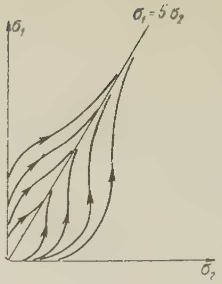

FIG. 1

$$\sigma_1 = 5\sigma_2, \qquad \sigma_2 = \left[1 - \frac{13}{8\pi^2}\,g_2^2 x\right]^{-1}. \tag{9}$$

With the help of (9) we find the form of the scalar functions S and G_i:

$$S_i = \left[1 - \frac{13}{8\pi^2}\,g_2^2 x\right]^{-\alpha_i/13}. \tag{10}$$

The constants α_i are

$S_i =$	$S_{N_1} = S_{N_2}$	S_Λ	S_Σ	S_K	$G_1 = G_3$	$G_2 = G_4$
$\alpha_i =$	2	5	1	16	−5	−3

B. $\epsilon = +1$. The integral curves in the (σ_1, σ_2) plane for this case are shown in Fig. 2. The particular solution for the straight line $\sigma_1 = \sigma_2$ is not stationary. The integral curves go either to the asymptotic $\sigma_1 = \sigma_2^5$ or to $\sigma_1 = \sigma_2^{3/7}$. We solve (8) for these asymptotes.

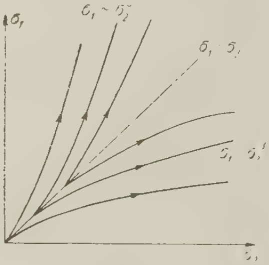

FIG. 2

a) The asymptote $\sigma_1 = \sigma_2^5$

$$\sigma_1 = g_1^2\left[1 - \frac{5}{32\pi^2}\,g_1^2 x\right]^{-1},$$

$$\sigma_2 = g_2^2\left[1 - \frac{5}{32\pi^2}\,g_1^2 x\right]^{-1/5}; \tag{11}$$

b) The asymptote $\sigma_1 = \sigma_2^{3/7}$

$$\sigma_1 = g_1^2\left[1 - \frac{7}{32\pi^2}\,g_2^2 x\right]^{-3/7},$$

$$\sigma_2 = g_2^2\left[1 - \frac{7}{32\pi^2}\,g_2^2 x\right]^{-1}. \tag{12}$$

The scalar functions S and G_i, found with the aid of (11) and (12), are respectively

S_i	α_i	β_i	α'_i	β'_i	S_i	α_i	βi	α'_i	β_i
$S_{N_1} = S_{N_2}$	1/5	3/4	3/7	1/4	S_K	8/5	6	24/7	2
S_Λ	4/5	0	0	1	$G_1 = G_3$	—4/5	—3	—12/7	—1
S_Σ	0	1	4/7	0	$G_2 = G_4$	—4/5	—3	—12/7	—1

$$S_i = \left[1 - \frac{5}{32\pi^2} g_1^2 x\right]^{-\alpha_i} \exp\left\{-\beta_i \frac{g_2^2}{g_1^2}\left[1 - \frac{5}{32\pi^2} g_1^2 x\right]^{4/5}\right\},$$

$$S_i = \left[1 - \frac{7}{32\pi^2} g_2^2 x\right]^{-\alpha'_i}$$

$$\times \exp\left\{-\beta'_i \frac{g_1^2}{g_2^2}\left[1 - \frac{7}{32\pi^2} g_2^2 x\right]^{4/7}\right\}. \tag{13}$$

The values α_i, β_i, α'_i, and β'_i are given in the table.

We shall find which curve is followed by a given point in the three-dimensional space $(\rho, \sigma_1, \sigma_2)$ when x goes to infinity. To do this we determine the integral curves of the system of equations got by dividing the third equation in (5) by the first and the second:

$$\frac{d\rho}{d\sigma_1} = \frac{3F_0[\sigma_1^2 + \sigma_1\sigma_2(2+\varepsilon) + 9\sigma_2^2] + 2F_1[\sigma_1 + 3\sigma_2]\rho + F_2\rho^2}{\beta_1^1\sigma_1^2 + \beta_1^2(\varepsilon)\sigma_1\sigma_2 + \varkappa_1\sigma_1\rho^2},$$

$$\frac{d\rho}{d\sigma_2} = \frac{3F_0[\sigma_1^2 + \sigma_1\sigma_2(2+\varepsilon) + 9\sigma_2^2] + 2F_1[\sigma_1 + 3\sigma_2]\rho + F_2\rho^2}{\beta_2^1(\varepsilon)\sigma_1\sigma_2 + \beta_2^2\sigma_2^2 + \varkappa_1\sigma_2\rho^2}. \tag{14}$$

The three dimensional space ρ, σ_1, σ_2 $(\sigma_1, \sigma_2 \geq 0)$ is divided into three regions by the surfaces ρ_1, ρ_2, the roots of the trinomials quadratic in ρ in the numerators in the right hand terms in (14); $\rho_1 > \rho_2$:

$$\begin{aligned} &\text{I)}\ \rho \geqslant \rho_1(\sigma_1, \sigma_2, \varepsilon), \\ &\text{II)}\ \rho_2(\sigma_1, \sigma_2, \varepsilon) \leqslant \rho \leqslant \rho_1(\sigma_1, \sigma_2, \varepsilon), \\ &\text{III)}\ \rho \leqslant \rho_2(\sigma_1, \sigma_2, \varepsilon). \end{aligned} \tag{15}$$

The derivatives $d\rho/d\sigma_1$, $d\rho/d\sigma_2$ are positive in region II and negative in regions I and III. Near the origin of the coordinates we neglect the $\sigma_1\rho^2$ and $\sigma_2\rho^2$ terms and write the solution of (14) in the form [see (A2)]

$$\sigma_1 = \lambda_1\rho, \qquad \sigma_2 = \lambda_2\rho. \tag{16}$$

For the ratio $\lambda = \lambda_1/\lambda_2$ we get three values $\lambda = 0$, $\lambda = \infty$, and $0 < \lambda(\epsilon) < \infty$. The first two give a family of integral curves corresponding to the planes (σ_2, ρ): $\sigma_1 = 0$ and (σ_1, ρ): $\sigma_2 = 0$. A detailed analysis shows that in these planes the family is qualitatively the same as in reference 8 (see Fig. 3). In the case $0 < \lambda(\epsilon) < \infty$ [see (A4)] we have a family of integral curves in the plane which includes the ρ axis and which forms with the (σ_2, ρ) plane an angle θ such that

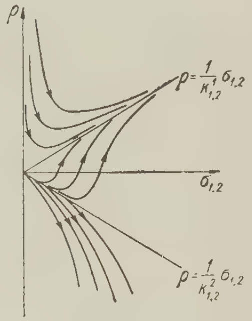

ρ
$\rho = \frac{1}{K^1_{1,2}}\sigma_{1,2}$
$\sigma_{1,2}$
$\rho = \frac{1}{K^2_{1,2}}\sigma_{1,2}$

FIG. 3

$$\tan\theta = \lambda(\varepsilon). \tag{17}$$

It appears that the integral curves in this plane are qualitatively the same as those in the (σ_1, ρ) for (σ_2, ρ) planes but the straight lines (A2) or (A3) should be respectively replaced by those given in (A4).

Points lying in the neighborhood of the origin on these three planes can only move along the integral curves as x goes to infinity and cannot leave these planes. Points somewhat away from the (σ_1, ρ) and (σ_2, ρ) planes will move along curves removed from these planes as x goes to infinity. This means that the (σ_1, ρ) and (σ_2, ρ) planes are not stationary. To clear up the stationary quality of the plane corresponding to $0 < \lambda(\epsilon) < \infty$, we look at the two cases $\epsilon = +1$ and $\epsilon = -1$. In the neighborhood of the origin the quantity $d\sigma_1/d\sigma_2$ does not depend on ρ and is equal to

$$d\sigma_1/d\sigma_2 = (\beta_1^1\sigma_1^2 + \beta_1^2(\varepsilon)\sigma_1\sigma_2)/(\beta_2^1(\varepsilon)\sigma_1\sigma_2 + \beta_2^2\sigma_2^2). \tag{18}$$

Equation (18) determines the lines of intersection of the integral curves of the system (14) with the plane $\rho = \text{const}$. In the $\epsilon = -1$ case they are shown in Fig. 1. We see that the plane forming the angle given by $\tan\theta = \lambda(-1) = 5$ with the (σ_2, ρ) plane is stationary. For the $\epsilon = +1$ case the analogous curves are shown in Fig. 2, from which it follows that the plane given by $\tan\theta = \lambda(+1) = 1$ is not stationary.

To get a fuller family of integral curves we solve (14) and (5) for the case $|\rho| \gg \sigma_1, \sigma_2$. The solution is

$$\rho = h/(1 - hF_2 x),$$

$$\sigma_1 = \sigma_2 = g_1^2 \exp\left[\frac{\varkappa_1}{F_2}\ (\rho - h)\right]$$

$$= g_1^2 \exp\left[h^2 \varkappa_1 x/(1 - hF_2 x)\right]. \tag{19}$$

A. Case $\epsilon = -1$. There exists a surface $\rho = \varphi(\sigma_1, \sigma_2, -1)$, in which the lines (A2) with $k_1^2 < 0$, (A3) with $k_2^2 < 0$, and (A4) with $\lambda_2^2(-1) < 0$ lie. This surface lies under the surface

$$\rho = \rho_2(\sigma_1, \sigma_2, -1), \qquad \varphi(\sigma_1, \sigma_2, -1) \leqslant \rho_2(\sigma_1, \sigma_2, -1).$$

There are two regions of the space $(\rho, \sigma_1, \sigma_2)$:

$$\text{I)}\ \rho \geqslant \varphi(\sigma_1, \sigma_2, -1); \qquad \text{II)}\ \rho \leqslant \varphi(\sigma_1, \sigma_2, -1)$$
$$(\sigma_1, \sigma_2 \geqslant 0). \tag{20}$$

Each point $(\rho, \sigma_1, \sigma_2)$ in region I moves onto the line (A4) with $\lambda_2^1(-1) > 0$, as x goes to ∞. Every point in region II, as x goes to ∞, moves along curves whose asymptotic form is given by formula (19) with $\rho < 0$. Since in this case the solution (A4) with $\lambda_2^1(-1) > 0$ is stationary, it is sufficient to solve Eq. (5) for this line. We get the formulas determining the invariant coupling constants (A4) with $\lambda_2^1(-1) > 0$ and Eq. (9). The functions S and G found with the aid of these formulas have the form (10). We add here the formula for the source

$$\square = \left[1 - \frac{13}{8\pi^2}\, g_2^2 x\right]^{\alpha_\square}, \qquad \alpha_\square > 0. \tag{21}$$

We note that the sources G_i depend on three arguments and that it is therefore possible to have various kinds of ultraviolet asymptotic values; but here the situation is the same as in meson theory: they all coincide. The source $\square$ depends on six arguments [see (2c)]. It seems that in this case the ultraviolet asymptotes do not all coincide and that $\alpha_\square$ depends on the kind of ultraviolet asymptote (for details, see the work of Ginzburg and Shirkov[9]).

B. Case $\epsilon = +1$. There exists a surface $\rho = \varphi(\sigma_1, \sigma_2, +1)$ in which lie the lines (A2) with $k_1^2 < 0$, (A3) with $k_2^2 < 0$, and (A4) with $\lambda_2^2(+1) < 0$. This surface lies under the surface

$$\rho = \rho_2(\sigma_1, \sigma_2, +1) < 0, \qquad \varphi(\sigma_1, \sigma_2, +1) \leqslant \rho_2(\sigma_1, \sigma_2, +1).$$

There are three regions of the space:

$$\begin{array}{ll} \text{I)}\ \rho \geqslant \varphi(\sigma_1, \sigma_2, +1), & \sigma_1 \geqslant \sigma_2 \geqslant 0; \\ \text{II)}\ \rho \geqslant \varphi(\sigma_1, \sigma_2, +1), & 0 \leqslant \sigma_1 \leqslant \sigma_2; \\ \text{III)}\ \rho \leqslant \varphi(\sigma_1, \sigma_2, +1), & \sigma_1, \sigma_2 > 0. \end{array} \tag{22}$$

As x goes to infinity, points in region I, moving along the integral curves, go onto the curves (A5), points in region II go onto curves (A6), and points in region III onto curves (19). In this case there is no stationary solution in the form of a straight line and therefore the source terms and Green's functions behave according to a law different from the one in electrodynamics or in meson theory.

4. CONCLUSION

1. The investigated integral curves in the $(\rho, \sigma_1, \sigma_2)$ space are not closed. This means that there exists for them, just as in electrodynamics and meson theory, a way of going beyond the limits of the weak coupling for increasing momenta. In our view the existence of closed integral curves in the theory considered is scarcely probable: we should be left inside the limits of the weak coupling theory. However, it is still useful to investigate in detail Eqs. (A1) or (5).

2. The behavior of Green's function and of the source terms essentially depends on the relative parity of the baryons. For some kinds of relative baryon parity (7) with $\epsilon = -1$ there exists a stationary solution in the form of a straight line in the space $(\rho, \sigma_1, \sigma_2)$, and then the Green's function and the source terms behave according to the standard law (10), (21).[1-4] For other sources (7) with $\epsilon = +1$ there is no stationary solution in the form of a line in the $(\rho, \sigma_1, \sigma_2)$ space. The connection between the invariant charges is shown by formulas, either (A5) or (A6). Here the Green's functions and the source terms behave entirely differently [see (13)].

3. The extent to which the assumption which we made of weak coupling is valid $(\rho, \sigma_1, \sigma_2 \ll 1)$ will be clear if one succeeds in determining exactly the magnitude of the constant g_i in (1). From the estimates got in references 5 and 6, it evidently follows that $g_i^2/4\pi \sim 1$. For such a value of the constant the poles of the invariant charges (9) and (11) are distributed in the neighborhood, respectively, of $|p| \sim E \sim 2.5$ Bev and $|p| \sim E \sim 9$ Bev.

4. In the investigation of the ultraviolet asymptotes, we should have taken into account the interaction of π mesons with baryons, which could change our results in an essential way. For the present we lay this question aside.

The author expresses his deep thanks to D. V. Shirkov for numerous remarks and for constant interest in the work.

APPENDIX

1. The Lie equations for the ultraviolet asymptotic case.

$$\frac{d\sigma_i}{dx} = \sigma_i \sum_{s=1}^{4} \varkappa_i^s \sigma_s + \varepsilon\varkappa_i^0 [\sigma_1\sigma_2\sigma_3\sigma_4]^{1/2} + \varkappa_1\sigma_i\rho^2 \qquad (i = 1, \ldots, 4),$$

$$\frac{d\rho}{dx} = F_0 [\sigma_1^2 + 3\sigma_1\sigma_2 + 9\sigma_2^2 + \sigma_1\sigma_3$$
$$+ 3\varepsilon [\sigma_1\sigma_2\sigma_3\sigma_4]^{1/2} + 9\sigma_2\sigma_4 + \sigma_3^2 + 3\sigma_3\sigma_4 + 9\sigma_4^2]$$
$$+ F_1 [\sigma_1 + 3\sigma_2 + \sigma_3 + 3\sigma_4]\rho + F_2\rho^2; \qquad \text{(A1)}$$

$$\varkappa_i^s = \frac{1}{32\pi^2}\begin{vmatrix} 3 & 3 & 2 & 12 \\ 1 & 5 & 4 & 2 \\ 2 & 12 & 3 & 3 \\ 4 & 2 & 1 & 5 \end{vmatrix};$$

$$\varkappa_1^0 = \varkappa_3^0 = -3/8\pi^2, \qquad \varkappa_2^0 = \varkappa_4^0 = -1/8\pi^2;$$

$$F_0 = 2F_1 = -2F_2/3 = 1/4\pi^2, \qquad \varkappa_1 > 0.$$

2. We look for the solution of (14) in the neighborhood of the origin in the form (16). For $\lambda = \lambda_1/\lambda_2$ we get

a) $\lambda = \infty, \qquad \sigma_1 = k_{1,2}^1\rho,$

$$k_{1,2}^1 = -\frac{2F_1 - \beta_1^1}{6F_0} \pm \left[\frac{(2F_1 - \beta_1^1)^2}{(6F_0)^2} - \frac{F_2}{3F_0}\right]^{1/2}; \qquad \text{(A2)}$$

b) $\lambda = 0, \ \sigma_2 = k_{1,2}^2\rho,$

$$k_{1,2}^2 = -\frac{6F_1 - \beta_2^2}{54F_0} \pm \left[\frac{(6F_1 - \beta_2^2)^2}{(54F_0)^2} - \frac{F^2}{27F_0}\right]^{1/2}; \qquad \text{(A3)}$$

c) $\sigma_1 = \lambda(\varepsilon), \qquad \lambda_2^{1,2}(\varepsilon)\rho, \qquad \sigma_2 = \lambda_2^{1,2}(\varepsilon)\rho, \quad \lambda(+1) = 1,$ $\lambda(-1) = 5,$

$$\lambda_2^{1,2}(+1) = \frac{(4F_1 - 1/8\pi^2)}{3F_0\cdot 13} \pm \left[\left(\frac{4F_1 - 1/8\pi^2}{3F_0\cdot 13}\right)^2 - \frac{F_2}{3F_0\cdot 13}\right]^{1/2},$$

$$\lambda_2^{1,2}(-1) = -\frac{[8F_1 - 13/16\pi^2]}{3F_0\cdot 39}$$
$$\pm \left[\left(\frac{8F_1 - 13/16\pi^2}{3F_0\cdot 39}\right)^2 - \frac{F_2}{3F_0\cdot 39}\right]^{1/2}. \qquad \text{(A4)}$$

3. The asymptotic solutions of systems (5) and (13). For the case $|\rho| \sim \sigma_1 \gg \sigma_2$

$$\sigma_1 = \sigma_2^5 = g_1^2\left[1 - \frac{5}{32\pi^2} g_1^2 x\right]^{-1},$$

$$[\rho/\sigma_1 - a_1]^{A/\alpha_2} [\rho/\sigma_1 - a_2]^{-A/\alpha_2} = c\sigma_1, \qquad \text{(A5)}$$

where

$$c = g_1^{-2} [h/g_1^2 - a_1]^{A/\alpha_2} [h/g_2^2 - a_2]^{-A/\alpha_2},$$

$$a_{1,2} = -\alpha_1/2\alpha_2 \pm [(\alpha_1/2\alpha_2)^2 - \alpha_0/\alpha_2]^{1/2},$$

$$A = [(\alpha_1/\alpha_2)^2 - 4\alpha_0/\alpha_2]^{1/2}, \qquad \alpha_0 = 3F_0/\beta_1^1,$$

$$\alpha_1 = 2F_1/\beta_1^1 - 1, \qquad \alpha_2 = F_2/\beta_1^1.$$

For the case $|\rho| \sim \sigma_2 \gg \sigma_1$

$$\sigma_1 = \sigma_2^{8/7}, \qquad \sigma_2 = g_2^2\left[1 - \frac{7}{32\pi^2} g_2^2 x\right]^{-1},$$

$$[\rho/\sigma_2 - a_1']^{A'/\alpha_2'} [\rho/\sigma_2 - a_2']^{-A'/\alpha_2'} = c'\sigma_2, \qquad \text{(A6)}$$

where A', c', $a_{1,2}'$ have the same structure as in the preceding case, but one must make the substitutions

$$\alpha_0 \to \alpha_0' = 27F_0/\beta_2^2, \qquad \alpha_1 \to \alpha_1' = 6F_1/\beta_2^2 - 1,$$
$$\alpha_2 \to \alpha_2' = F_2/\beta_2^2, \qquad g_1 \to g_2.$$

---

[1] Landau, Abrikosov, and Khalatnikov, Dokl. Akad. Nauk (U.S.S.R.) **95**, 497, 773, 1177 (1954); **96**, 262 (1954). L. D. Landau, in Niels Bohr and the Development of Physics, London (1955), Russian translation, IIL, 1958.

[2] Abrikosov, Galanin, and Khalatnikov, Dokl. Akad. Nauk (U.S.S.R.) **97**, 793 (1954).

[3] N. N. Bogolyubov and D. V. Shirkov, Nuovo cimento **3**, 845 (1956).

[4] N. N. Bogolyubov and D. V. Shirkov, Введение в теорию квантованных полей (Introduction to the Quantum Theory of Fields), Chapter 8, Gostekhizdat (1957).

[5] M. Gell-Mann, Phys. Rev. **106**, 1296 (1957).

[6] P. T. Matthews and A. Salam, Phys. Rev. **110**, 569 (1958).

[7] I. C. Polkinghorne, Nuovo cimento **4**, 864 (1956).

[8] I. F. Ginzburg, Dokl. Akad. Nauk SSSR **110**, 535 (1956), Soviet Phys. "Doklady" **1**, 560 (1957).

[9] I. F. Ginzburg and D. V. Shirkov, Докл. Высшей школы, серия физ.-мат., (Trans. of Higher Schools, Phys-Math Ser.) No. 2 (1958); Nuovo cimento **8**, 773 (1958).

Translated by W. Ramsay
15

π^--p INTERACTION AT 1.4 Bev

V. I. RUS' KIN

Institute for Nuclear Physics, Academy of Sciences, Kazakh S.S.R.

Submitted to JETP editor January 9, 1959; resubmitted March 31, 1959

J. Exptl. Theoret. Phys. (U.S.S.R.) **37**, 105-108 (July, 1959)

The statistical theory of Fermi, taking into account the resonance interaction between a pion and a nucleon as well as the resonance interaction between two π mesons, is used to explain the experimental results of the π-p interaction at 1.4 Bev. The results obtained are compared with the corresponding results of the "isobaric" model of Sternheimer and Lindenbaum.[1]

AT the present time, there is a large amount of experimental data on the π^--p interaction in the energy range 1.0 to 1.4 Bev.[2-4] A theoretical interpretation of this interaction is possible with the help of Fermi's statistical theory, but, as pointed out by Sternheimer and Lindenbaum,[1] the predictions of Fermi's original theory deviate considerably from experiment. These authors therefore proposed the "isobaric" model, in which it is assumed that the π^--p interaction takes place via an intermediate "isobaric" state. It was shown that the results obtained using this model, within the limit of statistical errors, are in accordance with the experimental results near 1.0 Bev. However, for incident π mesons with energy close to 1.4 Bev, there is a noticeable difference from experimental results. In the present work, we show that the π^--p interaction in this domain can be interpreted with the help of the statistical theory of Fermi, taking into account the resonance interaction of π mesons with nucleons and the resonance interaction between two π mesons.

The resonance interaction between particles, within the framework of Fermi's statistical theory, was considered in accordance with the method proposed by Belen'kiĭ.[5] The resonance interaction of π mesons with nucleons was taken into account using the isobar — "quasi-particle" — with effective mass 1.32,* isotopic spin $T = 3/2$ and intrinsic spin $S = 3/2$ — which decays into a π meson and nucleon.[6] (In the following, this isobar is denoted by the symbol N′.) The resonance interaction between two π mesons was accounted for with the help of a "quasi-particle" with effective mass $\mu = 0.47$, isotopic spin $T = 0$ and intrinsic spin $S = 0$, which decays quickly into two π mesons (this "quasi-particle" is denoted by the symbol Π and it is called the "Π-particle").[7]

The statistical weights of the possible types of reactions in π^--p collisions at 1.4 Bev was calculated according to the formula given in Belen'kiĭ et al.,[6] are as follows: (N2 — process taking place with the formation of a nucleon and two π mesons; N′1 — process proceeding with the formation of an isobar and one π meson, which we can consider to be free and different from the π meson formed on the decay of the isobar; NΠ — process, in which a nucleon and a Π particle are formed, etc.).

$N1$	$N2$	$N'1$	$N\Pi$	$N3$	$N'2$	$N\Pi 1$	$N'\Pi$	$N4$	Strange particles
12	18	18	7	5	8	8	2	0	22

Hence it is seen that the basic processes, determining the reactions (n + −) and (p − 0), are the two-particle processes NΠ and N′1. Moreover, the kinematic characteristics of each basic two-particle process is independent of the matrix element H_{if}. Therefore, the basic requirement of Fermi's statistical theory (independence of H_{if}) is known to be fulfilled for these processes.

Using the charge distribution in the final state of the π^--p collision mentioned in reference 7, we obtained the distribution of charge of the products according to the number of prongs:

two-prong collision	88 (94)
four-prong collision	12 (6),

It agrees, to within the statistical errors, with the experimental data (the numbers inside the parenthesis), obtained by Eisberg et al.[2] The statistical weight of the "strange" particles, although somewhat less than calculated according to the statistical theory with only isobars taken into account, is overestimated. Apparently, accounting for resonance interactions cannot reduce the statistical weight of "strange" particles down to the experimental value, making it necessary to introduce into the statistical theory supplementary assumptions regarding processes involving "strange" particle production (see, for example, reference 8).

---

*We always set $\hbar = c = M_{nuc} = 1$.

In calculating the momentum distributions it is assumed that the isobar and the Π particle decay isotropically in their rest frames. Then, in the decay of the isobar (Π particle) the momentum spectrum of the meson is given by[6]

$$N(p)\,dp = p\,dp/2p_c\gamma V\sqrt{p^2+\mu^2},$$

$$\gamma|p_c - VE_c| \leqslant p \leqslant \gamma|p_c + VE_c|,$$

$$\gamma = (1-V^2)^{-1/2};\qquad E_c = (p_c^2+\mu^2)^{1/2},$$

where p_c is the meson momentum at the decay of the isobar (Π particle) at rest; V is the velocity of the isobar (Π particle) in the center-of-mass frame of the meson plus nucleon. The momentum distributions of the mesons and nucleons in the reactions (n+−) and (p−0) in the center-of-mass system is presented in Figs. 1 and 2. The momentum distribution of the nucleon at impinging pion energies of 1.4 Bev is well explained by our calculations as well as by calculations using the "isobaric" model,[1] while at 1.0 Bev it has in the 300 − 350 Mev domain,[3] a characteristic maximum which cannot be explained by the "isobaric" model, see Fig. 1. In our case, there exists a uniquely possible process, which can bring out a similar maximum, the NΠ process. However, calculations give this maximum shifted by 100 Mev towards the higher momenta (see Fig. 1). Consequently, to make the theoretically-obtained maximum agree with experiment, it is necessary to increase the mass of the Π particle to 0.69.* It is necessary to note here that because of the very crude way of determining the momentum of the nucleon in the paper of Walker et al.,[3] the errors in the mass of the Π particle determined by this method, can turn out to be very considerable. Therefore, in spite of some quantitative disagreement, the effect can be considered as indicating the existence of resonance π-π interaction.

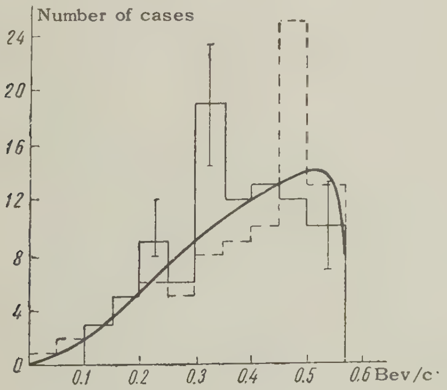

FIG. 1. Momentum distribution of nucleons in the reactions (n + −) and (p − 0) at 1.0 Bev. The continuous histogram is from experiment;[3] the dotted line represents the calculations of the statistical theory, taking resonance interactions into account; the continuous curve was calculated using the "isobar" model.[1]

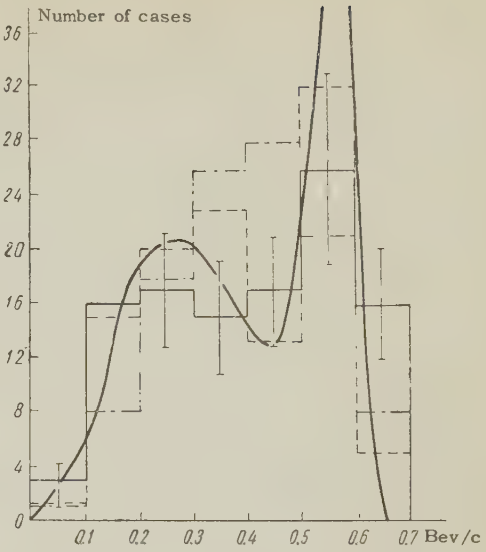

FIG. 2. Momentum distribution of all π-mesons in the reactions (n + −) and (p − 0) at 1.4 Bev. Continuous histogram – experiment,[2] dotted line – calculations using the statistical theory, taking resonance interactions into account (isobar and resonance $\pi-\pi$ interaction), dash-dot line – calculated according to the statistical theory, taking only the isobar into account.[6] The continuous curve – calculated with the "isobaric" model.[1]

Figure 2 shows the momentum distribution of the π mesons in the reactions (n+−) and (p−0), in the center of mass system. The theoretical histograms are normalized to the number observed in the experiment. The large experimental error in determining the momentum of the π meson does not allow a unique comparison; nevertheless the character of the experimental results can be explained.

The maximum in the high-momentum domain appears to be due to the process N′1, while the maximum in the domain of low momenta appears to be due to π mesons from the decay of the isobar in this same process. It is natural that the patterns observed and calculated on the "isobaric" model of Sternheimer and Lindenbaum, which takes into account only the process N′1, are similar. However, the maximum in the region of high momenta appears strongly overestimated and does not lie within experimental error.

---

*An analogous idea was expressed by Goto.[9]

In conclusion, it should be noted that the statistical theory, in which only the isobar is accounted for, gives a worse pion momentum distribution than ours, compared with experiment. Thus, a statistical theory that takes into account not only the isobar but also the resonance interaction of two pions is not contradicted by experimental data on the π^--p interaction at incident pion energies of 1.4 Bev, while the results obtained in this domain using the "isobaric" model begin to disagree with experiment.

The author expresses his sincere thanks to Professor Zh. S. Takibaev for his guidance in this work.

---

[1] R. Sternheimer and S. Lindenbaum, Phys. Rev. **109**, 1723 (1958).

[2] Eisberg, Fowler, Lea, Shephard, Shutt, Thorndike, and Whittemore, Phys. Rev. **97**, 797 (1955).

[3] Walker, Hushfar, and Shephard, Phys. Rev. **104**, 526 (1956).

[4] Cool, Piccioni, and Clark, Phys. Rev. **103**, 1082 (1956).

[5] S. Z. Belen'kiĭ, J. Exptl. Theoret. Phys. (U.S.S.R.) **32**, 1171 (1957), Soviet Phys. JETP **5**, 952 (1957).

[6] Belen'kiĭ, Maksimenko, Nikishov, and Rozental', Usp. Fiz. Nauk. **62**, 1 (1957).

[7] V. I. Rus'kin, J. Exptl. Theoret. Phys. (U.S.S.R.) **36**, 164 (1959), Soviet Phys. JETP **9**, 113 (1959).

[8] Barashenkov, Barbashev, and Bubelev, Nuovo cimento **7**, Suppl. **7**, 117 (1958); V. S. Barashenkov, J. Exptl. Theoret. Phys. (U.S.S.R.) **34**, 1016 (1958). Soviet Phys. JETP **7**, 701 (1958).

[9] T. Goto, Nuovo cimento **8**, 625 (1958).

Translated by Kenneth Smith
16

SOVIET PHYSICS JETP VOLUME 37(10), NUMBER 1 JANUARY, 1960

THEORY OF SPIN-LATTICE QUADRUPOLE RELAXATION IN LIQUID SOLUTIONS OF DIAMAGNETIC SALTS

K. A. VALIEV

Kazan' State Pedagogical Institute

Submitted to JETP editor January 10, 1959

J. Exptl. Theoret. Phys. (U.S.S.R.) **37**, 109-117 (July, 1959)

Quadrupole spin-lattice relaxation of nuclear spins in liquid solutions of diamagnetic salts is considered theoretically. The calculations are performed under the assumption that stable complexes are formed around ions, these complexes consisting of molecules of the solvent or of molecules of the solvent and anions (or cations) simultaneously. It is found that lattice relaxation of the nuclear spin of the central ion is due to normal vibrations of the complex if the addends of the complex are identical particles, and by diffuse rotation if the addends are different particles. The calculated magnetic resonance line widths agree with the experimental data for aqueous solutions of Al^{3+} and Ga^{3+} salts. The resonance line widths of weakly hydrated ions (Na^+, Br^-, I^-) are related to the times of stable existence of the corresponding complexes.

1. MECHANISM OF QUADRUPOLE SPIN-LATTICE RELAXATION IN DIAMAGNETIC IONIC SOLUTIONS

If the nucleus of a diamagnetic atom (or ion) possesses an electric quadrupole moment, energy is exchanged between the nuclear spin and the lattice (spin-lattice relaxation) as thermal motion causes changes in the quadrupole moment energy. Van Kranendonk[1] has calculated the quadrupole relaxation time of nuclear spins in crystals and Masuda[2] has performed a similar calculation for molecular liquids. In the present paper the quadrupole relaxation time is calculated for ionic liquid solutions of diamagnetic salts.

In ionic liquid solutions the immediate neighborhood of a positive (or negative) ion most frequently consists of six particles surrounding the ion in the form of an octahedron; these are molecules of the solvent or anions (or cations). We assume that a stable ionic complex endures longer than the spin-lattice relaxation time of the ionic nucleus. It is then evident that in studying the spin-lattice relaxation of the central ion we must first consider the thermal motions of members of the complex. The thermal motion of the complex consists of internal vibrations and diffuse rotation, both of which can result in relaxation of the nuclear spin. Diffuse rotation of the complex is found to play the principal part in quadrupole spin relaxation in mixed complexes consisting of different addends.* On the other hand, in complexes consisting of identical addends quadrupole relation results from the internal thermal vibrations of the complex.

Let us consider an ion located at the center of a mixed complex consisting of water molecules and anions. The strong inhomogeneous electric field at the center of the mixed complex will act on the nuclear quadrupole moment to induce quadrupole splitting of the ion's spin levels superposed on the Zeeman splitting. The magnitude of the quadrupole splitting depends on the orientation of the axes of the complex with respect to the external magnetic field; therefore Brownian rotation of the complex will change the splitting in a random fashion, which results in an energy exchange between the spin and thermal motion of the lattice.

When the addends of the complex are identical the electric field at the center of the octahedron will possess cubic symmetry and will not induce splitting of the nuclear spin levels. Therefore rotation of a complex with identical addends cannot result in spin relaxation. In this case we must consider the internal vibrations of the complex, as a result of which the symmetry of the electric field at the center of the octahedron is disturbed in a time-dependent manner. The splitting of the spin levels is consequently time-dependent, and spin relaxation results.

---

*An addend is a diamagnetic particle in the first coordination sphere of the ion.

In mixed complexes spin relaxation is obviously produced by both the rotation and internal vibrations of the complex, but we shall see below that the vibrations play a subordinate part.

In real solutions mixed and unmixed complexes exist simultaneously. Thus Connick and Poulson[3] have shown that aqueous solutions of NaF and $Al(NO_3)_3$ contain approximately identical numbers of the complexes $Al(H_2O)_6^{3+}$, $Al(H_2O)_5F^{2+}$ and $Al(H_2O)_4F_2^+$. It is noteworthy, however, that the intensity of magnetic resonance absorption in Al^{27} nuclei is proportional to the number of hydrated $Al(H_2O)_6^{3+}$ complexes. It is evident that Al^{27} quadrupole relaxation in mixed complexes is very rapid and that absorption by these nuclei is not observed because of the extremely large line width. This has been confirmed by our calculations for Al^{27} and a number of other ionic nuclei.

2. SPIN-LATTICE INTERACTION ENERGY OF NUCLEI HAVING AN ELECTRIC QUADRUPOLE MOMENT

The quadrupole part of the energy of any charge system (such as an atomic nucleus) in an inhomogeneous electric field induced by external charges is the scalar product of two symmetric second-order tensors — the tensor of the nuclear quadrupole moment, D_{ik}, and the tensor of the electric field gradient at the nucleus, $(\nabla E)^{ik} = \partial^2\varphi/\partial x_i \partial x_k$:[4]

$$H = \sum_{i,k} \frac{1}{6} D_{ik} \partial^2 \varphi / \partial x_i \partial x_k. \tag{1}$$

In the representation in which I^2 and I are diagonal the five independent components of the nuclear quadrupole moment tensor D_{ik} can be given in terms of the nuclear spin projection:

$$D_0 = \frac{1}{2} C (3I_z^2 - I(I+1)), \qquad D_{\pm 1} = -\frac{3}{2} C \{I_z I_\pm\},$$

$$D_{\pm 2} = 3CI_\pm^2, \qquad I_\pm = I_x \mp iI_y, \qquad \{I_i I_k\} = I_i I_k - I_k I_i,$$

$$C = eQ / I(2I-1), \tag{2}$$

where Q is the nuclear quadrupole moment.

With the coordinate origin at the center of mass of the given nucleus, $\mathbf{r}_A(x_A, y_A, z_A)$ will denote the radius vector of an outside charge e_A. The independent components of the tensor $(\nabla E)^{ik}$ are then

$$(\nabla E)^0 = \sum_A 3e_A r_A^{-5} (3z_A^2 - r_A^2),$$

$$(\nabla E)^{\pm 1} = \sum_A 3e_A r_A^{-5} z_A (x_A \pm iy_A)$$

$$(\nabla E)^{\pm 2} = \sum_A \frac{3}{4} e_A r_A^{-5} (x_A \pm iy_A)^2. \tag{3}$$

We now denote by $\mathbf{s}_A(X_A, Y_A, Z_A)$ the change of distance between the given nucleus and the charge e_A which results from internal thermal vibrations of the complex. $\mathbf{s}_A$ will obviously be small compared with the equilibrium distance $\mathbf{r}_A^0$ between the nucleus and charge; the tensor components $(\nabla E)^{ik}$ may therefore be expanded in powers of the projections of the $\mathbf{s}_A$, and for our purposes the linear term is sufficient. The form of the expansion is simple when the cubic axes of symmetry of the complex are the coordinate axes x, y, z; the equilibrium separation $\mathbf{r}_A^0$ is then represented by

$$r_1^0(a, 0, 0), \quad r_2^0(0, a, 0), \quad r_3^0(0, 0, a),$$

$$r_4^0(-a, 0, 0), \quad r_5^0(0, -a, 0), \quad r_6^0(0, 0, -a).$$

Furthermore, in an unmixed complex all addends are identical and possess identical effective charges $e_A = e'$, in which case we also have the identities

$$(\nabla E)^0_{s_A=0} = (\nabla E)^{\pm 1}_{s_A=0} = (\nabla E)^{\pm 2}_{s_A=0} = 0.$$

It follows easily from the foregoing that

$$(\nabla E)^0 = 18\sqrt{3}(1+\gamma) e' a^{-4} Q_3,$$

$$(\nabla E)^{\pm 1} = 6(1+\gamma) e' a^{-4} (Q_5 \pm iQ_6),$$

$$(\nabla E)^{\pm 2} = \frac{3}{2}(1+\gamma) e' a^{-4} (-3Q_2 \pm 2iQ_4). \tag{4}$$

Here Q_i are the orthogonal normal vibrational coordinates of the complex which were first introduced by Yost et al:[5]

$$Q_2 = (X_1 - X_4 - Y_2 + Y_5) / 2,$$

$$Q_3 = \left[\frac{1}{2}(X_1 - X_4 + Y_2 - Y_5) + (Z_6 - Z_3)\right] / \sqrt{3},$$

$$Q_4 = (X_2 - X_5 + Y_1 - Y_4) / 2,$$

$$Q_5 = (Z_1 - Z_4 + X_3 - X_6) / 2,$$

$$Q_6 = (Y_3 - Y_6 + Z_2 - Z_5) / 2. \tag{5}$$

The factor $(1+\gamma)$ in (4) takes antishielding into account; the inhomogeneous field of the outer particles distorts the electron shell of the central ion, creating an additional inhomogeneous field at the nucleus which is similar to the field of the outer particles. This effect must obviously be taken into account in calculating the relaxation time of nuclear spins. Antishielding factors γ have been calculated theoretically for a majority of ions possessing a nuclear quadrupole moment.[6]

The part of the energy of the quadrupole moment which is dependent on the lattice coordinates and on time may therefore be represented by the sum $\mathcal{H}' = \sum_{i=-2}^{2} \mathcal{H}'_i$, where

$$\mathcal{H}'_0 = 3\sqrt{3}\,\Lambda\,(3I_z^2 - I(I+1))\,Q_3,$$

$$\mathcal{H}'_{\pm} = \tfrac{3}{2}\,\Lambda\,\{I_zI_{\pm}\}\,(Q_5 \pm iQ_6),$$

$$\mathcal{H}'_{\pm 2} = \tfrac{3}{4}\,\Lambda I_{\pm}^2\,(-3Q_2 \pm 2iQ_4),$$

$$\Lambda = ee'(1+\gamma)\,Qa^{-4}/I(2I-1). \qquad (6)$$

In liquids only nuclear magnetic resonance can be observed since the quadrupole interaction of the nucleus varies randomly because of thermal motion and cannot induce constant splitting of the nuclear spin levels. The integrals of motion of a spin in a strong magnetic field are the values of I^2 and of the projection $I_{z'}$ in the external field direction. Therefore the spin variables in the right member of (6) must be transformed to the laboratory coordinate system $x'y'z'$ with z' in the external magnetic field direction. If θ and φ are the polar angles of the z' laboratory axis in the xyz coordinate system of the ionic complex, after a simple transformation of the components of I we obtain

$$I_{\pm}^2 = e^{\mp 2i\varphi}\,[I_{x'}^2\cos^2\theta - I_{y'}^2 + \{I_{x'}I_{z'}\}\sin\theta\cos\theta \mp i\,\{I_{x'}I_{y'}\}\cos\theta$$
$$\mp i\,\{I_{z'}I_{y'}\}\sin\theta + I_{z'}^2\sin^2\theta],$$

$$\{I_zI_{\pm}\} = e^{\mp i\varphi}\,[(I_{z'}^2 - I_{x'}^2)\sin 2\theta \mp i\,\{I_{x'}I_{y'}\}\sin\theta$$
$$+ \{I_{x'}I_{z'}\}\cos 2\theta \mp i\,\{I_{z'}I_{y'}\}\cos\theta],$$

$$I_z^2 = I_{x'}^2\sin^2\theta + I_{z'}^2\cos^2\theta - \{I_{x'}I_{y'}\}\sin\theta\cos\theta. \qquad (7)$$

The primes in (7) will hereinafter be omitted

3. RELAXATION TRANSITION PROBABILITIES

The perturbation (6) contains both spin variables and lattice variables of the system; the latter are the normal internal vibrational coordinates Q_i of the complex. The remaining lattice coordinates, which do not interact directly with the spin variables, interact with the Q_i coordinates and ultimately determine the character of their time dependence. Thus in liquids the Q_i interact with the random Brownian motion of particles surrounding the complex; this determines the random, fluctuating temporal variation of Q_i.[7]

The probability that the perturbation $\mathcal{H}'(t)$ induces a transition of the system from the state l to the state k in one second will be calculated by means of the familiar perturbation formula

$$w_{lk} = \frac{1}{t\hbar^2}\left|\int_0^t \mathcal{H}'_{lk}(t')\exp(-i\omega_{lk}t')\,dt'\right|^2, \qquad (8)$$

where $\omega_{lk} = (E_l - E_k)/\hbar$. When, as occurs in our problem, the matrix element $\mathcal{H}'_{lk}(t)$ is a random function of time, (8) can be transformed by introducing the correlation function[8]

$$G(\tau) = \overline{\mathcal{H}'_{lk}(t')\,\mathcal{H}'_{lk}(t'-\tau)}.$$

Then

$$w_{lk} = \hbar^{-2}\int_{-\infty}^{+\infty} G(\tau)\exp(-i\omega_{lk}\tau)\,d\tau. \qquad (9)$$

Denoting the characteristic correlation time by τ_c as usual, we represent the correlation function as decreasing exponentially:

$$G(\tau) = G(0)\exp(-|\tau|/\tau_c). \qquad (10)$$

The transition probability is then given by

$$w_{lk} = \hbar^{-2}\,\overline{|\mathcal{H}'_{lk}|^2}\,2\tau_c/(1+\omega_{lk}^2\tau_c^2). \qquad (11)$$

The bar denotes averaging over all possible values of the coordinates Q_i, θ, and φ. The time τ_c in (10) and (11) characterizes the damping of vibrations of Q_i. Al'tshuler and the present author[7] have shown that $\tau_c \sim 1/\gamma$, where γ is the vibrational line width in the optical spectra of liquid ions; τ_c is of the order 10^{-12} sec. The temperature variation of τ_c obeys a $T^{-1/2}$ law approximately; this reflects an increase in oscillator damping resulting from a temperature-associated increase in the number of collisions between the complex and neighboring Brownian particles.

We shall now calculate the coefficients in (11). The matrix element $\mathcal{H}'_{m,m-1}$ corresponding to the relaxation transition $m \rightarrow m-1$ is

$$\mathcal{H}'_{m,\,m-1} = \Lambda\,\{I_xI_z\}_{m,\,m-1}\,[Q_3(-9\sqrt{3}\sin\theta\cos\theta)$$
$$+ \tfrac{3}{2}(Q_5 + iQ_6)\,e^{-i\varphi}(\cos 2\theta - \cos\theta)$$
$$+ \tfrac{3}{2}(Q_5 - iQ_6)\,e^{i\varphi}(\cos 2\theta + \cos\theta)$$
$$- \tfrac{3}{4}(-3Q_2 - 2iQ_4)\,e^{-2i\varphi}\sin\theta(\cos\theta - 1)$$
$$+ \tfrac{3}{4}(-3Q_2 + 2iQ_4)\,e^{2i\varphi}\sin\theta(1 + \cos\theta)]. \qquad (12)$$

In averaging the square of this quantity the orthogonality of the Q_i coordinates must be taken into account. It is not actually possible to establish the differences between the normal frequencies ω_{0i} and masses m_i of individual Q_i oscillators; we therefore assume the following identical statistical mean square amplitude for all Q_i oscillators:[9]

$$\overline{Q_i^2} = \overline{Q^2} = (\hbar/2m\omega_0)\coth(\hbar\omega_0/2kT), \qquad (13)$$

where m and ω_0 are mean values, with m close to the mass of the entire complex. The normal vibrational frequencies ω_0 of octahedral complexes of transition group ions in liquids lie in the range[10] $(4-16)\times 10^{13}\ \text{sec}^{-1}$.

The result obtained by averaging is

$$\overline{|H'_{m,\,m-1}|^2} = (103/2)\,|\{I_xI_z\}_{m,\,m-1}|^2\,\Lambda^2\overline{Q^2}. \tag{14}$$

We obtain similarly:

$$\begin{aligned}\mathcal{H}'_{m,\,m-2} = \Lambda\,(I_x^2)_{m,\,m-2}\,[&Q_3\cdot 9\sqrt{3}\sin^2\theta\\ &-3\,(Q_5+iQ_6)\,e^{-i\varphi}\sin\theta\,(1+\cos\theta)\\ &+3\,(Q_5-iQ_6)\,e^{i\varphi}\sin\theta\,(1-\cos\theta)\\ &+{}^3/_4\,(-3Q_2+2iQ_4)\,e^{-2i\varphi}\,(1-\cos\theta)^2\\ &-{}^3/_4\,(3Q_2+2iQ_4)\,e^{2i\varphi}\,(1+\cos\theta)^2].\end{aligned} \tag{15}$$

$$\overline{|\mathcal{H}'_{m,\,m-2}|^2} = (1023/5)\,|(I_x^2)_{m,\,m-2}|^2\,\Lambda^2\overline{Q^2}. \tag{16}$$

Nonvanishing transition probabilities subject to the condition $\omega_{lk}^2\tau_c^2 \ll 1$ are

$$\begin{aligned}I={}^3/_2:\quad & w\,({}^3/_2,{}^1/_2) = w\,(-{}^1/_2,-{}^3/_2) = 309U,\\ & w\,({}^3/_2,-{}^1/_2) = w\,({}^1/_2,-{}^3/_2) = (3069/10)\,U.\end{aligned} \tag{17}$$

$$\begin{aligned}I={}^5/_2:\quad & w\,({}^5/_2,{}^3/_2) = w\,(-{}^3/_2,-{}^5/_2) = 2060U,\\ & w\,({}^3/_2,{}^1/_2) = w\,(-{}^1/_2,-{}^3/_2) = 824U,\\ & w\,({}^5/_2,{}^1/_2) = w\,(-{}^1/_2,-{}^5/_2) = 1023U,\\ & w\,({}^3/_2,-{}^1/_2) = w\,({}^1/_2,-{}^3/_2) = 4{,}5\cdot 1023U,\end{aligned} \tag{18}$$

where $U = \hbar^{-2}\Lambda^2\overline{Q}^2\tau_c$.

4. CALCULATION OF THE TIME T_1 AND OF THE LINE WIDTH

The table contains experimental data on relaxation times or magnetic resonance line widths for nuclei with quadrupole moments in aqueous ionic solutions. A resonance line whose width is determined by the spin-lattice interaction possesses Lorentz shape and width $\Delta\nu = 1/\pi T_1$.[11] In order to estimate the line width we calculate the time T_1, using the transition probabilities (17) and (18).

The spin-lattice relaxation time T_1 is obtained from the relation $T_1^{-1} = \alpha/C$, where α is the coefficient of thermal conductivity between the spin-system and the lattice, and C is the specific heat of the spin-system. Substituting the known formulas for α and C, we obtain[12]

$$T_1^{-1} = (2I+1)\sum_{l>k} w_{lk}\,(E_l-E_k)^2 \Big/ \sum_{l>k}(E_l-E_k)^2. \tag{19}$$

This equation is valid when $E_l - E_k \ll kT$, which is always fulfilled in our problem. By means of (17), (18), and (19) we obtain for spins $^5/_2$ and $^3/_2$, respectively:

$$T_1^{-1} = \frac{20312}{7}\left[\frac{ee'\,(1+\gamma)\,Q}{I\,(2I-1)\,a^4}\right]^2\overline{Q^2}\,h^{-2}\tau_c, \tag{20}$$

$$T_1^{-1} = \frac{15336}{25}\left[\frac{ee'\,(1+\gamma)\,Q}{I\,(2I-1)\,a^4}\right]^2\overline{Q^2}\,h^{-2}\tau_c. \tag{21}$$

We now proceed to evaluate the parameters in (20) and (21). These formulas were derived on the basis of a model in which the water molecule was regarded as a point charge; e′ and a are the effective charge of a dipolar water molecule and the effective distance between e′ and the nucleus of the central ion. The effective negative charge of the oxygen atom by which a water molecule is joined to the positive ion at the center of the complex is 0.66 e, judging from the dipole moment of water. The influence of the positive charges borne by the two hydrogen atoms may be neglected because the relaxation time is very strongly dependent on distance: $T_1 \backsim a^8$. It is clear from this relation that relaxation depends principally on the charge in the part of the oxygen atom electron shell which is closest to the central ion. The effective charge of the oxygen ion is displaced to the part of the electron shell closest to the central ion because of electric polarization induced by this positively charged central ion. Such polarization is of considerable magnitude because oxygen ions are highly polarizable ($\alpha = 3.88 \times 10^{-24}$ cm^3).[13] We therefore assume that the effective charge of the oxygen ion is not located on the oxygen nucleus but at a point where the field gradient falls off doubly compared with the gradient of the charges in the immediate vicinity of the central ion. Under this condition the distance a becomes $2^{1/3}r_u = 1.26\,r_u$ where r_u is the crystalline radius of the central ion.

The correlation time τ_c is taken to be 10^{-12} sec; T = 300°K. The values of I and Q given below were taken from reference 14, those of γ from reference 6 and those of r_u from reference 15. The following results were calculated:

Al^{27}: $I = {}^5/_2$, Q = 0.156 barn, $1+\gamma = 3.59$, r_u = 0.5 A. The complex $Al(H_2O)_6^{3+}$, because of the large charge of its central ion, is highly stable with a high natural frequency. Assuming $\omega_0 = 8 \times 10^{13}$ sec^{-1}, we have $T_1 = 1.22 \times 10^{-4}$ sec, $\Delta\nu = 2.6$ kcs.

Ga^{69}: $I = {}^3/_2$, Q = 0.2318 barn, $r_u = 0.62$ A, $1+\gamma = 9.75$. Assuming $\omega_0 = 8 \times 10^{13}$ sec^{-1}, we

Salts in aqueous solution	Ions	Experimental line width, kcs	Salts in aqueous solution	Ions	Experimental line width, kcs
$AlCl_3$ $Al_2(SO_4)_3$	$(Al^{27})^{3+}$	5 [16]	NaCl	$(Na^{23})^+$	⩽1 [18]
$GaCl_3$	$(Ga^{69})^{3+}$	7 [17]	LiBr NaBr	Br^-	10 [19]
$GaCl_3$	$(Ga^{71})^{3+}$	3 [17]	NaI	$(I^{127})^-$	14 [17]

have $T_1 = 10^{-4}$ sec, $\Delta\nu = 3$ kcs.

Ga^{71}: $I = 3/2$, $Q = 0.1461$ barn, $T_1 = 2.6 \times 10^{-4}$ sec, $\Delta\nu = 1.2$ kcs.

Na^{23}: $I = 3/2$, $Q = 0.1$ barn, $r_u = 0.95$ A, $1 + \gamma = 5.1$. The ion Na^+ is known to form a very weak solvate. The stability of a solvate complex determines its bond energies and its normal vibrational frequency. Assuming $\omega_0 = 4 \times 10^{13}$ sec^{-1}, we have $T_1 = 0.01$ sec, $\Delta\nu = 30$ kcs.

Spin relaxation of negative ions will now be calculated using the same model that gave T_1 for positive ions. The following results are obtained for I^- and Br^-:

I^{127}: $I = 5/2$, $Q = 0.7$ barn, $r_u = 2.16$ A, $1 + \gamma = 179.75$. Assuming $\omega_0 = 4 \times 10^{13}$ sec^{-1}, we have $T_1^{-1} = 2.6 \times 10^3$ sec^{-1}, $\Delta\nu \approx 1$ kcs.

Br^{79}: $I = 3/2$, $Q = 0.335$ barn, $r_u = 1.95$ A, $1 + \gamma = 100.0$. Assuming $\omega_0 = 4 \times 10^{13}$ sec^{-1}, we have $T_1^{-1} = 1300$ sec^{-1}, $\Delta\nu \approx 400$ cps.

5. QUADRUPOLE RELAXATION OF NUCLEAR SPIN INDUCED BY DIFFUSE ROTATION OF A MIXED COMPLEX

We shall limit our consideration to a mixed complex of the form $M(H_2O)_5Y$, where M is the central ion and Y is an ion that replaces one of the water molecules in the octahedron. With the z axis in the M-Y direction, Eq. (3) gives $(\nabla E)^{\pm 1} = (\nabla E)^{\pm 2} = 0$ and

$$(\nabla E)^0 = 6\,(e_B / b^3 - e_A / a^3), \tag{22}$$

where e_A and e_B are the effective charges of a water molecule and of the ion Y respectively. If Y is a singly charged ion, $e_B = e$ and $e_A = 0.66\,e$. In our model the separations a and b are both equal to $1.26\,r_u$. Taking the antishielding effect into account, we therefore obtain

$$(\nabla E)^0 = 1.02\,(1 + \gamma)\,e r_u^{-3}. \tag{23}$$

The nonvanishing matrix elements are easily calculated:

$$\mathcal{H}'_{m,\,m-1} = 3\,(\nabla E)^0 (1 + \gamma)\,eQ\,\{I_z I_x\}_{m,\,m-1} \sin^2\theta\,(t),$$

$$\mathcal{H}'_{m,\,m-2} = -\,(\nabla E)^0 (1 + \gamma)\,eQ\,(I_x^2)_{m,\,m-2} \sin\theta\,(t) \cos\theta\,(t). \tag{24}$$

Transition probabilities are calculated by means of (11); for spin 3/2 we obtain

$$w\,(3/2,\, 1/2) = w\,(-1/2,\, -3/2) = (144/5)\,|\,eQ\,(1 + \gamma)\,(\nabla E)^0\,|^2\,\hbar^{-2}\,\tau_r,$$

$$w\,(3/2,\, -1/2) = w\,(1/2,\, -3/2) = (1/5)\,|\,eQ\,(1 + \gamma)\,(\nabla E)^0\,|^2\,\hbar^{-2}\,\tau_r. \tag{25}$$

Here τ_r is the correlation time of diffuse rotation of the complex. From the theory of Brownian motion we know that

$$\tau_r = 4\pi\eta l^3 / 3kT, \tag{26}$$

where η is the viscosity of the liquid and l is the radius of the complex. By means of (19) and (25) we calculate the relaxation time:

$$(T_1^{-1})_r = (58/5)\,e^2Q^2\hbar^{-2}\,(1 + \gamma)^2\,|(\nabla E)^0|^2\,\tau_r. \tag{27}$$

The radius of the complex $Al(H_2O)_5Y^{++}$ is taken to be 2.85 A; then $\tau_r = 2.3 \times 10^{-11}$ sec. With the above-mentioned values of the other parameters we obtain $(T_1^{-1})_r = 7.7 \times 10^6$ sec^{-1}. A similar calculation for the ion Na^+ in the complex $Na(H_2O)_5Y$ gives $(T_1^{-1})_r = 7.8 \times 10^6$ sec^{-1}.

The spin relaxation time of the central ion will be even shorter if the complex contains two or more anions (located nonsymmetrically in the complex) because all components of the gradient tensor $(\nabla E)^{ik}$ are then nonvanishing and of greater magnitude.

6. CONCLUSION

1. The spin-lattice relaxation time of nuclei with a large electric quadrupole moment is of the order $10^{-6} - 10^{-7}$ sec in mixed complexes, corresponding to $\sim 10^6$ kc for the line width. Lines with this width can obviously not be observed experimentally. It follows that the observed magnetic resonance line intensity for a nucleus with large quadrupole moment is proportional to the number of purely aqueous complexes. This suggests that measurements of magnetic resonance intensities provide a convenient method for investigating complexing in liquid solutions of diamagnetic salts.

2. For aqueous complexes of the ions Al^{3+} and Ga^{3+} good agreement is obtained between the calculated and measured resonance line widths. It is known from chemical investigations that hydrated complexes of Al^{3+} and Ga^{3+} are very stable. This confirms the correctness of our model if the lifetime of the complexes exceeds the spin-lattice relaxation time.

3. For the ions Na^+, Br^-, and I^- the calculated and observed resonance line widths do not agree. This evidently results from the weak stability of the complexes that these ions form with water. The experimentally observed line widths for the nuclei Na^{23}, Br^{79}, Br^{81}, and I^{127} are related to the lifetime of the complex rather than to the spin-lattice relaxation time.

[1] J. Van Kranendonk, Physica **20**, 781 (1954).

[2] Y. Masuda, J. Phys. Soc. Japan **11**, 670 (1956).

[3] R. E. Connick and R. E. Poulson, J. Amer. Chem. Soc. **79**, 5153 (1957).

[4] L. D. Landau and E. M. Lifshitz, Теория поля GITTL, Moscow, 1948, p. 166, Engl. Transl. The Classical Theory of Fields, Addison-Wesley, Cambridge, Mass., 1951.

[5] Yost, Steffens, and Gross, J. Chem. Phys. **2**, 311 (1934).

[6] R. M. Sternheimer and H. M. Foley, Phys. Rev. **102**, 731 (1956); T. P. Das and R. Bersohn, Phys. Rev. **102**, 733 (1956); E. G. Wikner and T. P. Das, Phys. Rev. **109**, 360 (1958).

[7] S. A. Al'tshuler and K. A. Valiev, J. Exptl. Theoret. Phys. (U.S.S.R.) **35**, 947 (1958), Soviet Phys. JETP **8**, 661 (1959).

[8] A. Abragam and R. V. Pound, Phys. Rev. **92**, 943 (1953).

[9] L. D. Landau and E. M. Lifshitz, Статистическая физика (Statistical Physics), GITTL, Moscow, 1951, p. 107.

[10] M. L. Schultz, J. Chem. Phys. **10**, 194 (1942); M. Kobayashi and J. Fujita, J. Chem. Phys. **23**, 1354 (1955).

[11] J. H. Van Vleck and V. F. Weisskopf, Revs. Modern Phys. **17**, 227 (1945).

[12] C. J. Gorter, Paramagnetic Relaxation, Elsevier, New York, 1947; Russ. Transl. IIL, Moscow, 1949, p. 105.

[13] L. Pauling, Proc. Roy. Soc. (London) **A114**, 181 (1927).

[14] W. Gordy, W. Smith, and R. Trambarulo, Microwave Spectroscopy, Wiley, New York, 1953; Russ. Transl. GITTL, Moscow, 1955, p. 354.

[15] L. Pauling, The Nature of the Chemical Bond and the Structure of Molecules and Crystals, 2nd ed., Cornell Univ. Press, 1942; Russ. Transl. Goskhimizdat, Moscow, 1947, p. 337.

[16] J. R. Zimmerman and D. Williams, Phys. Rev. **75**, 198 (1949).

[17] R. V. Pound, Phys. Rev. **73**, 1247 (1948).

[18] L. H. Thomas and T. L. Collins, Phys. Rev. **79**, 226 (1950).

[19] R. V. Pound, Phys. Rev. **72**, 1273 (1947).

Translated by I. Emin
17

SOVIET PHYSICS JETP VOLUME 37(10), NUMBER 1 JANUARY, 1960

COHERENT ELECTRON RADIATION IN THE SYNCHROTRON. II.

L. V. IOGANSEN and M. S. RABINOVICH

P. N. Lebedev Physics Institute, Academy of Sciences, U.S.S.R. and V. I. Lenin Moscow State Pedagogical Institute

Submitted to JETP editor January 13, 1959

J. Exptl. Theoret. Phys. (U.S.S.R.) **37**, 118-124 (July, 1959)

The electromagnetic interaction of electrons in a thin relativistic bunch in coherent radiation in a synchrotron is considered. The tangential forces exerted on an individual electron by the bunch are considered for different particle phase distributions.

EARLIER[1] we have considered the coherent radiation spectrum of an electron bunch in a synchrotron. By summing the intensities of the individual harmonics for the entire spectrum it is possible to compute the total power associated with the coherent radiation for a given electron distribution in the bunch. This calculation has been carried out by Schiff for the case of a Gaussian distribution.[2] Schwinger has carried out this calculation for the case of a rectangular distribution and the results are given in reference 3. It is also of interest to compute the effect of the coherent radiation on the bunch. It is clear that when the coherent radiation becomes sizeable it must have an effect on the motion of the particles in the bunch. Coherent radiation arises as a result of the electromagnetic interaction of electrons within a bunch; hence the problem of determining the effect of coherent radiation on a bunch means essentially determining the tangential component of the electromagnetic forces exerted by the bunch on an individual electron. An accurate calculation of these forces for a bunch with an arbitrary distribution of particles, in which the phase and betatron oscillations are taken into account, is not feasible. However, two particular cases have been solved by Tamm[4] and Rytov.[5] These are for bunches which are segments of toroids or ellipsoids which move as a rigid body (common angular velocity) and which have a uniform electron density.

In the present paper it is assumed that all the particles in a bunch move in coaxial circles with a uniform linear velocity, $v \sim c$. This means that we can neglect betatron oscillations and the instantaneous spread in particle energy. This approach is justified because in practice the thickness of a bunch in a synchrotron is much smaller than its length. Hence, in the first approximation, the transverse dimensions do not appear in the expressions for the tangential forces.

We neglect the interaction of the bunch with the chamber walls, the pole pieces of the magnet, and the other constructional elements, assuming that the electrons move in an infinite free space. As long as the longitudinal dimensions of the bunch are small compared with the transverse dimensions of the chamber it is valid to neglect the effect of the wall on the inter-electron interaction. In cases in which the bunches are large compared with the cross section of the chamber the interaction with remote electrons is affected by the shielding of the walls and the present results cannot be applied directly.

The calculation of the tangential forces in coherent radiation has acquired new interest in connection with the experimental work being carried on in many laboratories on the formation and maintenance of electron bunches.[6]

1. INTERACTION BETWEEN TWO CHARGES IN A BUNCH

First we determine the interaction between two charges. We use the coordinate system used in reference 1. Call A the point of observation; at a given time t_A, this is the location of the charge which experiences the interaction with a second charge (radiating charge) located at point P. The effective source point of the field of the second charge, corresponding to the interaction at point A at time t_A, is designated Q; the corresponding time, which precedes t_A, we call t_Q. We use a four-dimensional notation and denote the corresponding world points by x_{Ai}; x_{Pi}; x_{Qi} ($i = 1, 2, 3, 4$). We introduce the 4-vector $R_i = x_{Ai} - x_{Qi}$. Since x_{Ai} and x_{Qi} lie on one light cone, $R_i^2 = 0$. Using the 4-dimensional Liénard-Wiechart potentials $A_i = -eu_i/R_k u_k$, where $u_i = dx_{Qi}/ds_Q$ is the 4-velocity of the charge Q, it is easy to obtain an expression for the Lorentz 4-force acting on the charge A:

$$f_i = -\frac{e^2}{c}\left\{\left[\frac{w_k \nu_k}{(R_k u_k)^2} - \frac{(1+R_k w_k)(u_k \nu_k)}{(R_k u_k)^3}\right] R_i + \frac{(1+R_k w_k)(R_k \nu_k)}{(R_k u_k)^3} u_i - \frac{R_k \nu_k}{(R_k u_k)^2} w_i\right\}. \tag{1}$$

Here $w_i = du_i/ds_Q$, while ν_i is the 4-velocity of charge A. We assume further that charges A and Q have the same velocity v and move in coaxial circles characterized by radii r_A and r_Q. In the case in which $r_A = r_Q$, i.e., when the orbits of the electrons lie on the common cylindrical surface, $f_i = -\partial\Phi/\partial x_{Ai}$, where the convection scalar potential

$$\Phi = -\frac{e^2}{c}\frac{1+R_k w_k}{R_k u_k} = \frac{\gamma}{c} e^2 \frac{1-\beta^2 (r_A/r_Q)\cos\xi}{R - \beta r_A \sin\xi}, \tag{2}$$

$$\beta = v/c; \quad \gamma = (1-\beta^2)^{-1/2}; \quad \xi = \psi_A - \psi_Q,$$
$$R = [(z_A - z_Q)^2 + (r_A - r_Q)^2 + 4r_A r_Q \sin^2(\xi/2)]^{1/2}, \tag{3}$$

and R is the distance between points A and Q. Equation (2) is similar to the potential derived by Tamm for motion with a common angular velocity.[4]

When $r_A \neq r_Q$ the force given by Eq. (1) is not deriveable from a potential. However one is easily convinced that the projection of (1) on the tangent to the orbit at A coincides in direction with the derivative of (2). The usual Lorentz force is given by $\mathbf{f} = (c/\gamma) f_\alpha$ $(\alpha = 1, 2, 3)$. It follows from the above that the tangential component of this force is

$$f_\tau = -\frac{e^2}{r_A}\frac{\partial}{\partial\psi_A}\frac{1-(\beta^2 r_A/r_Q)\cos\xi}{R - \beta r_A \sin\xi}. \tag{4}$$

Hence, although the force given in (1) cannot be derived from a potential the expression in Eq. (2) may be taken as a "potential for the tangential forces." One is easily convinced that the expression $(e^2/c)u_k\nu_k/R_k u_k$ is the "potential for the axial forces" for (1) in the same sense as (2). The phases at points A, P, and Q are related by the retardation condition

$$\psi_P - \psi_A + \xi = \beta R/r_Q. \tag{5}$$

Taking account of Eqs. (3) and (5) and the fact that $r_Q \equiv r_P$ and $z_Q \equiv z_P$, the force given by (4) may be considered a function of the coordinates of points A and P.

We derive an explicit expression for the force (4) for the simple relativistic case in which both electrons lie on one circle, i.e., $r_A = r_P = a$; $z_A = z_P = 0$ (the case considered by Tamm). Let $\psi_{AP} \equiv \psi_A - \psi_P > 0$, i.e., the charge A, on which the force is exerted, lies in front of the radiating charge P. If $^3/_2\gamma^3\psi_{AP} \ll 1$,

$$f_\tau \approx \frac{e^2}{\gamma^2 a^2 \psi_{AP}^2} - \frac{4}{3}\frac{e^2}{a^2}\gamma^4 + \frac{11}{3}\frac{e^2}{a^2}\gamma^{10}\psi_{AP}^2 \cdots \tag{6}$$

If $^3/_2\gamma^3\psi_{AP} \gg 1$, but $\psi_{AP} < 1$,

$$f_\tau \approx 2\cdot 3^{-4/3} e^2/a^2\psi_{AP}^{4/3}. \tag{7}$$

As is well known, $^3/_2\gamma^3 c/a = \omega_{\max}$ is the frequency at which the maximum radiation energy of a single electron is radiated. Hence the condition $^3/_2\gamma^3\psi_{AP} \gg 1$ is satisfied if points A and P are separated by a distance large compared with $\lambda\!\!\!^{-}_{\max} = c/\omega_{\max}$; in this case the coherent force (7) is greater than the Coulomb force $e^2/\gamma^2 a^2 \psi_{AP}^2$. When $\psi_{AP} < 0$,

$$f_\tau \approx -\frac{e^2}{\gamma^2 a^2 \psi_{AP}^2} + \frac{e^2}{8a^2} + \frac{e^2}{2^8 a^2}\psi_{AP}^2 \cdots \tag{8}$$

2. ACTION OF THE BUNCH UPON AN INDIVIDUAL ELECTRON

In order to obtain the total tangential force $\bar{f}_\tau$ exerted on charge A by the entire bunch, it is necessary to sum (4) over all electrons in the bunch. At distances much larger than the mean distance between the charges near point A the summation may be replaced by integration over the coordinates of point P.

Let the particle distribution in the bunch be given by the function $F(\psi, r, z)$. For the time being we neglect the region in the immediate proximity of A; thus

$$\bar{f}_\tau(\psi_A, r_A, z_A) = -e^2 \frac{\partial}{\partial\psi_A}\int_0^\infty dr_P \int_{-\infty}^{+\infty} dz_P \times \int_{-\pi}^{+\pi} \frac{r_P/r_A - \beta^2\cos\xi}{R - \beta r_A \sin\xi} F(\psi_P, r_P, z_P)\, d\psi_P. \tag{9}$$

In Eq. (9), carrying out the integration over ξ in place of ψ_P, using Eq. (5) we have

$$\bar{f}_\tau = -e^2 \frac{\partial}{\partial\psi_A}\int_0^\infty dr_P \int_{-\infty}^{\infty} dz_P \times \int_{-\pi}^{+\pi} \frac{r_P/r_A - \beta^2\cos\xi}{R} F\left\{\left[\psi_A - \xi + \beta\frac{R}{r_P}\right], r_P, z_P\right\} d\xi, \tag{10}$$

where R is given by Eq. (3).

We must now make certain assumptions as to the bunch. We assume that $F(\psi, r, z) = N\varphi(\psi)U(\rho, z)$, where $\rho = r - a$ (a is the radius of the stable orbit). We assume that $U(\rho, z)$ is an even function of ρ and z. Then the normalization condition is

$$a \int_{-\infty}^{\infty} \int_{-\infty}^{\infty} U(\rho, z)\, d\rho\, dz = 1.$$

We assume that the mean radius for the cross section of the bunch is

$$\sigma_0 = a \int_{-\infty}^{\infty} \int_{-\infty}^{\infty} \sqrt{\rho^2 + z^2}\, U(\rho, z)\, d\rho\, dz \ll a.$$

The effective angular dimensions of the bunch are characterized by the quantity $\vartheta_0 = 2 \int_0^{\pi} \psi\varphi(\psi)\, d\psi$. From reference 1 it follows that in the case of small oscillations $\vartheta_0 = 2\Phi_0/\pi$, where Φ_0 is the mean amplitude of the phase oscillations.

We consider an extended bunch, i.e., the case in which $a\vartheta_0 \gg \sigma_0$; we will be interested in points A close to the stable orbit, where $\rho_A \sim z_A \lesssim \sigma_0$. We assume that $\varphi(\psi)$ is a smooth function so that it does not vary significantly at distances $a\Delta\psi \sim \sigma_0$. Then, in Eq. (10) we change the argument:

$$[\psi_A - \xi + \beta R/r_\rho] \to [\psi_A - \xi + 2\beta\,|\sin(\xi/2)|\,].$$

We now expand (10) in a series in powers of $\rho_A/a \sim z_A/a \lesssim \sigma_0/a \ll 1$. We limit our consideration to the first and linear terms in the expansion. Because $U(\rho, z)$ is even, (10) is an even function of z_A. Hence in the expansion we eliminate the term which is linear in z_A. The linear term in ρ_A remains. First we consider the first term of the expansion

$$\bar{f}_\tau(\psi_A) = -Ne^2 \frac{d}{d\psi_A} \int_{-\infty}^{+\infty} \int_{-\infty}^{+\infty} d\rho\, dz U(\rho, z)$$

$$\times \int_{-\pi}^{\pi} \frac{1 - \beta^2 \cos\xi}{\sqrt{\rho^2 + z^2 + 4a^2 \sin^2(\xi/2)}}\, \varphi\left[\psi_A - \xi + 2\beta\left|\sin\frac{\xi}{2}\right|\right] d\xi. \tag{11}$$

For simplicity we assume that the bunch is circular in cross section with a radius σ and has a density which is constant over the cross section. Then we can carry out the integration over σ and z in Eq. (11). For values of ϑ_0 which are not too large, we replace the trigonometric functions in the first term by their series expansions. We have

$$\bar{f}_\tau = -\frac{Ne^2}{a^2}\, 2\left(\frac{a}{\sigma}\right)^2 \frac{d}{d\psi_A} \int_{-\pi}^{\pi} \left(\frac{1}{\gamma^2} + \beta^2\frac{\xi^2}{2}\right) \left\{\sqrt{\xi^2 + \left(\frac{\sigma}{a}\right)^2} - |\xi|\right\}$$

$$\times \varphi\left[\psi_A - \xi + \beta\left|\xi - \frac{\xi^3}{24}\right|\right] d\xi. \tag{12}$$

The term with γ^{-2} gives the Coulomb force; the term with $\beta^2\xi^2/2$ gives the coherent force. First we consider the latter: the quantity in the curly brackets in Eq. (12) can be replaced by its limiting value for $\sigma \to 0$: $\frac{1}{2}(\sigma/a)^2|\xi|^{-1}$. In the ultrarelativistic case $\gamma \gg 1$, the argument $\varphi(\psi)$ in (12) (with $\xi > 0$) assumes the form

$$\psi_A - \xi/2\gamma^2 - \xi^3/24 \approx \psi_A - \xi^3/24,$$

if $\xi \gg 1/\gamma$ and, if $\xi < 0$ it assumes the form $\psi_A - 2\xi$. Hence, for bunches characterized by $\gamma^{-3} \ll \vartheta_0 < 1$ the coherent force is

$$\bar{f}_\tau = -\frac{2}{3^{1/3}} \frac{Ne^2}{a^2} \frac{d}{d\psi_A} \int_0^{\infty} \varphi(\psi_A - \xi) \frac{d\xi}{\xi^{1/3}}$$

$$-\frac{1}{8} \frac{Ne^2}{a^2} \frac{d}{d\psi_A} \int_0^{\infty} \varphi(\psi_A + \xi)\, \xi d\xi. \tag{13}$$

The first term in Eq. (13) gives the contribution due to the interaction of charges lying behind charge A while the second term gives the contribution from charges lying in front of it. Since $\varphi(\psi) \sim 1/\vartheta_0$, in Eq. (13) the first term is of order $Ne^2/a^2\vartheta_0^{4/3}$ while the second term is approximately Ne^2/a^2. Consequently, when $\vartheta_0 \ll 1$ the second term can be neglected. Strictly speaking, directly at the end and behind of the bunch this procedure is not justified; however, for the main part of the bunch and the space in front of it, when $\gamma^{-3} \ll \vartheta_0 \ll 1$ we may assume

$$\bar{f}_\tau = -\frac{2}{3^{1/3}} \frac{Ne^2}{a^2} \frac{d}{d\psi_A} \int_0^{\infty} \varphi(\psi_A - \xi) \frac{d\xi}{\xi^{1/3}}. \tag{14}$$

For $\psi_A \gg \vartheta_0$, i.e., far in front of the bunch, from Eq. (14) we obtain the asymptotic expression for $\bar{f}_\tau$, which coincides with (7); behind the bunch we have $f_\tau \approx 0$. The Coulomb term in Eq. (12) is of order $(Ne^2/\gamma^2 a^2 \vartheta_0^2) \ln(a\vartheta_0/\sigma)$. Since the logarithm is always relatively small, the smallness of the Coulomb forces as compared with (14) gives the condition $(\vartheta_0\gamma^3)^{2/3} \gg 1$. This is almost the same as the condition $\vartheta_0 \gg \gamma^{-3}$.

Calculation of the term which is linear in ρ_A in the expansion in (10) shows that it makes a contribution of order $(\rho_A/a)\, Ne^2/a^2\vartheta_0^2$. As long as $\rho_A \ll a\vartheta_0$ this term can be neglected in comparison with (14). Consequently, (14) is the main component of the force being sought.

Summing the tangential forces which act on the individual electrons for the entire bunch we obtain the total reaction force on the bunch for the coherent radiation. Multiplying this force by the velocity of the bunch we find the total power of the coherent radiation. In particular, in the case $\gamma^{-3} \ll \vartheta_0 \ll 1$, using Eq. (14) we have

$$W_{\text{coher}} = -\frac{2}{3^{1/3}} \frac{Ne^2c}{a^2} \int_0^{\infty} \frac{d\xi}{\xi^{1/3}} \frac{d}{d\xi} \int_{-\infty}^{\infty} \varphi(\psi_A)\, \varphi(\psi_A - \xi)\, d\psi_A. \tag{15}$$

It is easier to compute the total power of the coherent radiation from Eq. (15) than by summing the intensities of the spectral harmonics. Furthermore, making the calculation by means of Eq. (15) serves as a good check on the validity of the expression for the tangential forces. For example, for a Gaussian distribution

$$\varphi(\psi) = \frac{1}{\pi\vartheta_0}\exp\left\{-\frac{1}{\pi}\left(\frac{\psi}{\vartheta_0}\right)^2\right\},$$

we have

$$W_{\mathbf{coher}} = \frac{2^{5/3}\,\Gamma\,(5/6)\,Ne^2c}{3^{1/6}\sqrt{\pi}\,a^2\,(2\sqrt{\pi}\,\vartheta_0)^{4/3}},$$

which coincides with the result obtained by Shiff.[2] For a rectangular distribution we also get exact agreement with the results obtained by Tamm[4] and Schwinger (cf. reference 3).

3. CALCULATION OF THE FORCES FOR CERTAIN MODELS

We now use Eq. (14) with various phase distributions, assuming that $\gamma^{-3} \ll \vartheta_0 \ll 1$.

For a rectangular distribution

$$\varphi(\psi) = {}^1/_4\,\vartheta_0, \quad |\psi| \leqslant 2\vartheta_0; \quad \varphi(\psi) = 0, \quad |\psi| > 2\vartheta_0,$$

and, using the notation $\psi_A/2\vartheta_0 = p_1$, we find

$$\bar{f}_\tau = -\frac{Nc^2}{3^{1/3}a^2\,(2\vartheta_0)^{4/3}}\,\chi(p_1);$$

$$\chi(p_1) = \begin{cases} 0; & p_1 < -1 \\ (p_1+1)^{-1/3}; & -1 < p_1 < 1. \\ -[(p_1-1)^{-1/3} - (p_1+1)^{-1/3}]; & p_1 > 1 \end{cases} \qquad (16)$$

The discontinuities at the points $\psi_A = \pm 2\vartheta_0$ are due to the fact that the assumption concerning the slow variation of the bunch are not satisfied at these points and Eq. (14) cannot be used. It is this distribution which was considered by Tamm and Rytov and they have shown that the region close to the ends of the bunch does not make an important change in the basic expression for the forces (16); at the discontinuities there are sharp maxima.

We consider a triangular bunch:

$$\varphi(\psi) = \frac{1}{3\vartheta_0}\left[1 - \frac{\psi}{3\vartheta_0}\right],$$

$$0 < \psi < 3\vartheta_0, \quad \varphi(\psi) = 0, \quad \psi > 3\vartheta_0, \qquad \varphi(-\psi) = \varphi(\psi).$$

Using the notation $p_2 = \psi_A/3\vartheta_0$, we have

$$\bar{f}_\tau = -\frac{3^{2/3}\,Ne^2}{a^2\,(3\vartheta_0)^{4/3}}\,\chi(p_2),$$

$$\chi(p_2) = \begin{cases} 0 & p_2 < -1 \\ (p_2+1)^{2/3} & -1 < p_2 < 0 \\ [(p_2+1)^{2/3} - 2p_2^{2/3}] & 0 < p_2 < 1 \\ [(p_2+1)^{2/3} - 2p_2^{2/3} + (p_2-1)^{2/3}] & p_2 > 1 \end{cases} \qquad (17)$$

For a Gaussian distribution

$$\bar{f}_\tau = -\frac{2}{3^{1/3}\sqrt{\pi}}\,\frac{Ne^2}{a^2\,(\sqrt{\pi}\,\vartheta_0)^{4/3}}\,\chi(p_3), \qquad p_3 = \frac{\psi_A}{\sqrt{\pi}\,\vartheta_0},$$

$$\chi(p_3) = \frac{d}{dp_3}\int_0^\infty \exp\{-(p_3-\xi)^2\}\,\frac{d\xi}{\xi^{1/3}}$$

$$= \frac{e^{-p^2}}{6}\sum_{n=0}^{\infty}\frac{\Gamma\,(n/2 - 1/6)}{n!}\,(2p_3)^n. \qquad (18)$$

The results obtained in (16) — (18) are shown in the three graphs. In each of these the dashed curves represent the distribution over phase for the particles in the bunch and ϑ_0 is identical in all cases. The force scale is the same throughout. The arrow indicates the direction of motion (to the right). It is apparent from these curves that the main losses in coherent radiation occur at the rear of the bunch. On the other hand, the electrons in the front part of the bunch may obtain additional energy by virtue of the interaction.

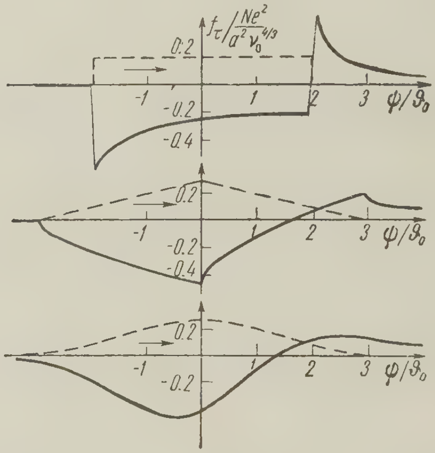

4. INTERACTION AT CLOSE DISTANCES

In conclusion we shall concern ourselves with calculating the interaction at close distances. Strictly speaking we can obtain the total force acting on the charge A if, in Eq. (9), we exclude from the region of integration a sphere with center at A and radius much larger than the mean distance between electrons δ and add the force due to the interaction of A with the remaining charges within the sphere. The latter force can be computed by means of Eq. (4). Carrying out this operation we find that in addition to the force indicated by (9) the electron at A experiences a force $f_{\delta\tau}$, directed along its line of motion. With $\delta \gg a/\gamma^3$: $f_{\delta\tau} \sim (e^2/a^2)(a/\delta)^{4/3}$ and when $\delta \ll a/\gamma^3$, $\gamma \gg 1$ this force approaches the value $(2e^2/3a^2)\gamma^4$, i.e., it compensates for the dissipation force due to radiation.

For a bunch characterized by $\vartheta_0 \ll 1$ the force $f_{\delta T}$ can be neglected compared with that given in (14) if $N^{5/9} \gg (a\vartheta_0/\sigma_0)^{8/9}$. On the other hand, for a circular current uniformly filling the entire circle, (9) vanishes and $f_{\delta T}$ determines the total force exerted on the electron at A by the bunch. Since there is no coherent radiation in this case, with $\delta \ll a/\gamma^3$ the radiation will be determined completely by the fluctuations in the density of electrons in the bunch. For present-day electron synchrotrons, in which $\gamma \sim 10^3$ and $a \sim 1$ m, the case $\delta \ll a/\gamma^3$ corresponds to a particle density of approximately 10^{21} cm^{-3}; this is far beyond what can be achieved. However, at smaller energies ($\gamma \sim 10$) and very small cross sections it is possible that $\delta \ll a/\gamma^3$. In this case (very small electron densities) there should be correlation in the distribution of the particles in the bunch and the fluctuation in the density should be smaller than for non-interacting particles. Hence the average losses due to radiation for one electron should be smaller than $(2e^2c/3a^2)\gamma^4$. However this problem requires further analysis.

The authors are indebted to Academician I. E. Tamm for making us acquainted with the results of his unpublished work.[4]

---

[1] L. V. Iogansen and M. S. Rabinovich, J. Exptl. Theoret. Phys. (U.S.S.R.) **35**, 1013 (1958), Soviet Phys. JETP **8**, 708 (1959).

[2] L. Schiff, Rev. Sci. Instr. **17**, 6 (1946).

[3] J. S. Nodvick and D. S. Saxon, Phys. Rev., **96**, 180 (1954).

[4] I. E. Tamm, Отчет ФИАН (Report of the Institute of Physics, Acad. of Sciences, U.S.S.R.), 1948.

[5] S. M. Rytov, Отчет ФИАН (Report of the Institute of Physics, Acad. Sci., U.S.S.R.), 1949.

[6] T. Ohkawa, Rev. Sci. Instr. **29**, 108 (1958).

Translated by H. Lashinsky
18

SOVIET PHYSICS JETP VOLUME 37 (10), NUMBER 1 JANUARY, 1960

ON HYDRODYNAMIC BOUNDARY CONDITIONS FOR EVAPORATION AND CONDENSATION

R. Ya. KUCHEROV and L. É. RIKENGLAZ

Submitted to JETP editor January 15, 1959

J. Exptl. Theoret. Phys. (U.S.S.R.) **37**, 125-126 (July, 1959)

The boundary conditions have been found for hydrodynamic equations in the presence of evaporation and condensation. For small evaporation rates the temperature jump and the deviation of the vapor pressure from the equilibrium value are shown to be of the order of the ratio between the speed of the vapor flow v and the mean speed of heat transfer c. It is shown that the expressions commonly used in the literature for the flow of materials and heat in the presence of evaporation and condensation contain an error.

IN the solution of hydrodynamic problems involving evaporation and condensation, the temperature T (0) and pressure p (0) of the vapor above the liquid (or solid) phase must be given as boundary conditions. Generally speaking, the vapor temperature is not the same as the temperature of the liquid surface, T_0, nor is its pressure equal to the saturated vapor pressure p_0 at the temperature T_0. This effect is analogous to the temperature jump at the boundary between a gas and a solid wall in the presence of heat flow.[1]

In the present work, the value of T (0) and p (0) are found on the basis of kinetic theory. For this purpose it is assumed that the vapor is an ideal gas, that the vapor molecules striking the liquid surface are completely captured, and that the molecules emitted from the liquid have the Maxwellian distribution corresponding to the temperature T_0 and the pressure p_0. The latter assumption is satisfactorily fulfilled in the case of monatomic gases,[2] which are the only ones we shall consider.

To simplify the calculations we limit ourselves to the case in which $v/c \ll 1$, and shall consider a one-dimensional flow of vapor at the plane liquid surface x = 0. (The x axis is directed out of the liquid into the vapor). To describe the state of the vapor we shall introduce the distribution function f (x, ξ), where ξ is the velocity of the molecules in the laboratory coordinate system.

Denoting the current density of the vapor molecules and the energy flux density by τ (x) and Q (x) respectively, we have, immediately outside the liquid surface x = 0,

$$\tau(0) = \tau_0 + \int_{-\infty}^{\infty}\!\!\int d\xi_z d\xi_y \int_{-\infty}^{0} \xi_x f(0, \xi)\, d\xi_x,$$

$$Q(0) = Q_0 + \frac{m}{2}\int_{-\infty}^{\infty}\!\!\int d\xi_z d\xi_y \int_{-\infty}^{0} \xi_x \xi^2 f(0, \xi)\, d\xi_x, \qquad (1)$$

where τ_0 and Q_0 are the molecular current density and the energy flux density for the vapor molecules emitted from the liquid.

Making the assumptions given above,

$$\tau_0 = p_0 / \sqrt{2\pi mkT_0}, \qquad Q_0 = 2kT_0\tau_0. \qquad (2)$$

To calculate τ (0) and Q (0) we use the distribution function in a "13 moment" approximation:[3]

$$f(x, \xi) = f_0\Big[1 + {\sum_{ij}}' \frac{p_{ij}}{2pRT} u_i u_j - \sum_i \frac{S_i u_i}{2pRT}\Big(1 - \frac{u^2}{5RT}\Big)\Big],$$
$$i, j = x, y, z, \qquad (3)$$

where

$$f_0 = n(m/2\pi kT)^{3/2} \exp(-mu^2/2kT),$$
$$\mathbf{u} = \xi - \mathbf{v}, \qquad R = k/m, \qquad (4)$$

n is the density of molecules, p_{ij} is the viscous stress tensor, **v** is the velocity of the local center of inertia, and $\mathbf{S} = m\int \mathbf{u}u^2 f\, d\mathbf{u}$ is twice the heat flow, related to the total energy flow by the formula

$$\mathbf{Q} = {}^1/_2\mathbf{S} + \tau c_p T,$$

where c_p is the heat capacity at constant pressure, equal to $^5/_2$k.

Substituting (2) and (3) into (1) and carrying out the integration to the accuracy of the terms linear in v/c, we obtain

$$\tau(0) = 2\{p_0/\sqrt{2\pi mkT_0} - p(0)/\sqrt{2\pi mkT(0)}\}, \qquad (5)$$
$$Q(0) = 2\{p_0\sqrt{2kT_0/\pi m} - p(0)\sqrt{2kT(0)/\pi m}\}. \qquad (6)$$

From this it can be seen that the flux of particles and energy, when $v/c \ll 1$, is equal to twice the difference between the corresponding Maxwellian currents directed out of and into the surface, and not to this difference itself, as it is usually taken to be (cf, for instance, references 2 and 4).

The appearance of the factor 2 is related to the fact that in determining the flux falling on the surface, the Maxwellian distribution function for a gas at rest has always been used as the zeroth-order approximation, whereas the proper form appears to be the Maxwellian distribution for a moving gas [Eq. (4)].

Solving Eqs. (5) and (6) for $p(0)$ and $T(0)$, we find the following expressions for the temperature and pressure of the vapor at the surface:

$$T(0)/T_0 = 1 - Q(0)/2Q_0 + \tau(0)/2\tau_0, \qquad (7)$$

$$p(0)/p_0 = 1 - Q(0)/4Q_0 - \tau(0)/4\tau_0. \qquad (8)$$

When $S/p\tau \gg 1$, (7) reduces to the well-known formula for the temperature jump at a non-absorbent surface.[3] In this case, it is known that the temperature jump is of the order of λ/a, the ratio between the free path and a characteristic dimension for the problem.

In the other limiting case, $S/p\tau \ll 1$, where convective heat transfer is much larger than molecular transfer, we have

$$T(0)/T_0 = 1 - \tau(0)/8\tau_0,$$

$$p(0)/p_0 = 1 - 9\tau(0)/16\tau_0, \qquad (9)$$

i.e., the temperature jump and the deviation of the vapor pressure from its equilibrium value are of order v/c.

Equations (5) and (6), or (7) and (8), can serve as boundary conditions for hydrodynamic equations involving evaporation and condensation.

The authors express their gratitude to M. I. Kaganov for profitable discussions, and to Yu. A. Shuander for his interest in the work.

---

[1] L. D. Landau and E. M. Lifshitz, Механика сплошных сред (Mechanics of Continuous Media), M. 1944.

[2] G. Wyllie, Proc. Roy. Soc. (London) **A197**, 383 (1949).

[3] H. Grad, Coll. Механика (Mechanics) **4**, IIL, M. 1952, p. 71.

[4] M. S. Plesset, J. Chem. Phys. **20**, 790 (1952).

Translated by D. C. West
19

RANGE-ENERGY RELATION FOR SOME SUBSTANCES

M. Z. MAKSIMOV

Submitted to JETP editor January 15, 1959

J. Exptl. Theoret. Phys. (U.S.S.R.) **37**, 127-130 (July, 1959)

From an analysis of the experimental and theoretical data on the stopping of charged particles in matter it is concluded that the specific loss and the range depend only on the ratio of E_a/a, the incident-particle energy per nucleon, to the mean excitation potential of atoms of the medium. Proceeding upon this assumption, a universal experimental curve is plotted from the experimental data, which yields the range for energies in the interval $0.5 \leqslant E_a/a \leqslant 200$ Mev for any substance whose excitation potential is known.

THE energy loss of a nonrelativistic particle with charge Z_a and mass number a upon passage through matter with atomic number Z and mass number A is given by the familiar formula

$$\varepsilon = \frac{dE}{dR} = \frac{4\pi Z_a^2 e^4}{mv^2} \frac{N_0 Z}{A} \ln \frac{2mv^2}{I_A}, \tag{1}$$

where R is the range in mg/cm^2, e and m are the electron charge and mass, N_0 is the Avogadro number, v is the velocity of the particle and I_A is the mean excitation potential of atoms of the stopping material.

In the Bloch approximation ($I_A \sim Z$) specific losses are a function of only the single parameter v^2/Z.[1,2] Subsequent investigations have shown[3] that this approximation is not entirely justified. If the energy properties of atoms of the stopping material are represented approximately by the mean excitation potential, then, in accordance with dimensional considerations and approximation (1), the specific loss must depend only on the ratio of the mean kinetic energy acquired by atomic electrons of the medium to the mean excitation potential. With the incident particle energy E_a given in Mev and I_A in kev, a convenient dimensionless parameter is

$$y = E_a / a I_A. \tag{2}$$

The formula obtained for the specific loss is then $\epsilon = cf(y)$, comparison of which with approximation (1) determines the constant c:

$$\varepsilon(E_a) = (Z / A I_A) Z_a^2 f(y). \tag{3}$$

The obvious expression for the range is then

$$R(E_a) = \frac{A I_A^2 a}{Z Z_a^2} F(y), \qquad F(y) = \int_0^y \frac{dt}{f(t)}, \tag{4}$$

where both f(y) and F(y) depend only on y and in approximation (1) f(y) is given by

$$f(y) \approx (145 / y) \ln (2.17 y) \text{ kev}^2\text{-cm}^2/\text{mg}. \tag{5}$$

We conclude from (3) and (4) that when experimental data are plotted on a graph with y along one axis and $F(y) = (ZZ_a^2/AI_A^2 a)R(E)$ or $f(y) = (I_A A/ZZ_a^2)\epsilon(E)$ along the other axis we obtain universal curves for determining ranges and specific losses in different media when the mean excitation potentials are known.

We are interested in the plot of F(y) which was based on the following experimental data: in the energy interval 0.2—2 Mev proton ranges were calculated from the experimental stopping powers of Be, Al, Cu, Au and Pb;[2,4] for 1—7 Mev, proton ranges were measured in Fe, Cu, Mo, Cd, Sn, Ta and Pb relative to Al;[5] for 6—18 Mev, absolute proton ranges were measured in Be, Al, Cu, Ag and Au;[6] for 40—120 Mev, the theoretical ranges in Al, Cu and Au were corrected experimentally;[7] finally, the ranges of 190-Mev deuterons (E_p = 95 Mev) were measured in Be, C, Cu, Ag, Pb, and U relative to Al.[8]

It is evident from (2) and (4) that the plotting of F(y) requires knowledge of the mean excitation potential, which has not been determined for all materials. The latest[3] of frequent[2,3,6,9] measurements for aluminum gives $I_{Al} \approx 0.166$ kev; therefore the experimental points for aluminum according to (2) and (4) were plotted first. Then from the data for other materials, making use of these same equations, suitable excitation potentials I_A were selected so that the experimental points would give the best fit to the curve obtained for aluminum. Closest agreement was obtained in the region 6—18 Mev, where absolute proton ranges were measured for several materials.

The results of the analysis are shown in the figure, where for convenience the mentioned experimental data are collected in the plot of $F(y)/y^2$.

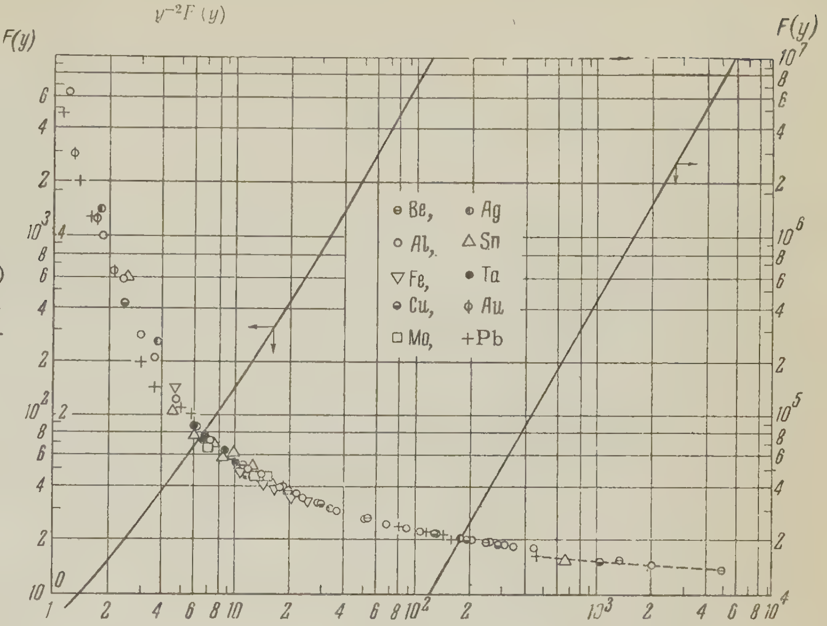

Solid curves – Plots of $F(y) = (ZZ_a^2 / AI_A^2 a) R(E)$ mg/cm²-kev² (outside scales on the left and right). Experimental points – values of $F(y)/y^2$ (inside non-logarithmic scale on the left)

As was expected, the experimental points lie in a satisfactory manner on a smooth curve over a wide range of y. The spread of the points results partly from experimental errors in determining ranges and energies $[F(y)/y^2 \approx R(E)/E^2]$. Thus, for example, the results obtained by Rybakov[5] show that the error in the function may be 5% or higher. Points (connected by the dashed line) were also plotted for protons with ≈ 340 Mev in Be, Al, Cu, Sn and Pb;[10] these also lie on a smooth curve but in a less satisfactory manner.

We also note, without giving the results, that experimental data on stopping powers[2,3,8] were used to plot $yf(y) = (A/ZaZ_a^2)\, E\epsilon(E)$ in the region $0.1 \leqslant y \leqslant 10^3$. The fit to a smooth curve is somewhat better than for $y^{-2}F(y)$; this may result from a smaller scattering effect. A calculation of yf(y) by means of the approximate formula (5) agrees with experiment even when $y \gtrsim 1$. However, the calculation of F(y), which is of interest here, by means of the same formula encounters difficulties since the region $y < 1$ is then included, where the formula is unsuitable [F(y) is obtained from (4) by an integration]. For sufficiently large y ($y \gtrsim 5$–10), where the effect of this region can be neglected, (5) gives satisfactory results for the calculation of F(y).

The figure contains the plot of F(y) while the table gives values of I_A for different materials; the plot and table combined enable us to calculate the range for any material at energies 0.5–200 Mev. The excitation potential of an univestigated material can be determined from the plot of $y^{-2}F(y)$, using the range at a single energy. In the absence of such information an estimate can be obtained from the table by means of linear interpolation in accordance with the Bloch approximation.

In conclusion the author wishes to thank M. M. Agrest for a discussion of the results.

Note added in proof, May 29, 1959. A satisfactory fit to the curve of $y^{-2}F(y)$ is also obtained with recently published experimental data on the range of 660-Mev protons in copper and of multiply charged ions with 40–100 Mev in copper and gold [V. P. Zrelov and G. D. Stoletov, J. Exptl. Theoret. Phys. (U.S.S.R.) **36**, 658 (1959), Soviet Phys. JETP **9**, 461

Element	Z/A	I_A, kev	Element	Z/A	I_A, kev	Element	Z/A	I_A, kev
H	1,000	0,017*	Al	0.483	0,166	Sn	0.421	0.450
Li	0,430	0.038*	Cl	0.481	0.169*	Ta	0.405	0.730
Be	0.445	0.067	Fe	0.465	0.286	W	0.402	0.770*
C	0,500	0,084*	Cu	0.457	0.320	Au	0.400	0.935
N	0.500	0.085*	Mo	0.433	0.450	Pb	0.395	0.730
Air	0.500	0.089*	Ag	0.436	0.530	U	0.386	0.995*
O	0.500	0.097*	Cd	0.427	0, 457			

---

*Data from reference 9, normalized to $I_{Al} = 0.166$ kev.

(1959), and Yu. Ts. Oganesyan, ibid, p. 936 (transl. p. 661)],

---

[1] J. Lindhard and M. Scharff, Kgl. Danske Videnskab. Selskab, Mat.-fys. Medd. **27**, No. 15 (1953).

[2] S. K. Allison and S. D. Warshaw, Revs. Modern Phys. **25**, 779 (1953).

[3] V. C. Burkig and K. R. MacKenzie, Phys. Rev. **100**, 734 (1955); **106**, 848 (1957).

[4] Bader, Pixley, Mozer, and Whaling, Phys. Rev. **103**, 32 (1956).

[5] V. V. Rybakov, J. Exptl. Theoret. Phys. (U.S.S.R.) **28**, 651 (1955), Soviet Phys. JETP **1**, 435 (1955).

[6] Bichsel, Mozley, and Aron, Phys. Rev. **105**, 1788 (1957).

[7] N. Bloembergen and P. J. Van Heerden, Phys. Rev. **83**, 561 (1951).

[8] E. Segre (ed.), Experimental Nuclear Physics, Wiley, New York, 1953; Russ. Transl. IIL, 1955, Vol. I. p. 172

[9] C. J. Bakker and E. Segre, Phys. Rev. **81**, 489 (1951).

[10] R. Mather and E. Segre, Phys. Rev. **84**, 191 (1951).

Translated by I. Emin
20

SOVIET PHYSICS JETP VOLUME 37(10), NUMBER 1 JANUARY, 1960

INELASTIC SCATTERING OF NUCLEONS ON Mg^{24} *AND* Si^{28} *NUCLEI*

V. I. MAMASAKHLISOV and T. I. KOPALEĬSHVILI

Institute of Physics, Academy of Sciences, Georgian S.S.R.

Submitted to JETP editor January 17, 1959

J. Exptl. Theoret. Phys. (U.S.S.R.) **37**, 131-136 (July, 1959)

Inelastic scattering of nucleons on Mg^{24} and Si^{28} nuclei is investigated with account of Coulomb interaction for 1) excitation of collective nuclear levels, and 2) single-particle excitation in the field of a deformed nucleus. An analysis is made of the relation between the character of the angular distribution and magnitude of the effective cross section on the one hand, and the magnitude and the sign of the deformation on the other.

1. Many recently published papers deal with experimental investigations of inelastic scattering of nucleons and deuterons by nuclei.[1,2] This problem becomes even more interesting because a comparison of the experimental data with the results of the theoretical investigations can lead to many conclusions concerning the character of excitation of nuclei.

The present paper is devoted to a theoretical investigation of inelastic scattering of nucleons by Mg^{24} and Si^{28}. Two cases of excitation, one-particle and collective, are considered.

Unlike Sawicki,[3] who recently considered this problem, we also take Coulomb interaction into account and investigate the dependence of the character of angular distribution and of the magnitude of the effective scattering cross section on the magnitude and sign of the deformation.

2. We first consider single-particle excitation. Here, as is known, it is assumed that only one of the nucleons above the closed shell is excited, and that this nucleon moves in the field of the deformed nucleus.

The wave functions for the nuclear system at the beginning and the end of the process are respectively[4]

$$\Phi_0 = \sqrt{\frac{2I+1}{16\pi^2}}\, \varphi_{n_\beta n_\gamma}(\beta,\gamma)\, [\chi_\Omega D^I_{MK}(\theta_i) + (-1)^p \chi_{-\Omega} D^I_{M-K}(\theta_i)], \tag{1}$$

$$\Phi = \sqrt{\frac{2I'+1}{16\pi^2}}\, \varphi_{n'_\beta n'_\gamma}(\beta,\gamma)\, [\chi_{\Omega'} D^{I'}_{M'K'}(\theta_i) + (-1)^{p'} \chi_{-\Omega'} D^{I'}_{M'-K'}(\theta_i)], \tag{2}$$

where I, K, and M is the angular momentum of the nucleus and its projections along the symmetry axis of the nucleus and a stationary axis respectively; $\Omega = \Sigma \Omega_i$, where Ω_i is the projection of the momentum of the i-th nucleon (from among the nucleons above the closed shell) on the axis of the nucleus; χ_Ω is the anti-symmetrized wave function of the nucleons above the closed shell; the wave functions $\varphi(\beta, \gamma)$ and $D(\theta_i)$ describe the collective (vibrational and rotational) states of the nucleus, β and γ being parameters that characterize the deformation of the nucleus, while θ_i $(\theta_1 \theta_2 \theta_3)$ are the Euler angles; $p = I + K - \Omega - (1/2) A$, where A is the mass number of the nucleus. (The primed symbols in Φ have the same meaning as in Φ_0, but pertain to the final states of the nuclear system.)

Since it is assumed that the incident nucleon interacts only with one nucleon of the nucleus, we can write

$$\chi_\Omega = \chi_{\Omega_i} \chi_{\Omega_0}, \tag{3}$$

where

$$\chi_{\Omega_i} = \sum_{l_i m_i \sigma_i} A_{l_i \Omega_i - \sigma_i} R_{N l_i}(r_i) \times Y_{l_i m_i}(\vartheta_i, \varphi_i)\, S(\sigma_i)\, D^{l_i}_{m_i \Omega_i - \sigma_i} \tag{4}$$

is the wave function of the excited nucleon, referred to a stationary system of coordinates, χ_{Ω_0} is the wave function of the remaining nucleons outside the closed shell, with $R_{Nl_i}(r_i)$ being the radial wave function, $S(\sigma_i)$ the spin function, and $A_{l_i \Omega_i - \sigma_i}$ the coefficients of diagonalization, tabulated by Nilsson.[4] We choose the energy of interaction between the incident nucleon and the i-th nucleon of the nucleus in the form

$$V = -V_0 \delta(\mathbf{r} - \mathbf{r}_i) + 4\pi e^2 \varepsilon \sum_{l'm'} \frac{r_i^{l'}}{(2l'+1)\, r^{l'+1}} Y^*_{l'm'}(\vartheta, \varphi)\, Y_{l'm'}(\vartheta_i, \varphi_i), \tag{5}$$

where $\epsilon = 1$ when the incident and i-th nucleon of the nucleus are protons, and $\epsilon = 0$ in all other cases. The Coulomb interaction in expression (5) is chosen in the form used in reference 5, where it is assumed, first, that the electric interaction occurs only when $r > r_0$ (where r_0 is the electric radius of the nucleus), and second, that the wave functions of the nuclear nucleons are real in the region $r_i < r_0$.

Taking plane wave functions for the incident nucleon at the beginning and the end of the process, we obtain for the differential cross section of inelastic scattering

$$\frac{d\sigma}{d\Omega} = \frac{\mu^2 V_0}{(2\pi\hbar^2)^2}\sqrt{1 + \frac{Q}{E_0'}}\,\frac{1}{2I+1}\sum |H_{if}|^2, \tag{6}$$

where

$$\begin{aligned} H_{if} = {} & \frac{1}{2}\sqrt{(2I+1)(2I'+1)} \\ & \times \sum_{Ll}\sum_{l_i l_i'}\sum_{m_i \sigma_i} [C(Lll_i l_i' m_i \sigma_i \Omega_i \Omega_i' K K') \\ & + (-1)^{p+p'} C(Lll_i l_i' m_i \sigma_i, -\Omega_i, -\Omega_i', \\ & -K, -K')]\,\delta_{MM'}\,\delta_{\Omega_i' + K', \Omega_i + K}, \end{aligned} \tag{7}$$

with

$$\begin{aligned} C(Lll_i l_i' m_i \sigma_i \Omega_i \Omega_i' K K') = {} & A_{l_i \Omega_i - \sigma_i} A'_{l_i' \Omega_i' - \sigma_i} \frac{i^l (2l+1)}{2L+1} J_{ll_i l_i'}(q) \\ & \times \sqrt{\frac{2l_i + 1}{2l_i' + 1}} (l_i l 00 \mid l 0)(l_i l m_i 0 \mid l_i' m_i)(l_i I m_i M \mid L m_i + M) \\ & \times (l_i' I' m_i M \mid L m_i + M)(l_i I \Omega_i - \sigma_i K \mid L \Omega_i + K - \sigma_i) \\ & \times (l_i' I' \Omega_i' - \sigma_i K \mid L \Omega' + K' - \sigma_i). \end{aligned} \tag{8}$$

In Eq. (6) μ is the reduced mass, E_0' the energy of the incident nucleon in the center of mass system, Q the energy absorbed by the nucleus in the reaction, and the function $J(q)$ which enters into (8) is equal to

$$\begin{aligned} J_{ll_i l_i'}(q) = {} & \int_0^\infty R_{Nl_i}(r_i) R_{Nl_i'}(r_i) f_l(qr_i) r_i^2 dr_i \\ & - \frac{e^2}{V_0}\frac{4\pi}{2l+1}\int_0^{r_0} r_i^{l+2} R_{Nl_i}(r_i) R_{Nl_i}(r_i)\, dr_i \\ & \times \int_{r_0}^\infty \frac{\exp(iqr)}{r^{l+1}} Y_{l0}(\vartheta, \varphi)\, d\mathbf{r}, \end{aligned} \tag{9}$$

where r_0 is the electric radius of the nucleus, $q = |\mathbf{k} - \mathbf{k}'|$, and $f_l(qr)$ is the spherical Bessel function ($\mathbf{k}$ and $\mathbf{k}'$ are the wave vectors of the incident and scattered nucleon).

3. Let us apply the derived formulas to the scattering of protons by Mg^{24} and Si^{28} with excitation of the first level. In both cases we have $I = 0$, $K = 0$, $M = 0$, $I' = 2$, $K' = 0$. Therefore, in accordance with the selection rules $\Omega_i' + K' = \Omega_i + K$, we can write $\Omega_i = \Omega_i'$. It is known that in Mg^{24} the nucleons above the O^{16} shell ($N = 2$) are in the state with $\Omega_i = \pm 1/2$ and $\pm 3/2$ at $\delta > 0$ and $\Omega_i = \pm 5/2$ and $\pm 1/2$ at $\delta < 0$ (δ is the deformation parameter). Consequently, the possible transitions in Mg^{24} are $1/2 \rightarrow 1/2$ and $3/2 \rightarrow 3/2$ (and also the transitions $-1/2 \rightarrow -1/2$ and $-3/2 \rightarrow -3/2$). We use the well known relation between the excitation energy and the deformation parameter

$$\Delta E = \varkappa\hbar\omega_0 [r_{\alpha_1}^{N\Omega_i}(\delta) - r_{\alpha_2}^{N\Omega_i}(\delta)], \tag{10}$$

where $\hbar\omega_0 = \hbar^2/2Mr_0'^2$, where r_0' is a parameter that enters into the expression for the oscillator potential, M the mass of the nucleon, and $r_\alpha^{N\Omega_i}$ the eigenvalue of the additional term in the interaction taking into account the deformation of the nucleus and the spin-orbit forces; the index α indicates the number of the level with given Ω_i according to Nilsson.[4] Nilsson also tabulated the values of $r_\alpha^{N\Omega}$ for different values of the deformation parameter δ (at $\kappa = 0.05$). By finding the density of the nucleons in the nucleus on the basis of the oscillator wave functions, and by stipulating that the point of maximum slope of the density curve correspond to the boundary of the nucleus, we can determine the value of the parameter r_0'. Assuming for the nuclear radius $R_0 = 1.45 A^{1/3} \times 10^{-13}$ cm, we find approximately the same value for Mg^{24} and Si^{28}, $r_0' = 1.9 \times 10^{-13}$ cm. Using the experimental value of the excitation energy ΔE, we can determine the deformation parameter δ from Eq. 10. In the case of Mg^{24} the excitation energy of the first level is 1.37 Mev. Assuming the transition $(1/2)_{\alpha_1} \rightarrow (1/2)_{\alpha_2}$ to take place, we obtain from Eq. (10) for the deformation parameter two values of δ, namely $\delta = 0.17$ and $\delta = -0.22$. If, on the other hand, we assume a $(3/2)_{\alpha_1} \rightarrow (3/2)_{\alpha_2}$ transition, then the deformation parameter is found to be practically zero. Thus, only a $1/2 \rightarrow 1/2$ transition is possible in the Mg^{24} deformed nucleus in the case of single-particle excitation.

A different result is obtained in the case of the Si^{28} nucleus, in which the levels $\pm 5/2$, $\pm 1/2$, $\pm 3/2$ are filled at $\delta < 0.17$ and the levels $\pm 1/2$, $\pm 3/2$, $\pm 1/2$ are filled at $\delta > 0.17$. On the basis of the selection rule $\Omega_i = \Omega_i'$ we have the same transitions as in the case of Mg^{24}, namely $1/2 \rightarrow 1/2$ and $3/2 \rightarrow 3/2$. (In the outer shell of Si^{28} there is only one level with $\Omega_i = \pm 5/2$.)

Considering that the excitation energy of the nearest level in Si^{28} is 1.77 Mev, we obtain for the deformation parameter $\delta = 0.1$ and $\delta = 0.3$

for the transition $1/2 \rightarrow 1/2$ and $\delta = 0.1$ for the transition $3/2 \rightarrow 3/2$

4. From (7) and (8) we have for the $1/2 \rightarrow 1/2$ transition

$$H_{if} = \tfrac{1}{2}\{J_{220}(q)\,[A_{00}(A'_{20} + A'_{21}) + A'_{00}(A_{20} + A_{21})] + (\sqrt{5}/7)\,J_{222}(q)\,(A_{20} + A_{21})\,(2A'_{20} + A'_{21})\}, \tag{11}$$

and for the $3/2 \rightarrow 3/2$ transition

$$H_{if} = (\sqrt{5}/7)\,J_{222}(q)\,(A_{21} + A_{22})\,(A'_{22} + A'_{21}), \tag{12}$$

where

$$J_{220} = \frac{1}{3\sqrt{10}}\Big\{(qr'_0)^2\,[(qr'_0)^2 - 4]\exp[-(qr'_0)^2/2] - \frac{12}{5}\,\frac{\sqrt{2\pi}e^2}{V'_0 R_0}\Big(\frac{r'_0}{R_0}\Big)^2 a\Big(\frac{r_0}{r'_0}\Big)\varepsilon\,\frac{f_1(qr_0)}{qr_0}\Big\}$$

and

$$J_{222} = \frac{1}{15}\Big\{(qr'_0)^2\,[7 - (qr'_0)^2]\exp[-(qr'_0)^2/2] - \frac{4}{5}\,\frac{\sqrt{2\pi}e^2}{V'_0 R_0}\Big(\frac{r'_0}{R_0}\Big)^2 a'\Big(\frac{r_0}{r'_0}\Big)\varepsilon\,\frac{f_1(qr_0)}{qr_0}\Big\},$$

with

$$V_0 = V'_0 R_0^3, \qquad a\Big(\frac{r_0}{r'_0}\Big) = \int_{r_0/r'_0}^{\infty} e^{-x^2/2}x^6\Big(1 - \frac{x^2}{3}\Big)dx,$$

$$a'\Big(\frac{r_0}{r'_0}\Big) = \int_{r_0/r'_0}^{\infty} e^{-x^2/2}x^8\,dx.$$

It is readily seen from (12) that in the $3/2 \rightarrow 3/2$ transition the relative angular distribution is independent of the deformation parameter, since the latter influences only the coefficients A_{ik} and A'_{ik}, which pertain to levels α_1 and α_2 respectively.

Let us compare the results obtained with the experimental data. In the case of Mg^{24}, as indicated above, only the $1/2 \rightarrow 1/2$ transition is possible in the presence of deformation. Curve 1 of Fig. 1 shows the theoretical angular distribution, obtained on the basis of Eq. (11) at $\delta = 0.2$; the vertical lines represent the experimental values of the cross section.[1] (We have replaced the exact value $\delta = 0.17$ by the approximate value $\delta = 0.2$, since the wave functions available in the literature[4] have been tabulated for δ in the interval from 0.3 to -0.3 in steps of 0.1). In plotting curve 1, we have assumed for the electric radius of Mg^{24} a value[5] $r_0 = 6 \times 10^{-13}$ cm. It is easy to see that the presence of a maximum in the angular distribution is determined essentially by the nuclear term of the interaction, and the location of the maximum depends substantially on R_0. We determine the parameter V'_0 from the condition that the maximum point on the theoretical curve coincide with the corresponding experimental value of the cross section at the same scattering angle. At $\delta = 0.2$ we obtain $V'_0 = 0.94$ Mev. The angular distribution at negative deformation, $\delta = -0.2$, differs little from the distribution at $\delta = 0.2$. Taking the same value $V'_0 = 0.94$ Mev, the only difference is that the magnitude of the maximum cross section in the case of $\delta = -0.2$ is approximately one order of magnitude less than for $\delta = 0.2$, and the position of the maximum is shifted approximately 10° towards the larger angles.

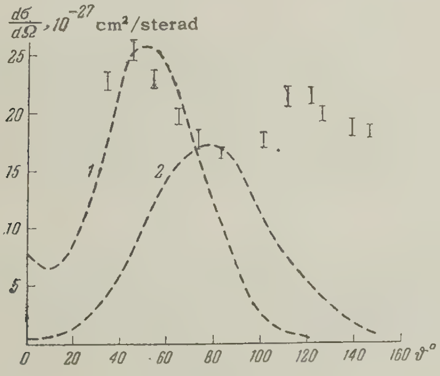

FIG. 1

As seen from Fig. 1, the theoretical curve 1 is in satisfactory agreement with the experimental data, both with respect to the position of the maximum and with respect to its shape, in the interval of angles from 0 to 70°. Thus, allowance for the Coulomb interaction has improved the agreement between theory and experiment in the region of small angles. It should be noted that we would obtain for the parameter δ a different value were we to stipulate that the experimental value of the maximum cross section coincide with the point of maximum not on the curve corresponding to the deformation parameter $\delta = 0.2$, but on the curve corresponding to the deformation parameter $\delta = -0.2$. It can be shown, however, that this would not influence the position of the maximum, since in this respect the angular distribution shows poorer agreement with experiment in the case of negative deformation.

Figure 2 shows the angular distribution of protons inelastically scattered by Si^{28}. As noted above, we have in this case $1/2 \rightarrow 1/2$ transitions with deformations $\delta = 0.1$ and $\delta = -0.3$, and $3/2 \rightarrow 3/2$ transitions with deformations $\delta = 0.1$. The theoretical angular distributions differ little from each other in all cases. We therefore show only one curve, corresponding to the $1/2 \rightarrow 1/2$ transition with a deformation parameter $\delta = 0.1$. If V'_0 is determined here, too, from the condition that the maximum point on the theoretical curve

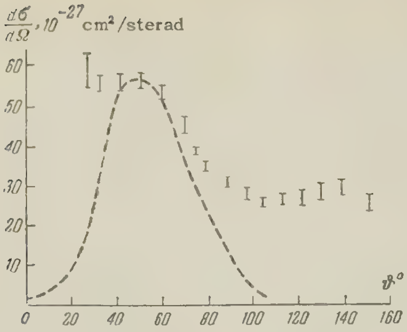

FIG. 2

correspond to the experimental value,[6] we find that, unlike Mg^{24}, allowance for the Coulomb interaction does not lead to any significant correction. (We obtain here $V_0' = 12.2$ Mev.) Therefore agreement is obtained with experiment only as regards the position of the principal maximum. As to the magnitude of the cross section, we indicate that the principal maximum value in the case of $1/2 \rightarrow 1/2$ and $3/2 \rightarrow 3/2$ transitions with deformation parameter $\delta = 0.1$ and the $1/2 \rightarrow 1/2$ transition with deformation parameter $\delta = -0.3$ are related approximately as 1:10:30 if we take for all the cases the same value of V_0', namely 12.2 Mev.

5. It is easy to obtain the angular distribution of inelastically scattered protons by Mg^{24} and Si^{28} under the assumption that the collective level is excited, provided we use the previously derived[5] formula, which pertains to the scattering of deuterons. Modifying this formula to account for the fact that we deal here with proton scattering, we obtain

$$\frac{d\sigma}{d\Omega} = \mu^2 \frac{(V_0 R_0^2)^2}{\pi \hbar^4} \beta^2 \sqrt{1 + \frac{Q}{E_0'}} \left[f_2(qR_0) + \frac{0{,}6 Z e^2}{R_0 V_0} \frac{f_1(qr_0)}{qr_0} \right]. \tag{13}$$

In reference 5 we used a value of β determined from energy of the rotational level. Considering, however, that the value of β thus obtained is approximately twice the experimental value of the deformation, we use for Mg^{24} $\beta = 0.42$.[3] It must be noted, that the deformation parameter $\delta = 0.95\beta$, determined from the energy of the single-particle level, differs from the deformation determined from the data on collective excitation. This is natural, since by attributing the entire excitation of the nucleus to one particle, it is necessary apparently to make a corresponding change in the field of deformation.

Curve 2 of Fig. 1 shows the angular distribution obtained from Eq. (13) for Mg^{24}. The first term of this equation corresponds to the nuclear interaction. The angular distribution due to this interaction has a maximum, something not obtained with the Coulomb interaction. The position of the maximum in the angular distribution, with allowance only of the nuclear term in the interaction, is independent of the parameter V_0' and is close to 80°. If we require here that the value of the cross section at the maximum of angular distribution coincide with the corresponding experimental value of the cross section, then the parameter V_0' is found to be such that the Coulomb term influences the distribution only at small angles, and does not change the position of the maximum. An analogous result is obtained also in the case of Si^{28}. Here, too, the position of the maximum of the angular-distribution curve is independent of the parameter V_0' and is close to 80°.

After comparing the results obtained for single-particle and collective excitations, we can arrive at the following conclusions:

1. For the same value of the radius of the equilibrium sphere, on which the angular distribution depends substantially, the position of the maxima in the distribution are found to be different, depending on the character of excitation of the nucleus. For the value we have assumed, $R_0 = 4.2 \times 10^{-13}$ cm, the maximum in the angular distribution for Mg^{24}, in single-particle excitation, is close to the origin and is in better agreement with the experimental data. When R_0 is increased, the maximum in the angular distribution shifts in both excitations towards the smaller angles. For example, at $R_0 = 6 \times 10^{-13}$ cm, the position of the maximum in the angular distribution, in the case of collective excitation, is in better agreement with experiment, but such a value of R_0 must be considered as excessive and not in agreement with other data.

2. In our method of analysis, the presence of a second maximum on the experimental curve of angular distribution cannot be explained for either case of excitation.

3. The relative angular distribution, connected with the collective excitation, is independent of the magnitude and sign of the deformation, whereas in the case of single-particle excitation such a dependence exists, although it is weak.

---

[1] Greenlees, Haywood, Kuo, and Petravic, Proc. Phys. Soc. **A70**, 331 (1957).

[2] Hinds, Middleton, and Parry, Proc. Phys. Soc. **A70**, 900 (1957).

[3] J. Sawicki, Nucl. Phys. **7**, 503 (1958).

[4] S. G. Nillson, Mat. Fys. Medd. Dan. Vid. Selsk. **29**, No. 16 (1955).

[5] V. I. Mamasakhilisov and T. I. Kopaleĭshvili, J. Exptl. Theoret. Phys. (U.S.S.R.) **34**, 1169 (1958), Soviet Phys. JETP **7**, 809 (1958).

[6] Greenlees, Kuo, Lowe, and Petravic, Proc. Phys. Soc. **A71**, 347 (1958).

Translated by J. G. Adashko
21

INTENSITY RULES FOR BETA TRANSITIONS TO DIFFERENT ROTATIONAL STATES OF EVEN-EVEN DAUGHTER NUCLEI

A. S. DAVYDOV

P. N. Lebedev Physics Institute, Academy of Sciences, U.S.S.R.

Submitted to JETP editor January 13, 1959

J. Exptl. Theoret. Phys. (U.S.S.R.) **37**, 137-142 (July, 1959)

Relative probabilities are computed for the β decay of an odd-odd nucleus with excitation of different rotational states of the non-axially-symmetrical even-even daughter nucleus. The theory is compared with experiment for the β decay of Re^{186}, Np^{238}, Eu^{154}, Re^{190}, and Ir^{190}.

1. INTRODUCTION

IT has been shown by Alaga, Alder, Bohr, and Mottelson[1] that the relative intensities of β transitions from a given initial nuclear state to different rotational states of a daughter nucleus obey rules that are analogous to the intensity rules for the fine structure and superfine structure of atomic spectra. These authors assumed axial symmetry for all nuclei, as a result of which the only rotational levels of even-even nuclei were given by the formula $E_J = AJ(J+1)$, $J = 0, 2, 4, \ldots$. It was further assumed that the wave functions of nuclear states can be represented by simple products of the functions φ_K, representing internal motion, and D^J_{MK}, which depend on the Euler angles that describe the spatial orientation of the nucleus:

$$\psi_{JMK} = \sqrt{(2J+1)/8\pi^2}\, \varphi_K D^J_{MK}.$$

The assumption of axial symmetry for all nuclei does not appear to be justified. It has been shown by the calculations of Geĭlikman,[2] Zaikin,[3] and Davydov and Filippov[4] that the equilibrium shape of a nucleus may not necessarily possess axial symmetry. In references 5 and 6 the energy levels of non-axisymmetric even-even nuclei were calculated for different values of a parameter γ which determines the departure from axial symmetry. It was shown that the rotational states of even-even nuclei include certain excited states which were previously regarded as γ and β vibrational levels. Since the relative energies and wave functions of all rotational levels can be determined unambiguously for each nucleus, when the energy ratio of two levels with spin 2 is known it becomes possible to estimate the relative probabilities of β transitions from a given state of the parent nucleus to different rotational states of a non-axisymmetric nucleus. Such relative probabilities of β transitions will be calculated in the present paper.

2. RATIO OF SQUARED ABSOLUTE VALUES OF MATRIX ELEMENTS FOR β DECAY TO DIFFERENT ROTATIONAL LEVELS

The β decay of an odd-odd parent nucleus with integral spin produces an even-even nucleus. β decay is characterized by the angular momentum L which is carried away by the electron and antineutrino and may be associated with the operator $\mathfrak{M}_{L\mu}$, where μ is the projection of L in some given direction.

To investigate the excitation of rotational states of the daughter nucleus in β decay it is convenient to express $\mathfrak{M}_{L\mu}$ in terms of multipole operators $\mathfrak{M}'_{L\nu}$ defined in the coordinate system fixed in the nucleus; we use the transformation

$$\mathfrak{M}_{L\mu} = \sum_{\nu} \mathfrak{M}'_{L\nu} D^L_{\nu\mu}(\theta_i). \tag{2.1}$$

Final rotational states of the even-even daughter nucleus can be represented in the adiabatic approximation by the wave functions

$$\psi_{Jmi} = \sum_{K} A_{Ki} \Phi_{JK}, \tag{2.2}$$

where

$$\Phi_{JK} = \varphi_J(r)\left[\frac{2J+1}{16\pi^2(1+\delta_{0K})}\right]^{1/2} \times (D^J_{mK} + (-1)^J D^J_{m,-K}), \tag{2.3}$$

and $\varphi_J(r)$ is an internal-state wave function of the daughter nucleus. The coefficients A_{Ki} which determine the rotational-state wave functions were calculated in references 5 and 6.

The initial-state wave function of a parent nucleus with spin I is represented in the adiabatic approximation by

$$\psi_{IM} = \varphi_I(r) \sum_K a_K D^I_{MK}. \tag{2.4}$$

The reduced probability of a β transition with angular momentum L carried away by the electron and antineutrino is given by

$$B(L;\ I \to Ji) = \frac{1}{2I+1} \sum_{m\mu M} |(Jmi\,|\,\mathfrak{M}_{L\mu}\,|\,IM)|^2. \tag{2.5}$$

Substituting (2.1), (2.2), and (2.4) into (2.5) and integrating over the Euler angles, we obtain (2.5) in the form of two factors, one of which depends on $\mathfrak{M}'_{L\nu}$ and the wave functions representing internal motion, while the other factor depends on the parameters a_K and A_{Ki} and the coefficients of vector addition which are dependent on the quantum numbers $IKJK'L$.

We consider the ratio of reduced probabilities for β transitions from a given initial state of the parent nucleus to different rotational states associated with the same internal state of the daughter nucleus. When

$$L < \begin{cases} \min(K+K'), & \text{for } K \neq 0,\quad K' \neq 0, \\ \min(K+K''), & \text{for } K \neq 0,\quad K'' \neq 0, \end{cases} \tag{2.6}$$

this ratio will not contain expressions relating to the internal state. Thus

$$B(L;\ I \to J'i') / B(L;\ I \to J''i'') = \frac{\left|\sum\limits_{KK'} a_K A^{J'}_{K'i'} (ILKK' - K\,|\,J'K')\right|^2}{\left|\sum\limits_{KK''} a_K A^{J''}_{K''i''} (ILKK'' - K\,|\,J''K'')\right|^2}. \tag{2.7}$$

At the present time we unfortunately do not know the coefficients a_K which determine the wave functions (2.4) of odd-odd nuclei. In some instances we must therefore express the initial-state wave function of the parent nucleus by

$$\psi_{IMK} = \Phi(r) D^I_{MK}.$$

The probability ratio (2.7) now becomes

$$B(L;\ IK \to J'i') / B(L;\ IK \to J''i'') = \frac{\left|\sum\limits_{K'} A^{J'}_{K'i'} (ILKK' - K\,|\,J'K')\right|^2}{\left|\sum\limits_{K''} A^{J''}_{K''i''} (ILKK'' - K\,|\,J''K'')\right|^2}, \tag{2.8}$$

if $K = 0$ or if (2.6) is fulfilled.

Finally, in a still rougher approximation, when definite values of the quantum number K' are assigned to the rotational states, the branching ratio (2.7) reduces to the following ratio that was derived in reference 1:

$$B(L;\ IK \to J'K') / B(L;\ IK \to J''K'') = (ILKK' - K\,|\,J'K')^2 / (ILKK' - K\,|\,J''K')^2, \tag{2.9}$$

when (2.6) is fulfilled or when $K = 0$ or $K' = 0$.

3. COMPARISON WITH EXPERIMENTS

It is well known that the probabilities of allowed β transitions are characterized conveniently by the quantity τf_0, where τ is the half-life and f_0 is the Fermi function which represents the integral of the electron energy distribution function. The Fermi function depends on the transition energy, nuclear charge and charge of the emitted particle.

The product τf_0 is inversely proportional to the square of the absolute value of the matrix element corresponding to an allowed transition ($L = 0$ or 1 with unchanged parity). In the general case of forbidden β transitions this simple relation does not exist; for these transitions it is evidently essential to use a combination of different types of interaction whose relative contributions are not easily determined. The so-called unique β transitions are exceptions.

In the case of unique n-th forbidden transitions ($L = n + 1$, with changing parity when n is odd) τf_n is inversely proportional to the square of the transition matrix element, where f_n is the integral of the electron energy distribution function for the given type of decay.

Davidson[7] has shown that, neglecting the influence of the Coulomb field, we may use the approximation

$$f_n = \bar{c}_n f_0. \tag{3.1}$$

where c_n depends on the transition energy E_0. In a rough approximation

$$\bar{c}_n \approx \{E_0^2 - m^2c^4\}^n, \tag{3.2}$$

Thus for allowed transitions ($n = 0$) or unique forbidden transitions it follows from the fact that $(\tau f_n)^{-1}$ is proportional to the square of the absolute value of the transition matrix element that the ratio of the values of τf_n for two β transitions from the same initial state of the parent nucleus to different rotational states of the daughter nucleus will be given by

$$\tau f_n(I \to J'i') / \tau f_n(I \to J''i'') = B(L;\ I \to J''i'') / B(L;\ I \to J'i'), \tag{3.3}$$

where $L = n + 1$ and the probability ratio must be calculated by means of (2.7) or the approximate formulas (2.8) and (2.9).

In comparing the experimental results with the theory it must be remembered that the experimental values of τf usually represent τf_0, since the Fermi formulas for allowed transitions are used to calculate f.

We shall now apply the foregoing results to the decay of Re^{186}. Figure 1 shows the decay scheme (reference 9, p. 539). The maximum electron energy (in kev) and the value of $\log_{10}(\tau f_0)$ are given near each arrow representing a transition. The spin and energy in kev are given for each rotational level. According to reference 10 the ground state of Re^{186} has zero spin and negative parity, and the transition to the first excited level of Os^{186} corresponds to $L = 2$ with changed parity, i.e., it is a unique singly forbidden transition. This conclusion is supported by the large value of $\log_{10}(\tau f)$ and the shape of the β spectrum, which results in a straight-line Kurie plot when the shape correction factor for a unique singly-forbidden transition is taken into account.

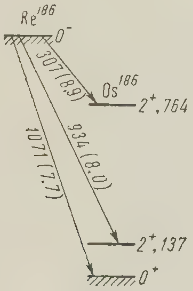

FIG. 1

Since according to the theory of non-axisymmetric nuclei the second excited 2^+ level also represents rotational excitation of Os^{186} the relative probabilities of β decay to these two levels can be calculated. From the energy ratio (5.56) of these two levels it follows that $\gamma = 18°$. Therefore, following reference 5, the wave functions of the rotational levels can be written as

$$\psi_{21} = 0.997\,\Phi_{20} + 0.065\,\Phi_{22}$$

$$\psi_{22} = -0.065\,\Phi_{20} + 0.997\,\Phi_{22}. \qquad (3.4)$$

Using (3.4) and the fact that the Re^{186} ground-state wave function corresponds to $J = K = 0$, we obtain the β-transition branching ratio from (2.7):

$$B(2; 0 \to 21)/B(2; 0 \to 22) = 1.3. \qquad (3.5)$$

The ratio $\tau f_0(0 \to 22)/\tau f_0(0 \to 21) = 7.94$ is obtained experimentally. Using (3.1) and (3.2), we obtain

$$\tau f_1(0 \to 22)/\tau f_1(0 \to 21) = 1.47.$$

According to (3.3) this ratio corresponds to the theoretical branching ratio (3.5).

Our second example is the decay of Np^{238}; the decay scheme is shown in Fig. 2 (see reference 9, p. 730), with the same notation as in Fig. 1. The energy ratio of levels with spin 2 is 23, which corresponds to $\gamma = 8°$. The rotational-state wave functions can be obtained from references 5 and 6.

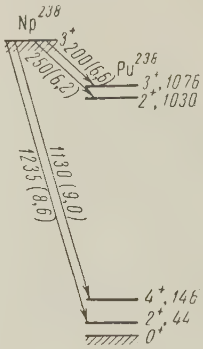

FIG. 2

The ground-state wave function of Np^{238}, with spin 3, is unknown and will be represented by the very simple form

$$\psi_J = \varphi_J\,(D^3_{m3} + \delta D^3_{m0}),$$

where δ is a parameter denoting the fractional share in the ground state of Np^{238} taken by states with $K = 0$ (for simplicity other possible values of K are disregarded). Branching ratios calculated from (2.7) for allowed β transitions (with $L = 1$) to levels of the rotational band of Pu^{238} are given in Table I for two values of δ, together with the inverse ratios of τf_0 for the same transitions.

TABLE I

j	$B(1; 3\to j)/B(1; 3\to 20)$		$\frac{\tau f_0\,(3\to 20)}{\tau f_0\,(3\to j)}$
	$\delta = 0$	$\delta = 0{,}047$	
41	0	2	0.4
22	10^4	800	250
3	10^3	100	100

We shall now consider the β decay of Eu^{154}. According to Juliano and Stephens[8] the decay of Eu^{154} to two excited levels of Gd^{154} having spin 2 and energies 123 and 998 kev, corresponds to the values 12.9 and 11.6, respectively, for $\log_{10}(\tau f_0)$. We obtain $\gamma = 14°$ from the energy ratio of these levels; the wave functions of both rotational states can then be determined from reference 5. The ground state of Eu^{154} has spin 3; assuming that its wave function is $\psi_{3m} = \varphi_3 (D^3_{m3} + \delta D^3_{m0})$, from (2.7) with $\delta = -0.26$ we obtain for β transitions with $L = 1$: $B(1;\ 3 \rightarrow 22) B^{-1}(1;\ 3 \rightarrow 20) = 20$, which agrees with the experimental ratio $\tau f_0 (3 \rightarrow 20)/\tau f_0 (3 \rightarrow 22) \approx 20$. With $\delta = 0$ this ratio would be 2500, and if K is a good quantum number for levels with spin 2 the ratio would become infinite.

We finally consider the excited rotational levels of Os^{190} resulting from the β decay of Re^{190} and K capture in Ir^{190}. The decay scheme is shown in Fig. 3 (see reference 9, p. 550). According to references 5 and 6 the rotational-state wave functions of Os^{190} can be obtained by assuming $\gamma = 21°$.

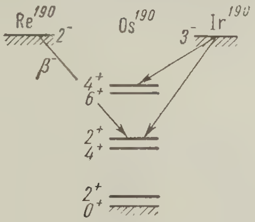

FIG. 3

Taking the wave functions φD^2_{m2} and φD^3_{m3} for the ground states of Re^{190} and Ir^{190}, respectively, (2.7) can be used to calculate the branching ratio for β decay $(L = 1)$ and K capture $(L = 1)$ to different rotational levels of Os^{190}. The results of these calculations are given in Table II, where the unit of measurement is the reduced probability of decay to the second excited level having spin 2.

Table II gives a qualitative explanation of the experimental findings that in β decay of Re^{190} only rotational level 22 is excited and that levels 22 and 42 are excited through K capture in Ir^{190}.

TABLE II

j	$\frac{B(1;\ 2\rightarrow j)}{B(1;\ 2\rightarrow 22)}$, $Re^{190}\rightarrow Os^{190}$	$\frac{B(1;\ 3\rightarrow j)}{B(1;\ 3\rightarrow 22)}$, $Ir^{190}\rightarrow Os^{190}$
41	0	$6 \cdot 10^{-4}$
21	$7.6 \cdot 10^{-3}$	$8 \cdot 10^{-4}$
61	0	0
42	0	$7.4 \cdot 10^{-2}$

The foregoing examples serve to illustrate the way in which (2.7) can be used. Ignorance of the wave function (2.4) of the parent nucleus (when $I \neq 0$) prevents a complete comparison of theory and experiment. When experimental values of τf_0 are available for allowed β transitions to different rotational levels of the daughter nucleus, (2.7) can be used to calculate the coefficients a_K, which determine the dependence of the parent-nucleus wave function on the Euler angles.

---

[1] Alaga, Alder, Bohr, and Mottelson, Kgl. Danske Videnskab. Selskab, Mat.-fys. Medd. **29**, No. 9 (1955).

[2] B. T. Geĭlikman, J. Exptl. Theoret. Phys. (U.S.S.R.) **35**, 989 (1958), Soviet Phys. JETP **8**, 690 (1959).

[3] D. A. Zaikin, J. Exptl. Theoret. Phys. (U.S.S.R.) **35**, 529 (1958), Soviet Phys. JETP **8**, 365 (1959).

[4] A. S. Davydov and G. F. Filippov, J. Exptl. Theoret. Phys. (U.S.S.R.) **36**, 1497 (1959), Soviet Phys. JETP **9**, 1061 (1959).

[5] A. S. Davydov and G. F. Filippov, J. Exptl. Theoret. Phys. (U.S.S.R.) **35**, 440 (1958), Soviet Phys. JETP **8**, 303 (1959).

[6] A. S. Davydov and V. S. Rostovskiĭ, J. Exptl. Theoret. Phys. (U.S.S.R.) **36**, 1788 (1959), Soviet Phys. JETP **9**, 1275 (1959).

[7] J. Davidson, Phys. Rev. **82**, 48 (1951).

[8] J. O. Juliano and F. Stephens, Phys. Rev. **108**, 341 (1958).

[9] B. S. Dzhelepov and L. K. Peker, Схемы распада радиоактивных ядер (Decay Schemes of Radioactive Nuclei), U.S.S.R. Acad. Sci. Press, 1958.

[10] Guss, Killion, and Porter, Phys. Rev. **95**, 627 (1954).

Translated by I. Emin
22

SOVIET PHYSICS JETP VOLUME 37 (10), NUMBER 1 JANUARY, 1960

THEORY OF WEAK SOLUTIONS OF He^4 IN LIQUID He^3

V. N. ZHARKOV and V. P. SILIN

Institute of Earth Physics, Academy of Sciences, U.S.S.R.

Submitted to JETP editor January 23, 1959

J. Exptl. Theoret. Phys. (U.S.S.R.) **37**, 143-153 (July, 1959)

A weak solution of He^4 in liquid He^3 is considered as a Boltzmann gas of impurity excitations (associated with the He^4 atoms) in a Fermi liquid. The spectrum of the impurity excitations and the thermodynamics of the solution are examined. Kinetic equations for Fermi and impurity excitations of the solution are derived. The dependences of the diffusion, thermal diffusion, viscosity and thermal conductivity coefficients on temperature and concentration are determined.

PURE liquid He^3 near absolute zero is a Fermi quantum liquid, for which Pomeranchuk[1] was the first to develop a qualitative theory that yielded the temperature dependence of both thermodynamic quantities (specific heat and entropy) and kinetic coefficients (viscosity and thermal conductivity). A theory constructed recently by Landau[2] provides a quantitative description of liquid He^3 as a system of Fermi "quasi-particles," the number of which equals that of the atoms in a unit of volume. Physically a quasi-particle is a He^3 atom in the self-consistent field of the surrounding atoms in the liquid He^3. At temperatures much below the degeneracy temperature most of the quasi-particles are condensed into a Fermi sphere [or into a Fermi layer or "bubble" in the case of the roton spectrum (3)] and only a negligible fraction is in the diffuse Fermi zone. In this temperature region the theory permits determination of the thermodynamic and kinetic properties of liquid He^3.[1,3,4]

An essential difference between the Landau theory of a Fermi liquid and the Fermi-gas theory is that the energy of a quasi-particle is a functional of the distribution function. At temperatures close to $T = 0$ this relation is given by[2,4]

$$\varepsilon = \varepsilon(\mathbf{p}) + \int f(\mathbf{p}, \mathbf{p}')\, \nu\, d\tau' \qquad d\tau = 2d\mathbf{p} / (2\pi h)^3, \tag{1}$$

where ν is the difference between the true distribution function and its value at $T = 0$ (f is Landau's function in reference 5). At sufficiently low temperatures the momentum dependence of the excitation energy may be of two types:

$$\varepsilon(\mathbf{p}) = a + |\mathbf{p} - \mathbf{p}_0|\, p_0 / m, \tag{2}$$

where p_0 is the momentum limit, and a and m are constants (this is equivalent to the gas spectrum $\epsilon = p^2/2m$), or

$$\varepsilon(\mathbf{p}) = a + (\mathbf{p} - \mathbf{p}_0)^2 / 2m. \tag{3}$$

The type of spectrum cannot be determined from presently available experimental data; we note only that spectrum (2) seems more natural.

When liquid He^3 contains a small number of foreign atoms, such as a small admixture of He^4, in the Boltzmann case these atoms will cause excitations with the spectrum

$$E = \Delta + q^2 / 2M \tag{4}$$

or

$$E = \Delta + (q - q_0)^2 / 2M, \tag{5}$$

where $\mathbf{q}$ is the momentum of the impurity excitation; Δ is the zero-point energy; q_0 and M are experimentally determined parameters. (4) and (5) may be supported by the same line of reasoning that was used by Landau and Pomeranchuk[6] for the spectrum of impurities in liquid He II.

We shall consider the thermodynamic and kinetic phenomena in weak solutions* of He^4 in liquid He^3. In addition to the coefficients of viscosity η and thermal conductivity κ the new kinetic factors which appear are the diffusion coefficient D and thermal diffusion coefficient Dk_T, where k_T is the thermal diffusion ratio. These coefficients will, as usual,[7] be determined by means of the equations

$$\mathbf{i} = -\rho D\left(\nabla c + \frac{k_T}{T}\nabla T\right) \quad \text{for } \mathbf{g} = \mathbf{g}_i + \mathbf{g}_f = 0, \tag{6}$$

$$\mathbf{Q} = -\varkappa \nabla T \qquad \text{for } \mathbf{i} = 0, \tag{7}$$

where $\mathbf{i}$ is the impurity current, $\mathbf{Q}$ is the heat flux, $\mathbf{g}$ is the total momentum flux in the solution, consisting of the momentum transported by impurity excitations (g_i) and the momentum transported by Fermi excitations (g_f).

---

*We are considering an unstratified region in which the solution is not a superfluid.

It was shown in reference 8 that the collision integrals due to the scattering of Fermi excitations contain, instead of the usual deviation δn_f of the Fermi-excitation distribution from equilibrium, the effective expression

$$\overline{\delta n}_f = \delta n_f - \frac{\partial n}{\partial \varepsilon} \int \delta n_f \, f(\mathbf{p}, \mathbf{p}') \, d\tau'. \tag{8}$$

This same expression replaces the usual δn_f in equations for the different fluxes resulting from Fermi excitations. For example, the momentum flux of Fermi excitations, which determines the Fermi portion of the solution's viscosity, is given by

$$\Pi_{ik}^{f} = \int p_i \frac{\partial \varepsilon}{\partial p_k} \overline{\delta n}_f \, d\tau. \tag{9}$$

Similarly, the energy flux, which determines the Fermi part of the thermal conductivity, is given by

$$Q_f = \int \varepsilon \frac{\partial \varepsilon}{\partial \mathbf{p}} \overline{\delta n}_f \, d\tau. \tag{10}$$

Therefore the fact that $\overline{\delta n}_f$ is given by (8) appears nowhere in the calculations.

1. THERMODYNAMICS OF WEAK SOLUTIONS OF He^4 IN LIQUID He^3

We now determine the conditions under which dissolved He^4 atoms can be described by Boltzmann statistics. Departures from classical statistics arise at temperatures where either the quantum degeneracy of the impurity gas or the interaction between impurity excitations is important. The spin of the atoms is zero, so that the degeneracy temperature T_0 of the impurity gas for spectrum (4) is[9,10]

$$T_0 = (\hbar^2 n_0^{2/3} \bar{c}^{2/3} / kM)(3^{2/3}\pi / 2), \tag{11}$$

where $n_0 = \rho/m_3$ is the number of atoms of pure He^3 in 1 cm^3, m_3 is the He^3 atomic mass and $\bar{c}$ is the He^4 concentration. We shall compare (11) with temperatures at which interactions between impurities play a part. The interaction energy of impurity particles is $\sim U\bar{c}$, where U is the characteristic energy of interactions between helium atoms and is of the order of a few degrees. Degeneracy occurs before the interaction becomes prominent[10] when the inequality $(kT_0/U\bar{c})^{1/2} \sim \bar{c}^{-1/3} \gg 1$ is satisfied. When $\bar{c} < 10^{-2}$ we have $T_0 < 0.2$°K. Pomeranchuk[10] has shown for bosons and spectrum (5) that the degeneracy temperature is given by

$$kT_0 \sim 2\bar{c}^2 \pi^4 \hbar^6 n_0^2 / q_0^4 M. \tag{11a}$$

In this case the departure from classical statistics results from the interaction of impurities and appears at temperatures $\sim U\bar{c}/\bar{k}$. Classical statistics will thus be applicable for $T \gtrsim 0.1$°K with $\bar{c} \lesssim 10^{-2}$.

The chemical potential of Fermi excitations in a weak solution of He^4 in liquid He^3 has the standard form[11]

$$\mu_f = \mu_0 - kT\bar{c}, \tag{12}$$

where μ_0 is the chemical potential of pure liquid He^3. Khalatnikov and Abrikosov[3] have considered the thermodynamics of pure liquid He^3. The presence of impurities results in additional contributions to the free energy F, entropy S and specific heat C, which are calculated by means of (12).

For a spectrum of type (4) we have

$$F_i = -N_4 kT \ln\left[\frac{eV}{N_4}\left(\frac{MkT}{2\pi\hbar^2}\right)^{3/2} e^{-\Delta/kT}\right],$$

$$S_i = N_4 k\left\{\ln\left[\frac{V}{N_4}\left(\frac{MkT}{2\pi\hbar^2}\right)^{3/2}\right] + \frac{5}{2}\right\}, \quad C_i = \frac{3}{2} N_4 k,$$

where N_4 is the number of impurities in a volume V. When $V = 1$ N_4 is related to the concentrations $c = N_4 m_4/(N_3 m_3 + N_4 m_4)$ and $\bar{c}$ as follows:

$$c = N_4 m_4 / \rho = N_4 m_4 / N_3 m_3 = \bar{c} m_4 / m_3, \quad N_4 / N_3 \ll 1.$$

Here m_3 and m_4 are the masses of He^3 and He^4 atoms; N_3 is the number of He^3 atoms per unit volume. For the spectrum (5) we have

$$F_i = -N_4 kT \ln\left[\frac{eV}{N_4} \frac{q_0^2}{\hbar^3} \sqrt{\frac{MkT}{2\pi^3}} e^{-\Delta/kT}\right],$$

$$S_i = N_4 k\left\{\ln\left(\frac{V}{N_4} \frac{q_0^2}{\hbar^3} \sqrt{\frac{MkT}{2\pi^3}}\right) + \frac{3}{2}\right\}, \quad C_i = \frac{1}{2} N_4 k.$$

S_i and C_i are proportional to the concentration and are therefore small at temperatures ~ 1°. On the other hand, at temperatures ~ 0.1° they may have an important influence on the entropy and specific heat of the solution.

2. THE KINETIC EQUATION

The kinetic equation which determines the distribution function n of elementary excitations in a solution of He^4 in liquid He^3 is

$$\frac{\partial n}{\partial t} + \frac{\partial \varepsilon}{\partial \mathbf{p}} \frac{\partial n}{\partial \mathbf{r}} - \frac{\partial \varepsilon}{\partial \mathbf{r}} \frac{\partial n}{\partial \mathbf{p}} = J(n). \tag{13}$$

We regard the solution as having macroscopic gradients of thermodynamic quantities and small gradients of the velocity $\mathbf{u}$. In this case the distribution functions n_f and n_i will differ slightly from their equilibrium values, as follows:

$$n_{\mathrm{f}} = n_{\mathrm{f}0} + \delta n_{\mathrm{f}}, \qquad n_{\mathrm{i}} = n_{\mathrm{i}0} + \delta n_{\mathrm{i}}, \tag{14}$$

where

$$n_{\mathrm{f}0} = [\exp\{(\varepsilon - \mathbf{pu} - \mu)/kT\} + 1]^{-1}, \tag{15}$$

$$n_{\mathrm{i}0} = A(c, T)\exp\{-(E - \mathbf{qu})/kT\},$$

$$A(c, T) = (c\rho/m_4)(2\pi MkT)^{-3/2} \tag{16}$$

for the impurity spectrum (4).

We shall now express the left member of the kinetic equation in terms of gradients of T, c, and u. For this purpose we shall, as is customary,[12,4] substitute n from (14) and (15) into (13) and shall make use of thermodynamic identities and hydrodynamic equations. We shall also assume that at the considered point of the liquid $\mathbf{u} = 0$. The kinetic equation for Fermi excitations therefore becomes

$$-\frac{1}{2}\frac{\partial n_{\mathrm{f}0}}{\partial \varepsilon}\left(p_i \frac{\partial \varepsilon}{\partial p_k} - \frac{1}{3} p_l \frac{\partial \varepsilon}{\partial p_l}\delta_{ik}\right)\left(\frac{\partial u_i}{\partial x_k} + \frac{\partial u_k}{\partial x_i} - \frac{2}{3}\delta_{ik}\frac{\partial u_l}{\partial x_l}\right)$$

$$+\frac{\partial n_{\mathrm{f}0}}{\partial \varepsilon} kT \frac{\partial \varepsilon}{\partial \mathbf{p}} \frac{m_3}{m_4}\nabla c$$

$$-\frac{\partial n_{\mathrm{f}0}}{\partial \varepsilon}\frac{\partial \varepsilon}{\partial \mathbf{p}}\left(\frac{\varepsilon - \mu}{T} - s\right)\nabla T = J_{\mathrm{ff}} + J_{\mathrm{fi}} \tag{17}$$

and similarly, the kinetic equation for impurities is

$$\frac{1}{2}\frac{n_{\mathrm{i}0}}{kT}\left(q_i \frac{\partial E}{\partial q_k} - \frac{1}{3} q_l \frac{\partial E}{\partial q_l}\delta_{ik}\right)\left(\frac{\partial u_i}{\partial x_k} + \frac{\partial u_k}{\partial x_i} - \frac{2}{3}\delta_{ik}\frac{\partial u_l}{\partial x_l}\right)$$

$$+ n_{\mathrm{i}0}\frac{\partial E}{\partial \mathbf{q}}\frac{\nabla c}{c} + n_{\mathrm{i}0}\frac{\partial E}{\partial \mathbf{q}}\left(\frac{E}{kT} - \frac{3}{2}\right)\frac{\nabla T}{T}$$

$$+ n_{\mathrm{i}0}\frac{\partial E}{\partial \mathbf{q}}\frac{\nabla \rho}{\rho} = J_{\mathrm{if}} + J_{\mathrm{ii}}. \tag{18}$$

In (17) and (18) we have omitted the term resulting in second viscosity, which will not be considered below. Furthermore, without affecting accuracy we may omit the term in (18) that contains $\nabla\rho$, which is relatively small.* J_{ff} and J_{fi} are the collision integrals for the scattering of Fermi excitations on other Fermi excitations and on impurities. J_{if} and J_{ii} have analogous meanings. By means of the substitutions†

$$\overline{\delta n}_{\mathrm{f}} = -n_{\mathrm{f}0}(1 - n_{\mathrm{f}0})\psi, \qquad \delta n_{\mathrm{i}} = -n_{\mathrm{i}0}\varphi \tag{19}$$

we reduce the collision integrals to the standard forms

$$J_{\mathrm{ff}} = \int w_{\mathrm{ff}}\, n_{\mathrm{f}01} n_{\mathrm{f}02}(1 - n'_{\mathrm{f}01})(1 - n'_{\mathrm{f}02})(\psi_1 + \psi_2 - \psi'_1 - \psi'_2)$$

$$\times\, \delta(\mathbf{p}_1 + \mathbf{p}_2 - \mathbf{p}'_1 - \mathbf{p}'_2)\,\delta(\varepsilon_1 + \varepsilon_2 - \varepsilon'_1 - \varepsilon'_2)\, d\tau_2 d\tau'_2 d\mathbf{p}'_2,$$

$$J_{\mathrm{fi}} = \int w_{\mathrm{fi}}\, n_{\mathrm{f}0} n_{\mathrm{i}0}(1 - n'_{\mathrm{f}0})(\psi + \varphi - \psi' - \varphi')$$

$$\times\, \delta(\mathbf{p} + \mathbf{q} - \mathbf{p}' - \mathbf{q}')\,\delta(\varepsilon + E - \varepsilon' - E')\, d\tau' d\mathbf{q} d\mathbf{q}',$$

$$J_{\mathrm{if}} = \int w_{\mathrm{fi}}\, n_{\mathrm{f}0} n_{\mathrm{i}0}(1 - n'_{\mathrm{f}0})(\psi + \varphi - \psi' - \varphi')$$

$$\times\, \delta(\mathbf{p} + \mathbf{q} - \mathbf{p}' - \mathbf{q}')\,\delta(\varepsilon + E - \varepsilon' - E')\, d\tau d\mathbf{p}' d\mathbf{q}',$$

$$J_{\mathrm{ii}} = \int w_{\mathrm{ii}}\, n_{\mathrm{i}0} n_{\mathrm{i}01}(\varphi + \varphi_1 - \varphi' - \varphi'_1)\,\delta(\mathbf{q} + \mathbf{q}_1 - \mathbf{q}' - \mathbf{q}'_1)$$

$$\times\, \delta(E + E_1 - E' - E'_1)\, d\mathbf{q}_1 d\mathbf{q}' d\mathbf{q}'_1. \tag{20}$$

We also require the cross sections for the scattering of impurities on Fermi excitations and on other impurities. The interaction law of these excitations is, of course, unknown, but just as in the theory[12] of weak solutions of He^3 in He II, it is reasonable for specific estimates to use a δ-function interaction law:

$$V_{\mathrm{fi}} = v_{01}\,\delta(\mathbf{x} - \mathbf{y}), \quad V_{\mathrm{ii}} = v_{02}\,\delta(\mathbf{y}_1 - \mathbf{y}_2),$$

where **x** is the coordinate of a Fermi excitation and **y** is the impurity coordinate. The unknown constants v_{01} and v_{02} are determined by comparing theory with experiment. The cross sections are calculated as in the theory of slow-neutron scattering by atoms,[12,13] and we obtain

$$\sigma_{\mathrm{fi}} = \left(\frac{mM}{m + M}\right)^2 \frac{|v_{01}|^2}{\pi\hbar^4}, \tag{21}$$

$$\sigma_{\mathrm{ii}} = M^2 |v_{02}|^2/\pi\hbar^4. \tag{22}$$

We also obtain the cross section for the scattering of an impurity on a Fermi particle with the spectrum (3). This is analogous to the scattering of an impurity on a roton and the total cross section is correspondingly[12]

$$\sigma_{\mathrm{fi}} = \frac{|v_{01}|^2 M}{2\pi\hbar^4}\frac{Mm}{m + M}. \tag{21a}$$

3. DIFFUSION

We consider first the diffusion of impurities. The kinetic equations (17) and (18) for Fermi excitations and impurities were derived above; with a non-zero concentration gradient in the system they are

$$kT\frac{\partial n_{\mathrm{f}0}}{\partial \varepsilon}\frac{\partial \varepsilon}{\partial \mathbf{p}}\frac{m_3}{m_4}\nabla c = J_{\mathrm{ff}} + J_{\mathrm{fi}}, \tag{22}$$

$$n_{\mathrm{i}0}\frac{\partial E}{\partial \mathbf{q}}\frac{\nabla c}{c} = J_{\mathrm{if}} + J_{\mathrm{ii}}. \tag{23}$$

---

*The independent variables are actually c and T. Therefore $\nabla\rho = (\partial\rho/\partial c)\nabla c + (\partial\rho/\partial T)\nabla T$.

†We shall hereinafter omit the bar above δn_f.

An exact general solution of the problem is hardly possible. We shall therefore consider the two limiting cases; results in the intermediate region can then be obtained by interpolation. The first limiting case is represented by the high-temperature region, where the effective number of excitations in the diffuse Fermi zone is much greater than the number of impurities. In the low-temperature region, on the other hand, the situation is reversed and the effective number of excitations in the diffuse Fermi zone is much smaller than the number of impurities.

It follows from symmetry that the deviations (19) of the distribution functions from equilibrium may be sought in the forms

$$\varphi = a(E)(\mathbf{q}\nabla c), \qquad \psi = b(\varepsilon)(\mathbf{p}\nabla c). \tag{24}$$

It is important here that the functions a and b are independent of angles. Spectrum (2) for Fermi excitations and spectrum (4) for impurity particles will be considered in greatest detail.

The High-Temperature Region. There is a relatively small number of impurity particles; collisions among these are unlikely and insignificant. The concentration region where this occurs is given more precisely by the condition $t_{ff} \ll t_{fi}$, i.e., the effective time for a collision between two Fermi particles is much shorter than the effective time for a collision between a Fermi particle and an impurity. The kinetic equation for impurities is therefore greatly simplified. Simple calculations show that the Fermi distribution function deviates considerably less from equilibrium than the impurity distribution function. The condition $t_{ff} \ll t_{fi}$ is sufficient so that in the mixed collision integrals J_{if} and J_{fi} in (20) we can neglect ψ compared with φ. Furthermore, the momenta of excited Fermi particles are much greater than those of impurities; we may therefore neglect the variation in the absolute value of the relative momentum of colliding particles. From all of these consideration we obtain

$$n_{i0}\frac{\partial E}{\partial \mathbf{q}}\frac{\nabla c}{c} = J_{if} = n_{i0}a(\mathbf{q}\nabla c)\int \sigma^*_{if}\,\frac{\partial \varepsilon}{\partial p}\,n_{0f}(1-n_{0f})\,d\tau_f,$$

where σ^*_{if} is the transport cross section for the scattering of an impurity on a Fermi excitation;

$$\sigma^*_{if} = -\frac{1}{2}\int \sigma_{if}(1-\cos\psi)\,d\cos\psi.$$

Here ψ is the angle between the vectors $\mathbf{q}$ and $\mathbf{q}'$. According to (21) σ^*_{if} does not depend on the energy of the colliding particles; we therefore obtain

$$\delta n_i = -\frac{n_{i0}}{c}\left\{\sigma^*_{if}(MkT)\left[\frac{\partial \varepsilon}{\partial p}\frac{d\tau_f}{d\varepsilon}\right]_{\varepsilon=\mu}\right\}^{-1}(\mathbf{q}\nabla c).$$

With the aid of δn_i it is easy to calculate the impurity current

$$\mathbf{i} = \int \mathbf{q}\,\delta n_i\,d\mathbf{q} = -\frac{\rho}{m_4\sigma^*_{if}(\partial\tau_f/\partial p)_{\varepsilon=\mu}}\nabla c. \tag{25}$$

A comparison of (25) with (6) yields the diffusion coefficient in this limiting case:

$$D = \frac{1}{m_4\sigma^*_{if}}\frac{1}{(\partial\tau_f/\partial p)_{\varepsilon=\mu}} = \pi^2\left(\frac{\hbar}{p_0}\right)^2\frac{\hbar}{\sigma^*_{if}m_4} = \frac{2kT}{3m_4}t_{if}, \tag{26}$$

where

$$t_{if}^{-1} = {}^3/_2\,\sigma^*_{if}\,kTN_3v_f/\mu \tag{27}$$

is the effective time for the scattering of impurities on Fermi particles; $v_f = p_0/m$; $N_f = {}^3/_2 N_3kT/\mu$ is the number of Fermi particles in the diffuse zone. As already noted, the high-temperature region is given by the condition $t_{ff} \ll t_{fi}$, i.e.,

$$\bar{c} \ll (T/T_0)^2, \qquad kT_0 = \mu. \tag{28}$$

According to (26) and (27), when (28) is satisfied the diffusion coefficient for a weak solution of He^4 in liquid He^3 is constant, being independent of both concentration and temperature.

The Low-Temperature Region. We now consider the opposite limit, when the number of impurity excitations is much greater than the effective number of excitations in the diffuse Fermi zone. This condition is represented more exactly by $t_{ii} \ll t_{if}$, where $t_{ii}^{-1} = \sigma^*_{ii}N_4\bar{v}_i$, $t_{if}^{-1} = \sigma^*_{fi}N_fv_f$ are the effective times for the scattering of impurities and Fermi excitations on impurities. The low-temperature region is therefore represented by the inequality

$$\bar{c} \gg (T/T_0)v_f/\bar{v}_i,\ v_f = p_0/m,\ \bar{v}_i \sim 2(2kT/\pi M)^{1/2} \tag{28a}$$

In this case the impurity distribution function departs from equilibrium much less than the Fermi function. Therefore φ may be neglected by comparison with ψ in the collision integrals J_{if} and J_{fi} in (20). To determine ψ we use the kinetic equation for Fermi excitations:

$$\frac{\partial n_{f0}}{\partial \varepsilon}kT\frac{\partial \varepsilon}{\partial \mathbf{p}}\frac{m_3}{m_4}\nabla c = J_{fi} + J_{ff}. \tag{29}$$

The two ways of determining ψ yield identical results: 1) by omitting J_{ff} in (29) as a small quantity because $t_{fi} \ll t_{ff}$; 2) by multiplying (29) by the Fermi-particle momentum $\mathbf{p}$ and integrating with respect to $d\tau_p$. Since $\int \mathbf{p}J_{ff}d\tau_p = 0$

we thus eliminate J_{ff}. We shall use the first method. In virtue of what has been stated above in connection with the solution in the high-temperature region, we now obtain

$$J_{fi} = -kT\frac{\partial n_{f0}}{\partial\varepsilon}\, b\,(\mathbf{p}\nabla c)\, N_4\sigma^*_{fi}\frac{\partial\varepsilon}{\partial p}.$$

Hence

$$\delta n_f = -\frac{m_3}{m_4}\frac{kT}{m}\frac{\partial n_{f0}}{\partial\varepsilon}\frac{1}{\sigma^*_{fi}v_f N_4}(\mathbf{p}\nabla c). \tag{30}$$

Using the momentum conservation law $\mathbf{g}_i + \mathbf{g}_f = 0$, we obtain for the impurity current

$$\mathbf{g}_i = -\int \mathbf{p}\,\delta n_f\, d\tau_f = -\rho D\nabla c. \tag{31}$$

(30) and (31) are used to give the diffusion coefficient

$$D = (km / p_0\sigma^*_{fi}\rho)\, T / c = (kT / m_4)\, t_{fi}, \tag{32}$$

where

$$t_{fi}^{-1} = \sigma^*_{if} N_4 v_f. \tag{33}$$

It is easily seen from (26) – (28) and (32) — (33) that an interpolation formula for the diffusion coefficient which includes both limiting cases is given by

$$D = tkT / m_4, \quad \text{where } 1/t = (3/2t_{if} + 1/t_{fi}).$$

We may treat analogously the case in which Fermi excitations are described by spectrum (3) and impurities by spectrum (4). The cross section (21a) must now be used; omitting the steps of the calculation we give the results: a) for high temperatures

$$D = \frac{4}{3}\sqrt{\frac{2}{\pi}}\left(\frac{k}{M}\right)^{1/2}\left(\frac{m_3}{\rho\sigma^*_{if}}\right)\frac{\mu_{lim}}{k}T^{-1/2}, \tag{34}$$

b) for low temperatures

$$D = \frac{1}{6}\frac{k}{\mu_{lim}}\frac{p_0}{\rho\sigma^*_{if}}\frac{T}{c}. \tag{35}$$

In (34) and (35) μ_{lim} denotes the Fermi energy limit for spectrum (3):

$$\mu_{lim} = [\rho(2\pi\hbar)^2 / m_3 16\pi p_0^2\sqrt{2m}]^2.$$

In liquid He^3, $\mu_{lim} = 1.05$° K when this spectrum is realized.[3]

4. THERMAL DIFFUSION

With non-zero concentration and temperature gradients in the solution at constant pressure, the impurity current $\mathbf{i}$ is defined by (6). The system of kinetic equations for thermal diffusion is

$$n_{i0}\frac{\partial E}{\partial \mathbf{q}}\left(\frac{E}{kT} - \frac{3}{2}\right)\frac{\nabla T}{T} = J_{if} + J_{ii},$$

$$-\frac{\partial n_{0f}}{\partial\varepsilon}\frac{\partial\varepsilon}{\partial\mathbf{p}}\left(\frac{\varepsilon-\mu}{T} - s\right)\nabla T = J_{ff} + J_{fi}.$$

The thermal diffusion ratio k_T is calculated just like the diffusion coefficient; for spectrum (2) we obtain $k_T = c$. Thus the thermal diffusion coefficient is smaller than the diffusion coefficient by a factor equal to the concentration.

5. VISCOSITY

At sufficiently low temperatures, for which alone the present theory is valid, the viscosity coefficient η of the solution will consist of the coefficient η_f of Fermi viscosity, resulting from momentum transfer by Fermi particles, and the coefficient η_i of impurity viscosity, resulting from momentum transfer by impurity particles:

$$\eta = \eta_f + \eta_i. \tag{36}$$

a) Fermi Viscosity of the Solution

The kinetic equation for Fermi excitations when the system contains non-zero gradients of the macroscopic velocity $\mathbf{u}$ is

$$-\frac{1}{2}\frac{\partial n_{0f}}{\partial\varepsilon}\left(p_i\frac{\partial\varepsilon}{\partial p_k} - \frac{1}{3}p_l\frac{\partial\varepsilon}{\partial p_l}\delta_{ik}\right)$$
$$\times\left(\frac{\partial u_i}{\partial x_k} + \frac{\partial u_k}{\partial x_i} - \frac{2}{3}\frac{\partial u_l}{\partial x_l}\delta_{ik}\right) = J_{ff} + J_{fi}.$$

We choose our z axis in the direction of the velocity and let the velocity gradient be perpendicular to the z axis along the x axis. In spherical coordinates with a polar z axis the kinetic equation then becomes

$$\frac{\partial n_{0f}}{\partial\varepsilon}p\frac{\partial\varepsilon}{\partial p}\frac{\partial u}{\partial x}\cos\theta\sin\theta\cos\varphi = J_{ff} + J_{fi}.$$

In accordance with the symmetry of the problem the solution of the kinetic equation will be sought in the form

$$\phi = p\frac{\partial\varepsilon}{\partial p}\frac{\partial u}{\partial x}\cos\theta\sin\theta\cos\varphi\, b(\varepsilon).$$

Since a general solution is hardly possible, we shall determine the dependence of n_f on temperature and concentration in the two limiting cases. 1) At high temperatures the number of Fermi particles in the diffuse zone is given by $N_f \gg N_4$ (more exactly: $t_{ff} \ll t_{fi}$, $t_{if} \ll t_{ii}$). In this case only the scattering of Fermi particles by each other is important and J_{fi} may be omitted from the kinetic equation. 2) At low temperatures the number of Fermi particles in the diffuse zone is given by $N_f \ll N_4$. Here only collisions between Fermi particles and impurities are important and collisions between Fermi particles may be neglected. The intermediate region can be obtained by interpolating between the two limiting cases.

The High-Temperature Region. The collision integral J_{ff} in (20) is

$$J_{ff} = \int w_{ff}\, n_{f01} n_{f02} (1 - n'_{f01})(1 - n'_{f02})(\psi_1 + \psi_2 - \psi'_1 - \psi'_2) \times \delta(\mathbf{p}_1 + \mathbf{p}_2 - \mathbf{p}'_1 - \mathbf{p}'_2)\,\delta(\varepsilon_1 + \varepsilon_2 - \varepsilon'_1 - \varepsilon'_2)\, d\tau_2 d\tau'_1 d\mathbf{p}'_2. \quad (37)$$

If we assume that the collision probability w_{ff} depends only on the angles between momenta, by transforming to dimensionless variables in the collision integral we find that it can be represented by

$$J_{ff} = \overline{\sigma^*_{ff}}\, n_{f01}(1 - n_{f01}) \times \cos\theta \sin\theta \cos\varphi \frac{\partial u}{\partial x} p \frac{\partial \varepsilon}{\partial p} \int b v_f n_{0f} (1 - n_{0f})\, d\tau, \quad (38)$$

where

$$\overline{\sigma^*_{ff}} = (kT/\mu)\, \overline{\sigma^*_{ff,0}}, \quad (39)$$

in which $\overline{\sigma^*_{ff0}}$ is the viscosity transport cross section.[4*] We shall, as usual, calculate the z component of the momentum transported in the x direction:

$$\Pi^f_{xz} = -\int p \frac{\partial \varepsilon}{\partial p} \cos\theta \sin\theta \cos\varphi\, \delta n\, d\tau = \eta_f \frac{\partial u}{\partial x}. \quad (40)$$

The result obtained is (see reference 14)

$$\eta_{fh} = \frac{2}{15} (p_0 / \overline{\sigma}_{ff\,0}) \left(\frac{\mu}{k}\right)^2 T^{-2} = \frac{1}{5} N_3 \frac{p_0^2}{m} \bar{t}_{ff}. \quad (41)$$

We have thus obtained the Pomeranchuk temperature law $\eta \sim T^{-2}$, as is not surprising since our initial premises agree with those of Pomeranchuk.

The Low-Temperature Region. Here only the scattering of Fermi particles by impurities is important; we therefore omit J_{ff} in the kinetic equation for Fermi excitations. In calculating J_{fi} we also consider that in this case $\delta n_i \ll \delta n_f$, and that therefore in J_{fi} n_i may be replaced by the equilibrium Maxwellian distribution function n_{i0}. As a result we have

$$J_{fi} = v_f \overline{\sigma^*_{fi}}\, n_{f0} (1 - n_{f0})\, p \frac{\partial \varepsilon}{\partial p} \frac{\partial u}{\partial x} \cos\theta \sin\theta \cos\varphi N_4 b.$$

In this case the effective deviation of the Fermi distribution function from equilibrium will be

$$\delta n_f = -\frac{1}{kT} n_{f0} (1 - n_{f0})\, p \frac{\partial \varepsilon}{\partial p} \frac{\partial u}{\partial x} \bar{t}_{fi} \cos\theta \sin\theta \cos\varphi, \quad (42)$$

where

$$\bar{t}_{fi} = 1 / \overline{\sigma^*_{if}} N_4 v_f. \quad (43)$$

Here $\overline{\sigma^*_{fi}}$ is the viscosity transport cross section. The ordinary transport cross section which is obtained when diffusion and thermal conductivity are considered is denoted by the same symbol without a bar. We use (42) and (40) to determine the Fermi part of the viscosity coefficient at low temperatures:

$$\eta_{fi} = p_0 / 5 \overline{\sigma^*_{fi}}\, \bar{c} = N_3 p_0^2 \bar{t}_{fi} / 5m. \quad (44)$$

We note that at low temperatures η_f is inversely proportional to the concentration.

An interpolation formula for η_f which gives correct values in both limiting cases is

$$\eta_f = N_3 p_0^2 \bar{t}_f / 5m, \quad 1/\bar{t}_f = (1/\bar{t}_{ff} + 1/\bar{t}_{fi}). \quad (45)$$

b) Impurity Viscosity of the Solution

The impurity viscosity of the solution is calculated in exactly the same manner as the Fermi part of the viscosity coefficient. The interpolation formula for η_i which gives correct values at the high-temperature and low-temperature limits is therefore

$$\eta_i = (cp/m_4) kT \bar{t}_i, \quad \bar{t}_i^{-1} = (\bar{t}_{if}^{-1} + \bar{t}_{ii}^{-1}),$$

where

$$1/\bar{t}_{ii} = \bar{v}_i \overline{\sigma^*_{ii}} N_4, \quad 1/\bar{t}_{if} = v_f \overline{\sigma^*_{if}} N_f,$$

$$N_f = (3T/2T_0) N_3. \quad (46)$$

In all of the foregoing calculations σ_{ff0}, σ^*_{if} and σ_{ii} [(21 and (22)] were constants, being independent of momentum. In the theory that has been developed here these quantities are unknown and are determined and normalized by comparing the theory with experiment. For a preliminary estimate of the contributions made by different processes to the viscosity of the solution we set

$$\overline{\sigma^*_{ff\,0}} \sim a_1 \cdot 10^{-15}\ \text{cm}^2, \quad \overline{\sigma^*_{if}} \sim a_2 \cdot 10^{-15}\ \text{cm}^2,$$

$$\overline{\sigma^*_{ii}} \sim a_3 \cdot 10^{-15}\ \text{cm}^2,$$

where a_1, a_2, and a_3 are constants of the order of unity.

Furthermore,[3]

$$\mu/k = p_0^2/2mk = 3.3°\text{K}, \quad m = 1.43\, m_3,$$

$$p_0/\hbar = 0.76 \cdot 10^{-8}\ \text{cm}^{-1}, \quad \rho = 0.078\ \text{g/cm}^3.$$

Unlike the ordinary transport cross section (which we denote by σ), the vicosity transport cross section $\overline{\sigma^*}$ is obtained by averaging the corresponding cross sections multiplied by $(1 - \cos\psi)^2 \sin^2\varphi$. This is shown in greater detail in reference 14.

Inserting these numerical values into (36), (45), and (46), we obtain the following expression for the viscosity of the solution:

$$\eta = 1.24 \cdot 10^{-4} / a_1 T^2 \{1 + 7.2 (a_2 / a_1) cT^{-2}\}$$

$$+ 2.1 \cdot 10^{-5} / a_2 \{1 + 1.1 (a_3 / a_2) cT^{-1/2}\}.$$

6. THERMAL CONDUCTIVITY

The thermal conductivity coefficient κ of the solution, like the viscosity coefficient, includes Fermi and impurity parts:

$$\varkappa = \varkappa_f + \varkappa_i. \quad (47)$$

The system of kinetic equations required to determine the thermal conductivity is the same as that used in discussing thermal diffusion and is given in Sec. 4. In accordance with the symmetry of the problem we seek a solution in the form

$$\varphi = \left[E / kT - \frac{3}{2}\right] \left(\frac{\partial E}{\partial \mathbf{q}} \frac{\nabla T}{T}\right) a, \quad \psi = \left\{\frac{\varepsilon - \mu}{T} - s\right\} \left(\frac{\partial \varepsilon}{\partial \mathbf{p}} \nabla T\right) b.$$

Further calculations are entirely analogous to those performed for the viscosity. We first calculate the Fermi part of the thermal conductivity coefficient in the high-temperature and low-temperature limits (κ_{fh} and κ_{fl}, respectively). An interpolation formula for κ_f is then constructed. The impurity part κ_i of the thermal conductivity coefficient is calculated similarly. The results are

$$\varkappa_{fh} = {}^5/_6 C_0 (p_0 / m)^2 t_{ff}, \quad \varkappa_{fl} = {}^5/_6 C_0 (p_0 / m)^2 t_{fi},$$

$$\varkappa_{ih} = 5 (\rho k^2 / m_4 M) cT t_{if}, \quad \varkappa_{il} = 5 (\rho k^2 / m_4 M) cT t_{ii}.$$

Interpolation formulas for κ_f and κ_i are

$$\varkappa_f = {}^5/_6 C_0 (p_0 / m)^2 t_f, \quad t_f^{-1} = t_{ff}^{-1} + t_{fi}^{-1},$$

$$\varkappa_i = 5 (\rho k^2 / m_4 M) cT t_i, \quad t_i^{-1} = t_{if}^{-1} + t_{ii}^{-1},$$

where C_0 is the specific heat of a unit volume of pure liquid He^3 and the other quantities have the same meanings as in (45) and (46) for the viscosity. The absence of bars indicates that we are here using the ordinary transport cross sections.[4] We note that at the high-temperature limit Pomeranchuk's law[1] for the thermal conductivity, $\kappa_f \sim T^{-1}$, is obtained.

In conclusion the authors wish to express their deep gratitude to B. I. Davydov for a valuable discussion.

---

[1] I. Ya. Pomeranchuk, J. Exptl. Theoret. Phys. (U.S.S.R.) **20**, 919 (1950).

[2] L. D. Landau, J. Exptl. Theoret. Phys. (U.S.S.R.) **30**, 1058 (1956), Soviet Phys. JETP **3**, 920 (1957).

[3] I. M. Khalatnikov and A. A. Abrikosov, J. Exptl. Theoret. Phys. (U.S.S.R.) **32**, 915 (1957), Soviet Phys. JETP **5**, 745 (1957).

[4] A. A. Abrikosov and I. M. Khalatnikov, J. Exptl. Theoret. Phys. (U.S.S.R.) **32**, 1083 (1957), Soviet Phys. JETP **5**, 887 (1957).

[5] L. D. Landau, J. Exptl. Theoret. Phys. (U.S.S.R.) **35**, 97 (1958), Soviet Phys. JETP **8**, 70 (1959).

[6] L. D. Landau and I. Ya. Pomeranchuk, Dokl. Akad. Nauk SSSR **59**, 669 (1948).

[7] L. D. Landau and E. M. Lifshitz, Механика сплошных сред (*Mechanics of Continuous Media*), Gostekhizdat, Moscow, 1953.

[8] V. P. Silin, J. Exptl. Theoret. Phys. (U.S.S.R.) **34**, 707 (1958), Soviet Phys. JETP **7**, 486 (1958).

[9] E. Schrödinger, *Statistical Thermodynamics*, Cambridge Univ. Press, 1946.

[10] I. Ya. Pomeranchuk, J. Exptl. Theoret. Phys. (U.S.S.R.) **19**, 42 (1949).

[11] L. D. Landau and E. M. Lifshitz, Статистическая физика (*Statistical Physics*), Gostekhizdat, M.-L., 1951.

[12] I. M. Khalatnikov and V. N. Zharkov, J. Exptl. Theoret. Phys. (U.S.S.R.) **32**, 1108 (1957), Soviet Phys. JETP 5, 905 (1957).

[13] L. D. Landau and E. M. Lifshitz, Квантовая механика (*Quantum Mechanics*), Gostekhizdat, Moscow, 1948, Engl. Transl. Addison-Wesley, 1958.

[14] A. A. Abrikosov and I. M. Khalatnikov, Usp. Fiz. Nauk **64**, 177 (1958).

Translated by I. Emin
23

SOVIET PHYSICS JETP VOLUME 37 (10), NUMBER 1 JANUARY, 1960

SECOND FORBIDDEN COULOMB β-DECAY TRANSITIONS

Yu. V. GAPONOV

Institute of Nuclear Physics, Moscow State University

Submitted to JETP editor January 27, 1959

J. Exptl. Theoret. Phys. (U.S.S.R.) **37**, 154-158 (July, 1959)

From a classification of the terms appearing in the series expansion of the β-decay interaction Hamiltonian, rules are obtained which make it possible to predict which nuclear matrix elements contribute to β transitions of a given type, and to estimate the values of these elements. It is shown that there exists a simple case of second forbidden Coulomb transitions, Δj = 2 (no), with properties similar to those of unique transitions. The angular β-ν correlation, the β-γ correlation with circularly polarized γ quantum, and the spectrum are found for this case.

THE study of the angular correlations in the general case of β decay is extremely complicated, since the theoretical formulas contain a large number of unknown nuclear matrix elements. The special cases in which the number of nuclear matrix elements is a minimum are the simplest from the point of view of the interpretation of the experimental results. Many papers have been devoted to the study of the correlations in allowed transitions, in which there are not more than two such unknown matrix elements. In particular, the angular β-ν correlation and the β-γ correlation with circularly polarized γ-ray quantum have been analyzed in a number of papers.[1-4] Cases of interest among the forbidden β-decay transitions are those of unique transitions and of the so-called first-forbidden Coulomb transitions. In the former case, the number of unknown nuclear matrix elements is one, and in the latter case, three, so that in the former case the correlations do not depend on the matrix elements at all, and in the latter case they depend on two ratios of matrix elements. These cases have been treated in a number of papers.[5-9]

In the present paper we derive simple rules that make it possible to predict which nuclear matrix elements will contribute to β-decay transitions of a given type, and to get approximate values of these elements. Second forbidden transitions are studied on the basis of these rules. It is shown that there is a simple case of Coulomb transitions, Δj = 2 (no), with properties similar to those of the unique transitions. The angular β-ν correlation and the β-γ correlation with circularly polarized γ-ray quantum are found for this case.

1. THE NUCLEAR MATRIX ELEMENTS

Let us take the Hamiltonian of the β-decay interaction in the form proposed by Gell-Mann and Feynman[10]

$$H = G\,[\overline{\Psi}_p\gamma_\mu(1+\lambda\gamma_5)\Psi_n]\left[\overline{\Phi}_e\gamma_\mu\frac{1}{\sqrt{2}}(1+\gamma_5)\,\Phi_\nu\right]. \qquad (1)$$

In the Coulomb field of a nucleus of charge Z, the wave function of an electron with momentum **p**, total energy E, and spin component ξ can be represented as the sum of two bispinors:

$$\Phi_{\mathbf{p},\xi} = 4\pi\sum_{j\mu}\begin{pmatrix}\sqrt{\frac{E+1}{2E}}N_j\left[(A_j+B_j)\,\Omega_{j\mu}^{(l)}\left(\frac{\mathbf{r}}{r}\right)(\Omega_{j\mu}^{(l)}(\mathbf{n}))_\xi^* + (A_j'+B_j)\,\Omega_{j\mu}^{(l')}\left(\frac{\mathbf{r}}{r}\right)(\Omega_{j\mu}^{(l')}(\mathbf{n}))_\xi^*\right]\\ \sqrt{\frac{E-1}{2E}}N_j\left[(A_j-B_j)\,\Omega_{j\mu}^{(l)}\left(\frac{\mathbf{r}}{r}\right)(\Omega_{j\mu}^{(l')}(\mathbf{n}))_\xi^* + (A_j'-B_j)\,\Omega_{j\mu}^{(l')}\left(\frac{\mathbf{r}}{r}\right)(\Omega_{j\mu}^{(l)}(\mathbf{n}))_\xi^*\right]\end{pmatrix}$$

$$l = j - {}^1/_2, \qquad l' = j + {}^1/_2, \qquad \mathbf{n} = \mathbf{p}/p;$$

$$A_j = \gamma_j + i\frac{\alpha ZE}{p} + \frac{\gamma_j - i\alpha ZE/p}{\gamma_j + i\alpha ZE/p}(j + {}^1/_2), \qquad B_j = \frac{\gamma_j - i\alpha ZE/p}{\gamma_j + i\alpha ZE/p}\,i\,\frac{\alpha ZE}{p}, \qquad A_j' = \gamma_j + i\frac{\alpha ZE}{p} - \frac{\gamma_j - i\alpha ZE/p}{\gamma_j + i\alpha ZE/p}(j + {}^1/_2),$$

$$N_j = \frac{2\Gamma(\gamma_j + i\alpha ZE/p)}{\Gamma(2\gamma_j + 1)}e^{\pi\alpha ZE/2p}(2pr)^{\gamma_j - 1}e^{i\pi(\gamma_j - 1)/2}, \qquad \gamma_j = \sqrt{(j + {}^1/_2)^2 - (\alpha Z)^2}, \qquad \alpha = 1/137. \qquad (2)$$

The first bispinor contains $\Omega_{j\mu}^{(l)}(\mathbf{r}/r)$ and can be regarded as the term corresponding to the emission of the electron with total angular momentum j and orbital angular momentum $l = j - \frac{1}{2}$. The second contains $\Omega_{j\mu}^{(l')}(\mathbf{r}/r)$ and can be regarded as the term corresponding to the emission of the electron with orbital angular momentum $l' = j + \frac{1}{2}$.

For $Z \rightarrow 0$, the terms of the second type go to zero, and the terms of the first type go over into the usual expansion of a plane wave in spherical functions. Similarly, the wave function of a neutrino with momentum $\mathbf{q}$ and spin component η is

$$\Phi_{\mathbf{q},\eta} = 4\pi \sum_{j_\nu \nu} \frac{1}{\sqrt{2}} (2 j_\nu + 1) M_{j_\nu} \begin{pmatrix} \Omega_{j_\nu \nu}^{(l_\nu)} (\mathbf{r}/r) [\Omega_{j_\nu \nu}^{(l_\nu)} (\mathbf{v})]_\eta^* \\ \Omega_{j_\nu \nu}^{(l_\nu)} (\mathbf{r}/r) [\Omega_{j_\nu \nu}^{(l'_\nu)} (\mathbf{v})]_\eta^* \end{pmatrix};$$

$$l_\nu = j_\nu - {}^1/_2, \qquad l'_\nu = j_\nu + {}^1/_2, \qquad \mathbf{v} = \mathbf{q}/q;$$

$$M_{j_\nu} = \frac{2\Gamma(j_\nu + {}^1/_2)}{\Gamma(2j_\nu + 2)} (2qr)^{j_\nu - {}^1/_2} \exp\{i\pi (j_\nu - {}^1/_2)/2\}. \tag{3}$$

The substitution of Eqs. (2) and (3) in Eq. (1) breaks the Hamiltonian up into a sum of terms; each contains one term from the expansion of the electron wave function and one from the neutrino function, and can be characterized by the two quantum numbers (j, l) of the electron and the two numbers (j_ν, l_ν) for the neutrino. In addition, the terms differ in the part referring to the nucleus. Here they are divided into the nonrelativistic terms with the operators γ_4 and $\boldsymbol{\gamma}\gamma_5$ between the wave functions of the initial and final states of the nucleus, and the relativistic terms, which have the operators $\gamma_4\gamma_5$ and $\boldsymbol{\gamma}$; the latter are of the order v_{nuc}/c compared with the former, where v_{nuc} is the average speed of the nucleons in the nucleus. The parity is $(-1)^{l+l_\nu}$ for the nonrelativistic terms and $(-1)^{l+l_\nu+1}$ for the relativistic terms.

Thus all the terms of the Hamiltonian can be classified in terms of four quantum numbers and the parity (cf. table). Their values can be found approximately with the factor $N_j M_{j_\nu}$. It is easy to see that as to their values, the terms are naturally divided into three groups: the ordinary type, the Coulomb type ($\sim \alpha Z$), and the relativistic terms (v_{nuc}/c).

j	l or l'	j_ν	l_ν	Parity	Estimate of value
1/2	0	1/2	0	no	1
3/2	1	1/2	0	yes	pR
1/2	1	1/2	0	yes	αZ
1/2	0	3/2	1	yes	qR
1/2	0	1/2	0	yes	v_{nuc}/c
5/2	2	1/2	0	no	$(pR)^2$
3/2	1	3/2	1	no	$pR\,(qR)$
1/2	0	5/2	2	no	$(qR)^2$
3/2	2	1/2	0	no	$\alpha Z\,(pR)$
1/2	1	3/2	1	no	$\alpha Z\,(qR)$
3/2	1	1/2	0	no	$(v_{\text{nuc}}/c)\,(pR)$
1/2	0	3/2	1	no	$(v_{\text{nuc}}/c)\,(qR)$
1/2	1	1/2	0	no	$(v_{\text{nuc}}/c)\,\alpha Z$

Each term of the expansion of the Hamiltonian can lead to several nuclear matrix elements. This is due to the fact that the classification has been carried out in terms of the quantum numbers of the individual particles (electron and neutrino), whereas the nuclear matrix element is characterized by the set of quantum numbers of the pair as a whole. In fact in the general case, a nuclear matrix element can be written

$$(j_2 | \overline{\Psi}_{j_2 m_2} O_s \Psi_{j_1 m_1} r^k Y_{LM}^* | j_1)_J \equiv \langle O_s r^k Y_{LM}^* \rangle_J. \tag{4}$$

Such "reduced" matrix elements are connected with the usual expressions written as integrals by the relation

$$\int \overline{\Psi}_{j_2 m_2}(\mathbf{r}) O_s \Psi_{j_1 m_1}(\mathbf{r}) r^k Y_{LM}^* \left(\frac{\mathbf{r}}{r}\right) d\mathbf{r}$$

$$= \frac{1}{\sqrt{4\pi}} \sum_{JN} C_{j_1 m_1}^{j_2 m_2 JN} C_{JN}^{LMS\sigma} \langle O_s r^k Y_{LM} \rangle_J. \tag{5}$$

Here $O_S = \gamma_4, \gamma_4\gamma_5, \boldsymbol{\gamma}$, and $\boldsymbol{\gamma}\gamma_5$, with the first two of these operators corresponding physically to the emission of the electron-neutrino pair in a singlet state, $S = 0$, and the other two to emission of the pair in a triplet state, $S = 1$. The order L of the spherical harmonic represents the orbital momentum of the pair, and J its total angular momentum, which is formed from S and L by the vector-addition rule $\mathbf{J} = \mathbf{L} + \mathbf{S}$, to which there corresponds the sum over J in Eq. (5). The parity of the nuclear matrix element is $(-1)^L$ for nonrelativistic elements and $(-1)^{L+1}$ for relativistic elements and, as will be seen shortly, is the same as the parity of the term in the expansion of the Hamiltonian that leads to the matrix element in question. The degree k is the power of R in the estimate given in the table for this term.

Thus any matrix element is fully characterized by the set of quantum numbers J, L, S. This set can be found from the quantum numbers of the electron and neutrino by the rules of vector addition. For this relationship we must require that the triangle rule hold for all rows and columns of the array

$$\begin{pmatrix} l & {}^1/_2 & j \\ l_\nu & {}^1/_2 & j_\nu \\ L & S & J \end{pmatrix}.$$

Furthermore, the additional condition $l + l_\nu + L$ = (even number), must be satisfied. By using these rules we can find for any term in the table the nuclear matrix elements that correspond to it.

A nuclear matrix element of a definite type contributes to the β-decay transition if two conditions are satisfied:

$$|j_2 - j_1| \leqslant J \leqslant j_2 + j_1,$$

$$\Pi = \begin{cases} (-1)^L & \text{for nonrelativistic nuclear matrix elements,} \\ (-1)^{L+1} & \text{for relativistic elements,} \end{cases}$$

where j_1 is the angular momentum of the initial nucleus, j_2 is that of the final nucleus, and Π is the change of parity in the β decay.

For example, the term of order $\alpha Z(qR)$ (no) leads to four types of nuclear matrix elements; two of them, with $J = 1$, give small corrections to allowed transitions, and the other two, with $J = 2$, contribute to forbidden transitions $\Delta j = 2$ (no).

2. THE SECOND-FORBIDDEN COULOMB TRANSITIONS

As has already been remarked, all the terms of the expansion of the Hamiltonian (1) fall naturally into three groups: terms of the ordinary type, those of the Coulomb type, and relativistic terms. The contribution of terms of the Coulomb type rises rapidly with increase of the charge of the nucleus, so that even for nuclei with $Z \geq 30$, all other terms can be neglected in comparison with Coulomb terms. Such β-decay transitions are called Coulomb transitions. They are realized when $\alpha Z \gg pR$ (or qR) and $\alpha Z \gg v_{\text{nuc}}/c$. In this case in the second order of the expansion of the Hamiltonian, there remain two terms: $\alpha Z(qR)$ and $\alpha Z(pR)$. For second-forbidden transitions $[\Delta j = 2, 3 \text{ (no)}]$ these terms lead to two nuclear matrix elements $\langle rY_{2M}\rangle_2$ and $\langle \gamma\gamma_5 rY_{2M}\rangle_2$. They do not contribute to the unique β-decay transitions.

The writer has made a calculation of the angular β-ν correlation and β-γ correlation with circularly polarized γ-ray quantum, neglecting the finite size of the nucleus. It was found that these two matrix elements always enter in the same combination,

$$\sqrt{2}\langle rY_{2M}\rangle_2 + \lambda\langle\gamma\gamma_5 rY_{2M}\rangle_2,$$

so that this case is like that of the unique β-decay transitions, whose angular correlation functions do not depend on nuclear matrix elements and can be found exactly.

We note that the correlation functions do not depend on the matrix elements also in the case of a Hamiltonian (1) of the most general form.

If the neutrino emerges at the angle φ with the direction of emission of the electron, the probability function is

$$W(\varphi) = \sum_r a_r P_r(\cos\varphi), \qquad 0 \leqslant r \leqslant 2;$$

$$a_0 = \tfrac{2}{5}[(|c_1|^2 + |c_2|^2) + (|c_3|^2 + |c_4|^2)|d|^2],$$

$$a_1 = \tfrac{2}{5}\,2\mathrm{Re}\,[(c_1c_3^* + c_2c_4^*)\,d] - \tfrac{2}{25}\,2\mathrm{Re}\,(c_1c_2^* + c_3c_4^*|d|^2),$$

$$a_2 = -\tfrac{2}{25}\,2\mathrm{Re}\,[(c_1c_4^* + c_2c_3^*)\,d]. \tag{5}$$

The probability of emission of a circularly polarized γ-quantum with polarization $\mu = \pm 1$ (right or left) at the angle θ with the direction of emission of the electron is given by

$$W(\theta) = \sum_R \beta_R \gamma_R P_R(\cos\theta), \qquad 0 \leqslant R \leqslant 3;$$

$$\beta_0 = a_0, \quad \beta_1 = -\frac{\sqrt{6}}{15}\,2\mathrm{Re}\left[c_1c_2^* - \tfrac{3}{5}c_3c_4^*|d|^2\right],$$

$$\beta_2 = \frac{\sqrt{70}}{20}(|c_3|^2 + |c_4|^2), \qquad \beta_3 = \tfrac{6}{25}\sqrt{\tfrac{2}{7}}\,2\mathrm{Re}\,(c_3c_4^*|d|^2). \tag{6}$$

We have found the quantity γ_R for an arbitrary γ-ray transition or cascade of γ-ray quanta in an earlier paper.[9] In the simplest case, in which β decay to an excited level j_2 is followed by a γ-ray transition with angular momentum L (of electric or magnetic type) to the level j_3,

$$\gamma_R = C_{L-\mu}^{L-\mu R0}\sqrt{(2j_2+1)(2L+1)}\,W(j_2j_3RL;\ Lj_2). \tag{7}$$

In Eqs. (5) and (6) the quantities c_1, c_2, etc. have the form

$$c_1 = 4\sqrt{(E+1)/E}\,(A'_{1/2} + B_{1/2}),$$

$$c_2 = 4\sqrt{(E-1)/E}\,(A'_{1/2} - B_{1/2}),$$

$$c_3 = 2\sqrt{(E+1)/E}\,(A'_{3/2} + B_{3/2}),$$

$$c_4 = 2\sqrt{(E-1)/E}\,(A'_{3/2} - B_{3/2}),$$

$$d = \frac{12\Gamma(\gamma_2 - i\alpha ZE/p)}{\Gamma(\gamma_1 - i\alpha ZE/p)}\,\frac{\Gamma(2\gamma_1+1)}{\Gamma(2\gamma_2+1)}\,\frac{p}{q}.$$

The β-ray spectrum of a second-forbidden Coulomb transition can be found from the usual formula

$$T = \frac{2\pi}{\hbar}|H|^2\rho(E), \qquad |H|^2 = \frac{\pi^2}{2}a_0|M|^2,$$

$$|M|^2 = \frac{32}{9}G^2p^2q^2\,\frac{|\Gamma(\gamma_1 - i\alpha ZE/p)|^2}{|\Gamma(2\gamma_1+1)|^2}\,e^{\pi\alpha ZE/p}$$

$$\times\,|\sqrt{2}\langle rY_{2M}\rangle_2 + \lambda\langle\gamma\gamma_5 rY_{2M}\rangle_2|^2.$$

The writer expresses his gratitude to Professor I. S. Shapiro for valuable suggestions and for his constant interest in this work.

---

[1] M. Morita and R. S. Morita, Phys. Rev. **107**, 139 (1957).

[2] Alder, Stech, and Winther, Phys. Rev. **107**, 728 (1957).

[3] M. Morita and R. S. Morita, Phys. Rev. **107**, 1316 (1957).

[4] Yu. V. Gaponov and V. S. Popov, J. Exptl. Theoret. Phys. (U.S.S.R.) **33**, 256 (1957), Soviet Phys. JETP **6**, 197 (1958).

[5] Berestetsky, Joffe, Rudik, and Ter-Martirosyan Nucl. Phys. **5**, 464 (1958).

[6] A. Z. Dolginov, Nucl. Phys. **5**, 512 (1958).

[7] M. Morita and R. S. Morita, Phys. Rev. **109**, 2048 (1958).

[8] Berestetsky, Joffe, Rudik, and Ter-Martirosyan, Phys. Rev. **111**, 522 (1958).

[9] Yu. V. Gaponov, J. Exptl. Theoret. Phys. (U.S.S.R.) **36**, 193 (1959), Soviet Phys. JETP **9**, 131 (1959).

[10] R. P. Feynman and M. Gell-Mann, Phys. Rev. **109**, 193 (1958).

Translated by W. H. Furry
24

SOVIET PHYSICS JETP VOLUME 37 (10), NUMBER 1 JANUARY, 1960

CAPTURE OF μ^- MESONS BY LIGHT NUCLEI

B. L. IOFFE

Institute for Theoretical and Experimental Physics, Academy of Sciences U.S.S.R.

Submitted to JETP editor January 29, 1959

J. Exptl. Theoret. Phys. (U.S.S.R.) 37, 159-163 (July, 1959)

Different effects in the capture of μ^- mesons by light nuclei, without neutron or proton emission, are calculated. It is assumed that the interaction is described by the A and V coupling variants. Corrections of first order in nucleon velocity and in $(R/\lambdabar)^2$ are taken into account and turn out to be quite significant. The results of the calculation contain one unknown constant, in addition to the usual matrix element, so that at least two experiments are necessary to verify the theory.

AT the present time there are all grounds for assuming that the interaction of μ mesons with nucleons is analogous to β decay and is described by the axial and vector coupling. We consider within this assumption the capture of μ^- mesons by light nuclei, in which the nucleus jumps into some excited level without emitting either a neutron or a proton.* If the changes in momentum and parity of the nucleus in such a transition have the form $\Delta j = 0, \pm 1$ (no), then the theory of this process is completely analogous to the theory of β decay. The essential difference is that the momentum of the emitted neutrino is of order m_μ (the mass of the muon), so that the corrections after expanding in powers of $R/\lambdabar$ (R is the nuclear radius and $\lambdabar$ the wavelength of the neutrino), and v/c of the nucleon, which are usually small in β decay, are very significant here. At the same time, if one confines oneself to muon capture in nuclei with $A \lesssim 16$, then the magnitude of these corrections is still quite small and it is sufficient (error ~ 5%) to consider terms linear in the nucleon velocity and quadratic in $R/\lambdabar$.

1. We start from the universal theory of weak interactions of Gell-Mann and Feynman[4] in which the β current of the nucleons and pions is conserved and the vector interaction is completely analogous to the electrodynamics. As shown by Gell-Mann,[3] this makes possible expressing the corrections with respect to v/c of the nucleons and $R/\lambdabar$ associated with the vector interaction in terms of the characteristics of the nuclei during γ transitions. The matrix element of the vector interaction, to an accuracy linear with respect to v/c of the nucleons, can be written

$$G_V\int dV\psi_f^*\Big\{J_0e^{-i\mathbf{qr}}-\frac{\mu_V}{2M}\sigma[\nabla\mathbf{J}e^{-i\mathbf{qr}}]$$

$$+\frac{i}{2M}(\nabla\mathbf{J}e^{-i\mathbf{qr}}+\mathbf{J}e^{-i\mathbf{qr}}\nabla)\Big\}\tau\psi_i,$$

$$J_0={}^1/_2\,\overline{\psi}_\nu\beta(1+\gamma_5)\psi_\mu,\qquad \mathbf{J}={}^1/_2\,\overline{\psi}_\nu\beta\boldsymbol{\alpha}(1+\gamma_5)\psi_\mu, \tag{1}$$

where ψ_i and ψ_f are the initial and final wave functions of the nucleus, $\mathbf{q}$ is the momentum of the neutrino, and M is the nucleon mass. The first term in (1) is analogous to an electric interaction with the nuclear charge distribution, the second term to the interaction of the magnetic field with the spin $\mu\boldsymbol{\sigma}\cdot\mathbf{H}$, and the third to the interaction of the electromagnetic field with the current. The quantity $e^{-i\mathbf{q}\cdot\mathbf{r}}$ in (1) is expanded in powers of $\mathbf{q}\cdot\mathbf{r}$ up to the second order. Then the first term in (1) becomes:

$$G_V\int dV\psi_f^*\left(1-\tfrac{1}{6}q^2r^2-\tfrac{1}{6}q_iq_kQ_{ik}\right)\tau\psi_iJ_0;$$

$$Q_{ik}=3r_ir_k-r^2\delta_{ik}. \tag{2}$$

Estimates based on a square-well potential[5,6] (and also experimental data on the magnitude of the quadrupole moment) show that the contribution from the quadrupole interaction in (2) does not exceed a few per cent, and, consequently, the term proportional to Q_{ik} can be omitted. An expansion of the second term of (1) in powers $\mathbf{q}\cdot\mathbf{r}$ contains no term linear in $\mathbf{r}$, by virtue of the selection rules, while the quadratic term is of the order of $^1/_6\,(m_\mu R)^2(m_\mu/M) \lesssim 5\%$ and can also be neglected. Finally, in the third term it is sufficient to keep only the expression in which the operator ∇ acts on the current of light particles

---

*Analogous calculations for the capture of μ mesons by protons was carried out by Wolfenstein[1] and Chou Kuang Chao and Maevskiĭ.[2] The former, however, did not take into account the corrections due to the vector interaction (of the "weak magnetic" type[3]) while the latter, on the contrary, did not take into account the pseudoscalar term, which has considerable practical importance.

$$i\nabla \mathbf{J}e^{-i\mathbf{qr}} = qJ_0.$$

The remaining expressions correspond either to the contribution of the orbital moment to the total magnetic moment of the transition in the nucleus, i.e., they have the same form as the second term in (1) and can be treated like it, or else they are of the order of $\frac{1}{6}(m_\mu R)^2(m_\mu/M)$. The entire matrix element of (1) takes the form

$$G_V\left\{\int dV\psi_f^*\tau\psi_i\left(1-\frac{1}{6}q^2\langle r^2\rangle_e+\frac{q}{2M}\right)J_0 + i\frac{\mu_V}{2M}\int dV\psi_f^*\sigma\tau\psi_i[\mathbf{q}\times\mathbf{J}]\right\}, \qquad (3)$$

where μ_V can be interpreted as the magnetic moment of the transition, while $<r^2>_e$ is the square radius of the nucleus corresponding to the given transition. The quantity μ_V is determined, according to Gell-Mann,[3] from the width of the nuclear γ-line belonging to the same isotopic multiplet, while $<r^2>_e$ can be calculated from experimental data on the inelastic scattering of electrons on nuclei.

2. The matrix element for the axial interaction can be written

$$\int dV\bar{\psi}_f\{G_A\gamma_\lambda\gamma_5 + b(k-q)_\lambda\gamma_5\}\tau\psi_i J_\lambda e^{-i\mathbf{qr}}, \qquad (4)$$

where

$$J_\lambda = \{J_0, \mathbf{J}\}, \quad \gamma_\lambda = \{\beta, \beta\boldsymbol{\alpha}\}, \quad q_\lambda J_\lambda = q_0 J_0 - \mathbf{qJ},$$

and k is the 4-momentum of the meson.* The pseudoscalar interaction — the second term in (4) — arises in the form of a correction to the axial interaction, owing to capture of the μ meson by the virtual π mesons.[1] The constant b was determined by Goldberger and Treiman[7] and found to be very large: $bm_\mu = 8\,G_A$, making allowance for the pseudoscalar term absolutely necessary. By virtue of the identities

$$(k-q)_\lambda J_\lambda = \frac{1}{2}m_\mu\bar{\psi}_\nu(1-\gamma_5)\psi_\mu$$

and $\beta\psi_\mu = \psi_\mu$ (μ meson at rest) it is possible to write (4) in the form:

$$\int dV\psi_f^*\{G_A\sigma\mathbf{J} + [G_A\gamma_5 + bm_\mu\beta\gamma_5]J_0\}\tau\psi_i e^{-i\mathbf{qr}}. \qquad (5)$$

In the nonrelativistic approximation with respect to the nucleon, both matrix elements $\psi_f^*\gamma_5\psi_i$ and $\psi_f^*\beta\gamma_5\psi_i$ must be proportional to the same expression $\psi_f^*\boldsymbol{\sigma}\cdot\psi_i\mathbf{q}$. For free nucleons we have

$$\psi_f^*\gamma_5\psi_i = (1/2M)\psi_f^*\sigma\psi_i\mathbf{q}, \qquad \psi_f^*\beta\gamma_5\psi_i = -(1/2M)\psi_f^*\sigma\mathbf{q}\psi_i.$$

Therefore, the entire expression in the square brackets in (5) can be written

$$\int dV\psi_f^*(G_A\gamma_5 + bm_\mu\beta\gamma_5)\tau\psi_i J_0 e^{-i\mathbf{qr}} = -\rho G_A\int dV\psi_f\sigma\mathbf{q}\tau\psi_i J_0 e^{-i\mathbf{qr}}, \qquad (6)$$

where ρ is some constant, whose magnitude depends on the magnitude of the spin-orbit interaction $V\boldsymbol{\sigma}\cdot\boldsymbol{l}$ of the nucleon in the nucleus: $\rho \sim VR^2bm_\mu/G_A \sim (3\text{ to }5)/M$. (For free nucleons $\rho = 7/2M$.) The expansion in powers of $R/\lambda\!\!\!{}^-$ is made in (5) in a manner analogous to that used in the vector interaction. We obtain as a result the following expression for the matrix element for the axial interaction:

$$G_A\int dV\psi_f^*\sigma\tau\psi_i\left\{\left(1-\frac{1}{6}q^2\langle r^2\rangle_A\right)\mathbf{J} - \rho\mathbf{q}J_0\right\}, \qquad (7)$$

where $<r^2>_A$ is the mean square radius of the nucleus in the transition due to axial interaction. In so far as the matrix element $\psi_f^*\sigma\psi_i$ has the same form as the matrix element of a magnetic dipole transition, then a better approximation is obtained if $<r^2>_A$ is taken equal to the square of the magnetic radius in the transition of a nucleus belonging to the same isotopic multiplet.

3. Making use of matrix elements (3) and (7), we calculate the total probability for μ^- capture and the magnitude of the longitudinal polarization of the nucleus in capture of an unpolarized meson, as well as the angular distribution and polarization of the nucleus in the direction of the meson spin, in capture of a polarized meson. It is possible to carry out the calculations by the same technique as described in reference 8. The total capture probability is:

$$W = (1/2\pi^2)a_\mu^{-3}q^2N_0,$$

$$N_0 = G_V^2|M_F|^2\left(1-\frac{1}{3}q^2\langle r^2\rangle_e + q/M\right) + G_A^2|M_{GT}|^2\left[1-\frac{1}{3}q^2\langle r^2\rangle_A + \frac{2}{3}(2a-\rho)q\right], \qquad (8)$$

where a_μ is the radius of the Bohr orbit of the meson, $M_F = (\int 1)$ and $M_{GT} = (\int\boldsymbol{\sigma})$ are the nuclear matrix elements, and $a = \mu_V G_V/2MG_A$. The probability $w(\mu')$, that on capture of an unpolarized meson the nucleus can have a spin μ' along the direction of the unit vector $\mathbf{n}_j$ is given by the formula

---

*In our notation G_V and G_A are positive; b is also positive.[7]

$$w(\mu') = 1 + Q_{j'j}\left[\tfrac{1}{3} - (\mathbf{n}_j\boldsymbol{\nu})^2\right](N'/N_0)$$

$$+ \boldsymbol{\nu}\mathbf{n}_j(\mu'/j')(N_\nu/N_0), \qquad Q_{j'j} = \Lambda_{j'j}\left(\frac{3\mu'^2}{j'(j'+1)} - 1\right),$$

$$\Lambda_{j'j} = \frac{j'+1}{2j'-1}\begin{cases} 1, & j = j'-1 \\ -(2j'-1)/(j'+1), & j = j' \\ j'(2j'-1)/(j'+1)(2j'+3), & j = j'+1 \end{cases}. \qquad (9)$$

Here

$$N' = -G_A^2|M_{GT}|^2(\rho + a)q,$$

$$N_\nu = G_A^2|M_{GT}|^2\lambda_{j'j}\left(1 + 2aq - \tfrac{1}{3}q^2\langle r^2\rangle_A\right)$$

$$+ 2\delta_{jj'}\sqrt{j/(j+1)}\,G_AG_V\,\mathrm{Re}\,M_FM_{GT}^*\left[1 - \rho q - \tfrac{1}{6}q^2(\langle r^2\rangle_e\right.$$

$$\left.+ \langle r^2\rangle_A) + q/2M\right],$$

$$\lambda_{j'j} = [j'(j'+1) - j(j+1) + 2]/2(j'+1), \qquad (10)$$

j and j′ are the spins of the initial and final nuclei, respectively, and $\boldsymbol{\nu} = \mathbf{q}/q$. Upon capture of a polarized meson, the angular distribution of the recoil nuclei has the form

$$w = 1 - \langle\sigma\rangle\boldsymbol{\nu}N_3/N_0, \qquad (11)$$

and the polarization of the final nucleus, averaged over the directions of the emitted neutrino, is determined by

$$w_\sigma(\mu') = 1 + \mathbf{n}_j\langle\sigma\rangle(\mu'/j')(N_1/N_0), \qquad (12)$$

where $<\sigma>$ is the expectation value of the spin of the μ meson in the K-orbit, and:

$$N_3 = G_V^2|M_F|^2[1 - {}^1\!/_3\,q^2\langle r^2\rangle_e + q/M]$$

$$- {}^1\!/_3\,G_A^2|M_{GT}|^2[1 - {}^1\!/_3\,q^2\langle r^2\rangle_A + 2(a+\rho)q],$$

$$N_1 = G_A^2|M_{GT}|^2\lambda_{j'j}[1 + {}^2\!/_3(2a - \rho)q - {}^1\!/_3\,q^2\langle r^2\rangle_A]$$

$$- 2\delta_{jj'}\sqrt{j/(j+1)}\,G_AG_V\,\mathrm{Re}\,M_FM_{GT}^*[1 + q/2M$$

$$- (q/3)(2a - \rho) - (q^2/6)(\langle r^2\rangle_e + \langle r^2\rangle_A)]. \qquad (13)$$

In the calculation of (8) to (13), only terms linear in v/c of the nucleons and in $(q^r)^2$ were taken into account. The hyperfine structure of the mesic atom was not taken into account. Therefore, strictly speaking,[9] our results are correct only for the capture of muons by nuclei with zero spin. If we pass in (8) to (13) to the case of μ capture by protons ($M_F = 1$, $M_{GT} = \sqrt{3}$) and neglect the pseudoscalar term ($\rho = -1/2M$), then the equations agree with the results of reference 2. In neglecting terms $\sim (v/c)_{\mathrm{nuc}}$ and $\sim (R/\lambda\!\!\!^{-})^2$, relations (8) to (11) become the usual relations for K capture (see for example, reference 10). However, these terms are quite significant.

4. We consider the more interesting case of the capture of μ^- mesons in C^{12}, with production of B^{12}, which then β-decays back into C^{12}. The quantity a for the transition $C^{12} \rightarrow B^{12}$ (transition $0 \rightarrow 1$, no) was calculated by Gell-Mann:[3] a = 2.34 ± 0.25/M. Taking $<r^2>_A^{1/2}$ to be the electrostatic radius of the nucleus* C^{12}, see reference 11 ($<r^2>_A^{1/2} = 2.4 \times 10^{-13}$ cm) and q = 90 Mev, we find $q^2<r^2>_A/3 = 0.37$, $4aq/3 = 0.3$. The constant ρ cannot be calculated theoretically. It is possible to determine it from experimental data[12] on the lifetime of the μ mesons relative to capture by C^{12}, according to which $N_0/G_A^2|M_{GT}|^2 = 1.37 \pm 0.08$. Hence $2\rho q/3 = -0.44$, which agrees with the theoretical estimate ($2q\rho/3 = 0.95$ for free protons) and leads one to believe that the pseudoscalar term has the order of magnitude predicted by Goldberger and Treiman.[7]†

Since the theory includes one more constant to be determined from experiment, besides the constants and matrix elements that are known from β decay, a verification of the theory, and, in particular, a verification of the hypothesis of renormalizability of the vector interaction can be achieved if at least one more experiment is performed in addition to measuring the capture probability. Measurement of the polarization of the B^{12} nucleus along the direction of the spin of the μ meson in the capture of a polarized meson in C^{12} is unsuitable for this purpose, since it follows from (13) and (8) that the magnitude of this polarization in the Gamow-Teller transition does not depend on terms containing a or ρ. (The absence of such a dependence denotes, on the other hand, that measurement of the polarization of B^{12} may be a good verification of the two-component μ-meson hypothesis in μ capture, see reference 10). The hypothesis of renormalizability of the vector interaction can be verified in experiments on the measurement of the longitudinal polarization of the nucleus in capture of unpolarized mesons or by measuring the angular distribution of the recoil nuclei in capture of polarized mesons. In both these cases the effect of the terms proportional to a and ρ is sufficiently large, reaching 30 to 50%. The polarization of the product nuclei can be determined experimentally from the asymmetry of the electrons of the subsequent β decay. The coefficient of asymmetry of the electrons contains also a correction term $\sim (v/c)_{\text{nuc}}$. This correction, however, is very small, of the order of 2 or 3%.

---

*It follows from the experimental data of Fregeau[11] that the magnitude of the radius of the C^{12} nucleus changes very little on passing from elastic to inelastic processes.

†It is somewhat strange that ρ appears to be negative for μ^- capture in C^{12}, and positive for the capture by protons. Estimates with relativistic-interaction models indicate that $\rho < 0$ might arise with the same interactions that cause spin-orbit coupling, but should not be as negative as is required by experiment.[12]

The author expresses his deep gratitude to A. I. Alikhanov and I. S. Shapiro for remarks that have stimulated the author to perform this work, and to V. B. Berestetskiĭ and L. B. Okun' for valuable discussions.

---

[1] L. Wolfenstein, Nuovo cimento **8**, 882 (1958).

[2] Chou Kuang Chao and V. Maevskiĭ, J. Exptl. Theoret. Phys. (U.S.S.R.) **35**, 1581 (1958), Soviet Phys. JETP **8**, 1106 (1959).

[3] M. Gell-Mann, Phys. Rev. **111**, 362 (1958).

[4] R. P. Feynman and M. Gell-Mann, Phys. Rev. **109**, 193 (1958).

[5] H. A. Tolhoek and J. R. Luyten, Nucl. Phys. **3**, 679 (1957).

[6] É. I. Dolinskiĭ and L. D. Blokhintsev, J. Exptl. Theoret. Phys. (U.S.S.R.) **35**, 1488 (1958), Soviet Phys. JETP **8**, 1040 (1959).

[7] M. L. Goldberger and S. B. Treiman, Phys. Rev. **111**, 354 (1958).

[8] Berestetskiĭ, Ioffe, Rudik, and Ter-Martirosyan, Nucl. Phys. **5**, 464 (1958).

[9] I. M. Shmushkevich, J. Exptl. Theoret. Phys. (U.S.S.R.) **36**, 953 (1959), Soviet Phys. JETP **9**, 673 (1959).

[10] S. B. Treiman, Phys. Rev. **110**, 448 (1958); Frauenfelder, Jackson, and Wyld, Phys. Rev. **110**, 452 (1958); B. L. Ioffe and V. A. Lyubimov, J. Exptl. Theoret. Phys. (U.S.S.R.) **34**, 1321 (1958), Soviet Phys. JETP **7**, 911 (1958).

[11] J. H. Fregeau, Phys. Rev. **104**, 225 (1956).

[12] Bargman, Fischer, Leontic, Lundby, Meunier, Strout, and Teja, Phys. Rev. Lett. **1**, 469 (1958).

Translated by K. Smith
25

RADIATIVE PROCESSES AHEAD OF A SHOCK-WAVE FRONT

L. M. BIBERMAN and B. A. VEKLENKO

Moscow Energetic Institute

Submitted to JETP editor January 29, 1959

J. Exptl. Theoret. Phys. (U.S.S.R.) 37, 164-169 (July, 1959)

The distribution of excited atoms or molecules ahead of a shock wave front is considered. The excitation is produced by radiation coming from the shock front. The process of nonstationary diffusion of the radiation is taken into account. It is shown that concentrations of excited atoms or molecules corresponding to excitation temperatures close to the temperature of the shock wave are formed in the cold gas ahead of the wave front.

THERE are a number of papers in the literature (see, for instance, reference 1) devoted to the influence of radiation from a shock wave on the state of the gas ahead of it. These papers discuss the photoelectric absorption of radiation from the shock wave by atoms or molecules which are in the lowest energy state. Thus, only the shortwave region of the absorption spectrum is taken into account; for radiations whose wavelength is greater than the red limit for the photoeffect from the ground state, the gas is considered to be transparent.

In the present communication we treat the absorption of radiation that causes excitation of the atoms or molecules. The treatment takes into account the subsequent process of nonstationary diffusion of the radiation. We show that there is a wave of atomic or molecular excitation ahead of the shock wave front.

1. THE BASIC EQUATIONS AND THEIR APPROXIMATE SOLUTION

Assume a plane shock wave whose temperature is T, propagating with velocity v in the direction of the x axis. We set up the equations describing the distribution of excited atoms in space and time.* We are interested here only in the concentration of atoms excited to resonance levels. We take into account the possibility of extinction as the result of kinetic processes. The time of flight of the photons will be neglected in comparison with the mean lifetime τ of the excited state of the atom.

Using the previously developed theory of the diffusion of resonance radiation,[2] we find that the concentration of excited atoms $n_a(x, t)$ ahead of the shock wave front is given by the following equation:

$$\frac{\partial n_a(x,t)}{\partial t} = v\frac{\partial n_a(x,t)}{\partial x} + \frac{1}{\tau}\int_0^\infty n_a(\xi, t)\,K(|x-\xi|)\,d\xi - n_a(x;t)\left[\frac{1}{\tau} + \sigma(x)\right] + B(x). \tag{1}$$

Here

$$K(|x-\xi|) = \frac{1}{2}\int_1^\infty\int_0^\infty \varepsilon_\nu k_\nu \exp\{-k_\nu|x-\xi|u\}\,d\nu\,\frac{du}{u}, \tag{2}$$

where the x coordinate is measured from the front of the shock wave. The functions ϵ_ν and k_ν characterize the shapes of the emission and absorption lines, respectively; $\sigma(x)$ is the probability of extinction per unit time, calculated for a single excited atom; $B(x)$ is the number of excitation events per unit volume per second caused by the absorption of radiation coming directly from the shock wave. The shock-wave radiation, at least in the portions of the spectrum adjacent to the resonance lines, can be considered as black-body radiation. It is then easy to show that

$$B(x) = \int_0^\infty \frac{E_\nu(T)}{2h\nu}\int_1^\infty k_\nu e^{-k_\nu xu}\,\frac{du}{u^2}\,d\nu. \tag{3}$$

The Planck function $E_\nu(T)$ changes slowly with frequency, compared with k_ν. Making use of this fact, we obtain

$$B(x) = \frac{n^0(T)}{\tau}\left[1 - \int_0^\infty K(|x-\xi|)\,d\xi\right], \tag{4}$$

where $n^0(T)$ is the Boltzmann concentration corresponding to the temperature T. This expression is valid for not too large values of x, i.e., when a linear approximation of the function $E_\nu/h\nu$ is possible over the frequency interval corresponding to the absorption line of a layer of gas of thickness x.

---

*The assumptions used in Secs. 1 and 2 can be used to obtain results for either an atomic or a molecular gas. However, for simplicity we use arbitrarily the terms "atomic" and "spectral line" in these sections.

The solution of the integro-differential equation (1) entails great mathematical difficulties, and can hardly be solved at all in the general form. At the same time it has been shown previously[3] that, in the case of integral equations with the kernel (2), good results have followed from the use of an approximate method involving the introduction of the concept of an effective lifetime of the excited state of the atom

$$\tau_{eff}(x) = \tau / \Theta(x), \tag{5}$$

where $\Theta(x)$ is the total probability that a photon emitted from the point x will reach the boundaries of the space under consideration without being absorbed. In our case,

$$\Theta(x) = 1 - \int_0^\infty K(|x-\xi|)\,d\xi. \tag{6}$$

Making use of the approximate method, we obtain instead of Eq. (1)

$$\partial n_a(x,t)/\partial t = v\partial n_a(x,t)/\partial x$$
$$- n_a(x,t)\,[\Theta(x)/\tau + \sigma(x)]. \tag{7}$$

The solution of Eq. (7), with the initial conditions $n_a(x, t) = 0$ for $t \le 0$, is the function

$$n_a(x,t) = \frac{n^0(T)}{\tau}\int_0^t \Theta(x+vt')\exp\left\{-\frac{1}{\tau}\int_0^{t'}[\Theta(x+vt'')\right.$$
$$\left. + \sigma(x+vt'')]\partial t''\right\}dt'. \tag{8}$$

This function can be written in the somewhat different form

$$n_a(x,t) = n_a(x,\infty)\left\{1 - \frac{\varphi(x,t)}{\varphi(x,0)}e^{-f(x,t)}\right\}, \tag{9}$$

where

$$f(x,t) = \int_0^t [\Theta(x+vt')/\tau + \sigma(x+vt')]\,dt', \tag{10}$$

$$\varphi(x,t) = n^0(T)\left[1 - e^{f(x,t)}\int_t^\infty \sigma(x+vt')e^{-f(x,t')}\,dt'\right], \tag{11}$$

with

$$n_a(x,\infty) = \varphi(x,0) = n^0(T)\left[1 - \int_0^\infty \sigma(x+vt')\,e^{-f(x,t')}\,dt'\right].$$

2. DISCUSSION OF THE APPROXIMATE SOLUTION

In certain special cases the expression (9) can be written in simpler forms.

a. $\sigma = 0$, $v \neq 0$:

$$n_a(x,t) = n^0(T)\left[1 - \exp\left\{-\frac{1}{\tau}\int_0^t \Theta(x+vt')\,dt'\right\}\right]. \tag{12}$$

Consequently, in the absence of extinction, a wave of excited atoms is gradually formed in the cold gas ahead of the shock wave front, with a concentration equal to the Boltzmann value for the temperature T. This result holds for any value of the velocity v.

The latter fact is explained by noting that the exciting radiation contains a great many photons corresponding to the "tails" of the absorption line. A finite fraction of these photons undergo their first absorption so far from the shock wave front that the excited atoms so formed cannot reach the plane x = 0 within the time τ.

b. $v = 0$, $\sigma \neq 0$:

$$n_a(x,t) = \frac{n^0(T)}{1+\sigma(x)\,\tau_{eff}(x)}\left\{1 - \exp\{-[1\right.$$
$$\left. + \sigma(x)\tau_{eff}(x)]\,t/\tau_{eff}\}\right\}. \tag{13}$$

As $t \to \infty$ we have the following distribution:

$$n_a(x,\infty) = n^0(T)/[1+\sigma(x)\tau_{eff}(x)]. \tag{14}$$

The ratio of the extinction probability to $1/\tau_{eff}(x)$, the effective probability of a radiative transition, serves as a parameter in expressions (13) and (14). As a criterion of the time t^* required to establish a stationary distribution, we may take the condition that the argument of the exponential function in (13) be equal to unity:

$$t^* = \tau_{eff}(x)/[1+\sigma(x)\tau_{eff}(x)]. \tag{15}$$

$\tau_{eff}(x)$ increases with increasing distance from the wave front so that for constant σ at large values of x the quantity t^* becomes of the order of $1/\sigma$. When x is so small that $\sigma(x)\tau_{eff}(x) \ll 1$, the rise time is $t^* \sim \tau_{eff}(x)$.

c. $\sigma \neq 0$, $v \neq 0$. In this case substantial simplification of expression (9) can be obtained only by choosing a specific form for the functions $\sigma(x)$ and $\Theta(x)$. It is natural to assume that the extinction does not depend on the coordinates (σ = const.). Then, bearing in mind that $\Theta(x)$ decreases with increasing x, it is easy to show that $n_a(x, t)$ is less when $v \neq 0$ than when $v = 0$, i.e., that (13) is the upper limit of (9).

Furthermore, with constant σ, the region of integration in (9) is restricted in practice by the exponential term $\exp(-\sigma t')$. Hence for sufficiently large values of x the function $\Theta(x+vt')$ is very little different from $\Theta(x)$. In this case Eqs. (9) and (13) lead to identical results, so that at sufficiently large distances the relative distribution of excited atoms does not depend on the speed of the wave. It can be shown that as t increases, the function $\varphi(x, t)$ decreases. Thus in the course of time a stationary distribution of excited atoms builds up ahead of the shock-wave front. The build-up time will be shorter than the value determined from the equation

$$f(x, t^*) = 1. \tag{16}$$

If σ is constant, then for any x and v the inequality $t^* < 1/\sigma$ holds.

3. PROPAGATION OF A SHOCK WAVE IN AN ATOMIC GAS

In the case of an atomic gas the interaction between radiation and the atoms is characterized by linear absorption, whose form is usually determined by the Doppler effect and shock or resonance interactions, the Doppler effect determining the intensity distribution in the central portion of the absorption line. The appearance of excited atoms at considerable distances ahead of the shock wave front is connected with the long free path of the photons corresponding to the tails of the spectral line. Therefore, assuming that the absorption line is of the pure dispersion type, we obtain a solution which to a good approximation applies to the general case.

For a dispersion line

$$k_\nu = \frac{k_0}{1 + [2(\nu - \nu_0)/\Delta\nu]^2},$$

where ν_0 is the frequency corresponding to the center of the line and $\Delta\nu$ is the line width,

$$K(|x|) = \frac{k_0}{2\pi} \int_{-\infty}^{\infty} \int_{1}^{\infty} \frac{\exp\{-k_0 |x| u/(1+y^2)\}}{(1+y^2)^2} \frac{du}{u} dy. \tag{17}$$

Substituting (17) into (6), we obtain an expression for $\Theta(x)$. If $k_0 x \geq 1$, then to a good approximation,

$$\Theta(x) \approx (3\sqrt{\pi k_0 x})^{-1}. \tag{18}$$

When $x = 0$, $\Theta(x) = 0.5$. Consequently $\tau_{\text{eff}}(0) = 2\tau$. Making use of (18) and assuming σ to be constant, we find

$$n_a(x, t) = \frac{n^0(T)}{\tau_{eff}(x)} \sqrt{\frac{x}{v\sigma}} \exp\left\{\frac{x\sigma}{v}\left[1 + \frac{\Theta(x)}{\tau\sigma}\right]^2\right\}$$
$$\times \left\{\Phi\left[\sqrt{\frac{(x+vt)\sigma}{v}}\left(1 + \frac{\Theta(x+vt)}{\sigma\tau}\right)\right] - \Phi\left[\sqrt{\frac{x\sigma}{v}}\left(1 + \frac{\Theta(x)}{\sigma\tau}\right)\right]\right\}, \tag{19}$$

where $\Phi(z)$ is the probability integral. As $t \to \infty$, the first term tends to unity.

We now estimate the distribution of excited atoms in front of a shock wave in argon, starting with the wave parameters derived in the paper by Resler et al.[4] (wave velocity = 18 M; temperature = 14,000° K behind the wave front and 300° K ahead of it; pressure = 10 mm Hg ahead of the front). The resonance lines 1049 A and 1067 A correspond to transitions from the ground state to the excited states $3p^5\,(^2P^0_{1/2})\,4s$ and $3p^5\,(^2P^0_{3/2})\,4s$. The oscillator strengths for these transitions are equal to 0.2 and 0.05, respectively.[5]

Under the above conditions, the intensity distribution in the tails of the lines depends upon the resonance broadening, which gives $k_0 \approx 1.5 \times 10^5$ cm^{-1} in both cases (see reference 6).

The extinction depends on the collisions of excited argon atoms with molecules of air which are present as an impurity in the argon. The effective cross sections for extinction of excited argon atoms by N_2 and O_2 molecules are not to be found in the literature. Using data on the extinction of other atoms, and assuming that the concentration of excited atoms does not affect the estimate, we obtain an effective cross section of 10^{-14} cm^2 for extinction. Thus, for an impurity content of 0.01%, $\sigma \sim 10^4$ sec^{-1}.

The figure shows the concentration of argon atoms in the state $3p^5\,(^2P^0_{1/2})\,4s$ as a function of the distance x ahead of the shock front, determined from the above parameters. It will be seen that there is a noticeable concentration of excited atoms ($\sim 5 \times 10^{13}$ cm^{-3}) at a distance of one meter from the shock front. The excitation temperature is equal to 13,500° K, only slightly less than the temperature in the shock wave. The concentration of atoms in the state $3p^5\,(^2P^0_{3/2})\,4s$ cannot differ essentially from that shown in the figure, since the lower oscillator strength is to a certain extent compensated by the higher statistical weight.

Because of the relatively small energy difference between the $P_{1/2}$ and $P_{3/2}$ states, direct transitions between them are possible as a result of interactions with unexcited argon atoms. Taking such processes into account should not seriously alter our estimates.

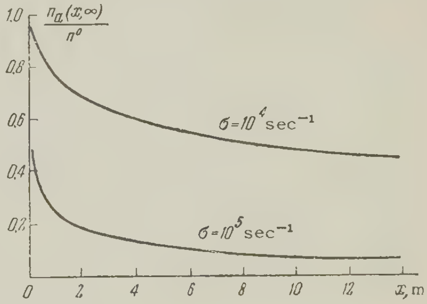

In estimating the concentrations of excited atoms we have used the approximate expression (4). As already mentioned above, the transition from (3) to (4) is valid if a linear approximation to the function $E_\nu(T)/h\nu$ is permissible over the frequency interval corresponding to the absorption line for a layer of thickness x. In our example, the limiting value of x is found to be of the order of hundreds of meters.

The distribution shown in the figure was obtained without taking into account the effect of the shock tube walls. At distances less than the radius of the shock tube, this factor can be neglected. At greater distances, two factors must be considered: (1) the reduction in excited atoms due to the absorption of radiation by the walls; (2) an additional weakening of the quantity $B(x)$ as x increases. The latter factor is connected with the decrease in the solid angle through which the primary incident radiation arrives from the shock wave.

Polishing or chrome-plating the interior surface of the shock tube, which is usually done to eliminate contamination, greatly reduces the effect of the above factors. Furthermore, under our conditions the first factor is not serious, since the extinction due to impurities was an order of magnitude larger than the reduction in the number of excited atoms due to radiation absorption by the tube walls.

In constructing the curves it was assumed that the extinction depended on the interaction of excited atoms with impurity molecules, and therefore did not depend on the coordinates. It must however be borne in mind that an appreciable number of free electrons are formed as a result of the photo-ionization of argon atoms by short-wave radiation ahead of the shock front. The concentration of free electrons, taking into account the motion of the wave, will fall off with increase in the x coordinate according to the law e^{-snx}, where s is the cross section for photo-ionization and n is the concentration of argon atoms in the free state.

An evaluation shows that at distances $x < 1$ cm extinction by electrons is dominant. Since this form of extinction increases with proximity to the wave front, there is a possibility of a maximum occurring in the distribution of excited atoms. It is obvious that atoms excited to more highly energetic states would also have a nonmonotonic distribution.

Several reports have been given in the literature of luminosity in the gas ahead of a shock front. In addition, in some cases a maximum has been observed in this luminosity.[7] Up to the present time, this phenomenon has not had any theoretical explanation. It is possible that this maximum can be explained as a nonmonotonic dependence of the excited atom concentration ahead of the shock wave upon the x coordinate. The absence of sufficiently complete experimental data prevents us from carrying out a quantitative comparison of theory with experiment.

In conclusion it should be mentioned that the presence of considerable numbers of excited atoms or molecules ahead of a shock wave front may lead to the appearance of secondary effects. Thus, for example, the formation of ions at considerable distances from the shock front appears to be the result of photo-ionization of excited atoms or molecules. In certain cases serious energetic effects may arise due to the absorption of radiation from the shock wave by excited atoms.

---

[1] Ya. B. Zel'dovich and Yu. P. Raĭzer, Usp. Fiz. Nauk **63**, 613 (1957).

[2] L. M. Biberman, J. Exptl. Theoret. Phys. (U.S.S.R.) **17**, 416 (1947).

[3] L. M. Biberman, Dokl. Akad. Nauk SSSR **59**, 659 (1948).

[4] Resler, Lin, and Kantrowitz, J. Appl. Phys. **23**, 1390 (1952).

[5] R. S. Knox, Phys. Rev. **110**, 375 (1958).

[6] A. A. Vlasov and V. S. Fursov, J. Exptl. Theoret. Phys. (U.S.S.R.) **6**, 751 (1936).

[7] A. Kantrowitz, Sci. American, Sept. 1954, p. 132.

Translated by D. C. West
26

SOVIET PHYSICS JETP VOLUME 37(10), NUMBER 1 JANUARY, 1960

ON THE LAGRANGIAN FORMALISM FOR SPIN VARIABLES

D. V. VOLKOV and S. V. PELETMINSKIĬ

Physical and Technological Institute, Academy of Sciences, Ukrainian S.S.R.

Submitted to JETP editor January 29, 1959

J. Exptl. Theoret. Phys. (U.S.S.R.) 37, 170-178 (July, 1959)

It is shown that a change of the class of allowable variations in the Schwinger variation principle[1] makes it possible to include the spin variables in the general Lagrangian formalism in both the nonrelativistic and relativistic cases.

THE transition from classical mechanics to quantum mechanics is usually made by means of the correspondence principle, which consists of replacement of the classical Poisson brackets by the quantum commutation relations. Despite the great generality of the correspondence principle, it has well-known limitations, owing to the requirement that a classical Lagrangian function exist for the system in question. Because of this limitation the spin variables, which, as is well known, have no classical analogues, are introduced into the general scheme of quantum mechanics not on the basis of the correspondence principle, but by means of a formal increase of the number of components of the wave function and the requirement that under transformations of rotation these components shall transform according to some irreducible representation of the rotation group.

Schwinger has proposed a Lagrangian formulation of quantum mechanics, based on the application of a variation principle to an operator action function.[1] Because of the operator character of the Schwinger variation principle, the existence of a classical (nonoperator) Lagrangian function is not a necessary condition for its use. In this sense the Schwinger variation principle is broader than the correspondence principle.

Owing, however, to the limitations imposed by Schwinger on the class of allowable variations,* the spin variables cannot be included in this more general scheme.

In the present paper it is shown that the limitations on the class of allowable variations postulated by Schwinger are not necessary (cf. also reference 2). A change of the class of allowable variations makes it possible to include the spin variables (for an arbitrary value of the spin) in the general scheme of the Schwinger variation principle, both in the nonrelativistic case and also in the relativistic case. The Lagrangian formalism for the spin variables in the relativistic case leads to a natural introduction of the proper time into the theory.

1. THE NONRELATIVISTIC CASE

In the nonrelativistic case we shall describe the spin variables by a vector $\mathbf{s}$. We shall determine the equations of motion and the operator properties of the vector $\mathbf{s}$ on the basis of the application of the operator action principle to the following Lagrangian function:

$$L = \tfrac{1}{2} i [\mathbf{s}, \dot{\mathbf{s}}] - H(\mathbf{s}), \tag{1}$$

where $H(\mathbf{s})$ is an arbitrary function of $\mathbf{s}$, which is the Hamiltonian of the system, $\dot{\mathbf{s}}$ is the time derivative of the operator $\mathbf{s}$ in the Heisenberg representation, and the square brackets denote the commutator (we shall use a system of units in which $\hbar = 1$).

The first term in the expression (1) corresponds to the kinematic part of the Lagrangian function. This term is uniquely determined from the condition of invariance under rotation transformations and the requirement that the equations of motion for the spin vector be equations of the first order.

We note that in the classical case, in which the components of the vector $\mathbf{s}$ are c-numbers and not operators, the scalar product $\mathbf{s}\dot{\mathbf{s}}$ is a total derivative with respect to time, so that the addition of such a term to the Lagrangian function does not enable us to get equations of motion for the spin vector in the classical case.

An arbitrary variation of the action integral for this Lagrangian function can be written in the form

---

*Schwinger restricted the class of allowable variations to those commuting or anticommuting with all other operators. Such a limitation seemed to Schwinger to be necessary for the obtaining of the equations of motion from the condition that the action integral be stationary.

$$\delta W_{21} = \delta \int_{t_1}^{t_2} L dt = \int_{t_1}^{t_2} \{ i [\delta^* \mathbf{s}, \dot{\mathbf{s}}] - \delta^* H \} dt$$
$$[\tfrac{1}{2} i [\mathbf{s}, \delta^* \mathbf{s}] + L \delta t]_{t_1}^{t_2}. \tag{2}$$

According to the Schwinger variation principle[1] the variation δW_{21} for fixed "external" parameters has the form

$$\delta W_{21} = G(t_2) - G(t_1), \tag{3}$$

where the operators $G(t_1)$ and $G(t_2)$ depend only on the dynamical variables referring to the times t_1 and t_2, respectively, and are interpreted as operators generating infinitesimal unitary transformations corresponding to the variations in question; that is, for a fixed time:*

$$\delta^* \mathbf{s} = i [G, \mathbf{s}], \tag{4}$$

where

$$G = \tfrac{1}{2} i [\mathbf{s}, \delta^* \mathbf{s}] + L \delta t. \tag{5}$$

The last expression, which defines the explicit form of the generating operator $G(t)$, is obtained by comparing Eqs. (2) and (3) under the condition that

$$\int_{t_1}^{t_2} \{ i [\delta^* \mathbf{s}, \dot{\mathbf{s}}] - \delta^* H \} dt = 0. \tag{6}$$

The variation $\delta^* \mathbf{s}$ in the formulas (2), (4), (5), and (6) does not contain the changes caused by the variation δt. The total variation, including these changes also, has the form:

$$\delta \mathbf{s} = \delta^* \mathbf{s} + \dot{\mathbf{s}} \delta t. \tag{7}$$

(We note that in the interior of the region of integration [Eq. (2)] the time t is not varied, so that the variation $\delta \mathbf{s}$ coincides with the variation $\delta^* \mathbf{s}$.) Using Eq. (7), we rewrite Eq. (5) in the form

$$G = G_{\mathbf{s}} + G_t,$$

where

$$G_{\mathbf{s}} = \tfrac{1}{2} i [\mathbf{s}, \delta \mathbf{s}], \qquad G_t = -H \delta t \tag{5$'$}$$

and

$$\delta \mathbf{s} - \mathbf{s} \delta t = i [G_{\mathbf{s}} + G_t, \mathbf{s}]. \tag{4$'$}$$

Because of the independence of the variations $\delta \mathbf{s}$ and δt, the relation (4′) separates into two independent relations

$$\delta \mathbf{s} = i [G_{\mathbf{s}}, \mathbf{s}], \tag{8}$$
$$\dot{\mathbf{s}} = i [H, \mathbf{s}]. \tag{9}$$

The relation (9) defines the equation of motion for the vector $\mathbf{s}$.

To establish the commutation relations between the different components of the vector $\mathbf{s}$, let us consider the rotation transformation

$$s_i \to s_i + \varepsilon_{ikl} \omega_k s_l$$

(ϵ_{ikl} is the antisymmetric unit tensor).

We obtain the generating operator G_ω for this transformation by substituting

$$\delta s_i' = \varepsilon_{ikl} \omega_k s_l$$

in the general expression (5′):

$$G_{\boldsymbol{\omega}} = -\tfrac{1}{2} i \omega_i \varepsilon_{ikl} [s_k, s_l]. \tag{10}$$

In virtue of (8), the commutator of the operator G_ω with an arbitrary vector function $\mathbf{A}(\mathbf{s})$ (under the condition that no "external" vectors are involved in this function) is given by

$$[G_{\boldsymbol{\omega}}, A_i(\mathbf{s})] = -i \varepsilon_{ikl} \omega_k A_l(\mathbf{s}),$$

or, since the vector $\boldsymbol{\omega}$ is arbitrary, we have

$$[M_i, A_k(\mathbf{s})] = i \varepsilon_{ikl} A_l(\mathbf{s}), \tag{11}$$

where

$$M_i = -\tfrac{1}{2} i \varepsilon_{ikl} [s_k, s_l]. \tag{12}$$

If we take as the vector $\mathbf{A}$ the vector $\mathbf{M}$ defined by (12), then Eq. (11) leads to the well-known commutation relations for the components of the angular momentum operator,

$$[M_i, M_k] = i \varepsilon_{ikl} M_l. \tag{13}$$

This also establishes the well-known connection between the operator for an infinitesimal rotation and the angular momentum operator,

$$G_{\boldsymbol{\omega}} = \boldsymbol{\omega} \mathbf{M}. \tag{14}$$

The vector $\mathbf{s}$ is connected with the angular momentum vector by the relation (12). Using Eqs. (12) and (13) together with the relation

$$[M_i, s_k] = i \varepsilon_{ikl} s_l, \tag{15}$$

which is a special case of Eq. (11) for $\mathbf{A} = \mathbf{s}$, and assuming that the operator $\mathbf{s}$ acts in a space with a finite number of dimensions, one can easily show that

$$\mathbf{s} = \mathbf{M}, \tag{16}$$

---

*The limitation to variations that commute or anticommute has the consequence that relations of the type (4) are not always satisfied for the general case of quantum-mechanical variables. The difficulties that thus arise in the interpretation of the derivatives of operators have been noted in a paper by Burton and Touschek.[3] The removal of these difficulties required the bringing in of additional nontrivial arguments.[4] The broadening of the class of allowable variations makes it possible to obtain a unique interpretation of the derivatives of operators, without the difficulties that have been mentioned.

i.e., the operator properties of the vector $\mathbf{s}$ coincide with those of the angular momentum operator

$$[s_i, s_k] = i\varepsilon_{ikl} s_l. \tag{17}$$

Thus the vector $\mathbf{s}$ actually describes the spin degrees of freedom of the particle.

In the derivation of the equations of motion (9) and the commutation relations (17), we have used only the properties of the generating operator G [Eqs. (4) and (8)]. We have established the explicit form of the operator G on the basis of the assumption that the variation of the action integral vanishes in the entire internal region of integration in the interval between t_1 and t_2 [Eq. (3)].

A little later we shall show that this assumption is satisfied as a consequence of the equations of motion (9) if the variation $\delta\mathbf{s}$ we are considering belongs to a definite class.

For the definition of the class of allowable variations, let us adopt the natural requirement that the operator

$$G_{\mathbf{s}}(t) = \tfrac{1}{2} i\,[\mathbf{s}(t), \delta\mathbf{s}(t)] \tag{18}$$

is to be the generating operator for the change $\delta\mathbf{s}(t)$; i.e., that

$$\delta\mathbf{s}(t) = i\,[G_{\mathbf{s}}(t), \mathbf{s}(t)] \tag{19}$$

also for variations in the entire internal region of integration.

Substituting Eq. (19) in Eq. (18), we get the relation

$$G_{\mathbf{s}} = -\tfrac{1}{2}[\mathbf{s}, [G_{\mathbf{s}}, \mathbf{s}]], \tag{20}$$

in which, for brevity, we have omitted the variable t. To find the general form of the generating operator $G_{\mathbf{s}}$ compatible with Eq. (20), let us expand $G_{\mathbf{s}}$ in terms of the irreducible tensors $Y^{lm}(\mathbf{s})$

$$G_{\mathbf{s}} = \sum_{l,m} a_{lm} Y^{lm}(\mathbf{s}).$$

Using the commutation rules for the vector $\mathbf{s}$, one can easily show that

$$[\mathbf{s}, [\mathbf{s}, Y^{lm}(\mathbf{s})]] = l(l+1)\,Y^{lm}(\mathbf{s}). \tag{21}$$

The relation (21) is compatible with Eq. (20) only for $l = 1$, from which it follows that the most general expression for the operator $G_{\mathbf{s}}$ has the form

$$G_{\mathbf{s}} = \sum_{m=-1}^{1} a_{1m} Y^{1m}(\mathbf{s}) = \boldsymbol{\omega}\mathbf{s}. \tag{22}$$

Substituting Eq. (22) in Eq. (19), we get the general expression characterizing the class of allowable variations,

$$\delta s_i(t) = i\,[\omega_k(t)\, s_k(t), s_i(t)] = \varepsilon_{ikl}\,\omega_k(t)\, s_l(t), \tag{23}$$

where the $\omega_k(t)$ are arbitrary functions of the time.

We note that the variations $\delta\mathbf{s}$ that we used for the derivation of the commutation relations also belong to this class of variations.

We shall now show that the principle of stationary action, which is the condition that the integral in Eq. (2) vanish,

$$\int_{t_1}^{t_2} \{i\,[\delta\mathbf{s}, \dot{\mathbf{s}}] - \delta H\}\, dt = 0, \tag{24}$$

is satisfied for the class of allowable variations that we are considering.

In fact, if the variation δH occurs only on account of variation of the vector $\mathbf{s}$, it can be put in the form

$$\delta H = i\,[G_{\mathbf{s}}, H] = -\tfrac{1}{2}[[\mathbf{s}, \delta\mathbf{s}], H]. \tag{25}$$

Using the operator Jacobi identity, we can write the last expression in another form

$$\delta H = -\tfrac{1}{2}[\mathbf{s}, [\delta\mathbf{s}, H]] - \tfrac{1}{2}[\delta\mathbf{s}, [H, \mathbf{s}]]. \tag{26}$$

For an arbitrary operator X we have as a consequence of Eq. (23) the relation

$$s_i X \delta s_i = s_i X \varepsilon_{ikl}\,\omega_k s_l = -\delta s_i X s_i, \tag{27}$$

which enables us to transform the first term in the expression (26) to the form

$$-\tfrac{1}{2}[\mathbf{s}, [\delta\mathbf{s}, H]] = \tfrac{1}{2}[\delta\mathbf{s}, [\mathbf{s}, H]]. \tag{28}$$

Substituting Eq. (28) in Eq. (26), we get the following expression for δH

$$\delta H = -[\delta\mathbf{s}, [H, \mathbf{s}]], \tag{29}$$

and a corresponding expression for the integral in Eq. (24),

$$\int_{t_1}^{t_2} i\,[\delta\mathbf{s}, \dot{\mathbf{s}} - i\,[H, \mathbf{s}]]\, dt. \tag{30}$$

It can be seen at once from Eq. (30) that the principle of stationary action for the class of allowable variations under consideration is a consequence of the equations of motion (9).

The results of this section show that the information about the equations of motion and the operator properties of the vector $\mathbf{s}$ obtained by the application of the operator action principle to the Lagrangian function (1) are internally consistent and correctly describe the properties of the spin variables.

2. THE RELATIVISTIC CASE

The Schwinger variation principle permits us to introduce the spin variables into the Lagrangian formalism also in the relativistic case.

As the natural relativistic generalization of the spin vector **s** let us consider the four-dimensional vector Γ_μ. We denote the coordinate and momentum four-vectors by x_μ and p_μ, respectively. Relativistic invariance of the formulation of the theory can be achieved by the introduction of an invariant parameter τ, on which the dynamical variables Γ_μ, x_μ, p_μ depend, and which we shall call hereafter the "proper" time of the particle.*

The operator Lagrangian function, on the basis of which one obtains the equations of motion and the commutation relations for the dynamical variables Γ_μ, x_μ, p_μ, is now chosen in the form†

$$\mathscr{L} = \tfrac{1}{8} i[\Gamma_\mu, \dot{\Gamma}_\mu] - \tfrac{1}{4}(\{x_\mu, \dot{p}_\mu\} - \{\dot{x}_\mu, p_\mu\}) - \mathscr{H}, \qquad (31)$$

where $\mathscr{H}$ is a certain function of Γ_μ, x_μ, p_μ; the dot denotes differentiation with respect to the proper time τ, and the braces denote anticommutators. The kinematic part of the Lagrangian function is written in relativistically invariant form.

The action operator corresponding to the Lagrangian function (31) is given by

$$W_{21} = \int_{\tau_1}^{\tau_2} \mathscr{L}(\tau)\, d\tau. \qquad (32)$$

Varying both the dynamical variables and the proper-time parameter in the action integral, we get

$$\delta W_{21} = \int_{\tau_1}^{\tau_2} d\tau \left(\tfrac{1}{4} i [\delta\Gamma_\mu, \dot{\Gamma}_\mu] - \tfrac{1}{2}\{\delta x_\mu, \dot{p}_\mu\} + \tfrac{1}{2}\{\delta p_\mu, \dot{x}_\mu\} - \delta\mathscr{H}\right)$$
$$+ G(\tau_2) - G(\tau_1), \qquad (33)$$

where

$$G(\tau) = G_\Gamma + G_{xp} + G_\tau, \quad G_\Gamma = \tfrac{1}{8} i [\Gamma_\mu, \delta\Gamma_\mu],$$
$$G_{xp} = \tfrac{1}{4}(\{\delta x_\mu, p_\mu\} - \{\delta p_\mu, x_\mu\}), \quad G_\tau = -\mathscr{H}\delta\tau. \qquad (34)$$

Just as in the preceding section, the equations of motion and the commutation relations for the quantities Γ_μ, x_μ, p_μ are obtained by means of the operators G that generate infinitesimal unitary transformations of the dynamic variables:

$$i[G, \Gamma_\mu] = \delta\Gamma_\mu - \dot{\Gamma}_\mu\delta\tau, \qquad i[G, x_\mu] = \delta x_\mu - \dot{x}_\mu\delta\tau,$$
$$i[G, p_\mu] = \delta p_\mu - \dot{p}_\mu\delta\tau. \qquad (35)$$

In Eqs. (34) and (35) $\delta\Gamma_\mu$, δx_μ, δp_μ are the total variations of the quantities Γ_μ, x_μ, p_μ.

The allowable class of variations is defined by the requirement that (35) be compatible with the principle of stationary action, i.e., with the assumption that for arbitrary $\mathscr{H}$ the variation δW_{21} of Eq. (33) have the form‡

$$\delta W_{21} = G(\tau_2) - G(\tau_1). \qquad (33')$$

For the Lagrangian function (31) this class of variations has the form

$$\delta\Gamma_\mu = \varepsilon_{\mu\nu}\Gamma_\nu, \qquad \delta x_\mu = A_{\mu\nu}x_\nu + B_{\mu\nu}p_\nu,$$
$$\delta p_\mu = -A_{\nu\mu}p_\nu + C_{\mu\nu}x_\nu, \qquad (36)$$

where

$$\varepsilon_{\mu\nu} = \overset{*}{\varepsilon}_{\mu\nu} = -\varepsilon_{\nu\mu}, \qquad B_{\mu\nu} = \overset{*}{B}_{\mu\nu} = B_{\nu\mu}, \qquad C_{\mu\nu} = \overset{*}{C}_{\mu\nu} = C_{\nu\mu},$$
$$A_{\mu\nu} = \overset{*}{A}_{\mu\nu}, \qquad (37)$$

for μ, $\nu = 0, 1, 2, 3$. The matrices ϵ, A, B, C have arbitrary time dependences.

Since the variations $\delta\tau$ and $\delta\Gamma_\mu$, δx_μ, δp_μ are independent, Eqs. (34) and (35) lead to the following equations of motion for the quantities Γ_μ, x_μ, p_μ:

$$\dot{\Gamma}_\mu = i^{-1}[\Gamma_\mu, \mathscr{H}], \qquad \dot{p}_\mu = i^{-1}[p_\mu, \mathscr{H}],$$
$$\dot{x}_\mu = i^{-1}[x_\mu, \mathscr{H}]. \qquad (38)$$

It can be seen from these equations that $\mathscr{H}$ plays the part of the Hamiltonian with respect to the proper time (and not with respect to the ordinary time, as in the nonrelativistic case).

Let us now verify that with the class of allowable variations (36) the principle of stationary action is satisfied in virtue of the equations of motion (38).

Using Eqs. (36) and (37), by means of the generating operator $G_\Gamma + G_{xp}$ we can transform the variation $\delta\mathscr{H}$ to the form:

$$\delta\mathscr{H} = \delta_\Gamma\mathscr{H} + \delta_{xp}\mathscr{H},$$

where

$$\delta_\Gamma\mathscr{H} = i[G_\Gamma, \mathscr{H}] = \tfrac{1}{4}[\delta\Gamma_\nu, [\Gamma_\nu, \mathscr{H}]], \quad \delta_{xp}\mathscr{H} = i[G_{xp}, \mathscr{H}]$$
$$= \tfrac{1}{2} i^{-1}\{\delta x_\mu, [\mathscr{H}, p_\mu]\} - \tfrac{1}{2} i^{-1}\{\delta p_\mu, [\mathscr{H}, x_\mu]\}. \qquad (39)$$

Substituting Eq. (39) in Eq. (33), we easily verify that the principle of stationary action in the form (33′) is in fact satisfied.

Let us go on to the determination of the commutation relations for the operators of the dynamical variables.

By Eq. (36) the variation $\delta\Gamma_\mu$ is independent of the variations δx_μ, δp_μ, so that the first of the formulas (35) can be written in the form

---

*Wave equations with the proper time have been considered by Fock, Nambu, Feynman, and Schwinger,[5-9] but the Lagrangian formulation for the equations of motion with the proper time was carried through only for the classical case (cf., e.g., reference 5) and for the Klein-Gordon equation.[7]

†In the present section we use a system of units in which ħ = c = 1.

‡A detailed investigation of the class of allowable variations will be made in another paper. Here we note only that the class of allowable variations preserves the invariance of the kinematic part of the Lagrangian function.

$$\delta\Gamma_\mu = i\,[G_\Gamma, \Gamma_\mu] = \tfrac{1}{8}\,[\Gamma_\mu, [\Gamma_\nu, \delta\Gamma_\nu]].$$

Using the formulas (36) and (37), which define the allowable variations $\delta\Gamma_\mu$, we easily obtain the following commutation relations for the quantities Γ_μ:*

$$\tfrac{1}{4}\,[\Gamma_\nu, [\Gamma_\mu, \Gamma_\lambda]] = \delta_{\mu\nu}\Gamma_\lambda - \delta_{\lambda\nu}\Gamma_\mu. \tag{40}$$

If we introduce the notation

$$I_{\mu\lambda} = \tfrac{1}{4}\,[\Gamma_\mu, \Gamma_\lambda], \tag{41}$$

Equation (40) takes the form

$$[\Gamma_\nu, I_{\mu\lambda}] = \delta_{\mu\nu}\Gamma_\lambda - \delta_{\lambda\nu}\Gamma_\mu. \tag{42}$$

If follows at once from Eqs. (41) and (42) that

$$[I_{\mu\lambda}, I_{\sigma\nu}] = \delta_{\mu\sigma}I_{\nu\lambda} + \delta_{\lambda\sigma}I_{\mu\nu} + \delta_{\lambda\nu}I_{\sigma\mu} + \delta_{\mu\nu}I_{\lambda\sigma}. \tag{43}$$

Thus the $I_{\mu\lambda}$ are the infinitesimal operators of the four-dimensional rotation group, and according to Eqs. (34) and (36) the generating operator for four-dimensional rotations has the form

$$G_\Gamma \equiv G_\varepsilon = \tfrac{1}{2}\,i\varepsilon_{\mu\nu}I_{\mu\nu}. \tag{44}$$

The commutation relations between the x_μ and p_μ are obtained by means of the generating operator G_{xp} on the class of allowable variations (36) in the same way as the commutation relations for the Γ_μ, and have the following rather complicated form

$$\begin{gathered}
2\delta_{\lambda\mu}x_\nu = i^{-1}\,[x_\mu, \{x_\nu, p_\lambda\}], \qquad 2\delta_{\lambda\mu}p_\nu = -i^{-1}\,[p_\mu, \{x_\lambda, p_\nu\}], \\
[p_\mu, \{p_\nu, p_\lambda\}] = 0, \quad \delta_{\lambda\mu}p_\nu + \delta_{\nu\mu}p_\lambda = \tfrac{1}{2}\,i^{-1}\,[x_\mu, \{p_\nu, p_\lambda\}], \\
[x_\mu, \{x_\nu, x_\lambda\}] = 0, \quad \delta_{\lambda\mu}x_\nu + \delta_{\nu\mu}x_\lambda = -\tfrac{1}{2}\,i^{-1}\,[p_\mu, \{x_\nu, x_\lambda\}].
\end{gathered} \tag{45}$$

These commutation relations are compatible with each other and with the usual commutation relations between x_μ and p_ν,

$$[p_\mu, p_\nu] = 0, \qquad [x_\mu, x_\nu] = 0, \qquad [x_\mu, p_\nu] = i\delta_{\mu\nu}. \tag{46}$$

These latter relations can be obtained directly by means of the generating operators if we add to the Lagrangian function (31) the total derivative $\frac{1}{4}(d/d\tau)\{x_\mu, p_\mu\}$.[4]

The kinematic term of the altered Lagrangian function, depending on x_μ, p_ν, then takes the form

$$\tfrac{1}{2}\,\{\dot{x}_\mu, p_\mu\}. \tag{47}$$

It follows from Eq. (47) that the new generating operator G'_{xp} is defined by the equation

$$G'_{xp} = \tfrac{1}{2}\,\{\delta x_\mu, p_\mu\}. \tag{48}$$

The class of allowable variations for the altered Lagrangian function has the form†

$$\delta\Gamma_\mu = \varepsilon_{\mu\nu}\Gamma_\nu, \qquad \delta x_\mu = \varepsilon_\mu, \qquad \delta p_\mu = 0. \tag{49}$$

With this class of variations the principle of stationary action in the form (33′) is also satisfied. From Eqs. (48) and (49) and the independence of the variations $\delta\Gamma_\mu$ and δx_μ, we get the following commutation relations:

$$[p_\nu, p_\mu] = 0, \qquad [x_\mu, p_\nu] = i\delta_{\mu\nu}, \qquad [\Gamma_\mu, p_\nu] = 0. \tag{50}$$

If we add to the Lagrangian function (31) the total derivative $-\frac{1}{4}(d/d\tau)\{x_\mu, p_\mu\}$, then in a similar way we get two new commutation relations:

$$[x_\mu, x_\nu] = 0, \qquad [\Gamma_\mu, x_\nu] = 0. \tag{51}$$

Equations (42), (43), (50), and (51) are the final form of the commutation relations between Γ_μ, x_μ, p_μ.

All of the operators considered in the present section are taken in the Heisenberg representation, in which the state vector ψ does not depend on the proper time τ.

In the Schrödinger representation, in which the operators do not depend on the proper time τ, the state vector satisfies the following Schrödinger equation:

$$i\partial\psi(\tau)/\partial\tau = \mathscr{H}\psi(\tau). \tag{52}$$

For a free particle the Lagrangian function must be invariant with respect to displacements of the four-vector x_μ. The only relativistically invariant combination that satisfies this requirement and does not contain any dimensional constants is the quantity $\Gamma_\mu p_\mu$. Therefore it is natural to take as the function $\mathscr{H}$ for the case of free particles:

$$\mathscr{H} = -\tfrac{1}{2}\,\{\Gamma_\mu, p_\mu\}. \tag{53}$$

Then in virtue of the commutation relations the equations of motion (8) of the Heisenberg representation take the form

$$\dot{\Gamma}_\mu = 4iI_{\mu\nu}p_\nu, \qquad \dot{x}_\mu = -\Gamma_\mu, \qquad \dot{p}_\mu = 0. \tag{54}$$

The equations of motion and the commutation relations in the presence of an electromagnetic field are obtained from the Lagrangian function (31) with the Hamiltonian

---

*The algebra of the matrices Γ_μ, as defined by the commutation relations (40), has been studied in detail by Bhabha.[10] If we include in the kinematic part of the Lagrangian function arbitrary functions of the operators Γ_μ of the forms $f_\mu(\Gamma)\,\Gamma_\mu$, then Eqs. (42) and (43) remain unchanged, and Eq. (41) takes a more general form, which depends on the concrete form of the functions $f_\mu(\Gamma)$. This corresponds to the passage to an algebra that arises in the consideration of general relativistically invariant equations (cf., e.g., reference 11).

*These variations also leave invariant the kinematic part of the altered Lagrangian function (cf. footnote ‡, p. 124).

$$\mathscr{H} = -\tfrac{1}{2}\{\Gamma_\mu,\ \pi_\mu\}, \qquad \pi_\mu = p_\mu - eA_\mu$$

and are

$$\dot{\Gamma}_\mu = 4iI_{\mu\nu}\pi_\nu, \qquad \dot{x}_\mu = -\Gamma_\mu, \qquad \dot{\pi}_\mu = -eF_{\mu\nu}\Gamma_\nu,$$
$$[\pi_\mu,\ \pi_\nu] = ieF_{\mu\nu}, \quad [\pi_\mu,\ x_\nu] = -i\delta_{\mu\nu}, \quad [x_\mu,\ x_\nu] = 0. \tag{55}$$

The commutation relations for the matrices Γ_μ are those shown in Eq. (40). The Hamiltonian $\mathcal{H}$ does not depend explicitly on τ, so that there exist solutions of Eq. (52) in the form[7]

$$\psi(\tau) = e^{-im\tau}\psi,$$

where ψ satisfies the equation

$$\mathscr{H}\psi = m\psi. \tag{56}$$

For the case of free particles, Eq. (56) can be written in the form

$$(\Gamma p + m)\psi = 0 \tag{57}$$

and coincides with the relativistically invariant equations studied by Bhabha[10] (cf. footnote* p. 125).

In conclusion, the writers express their gratitude to A. I. Akhiezer and P. I. Fomin for helpful discussions.

---

[1] J. Schwinger, Theory of Quantized Fields (Russian transl.) IIL, 1956. Phys. Rev. **91**, 713, 729 (1953); **92**, 1283 (1953); **93**, 615 (1954); **94**, 1362 (1954).

[2] D. V. Volkov, J. Exptl. Theoret. Phys. (U.S.S.R.) **36**, 1560 (1959), Soviet Phys. JETP **9**, 1107 (1959).

[3] W. K. Burton and B. F. Touschek, Phil. Mag. **44**, 161 (1953).

[4] J. Schwinger, Phil. Mag. **44**, 1171 (1953).

[5] V. A. Fock, Работы по квантовой теории поля (Papers on Quantum Field Theory), Leningr. State Univ., 1957, p. 141.

[6] Y. Nambu, Prog. Theor. Phys. **5**, 82 (1950).

[7] R. P. Feynman, Phys. Rev. **80**, 440 (1950).

[8] J. Schwinger, Phys. Rev. **82**, 664 (1951).

[9] R. P. Feynman, Phys. Rev. **84**, 108 (1951).

[10] H. J. Bhabha, Revs. Modern Phys. **17**, 200 (1945).

[11] I. M. Gel'fand and A. M. Yaglom, J. Exptl. Theoret. Phys. (U.S.S.R.) **18**, 703 (1948).

Translated by W. H. Furry
27

SOVIET PHYSICS JETP VOLUME 37 (10), NUMBER 1 JANUARY, 1960

*ON TAKING THE COULOMB EFFECTS INTO ACCOUNT IN THE THEORY OF SUPERCONDUCTIVITY**

D. V. SHIRKOV

Joint Institute for Nuclear Research

Submitted to JETP editor January 29, 1959

J. Exptl. Theoret. Phys. (U.S.S.R.) **37**, 179-186 (July, 1959)

Through a transition from the energy operator to the S matrix the compensation equation for dangerous electron diagrams is brought into a symmetric form, which is expressed in terms of the usual Green functions. In the high-density electron gas approximation the summation of the Coulomb singularities in the kernel of the compensation equation is performed by the renormalization group method. In the lowest approximation the result of the summation is the same as the formulas obtained previously by qualitative means.

1. THE SYMMETRIC COMPENSATION EQUATION

THE compensation equation for the dangerous electron diagrams in the theory of superconductivity can [according to Eq. (5.19) of the book by Bogolyubov, Tolmachev, and the author[1]] be written in the form

$$\int_{-\infty}^{0} \left\langle \frac{\delta^2 R}{\delta \alpha_{k1}^{+}(t)\, \delta \alpha_{k0}^{+}(t')} \right\rangle_c e^{i\tilde{\varepsilon}(k)(t+t')} dt\, dt' = 0, \qquad (1.1)$$

where R is the energy operator

$$R = H_{int} T \left(\exp \left\{ -i \int_{-\infty}^{0} H_{int}(t)\, dt \right\} \right) = H_{int} S_{-\infty}^{0},$$

$\alpha_{k_1}^{+}$, $\alpha_{k_0}^{+}$ are the creation operators for quasi-electrons, $\tilde{\epsilon}(k)$ the energy of the single fermion excitations relative to the Fermi surface, and the index "c" indicates an average over the strongly connected diagrams (see reference 1).

In a previous paper[2] we formulated a rule for going over from matrix elements of the variational derivatives of the energy operator R to the matrix elements of the variational derivatives of the Feynman matrix

$$S = S_{-\infty}^{\infty} = T \left(\exp \left[-i \int_{-\infty}^{\infty} H_{int}(t)\, dt \right] \right).$$

According to Eq. (2.9) of that paper, Eq. (1.1) can be replaced for small $\tilde{\epsilon}(k)$ (i.e., the immediate vicinity of the Fermi surface) by

$$i \int_{-\infty}^{\infty} \left\langle \frac{\delta^2 S}{\delta \alpha_{k1}^{+}(0)\, \delta \alpha_{k0}^{+}(t)} \right\rangle_c e^{-i\tilde{\varepsilon}(k)|t|} dt = 0. \qquad (1.2)$$

Going over to derivatives with respect to the electron-hole operators $a_{k,s}$ (just as this was done in references 1 and 2), we rewrite (1.2) in the form

$$2\xi(k) u_k v_k = (u_k^2 - v_k^2) \sum_{k'} u_{k'} v_{k'} Q(k, k'), \qquad (1.3)$$

where u_k, v_k are the parameters of the canonical transformation from a to α, and

$$\xi(k) = E(k) - \lambda$$
$$+ i \int_{-\infty}^{\infty} e^{-i\tilde{\varepsilon}(k)|t|} \left\{ \left\langle \frac{\delta^2 S}{\delta a_{k,+}(0)\, \delta a_{k,+}^{+}(t)} \right\rangle_c - \left\langle \frac{\delta^2 S}{\delta a_{-k,-}^{+}(0)\, \delta a_{-k,-}(t)} \right\rangle_c \right\} dt,$$

$$Q(k, k') = Q_c(k, k') + Q_{ph}(k, k'),$$
$$Q_c(k, k') = \begin{cases} q(k, k') & \text{for } k > k_F \\ q(k', k) & \text{for } k < k_F \end{cases}, \qquad (1.4)$$

$$q(k, k') = i \int_{-\infty}^{\infty} d\tau\, d\theta\, dt \exp\{-i\tilde{\varepsilon}(k)\, \tau - \theta - i\tilde{\varepsilon}(k')\, t\}$$
$$\times \left\langle \frac{\delta^4 S_c}{\delta a_{k',+}(0)\, \delta a_{-k',-}(t)\, \delta a_{k,+}^{+}(\tau)\, \delta a_{-k,-}^{+}(0)} \right\rangle_c,$$

$$Q_{ph}(k, k') = \frac{2\tilde{g}^2(q)\, \tilde{\omega}(q)}{\tilde{\omega}(q) + \tilde{\varepsilon}(k') + \tilde{\varepsilon}(k)} \Lambda(k, k', q) \Lambda$$
$$\times (-k, -k', -q), \quad q = k - k'. \qquad (1.5)$$

The details of this calculation are contained in reference 2. We abide also by the notation used in references 1 and 2.

The vertex function Λ is defined by Eq. (3.15) of reference 2. It will be essential for us in the following that in the region of the infrared Coulomb singularity for $q^2 \sim 0$ it has the form

---

*The main results of this paper were communicated at the Fifth All-Union Conference on Low Temperature Physics (Tbilisi, October 1958).

$$\Lambda(k, k'; q) = \frac{1}{\sqrt{2V}}\left\{1 - \frac{\nu(q)\,F(q)}{2}\sum_{s}\int_{-\infty}^{\infty} dt\,\Psi_{s,q}(t)\right\}. \quad (1.6)$$

Here $\nu(q)$ is the kernel of the Coulomb interaction,

$$F(q) \quad \frac{4}{V}\sum_{\substack{l+q>k_F\\ l<k_F}} \frac{1}{\tilde{\varepsilon}(l+q)+\tilde{\varepsilon}(l)}\,,$$

and $\Psi_{s,q}(t)$ is the coefficient for the main part of the fourth variational derivative

$$\left\langle \frac{\delta^4 S_c}{\delta a^{+}_{l,s}(\tau)\,\delta a^{+}_{k,+}(\theta)\,\delta a_{l+q,s}(0)\,\delta a_{k',+}(t)} \right\rangle_c = \frac{i\nu(q)}{V}\,\delta(\tau)\,\delta(t-\theta)\,\Psi_{s,q}(t). \quad (1.7)$$

2. THE PROBLEM OF THE SUMMATION OF THE COULOMB SINGULARITIES

The expressions (1.5), (1.6), and (1.7) which we have obtained for the kernels Q_c and Q_{ph} of the integral compensation equation contain fourth variational derivatives of the Coulomb matrix S_c, the expressions for which can be analyzed completely in the approximation of a high-density electron gas when the effective parameter for the Coulomb interaction $\nu(k_F)N/V$ is small compared to the electron energy at the Fermi surface $k_F^2/2m$, i.e., when

$$\frac{4\pi\hbar^2 e^2 N}{k_F^2 V}\Bigg/\frac{k_F^2}{2m} = \frac{8}{\pi^3}\,r_s\alpha \ll 1. \quad (2.1)$$

Here $\alpha = (4/9\pi)^{1/3}$, and r_s is a dimensionless interelectron distance expressed in units of the Bohr radius.

In that case the Coulomb energy is small compared to the kinetic energy everywhere except in the region of small momentum transfers:

$$q^2 \ll k_F^2 \quad (2.2)$$

the so-called "infrared region." We can therefore use the usual perturbation theory everywhere except in the infrared region. In the infrared region, where the effective expansion parameter $r_s k_F^2/q^2$ is not small, it is necessary to sum the infinite series of "main" Coulomb terms which are proportional to the powers $(r_s k_F^2/q^2)^n$.

We meet here with a situation which is well-known in relativistic quantum electrodynamics where, notwithstanding the smallness of the dimensionless coupling constant (the fine structure constant $e^2/4\pi = 1/137$) in the so-called "ultraviolet" and "infrared" regions of the momentum variables, the actual expansion parameter is a product of $e^2/4\pi$ and a large logarithm. In quantum electrodynamics there are several well-known methods that allow us to sum the infinite sequence of main terms. We have here in mind the method of the summation of the main diagrams by Landau, Abrikosov, and Khalatnikov[3] and the method of the renormalization group.[4]

There are also a few methods, proposed in quantum statistics, which give similar results. The procedure of summing the main Coulomb diagrams developed by Gell-Mann, Brueckner and Sawada[5] is, thus, essentially equivalent to the method stated in reference 3. The well-known method of approximate second quantization[6] in the problem of the high-density electron gas leads also to similar results.[1,7] Finally, one can use for the summation of the Coulomb singularities in the Green functions the technique of the renormalization group. (Such a possibility was first indicated in reference 8.)

An important advantage of the renormalization group method is its regularity. It will be shown that the first approximation of the renormalization group method leads to the same equations as result from the summation of the main diagrams (similar to what happens in quantum field theory) and to the equations of the method of approximate second quantization.

The results of higher approximations in the renormalization group method may be of interest for a study of the problem of extending the region of applicability of the high-density electron gas approximation.

3. THE RENORMALIZATION GROUP IN THE PROBLEM OF THE COULOMB INTERACTION BETWEEN ELECTRONS

The possiblity of using the method of the renormalization group in the problem of the Coulomb interaction between electrons is based upon (see references 8 and 9 for more detail) the group character of a finite multiplicative transformation of the basic quantities: the one-electron Green function G, the two-electron (four-vertex) Green function Γ, and the dimensionless Coulomb interaction parameter r [see (2.1)]

$$G \to G' = z_2 G, \quad \Gamma \to \Gamma' = z_1^{-1}\Gamma, \quad r \to r' = z_1 z_2^{-2} r. \quad (3.1)$$

The meaning of the transformation (3.1) consists in the fact that the totality of the quantities (G', Γ', r') describes the same physical picture as the triplet (G, Γ, r).

The main instrument of the renormalization group method are the Lee differential equations. To get these we must first of all write down the functional group equations corresponding to (3.1).

As a first step we must choose a representation of the Green functions G and Γ.

For this purpose we go over to the symmetric energy-momentum representation of the electron operators (see, for instance, reference 10)

$$a_s(p) = a_s(p_0, \mathbf{p}) = \frac{1}{\sqrt{2\pi}} \int\limits_{-\infty}^{\infty} e^{ip_0\tau} a_{p,\,s}(\tau)\, d\tau,$$

$$a_s^+(p) = \frac{1}{\sqrt{2\pi}} \int\limits_{-\infty}^{\infty} e^{-ip_0\tau} a_{p,\,s}^+(\tau)\, d\tau. \qquad (3.2)$$

The chronological pairing has the following form in that representation

$$\overbracket{a_s(p)\; a_\sigma^+}(k) = i\delta(p-k)\,\delta_{s\sigma} G_0(p),$$

$$\delta(p-k) \equiv \delta_{\rho\mathbf{k}}\,\delta(p_0 - k_0),$$

$$G_0(p) = 1/[p_0 - |\tilde{\varepsilon}(\mathbf{p})| + i\alpha\, \mathrm{sign}\, \tilde{\varepsilon}(\mathbf{p})]. \qquad (3.3)$$

In the case under consideration we get for the total Green function, because of the definition of the renormalized energy $\tilde{\epsilon}$,

$$\langle T a_s(p)\, a_\sigma^+(k)\, S\rangle_0 / S_0 = i\delta(p-k)\,\delta_{s\sigma} G(p)$$

also

$$G(p) = s(p)/[p_0 - |\tilde{\varepsilon}(\mathbf{p})| + i\alpha\, \mathrm{sign}\, \tilde{\varepsilon}]. \qquad (3.4)$$

The two-electron (four-vertex) Green function Γ is defined as

$$i\left\langle \frac{\delta^4 S}{\delta a_{s_1}(p_1)\, \delta a_{s_2}(p_2)\, \delta a_{\sigma_1}^+(k_1)\, \delta a_{\sigma_2}^+(k_2)} \right\rangle_c$$

$$= \delta(p_1 + p_2 - k_1 - k_2)\, \Gamma_{s_1 s_2 \sigma_1 \sigma_2}(p_1, p_2, k_1, k_2).$$

Here

$$\Gamma_{s_1 s_2 \sigma_1 \sigma_2}(p_1, p_2, k_1, k_2)$$

$$= \frac{i}{2\pi} \int\limits_{-\infty}^{\infty} d\tau\, dt_1\, dt_2 \exp\{-ip_2^0\tau + ik_1^0 t_1 + ik_2^0 t_2\}$$

$$\times \left\langle \frac{\delta^4 S}{\delta a_{s_1\mathbf{p}_1}(0)\, \delta a_{s_2\mathbf{p}_2}(\tau)\, \delta a_{\sigma_1\mathbf{k}_1}^+(t_1)\, \delta a_{\sigma_2\mathbf{k}_2}^+(t_2)} \right\rangle_c,$$

$$p_1^0 + p_2^0 = k_1^0 + k_2^0, \qquad \mathbf{p}_1 + \mathbf{p}_2 = \mathbf{k}_1 + \mathbf{k}_2. \qquad (3.5)$$

The function Γ has a simple matrix structure

$$\Gamma_{s_1 s_2 \sigma_1 \sigma_2}(p_1, p_2, k_1, k_2) = \delta_{s_2\sigma_1}\delta_{s_1\sigma_2}\Gamma(k_1, k_2, p_1, p_2)$$

$$- \delta_{s_1\sigma_1}\delta_{s_2\sigma_2}\Gamma(k_1, k_2, p_2, p_1).$$

In our case of the infrared Coulomb asymptotic behavior, the one-electron Green function G has no singularity, and we can thus put s(p) = 1. If we also take into account that for the compensation equation only the vicinity of the Fermi surface is of importance, we can restrict our consideration to the function Γ with $k_1^0 = k_2^0 = p_1^0 = p_2^0 = 0$, i.e.,

$$\Gamma(\mathbf{k}_1, \mathbf{k}_2, \mathbf{p}_1, \mathbf{p}_2)$$

$$= \frac{i}{2\pi} \int\limits_{-\infty}^{\infty} d\tau\, dt_1\, dt_2 \left\langle \frac{\delta^4 S_c}{\delta a_{\mathbf{p}_1,+}(0)\, \delta a_{\mathbf{p}_2,-}(\tau)\, \delta a_{\mathbf{k}_1,-}^+(t_1)\, \delta a_{\mathbf{k}_2,+}^+(t_2)} \right\rangle_c.$$

$$(3.6)$$

with $\mathbf{p}_1 + \mathbf{p}_2 = \mathbf{k}_1 + \mathbf{k}_2$. Indeed, we get from Eq. (1.5)

$$q(k, k') = -2\pi\Gamma(-\mathbf{k}, \mathbf{k}, \mathbf{k} - \mathbf{q}, \mathbf{q} - \mathbf{k}). \qquad (3.7)$$

On the other hand, it follows from (1.6) and (1.7) that

$$\Lambda(k, k'; q) = \{1 - 2\pi V F(\mathbf{q})\Gamma(\mathbf{q})\}/\sqrt{2V}, \qquad (3.8)$$

where Γ(**q**) is the "main" part of the function Γ(*l*+**q**, **k**−**q**, **k**, *l*), in the limit of small **q** independent of **k** and *l*.

In the lowest order of perturbation theory

$$\Gamma_0(k, l, l+q, k-q) = \nu(q)/2\pi V.$$

It is therefore convenient to introduce a new function g defined by the relation

$$\Gamma(k, l, l+q, k-q)$$

$$= \frac{\nu(q)}{2\pi V} g(k, l, l+q, k-q). \qquad (3.9)$$

This function possesses the following important properties:

a) It transforms under the transformation (3.1) as

$$g \to g' = z_1^{-1} g; \qquad (3.10)$$

b) It tends to a constant in the limit of switching off the Coulomb interaction.

c) If it is written as a perturbation-theory series, it contains terms proportional to powers of the ratio $(r_S k_F^2/q^2)$.

In such a case it is not difficult to write down the functional group equation for the vertex function g in the infrared region. To do this we shall introduce a normalizing momentum λ and go over to dimensionless variables

$$g(q^2, k_F^2, \ldots, r) = f(q^2/\lambda^2, k_F^2/\lambda^2; r).$$

The dots indicate here the unimportant momentum variables k^2, l^2, $(k-l)^2, \ldots$. We must also include in their number the energy variables k_0, q_0, l_0. We can omit writing all these variables explicitly, considering them as fixed parameters. Taking (3.1) and (3.10) into account we get

$$f(q^2/\lambda_1^2, k_F^2/\lambda_1^2, r_1)$$

$$= z_1^{-1} f(q^2/\lambda^2, k_F^2/\lambda^2, r), \quad r_1 = z_1 r. \qquad (3.11)$$

Choosing the normalizing momentum λ in such a way that

$$f(1, y, r) = 1, \qquad (3.12)$$

we go over to the functional group equation

$$f(x,\ y,\ r)=f(t,\ y,\ r)\,f(x/t,\ y/t,\ rf(t,\ y,\ r)). \tag{3.13}$$

Differentiating (3.12) with respect to x and afterwards putting t = x we get Lee's equation

$$\frac{\partial f(x,\ y,\ r)}{\partial x}=\frac{f(x,\ y,\ r)}{x}\,\Phi\left(\frac{y}{x},\ rf(x,\ y,\ r)\right), \tag{3.14}$$

where the function

$$\Phi(y,\ r)=\left.\frac{\partial f(x,\ y,\ r)}{\partial x}\right|_{x=1}, \tag{3.15}$$

according to the usual correspondence requirements must be evaluated by perturbation theory.

4. THE INFRARED ASYMPTOTIC BEHAVIOR OF THE VERTEX FUNCTION

The perturbation-theory evaluation of the function f which enters into the right-hand side of (3.15) must be performed with account of the multiplicative arbitrariness of (3.11), which insures the satisfying of the normalization condition (3.12).

In this way we get, up to terms of the third order,

$$f_{\text{pert. th.}}(x,\ y,\ r)=1-ar\left(\frac{y}{x}-1\right)+br^2\left(\frac{y}{x}-1\right)^2$$
$$-\,cr^2\left(\frac{y}{x}-1\right)+\cdots, \tag{4.1}$$

where a, b, and c are certain numbers (which may depend on the above-mentioned parameters). Substituting (4.1) into (3.15) and (3.14) and evaluating the quadrature, we get successively

$$\Phi(y,\ r)=ary+cr^2y,$$
$$\frac{df}{f^2(1+rf\,c/a)}=ary\frac{dx}{x^2},$$
$$r\frac{c}{a}\ln\left|\frac{a+rcf}{(a+rc)f}\right|+1-\frac{1}{f}=ary\left(1-\frac{1}{x}\right). \tag{4.2}$$

We obtain here for f a transcendental equation which can be solved by successive approximations, taking into account the fact that r is small. This gives

$$f(x,\ y,\ r)=\left\{1+ary\left(\frac{1}{x}-1\right)\right.$$
$$\left.+\,r\frac{c}{a}\ln\left|\frac{1+ary(1/x-1)+rc/a}{1+rc/a}\right|\right\}^{-1}. \tag{4.3}$$

We note that the constant b in (4.1) does not enter into Eqs. (4.2) and (4.3). The point is that this constant is not independent. Expanding (4.3) in a power series in r and comparing it with (4.1), we find that

$$b=a^2. \tag{4.4}$$

We must now still perform the transition to the usual unnormalized function f_0, which depends on the observed value of the coupling constant $r = r_s$ and which does not contain the normalization momentum λ.

Perturbation theory gives for f_0

$$f_0^{\text{pert. th.}}(q^2,\ r_s)=1-ar_s\left(\frac{k_F^2}{q^2}+d\right)+a^2r_s^2\left(\frac{k_F^2}{q^2}+d\right)^2$$
$$-\,cr_s^2\frac{k_F^2}{q^2}+\cdots. \tag{4.5}$$

Here d is a constant, just as a and c.

To perform the above-mentioned transition we use a standard method (see Sec. 42.3 of reference 4) based upon the property of the invariant charge rf:

$$rf(q^2/\lambda^2,\ k_F^2/\lambda^2,\ r)=r_sf_0(q^2,\ k_F^2,\ r_s). \tag{4.6}$$

Putting $q^2 = \lambda^2$ in (4.6) we get for r the explicit expression

$$r=r_sf_0^{\text{pert. th.}}(\lambda^2,\ k_F^2,\ r_s).$$

Substituting this value into the left-hand side of (4.6) and taking (4.3) into account we obtain, after some simple calculations,

$$f_0(q^2,\ r_s)=\left[1+ar_s\left(\frac{k_F^2}{q^2}+d\right)\right.$$
$$\left.+\,r_s\frac{c}{a}\ln\left(1+ar_s\frac{k_F^2}{q^2}\right)\right]^{-1}. \tag{4.7}$$

One can easily verify that (4.5) is just the expansion of (4.7) in powers of small r_s.

5. DISCUSSION OF THE RESULTS

Let us discuss Eq. (4.7) which we have obtained and which describes the behavior of the Coulomb four-vertex function in the infrared region.

Recalling that according to (3.9)

$$\Gamma(q)=\frac{\nu(q)}{2\pi V}f_0(q^2,\ r_s)=\frac{2e^2}{V|q|^2}f_0(q^2,\ r_s), \tag{5.1}$$

we consider the expression

$$Q^{-2}=\frac{1}{q^2}f_0(q^2,\ r_s)=\left[q^2+ar_sk_F^2+q^2ar_sd\right.$$
$$\left.+\,r_s\frac{c}{a}q^2\ln\left(1+ar_s\frac{k_F^2}{q^2}\right)\right]^{-1}. \tag{5.2}$$

In the limits of small r_s and q^2 we get

$$Q^{-2}=\frac{1}{q^2+ar_sk_F^2}=\frac{1}{q^2+q_s^2}, \tag{5.3}$$

where $q_s = 0.814\,r_s^{1/2}k_F$ is the inverse Thomas-Fermi screening length.

In the lowest approximation (in powers of r_s), Eq. (5.2) leads to the well-known formula of the Coulomb screening. We have thus shown that the results of the summation of the main Coulomb diagrams by Gell-Mann, Brueckner, and Sawada[5] can be obtained by the renormalization group method by far simpler means.

We note also that substituting (5.3) into (5.1) and into (3.8) and taking into account that

$$\lim_{q^2 \to 0} q^2 F(q)\,\nu(q) = q_s^2,$$

we get*

$$\Lambda(q) = \frac{1}{\sqrt{2V}}\left\{1 - \frac{q_s^2}{q^2 + q_s^2}\right\} = \frac{1}{\sqrt{2V}}\,\frac{q^2}{q^2 + q_s^2}\,. \qquad (5.4)$$

Equations (5.3) and (5.4) are the same as the results of Sec. 6.2 of reference 1 obtained there by qualitative arguments.

The significance, however, of Eqs. (5.2) and (4.7) and also of the possibilities of the renormalization group method in the problem of interacting electrons is not exhausted by this. The renormalization group technique gives us a regular method to improve the asymptotic properties of the expansions of the usual perturbation theory. This fact is well-known in quantum field theory. The present investigation illustrates this fact for quantum statistics.

Equations (4.7) and (5.2) appropriately generalized to the case where the energy arguments are not equal to zero are thus the second approximation to the results of reference 5. A further generalization of these equations to higher orders can very simply be performed by means of taking higher terms in powers of r_s into account in (4.1).

Such a generalization can be of interest, for instance, to make the criterion for superconductivity (see Sec. 5.4 of reference 1) more precise and also to make the expansions for the correlation energy more precise in the region of not-very-small r_s.

We note in this connection that at the last moment we learned of the thesis by Dubois[12] in which there is an attempt to make the formulas of reference 5 more exact by summing the main diagrams of the second order. Without going into a detailed comparison, we note that the structure of the expressions obtained by Dubois[12] [Eqs. (2.7), (2.5), and (A.3) of that paper] correspond at first sight to the following substitution into (4.7);

$$r_s \frac{c}{a} \ln\left(1 + a r_s \frac{k_F^2}{q^2}\right) \to r_s^2 c \frac{k_F^2}{q^2}\,,$$

which is valid only for small r_s and not too small q^2.

---

*This formula is in agreement with the result of reference 11.

---

[1] Bogolyubov, Tolmachev, and Shirkov, Новый метод в теории сверхпроводимости, (*A New Method in the Theory of Superconductivity*), U.S.S.R. Acad. Sci. Press, 1958, Fortschr. Phys. **6**, 605 (1958).

[2] D. V. Shirkov, J. Exptl. Theoret. Phys. (U.S.S.R.) **36**, 607 (1959), Soviet Phys. JETP **9**, 421 (1959).

[3] Landau, Abrikosov, and Khalatnikov, Dokl. Akad. Nauk SSSR **95**, 773, 1177 (1954). **96**, 261 (1954).

[4] N. N. Bogolyubov and D. V. Shirkov, *Introduction to the Theory of Quantum Fields*, Interscience, 1959.

[5] M. Gell-Mann and K. A. Brueckner, Phys. Rev. **106**, 364 (1957); K. Sawada, Phys. Rev. **106**, 372 (1957).

[6] N. N. Bogolyubov, Лекции по квантовой статистике (*Lectures on Quantum Statistics*), Kiev, 1947.

[7] Chen Chun-Sian and Chow Shih-Hsun, J. Exptl. Theoret. Phys. (U.S.S.R.) **34**, 1566 (1958), Soviet Phys. JETP **7**, 1080 (1958).

[8] Blank, Bonch-Bruevich, and Shirkov, J. Exptl. Theoret. Phys. (U.S.S.R.) **33**, 265 (1957), Soviet Phys. JETP **6**, 204 (1958).

[9] V. L. Bonch-Bruevich, Физика металлов и металловедение (Phys. of Metals and Metallography) **6**, 769 (1958).

[10] V. M. Galitskiĭ and A. B. Migdal, J. Exptl. Theoret. Phys. (U.S.S.R.) **34**, 139 (1958), Soviet Phys. JETP **7**, 96 (1958); V. M. Galitskiĭ, J. Exptl. Theoret. Phys. (U.S.S.R.) **34**, 151 (1958), Soviet Phys. JETP **7**, 104 (1958).

[11] Chen Chun-Sian and Chow Shih-Hsun, J. Exptl. Theoret. Phys. (U.S.S.R.) **36**, 1246 (1959), Soviet Phys. JETP **9**, 885 (1959).

[12] D. F. Dubois, Electron Interactions, Doctoral Thesis, California Institute of Technology, 1958.

Translated by D. ter Haar
28

SOVIET PHYSICS JETP VOLUME 37 (10), NUMBER 1 JANUARY, 1960

ANALYSIS OF EXPERIMENTAL DATA RELATING TO THE SURFACE IMPEDANCE OF SUPERCONDUCTORS

A. A. ABRIKOSOV, L. P. GOR' KOV, and I. M. KHALATNIKOV

Institute for Physical Problems, Academy of Sciences, U.S.S.R.

Submitted to JETP editor February 3, 1959

J. Exptl. Theoret. Phys. (U.S.S.R.) **37**, 187-191 (July, 1959)

The results of experimental measurement of the surface impedance of superconductors at various frequencies are compared with the new theory of superconductivity. Satisfactory agreement with the experiments has been found for all frequencies excluding the very lowest ones. At low frequencies the experimental values for the real part of the impedance near the critical temperature are several times larger than the theoretical values.

THE properties of superconductors in a high-frequency field have been discussed by the present authors[1] and by Mattis and Bardeen.[2] In this paper the theory will be compared with experimental results on the surface impedance of superconductors.

We first derive formulae for the surface impedance in various limiting conditions, which are appropriate for making comparison with experiment.* It is usual in experiments to measure the ratio of the impedance in the superconducting state $Z(\omega)$, to the real part of the impedance in the normal state, R_n. This ratio is given (in the Pippard limiting case) by the formula

$$Z(\omega)/R_n = -2i\left(\pi\omega/\Delta Q(\omega)\right)^{1/3}. \tag{1}$$

The complex function $Q(\omega)$ is given by

$$\begin{aligned} Q(\omega) = \pi \int\limits_{\max(1,\,\tilde{\omega}-1)}^{1+\tilde{\omega}} \tanh\frac{\varepsilon\Delta}{2T}\, \frac{\varepsilon(\varepsilon-\tilde{\omega})+1}{\sqrt{(\varepsilon^2-1)(1-(\varepsilon-\tilde{\omega})^2)}}\, d\varepsilon \\ - i\pi\theta(\tilde{\omega}-2) \int\limits_{1}^{\tilde{\omega}-1} \tanh\frac{\varepsilon\Delta}{2T}\, \frac{\varepsilon(\tilde{\omega}-\varepsilon)+1}{\sqrt{(\varepsilon^2-1)((\tilde{\omega}-\varepsilon)^2-1)}}\, d\varepsilon \\ - i\pi\int\limits_{1}^{\infty} \left\{\tanh\frac{(\varepsilon+\tilde{\omega})\Delta}{2T}\right. \\ \left. - \tanh\frac{\varepsilon\Delta}{2T}\right\} \frac{\varepsilon(\varepsilon+\tilde{\omega})+1}{\sqrt{(\varepsilon^2-1)((\varepsilon+\tilde{\omega})^2-1)}}; \end{aligned} \tag{2}$$

$$\theta(x) = \begin{cases} 1; & x > 0 \\ 0; & x < 0 \end{cases}; \quad \tilde{\omega} = \omega/\Delta.$$

The magnitude of 2Δ gives the energy gap at the given temperature.

According to Eq. (1) the frequency dependence of the impedance is given by the expression

$$\begin{aligned} \frac{Z(\omega)}{R_n} = 2\left[\frac{\pi\omega}{\Delta|Q(\omega)|}\right]^{1/3} \left\{\sin\left(\frac{1}{3}\tan^{-1}\frac{\operatorname{Im} Q}{\operatorname{Re} Q}\right)\right. \\ \left. - i\cos\left(\frac{1}{3}\tan^{-1}\frac{\operatorname{Im} Q}{\operatorname{Re} Q}\right)\right\}. \end{aligned} \tag{3}$$

For $T = 0$ the function Q has the values

$$\begin{aligned} Q(\omega, 0) = \begin{cases} 2\pi E\left(\frac{\tilde{\omega}}{2}\right), & \tilde{\omega} < 2 \\ \pi\left[\tilde{\omega} E\left(\frac{2}{\tilde{\omega}}\right) - \frac{\tilde{\omega}^2-4}{\tilde{\omega}} K\left(\frac{2}{\tilde{\omega}}\right)\right] \end{cases} \\ + i\pi\theta(\tilde{\omega}-2)\left[\tilde{\omega} E\left(\sqrt{1-\left(\frac{2}{\tilde{\omega}}\right)^2}\right)\right. \\ \left. - \frac{4}{\tilde{\omega}} K\left(\sqrt{1-\left(\frac{2}{\tilde{\omega}}\right)^2}\right)\right], \quad \tilde{\omega} > 2. \end{aligned} \tag{4}$$

Here E and K are complete elliptical integrals. Figure 1 shows the dependence of $Z/R_n = R/R_n + iX/R_n$ on $\tilde{\omega}$ at $T = 0$.

The temperature dependence for temperatures other than absolute zero will be analyzed for various frequencies:

a) $\omega \ll \Delta(0)$. At the lowest temperatures

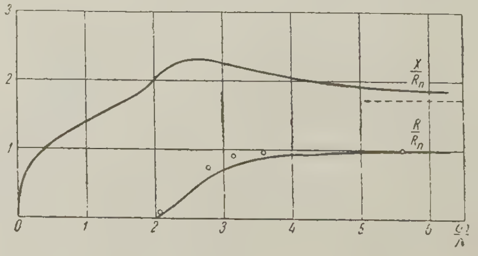

FIG. 1

---

*We take this opportunity to point out that in Eq. (14) of reference 1 the real part of Q(ω) was incorrectly calculated. This error affects some limiting expressions for the impedance derived in reference 1. The present nomenclature is the same as in reference 1.

there is a region where $T \ll \omega \ll \Delta$ in which Eqs. (3) and (4) apply. After the region where $T \sim \omega$ we arrive at $\omega \ll T \ll \Delta$, and the variation with T is given by

$$\frac{Z(\omega)}{R_n} = 2\left(\frac{\omega}{\pi\Delta}\right)^{1/3}\left\{\frac{4}{3}\sinh\frac{\omega}{2T}K_0\left(\frac{\omega}{2T}\right)e^{-\Delta/T}\right.$$
$$\left.-i\left[1+\frac{1}{3}\left(\frac{\omega}{4\Delta}\right)^2+\frac{2}{3}e^{-\omega/2T}I_0\left(\frac{\omega}{2T}\right)e^{-\Delta/T}\right]\right\}. \qquad (5)$$

On increasing T further we first have $\omega \ll \Delta \sim T$ and then the small region where $\omega \ll \Delta \ll T$. Here, until $\Delta/T \gg \omega/\Delta$, Q is little different from its value at $T = 0$, and we then obtain

$$\frac{Z(\omega)}{R_n} = 2\left[\frac{\omega}{\pi\Delta\tanh(\Delta/2T)}\right]^{1/3}\left\{\frac{2}{3\pi}\frac{\omega}{T\sinh(\Delta/T)}\ln\left(2\sqrt{\frac{2\Delta}{\omega}}\right)\right.$$
$$+\frac{1}{3\pi}\frac{\omega}{\Delta}\left(\coth\frac{\Delta}{2T}-1\right)$$
$$\left.-\frac{2}{3\pi}\frac{\omega}{T}P\left(\frac{\Delta}{T}\right)\coth\frac{\Delta}{2T}-i\left[1+\frac{1}{3}\left(\frac{\omega}{4\Delta}\right)^2\right]\right\}, \qquad (6)$$

where the function P (x) is the integral

$$P(x) = \int_1^\infty \frac{d\varepsilon}{\varepsilon^2-1}\frac{\cosh x\varepsilon - \cosh x}{(\cosh x\varepsilon+1)(\cosh x+1)}$$
$$= \begin{cases} e^{-x}\ln 2\gamma x; & \text{for. } x \gg 1 \\ (7/2\pi^2)\zeta(3)\,x; & \text{for. } x \ll 1. \end{cases} \qquad (6')$$

When this condition does not hold, one can obtain the following formula by making use of the fact that Δ is small:

$$Z(\omega)/R_n = -2i\left(-i+\pi\Delta^2/2T\omega\right)^{-1/3}. \qquad (7)$$

b) $\omega \sim \Delta(0)$. It is much more difficult to compare theory and experiment in this case, since in most of the temperature range $0 < T < T_c$, Δ, ω and T are of the same order of magnitude. The expression for $Q(\omega)$ can only be simplified at low temperatures, such that $T \ll \omega \sim \Delta$. There are then two possibilities: $\omega < 2\Delta(0)$ and $\omega > 2\Delta(0)$. In the first case $Q(\omega)$ is little different from the value of $\operatorname{Re} Q(\omega)$ at $T = 0$, equal to $2\pi E(\omega/2\Delta)$, and the impedance is given by

$$\frac{Z(\omega)}{R_n} = 2\left[\frac{\omega}{2\Delta E(\omega/2\Delta)}\right]^{1/3}\left\{\frac{e^{-\Delta/T}}{3E(\omega/2\Delta)}\sqrt{\pi T\left(\frac{1}{\omega}+\frac{1}{2\Delta}\right)}\right.$$
$$\left.-i\left[1+\frac{e^{-\Delta/T}}{3E(\omega/2\Delta)}\sqrt{\pi T\left(\frac{1}{\omega}-\frac{1}{2\Delta}\right)}\right]\right\}. \qquad (8)$$

For $\omega > 2\Delta(0)$ both parts of $Q(\omega)$ are of comparable magnitude, and it is simplest to use the general formula (3) with $Q(\omega)$ given by

$$Q(\omega, T) = Q(\omega, 0) + 2\pi e^{-(\omega-\Delta)/T}\sqrt{\pi T(1/2\Delta - 1/\omega)}$$
$$-2\pi i e^{-\Delta/T}\sqrt{\pi T}\left[\sqrt{1/\omega + 1/2\Delta}\right.$$
$$\left.-\sqrt{1/2\Delta - 1/\omega}\right]. \qquad (9)$$

With increasing temperature we pass the region where $\omega \sim \Delta \sim T$ and reach the region $\Delta \ll T \sim \omega$. Here we can make use of the fact that the limiting value of the impedance for $\omega \gg \Delta$ is independent of temperature and corresponds to the normal metal. Equation (9) can, therefore, be used for extrapolation purposes without appreciable error.

c) $\omega \gg \Delta(0)$. In this case only the relation between T and Δ varies, while ω is always large compared with them both. Bearing in mind that the real part of $Q(\omega)$ is small compared with the imaginary part, we obtain

$$\frac{Z(\omega)}{R_n} = 1 + \left(\frac{\Delta}{\omega}\right)^2\left[\frac{2}{3}\ln\frac{2\omega}{\Delta(0)}+\frac{1}{3}-\frac{\pi}{\sqrt{3}}\right]$$
$$-i\sqrt{3}\left[1+\left(\frac{\Delta}{\omega}\right)^2\left(\frac{2}{3}\ln\frac{2\omega}{\Delta(0)}+\frac{1}{3}-\frac{\pi}{3\sqrt{3}}\right)\right]. \qquad (10)$$

The formulae we have derived make it possible to compare theory with the many experimental results in detail.

For this comparison we have used the data of several authors.[3-6]

There are no experimental data for very high frequencies $\omega \gg \Delta(0)$. The largest "effective frequency" $\omega/T_c = 3.04$ was used in the measurement of R for aluminum.[3] Since Δ decreases on approaching T_c, we may assume that the conditions for the applicability of Eq. (10) are approximately satisfied for $1 - T/T_c < 0.9$. Figure 2 shows the comparison between this equation and the experimental data, and it can be seen that near T_c there is agreement (the full curve is the theoretical curve for $\omega \gg \Delta$, T).

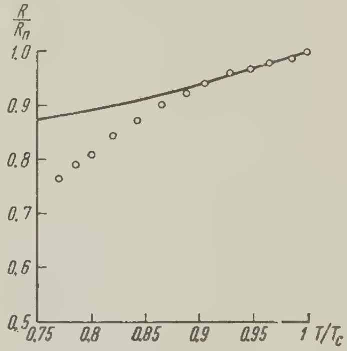

FIG. 2

In Khaĭkin's work[4] the surface impedance of single crystals of cadmium was measured at temperatures between 0.1° and $T_c = 0.56$°K at a frequency $\omega = 0.9\,T_c$ ($\Delta = 0.985$°K). In practice, the whole temperature range, except near T_c, is covered by Eq. (8) ($\omega \sim \Delta$). The theoretical curves for R/R_n and X/R_n are shown in Fig. 3, and the experimental data are plotted with the er-

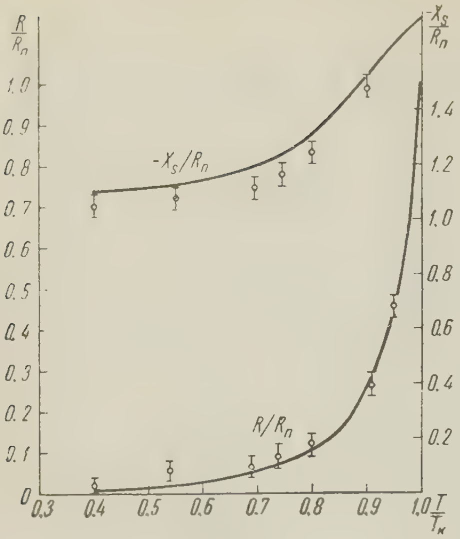

FIG. 3

ror limits indicated by the lines. The agreement between theory and experiment is quite good. It must be borne in mind that the effects of anisotropy, which may influence the results, are not considered in the theory.

The situation is worse when we analyze the low-frequency data of Pippard[5] and Prozorova.[6] There is considerable disagreement between the results for mercury ($\omega = 0.014\,T_c$) and tin ($\omega = 0.0155\,T_c$ in reference 5; $\omega = 0.11\,T_c$ in reference 6) and the theory, near the transition temperature.

At these low frequencies we are, near T_c, in the region where $\Delta/T \ll 1$, but the condition $\Delta/T \gg \omega/\Delta$ is not satisfied. For example, for mercury[5] the two conditions hold at $T - T_c \sim 10^{-3\circ}$ K. Equation (7) then simplifies to

$$\frac{R}{R_n} = 0.019\left(\frac{\omega/T_c}{1-T/T_c}\right)^{4/3}, \qquad \frac{X}{R_n} = 0{,}82\left(\frac{\omega/T_c}{1-T/T_c}\right)^{1/3},$$

$$\Delta \approx 3.06\ T_c(1 - T/T_c)^{1/2}. \tag{11}$$

These equations for T near T_c could have been obtained independently of the previous calculation, as can be seen from Eq. (7), which can really be considered an interpolation between a superconductor at $\omega = 0$ and the normal metal.

Equation (6) must be used for temperatures further away from T_c.

The following results come out of the calculation. R/R_n at $T/T_c \sim 0.6 - 0.7$ for Hg at 1200 Mcs,[5] calculated according to Eq. (6) is just half the experimental value. This discrepancy increases on approaching T_c, and where Eq. (11) is applicable, for $T - T_c \sim 0.01$°K, the value of R/R_n obtained from Eq. (11) is one sixth of the measured value. The discrepancy for tin measured by Pippard is even greater. We may note that at these frequencies tin, unlike mercury, is not a clear example of a Pippard metal, but is, rather, an intermediate case.

A similar discrepancy is found between the calculated values and Prozorova's results for tin at higher frequencies, $\omega \simeq 0.11\,T_c$. At $T/T_c \sim 0.75$ the experimental value of R/R_n is only 30% higher than the calculated value, and this difference increases to a factor of 3 or 4 near T_c. Both curves, naturally, agree at $T = T_c$ with the normal metal. Comparison with the experimental data for X shows somewhat better agreement. The experimental[6] and theoretical values for $|X_n - X|/R_n$ do not differ by more than a factor of 2.

The reason for the discrepancy between the experimental data and the impedance calculated according to the new theory of superconductivity is at present not clear. We should point out that for mercury, near $T_c - T \sim 0.1 - 0.005°$, the data fit the relation $R/R_n \sim (1 - T/T_c)^{-4/3}$. This range is also described by Eq. (6) in the region $\Delta \sim T$, where the discrepancy with experiment is less. If the ratio R/R_n were calculated on the assumption that for this range of temperature and frequency the metal were of the London type, which is justifiable for tin, then the temperature dependence would essentially be $R/R_n \sim (1 - T/T_c)^{-2}$. As can be seen, this does not agree with Pippard's experimental results.

---

[1] Abrikosov, Gor'kov, and Khalatnikov, J. Exptl. Theoret. Phys. (U.S.S.R.) **35**, 265 (1958), Soviet Phys. JETP **8**, 182 (1959).

[2] D. C. Mattis and J. Bardeen, Phys. Rev. **111**, 412 (1958).

[3] Biondi, Garfunkel, and McCoubrey, Phys. Rev. **108**, 495 (1957).

[4] M. S. Khaĭkin, J. Exptl. Theoret. Phys. (U.S.S.R.) **34**, 1389 (1958), Soviet Phys. JETP **7**, 961 (1958).

[5] A. B. Pippard, Proc. Roy. Soc. **A191**, 370, 399 (1947).

[6] L. A. Prozorova, Thesis, Institute for Physical Problems, Academy of Sciences, U.S.S.R. (1958).

Translated by R. Berman
29

SOVIET PHYSICS JETP VOLUME 37(10), NUMBER 1 JANUARY, 1960

ON THE CALCULATION OF THE INTERACTION CONSTANT IN A NONLINEAR THEORY

Ya. I. GRANOVSKIĬ

Institute of Nuclear Physics, Academy of Sciences, Kazakh S.S.R.

Submitted to JETP editor, February 6, 1959

J. Exptl. Theoret. Phys. (U.S.S.R.) **37**, 192-196 (July, 1959)

The coupling constant is expressed in terms of the proton mass in the second approximation of the Tamm-Dancoff method. The formulas obtained can be used in the case in which the Lagrangian is an arbitrary linear combination of the five basic invariants.

CALCULATION of various physical quantities in the theory with the Lagrangian

$$L=\bar{\psi}\gamma_\mu\nabla_\mu\psi+\tfrac{1}{2}l^2\sum_n C_nN\,(\bar{\psi}O_n\psi\cdot\bar{\psi}O_n\psi) \qquad (1)$$

requires a knowledge of the coupling constant l. Various methods exist for its determination: from the meson-nucleon interaction,[1] from the mass of the π meson,[1, 2] and so on. In the present paper we shall determine it from a calculation of the mass of the nucleon.[3]

The equation for a Fourier component of the nucleon wave function,

$$\psi(p)=\int\langle 0\,|\,\psi(x)\,|\,\Phi\rangle\, e^{-ipx}d^4x \qquad (2)$$

can be derived in the same way as in the paper of Heisenberg, Kortel, and Mitter.[3] It has the form

$$\begin{aligned}\psi(p)=&-\frac{l^4}{3(2\pi)^8}G(p)\sum_{m,n}C_mC_nO_m\int d^4q\,d^4r\\&\times\{G(p+q-r)\,O_n\,S(q)\,O_mS(r)\\&-G(p+q-r)\,\mathrm{Sp}\,O_nS(q)\,O_mS(r)\\&+S(r)\,O_nS(q)\,O_m\,G(p+q-r)\\&-S(r)\,\mathrm{Sp}\,O_nS(q)\,O_mG(p+q-r)\\&-S(r)\,O_n\,G(p+q-r)\,O_mS(-q)\\&+S(r)\,\mathrm{Sp}\,O_nG(p+q-r)\,O_mS(r)\}\,O_n\psi(p).\end{aligned} \qquad (3)$$

In this integral the path is taken around the poles of the Green's function

$$G(p+q-r)=\gamma_\mu\frac{(p+q-r)_\mu}{(p+q-r)^2}\equiv\frac{\hat{S}}{(p+q-r)^2} \qquad (4)$$

and the propagation function

$$\begin{aligned}S(q)&=\frac{\varkappa^3}{q^2(q^2+\varkappa^2)}\left(\varkappa\frac{\gamma_\nu q_\nu}{q^2}-i\right)\\&\equiv\frac{\varkappa^3}{q^2(q^2+\varkappa^2)}(\hat{Q}-i)\end{aligned} \qquad (5)$$

as prescribed by Feynman's rules.

Using the identity[4,5]

$$\begin{aligned}(O_nMO_n)_{\alpha\beta}&=O^n_{\alpha\gamma}M_{\gamma\delta}O^n_{\delta\beta}\\&=\tfrac{1}{4}M_{\gamma\delta}\sum_k A_{nk}O^k_{\alpha\beta}O^k_{\delta\gamma}=\tfrac{1}{4}\sum_k A_{nk}O^k_{\alpha\beta}\mathrm{Sp}\,MO^k,\end{aligned} \qquad (6)$$

we can reduce all the terms of Eq. (3) to calculations of traces:

$$\begin{aligned}\psi(p)=&-\frac{l^4\varkappa^6}{3(2\pi)^8}G(p)\sum_{m,n,k}C_mC_n\left(\frac{1}{4}A_{nk}-\delta_{nk}\right)\\&\times\int\frac{d^4q\,d^4r}{N_1}\{O_m\hat{S}O_k\,\mathrm{Sp}\,(\hat{Q}-i)\,O_m\,(\hat{R}-i)\,O_k\\&+O_m\,(\hat{R}-i)\,O_k\mathrm{Sp}\,(\hat{Q}-i)\,O_m\hat{S}O_k\\&+O_m\,(\hat{R}-i)\,O_k\,\mathrm{Sp}\,\hat{S}O_m\,(\hat{Q}+i)\,O_k\}\,\psi(p)\\=&-\frac{l^4\varkappa^6}{3(2\pi)^8}G(p)\sum_{m,n}C_mC_n\int\frac{d^4q\,d^4r}{N_1}\sum_k\left(\frac{1}{4}A_{nk}-\delta_{nk}\right)\\&\times\{O_m\hat{S}O_k[\mathrm{Sp}\,O_k\hat{Q}O_m\hat{R}-i\,\mathrm{Sp}\,O_kO_m\hat{R}-i\,\mathrm{Sp}\,O_k\,\hat{Q}O_m\\&-\mathrm{Sp}\,O_kO_m]+O_m\,(\hat{R}-i)\,O_k\,[\mathrm{Sp}\,O_k\hat{Q}O_m\hat{S}-i\,\mathrm{Sp}\,O_kO_m\,\hat{S}\\&+i\,\mathrm{Sp}\,O_k\hat{S}O_m+\mathrm{Sp}O_k\hat{S}O_m\hat{Q}]\}\,\psi(p).\end{aligned} \qquad (7)$$

Here we have for brevity introduced the notation

$$N_1=(p+q-r)^2\,q^2\,(q^2+\varkappa^2)\,r^2\,(r^2+\varkappa^2). \qquad (8)$$

The calculation of the traces is based on the following observation: since the trace of any of the 16 Dirac matrices, except the unit matrix, is zero, $\mathrm{Sp}O_k\gamma_\mu O_m\gamma_\nu$ is different from zero (and is then equal to 4) only if $O_k=\gamma_\nu O_m\gamma_\mu=O_{m_1}$. Thus we have

$$\mathrm{Sp}\,O_k\gamma_\mu O_m\gamma_\nu=4\delta_{km_1}. \qquad (9)$$

Owing to the factor δ_{km_1} the sum over k can be found; in doing so we must keep in mind that $A_{nm_1}=A_{nm}$. Thus we have

$$\begin{aligned}\sum_k\left(\tfrac{1}{4}A_{nk}-\delta_{nk}\right)O_k\,\mathrm{Sp}\,O_k\hat{Q}O_m\hat{R}&=\left(\tfrac{1}{4}A_{nm}-\delta_{nm}\right)4\gamma_\nu O_m\gamma_\mu Q_\mu R_\nu\\&=(A_{nm}-4\delta_{nm})\hat{R}O_m\hat{Q}.\end{aligned} \qquad (10)$$

Similarly,

$$\sum_k\left(\tfrac{1}{4}A_{nk}-\delta_{nk}\right)O_k\,\mathrm{Sp}\,O_k\hat{Q}O_m=-(A_{nm'}-4\delta_{nm'})\,O_m\hat{Q}, \qquad (11)$$

where the index m′ comes from the matrix $O^{m'} = O^m \gamma_\nu$. Multiplication of the matrix O^m by γ_ν transfers it from one class to another, the correspondence being

$$\begin{array}{llllll} O^m: & S & V & T & A & P \\ O^{m'}: & V & T & A & P & A \end{array}$$

In Eq. (7) the first and fourth terms in each set of square brackets give traces of the first type; all the other terms give traces of the second type. Applying Eqs. (10) and (11), we reduce the sum over k to the form

$$\begin{aligned}(A_{nm} - 4\delta_{nm})[O_m\hat{S}\hat{R}O_m\hat{Q} - O_m\hat{S}O_m + O_m(\hat{R} - i)\hat{S}O_m\hat{Q} \\ + O_m(\hat{R} - i)\hat{Q}O_m\hat{S}] - (A_{nm'} - 4\delta_{nm'})[-iO_m\hat{S}\hat{R}O_m \\ - iO_m\hat{S}O_m\hat{Q} - iO_m(\hat{R} - i)\hat{S}O_m + iO_m(\hat{R} - i)O_m\hat{S}]. \quad (12)\end{aligned}$$

The expressions in square brackets can be simplified if we use the formulas

$$\begin{aligned}O_m\hat{R}\hat{S}O_m + O_m\hat{R}\hat{S}O_m = 2(RS)O_mO_m = 2(RS)A_{mS}, \\ O_m\hat{S}O_m = \hat{S}A_{mV} \quad (13)\end{aligned}$$

and note that the momentum integrals in Eq. (7) are invariant under the interchange q ⇄ − r, which makes $\hat{Q}\hat{R} \to \hat{R}\hat{Q}$. This enables us to use here the equation

$$\hat{Q}\hat{R} = (QR). \quad (14)$$

Thus Eq. (12) can be reduced to

$$\begin{aligned}(A_{nm} - 4\delta_{nm})[2\hat{Q}(RS)A_{mS} + \hat{S}(QR)A_{mS} - \hat{S}A_{mV} \\ - 2i(QS)A_{mV}] - (A_{nm'} - 4\delta_{nm'})[-2i(RS)A_{mS} \\ - 2i(QS)A_{mV} - \hat{S}A_{mV} + \hat{S}A_{mS}] \\ = a_1\hat{S} + 2a_1 i(QS) + b_1\hat{S}(QR), \quad (15)\end{aligned}$$

where

$$\begin{aligned}a_1 = -A_{mV}(A_{nm} - 4\delta_{nm}) + (A_{mV} - A_{mS})(A_{nm'} - 4\delta_{nm'}). \\ b_1 = 3A_{mS}(A_{nm} - 4\delta_{nm}). \quad (16)\end{aligned}$$

Here we have used the equality of the momentum integrals with integrands $\hat{S}(QR)$ and $\hat{Q}(RS)$, and in some terms have made the interchange q ⇄ − r.

Substitution of Eq. (15) in Eq. (7) gives

$$\begin{aligned}\psi(p) = -\frac{l^4\varkappa^6}{3(2\pi)^8}G(p) \\ \times \int \frac{d^4q\,d^4r}{N_1}[a\hat{S} + b\hat{S}(QR) + 2ai(QS)]\psi(p), \quad (17)\end{aligned}$$

with

$$\begin{aligned}a = \sum_{m,n} C_mC_n[-A_{mV}(A_{nm} - 4\delta_{nm}) \\ + (A_{mV} - A_{mS})(A_{nm'} - 4\delta_{nm'})] \\ = \sum_m C_m[-B_mA_{mV} + B_{m'}(A_{mV} - A_{mS})], \quad (18a)\end{aligned}$$

$$b = 3\sum_{m,n} C_mC_nA_{mS}(A_{nm} - 4\delta_{nm}) = 3\sum_m C_mB_mA_{mS}. \quad (18b)$$

As is clear from the derivation, the terms in δ_{nm} have come from the terms in Eq. (3) that contain traces. A characteristic peculiarity of Eq. (17) is the presence in it of only two (and not three) independent quadratic combinations of the coefficients C_n.

It is well-known that the way the Lagrangian is written in Eq. (1) is not the only possibility.[4] Interchange of two operators ψ in the expression under the sign of the normal product, followed by application of Eq. (6) brings the nonlinear term to the previous form, but with different values of the constants:

$$C_k' = -\tfrac{1}{4}\sum_n C_nA_{nk}. \quad (19)$$

A consequence of this is the fact that of the five possible invariants only three are linearly independent.

It can be verified that the expressions (18) for the quadratic forms a and b are invariant with respect to the transformation (19). This property is possessed by the linear combinations

$$\begin{aligned}B_l' = \sum_k C_k'(A_{kl} - 4\delta_{kl}) = -\tfrac{1}{4}\sum_{k,n} C_nA_{nk}(A_{kl} - 4\delta_{kl}) \\ = \sum_n C_n(A_{nl} - 4\delta_{nl}) = B_l \quad (20)\end{aligned}$$

(the orthogonality of the coefficients A_{nk} has been used). Writing Eq. (19) in the form

$$C_k' = -\tfrac{1}{4}B_k - C_k, \quad (19a)$$

we see that this transformation brings the quadratic form (18b) to the form

$$\begin{aligned}b' = -\tfrac{3}{4}\sum_m B_m^2A_{mS} - 3\sum_m C_mB_mA_{mS} \\ = -\tfrac{3}{4}\sum_m B_m^2A_{mS} - b. \quad (21)\end{aligned}$$

It can easily be shown that the first term in this formula is twice the second, so that the invariance b′ = b holds. Along with this, Eq. (21) makes it possible to give for b the obviously invariant expression

$$\begin{aligned}b = -\tfrac{3}{8}\sum_m B_m^2A_{mS} \\ = -\tfrac{3}{8}(B_S^2 + 4B_V^2 + 6B_T^2 + 4B_A^2 + B_P). \quad (22)\end{aligned}$$

The quadratic form (18a) can be handled in a similar way; for this purpose it is convenient to rewrite it in the form

$$a = \sum_m C_m(B_{m'} - B_m)(A_{mV} - A_{mS}) - b/3. \quad (23)$$

The first term of this expression is also changed by the transformation (19a) into two terms, one of which is twice as large as the other. We get finally

$$a = -\tfrac{1}{8}\sum_m B_m(B_{m'} - B_m)(A_{mV} - A_{mS}) - b/3$$

$$= \tfrac{1}{4}(3B_V B_V' + 3B_T B_T' + B_A B_A' + B_P B_P') - b/3 \qquad (24)$$

Here

$$B_m' = B_{m'} - B_m. \qquad (24a)$$

The values of the constants a and b for the pure interaction types are given in the table.

Interaction type	a	b	$(4\pi/\varkappa l)^2$
S	3	—9	2.897
V	—12	—72	5.078
T	0	—108	4.738
A	20	—72	7.644
P	—1	—9	1.665

The further treatment of Eq. (17) consists of the calculation of the momentum integrals. For this purpose let us introduce the following invariant functions of the momentum p (private communication from H. Mitter).

$$\int \frac{d^4q\,d^4r}{N_1}\hat{S} = -\frac{\pi^4}{\varkappa^2}\hat{p}\,M\left(-\frac{p^2}{\varkappa^2}\right),$$

$$\int \frac{d^4q\,d^4r}{N_1}\hat{S}\,(QR) = -\frac{\pi^4}{\varkappa^2}\hat{p}\,L\left(-\frac{p^2}{\varkappa^2}\right),$$

$$\int \frac{d^4q\,d^4r}{N_1}(QS) = -\frac{\pi^4}{\varkappa}N\left(-\frac{p^2}{\varkappa^2}\right) \qquad (25)$$

With these and the relation $G(p) = \hat{p}/p^2$, we rewrite Eq.(17) in the form

$$\psi(p) = \frac{1}{3}\left(\frac{\varkappa l}{4\pi}\right)^4\left[aM\left(-\frac{p^2}{\varkappa^2}\right) + bL\left(-\frac{p^2}{\varkappa^2}\right)\right.$$

$$\left. + 2ai\varkappa\frac{\hat{p}}{p^2}N\left(-\frac{p^2}{\varkappa^2}\right)\right]\psi(p). \qquad (26)$$

Squaring this equation, we bring it to the scalar form

$$\frac{1}{3}\left(\frac{\varkappa l}{4\pi}\right)^4\left[aM\left(-\frac{p^2}{\varkappa^2}\right) + bL\left(-\frac{p^2}{\varkappa^2}\right)\right.$$

$$\left. \pm 2a\sqrt{\frac{\varkappa^2}{-p^2}}N\left(-\frac{p^2}{\varkappa^2}\right)\right] = 1. \qquad (27)$$

Since p is the momentum of the proton,

$$p^2 = -m_p^2, \qquad (28)$$

and from Eq. (27) we find

$$\left(\frac{4\pi}{\varkappa l}\right)^4 = \frac{1}{3}\left[aM\left(\frac{m_p^2}{\varkappa^2}\right) + bL\left(\frac{m_p^2}{\varkappa^2}\right)\right.$$

$$\left. \pm 2a\frac{\varkappa}{m_p}N\left(\frac{m_p^2}{\varkappa^2}\right)\right]. \qquad (29)$$

From this it is clear that the value of the constant $(4\pi/\kappa l)^4$ depends essentially on the choice of the quantity κ appearing in the propagation function. Values of the constants for $\kappa = m_p$ are shown in the table.

In conclusion I express my sincere gratitude to Prof. W. Heisenberg and Dr. H. Mitter for their interest in this work and for supplying numerical data omitted from their paper.[3]

---

[1] Z. Maki, Prog. Theor. Phys. **16**, 667 (1956).

[2] I. V. Polubarinov, Joint Institute of Nuclear Studies, Preprint P-177, 1958.

[3] Heisenberg, Kortel, and Mitter, Z. Naturforsch. **10a**, 425 (1955).

[4] H. Umezawa, Quantum Field Theory (Russian transl.), Moscow 1958 [North-Holland, Amsterdam, 1956]

[5] Ya. I. Granovskiĭ, J. Exptl. Theoret. Phys. (U.S.S.R.) **37**, 442, 1959, Soviet Phys. JETP **10**, in press.

Translated by W. H. Furry
30

SOVIET PHYSICS JETP VOLUME 37 (10), NUMBER 1 JANUARY, 1960

DECAY PROCESSES IN THE DEVELOPMENT OF NUCLEAR CASCADES IN THE ATMOSPHERE

G. T. ZATSEPIN, S. I. NIKOL'SKIĬ, and A. A. POMANSKIĬ

P. M. Lebedev Physics Institute, Academy of Sciences, U.S.S.R.

Submitted to JETP editor February 7, 1959

J. Exptl. Theoret. Phys. (U.S.S.R.) **37**, 197-201 (July, 1959)

A general method is presented for the solution of the equations describing the nuclear-cascade process in the atmosphere for initial conditions prescribed at an arbitrary depth. The fraction of energy expended by nuclear cascade showers as a result of the $\pi \rightarrow \mu + \nu$ decay is estimated.

PREVIOUS experimental data show that, in the development of air showers, a considerable fraction of the energy of the primary particle is transferred to the μ-meson component of the shower.[1-2] The large role of decay processes in the development of showers in the depth of the atmosphere as well follows from the results of reference 3.

The method of solution of nuclear cascade equations, taking into account the decay processes for an event where the initial conditions are given at the top of the atmosphere, was found in the form of a method of successive generations.[4-5] The fact that in experiments on atmospheric showers the energy of the primary is not measured directly leads to the necessity of calculating the development of showers, assuming certain initial conditions in the depth of the atmosphere. However, the usual method of successive generations is not adaptable for the solution of such problems.

Let nucleons and π mesons take part in a nuclear cascade process. The effective cross section for nuclear collisions for nucleons and π mesons is assumed to be identical. In such a case, it is convenient to measure the path of particles and the depth in the atmosphere not in units of g/cm^2 but in units of the mean free path of particles λ_0. If the atmospheric depth, measured in g/cm^2, equals z, then, in the new units, the depth corresponds to $x = z/\lambda_0$, where λ_0 is expressed in g/cm^2.

We shall consider the initial conditions to be prescribed at the depth x_0. The number of nucleons and π mesons with energy in the interval between E, $E+dE$ at a depth x_0 is $N(E, x_0)\,dE$ and $\Pi(E, x_0)\,dE$ respectively.

The kinetic equations can be written in the form

$$\frac{\partial N(E, x)}{\partial x} = -N(E, x) + \int_0^\infty [N(E', x) W_{NN}(E', E) + \Pi(E', x) W_{\pi N}(E', E)]\,dE',$$

$$\frac{\partial \Pi(E, x)}{\partial x} = -\Pi(E, x)\left(1 + \frac{E_\pi}{Ex}\right) + \int_0^\infty [N(E', x) W_{N\pi}(E', E) + \Pi(E', x) W_{\pi\pi}(E', E)]\,dE', \tag{1}$$

where W_{NN}, $W_{N\pi}$, $W_{\pi N}$, $W_{\pi\pi}$ are the energy spectra of particles corresponding to the second index produced in a nuclear collision with a particle of energy E', denoted by the first index; $E_\pi = Mcz_0/\tau_0\rho(z_0) = 1.4 \times 10^{11}$ ev is the critical energy of $\pi^\pm$ mesons for which the probability of a nuclear collision and of decay at the depth $x = 1$ are the same; $\rho(z_0)$ is the air density in g/cm^3 at depth z_0.

We represent the solution in the form of the series

$$N(E, x) = e^{-(x-x_0)} \sum_{i=0}^\infty N_i(E, x),$$

$$\Pi(E, x) = e^{-(x-x_0)} \sum_{i=0}^\infty \Pi_i(E, x). \tag{2}$$

Substituting these series in Eq. (1), we obtain

$$\sum_{i=0}^\infty \frac{\partial N_i(E, x)}{\partial x} = \sum_{i=0}^\infty G_i^{(N)}(E, x),$$

$$\sum_{i=0}^\infty \frac{\partial \Pi_i(E, x)}{\partial x} = -\sum_{i=0}^\infty \Pi_i(E, x)\frac{E_\pi}{Ex} + \sum_{i=0}^\infty G_i^{(\pi)}(E, x), \tag{3}$$

where

$$G_i^{(N)}(E,\ x)=\int_E^\infty [N_i(E',\ x)\,W_{NN}(E',\ E)$$

$$+\Pi_i(E',\ x)\,W_{\pi N}(E',\ E)]\,dE',$$

$$G_i^{(\pi)}(E,\ x)=\int_E^\infty [N_i(E',\ x)\,W_{N\pi}(E',\ E)$$

$$+\Pi_i(E',\ x)\,W_{\pi\pi}(E',\ E)]\,dE'. \qquad (4)$$

Equations (3) are identically satisfied if we require, for $i = 0$:

$$\partial N_0(E,\ x)/\partial x=0,$$
$$\partial\Pi_0(E,\ x)/\partial x=-\Pi_0(E,\ x)\,E_\pi/Ex, \qquad (5)$$

where

$$N_0(E,\ x_0)=N(E,\ x_0), \qquad \Pi_0(E,\ x_0)=\Pi(E,\ x_0),$$

and for $i > 0$:

$$\partial N_i(E,\ x)/\partial x=G_{i-1}^{(N)}(E,\ x),$$
$$\partial\Pi_i(E,\ x)/\partial x=-\Pi_i(E,\ x)\,E_\pi/Ex+G_{i-1}^{(\pi)}(E,\ x), \qquad (5')$$

where

$$N_i(E,\ x_0)=0, \qquad \Pi_i(E,\ x_0)=0.$$

Equations (5) corresponds to the physical representation of successive generations.

The solutions of Eqs. (5) and (5′) are elementary. For $i = 0$:

$$N_0(E,\ x)=N(E,\ x_0), \quad \Pi_0(E,\ x)=\Pi(E,\ x_0)\,(x_0/x)^{E_\pi/E};$$

For $i > 0$:

$$N_i(E,\ x)=\int_{x_0}^{x} G_{i-1}^{(N)}(E,\ \xi)\,d\xi,$$

$$\Pi_i(E,\ x)=\int_{x_0}^{x}\left(\frac{\xi}{x}\right)^{E_\pi/E} G_{i-1}^{(\pi)}(E,\ \xi)\,d\xi,$$

where the integration over ξ for any generation can be carried out in final form. In the particular case $x_0 = 0$, the solutions become the well known solution of the successive generation method.

In our solution all the terms of the series are positive. The series is always convergent when the total energy of particles at x_0 is finite. The solution, however, is more complicated than for the case $x_0 = 0$, since, in order to obtain each i-th term, it is necessary, in general, to integrate i times.

However, for several cases which are of interest for the interpretation of experimental data, the role of the cascade process can be taken into account in a much simpler manner. We shall estimate the fraction of the energy of the nuclear-active component present in showers at the level of the Pamir station that is lost in the production of μ mesons and neutrinos in its further passage through the atmosphere.

According to experimental data, the form of the energy spectrum of nuclear-active particles in showers depends little on the depth, and can be represented by a power law with a differential spectrum exponent close to 2. We shall assume that the absorption of all particles in showers follows an experimental law with a mean free path of about 200 g/cm^2. Furthermore, in the depth of the atmosphere, the air density varies slowly with depth, and can be assumed to be constant, corresponding to a certain effective depth x_{eff}.

The number of $\pi^\pm$ mesons of given energy decaying per unit length is equal to

$$-(\partial\Pi(E,\ x)/\partial x)_{\mathrm{dec}}=(E_\pi/Ex_{\mathrm{eff}})\,\Pi(E,\ x), \qquad (6)$$

where x_{eff} is the effective depth in the atmosphere. The energy lost by decay of π mesons of given energy per unit path is equal to

$$-E\,(\partial\Pi(E,\ x)/\partial x)_{\mathrm{dec}}=(E_\pi/x_{\mathrm{eff}})\,\Pi(E,\ x). \qquad (7)$$

Under the assumptions made above, we have

$$\Pi(E,\ x)=\Pi(E,\ x_0)\,e^{-\mu(x-x_0)}, \qquad (8)$$

and the total energy lost by the nuclear cascade because of the $\pi \to \mu + \nu$ decay on the path from x_0 to x, is equal to

$$\mathscr{E}_{\mu,\nu}(x_0,\ x)=\frac{E_\pi}{x_{\mathrm{eff}}\,\mu}(1-e^{-\mu(x-x_0)})\int_0^\infty \Pi(E,\ x)\,dE, \qquad (9)$$

where x_{eff} for $\mu\,(x - x_0) \gg 1$ should be taken from the relation

$$x_{\mathrm{eff}}=x_0+\ln 2/\mu. \qquad (10)$$

Thus, the energy lost by the cascade in the decay process on the path from x_0 to x is determined by the total number of π mesons present in the shower at the depth x_0, in consequence of which the problem reduces to the finding of $\Pi\,(E,\ x_0)$.

In order to carry out a numerical estimate, we assume, according to experimental data, that nuclear-active particles in the shower are essentially nucleons, the number of which at the depth x and in the energy interval $E,\ E + dE$ is equal to

$$N(E,\ x)\,dE=Ae^{-\mu(x-x_0)}E^{-2}dE, \qquad E_1<E<E_2. \qquad (11)$$

If we assume a mean free path of nuclear-active particles in the air equal to $\lambda_0 = 80$ g/cm^2, then the absorption mean free path of the shower $\lambda = 200$ g/cm^2 corresponds to the value

$$\mu = 0.4. \tag{12}$$

We assume further that $W_{\pi N}(E', E) \equiv 0$, i.e., we neglect the production of fast high-energy nucleons in nuclear collisions of π mesons.

Substituting Eq. (11) into Eq. (1), we obtain

$$\mu = 1 - \int_{E}^{E_2} (E/E')^2 W_{NN}(E', E)\, dE. \tag{13}$$

Equation (13) satisfies the value $\mu = 0.4$ in the region* $E \ll E_2$ if, in the collision of a nucleon of energy E' with the nucleus, the energy spectrum of secondary nucleons can be described by a homogeneous function of E/E', and if the energy of secondary nucleons amounts to $0.6\,E'$. In particular, the equation is satisfied if we assume that $W_{NN}(E', E)\,dE = \delta(E - 0.6\,E')\,dE$, i.e., that the colliding nucleon conserves the fraction of energy equal to 0.6 of the primary energy, and that no additional nucleons are produced.[6] We shall assume that, in nuclear collisions of nucleons, $0.4\,E'$ is transferred on the average to π mesons, and out of this energy, $\frac{2}{3}$ goes to $\pi^{\pm}$ mesons. Substituting the solutions for $N(E, x)$ and $\Pi(E, x)$ written in the form

$$N(E, x) = N(E, x_0)\, e^{-\mu(x - x_0)},$$

$$\Pi(E, x) = \Pi(E, x_0)\, e^{-\mu(x - x_0)},$$

[which corresponds to Eqs. (8) and (11)] into the second of Eqs. (1), we obtain an integral equation from which we find $\Pi(E, x_0)$:

$$\Pi(E, x_0) = \frac{1}{1 - \mu + E_\pi / E x_0} \int_{E}^{E_1} [N(E', x_0)\, W_{N\pi}(E', E) + \Pi(E', x_0)\, W_{\pi\pi}(E', E)]\, dE'. \tag{14}$$

We have carried out a numerical estimate of the energy fraction of the nuclear-active component of the shower lost in the $\pi^{\pm} \to \mu^{\pm} + \nu$ decay in the lower third of the atmosphere (from the depth of 655 g/cm^2 corresponding to the altitude of the Pamir station to sea level). To explain the dependence of this fraction on the mechanism of the elementary act of the nuclear interactions, the calculations were carried out for different assumptions regarding the character of the elementary act and, consequently, the form of the functions $W_{N\pi}$ and $W_{\pi\pi}$. In the first approximation, which is more in line with present ideas, the assumed model has been close to the statistical model of Fermi-Landau. In the second assumption, a substantially lower multiplicity was assumed.

The energy spectrum of the nuclear-active component at the altitude of 655 g/cm^2 was assumed in the form $E^{-2}\,dE$ for the energy range from E_1 to E_2, and the estimates were carried out for different values of the upper limit of the spectrum E_2 of nucleons in the shower. The lower limit of the energy spectrum of nucleons was assumed to be equal to $E_1 = 3 \times 10^9$ ev. All produced particles were assumed to be π mesons, out of which one third were π^0 mesons. Thus, two variants were considered.

1. It was assumed that the total multiplicity of produced mesons in a collision between a nucleon of energy E' with the nucleus of an air atom is equal to

$$n(E') = 4(E'/2Mc^2)^{1/4}. \tag{15}$$

A total of 40% of the energy of the incident nucleons is transferred to the meson in the collisions. The energy spectrum represents two monoenergetic meson groups, and one quarter of the mesons obtain 0.75 of all energy, while the remaining three quarters obtain 0.25 of the total energy transferred to mesons. In collisions of mesons with the nucleus, the number of produced mesons is determined by the same relation (15), but the whole energy is transferred to mesons. The energy spectrum of meson-produced mesons has a form analogous to the spectrum of mesons produced by a nucleon.

Thus, it was assumed that

$$W_{N\pi}(E', E)\, dE = \frac{2}{3}\left(\frac{E'}{2Mc^2}\right)^{1/4}\left[\delta\left(E - \frac{0.75 \cdot 0.4E'}{(E'/2Mc^2)^{1/4}}\right) + 3\delta\left(E - \frac{0.25 \cdot 0.4E'}{3\,(E'/2Mc^2)^{1/4}}\right)\right],$$

$$W_{\pi\pi}(E', E)\, dE = \frac{2}{3}\left(\frac{E'}{2Mc^2}\right)^{1/4}\left[\delta\left(E - \frac{0.75\,E'}{(E'/2Mc^2)^{1/4}}\right) + 3\delta\left(E - \frac{0.25E'}{(E'/2Mc^2)^{1/4}}\right)\right]. \tag{16}$$

The calculation of the energy spectrum of mesons according to formula (14) by means of successive approximations gives fast convergence.

2. In addition, a calculation was carried out under the assumption of an essentially different mechanism of π-meson production. It was assumed that the multiplicity of meson production is constant: $n(E') = 3$. The production functions $W_{N\pi}$ and $W_{\pi\pi}$ were assumed to be of the form

---

*Since Eq. (13) cannot be correct in the range where the condition $E \ll E_2$ is not satisfied, the absorption coefficient will, in fact, depend both on E and on x, increasing with both E and x. However, in calculating the energy lost because of the $\pi \to \mu + \nu$ decay, neglect of the dependence of μ on E and x leads to an overestimate of this energy by certainly not more than 10%, as has been shown by check estimates.

$$W_{N\pi}(E', E)\,dE = 2\delta(E - 0.4E'/3),$$
$$W_{\pi\pi}(E', E)\,dE = 2\delta(E - E'/3). \qquad (17)$$

The calculation was carried out only for $E_2 = 10^{12}$ ev. The results are given in the table for both variants. The number in the table gives the relative fraction of the energy lost for the $\pi \rightarrow \mu + \nu$ decay in the passage of the shower from $z_0 = 655$ g/cm^2 to $z = 1033$ g/cm^2, i.e., $\mathscr{E}_{\mu\nu}(x - x_0)/E_0$, where $\mathscr{E}_{\mu\nu}$ is given by Eq. (9) and

$$E_0 = \int_{E_1}^{E_2} E\,[N(E, x_0) + \Pi(E, x_0)]\,dE.$$

At an intermediate stage of the calculations we obtained the fraction of all nuclear-active particles consisting of π mesons. This fraction clearly depends sharply on the energy range. For the energy of 5 Bev and for different variants it amounts to 11 — 13% increasing, in the energy range of 100 Bev, to 30 — 40% (slow increase with increasing E_2).

Thus, as a result of the calculations, it was found that, for the energy spectrum of the nuclear-active shower component of the type $E^{-2}dE$ at mountain altitudes, a considerable fraction of the energy of that component (of the order of 50%) should be lost for the production of μ mesons and neutrinos, and thus, were lost for the development of the cascade. Such a conclusion, clearly, is almost independent of the mechanism of the elementary act of nuclear collision, which is indicated by the similarity of results of the calculations of the first and second variants.

E_2	1	2
10^{12}	0.57	0.55
10^{13}	0.5	—
10^{14}	0.42	—

---

[1] Dobrotin, Zatsepin, Rozental', Sarycheva, Khristiansen, and Éĭdus, Usp. Fiz. Nauk **49**, 185 (1953).

[2] K. Greisen, Progress in Cosmic Ray Physics, (North Holland Publishing Co., Amsterdam, 1958) Vol. 3.

[3] S. I. Nikol'skiĭ and A. A. Pomanskiĭ, J. Exptl. Theoret. Phys. (U.S.S.R.) **35**, 618 (1958), Soviet Phys. JETP **8**, 430 (1959).

[4] G. T. Zatsepin and I. L. Rozental', Dokl. Akad. Nauk SSSR **99**, 369 (1954).

[5] U. Haber-Schaim and G. Yekutieli, Nuovo cimento **11**, 172 (1954).

[6] Vernov, Grigorov, Zatsepin, and Chudakov, Izv. Akad. SSSR, Ser. Fiz. **19**, 493 (1955), Columbia Tech. Transl. p. 445.

Translated by H. Kasha
31

SOVIET PHYSICS JETP VOLUME 37 (10), NUMBER 1 JANUARY, 1960

OPTICAL ANISOTROPY OF ATOMIC NUCLEI

A. M. BALDIN

P. N. Lebedev Physics Institute, Academy of Sciences, U.S.S.R.

Submitted to JETP editor February 7, 1959

J. Exptl. Theoret. Phys. (U.S.S.R.) **37**, 202-211 (July, 1959)

Concepts of molecular optics are extended to photonuclear reactions. The consequences of the existence of tensor polarizability of atomic nuclei, not yet discovered experimentally, are discussed. Various models of tensor polarizability are examined and estimates are given for the magnitudes of the effects that could be observed with present experimental capabilities.

1. INTRODUCTION

IN preceding studies[1,2] it has been shown that the cross section for the interaction of γ-ray quanta with nuclei can depend substantially upon the spin orientation of the nucleus with respect to the wave vector of the photon and that the detection of such dependence would furnish proof of the existence of a tensor component in the electric dipole polarizability of atomic nuclei. As already pointed out,[2] a possible model for such polarizability is contained in the successful interpretation of the giant resonance widths, given by Okamoto[3] and Danos;[4] in addition, other models of tensor polarizability are also possible.

The study of this new property of asymmetry in the electromagnetic radiation of atomic nuclei possesses indubitable interest. The object of the present work is a systematic formulation of the theory of the electric dipole polarizability of atomic nuclei, a discussion of experiments by means of which it might be possible to obtain information about the tensor component of the electric polarizability, and an estimate of the magnitude of the effects with the aid of two different nuclear models — the independent-particle model and the collective model.[3,4]

A theory of the polarizability of atomic nuclei can be constructed by analogy with the theory of molecular polarizability.[5] It should be remarked that, in general, many of the methods of molecular optics can be applied to photonuclear reactions. Thus, for example, it would undoubtedly be interesting to study the combination scattering of γ-ray quanta by nuclei or the effects of the depolarization of scattered radiation for the purpose of securing a series of important nuclear parameters. The scope of this article does not comprise the broad extension of the theory of the interaction of light with molecules to the interaction of γ-ray quanta with nuclei. We shall consider only the elastic scattering of γ-ray quanta by nuclei and the photonuclear reactions (total cross section for the absorption of dipole γ-ray quanta by nuclei).

2. GENERAL CONSIDERATIONS

As is well known, electric dipole absorption plays a principal role in the interaction of γ-ray quanta with nuclei in an energy range up to ~ 20 Mev. We shall therefore confine ourselves to this part of the interaction.

The possible existence of tensor polarization in nuclei signifies that the scattering amplitude may depend upon the spin of the system, i.e., the induced dipole moment of the nucleus can depend upon the orientation of the nucleus with respect to the electric field. The most general formula for the scattering amplitude, as a function of the nuclear spin operator $\hat{\mathbf{J}}$ and of the polarizations of the incident photon $\boldsymbol{\lambda}$ and the scattered photon $\boldsymbol{\lambda}'$, is written in the form

$$\hat{R} = R^{(1)}(\hat{\mathbf{J}}\boldsymbol{\lambda})(\hat{\mathbf{J}}\boldsymbol{\lambda}') + R^{(2)}(\hat{\mathbf{J}}\boldsymbol{\lambda}')(\hat{\mathbf{J}}\boldsymbol{\lambda}) + R^{(3)}(\boldsymbol{\lambda}'\boldsymbol{\lambda}) + T(\boldsymbol{\lambda}'\boldsymbol{\lambda}), \quad (1)$$

where $T = \omega Z^2 e^2 / 2\pi AM$ is the amplitude of Thomson scattering, which may make a substantial contribution (we assume that $\hbar = c = 1$ everywhere).* The amplitudes, $R^{(1)}$, $R^{(2)}$, $R^{(3)}$, being functions of the photon frequency, are proportional to the polarizability of the system. Thus, if only scalar polarizability of the system is present ($R^{(1)} = R^{(2)} = 0$), we have $R^{(3)} = -(\omega^3/2\pi)\,\alpha(\omega)$, where α is the electric dipole polarizability, through which the Rayleigh cross section for scattering by a small particle (nucleus) is expressed in accordance* with

---

*Of course, we neglect Delbrück scattering and scattering by the magnetic moment.

$$d\sigma / d\Omega = \omega^4 |\alpha(\omega)|^2 (\boldsymbol{\lambda}'\boldsymbol{\lambda}).$$

The expression (1) can be simplified. In molecular optics the case usually considered is that for which the polarizability tensor is Hermitian, or $\hat{R}^+ = \hat{R}$. This case is of little interest for the nucleus, since its energy levels have large widths, owing to the strong interaction between the constituent particles. Therefore, $R^{(1)}$, $R^{(2)}$, $R^{(3)}$ have real and imaginary parts over a broad frequency range.

We shall utilize the invariance of the S-matrix under time reversal, which gives $R^{(1)} = R^{(2)}$. Thus, (1) may be rewritten in the form

$$\hat{R} = R^T \frac{3}{J(2J-1)} \left\{ \frac{1}{2} [(\hat{\mathbf{J}}\boldsymbol{\lambda}')(\hat{\mathbf{J}}\boldsymbol{\lambda}) + (\hat{\mathbf{J}}\boldsymbol{\lambda})(\hat{\mathbf{J}}\boldsymbol{\lambda}')] - \frac{1}{3} \hat{\mathbf{J}}^2 (\boldsymbol{\lambda}'\boldsymbol{\lambda}) \right\}$$
$$+ (R^S + T)(\boldsymbol{\lambda}'\boldsymbol{\lambda}). \qquad (2)$$

The expediency of introducing R^T and R^S will become clear in the sequel. In accordance with references 1 and 2, we shall call $\alpha^S = -(2\pi/\omega^3)R^S$ and $\alpha^T = -(2\pi/\omega^3)R^T$ the scalar and tensor polarizabilities. Obviously, they are complex parameters. The imaginary and real parts of these parameters are not independent, but connected by dispersion relationships.

In order to express the imaginary part of the amplitude, we make use of the unitarity of the S-matrix:

$$i(\hat{R}^+ - \hat{R}) = \hat{R}\hat{R}^+. \qquad (3)$$

We shall take the matrix element of matrix equation (3) for the state $(\alpha m j)\, 2\pi/\omega$, where m is the projection of the nuclear spin on the z axis and j is the vector projection of the photon polarization, while α represents all the remaining quantum numbers of the nuclear ground state; we get

$$i(2\pi/\omega)^2 [(m'j'\alpha|R^+|\alpha m j) - (m'j'\alpha|R|\alpha m j)]$$
$$= (2\pi/\omega)^2 \sum_N (m'j'\alpha|R|N)(N|R^+|\alpha j m). \qquad (4)$$

The summation includes all the states permissible from the viewpoint of the law of the conservation of energy. We define the cross-section operator $\hat{\sigma}$ as that for which the mean value corresponding to the polarized state of the target nuclei and the incident photons gives the cross section

$$\sigma = \mathrm{Sp}\, \hat{\rho}\hat{\sigma}$$

(here ρ is the density matrix). Substituting (2) into (4), we obtain

$$2\frac{4\pi^2}{\omega^2} \left\{ \frac{3}{J(2J-1)} (m'| \frac{1}{2} (\hat{J}_{j'}\hat{J}_j + \hat{J}_j\hat{J}_{j'}) - \frac{1}{3} \hat{J}^2 \delta_{jj'} | m) \,\mathrm{Im}\, R^T \right.$$
$$\left. + \delta_{jj'} \mathrm{Im} R^S \right\} = (m'j'|\hat{\sigma}|mj). \qquad (5)$$

Thus, the imaginary parts of R^T and R^S are simply related to the absorption cross section. At the same time Eq. (5) leads to a more general dependence of the absorption cross section upon the nuclear spin. For instance, let the polarization of the photon be given rigorously, i.e., the density matrix expressing the polarization state of the photon has the form $\rho = \delta_{jz}\delta_{j'z}$ (the z axis is oriented along the photon polarization). Then the cross section of the photon absorption is expressed in the form

$$\sigma = \mathrm{Sp}\, \hat{\rho}\hat{\sigma} = \frac{4\pi^2}{\omega^2} 2 \left\{ \frac{3(J+1)}{(J-1)} \left[\frac{\overline{J_z^2}}{J(J+1)} - \frac{1}{3} \right] \mathrm{Im}\, R^T + \mathrm{Im}\, R^S \right\}; \qquad (6)$$

and for the unpolarized photon beam we get

$$\bar{\sigma} = \frac{8\pi^2}{\omega^2} \left\{ \frac{3(J+1)}{(2J-1)} \left[\frac{1}{6} - \frac{\overline{J_\varkappa^2}}{2J(J+1)} \right] \mathrm{Im}\, R^T + \mathrm{Im}\, R^S \right\}. \qquad (7)$$

Here $\overline{J}_\kappa^2$ is the mean square of the spin projection on the wave vector of the photon.

For unoriented nuclei $[\rho_{m'm} = \delta_{m'm}/(2J+1)]$ the terms with R^T in formulas (6) and (7) vanish. Therefore, as evident from (6) and (7), to prove the existence of the tensor part of the polarizability of atomic nuclei it is necessary to demonstrate the dependence of the cross section for photon absorption upon the orientation of the nucleus.

From formula (7) it is easy to derive that

$$\mathrm{Im}\, R^T = \tfrac{2}{3} (\omega/2\pi)^2 (\sigma_\perp - \sigma_\parallel),$$

where $\sigma_\parallel$ and $\sigma_\perp$ are the total absorption cross sections for γ-ray quanta when the nuclei are completely oriented parallel to the wave vector of the photons and perpendicular thereto, respectively. Having determined the imaginary part of R^T, it is possible to find its real part by using the dispersion relationships.

As noted earlier,[1] the influence of the R^T effect must be especially strong both on the absolute magnitude of the cross section for scattering by unoriented nuclei and on the azimuthal asymmetry of scattering by oriented nuclei. We present here more detailed estimates.

Let us find how the cross section for the elastic scattering of γ-ray quanta by nuclei depends upon the parameter R^T introduced by us or upon the tensor polarizability, which is proportional to R^T. We denote

---

*We stress the fact that we mean everywhere not the local polarizability, but the polarizability of the whole particle.

$$\hat{\varepsilon}_{ik} = \frac{3}{J(2J-1)}\left[\frac{1}{2}(\hat{J}_i\hat{J}_k + \hat{J}_k\hat{J}_i) - \frac{1}{3}\hat{J}^2\delta_{ik}\right].$$

Then the scattering cross-section operator is written

$$\hat{\sigma}_{ikjq} = (2\pi/\omega)^2\,[R^{T*}\hat{\varepsilon}^*_{ik} + R'^*\delta_{ik}]\,[R^T\hat{\varepsilon}_{jq} + R'\delta_{jq}]. \qquad (8)$$

Here $R' = R^S + T$.

Let us find the cross sections for scattering by unoriented nuclei. For this purpose we average (8) over the state $\rho_{m'm} = \delta_{m'm}/(2J+1)$. The mean value of the product $\hat{\epsilon}_{ik}\hat{\epsilon}_{jq}$ must have the form

$$\overline{\hat{\varepsilon}_{ik}\,\hat{\varepsilon}_{jq}} = A_1\delta_{ik}\delta_{jq} + A_2[\delta_{iq}\delta_{kj} + \delta_{kq}\delta_{ij}].$$

Finding the convolutions for the right-hand and left-hand parts of the tensors, first with respect to the indices $i = k$ and $j = q$, and then for $i = j$ and $k = q$, and utilizing the commutation relation for the components of the spin operator, we readily obtain

$$A_1 = -2A_2/3, \qquad A_2 = 3(J+1)(2J+3)/20J(2J-1).$$

The mean value of $\hat{\epsilon}_{ik}$ is equal to zero. The final result for the cross section, averaged over the orientation of the nuclei, but for a definite orientation of the polarization of the photon in its initial and terminal states, has the form

$$\frac{d\sigma}{d\Omega} = \frac{4\pi^2}{\omega^2}\left\{|R^T|^2\,\frac{3(J+1)(2J+3)}{20(2J-1)J}\left[1 + \frac{1}{3}(\boldsymbol{\lambda}'\boldsymbol{\lambda})^2\right] + |R'|^2(\boldsymbol{\lambda}'\boldsymbol{\lambda})^2\right\}. \qquad (9)$$

Averaging over the photon polarizations in the initial state and summing over the final states, we get for the angular distribution of the scattered photons

$$\overline{\frac{d\sigma}{d\Omega}} = \frac{2\pi^2}{\omega^2}\left\{|R^T|^2\,\frac{(2J+3)(J+1)}{20J(2J-1)}(13 + \cos^2\theta) + |R'|^2(1 + \cos^2\theta)\right\}. \qquad (10)$$

Thus, as already pointed out,[1] the existence of the tensor polarizability can be revealed by the magnitude of the cross section for elastic scattering and by the angular distribution of the scattering (the existence of a large isotropic component in the angular distribution).

The elastic scattering of γ-ray quanta by oriented nuclei has been discussed earlier.[1] As shown, the existence of tensor polarizability brings about azimuthal asymmetry of scattering. The greatest asymmetry occurs when the nuclei are oriented perpendicularly to the wave vector of the incident photon. The angular distribution in the plane normal to the incident beam has the form (in the notation of the present article):

$$d\sigma/d\Omega = (2\pi^2/\omega^2)\{[\tfrac{3}{4}|R^T|^2 + \tfrac{3}{2}(R^{T*}R' + R'^*R^T)]\sin^2\varphi + [\tfrac{1}{4}|R^T|^2 - \tfrac{1}{2}(R^{T*}R' + R'^*R^T) + R'^2]\}. \qquad (11)$$

Formula (11) has been derived from classical considerations and is valid only for J → ∞. Quantum corrections for it are very substantial. For $J = 0$ or $J = \frac{1}{2}$, the azimuthal asymmetry vanishes in general.

Apart from the effects mentioned, the existence of tensor polarizability can be disclosed by measurements of the static polarizability and of the quadratic fluctuation of the dipole moment in the ground state for oriented nuclei on the basis of the application of the summation rules. These effects have been discussed previously.[2]

Thus, there are many effects upon which tensor polarizability can exert an influence and which can be fully observed by existing experimental means. To estimate the measureability of the effects under discussion, it is necessary to calculate R^T and R^S on the basis of models.

3. MODELS FOR TENSOR POLARIZABILITY

Tensor polarizability models have been discussed in part before.[2] By analogy with molecular optics, we introduce the concept of the "internal" tensor polarizability, i.e., the polarizability in a coordinate system rotating together with the nucleus. In the coordinate system affixed to the nucleus, let the tensor part of the polarizability have the form

$$\alpha^{0T}_{ik} = \tfrac{3}{2}\alpha^T_0\,(n_i n_k - \tfrac{1}{3}\delta_{ik}). \qquad (12)$$

We have assumed that this tensor has axial symmetry; n_i is the component of the unit vector along the axis of symmetry. Generalization to the axially unsymmetric case presents no particular difficulties. In addition, we assume that $\mathbf{n}$ coincides with the direction of the nuclear-surface symmetry axis, along which the nuclear spin is directed in the ground state. Under these assumptions there is a direct analogy, on the one hand, between α^T_0 and α^T, and, on the other hand, between the "internal" and the spectroscopic quadrupole moments. Hence we have

$$\alpha^T = \alpha^T_0\,J(2J-1)/(J+1)(2J+3). \qquad (13)$$

Thus, the amplitude R^T of photon scattering by the nucleus in the laboratory system of coordinates is expressed through the "internal" polarizability by the following formula:

$$R^T = -\frac{\omega^3}{2\pi}\,\frac{J(2J-1)}{(J+1)(2J+3)}\,\alpha^T_0 = R^T_0\,\frac{J(2J-1)}{(J+1)(2J+3)}, \qquad (14)$$

i.e., the tensor polarizability vanishes for nuclei with spins 0 or $\frac{1}{2}$.

A model of tensor polarizability is contained in an extension of the hydrodynamic model of dipole vibrations of nuclei to nonspherical forms (Okamato[3] and Danos[4]). These authors have called attention to the fact that in a deformed nucleus the fluctuations of the densities of the neutron and proton liquids must take place with two neighboring characteristic frequencies. The order of magnitude of the ratio of these frequencies follows from the dimensional consideration, namely $\omega_1/\omega_2 \sim R_2/R_1$, where R_2 and R_1 are the smallest and largest radii of the nuclear surface. A detailed hydrodynamic analysis yields $\omega_1/\omega_2 = 0.91\, R_2/R_1$ if the surface is an ellipsoid with small eccentricity. This idea enabled the two authors mentioned to reach the conclusion that the experimentally observed giant resonance corresponds not to one characteristic frequency, but to two. Hence followed the successful explanation of the "line broadening" in the giant resonance for deformed nuclei. From this model it also follows that the wave of the fluctuations of the density differences of the neutron and proton liquids is propagated in the direction of the electric field of the photon. The latter inference signifies that the frequency ω_1 is excited when the electric vector of the photon is directed along the radius R_1, and ω_2 when the electric vector is directed along R_2. We do not adhere to the hydrodynamic model, but use the results of molecular optics and consider the nucleus as an aggregate of three linear oscillators, arranged perpendicularly to each other, with the oscillation frequencies ω_1 and $\omega_2 = \omega_3$, and the damping ratios γ_1 and $\gamma_2 = \gamma_3$. In this case the scattering amplitude in the coordinate system affixed to the nucleus is expressed by

$$R_0^T = \frac{\omega^3}{2\pi}\,\frac{2}{3}\left\{f_1\,\frac{\omega_1^2-\omega^2+i\gamma_1\omega}{(\omega_1^2-\omega^2)^2+\gamma_1^2\omega^2}-f_2\,\frac{\omega_2^2-\omega^2+i\gamma_2\omega}{(\omega_2^2-\omega^2)^2+\gamma_2^2\omega^2}\right\},$$

$$R_0^S = \frac{\omega^3}{2\pi}\left\{\frac{1}{3}f_1\,\frac{\omega_1^2-\omega^2+i\gamma_1\omega}{(\omega_1^2-\omega^2)^2+\gamma_1^2\omega^2}+\frac{2}{3}f_2\,\frac{\omega_2^2-\omega^2+i\gamma_2\omega}{(\omega_2^2-\omega^2)^2+\gamma_2^2\omega^2}\right\}. \tag{15}$$

The expression for the amplitude in the laboratory coordinate system follows from Eqs. (15), (14), and (2). The imaginary part of the amplitude determines the cross section for the absorption of γ-ray quanta by the nucleus in accordance with (6) and (7). From formula (15) it is seen that with $\omega_1 - \omega_2 \gtrsim \gamma_{1,2}$ the tensor polarizability for frequencies within the range of the giant resonance can exceed the scalar polarizability twofold, whence it follows that the above-mentioned effects can be observed fully.

As seen from (10) and (14), in comparatively simple experiments with elastic scattering by unoriented nuclei (R_0^T) the tensor polarizability will be manifested only for nuclei with sufficiently high spins. Thus, for example, in the case of In^{115}, which has a spin of $9/2$, the ratio of the contributions by the first and second components can be expected to reach 0.5. In this connection, as evident from formula (10), the anticipated angular distribution in elastic scattering is of the type $a + \cos^2\theta$, where $a = 1.5$, not 1 (the latter value corresponds to $R^T = 0$).*

The quantities γ_1, ω_1, γ_2, ω_2 and the oscillator strengths f_1 and f_2 are of substantial importance in all the estimates.

Perhaps the most thorough hydrodynamic estimate of ω_1, ω_2 is that by Levinger,[6] who utilized a summation rule similar to the known Kramers-Heisenberg formula,

$$\alpha = \frac{1}{2\pi^2}\int\frac{\sigma}{\omega^2}\,d\omega$$

and evaluated the static polarizability of the nucleus in the coordinate system affixed to the nucleus. The results coincided with the calculations by Okamoto and Danos: $\omega_1 \sim 1/R_1$ and $\omega_2 \sim 1/R_2$. With regard to γ_1 and γ_2 it is impossible to say anything definite at the present time. Experiment appears to indicate that γ_1 and γ_2 are substantially different. This circumstance cannot be explained within the framework of the simple hydrodynamic model. In view of this, a consideration of other models is warranted.

Soga and Fujita[7] calculated the one nucleon electric dipole transitions in deformed nuclei, using the shell model, and showed that the transitions are grouped around the two frequencies $\omega_1 \sim 1/R_1$ and $\omega_2 \sim 1/R_2$. Of course, such an approach employs many detailed assumptions about the form of the wave functions for the ground and excited states of the nuclei. We shall show that in the independent-particle model the conclusion that $\omega_1 \sim 1/R_1$ and $\omega_2 \sim 1/R_2$ follows from very general notions about the nucleus, without recourse to the mentioned assumptions.

---

*Recently E. Fuller and E. Hayward (preprint and private communication from D. Levinger) made an attempt to interpret their data on the elastic scattering of γ-ray quanta from Ta from the viewpoint of the existence of tensor polarizability in this nucleus (on the basis of the Okamoto-Danos hydrodynamic model). However, they used classical averaging for the nuclear orientation. Our Eqs. (10) and (14) differ from theirs, by the factor $J(2J-1)(2J+3)(J+1)$. Inclusion of this factor will substantially change the result of their analysis. The author avails himself of this occasion to thank D. Levinger and E. Fuller for the interesting information.

We consider the summation rule

$$\sigma_{-1} = \int \frac{\sigma}{\omega}\, d\omega = 4\pi^2 \langle 0 | d_z^2 | 0 \rangle \tag{16}$$

in a coordinate system affixed to the nucleus; $\mathbf{d} = \sum_i e_i \mathbf{r}_i$ is the nuclear dipole moment operator and $|0\rangle$ represents the ground state of the nucleus. The right-hand part can be written

$$\langle 0 | d_z^2 | 0 \rangle = e^2 \langle 0 | \sum_i (z_i^2 - \tfrac{1}{3} r_i^2) | 0 \rangle + \tfrac{1}{3} \langle 0 | d^2 | 0 \rangle$$

$$- \langle 0 | \sum_{i \neq j} z_i z_j - \tfrac{1}{3} r_i r_j | 0 \rangle. \tag{17}$$

As can be seen without difficulty, in this expression the first term is proportional to the quadrupole moment of the nucleus, the second term to the first moment of the cross section σ_{-1} for unoriented nuclei, and the last term is connected with the positional correlations of the protons in the nucleus. As is well known, the basic sources of correlation of the type interesting to us are the relationship $\sum \mathbf{r}_k = 0$ (where $\mathbf{r}_k$ represents the coordinates of both protons and neutrons) and Pauli's exclusion principle. We shall take these effects into account and estimate the last term. To take the relationship $\sum \mathbf{r}_k = 0$ into account, we introduce, as usual, the effective charges $e_p = eN/A$ for the proton and $e_n = -eZ/A$ for the neutron; and since Pauli's principle imposes a restriction only upon similar particles, we discard terms associated with proton-neutron correlations:

$$e^{-2} \langle 0 | d_z^2 | 0 \rangle = (N/A)^2 \langle 0 \Big| \sum_{i}{}_p (z_i^2 - \tfrac{1}{3} r_i^2) \Big| 0 \rangle$$

$$+ (Z/A)^2 \langle 0 \Big| \sum_{i}{}_n (z_i^2 - \tfrac{1}{3} r_i^2) \Big| 0 \rangle + \langle 0 \Big| \sum_{i \neq j}{}_p [z_i z_j - \tfrac{1}{3} r_i r_j] \Big| 0 \rangle$$

$$+ \langle 0 \Big| \sum_{i = j}{}_n [z_i z_j - \tfrac{1}{3} r_i r_j] \Big| 0 \rangle + \tfrac{1}{3} \langle 0 | d^2 | 0 \rangle, \tag{18}$$

where $\sum_{p(n)}$ indicates summation over all the protons (or neutrons) in the nucleus.

To estimate the correlations associated with Pauli's principle, we employ a method first applied by Khokhlov[8]* to an analogous problem. We introduce a function expressing the distribution of the coordinates of two protons

$$n(\mathbf{r}', \mathbf{r}) = \frac{1}{Z(Z-1)} \sum_{p_1 \neq p_2} \langle 0 | \delta(\mathbf{r} - \mathbf{r}_{p_1})\, \delta(\mathbf{r}' - \mathbf{r}_{p_2}) | 0 \rangle$$

(the summation extends over all the protons in the nucleus).

We shall define

$$\overline{r_\mu r'_\nu} = \int r_\mu r'_\nu n(\mathbf{r}', \mathbf{r})\, d\mathbf{r} d\mathbf{r}',$$

$$\overline{r_\mu^2} = \int r_\mu^2 n(\mathbf{r})\, d\mathbf{r}, \qquad n(\mathbf{r}) = \int n(\mathbf{r}', \mathbf{r}) d\mathbf{r}', \tag{19}$$

where $\overline{r}_\mu$ is manifestly equal to zero. Inasmuch as the dimension a of the region in which the correlations due to Pauli's principle make themselves felt is much smaller than the dimensions of the nucleus, it is possible to adopt the following expression for $n(\mathbf{r}', \mathbf{r})$

$$n(\mathbf{r}', \mathbf{r}) = n(\mathbf{r})\, n(\mathbf{r}')$$

$$- \Omega \left[\delta(\mathbf{r}' - \mathbf{r}) n\left(\frac{\mathbf{r}' + \mathbf{r}}{2}\right) - n(\mathbf{r})\, n(\mathbf{r}') \right] \tag{20}$$

and to consider that this function is the same for neutrons as for protons. The quantity $\Omega \sim (a/R)^3$ can be found by using the actual form of the wave functions of the nucleus. However, as will be shown below, for our purposes the value of this quantity is generally insignificant. If the expression (20) and our definitions (19) are employed, then, as easily verified, Eq. (18) assumes the form

$$e^{-2} \langle 0 | d_z^2 | 0 \rangle = [(N/A)^2 Z + (Z/A)^2 N]\, \overline{(z^2 - {}^1\!/_3 r^2)}$$

$$- \Omega [(N/A)^2 Z (Z - 1) + (Z/A)^2 N (N - 1)]\, \overline{(z^2 - {}^1\!/_3 r^2)}$$

$$+ {}^1\!/_3 \overline{r^2} [(N/A)^2 Z + (Z/A)^2 N] - \Omega [(N/A)^2 Z (Z - 1)$$

$$+ (Z/A)^2 N (N - 1)]\, \overline{r^2}/3. \tag{21}$$

Hence we find the dependence of σ_{-1} on the angle between the electric vector of the photon and the symmetry axis of the nucleus:

$$\frac{1}{4\pi^2} \sigma_{-1} = F(Z, A, \Omega) \left[\frac{1}{2Z} Q^0 \left(\cos^2\beta - \frac{1}{3} \right) + \frac{1}{3} \overline{r^2} \right], \tag{22}$$

where $F(Z, A, \Omega)$ is a general factor the form of which follows from (21) and Q^0 is the "internal" quadrupole moment of the nucleus.

From (22) it is easy to get for oriented nuclei

$$\frac{1}{4\pi^2} \hat{\sigma}_{-1} = F(Z, A, \Omega)$$

$$\times \left[\frac{1}{2Z} Q \frac{2(J+1)}{(2J-1)} \left(\frac{\hat{J}_z^2}{J(J+1)} - \frac{1}{3} \right) + \frac{1}{3} \overline{r^2} \right], \tag{23}$$

where Q denotes the spectroscopic quadrupole moment of the nucleus. As already[2] pointed out, formula (23) is exact for deuterium, with F = 1.*

---

*The author is grateful to Yu. K. Khokhlov for pointing out that the effect of the correlations connected with Pauli's principle can be easily estimated by this method.

*The static tensor polarizability of the deuteron was calculated by Yu. I. Bregadze. The ratio of the tensor part of the polarizability to the scalar one came out equal to ~ 1.5%.

From (22) we obtain

$$(\sigma^{(1)}_{-1} - \sigma^{(2)}_{-1})/\sigma^{0}_{-1} = 3Q^0/2Z\overline{r^2} \approx 5Q^0/2ZR^2. \qquad (24)$$

Here $\sigma^{(1)}_{-1}$ is the greatest value of σ_{-1} (at $\beta = 0$) while $\sigma^{(2)}_{-1}$ is its least value (at $\beta = \pi/2$); σ^{0}_{-1} is the moment of the cross section for unoriented nuclei, and R is the radius of the nucleus.

If, as usual, the "position of the maximum" of the giant resonance is defined as

$$\bar{\omega} = \int \sigma d\omega \Big/ \int \frac{\sigma}{\omega} d\omega,$$

then the width of the maximum for the giant resonance follows from (24):

$$(\overline{\omega^{(1)}} - \overline{\omega^{(2)}})/\bar{\omega}_0 \approx 5Q^0/2ZR^2.$$

Comparing this formula with the results secured by Okamoto and Danos, we find that the results of a calculation based on the independent-particle model agree, accurate to a numerical factor, with those obtained on the basis of the collective hydrodynamic model.

Analogous calculations with the aid of formula (23) yield an expression for the "shift of the maximum"[2] for completely oriented nuclei:

$$(\omega_{\parallel} - \omega_{\perp})/\omega_0 \approx 5Q/4ZR^2.$$

Here Q is the spectroscopic quadrupole moment. It must be emphasized that essentially we have made use here of the assumption about the absence in the nucleus of any correlations other than those with a radius much smaller than the nuclear dimensions.*

Thus, the use of various models and very general assumptions yields one and the same result, $\omega_1 \sim 1/R_1$ and $\omega_2 \sim 1/R_2$. The calculation of the widths γ_1 and γ_2 on the basis of the independent-particle model requires special investigations.

4. DISCUSSION

An examination of the various models of the nucleus shows that it is hardly possible to doubt the existence of tensor polarizability in atomic nuclei. In any event, it can be affirmed that tensor polarizability exists in the nucleus of deuterium.

The theory of the polarizability of atomic nuclei ensues as an extension of the theory of molecular polarizability.[5] Its non-Hermitian character is an important distinguishing feature of the tensor polarizability of atomic nuclei in comparison with that of molecules. Another distinction of the theory of nuclear polarizability is that the effects considered correspond to the experimental methods of nuclear physics. For example, one of the basic methods for the investigation of molecular polarizability — the study of the depolarization of scattered radiation — is hardly likely to be applied to the investigation of nuclear polarizability in the near future.

It seems to us that experiments with oriented nuclei must be considered the principal source of information about the tensor polarizability of atomic nuclei, although experiments with the elastic scattering of γ-ray quanta by nuclei might compete with this method. At the same time it is necessary to consider the possibility of an experimental study of Raman scattering of γ-ray quanta by nuclei. This method might yield a great deal of valuable information about nuclear parameters. A recently initiated study[9] of (γ, γ') reactions (which are equivalent to "nuclear luminescence" in the terminology of molecular optics), may also furnish many very valuable facts about the tensor polarizability of atomic nuclei. However, the interpretation of these experiments is rather ambiguous (it is not clear how many and what kind of transitions have occurred before the nucleus reaches its metastable level).

Quantitative estimates of the order of magnitude of the effects follow from Eqs. (2), (7), (10), (14), and (15). As can be seen from (15), at $\gamma_{1,2} \lesssim \Delta\omega$, the value of R_0^T exceeds R^S twofold in the frequency range $\omega \sim \omega_1$, whereas in the frequency range $\omega \sim \omega_2$ the value of R_0^T is equal to R^S but is opposite in sign. Hence comes the very peculiar dependence of the difference of the cross sections $\sigma_{\perp} - \sigma_{\parallel}$ for the absorption of γ-ray quanta by completely oriented nuclei [see formulas (7) and (8)]. For nuclei with spins > $5/2$ this difference is of the same order of magnitude as the cross sections themselves. This effect is certainly measurable even if the degree of nuclei orientation has been established meagerly and unreliably, since the energy dependence of the quantity R^T is of prime interest.

In the experiments on elastic scattering, the effects are also large (see text for estimates). These conclusions are almost independent of the models used. Identical values of the two Okamoto-Danos frequencies, $\omega_1 \sim 1/R_1$ and $\omega_2 \sim 1/R_2$, were secured from very different models. A discussion of the remaining parameters of formula (15) on the basis of the models is difficult at present because of the lack of experimental data.

---

*We note that our results will not be altered if the existence of strong neutron-proton correlations with a small radius is assumed.

At any rate, the investigation of tensor polarizability will provide more precise and more complete information about the shape of the nucleus than any other existing methods. In addition, experimental data on the quantities γ_1 and γ_2 can help substantially in understanding the mechanism of the absorption of γ-ray quanta by nuclei.

It must be emphasized that the effects under discussion can be observed only with nuclei possessing large spins. In this regard we point out once more the necessity of exploring the experimental possibilities in the study of Raman scattering, which is not subject to this restriction.

---

[1] A. M. Baldin, Материалы конференции по ядерным реакциям в области малых и средних энергий (Proceedings of the Conference on Nuclear Reactions at Low and Medium Energies), M., 1957.

[2] A. M. Baldin, Nucl. Phys. **9**, 237 (1958).

[3] K. Okamoto, Progr. Theor. Phys. **15**, 75 (1956); Phys. Rev. **110**, 143 (1958).

[4] M. Danos, Bull. Amer. Phys. Soc., Ser. II, **1**, 35 (1956).

[5] G. Placzek and E. Teller, Z. Physik **81**, 209 (1933).

[6] J. S. Levinger, Nucl. Phys., Preprint (1958).

[7] M. Soga and J. Fujita, Nuovo cimento **7**, 1494 (1957).

[8] Yu. K. Khokhlov, J. Exptl. Theoret. Phys. (U.S.S.R.) **32**, 124 (1957), Soviet Phys. JETP **5**, 88 (1957).

[9] J. Goldenberg and L. Katz, Phys. Rev. **90**, 308 (1953); Bogdankevich, Lazareva, and Nikolaev, J. Exptl. Theoret. Phys. **31**, 405 (1956), Soviet Phys. JETP **4**, 320 (1957).

Translated by J. E. Viscardi
32

SOVIET PHYSICS JETP VOLUME 37(10), NUMBER 1 JANUARY, 1960

ON CONVECTIVE MOTION OF A CONDUCTING FLUID BETWEEN PARALLEL VERTICAL PLATES IN A MAGNETIC FIELD

S. A. REGIRER

Northern Division of the Frost-Science Institute, Academy of Sciences, U.S.S.R.

Submitted to JETP editor February 7, 1959

J. Exptl. Theoret. Phys. (U.S.S.R.) **37**, 212-216 (July, 1959)

Stationary convective motion of a conducting fluid between vertical parallel plates in a magnetic field is considered. An exact solution of the magnetohydrodynamic equations is obtained for the case of a constant vertical temperature gradient. The critical value of Grasshof's number is determined for the case when the temperature of both plates is the same.

1. The free convective motion of a conducting fluid between vertical plates maintained at a constant temperature in the presence of an external magnetic field was studied in detail by Gershuni and Zhukhovitskiĭ.[1,2] In this paper we shall generalize the results referring to stationary flow to the case when the temperature varies in the vertical direction. We shall also discuss the problem of the superposition of free and forced convection, thereby generalizing the well-known solution due to Hartmann.[3]

We consider the case of stationary convective motion of a fluid between vertical infinite plates $x = \pm\delta$, whose temperatures are respectively $T_-(z)$ and $T_+(z)$. We take the flow lines to be parallel to the plates, i.e., to the z axis. An external homogeneous transverse magnetic field $H_x = H_0$ is applied to the plates.

We write the general equations of magnetohydrodynamics:[4]

$$\frac{\partial \mathbf{v}}{\partial t} + (\mathbf{v}\nabla)\mathbf{v} = -\frac{1}{\rho}\nabla\left(p + \frac{\mu H^2}{8\pi}\right) + \nu\nabla^2\mathbf{v} + \frac{\mu}{4\pi\rho}(\mathbf{H}\nabla)\mathbf{H} - \beta\mathbf{g}T, \tag{1.1}$$

$$\frac{\partial \mathbf{H}}{\partial t} + (\mathbf{v}\nabla)\mathbf{H} = (\mathbf{H}\nabla)\mathbf{v} + \frac{c^2}{4\pi\sigma\mu}\nabla^2\mathbf{H}, \tag{1.2}$$

$$\frac{\partial T}{\partial t} + \mathbf{v}\nabla T = a\nabla^2 T, \tag{1.3}$$

$$\operatorname{div}\mathbf{v} = 0, \qquad \operatorname{div}\mathbf{H} = 0, \tag{1.4}$$

where T is the temperature, p is the pressure, **v** and **H** are the velocity and field vectors, ρ, ν, μ, σ, a, β are, respectively, the density, the kinematic viscosity, the magnetic permeability, the conductivity, the thermal conductivity, and the coefficient of thermal expansion of the fluid. The problem under consideration has an exact solution of the form $v_x = v_y = 0$, $v_z = v(x)$, $H_x = H_x(x)$, $H_y = 0$, $H_z = H_z(x)$, $T = T(x, z)$, $p = p(x, z)$. If we take the positive direction of the z axis in the opposite direction to the force of gravity vector **g**, we obtain from Eqs. (1.1) – (1.4), the system of equations

$$0 = -\frac{1}{\rho}\frac{\partial}{\partial z}\left(p + \frac{\mu H^2}{8\pi}\right) + \nu\frac{\partial^2 v}{\partial x^2} + \frac{\mu H_x}{4\pi\rho}\frac{\partial H_z}{\partial x} + \beta g T,$$

$$\frac{\partial}{\partial x}\left(p + \frac{\mu H^2}{8\pi}\right) = 0, \tag{1.5}$$

$$0 = H_x\frac{\partial v}{\partial x} + \frac{c^2}{4\pi\sigma\mu}\frac{\partial^2 H_z}{\partial x^2}, \tag{1.6}$$

$$v\frac{\partial T}{\partial z} = a\frac{\partial^2 T}{\partial x^2}, \tag{1.7}$$

where $H_x = \text{const}$, which follows from the equation $\operatorname{div}\mathbf{H} = 0$; $g = -g_z$.

Since the component of the field normal to the boundary must be continuous at $x = \pm\delta$, we have $H_x \equiv H_0$. On substituting T from (1.5) into (1.7) and on differentiating the resultant equation with respect to z we see that when $v \neq \text{const}$ we necessarily have $(\partial^2/\partial z^2)(p + \mu H^2/8\pi) = \text{const}$ and, consequently, $\partial T/\partial z = A = \text{const}$ (see reference 5). From this it follows that $T = Az + T_0(x)$. The expressions for the given plate temperatures may now be written in the form

$$T_-(z) = Az + T_0(+\delta), \qquad T_+(z) = A_z + T_0(-\delta).$$

For the sake of definiteness we assume $T_-(z) < T_+(z)$. Then, on taking $T_0(0)$ as the reference point on the temperature scale, we have

$$T_-(z) = T(z, \delta) = Az - T_{w1},$$
$$T_+(z) = T(z, -\delta) = Az + T_{w2}, \tag{1.8}$$

where $T_{w_1} + T_{w_2}$ is the temperature difference between the plates which remains constant along the z axis. We shall subsequently use formulas (1.8) as the boundary conditions for the temperature.

Over the boundaries (at $x = \pm\delta$) the conditions of absence of slipping and of the continuity of the tangential component of the vector H must also be fulfilled, and reduce to the equalities

$$v(\pm\delta) = H_z(\pm\delta) = 0. \tag{1.9}$$

In addition we shall assume that the flow of fluid over the cross section of the gap between the plates is specified

$$Q = \int_{-\delta}^{\delta} v(x)\,dx. \tag{1.10}$$

If $Q = 0$, then Eq. (1.10) will be the condition that the lines of flow are closed, and the flow is free, since it will be due only to the force of buoyancy. However, if $Q \neq 0$ then the flow will be mixed, and forced convection will be superimposed on the free convection.

We now introduce the following dimensionless quantities

$$\xi = x/\delta, \quad \zeta = z/\delta, \quad u = v\delta/\nu, \quad h = H_z/H_0,$$
$$q = p\delta^2/\rho\nu^2, \quad \theta = T/A\delta = \zeta + \theta_0(\xi),$$
$$P = \nu/a, \quad P_m = 4\pi\sigma\nu/c^2, \quad M = (\mu H_0\delta/c)\sqrt{\sigma/\rho\nu},$$
$$G = \beta g A\delta^4/\nu^2, \tag{1.11}$$

where P and P_m are the ordinary and the magnetic Prandtl numbers, M is the Hartmann number, G is the Grasshof number. In terms of these new variables, the equations and the boundary conditions of our problem assume the following form

$$0 = -\frac{\partial q^*}{\partial\zeta} + \frac{\partial^2 u}{\partial\xi^2} + \frac{M^2}{P_m}\frac{\partial h}{\partial\xi} + G\theta, \quad \frac{\partial q^*}{\partial\xi} = 0, \tag{1.12}$$

$$0 = \frac{\partial u}{\partial\xi} + \frac{1}{P_m}\frac{\partial^2 h}{\partial\xi^2}, \tag{1.13}$$

$$u\,\frac{\partial\theta}{\partial\zeta} = \frac{1}{P}\,\Delta\theta, \tag{1.14}$$

$$u(\pm 1) = h(\pm 1) = 0, \quad Q^* = \int_{-1}^{1} u(\xi)\,d\xi,$$
$$\theta(\zeta, 1) = \zeta - \theta_{w1}, \quad \theta(\zeta, -1) = \zeta + \theta_{w2}, \tag{1.15}$$

where

$$q^* = q + M^2(h^2+1)/2P_m, \quad \theta_{wi} = T_{wi}/A\delta, \quad Q^* = Q/\nu.$$

Further analysis of our problems will be based on the system of equations (1.12) — (1.15).

2. In order to solve the system of equations (1.12) — (1.15) we substitute the expression $\theta = \zeta + \theta_0(\xi)$ into the first equation of (1.12) and into (1.14). We then obtain

$$0 = -\frac{\partial q^*}{\partial\zeta} + \frac{\partial^2 u}{\partial\xi^2} + \frac{M^2}{P_m}\frac{\partial h}{\partial\xi} + G\zeta + G\theta_0, \tag{2.1}$$

$$u = \frac{1}{P}\,\frac{\partial^2\theta_0}{\partial\xi^2}. \tag{2.2}$$

On the one hand, since u and h do not depend on ζ, it follows from (2.1) that $G\zeta - \partial q^*/\partial\zeta = D =$ const and

$$q^* = G\zeta^2/2 - D\zeta + D_1(\xi).$$

The second equation of (1.12) immediately shows that $D_1 =$ const

$$q^*(\zeta) - q^*(0) = G\zeta^2/2 - D\zeta. \tag{2.3}$$

On the other hand, on eliminating the unknowns h and θ_0, from Eqs. (2.1), (2.2), and (1.13) we obtain the equation

$$u^{\mathrm{IV}} - M^2 u'' + GPu = 0, \tag{2.4}$$

whose general solution is

$$u = C_1\cosh m\xi + C_2\sinh m\xi + C_3\cosh n\xi + C_4\sinh n\xi, \tag{2.5}$$

where m, n are in the general case complex parameters:

$$m = [M^2/2 + \sqrt{M^4/4 - GP}]^{1/2},$$
$$n = [M^2/2 - \sqrt{M^4/4 - GP}]^{1/2}. \tag{2.6}$$

Now with the aid of Eqs. (1.13), (2.1), and (2.3) we obtain in turn

$$h = -P_m\Big(C_1\frac{\sinh m\xi}{m} + C_2\frac{\cosh m\xi}{m} + C_3\frac{\sinh n\xi}{n}$$
$$+ C_4\frac{\cosh n\xi}{n} - C_5\xi - C_6\Big); \tag{2.7}$$

$$\theta_0 = \frac{1}{G}\Big(C_1 n^2\cosh m\xi + C_2 n^2\sinh m\xi + C_3 m^2\cosh n\xi$$
$$+ C_4 m^2\sinh n\xi - M^2 C_5 - D\Big). \tag{2.8}$$

For the derivation of the last formula we made use of the obvious equality $m^2 + n^2 = M^2$.

On satisfying conditions (1.15) we obtain seven equations for the determination of the constants C_i $(i = 1, 2, \ldots, 6)$ and D.

Let us dwell on certain pecularities of this system, which are connected with the boundary conditions of the initial problem.

a) In the case of free convection with the two plates unequal in temperature, i.e., for $Q^* = 0$, $\theta_{w_1} + \theta_{w_2} \neq 0$, the system has a unique solution for all values of M and G.

b) In the case of free convection with the temperature of the plates the same, i.e., for $Q^* = 0$, $\theta_{w_1} + \theta_{w_2} = 0$, the system has a solution only when a definite relation exists between G and M. The smallest possible value of G characterizes the threshold of convection.

c) In the case of mixed flow, i.e., for $Q^* \neq 0$, the system has a unique solution for arbitrary G and M.

We shall now discuss each one of these problems separately.

3. In the case that $Q^* = 0$ and $\theta_{w_1} + \theta_{w_2} \neq 0$, we first find that $C_1 = C_3 = C_5 = D = 0$, so that the temperature distribution is expressed by means of an odd function. Therefore for the case of free

stationary convection we should take $\theta_{W_1} = \theta_{W_2} = \theta_W$. Then on finding the constants C_2, C_4, and C_6 we obtain the following formulas for the velocity, for the induced field component, and for the temperature:

$$u = \frac{G\theta_w}{m^2 - n^2}\left(\frac{\sinh m\xi}{\sinh m} - \frac{\sinh n\xi}{\sinh n}\right), \qquad (3.1)$$

$$h = \frac{P_m G\theta_w}{m^2 - n^2}\left(\frac{\cosh m - \cosh m\xi}{m \sinh m} - \frac{\cosh n - \cosh n\xi}{n \sinh n}\right), \qquad (3.2)$$

$$\theta = \zeta + \theta_0(\xi) = \zeta + \frac{\theta_w}{m^2 - n^2}\left(\frac{n^2 \sinh m\xi}{\sinh m} - \frac{m^2 \sinh n\xi}{\sinh n}\right). \qquad (3.3)$$

From these formulas it is possible to obtain the well-known result of reference 1 by means of a limiting transition for $A \to 0$, when $m \to M$ and $n \to 0$, taking into account the fact that $G\theta_W = \beta g T_W \delta^3/\nu^2$. Moreover, by noting that in the case where the ratio $M^4/4|G|P$ increases without limit we have $m/M \to 1$ and $n \to 0$, it can be easily shown that in this case the values of $u(\xi)$, $h(\xi)$, and $\theta_0(\xi)$ approach asymptotically the corresponding expressions found by Gershuni and Zhukhovitskiĭ. Therefore when $M_4/4|G|P \gg 1$ their conclusions with respect to the existence of a boundary layer, the behavior of the thermal flux, and of the induced field are approximately valid.

If the ratio $M^4/4GP$ is close to unity, then by means of a limiting transition with $m \to n$ it is possible to obtain from (3.1) – (3.3) the following approximate formulas:

$$u \approx \frac{G\theta_w}{2n \sinh^2 n}(\xi \cosh n\xi \sinh n - \sinh n\xi \cosh n), \qquad (3.4)$$

$$h \approx \frac{P_m G\theta_w}{2n^3 \sinh^2 n}[(\sinh n - \xi \sinh n\xi)\, n \sinh n - (\cosh n - \cosh n\xi)(\sinh n - n \cosh n)], \qquad (3.5)$$

$$\theta \approx \zeta + \theta_w\left(\frac{n}{2}\, \frac{\xi \cosh n\xi \sinh n - \sinh n\xi \cosh n}{\sinh^2 n} - \frac{\sinh n\xi}{\sinh n}\right). \qquad (3.6)$$

On investigating Eq. (3.4) we find that the extremum points of the velocity profile satisfy the equation

$$n\xi \tanh n\xi = n \coth n - 1, \qquad (3.7)$$

whose solution tends to $\xi = \pm 1$ when $n \to \infty$. This proves the formation of a boundary layer also in the case of comparable values of M^4 and GP.

4. When the temperature of the two plates is the same and $\theta_W = 0$, free convective motion is possible only when a certain relation holds between M and G. This relation consists of the vanishing of the determinant of the system of equations with respect to C_i and D. By bringing it to diagonal form we obtain

$$(m^2 - n^2)\sinh m \sinh n\left(\cosh m \frac{\sinh m}{n} - \cosh n \frac{\sinh n}{m}\right) = 0. \qquad (4.1)$$

The only family of solutions of this equation which leads to a nontrivial solution of the problem is $n = ik\pi$ $(k = 1, 2 \ldots)$, where G must be negative.

Thus, if $G > 0$, when the temperature increases in the direction of positive z, the equilibrium of the liquid at rest is always stable. In the opposite case, when $G < 0$, the equilibrium is stable only for $|n^2| < \pi^2$, i.e., for $|GP| < \pi^2(M^2 + \pi^2)$. In the case $GP = -\pi^2(M^2 + \pi^2)$, stationary laminar flow is possible, characterized by the formulas

$$u = C\pi \sin \pi\xi, \qquad h = -CP_m(\cos \pi\xi + 1),$$
$$\theta = \zeta - \frac{PC}{\pi} \sin \pi\xi, \qquad (4.2)$$

where C is an arbitrary constant.

The formula obtained above for the dependence of the critical value of the number G on M confirms the fact that the presence of a magnetic field significantly postpones the beginning of instability of the equilibrium. This result naturally applies only to the case of plane motion.

5. Finally, we consider the case of mixed flow when the quantity $\theta_{W_1} + \theta_{W_2}$ is arbitrary, while $Q^* \neq 0$.

In accordance with this, the solution of our problem, based on Eqs. (2.5), (2.7), and (2.8), assumes the following form

$$u = \frac{mnQ^*(\cosh m \cosh n\xi - \cosh n \cosh m\xi)}{2(m \cosh m \sinh n - n \cosh n \sinh m)} + \frac{G(\theta_{w1} + \theta_{w2})(\sinh n \sinh m\xi - \sinh m \sinh n\xi)}{2(m^2 - n^2)\sinh m \sinh n}, \qquad (5.1)$$

$$h = -P_m\left[\frac{Q^*(m \cosh m \sinh n\xi - n \cosh n \sinh m\xi)}{2(m \cosh m \sinh n - n \cosh n \sinh m)} + \frac{G(\theta_{w1} + \theta_{w2})(n \sinh n \cosh m\xi - m \sinh m \cosh n\xi)}{2mn(m^4 - n^4)\sinh m \sinh n} - \frac{Q^*\xi}{2} - \frac{G(\theta_{w1} + \theta_{w2})}{2(m^2 - n^2)mn}(n \coth m - m \coth n)\right], \qquad (5.2)$$

$$\theta = \zeta + \frac{1}{G}\left[\frac{mnQ^*(m^2 \cosh m \cosh n\xi - n^2 \cosh n \cosh m\xi)}{2(m \cosh m \sinh n - n \cosh n \sinh m)} + \frac{G(\theta_{w1} + \theta_{w2})(n^2 \sinh n \sinh m\xi - m^2 \sinh m \sinh n\xi)}{2(m^2 - n^2)\sinh m \sinh n} - \frac{mn(m^2 - n^2)Q^*}{2(m \tanh n - n \tanh m)} + \frac{G(\theta_{w2} - \theta_{w1})}{2}\right]. \qquad (5.3)$$

When $G \rightarrow 0$, $\theta_{wi} \rightarrow 0$, the formulas (5.1) and (5.2) reduce to the well-known solution of Hartmann's problem.[3]

---

[1] G. Z. Gershuni and E. M. Zhukhovitskiĭ, J. Exptl. Theoret. Phys. (U.S.S.R.) **34**, 670 (1958), Soviet Phys. JETP **7**, 461 (1958).

[2] G. Z. Gershuni and E. M. Zhukhovitskiĭ, J. Exptl. Theoret. Phys. (U.S.S.R.) **34**, 675 (1958), Soviet Phys. JETP **7**, 465 (1958).

[3] J. Hartmann, Kgl. Danske Videnskab. Selskab. Math-fys. Medd. **15**, 6 (1937).

[4] L. D. Landau and E. M. Lifshitz, Электродинамика сплошных сред (Electrodynamics of Continuous Media), Gostekhizdat, 1957.

[5] G. A. Bugaenko, Прикладная математика и механика (Applied Math. and Mechanics) **17**, 496 (1953).

Translated by G. Volkoff
33

SOVIET PHYSICS JETP VOLUME 37(10), NUMBER 1 JANUARY, 1960

ANGULAR AND POLARIZATION ANALYSES OF REACTIONS OF THE TYPE $a + b \rightarrow a' + b' + c'$

V. I. RITUS

P. N. Lebedev Physics Institute, Academy of Sciences, U.S.S.R.

Submitted to JETP editor February 7, 1959

J. Exptl. Theoret. Phys. (U.S.S.R.) 37, 217-223 (July, 1959)

A study is made of the invariant angular operators in terms of which the scattering matrix for reactions of the type $a + b \rightarrow a' + b' + c'$ can be expanded, and which are convenient for angular and polarization analyses of such reactions. The angular operators are obtained in explicit form for reactions in which the spin of the system does not exceed unity, and also for analogous reactions involving γ-ray quanta.

1. INTRODUCTION

IT is convenient to carry out angular and polarization analyses of nuclear reactions by means of the invariant angular operators in terms of which the scattering matrix or scattering amplitude can be expanded. We have previously[1] studied and constructed such operators for reactions of the type $a + b \rightarrow a' + b'$. Ciulli and Fischer[2] have constructed the first few angular operators for reactions of the type $a + b \rightarrow a' + b' + c'$ in which the spins of the initial and final system are equal to ½. In the present paper the angular operators are constructed for reactions $a + b \rightarrow a' + b' + c'$ in which the spins of the initial and final systems do not exceed unity, and also for analogous reactions involving γ-ray quanta.

2. GENERAL REMARKS

The initial and final states of the system in the reaction $a + b \rightarrow a' + b' + c'$ are defined by the momenta $\mathbf{p}_a$, $\mathbf{p}_b$ and $\mathbf{p}'_a$, $\mathbf{p}'_b$, $\mathbf{p}'_c$ of the particles a, b and a′, b′, c′, and the spin coordinates α and α' of the spin of the system. The momenta of the particles are connected by the relations

$$\mathbf{p}_a + \mathbf{p}_b = \mathbf{p}'_a + \mathbf{p}'_b + \mathbf{p}'_c = \mathbf{P},$$
$$E_a + E_b = E'_a + E'_b + E'_c = E, \tag{1}$$

where $E_a = (p_a^2 + m_a^2)^{1/2}$ is the energy of particle a, and so on, and E and $\mathbf{P}$ are the energy and momentum of the system. In the center-of-mass system ($\mathbf{P} = 0$) we can introduce, instead of the momenta of the particles, the momenta

$$\mathbf{p} = \mathbf{p}_a - \mathbf{p}_b \tag{2}$$

and (cf. reference 3)

$$\mathbf{p}_1 = \mathbf{p}'_a - \mathbf{p}'_b, \qquad \mathbf{p}_2 = -(\mathbf{p}'_a + \mathbf{p}'_b) = \mathbf{p}'_c. \tag{2'}$$

To the momenta $\mathbf{p}$, $\mathbf{p}_1$, $\mathbf{p}_2$ there correspond the orbital angular momenta $\mathbf{l}$, $\mathbf{l}_1$, $\mathbf{l}_2$ ($\mathbf{l}$ is the orbital angular momentum of the system a + b, $\mathbf{l}_1$ that of the system a′ + b′, and $\mathbf{l}_2$ that of particle c′), and the total angular momenta $\mathbf{J}$, $\mathbf{J}'$ of the initial and final systems are connected with these orbital angular momenta by the relations $\mathbf{J} = \mathbf{l} + \mathbf{S}$, $\mathbf{J}' = \mathbf{l}_1 + \mathbf{l}_2 + \mathbf{S}'$, where $\mathbf{S}$, $\mathbf{S}'$ are the spins of the initial and final systems. Using the momenta (2), (2′) and the relations (1), we can see without difficulty that, as the independent variables of the initial system, we can choose the quantities

$$E,\ \mathbf{k},\ \alpha, \tag{3}$$

where $\mathbf{k} = \mathbf{p}/p$, and as the independent variables of the final system the quantities

$$E,\ p'_c,\ \mathbf{k}_1,\ \mathbf{k}_2,\ \alpha', \tag{3'}$$

where $\mathbf{k}_1 = \mathbf{p}_1/p_1$, $\mathbf{k}_2 = \mathbf{p}_2/p_2$.

In the center-of-mass system the scattering matrix S for the reaction $a + b \rightarrow a' + b' + c'$ depends on the variables (3) and (3′); it is a matrix (operator) in the spin variables α, α' and a function of the remaining variables. We shall be interested in the dependence of the scattering matrix on the variables $\mathbf{k}$, α and $\mathbf{k}_1$, $\mathbf{k}_2$, α'. Therefore we shall write the S matrix in the form $S(\mathbf{k}_1\mathbf{k}_2\alpha'; \mathbf{k}\alpha) \equiv [S(\mathbf{k}_1\mathbf{k}_2; \mathbf{k})]_{\alpha\alpha'}$, omitting the variables E, p'_c. If the matrix S is invariant with respect to rotations and reflections, it can be expanded in a series in the angular operators invariant with respect to rotations and reflections, $L_{J\nu'\nu}(\mathbf{k}_1, \mathbf{k}_2; \mathbf{k})$:

$$S(\mathbf{k}_1, \mathbf{k}_2; \mathbf{k}) = \sum_{J\nu\nu'} S_{J\nu'\nu} L_{J\nu'\nu}(\mathbf{k}_1, \mathbf{k}_2; \mathbf{k}). \tag{4}$$

The coefficients $S_{J\nu'\nu}$ in this expansion are functions only of the total energy E and the absolute value p'_c of the momentum of particle c′.

The angular operators are scalar products of the J vectors $\psi_{JM\nu}(\mathbf{k})$ and $\psi_{JM\nu'}(\mathbf{k}_1\mathbf{k}_2)$ of the initial and final states:

$$L_{J\nu'\nu}(\mathbf{k}_1\mathbf{k}_2;\ \mathbf{k}) = \sum_M \psi_{JM\nu'}(\mathbf{k}_1\mathbf{k}_2)\,\psi^*_{JM\nu}(\mathbf{k}). \tag{5}$$

The numbers J, M, ν denote respectively the total angular momentum, its projection, and a set of eigenvalues of operators commuting with the total angular momentum, for example the spin of the system, the orbital angular momenta, etc. The general properties of the operators (5) are the same as in the case of the reactions a + b → a′ + b′ (cf. reference 1). In particular, these operators are Hermitian:

$$L^+_{J\nu'\nu}(\mathbf{k}_1\mathbf{k}_2;\ \mathbf{k}) = L_{J\nu\nu'}(\mathbf{k};\ \mathbf{k}_1\mathbf{k}_2), \tag{6}$$

are orthogonal and normalized:

$$\int L^+_{J'\nu''\nu}(\mathbf{k}_1\mathbf{k}_2;\mathbf{k})\,L_{J\nu'\nu_0}(\mathbf{k}_1\mathbf{k}_2;\mathbf{k}_0)\,\frac{d\mathbf{k}_1}{4\pi}\,\frac{d\mathbf{k}_2}{4\pi} = \delta_{JJ'}\,\delta_{\nu''\nu'}\,L_{J\nu\nu_0}(\mathbf{k},\ \mathbf{k}_0), \tag{7}$$

$$\int L_{J'\nu\nu'}(\mathbf{k}'_1\mathbf{k}'_2;\ \mathbf{k})\,L^+_{J\nu_0\nu''}(\mathbf{k}_1\mathbf{k}_2;\mathbf{k})\,\frac{d\mathbf{k}}{4\pi} = \delta_{JJ'}\,\delta_{\nu''\nu'}\,L_{J\nu\nu_0}(\mathbf{k}'_1\mathbf{k}'_2;\ \mathbf{k}_1\mathbf{k}_2) \tag{7$'$}$$

and have the property of completeness:

$$\sum_{J\nu}\int L^+_{J\nu'\nu}(\mathbf{k}_1\mathbf{k}_2;\ \mathbf{k}')\,L_{J\nu'\nu}(\mathbf{k}_1\mathbf{k}_2;\ \mathbf{k})\,\frac{d\mathbf{k}_1}{4\pi}\,\frac{d\mathbf{k}_2}{4\pi} = \delta(\mathbf{k}' - \mathbf{k}), \tag{8}$$

$$\sum_{J\nu}\int L_{J\nu'\nu}(\mathbf{k}'_1\mathbf{k}'_2;\ \mathbf{k})\,L^+_{J\nu'\nu}(\mathbf{k}_1\mathbf{k}_2;\ \mathbf{k})\,\frac{d\mathbf{k}}{4\pi} = \delta(\mathbf{k}'_1 - \mathbf{k}_1)\,\delta(\mathbf{k}'_2 - \mathbf{k}_2), \tag{8$'$}$$

where

$$\int \delta(\mathbf{k}' - \mathbf{k})\,d\mathbf{k}/4\pi = 1 \text{ and so on}$$

Since

$$\mathrm{Sp}\,L_{J\nu\nu_0}(\mathbf{k},\ \mathbf{k}) = (2J + 1)\,\delta_{\nu\nu_0}.$$

$$\mathrm{Sp}\int L_{J\nu\nu_0}(\mathbf{k}_1\mathbf{k}_2;\ \mathbf{k}_1\mathbf{k}_2)\,d\mathbf{k}_i\,4\pi = (2J + 1)\,\delta_{\nu\nu_0}, \qquad i = 1.2,$$

the coefficients $S_{J\nu'\nu}$ of the expansion (4) can be calculated by the formulas

$$S_{J\nu'\nu} = \frac{1}{2J+1}\,\mathrm{Sp}\int \frac{d\mathbf{k}_1}{4\pi}\,\frac{d\mathbf{k}_2}{4\pi}\,L^+_{J\nu'\nu}(\mathbf{k}_1\mathbf{k}_2;\ \mathbf{k})\,S(\mathbf{k}_1\mathbf{k}_2;\ \mathbf{k}); \tag{9}$$

$$S_{J\nu'\nu} = \frac{1}{2J+1}\,\mathrm{Sp}\int \frac{d\mathbf{k}}{4\pi}\,\frac{d\mathbf{k}_i}{4\pi}\,S(\mathbf{k}_1\mathbf{k}_2;\ \mathbf{k})\,L^+_{J\nu'\nu}(\mathbf{k}_1\mathbf{k}_2;\ \mathbf{k}), \qquad i = 1.2. \tag{9$'$}$$

We shall describe the system a + b by the J vector

$$\psi_{JMlS}(\mathbf{k}) = \sum_\mu C^{lM-\mu;\ S\mu}_{JM}\,Y_{lM-\mu}(\mathbf{k})\,Q_{S\mu}, \tag{10}$$

where $Y_{lm}(\mathbf{k})$ is the orbital function and $Q_{S\mu}$ the spin function of the system; $\mathbf{J} = \mathbf{l} + \mathbf{S}$. We shall describe the system a′ + b′ + c′ either by the J vector

$$\psi_{JM\nu'}(\mathbf{k}_1\mathbf{k}_2) = \sum_{\mu'} C^{l'M-\mu';\ S'\mu'}_{JM}\,D^{l_1l_2}_{l'M-\mu'}(\mathbf{k}_1\mathbf{k}_2)\,Q_{S'\mu'},$$

$$D^{l_1l_2}_{l'm'} = \sum_{m_2} C^{l_1m_1;\ l_2m_2}_{l'm'}\,Y_{l_1m_1}(\mathbf{k}_1)\,Y_{l_2m_2}(\mathbf{k}_2), \tag{11a}$$

where S′ is the spin of the system, l_1, l_2 are the orbital angular momenta, $\mathbf{l}' = \mathbf{l}_1 + \mathbf{l}_2$ is the total orbital angular momentum, and $\mathbf{J} = \mathbf{l}' + \mathbf{S}'$ is the total angular momentum, or else by the J vector

$$\psi_{JM\nu'}(\mathbf{k}_1\mathbf{k}_2) = \sum_m C^{l_2M-m;\ jm}_{JM}\,Y_{l_2M-m}(\mathbf{k}_2)\,D^{S'}_{jl_1m}(\mathbf{k}_1),$$

$$D^{S'}_{jl_1m}(\mathbf{k}_1) = \sum_{\mu'} C^{l_1m-\mu';\ S'\mu'}_{jm}\,Y_{l_1m-\mu'}(\mathbf{k}_1)\ Q_{S'\mu'}, \tag{11b}$$

where S′ is the spin of the system, l_1, l_2 are the orbital angular momenta,* $\mathbf{j} = \mathbf{l}_1 + \mathbf{S}'$, $\mathbf{J} = \mathbf{j} + \mathbf{l}_2$.

By means of Eqs. (5), (10) and (11) one can construct the angular operators $L_{J\nu'\nu}(\mathbf{k}_1\mathbf{k}_2;\ \mathbf{k})$. For this purpose it is convenient to use the coordinate system with its x, y and z axes along the vectors $[\mathbf{k}\times\mathbf{k}_1]\times\mathbf{k}$, $[\mathbf{k}\times\mathbf{k}_1]$, $\mathbf{k}$ and the invariance of the angular operators.

3. THE EXPLICIT FORM OF THE ANGULAR OPERATORS

We shall present first the form of the angular operators (polynomials) for spinless particles.

Case S = S′ = 0:

$$L_{l_1l_2l}(\mathbf{k}_1\mathbf{k}_2;\ \mathbf{k}) = \sqrt{(2l_1 + 1)(2l_2 + 1)(2l + 1)}\,\Big[C^{l_10;\ l_20}_{l0}\,P_{l_1}(x_1)\,P_{l_2}(x_2) + 2\sum_{m=0}^{l_2} C^{l_1-m;\ l_2m}_{l0}\sqrt{\frac{(l_1-m)!\,(l_2-m)!}{(l_1+m)!\,(l_2+m)!}} \times a^{(q)}_m\,P^{(m)}_{l_1}(x_1)\,P^{(m)}_{l_2}(x_2)\Big], \tag{12}$$

where

$$a^{(q)}_m = \tfrac{1}{2}\{(x_1x_2 - x_{12} - i([\mathbf{k}_1\times\mathbf{k}_2]\,\mathbf{k}))^m + q\,(x_1x_2 - x_{12} + i([\mathbf{k}_1\times\mathbf{k}_2]\,\mathbf{k}))^m\},$$

$$x_1 = (\mathbf{k}\mathbf{k}_1),\quad x_2 = (\mathbf{k}\mathbf{k}_2),\quad x_{12} = (\mathbf{k}_1\mathbf{k}_2),$$

$$q = (-1)^{l_1+l_2-l};\quad P^{(m)}_l = d^mP_l/dx^m; \tag{13}$$

---

*We shall not consider here the coupling $\mathbf{j} = \mathbf{l}_2 + \mathbf{S}'$, $\mathbf{J} = \mathbf{j} + \mathbf{l}_1$, since it is equivalent to the coupling $\mathbf{j} = \mathbf{l}_1 + \mathbf{S}'$, $\mathbf{J} = \mathbf{j} + \mathbf{l}_2$ and the notations $\mathbf{p}_1 = -(\mathbf{p}'_a + \mathbf{p}'_b) \equiv \mathbf{p}'_c$, $\mathbf{p}_2 = \mathbf{p}'_a - \mathbf{p}'_b$ instead of Eq. (2′).

$q = +1$ or -1, corresponding to conservation or change of the intrinsic parity of the system in the reaction. The angular polynomials (12) satisfy the conditions

$$\begin{aligned} L_{l_1 l_2 l}(\mathbf{k}_1\mathbf{k}_2;\ \mathbf{k}) &= (-1)^{l_1-l}\sqrt{\frac{2l+1}{2l_1+1}}\,L_{l_2 l l_1}(\mathbf{k}_2\mathbf{k};\ \mathbf{k}_1) \\ &= (-1)^{l_2-l}\sqrt{\frac{2l+1}{2l_2+1}}\,L_{l l_1 l_2}(\mathbf{k}\mathbf{k}_1;\ \mathbf{k}_2) \\ &= (-1)^{l_1+l_2-l}\,L_{l_2 l_1 l}(\mathbf{k}_2\mathbf{k}_1;\ \mathbf{k}). \end{aligned} \qquad (14)$$

A. Coupling $\mathbf{l}_1 + \mathbf{l}_2 = \mathbf{l}'$, $\mathbf{l}' + \mathbf{S}' = \mathbf{J}$

We now note that the angular operators $L_{J\nu'\nu}(\mathbf{k}', \mathbf{k})$ for the reaction $a + b \to a' + b'$ can be represented in the form of a certain invariant differential operator $O_{J\nu'\nu}(\mathbf{L}', \mathbf{T})$, which depends on the orbital angular momentum operator $\mathbf{L}' = -i[\mathbf{k}'\partial/\partial\mathbf{k}']$ and the vector matrix $\mathbf{T}$ in the spin space of the system, and acts on the angular polynomial for spinless particles:

$$L_{Jl'S'lS}(\mathbf{k}', \mathbf{k}) = O_{Jl'S'lS}(\mathbf{L}', \mathbf{T})\,L_{l'}(\mathbf{k}', \mathbf{k}). \qquad (15)$$

Starting from Eqs. (11a), (10), and (5), we can show without difficulty that the angular operators for reactions $a + b \to a' + b' + c'$ can be represented in the form

$$L_{Jl'l_1l_2S'lS}(\mathbf{k}_1\mathbf{k}_2;\ \mathbf{k}) = O_{Jl'S'lS}(\mathbf{L}', \mathbf{T})\,L_{l_1l_2l'}(\mathbf{k}_1\mathbf{k}_2;\ \mathbf{k}), \qquad (16)$$

where $O_{Jl'S'lS}$ is the same operator as in Eq. (15), $\mathbf{L}' = \mathbf{L}_1 + \mathbf{L}_2$, and $L_{l_1l_2l'}(\mathbf{k}_1\mathbf{k}_2;\ \mathbf{k})$ is the angular polynomial (12) for spinless particles.* With regard to Eq. (16) we note the following. Since parity is conserved in the reaction $a + b \to a' + b' + c'$, the quantity $l_1 + l_2 - l$ is either even or odd, depending on whether the intrinsic parity of the system is conserved or changes in the reaction. Therefore the angular operators $L_{J\nu'\nu}(\mathbf{k}_1\mathbf{k}_2;\ \mathbf{k})$ are either scalars (if the intrinsic parity is conserved and the quantity $q \equiv (-1)^{l_1+l_2-l}$ is equal to +1) or pseudoscalars (if the intrinsic parity changes and $q = -1$). As for the angular polynomials $L_{l_1l_2l'}$ and the operators $O_{Jl'S'lS}$ that appear in Eq. (16), they can be either scalars or pseudoscalars, independently of the conservation or change of the intrinsic parity in the reaction; namely, $L_{l_1l_2l'}$ is a scalar (pseudoscalar) if $q' \equiv (-1)^{l_1+l_2-l}$ is equal to $+1(-1)$, and $O_{Jl'S'lS}$ is a scalar (pseudoscalar) if $q_0 \equiv (-1)^{l'-l}$ is equal to $+1(-1)$. We note that $q = q_0q'$.

We shall give the explicit forms of the operators $O_{Jl'S'lS}(\mathbf{L}', \mathbf{T})$ for the cases in which S and S′ do not exceed 1.

Case $S = S' = \tfrac{1}{2}$:

$$O_{Jl'\frac{1}{2}l\frac{1}{2}}(\mathbf{L}', \sigma) = \frac{1}{2(2l'+1)}\left[J + \frac{1}{2} + (-1)^{l'-J+\frac{1}{2}}(\sigma\mathbf{L}')\right][(q_0+1) + (q_0-1)(\sigma\mathbf{k})]; \qquad (17)$$

Case $S = 0$, $S' = 1$:

$$O_{Jl'1l}(\mathbf{L}', \mathbf{T}) = \begin{cases} \dfrac{1}{2l'+1}\sqrt{\dfrac{2J+1}{J+\frac{1}{2}\mp\frac{1}{2}}}\left[-i(\mathbf{T}[\mathbf{k}\times\mathbf{L}']) \pm \left(J+\dfrac{1}{2}\mp\dfrac{1}{2}\right)(\mathbf{T}\mathbf{k})\right], & J = l = l' \pm 1, \qquad (18) \\ \dfrac{1}{\sqrt{J(J+1)}}(\mathbf{T}\mathbf{L}'), & J = l = l'; \qquad (19) \end{cases}$$

Case $S = 1$, $S' = 0$:

$$O_{Jl'l1}(\mathbf{L}', \mathbf{T}) = \begin{cases} \dfrac{1}{2l'+1}\sqrt{\dfrac{2J+1}{J+\frac{1}{2}\mp\frac{1}{2}}}\left[i(\mathbf{T}[\mathbf{k}\times\mathbf{L}']) \pm \left(J+\dfrac{1}{2}\mp\dfrac{1}{2}\right)(\mathbf{T}\mathbf{k})\right], & J = l \pm 1 = l', \qquad (20) \\ \dfrac{1}{\sqrt{J(J+1)}}(\mathbf{T}\mathbf{L}'), & J = l = l'; \qquad (21) \end{cases}$$

Case $S = S' = 1$:

a) $q_0 = +1$,

$$O_{Jl'1l1}(\mathbf{L}', \mathbf{S}) = \begin{cases} \dfrac{1}{(2l'+1)(J+\frac{1}{2}\mp\frac{1}{2})}\left\{\pm\left(J+\dfrac{1}{2}\mp\dfrac{1}{2}\right)[1+(\mathbf{S}\mathbf{L}')] + (\mathbf{S}\mathbf{L}')(\mathbf{S}\mathbf{L}')\right\}, & J = l \pm 1 = l' \pm 1, \\ \dfrac{1}{(2l'+1)\sqrt{J(J+1)}}\left\{-2\left(J+\dfrac{1}{2}\pm\dfrac{1}{2}\right)^2 + (2J+1)\left[\left(J+\dfrac{1}{2}\pm\dfrac{1}{2}\right)(\mathbf{S}\mathbf{k})\right.\right. & \\ \left.\left.\pm i(\mathbf{S}[\mathbf{k}\times\mathbf{L}'])\right](\mathbf{S}\mathbf{k}) \pm \left(J+\dfrac{1}{2}\mp\dfrac{1}{2}\right)(\mathbf{S}\mathbf{L}') + (\mathbf{S}\mathbf{L}')(\mathbf{S}\mathbf{L}')\right\}, & J = l \pm 1 = l' \mp 1, \\ \dfrac{1}{J(J+1)}\{J(J+1) - (\mathbf{S}\mathbf{L}')(\mathbf{S}\mathbf{L}')\}, & J = l = l'; \end{cases} \qquad (22)$$

---

*A similar representation for $S = S' = \tfrac{1}{2}$ is used in reference 2.

b) $q_0 = -1$,

$$O_{Jl'1l1}(\mathbf{L}',\mathbf{S}) = \begin{cases} \dfrac{1}{(2l'+1)(J+{}^1/_2\mp{}^1/_2)}\sqrt{\dfrac{2J+1}{J+{}^1/_2\pm{}^1/_2}}\Big[\mp\Big(J+\dfrac{1}{2}\mp\dfrac{1}{2}\Big)(\mathbf{Sk}) - \\ \qquad -i(\mathbf{S}[\mathbf{k}\times\mathbf{L}'])\Big](\mathbf{SL}'), \qquad J = l\pm 1 = l'. \\ \dfrac{1}{(2l'+1)(J+{}^1/_2\mp{}^1/_2)}\sqrt{\dfrac{2J+1}{J+{}^1/_2\pm{}^1/_2}}\Big[\mp\Big(J+\dfrac{1}{2}\mp\dfrac{1}{2}\Big)(\mathbf{Sk})\mp \\ \mp\Big(J+\dfrac{1}{2}\pm\dfrac{1}{2}\Big)(\mathbf{SL}')(\mathbf{Sk}) + i(\mathbf{SL}')(\mathbf{S}[\mathbf{k}\times\mathbf{L}'])\Big], \; J = l = l'\pm 1. \end{cases} \tag{23}$$

B. Coupling* $l_1 + S' = j$, $j + l_2 = J$

If, on the other hand, we use the formulas (11b), (10), and (5), then for integral S and S′ the angular operator for the reaction a + b → a′ + b′ + c′ can again be reduced to a certain invariant differential operator acting on an angular polynomial of the form $L_{jl_2J}(\mathbf{k}_1\mathbf{k}_2; \mathbf{k})$ [Eq. (12)]; we have

$$L_{Jjl_1S'l_2lS}(\mathbf{k}_1\mathbf{k}_2;\mathbf{k}) = O_{jl_1S',\,JlS}(\mathbf{L},\mathbf{L}_1,\mathbf{T})\,L_{jl_2J}(\mathbf{k}_1\mathbf{k}_2;\mathbf{k}). \tag{24}$$

In particular, we get for the operators $O_{jl_1S';\,JlS}$

Cases S = 0, S′ = 1 and S = 1, S′ = 0:

$$O_{jl_11} = (\mathbf{O}_{jl_1}(\mathbf{k}_1,\mathbf{L}_1)\mathbf{T}), \qquad O_{Jl1} = (\mathbf{O}_{Jl}(\mathbf{k},\mathbf{L})\mathbf{T}); \tag{25}$$

Case S = S′ = 1:

$$O_{jl_11;\,Jl1} = (\mathbf{O}_{Jl}(\mathbf{k},\mathbf{L})\,\mathbf{O}_{jl_1}(\mathbf{k}_1,\mathbf{L}_1)) - (\mathbf{O}_{Jl}(\mathbf{k},\mathbf{L})\mathbf{S})(\mathbf{O}_{jl_1}(\mathbf{k}_1,\mathbf{L}_1)\mathbf{S}), \tag{26}$$

where

$$\mathbf{O}_{JJ\pm1}(\mathbf{k},\mathbf{L}) = \frac{1}{\sqrt{(2J+1)(J+{}^1/_2\pm{}^1/_2)}}\Big[-i[\mathbf{k}\times\mathbf{L}]\mp\Big(J+\frac{1}{2}\pm\frac{1}{2}\Big)\mathbf{k}\Big],$$

$$\mathbf{O}_{JJ}(\mathbf{k},\mathbf{L}) = \frac{\mathbf{L}}{\sqrt{J(J+1)}}. \tag{27}$$

If, on the other hand, S and S′ are half-integral, the angular operator can be constructed directly, as in Eq. (12). In particular we have:

Case S = S′ = ½:

$$\begin{aligned} L_{Jjl_1{}^1/_2\,l_2l\,{}^1/_2}(\mathbf{k}_1\mathbf{k}_2;\mathbf{k}) &= (-1)^{j+l_2-J}\sqrt{\Big(J+\tfrac{1}{2}\Big)(2l_2+1)}\sum_{m={}^1/_2}^{j}\left\{\frac{(j-m)!(l_2-m+{}^1/_2)!}{(j+m)!(l_2+m-{}^1/_2)!}\right\}^{{}^1/_2} \\ &\times\Big\{\Big(l_1\pm m+\tfrac{1}{2}\Big)P_{l_1}^{(m-{}^1/_2)}(x_1)\mp i(\boldsymbol{\sigma}[\mathbf{k}_1\times\mathbf{k}])P_{l_1}^{(m+{}^1/_2)}(x_1)\Big\} \\ &\times\Big\{a_{m-{}^1/_2}^{(q)}-(\boldsymbol{\sigma}\mathbf{k})\,a_{m-{}^1/_2}^{(-q)}\Big\}\Big\{C_{J\,{}^1/_2}^{l_2\,{}^1/_2-m;\,jm}P_{l_2}^{(m-{}^1/_2)}(x_2) \\ &+(-1)^{J+{}^1/_2-l}\Big[\Big(l_2-m+\tfrac{1}{2}\Big)\Big(l_2+m+\tfrac{1}{2}\Big)\Big]^{-{}^1/_2} \\ &\times C_{J-{}^1/_2}^{l_2-{}^1/_2-m;\,jm}\,i(\boldsymbol{\sigma}[\mathbf{k}_2\times\mathbf{k}])P_{l_2}^{(m+{}^1/_2)}(x_2)\Big\}. \end{aligned} \tag{28}$$

The signs ± correspond to $j = l_1 \pm ½$.

We note that for the reactions π + N → 2π′ + N′ and $N_1 + N_2 \to N_1' + N_2' + \pi'$ the formulas more convenient in practice are Eqs. (28) and (24), and not Eq. (16), since in this case the quantum numbers l_1, j describing the final system correspond to the quantum numbers l', J describing the final system in the reactions π + N → π′ + N′ and $N_1 + N_2 \to N_1' + N_2'$. Therefore if the matrix elements $S_{J_0l_0'S_0'l_0S_0}$ are important for the reactions π + N → π′ + N′ and $N_1 + N_2 \to N_1' + N_2'$, it can be assumed that an important part in the expansions (4) for the reactions π + N → 2π′ + N′ and $N_1 + N_2 \to N_1' + N_2' + \pi'$ is played by the matrix elements $S_{Jjl_1S'l_2lS}$ for which $j = J_0$, $l_1 = l_0'$, $S' = S_0'$, $l = l_0$, $S = S_0$.

4. REACTIONS INVOLVING γ-RAY QUANTA

The wave function $(\mathbf{eD}_{lm}^{(\lambda)}(\mathbf{k}))$ of a photon with momentum **k**, angular momentum l, polarization **e**, and multipole character λ (λ = 1 or 0 for multipoles of electric or magnetic type, respectively) is connected with the function $Y_{lm}(\mathbf{k})$ of a particle of spin zero by the relation

$$(\mathbf{eD}_{lm}^{(1)}(\mathbf{k})) = \frac{1}{\sqrt{l(l+1)}}\Big(\mathbf{e}\frac{\partial}{\partial\mathbf{k}}\Big)Y_{lm}(\mathbf{k}), \qquad \text{parity} = (-1)^l,$$

$$(\mathbf{eD}_{lm}^{(0)}(\mathbf{k})) = \frac{1}{\sqrt{l(l+1)}}\Big(i[\mathbf{k}\times\mathbf{e}]\frac{\partial}{\partial\mathbf{k}}\Big)Y_{lm}(\mathbf{k}),$$

$$\text{parity} = (-1)^{l+1}. \tag{29}$$

Therefore the construction of the angular operators for a reaction involving a photon reduces to the application of the "polarization" operator $[l(l+1)]^{-1/2}(\mathbf{e}\partial/\partial\mathbf{k})$ or $[l(l+1)]^{-1/2}(i[\mathbf{k}\times\mathbf{e}]\partial/\partial\mathbf{k})$ to the angular operators of the analogous reaction, in which the photon is replaced by a scalar or pseudoscalar particle with spin zero (cf. reference 1). That is, if one has to construct the angular operators $L_{J\nu'\nu\lambda}(\mathbf{k}_1\mathbf{k}_2;\mathbf{k})$ for the reaction γ + b → a′ + b′ + c′, one must construct the angular operators $L_{J\nu',\nu}^{(q)}(\mathbf{k}_1\mathbf{k}_2;\mathbf{k})$ or $L_{J\nu',\nu}^{(-q)}(\mathbf{k}_1\mathbf{k}_2;\mathbf{k})$ for the reaction a + b → a′ + b′ + c′, where a is a scalar or pseudoscalar particle with spin zero, and then apply to them the operators $[l(l+1)]^{-1/2}(\mathbf{e}\partial/\partial\mathbf{k})^*$ or $[l(l+1)]^{-1/2}\cdot(i[\mathbf{k}\times\mathbf{e}]\partial/\partial\mathbf{k})^*$, respectively:

---

*Cf. footnote *, page 154.

$$L_{J\nu'\nu\lambda}(\mathbf{k}_1\mathbf{k}_2;\ \mathbf{k}) = \begin{cases} [l(l+1)]^{-1/2}(\mathbf{e}\,\partial/\partial\mathbf{k})^* L^{(q)}_{J\nu'\nu}(\mathbf{k}_1\mathbf{k}_2;\ \mathbf{k}), & \lambda = 1, \\ [l(l+1)]^{-1/2}(i\,[\mathbf{k}\times\mathbf{e}]\,\partial/\partial\mathbf{k})^* L^{(-q)}_{J\nu'\nu}(\mathbf{k}_1\mathbf{k}_2;\ \mathbf{k}), & \lambda = 0. \end{cases} \quad (30)$$

Similarly, the angular operators $L_{J\nu'\lambda'\nu}(k_1k_2;\ k)$ for the reaction $a + b \rightarrow a' + b' + \gamma'$ are connected with the operators $L^{(q)}_{J\nu'\nu}(k_1k_2;\ k)$ and $L^{(-q)}_{J\nu'\nu}(k_1k_2;\ k)$ of the reaction $a + b \rightarrow a' + b' + c'$, where c' is a scalar or pseudoscalar particle with spin zero, by the relations

$$L_{J\nu'\lambda'\nu}(\mathbf{k}_1\mathbf{k}_2;\ \mathbf{k}) = \begin{cases} [l_2(l_2+1)]^{-1/2}(\mathbf{e}'\partial/\partial\mathbf{k}_2)\, L^{(q)}_{J\nu'\nu}(\mathbf{k}_1\mathbf{k}_2;\ \mathbf{k}), & \lambda' = 1, \\ [l_2(l_2+1)]^{-1/2}(i\,[\mathbf{k}_2\times\mathbf{e}']\,\partial/\partial\mathbf{k}_2)\, L^{(-q)}_{J\nu'\nu}(\mathbf{k}_1\mathbf{k}_2;\ \mathbf{k}), & \lambda' = 0. \end{cases} \quad (31)$$

Here it is assumed that the angular momentum and momentum of the photon are l_2 and $\mathbf{p}_2$. Finally, the angular operators $L_{J\nu'\lambda'\nu\lambda}(k_1k_2;\ k)$ for the reaction $\gamma + b \rightarrow a' + b' + \gamma'$ are obtained by applying the operators

$$[l_2(l_2+1)\,l(l+1)]^{-1/2}(\mathbf{e}'\partial/\partial\mathbf{k}_2)(\mathbf{e}\,\partial/\partial\mathbf{k})^*$$

and $[l_2(l_2+1)\,l(l+1)]^{-1/2}(i\,[\mathbf{k}_2\times\mathbf{e}']\,\partial/\partial\mathbf{k}_2)(i\,[\mathbf{k}\times\mathbf{e}]\,\partial/\partial\mathbf{k})^*$

to the angular operators for the reaction $a + b \rightarrow a' + b' + c'$, in which the particles a and c′ have spin zero and the same parity and by applying the operators

$$[l_2(l_2+1)l(l+1)]^{-1/2}(\mathbf{e}'\partial/\partial\mathbf{k}_2)(i[\mathbf{k}\times\mathbf{e}]\partial/\partial\mathbf{k})^*$$

and $[l_2(l_2+1)\,l(l+1)]^{-1/2}\ (i[\mathbf{k}_2\times\mathbf{e}']\,\partial/\partial\mathbf{k}_2)\,(\mathbf{e}\partial/\partial\mathbf{k})^*$

to the angular operators for the reaction $a + b \rightarrow a' + b' + c'$, in which particles a and c′ have spin zero and opposite parities.

5. CONCLUSION

The angular operators completely determine the angular distribution and polarization of the particles in the transition $J\nu \rightarrow J\nu'$. Since the differential cross section $d\sigma/d\Omega$ and the polarization of the scattered particles (i.e., the mean values $\langle\Omega\rangle'$ of certain spin operators Ω) are connected with the scattering amplitude $T = S - 1$ by the relations

$$d\sigma/d\Omega = \mathrm{Sp}\,(T\rho T^+), \qquad \langle\Omega\rangle' = \mathrm{Sp}\,(\Omega T\rho T^+)\,/\,\mathrm{Sp}\,(T\rho T^+),$$

where ρ is the density matrix of the incident particles, by measuring $d\sigma/d\Omega$ and $\langle\Omega\rangle'$ experimentally and using the expansion (4) for the scattering matrix, one can find the coefficients $S_{J\nu'\nu}(E,\ p'_c)$, i.e., carry out the phase-shift analysis.

On the other hand, if the scattering matrix obeys some known equation, the problem of finding this matrix is made easier if, by means of the expansion (4), one effects a separation of the angular and spin variables from the variables E, p'_c, and reduces the problem to that of finding the $S_{J\nu'\nu}(E,\ p'_c)$, which depend only on E and p'_c.

The writer is grateful to I. E. Tamm, who stimulated this research, and also to J. Fischer and S. Ciulli, who made their work available before its publication.

---

[1] V. I. Ritus, J. Exptl. Theoret. Phys. (U.S.S.R.) **32**, 1536 (1957), Soviet Phys. JETP **5**, 1249 (1957).

[2] S. Ciulli and J. Fischer, Nuovo cimento (in press).

[3] E. Fabri, Nuovo cimento **11**, 479 (1954).

Translated by W. H. Furry
34

SOVIET PHYSICS JETP VOLUME 37 (10), NUMBER 1 JANUARY, 1960

DYNAMICS OF A CONDUCTING GASEOUS SPHERE IN A QUASI-STATIONARY ELECTROMAGNETIC FIELD

V. V. YANKOV

P. N. Lebedev Physics Institute, Academy of Sciences, U.S.S.R.

Submitted to JETP editor, February 10, 1959

J. Exptl. Theoret. Phys. (U.S.S.R.) **37**, 224-228 (July, 1959)

An investigation is made of the small oscillations of a plasma sphere of infinite conductivity.

VEKSLER[1] and Knox[2] have called attention to the possibility of using ac electromagnetic fields for the stabilization of hot plasmas.

Below we consider a uniform gaseous sphere with sharp boundaries located in a quasi-stationary, spatially homogeneous electromagnetic field

$$H_k = H_0 \exp(i\Omega_k^H t), \quad E_k = E_0 \exp(i\Omega_k^E t), \qquad (1)$$

$(k = x, y, z)$ where the frequencies Ω_k^H and Ω_k^E are all assumed to be different from each other. If the skin effect is large the ac field does not penetrate the plasma, the electrical conductivity of which is assumed to be infinite. The time-average of the pressure at the surface of a weakly deformed, ideally conducting sphere in an ac field (1) has been determined in reference 3:

$$\bar{p}(\vartheta, \varphi) = \frac{9H_0^2}{32\pi}\left[\left(1 - 2\frac{E_0^2}{H_0^2}\right) + \sum_{l=2}^{\infty}\sum_{m=-l}^{l}\frac{(2l-1)(l-1)}{2l+1}\right.$$
$$\left.\times\left(1 - \frac{4}{3}\frac{l(l+1)}{l-1}\frac{E_0^2}{H_0^2}\right)\alpha_{lm}Y_l^m(\vartheta, \varphi)\right]. \qquad (2)$$

Here the α_{lm} are the coefficients in the expansion, in spherical functions, for the radial deviation from a sphere of radius r_0 of points at the surface of the plasma:

$$\delta r(\vartheta, \varphi)/r_0 = \sum_{l=0}^{\infty}\sum_{m=-l}^{l}\alpha_{lm}Y_l^m(\vartheta, \varphi).$$

For equilibrium the internal gas kinetic pressure at the boundary of the plasma must be equal to the electromagnetic forces:

$$(9H_0^2/32\pi)(1 - 2E_0^2/H_0^2) = p > 0.$$

Since there is no electromagnetic field inside the bunch, in analyzing small deviations we start with the usual hydrodynamic equation (neglecting viscosity). Then, a monochromatic component of the displacement potential

$$\xi(r, \vartheta, \varphi)e^{i\omega t} = \nabla\Phi(r, \vartheta, \varphi)e^{i\omega t}$$

of an individual particle obeys the following wave equation in the linear perturbation approximation:

$$\omega^2\Phi + c^2\Delta\Phi = 0,$$

where the adiabatic velocity of sound is $c^2 = \gamma p/\rho$. The particular solution

$$\Phi_{lm}(r, \vartheta, \varphi) = \mathrm{const}\cdot r^{-1/2}J_{l+1/2}(\omega r/c)Y_l^m(\vartheta, \varphi), \qquad (3)$$

in which the frequency ω is still arbitrary, must satisfy the boundary condition

$$-\gamma p\{\operatorname{div}\xi\}_{r=r_0} = \frac{9H_0^2}{32\pi}\frac{(2l-1)(l-1)}{2l+1}f_l\left\{\frac{\xi_r}{r_0}\right\}_{r=r_0} \quad (l \geqslant 2),$$

$$f_l(E_0/H_0) = 1 - \frac{4}{3}\frac{l(l+1)}{l-1}\frac{E_0^2}{H_0^2}, \qquad (4)$$

which states that the Lagrangian variations of the hydrodynamic and electromagnetic pressures at the surface of the perturbed sphere must be equal. Converting from the displacement amplitude to the potential in Eq. (4) we obtain the dispersion relation

$$\omega^2 = F_l(\omega) \equiv \frac{9H_0^2}{32\pi}\frac{c^2}{\gamma p r_0}\frac{(2l-1)(l-1)}{2l+1}f_l\frac{\sqrt{r_0}}{J_{l+1/2}(\omega r_0/c)}$$
$$\times\left\{\frac{d}{dr}\frac{J_{l+1/2}(\omega r/c)}{\sqrt{r}}\right\}_{r=r_0}, \quad l \geqslant 2. \qquad (5)$$

For radial spherically symmetric oscillations of the sphere $(l = 0)$ and reciprocating displacements of the sphere as a whole $(l = 1)$ the internal pressure remains unchanged. Consequently we have the boundary condition

$$J_{l+1/2}(\omega r_0/c) = 0, \quad l = 0,1. \qquad (6)$$

The roots of the transcendental equations (5) and (6) determine the spectrum of eigenvalues ω_l for a given perturbation (3). The absence of solutions with $\omega^2 < 0$ for positive f_l indicates that the bunch is stable against perturbations characterized by wavelengths $\lambda_s = 2\pi r_0/l$ along the surface of the sphere for which $f_l(E_0/H_0) > 0$. Instability is possible for a perturbation characterized by $f_l < 0$. In this case the solution with $\omega^2 < 0$ signifies random deviations which increase exponentially in the course of time. In the particular case[2] $E_0 = 0$ and $f_l = 1$ a spherical plasma has internal stability against arbitrary perturbations. The limiting case $c \to \infty$ in Eq. (5) gives the simple formula

$$\omega_l^2 = \frac{9H_0^2}{32\pi}\frac{1}{\rho r_0^2}\frac{(2l-1)(l-1)l}{2l+1} f_l,$$

which characterizes the dynamics of a highly conducting incompressible fluid.* The equilibrium criteria formulated do not apply when λ_s becomes comparable with the skin depth (for large values of l) since a perturbation of this kind is not compatible with the original assumption of infinite conductivity for the deformed sphere.

We have discussed here the behavior of a plasma sphere when the pressure of the external electromagnetic field is constant (time average). In order to calculate the effect of the alternating component of the high-frequency field we consider rapid motion of a plasma produced, for example, by the z component of the magnetic field (E_0 is assumed to be zero). As before we assume that $\alpha_{lm} \ll 1$. The magnetic pressure

$$p_{H_z}(\vartheta, \varphi, t) = \frac{3H_z^2}{16\pi}\left[1 - Y_2^0 + \sum_{l=2}^{\infty}\sum_{m=-l}^{l} \Lambda_{lm}\alpha_{lm}Y_l^m\right],$$

$$\Lambda_{lm} = \frac{12l^3(l^2-m^2) + 2l^2(l^2-3m^2) - 18l(l^2-m^2) + 10l^2 - 9m^2}{(2l+3)(2l+1)l(2l-1)} \tag{7}$$

is computed in the same way as for (2). In Eq. (7) we separate out the harmonic time component

$$\tilde{p}_{H_z}(\vartheta, \varphi, t) = \frac{p}{3}\Big[1 - Y_2^0 + \sum_{l=2}^{\infty}\sum_{m=-l}^{l} \Lambda_{lm}\alpha_{lm}Y_l^m(\vartheta, \varphi)\Big]\cos 2\Omega_z t,$$

and, in the acoustic approximation, obtain the boundary condition for the displacement potential $\zeta(r, \vartheta, \varphi, t) = \nabla\Psi$, which is governed by the wave equation $c^2\Delta\Psi = \partial^2\Psi/\partial t^2$:

$$\frac{3\gamma}{c^2}\left\{\frac{\partial^2\Psi}{\partial t^2}\right\}_{r=r_0} = \begin{cases} -\cos 2\Omega_z t \quad \text{for } l = 0; \\ Y_2^0\cos 2\Omega_z t - \left(\frac{52}{35}\cos 2\Omega_z t + \frac{9}{5}\right)\frac{1}{r_0}\left\{\frac{\partial\Psi}{\partial r}\right\}_{r=r_0} \\ \qquad \text{for } l = 2,\ m = 0; \\ -\left(\Lambda_{lm}\cos 2\Omega_z t + \frac{3(2l-1)(l-1)}{2l+1}\right)\frac{1}{r_0}\left\{\frac{\partial\Psi}{\partial r}\right\}_{r=r_0} \\ \qquad \text{for } l = 2,\ m \neq 0;\ l \geqslant 3. \end{cases} \tag{8}$$

Whence we find the solution for $l = 0$:

$$\frac{\zeta_r(r_0, t)}{r_0} = \frac{1}{3\gamma\nu_0}\frac{\sqrt{\nu_0}}{J_{1/2}(\nu_0)}\left\{\frac{d}{d\nu}\frac{J_{1/2}(\nu)}{\sqrt{\nu}}\right\}_{\nu=\nu_0} Y_0\cos 2\Omega_z t,$$

where the following notation has been introduced:

$$2\Omega_z r/c = \nu, \quad 2\Omega_z r_0/c = \nu_0.$$

An investigation of the other equations ($l \geq 3$; $l = 2$, $m \neq 0$) by the method of successive approximations shows that the oscillations are stable for frequencies characterized by $\Omega_Z > \omega_l$. Unstable solutions are possible close to the values $\Omega_Z = \omega_l/n$, where $n = 1, 2, 3, \ldots$ (parametric resonance). In the region of stable solutions for spheroidal perturbation ($l = 2$, $m = 0$) the motion of the sphere boundary is given approximately by the expression

$$\frac{\zeta_r(r_0, t)}{r_0} = \frac{5}{9}\frac{F_2(2\Omega_z)}{F_2(2\Omega_z) - (2\Omega_z)^2} Y_2^0(\vartheta, \varphi)\cos 2\Omega_z t,$$

$$F_2 \neq n^2(2\Omega_z)^2.$$

By proper choice of the frequency Ω_Z it should be possible to meet the requirements for small induced surface oscillations with respect to simple Y_0 and Y_2^0-deformation. For example, with $x_0 \gg 1$ the oscillations of the volume and the shape of the plasma are insignificant $[r_0^{-1}|\zeta_r(r_0, t)|_{\max} \ll 1]$ if the inequality $|\nu_0 \cot \nu_0 - 1| \ll \nu_0^2$ is satisfied.

If we assume that the plasma is incompressible the boundary conditions in (8) reduce to Mathieu equations (with a right-hand member in the case of a spheroidal deformation)

$$\frac{d^2\alpha_{20}}{d\tau^2} + (a_2 + 16q_{20}\cos 2\tau)\alpha_{20} = \frac{2p\cos 2\tau}{3\rho\Omega_z^2 r_0^2},$$

$$\frac{d^2\alpha_{lm}}{d\tau^2} + (a_l + 16q_{lm}\cos 2\tau)\alpha_{lm} = 0, \quad l = 2, \quad m \neq 0; \quad l \geqslant 3,$$

where

$$\tau = \Omega_z t, \ a_l = \omega_l^2/\Omega_2^2, \qquad q_{lm} = l\Lambda_{lm}p/48\rho\Omega_z^2 r_0^2.$$

The motion of the surface of an incompressible liquid is stable with respect to the first three harmonics ($l = 2, 3, 4$) for example with $\Omega_Z^2 \approx p/3\rho r_0^2$. In general, with increasing values of m and l the instability zones become smaller.

The stability criteria for high frequencies in the presence of an electric field may be obtained in a similar manner if, in place of Eq. (7), we use

$$p_{E_z}(\vartheta, \varphi, t) = -\frac{3E_z^2}{4\pi}\left[\frac{1}{2} + Y_2^0 + \sum_{l=2}^{\infty}\sum_{m=-l}^{l} \Xi_{lm}\alpha_{lm}Y_l^m\right], \tag{9}$$

where

---

*The lowest limiting frequency found (ω_2) is approximately the same as that determined by Eq. (5) in the general case of a compressible fluid.

$$\Xi_{lm} = \frac{4l^3(l^2 - m^2) + 8l^2(l^2 - m^2) - l(l^2 - 5m^2) - 6(l^2 - m^2) - l}{(2l - 1)(2l + 1)(2l + 3)}.$$

We can now consider the qualitative features of the physical results. First we consider the mechanism for stabilization of a plasma by a magnetic field. The application of one field (for example H_z) causes, in addition to the anisotropic pressure $p(\vartheta) = 3H_0^2(1 - Y_2^0)/32\pi$, an instability for perturbations characterized by $m = l$ [cf. Eq. (7)]. In these deformations the magnetic force lines which bend around the sphere along the meridians, are, (without twisting) spread apart at protruding regions of the surface and concentrated in regions of indentation; as a result a magnetic pressure differential is created, which tends to increase the deformation. With $m \neq l$ another effect predominates; this is the increase in the magnetic pressure as a consequence of twisting of the force lines, which provides stability for all simple perturbations. A rapid change in the direction of the field, realized above by superposition of three fields, breaks up the correlation of the motion produced by the instability with $m = l$, and the field configuration; rotation of the field leads to a time average dynamic stability with respect to a weak perturbation.* The application of electric fields only weakens the stability of the spherical shape. This is because the electric force lines formed at the induced surface charges are concentrated in surface regions of high curvature and any deformation leads to an additional negative electric pressure which tends to increase the deformation [cf. Eq. (9)].

In an inhomogeneous magnetic field a plasma of infinite conductivity is diamagnetic; in an inhomogeneous electric field it behaves like a pure dielectric. Thus, the average force acting on the sphere is given by

$$\mathbf{F} = r_0^3 \operatorname{grad}(2\overline{E}^2 - \overline{H}^2)/4.$$

By satisfying the stability requirements of the position of the sphere as a whole as well as those for volume and shape it is possible to make an isolated plasma stable in a given region of the external field.

The author is indebted to M. S. Rabinovich for valuable discussions of the present work.

---

*The containment of a plasma by a rotating magnetic field has also been considered by Butler et al.[4]

[1] Veksler, Kovrizhnykn, Rabinovich, and Yankov, Possibility of Using an Electromagnetic Wave for Stabilization of High Temperature Plasmas, Отчет ФИАН Report, Inst. of Physics, U.S.S.R. Acad. Sci. August, 1956.

[2] F. B. Knox, Austr. J. Phys., **10**, 221 (1957).

[3] V. V. Yankov, J. Exptl. Theoret. Phys. (U.S.S.R.) **36**, 560 (1959), Soviet Phys. JETP **9**, 388 (1959).

[4] Butler, Hatch, and Ulrich, Second United Nations Intern. Conf. on the Peaceful Uses of Atomic Energy, p. 350, U.S.A., 1958.

Translated by H. Lashinsky
35

SOVIET PHYSICS JETP VOLUME 37(10), NUMBER 1 JANUARY, 1960

VAN DER WAALS FORCES IN LIQUID FILMS

I. E. DZYALOSHINSKIĬ, E. M. LIFSHITZ, and L. P. PITAEVSKIĬ

Institute for Physical Problems, Academy of Sciences, U.S.S.R.

Submitted to JETP editor February 12, 1959; resubmitted March 27, 1959

J. Exptl. Theoret. Phys. (U.S.S.R.) **37**, 229-241 (July, 1959)

A previously developed theory[1] of the molecular forces of interaction between solid bodies, the surfaces of which are brought to very small distances of one another, is extended to the case where the space between the bodies is filled with a liquid medium. It is shown, in particular, that two identical bodies always attract one another whatever the "layer" between them.

We have obtained general formulas for the thermodynamic quantities (chemical potential) of the liquid film from the knowledge of the spectral properties [the dielectric constant $\epsilon(\omega)$] of the liquid and the solid substratum. We have found limiting laws for the dependence of the chemical potential on the film thickness. The problem of the stability of films is considered and different possible cases of instability in well determined ranges of film thickness are noted. The possibility of the existence of very small, but non-zero, contact angles is noted. Liquid helium films are discussed.

1. INTRODUCTION

WE have developed earlier[1] a theory of the attractive molecular forces between solid bodies separated by a narrow gap. This theory was macroscopic in character, and in it the interaction between the bodies was considered to be caused through the intermediary of the fluctuating electromagnetic field. The attractive force itself was then evaluated as the appropriate component of the Maxwell stress tensor of the electromagnetic field at the surface of the body.

In reference 1 it was assumed that the space between the bodies was a vacuum, so that the evaluation of the Maxwell stresses was carried out using the usual formulas for the field in vacuo. A generalization of the theory to the case where the gap between the bodies is also filled with some medium was difficult because there were no formulas for the stress tensor in a variable field in absorbing media.

This difficulty is now no longer present, thanks to the fact that recently[2] there have been obtained general formulas for that part of the thermodynamic quantities (including the stress tensor) of an arbitrary absorbing medium which is due to the fluctuating electromagnetic field with wavelengths $\lambda \gg a$ (a being the interatomic distance). This field corresponds exactly to forces that have the same nature as the van der Waals forces between individual molecules large distances apart.

A general formula for the tensor of the stresses arising from the fluctuations of the electromagnetic field in an absorbing medium is given in Sec. 2. We shall see, however, that it is unnecessary in practice to use it again for explicit calculations, since it turns out to be possible to obtain the required formula for the interaction force between bodies separated by a "layer" through a simple transformation of the formula for bodies separated by a vacuum.

Different cases which may occur when two bodies interact are analyzed in Sec. 3. The indices 1 and 2 distinguish in all equations quantities referring to these two bodies, and the index 3 identifies quantities referring to the medium filling the gap (of width l) between the bodies. Although in all this we have assumed the gap to be plane-parallel, we must nevertheless bear in mind that in reality, for a correct statement of the problem of the interaction force between bodies, we must consider that at least one of them has finite dimensions and is surrounded on all sides by the medium 3, and we must determine the total force acting upon it. In view of the very steep decrease of molecular forces with distance, this resultant force can, in actual fact, be completely attributed to the forces acting across the narrow gap between the two bodies.

If one of the media 1 or 2 is replaced by a vacuum we then have the case of a thin film on the surface of a solid body. The thermodynamic quantities (the chemical potential) of a film are evaluated in Sec. 4, which also includes an investigation of the stability of films of different thicknesses. Liquid helium films are considered separately in Sec. 6.

In the case of a vacuum gap between bodies, the forces of the interaction between them can completely be reduced to the forces described by the fluctuating electromagnetic fields. When, however, the gap is filled with a liquid medium, there are forces of yet another origin, which are connected with the energies of the acoustic sound vibrations in that medium. Moreover, fluctuating surface vibrations at the interface of different media can also lead to a definite contribution. The same holds also for the evaluation of the chemical potential of the film. In actual fact, however, these additional contributions are small (as will be shown in Sec. 5) compared with the contribution from the electromagnetic fluctuations, i.e., from the van der Waals forces.

2. THE STRESS TENSOR IN A LAYER OF AN ABSORBING MEDIUM

It was shown in reference 2 that the additional stresses arising in an absorbing medium in which there is a fluctuating electromagnetic field can be expressed in terms of temperature Green's functions $\mathfrak{D}_{ik}(\mathbf{r}, \mathbf{r}'; \xi_n)$ of the electromagnetic field, which depend on a discrete imaginary frequency. These functions were introduced by Gor'kov, Abrikosov, and Dzyaloshinskiĭ and by Fradkin[3] and are Fourier expansions of the well-known temperature Green's functions of Matsubara.[4]

The general formula for the stress tensor of a fluctuating electromagnetic field has the following form:*

$$\sigma_{ik} = -\frac{\hbar T}{2\pi} \sum_{n=0}^{\infty}{}' \Big\{ -\frac{1}{2}\delta_{ik}\Big(\varepsilon - \rho\frac{\partial\varepsilon}{\partial\rho}\Big)\mathfrak{D}_{ll}^{E}(\mathbf{r}, \mathbf{r};\ \xi_n) + \varepsilon\mathfrak{D}_{ik}^{E}(\mathbf{r}, \mathbf{r};\ \xi_n) - \frac{1}{2}\delta_{ik}\mathfrak{D}_{ll}^{H}(\mathbf{r}, \mathbf{r};\ \xi_n) + \mathfrak{D}_{ik}^{H}(\mathbf{r}, \mathbf{r};\ \xi_n)\Big\} - \delta_{ik}p_0. \tag{1}$$

Here $\epsilon = \epsilon(\mathbf{r}, i\xi_n)$ is the dielectric constant of the substance as a function of the imaginary frequency $\omega = i\xi$; the summation is taken over the values $\xi_n = 2\pi nT/\hbar$ (where the term with $n = 0$ is taken with a factor $\frac{1}{2}$); T is the temperature; ρ is the density of the substance; $p_0 = p_0(\rho, T)$ is that density which would be present in the medium if there were no field for the given values of ρ and T. The functions $\mathfrak{D}_{ik}^{E}$ and $\mathfrak{D}_{ik}^{H}$ play the role of the average values of the derivatives of the corresponding stress components of the fluctuating field, and are connected with the temperature Green's functions $\mathfrak{D}_{ik}$ which play a similar role for the vector potential of the field through the relations

$$\mathfrak{D}_{ik}^{E}(\mathbf{r}, \mathbf{r}'; \xi_n) = -\xi_n^2\mathfrak{D}_{ik}(\mathbf{r}, \mathbf{r}';\ \xi_n),$$
$$\mathfrak{D}_{ik}^{H}(\mathbf{r}, \mathbf{r}'; \xi_n) = \operatorname{curl}_{il}\operatorname{curl}'_{km}\mathfrak{D}_{lm}(\mathbf{r}, \mathbf{r}'; \xi_n) \tag{2}$$

The latter Green's function satisfies the equation

$$\varepsilon\xi_n^2\mathfrak{D}_{ik}(\mathbf{r}, \mathbf{r}'; \xi_n) + \operatorname{curl}_{il}\operatorname{curl}_{lm}\mathfrak{D}_{mk}(\mathbf{r}, \mathbf{r}';\ \xi_n) = -4\pi\delta(\mathbf{r} - \mathbf{r}')\,\delta_{ik}. \tag{3}$$

At the interface between two media, the components of $\mathfrak{D}_{ik}$ must satisfy boundary conditions corresponding to the continuity of the tangential components of the electrical and magnetic fields (it is unnecessary to write these out explicitly here).

Let body 2 be separated from body 1 by a gap of width l and be surrounded on all sides by the medium 3. The total force acting upon body 2 can be evaluated as being the total momentum flux flowing from the medium 3 into the body, i.e., in the form of an integral $\oint \sigma_{ik} df_k$ of the stress tensor in the above mentioned medium taken over the surface of the body. From the condition that the chemical potential should be constant in a medium in equilibrium we have, however, (see reference 5, §15)*

$$p_0 + \frac{\hbar T}{2\pi} \sum_{n=0}^{\infty}{}' \frac{1}{2}\rho\frac{\partial\varepsilon_3}{\partial\rho}\mathfrak{D}_{ll}^{E} = \text{const.} \tag{4}$$

Because of this condition, part of the stress tensor turns out to be a uniform pressure which is constant in the medium and which does not contribute anything to the total force acting upon the body. To determine this force it is, thus, in fact sufficient to write the stress tensor in the medium 3 in the form (compare a similar derivation in reference 5, §16)

$$\sigma'_{ik} = -\frac{\hbar T}{2\pi} \sum_{n=0}^{\infty}{}' \Big\{\varepsilon_3\Big[\mathfrak{D}_{ik}^{E} - \frac{1}{2}\delta_{ik}\mathfrak{D}_{ll}^{E}\Big] + \Big[\mathfrak{D}_{ik}^{H} - \frac{1}{2}\delta_{ik}\mathfrak{D}_{ll}^{H}\Big]\Big\}. \tag{5}$$

This expression differs from the one which would be valid for a field in a vacuum only by the factor ϵ_3 in the first term. This fact enables us to reduce the problem to the case considered in reference 1, where the bodies were separated by a vacuum, through a simple transformation.

---

*It must be understood that we have removed from this expression the divergent part that is connected with the equilibrium heat radiation in a homogenous medium.

*This condition assumes, in this form, that one may neglect the change in density of the medium itself under the influence of the field; taking this into account would lead to quantities of higher order in the field.

To do this we perform a coordinate transformation $\mathbf{r} = \tilde{\mathbf{r}}/\sqrt{\epsilon_3}$, at the same time introducing new $\mathfrak{D}$ functions by $\mathfrak{D}_{ik} = \tilde{\mathfrak{D}}_{ik}\sqrt{\epsilon_3}$; then, because of the definitions (2), we have

$$\mathfrak{D}^E_{ik} = \tilde{\mathfrak{D}}^E_{ik}\,\varepsilon_3^{1/2}, \qquad \mathfrak{D}^H_{ik} = \tilde{\mathfrak{D}}^H_{ik}\varepsilon_3^{3/2},$$

so that

$$\sigma'_{ik} = -\frac{\hbar T}{2\pi}\sum_{n=0}^{\infty}{}' \varepsilon_3^{3/2}\left[\tilde{\mathfrak{D}}^E_{ik} - \frac{1}{2}\delta_{ik}\tilde{\mathfrak{D}}^E_{ll} + \tilde{\mathfrak{D}}^H_{ik} - \frac{1}{2}\delta_{ik}\tilde{\mathfrak{D}}^H_{ll}\right]. \tag{6}$$

One sees easily that for the new functions $\tilde{\mathfrak{D}}_{ik}$ in the new coordinates we obtain equations of the same form as Eq. (3) in the regions 1, 2, and 3, where ϵ_1/ϵ_3, ϵ_2/ϵ_3, and 1 play, respectively, the role of ϵ in these equations. The interaction force between two bodies with dielectric constants ϵ_1 and ϵ_2 separated by a gap of width l filled with a medium ϵ_3 can thus be obtained from the expression for the interaction force of two bodies separated by a vacuum region by multiplying each term of the sum over n by $\epsilon_3^{3/2}$ and by replacing in all terms ϵ_1 and ϵ_2 by ϵ_1/ϵ_3 and ϵ_2/ϵ_3, respectively, and l by $l\sqrt{\epsilon_3}$.

3. THE MOLECULAR INTERACTION FORCES BETWEEN SOLID BODIES

One can usually neglect the influence of the temperature on the attractive force (compare reference 1) for those distances l which will be considered in connection with the problem under consideration. We then get a general formula for the attractive force F (per one cm^2 surface area of the body) by means of the above mentioned transformation from Eq. (2.9) of reference 1. This formula has the form

$$F = \frac{\hbar}{2\pi^2 c^3}\int_0^\infty\int_1^\infty p^2\xi^3\varepsilon_3^{3/2}\left\{\left[\frac{(s_1+p)(s_2+p)}{(s_1-p)(s_2-p)}\exp\left(\frac{2p\xi}{c}l\sqrt{\varepsilon_3}\right)-1\right]^{-1}\right.$$
$$\left.+\left[\frac{(s_1+p\varepsilon_1/\varepsilon_3)(s_2+p\varepsilon_2/\varepsilon_3)}{(s_1-p\varepsilon_1/\varepsilon_3)(s_2-p\varepsilon_2/\varepsilon_3)}\exp\left(\frac{2p\xi}{c}l\sqrt{\varepsilon_3}\right)-1\right]^{-1}\right\}dp\,d\xi, \tag{7}$$

where

$$s_1 = \sqrt{\varepsilon_1/\varepsilon_3 - 1 + p^2}, \qquad s_2 = \sqrt{\varepsilon_2/\varepsilon_3 - 1 + p^2},$$

and ϵ_1, ϵ_2, ϵ_3 are functions of imaginary frequency $\omega = i\xi$.

It will be remembered in this connection that $\epsilon(i\xi)$ is a real function, monotonically decreasing from the electrostatic value ϵ_0 (when $\xi = 0$) to 1 (when $\xi = \infty$). If the function $\epsilon''(\omega)$ (the imaginary part of the dielectric constant for real frequencies ω) is known from experiment, the function $\epsilon(i\xi)$ can be calculated from the formula (see reference 5, Sec. 62)

$$\varepsilon(i\xi) - 1 = \frac{2}{\pi}\int_0^\infty \frac{\omega\varepsilon''(\omega)}{\omega^2+\xi^2}\,d\omega \tag{8}$$

The transition to the limiting cases of "small" and "large" distances takes place in the same way as in reference 1. We thus get at small distances

$$F = \frac{\hbar}{16\pi^2 l^3}\int_0^\infty\int_0^\infty x^2\left[\frac{(\varepsilon_1+\varepsilon_3)(\varepsilon_2+\varepsilon_3)}{(\varepsilon_1-\varepsilon_3)(\varepsilon_2-\varepsilon_3)}e^x - 1\right]^{-1}dx\,d\xi. \tag{9}$$

At large distances, on the other hand,

$$F = \frac{\hbar c}{32\pi^2 l^4\sqrt{\varepsilon_{30}}}\int_0^\infty\int_1^\infty \frac{x^3}{p^2}\left\{\left[\frac{(s_{10}+p)(s_{20}+p)}{(s_{10}-p)(s_{20}-p)}e^x - 1\right]^{-1}\right.$$
$$\left.+\left[\frac{(s_{10}+p\varepsilon_{10}/\varepsilon_{30})(s_{20}+p\varepsilon_{20}/\varepsilon_{30})}{(s_{10}-p\varepsilon_{10}/\varepsilon_{30})(s_{20}-p\varepsilon_{20}/\varepsilon_{30})}e^x - 1\right]^{-1}\right\}dp\,dx,$$

$$s_{10} = \sqrt{\varepsilon_{10}/\varepsilon_{30} - 1 + p^2}, \qquad s_{20} = \sqrt{\varepsilon_{20}/\varepsilon_{30} - 1 + p^2}, \tag{10}$$

where ϵ_{10}, ϵ_{20}, ϵ_{30} are the electrostatic values of the dielectric constants. If both bodies are the same ($\epsilon_{10} = \epsilon_{20}$), one can put Eq. (10) in the form

$$F = \frac{\hbar c}{l^4}\frac{\pi^2}{240\sqrt{\varepsilon_{30}}}\left(\frac{\varepsilon_{10}-\varepsilon_{30}}{\varepsilon_{10}+\varepsilon_{30}}\right)^2\varphi\left(\frac{\varepsilon_{10}}{\varepsilon_{30}}\right), \tag{11}$$

where $\varphi(x)$ is the function the numerical values of which are given in Fig. 4 of reference 1 for arguments ranging from 1 to ∞; in addition we mention that $\varphi(0) = 0.52$.

With an accuracy which is completely sufficient for practical purposes, we can write Eqs. (9) and (10) in a simpler form by neglecting within the square brackets the quantity 1 compared to the terms with e^x. After this, the integration over dx is elementary, and there remains only a single integral* over $d\xi$ or dp. We get thus instead of Eq. (9)

$$F = \frac{\hbar\bar{\omega}}{8\pi^2 l^3}, \quad \text{where } \bar{\omega} = \int_0^\infty \frac{(\varepsilon_1-\varepsilon_3)(\varepsilon_2-\varepsilon_3)}{(\varepsilon_1+\varepsilon_3)(\varepsilon_2+\varepsilon_3)}\,d\xi. \tag{12}$$

The quantity $|\bar{\omega}|$ plays the role of some frequency characteristic of the absorption spectra of all three media.

When $\epsilon_{30} \to \infty$, expression (10) tends to zero. This means that when the gap between the bodies is filled by a liquid metal, the interaction force varies (at "large" distances) as a higher power

---

*The accuracy of such a simplification is connected with the fact that an integral of the form

$$\frac{a}{n!}\int_0^\infty \frac{x^n dx}{ae^x - 1}$$

does not change appreciably when a changes from ∞ to 1; it changes from 1 to 1.2 if n = 2, to 1.08 if n = 3, to 1.04 if n = 4, and so on.

of $1/l$. To consider this case it is necessary to turn to the original Eq. (7) and to take into account the actual law according to which the dielectric constant of a metal increases when the frequency is decreased.

The variation of $\epsilon(\omega)$ of a metal in the infrared region of the spectrum is given by

$$\varepsilon(\omega) = -4\pi e^2 N / m\omega^2,$$

where N is the number density of the free electrons. When we substitute $\epsilon_3(i\xi) = 4\pi e^2 N/m\xi^2$ into Eq. (7), the exponential factors in the denominators of the integrand take on the form

$$\exp\{(2pl/c)\sqrt{4\pi e^2/Nm}\},$$

i.e., ξ disappears from them, and since $p \geq 1$, we are led to the conclusion that the contribution to the force F from the region of frequencies under consideration decreases exponentially with the distance l.

But the main contribution to the interaction force is given in this case by the region of even smaller frequencies where $\epsilon(\omega)$ is connected with the usual electrical conductivity of the metal σ by the well-known formula

$$\varepsilon(\omega) = 4\pi i\sigma/\omega.$$

Substituting $\epsilon_3(i\xi) = 4\pi\sigma_3/\xi$ into the integrand in Eq. (7) (in the exponents and in the factor $\epsilon_3^{3/2}$; in other places it is sufficient to put $\epsilon_3 = \infty$), and introducing the variable $x = 4pl\sqrt{\pi\sigma_3\xi/c^2}$ instead of the integration variable ξ, we get

$$F = \frac{\hbar c^2}{2^7\pi^3\sigma_3 l^5}\int_0^\infty\int_1^\infty \frac{x^4}{p^2}\left\{\left[\left(\frac{\sqrt{p^2-1}+p}{\sqrt{p^2-1}-p}\right)^2 e^x - 1\right]^{-1} + \frac{1}{e^x-1}\right\} dp\, dx.$$

The value of the double integral (evaluated by the method mentioned in footnote* of page 163) is 13.5 and, as a result, we obtain

$$F = 0.0034\cdot\hbar c^2/\sigma_3 l^5. \qquad (13)$$

The force of molecular attraction thus goes, in the case of a metallic "layer" between bodies, from an l^{-3} law at "small" distances to an l^{-5} law at "large" distances; the beginning of the latter is delayed, though, by the occurrence in Eq. (13) of a small numerical coefficient.

Returning to the general Eq. (7), we note that if both bodies are the same ($\epsilon_1 = \epsilon_2$) the integrand in Eq. (7) is always positive* and decreases monotonically with increasing l for all values of p and ξ. It follows hence that both $F > 0$ and $dF/dl < 0$, i.e., identical bodies attract one another whatever the layer is between them, and the force F decreases monotonically with increasing distance.*

If, however, the bodies are different, the force acting between them can be either attractive or repulsive. It is clear from Eq. (12) that if the differences $\epsilon_1 - \epsilon_3$ and $\epsilon_2 - \epsilon_3$ have different signs in the essential frequency region, we have $F < 0$, that is, at "small" distances the bodies repel one another. At "large" distances, however, the character of the force is determined by the relative magnitude of the electrostatic values of the dielectric constants: if the signs of the differences $\epsilon_{10} - \epsilon_{30}$ and $\epsilon_{20} - \epsilon_{30}$ are the same we have $F > 0$, and if they are different $F < 0$. Moreover, since the relative magnitudes of ϵ_{10}, ϵ_{20}, and ϵ_{30} are, generally speaking, not connected with the behavior of the functions $\epsilon_1(i\xi)$, $\epsilon_2(i\xi)$, and $\epsilon_3(i\xi)$ in those frequency regions which are essential for the given bodies, it is possible, in principle, that there are cases where the function $F(l)$ changes sign for some l. (This is discussed in more detail in Sec. 4.)

4. A THIN FILM ON THE SURFACE OF A SOLID BODY

We can also apply Eq. (7) to evaluate the thermodynamic quantities of a thin liquid film on the surface of a solid body (Fig. 1). We assume here that the thickness l of the film (as the gap width in the previous case) is large compared with interatomic distances.

FIG. 1

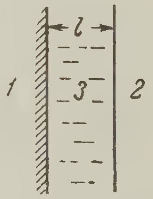

We consider a film on a solid wall situated vertically in the gravitational field. The condition that the chemical potential be constant in the film (medium 3) (which is in equilibrium) is expressed by Eq. (4), where we must add in the left-hand side a term ρgz (where z is the height). One other condition must express the fact that at any free surface of the film a constant pressure, the black-body radiation pressure acts from the direction of the vacuum. The σ_{xx} component (x is the normal to the surface of the film) of the stress tensor, Eq. (1), evaluated in the film, must therefore also be constant (independent of z). Combining these two conditions we get

---

*This is easily checked if we note that for $s = \sqrt{\varepsilon - 1 + p^2}$ (where $p \geq 1$) the inequality $\varepsilon p > s > p$ holds if $\varepsilon > 1$, and $\varepsilon p < s < p$ if $\varepsilon < 1$.

*This statement was already made by Hamaker,[6] based upon an assumption about the additivity of molecular forces (which in actual fact does not take place).

$$\sigma'_{xx} + \rho g z = \text{const},$$

where σ'_{xx} is the component of the "truncated" stress tensor, Eq. (5). However, σ'_{xx} in medium 3 is none other than the quantity $F(l)$ evaluated above, so that we have

$$F(l) + \rho g z = \text{const}. \tag{14}$$

Equation (14) is nothing but the condition that the chemical potential be constant in the system, so that $F(l)$ is that part of its chemical potential μ which depends on the film thickness. (We define μ here as the thermodynamic potential referred to the mass ρ; we consider the liquid density to be constant.) Thus $\mu = \mu_0 + F(l)$, where μ_0 is the chemical potential of the "bulk" liquid (compare reference 7, Sec. 141). If we measure the chemical potential from the value μ_0, we can simply write $\mu(l)$ instead of $F(l)$.* Measuring also the height z from the surface of the liquid in the vessel, the constant of Eq. (14) vanishes, so that

$$\mu(l) + \rho g z = 0. \tag{15}$$

The function $\mu(l)$ determines all the thermodynamic properties of the film; it is defined by Eqs. (7) to (10), in which we must put $\epsilon_2 = 1$ (the medium 2 is vacuum).† We must also introduce an "effective" coefficient of surface tension α at the boundary of the phases 1 and 2, taking into account the existence of a liquid film between them. This can be done by formally using the well-known formula from adsorption theory $\gamma = -(\partial\alpha/\partial\mu')_T$ where γ is the surface concentration of the adsorbed substance (number of particles per cm^2) and μ' its chemical potential (defined as the thermodynamical potential referred to one particle; see, e.g., reference 7, Sec. 139). When we use the definition of μ given here this relation can be written

$$l = -(\partial\alpha/\partial\mu)_T, \tag{16}$$

which is applicable both to macroscopically thick ("wetting") films and to adsorption films of "molecular thickness," in the latter case, finally, l has only a formal meaning as a quantity proportional to the surface concentration ($l = \gamma m/\rho$, m being the mass of a molecule). Integrating Eq. (16) and taking into account that as $l \to \infty$ the function $\alpha(l)$ must go over into $\alpha_{13} + \alpha_{32}$ (the sum of the surface tensions at the boundaries of the "bulk" phases 1, 2, and 3, we get

$$\alpha(l) = \int_l^\infty l \frac{d\mu}{dl}\, dl + \alpha_{13} + \alpha_{32}. \tag{17}$$

As $l \to 0$, $\alpha(l)$ must tend to the surface tension at the boundary of the "pure" phases 1 and 2, so that

$$\int_0^\infty l \frac{d\mu}{dl}\, dl = \alpha_{12} - \alpha_{13} - \alpha_{32}. \tag{18}$$

We recall also that the necessary condition for the thermodynamic stability of the film is that the inequality

$$(\partial\mu/\partial l)_T > 0 \tag{19}$$

be satisfied, or $(\partial\alpha/\partial l)_T < 0$ (compare reference 7, Sec. 139). If that condition is satisfied a film will be in equilibrium with the vapor if its thickness is such that $\mu(l) = \mu_{\text{vap}}$ (for a saturated vapor $\mu_{\text{vap}} = 0$, for an unsaturated vapor $\mu_{\text{vap}} < 0$). If there are more than one such values of l the film with the smallest value of α will correspond to the stable state; a larger value of α will then correspond to a metastable state.

We shall consider some typical cases that may occur, depending on the character of the function $\mu(l)$. It is necessary to bear particularly in mind that the function $\mu(l)$ may change sign and may not be monotonic; this is already clear from the fact that the signs in the limiting expressions for $\mu(l)$, for large and for small l, are practically independent of one another (compare the end of Sec. 3).

a) If $\mu(l)$ is a monotonically decreasing, everywhere positive function (Fig. 2a), the liquid will not, in general, wet the solid surface; hence

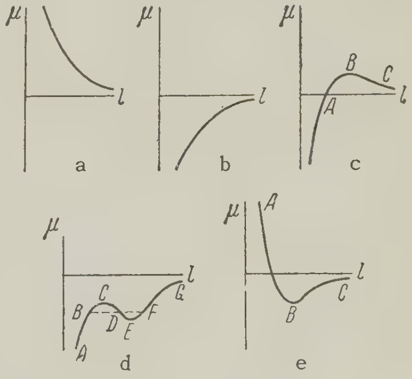

FIG. 2

---

*For a convenient comparison we note that the quantity μ defined in this way is the same (with the opposite sign) as the "separating pressure" P used in the papers by Deryagin and his collaborators (see, e.g., reference 8).

†Region 2 is actually filled with the vapor of substance 3 which is in thermodynamic equilibrium with the liquid in the vessel and in the film; in view of the rareness of this medium, we can fully consider it to be a vacuum in the electrodynamic sense.

no film is formed at all. We emphasize that we are dealing here just with macroscopically thick films, to which the whole of the theory developed here refers. As regards adsorption in the narrow sense of the word, this always takes place to some extent as is well-known. This corresponds to the fact that whatever the behavior of the function $\mu(l)$, in the region of molecular distances (not depicted in Fig. 2) it ultimately tends to $-\infty$ according to the law $\mu \sim \ln l$, which corresponds to a "weak solution" of the adsorbed substance on the surface.

b) If $\mu(l)$ is a monotonically increasing everywhere negative function (Fig. 2b), this will normally correspond to a liquid which fully wets the solid surface and (depending on the vapor pressure above it) forms a stable film of arbitrary thickness. In particular, there will be formed on a vertical wall a film with a thickness which tends to zero as $z \to \infty$; the decrease goes at first as $l \sim z^{-1/4}$ and later as $z^{-1/3}$.

However, also in that case, the liquid may turn out to be nonwetting if the behavior of $\mu(l)$ in the microscopic region is such that it leads there to a smaller value of the surface tension α; a molecular adsorption film, and not a wetting film will then be the stable one.*

c) $\mu(l)$ goes through zero and possesses a maximum as shown in Fig. 2c. With the same reservation as in the case b), we shall have here a case of wetting, but with formation of a film that is stable only for thicknesses less than a well-defined limit. A film of finite thickness corresponding to the point A is in equilibrium with the saturated vapor. This state is separated from another stable state — the equilibrium of the solid wall with the "bulk" liquid — by a metastable region AB and a region of total instability BC.

A $\mu(l)$ curve of such a type must lead to interesting features in the formation of a contact angle θ of drops of liquid on a solid surface. In this case a drop will be in equilibrium with a film of finite thickness $l_{\max}$ (Fig. 3), and from the usual elementary formula we have

$$\cos\theta = [\alpha(l_{max}) - \alpha_{13}] / \alpha_{23}, \tag{20}$$

where $\alpha(l_{\max})$ [with $\alpha(l)$ from Eq. (17)] plays the role of the coefficient of the surface tension between phases 1 and 2. Since the first term in Eq. (17) is a small quantity, we get from Eq. (20)

$$\theta^2 \approx -\frac{2}{\alpha_{23}} \int_{l_{max}}^{\infty} l \frac{d\mu}{dl}\, dl = \frac{2}{\alpha_{23}} \int_{l_{max}}^{\infty} \mu\, dl. \tag{21}$$

FIG. 3

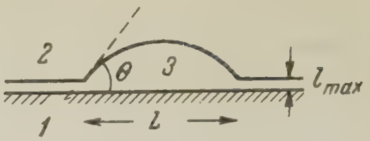

Interpolating between the $\mu \sim l^{-3}$ and the $\mu \sim l^{-4}$ laws, we get as an estimate

$$\theta \sim (1/10\, l_{max}) \sqrt{\hbar |\overline{\omega}| / \alpha_{23}} \tag{22}$$

with $\overline{\omega}$ from Eq. (12). Thus if $\hbar\overline{\omega} \sim 10$ ev, $\alpha_{23} \sim 20$ erg cm^{-2}, and $l_{\max} \sim 5 \times 10^{-5}$ cm we get $\theta \sim 0.1°$.

In our case the contact angle must thus have a finite, but very small, value (in contradistinction to the value $\theta = 0$ for complete wetting and $\theta \sim 1$ for the usual cases of nonwetting). Such a statement has, of course, a really specific meaning only if the thickness of the drop is large compared to the thickness of the film, i.e., if $L\theta \gg l_{\max}$, where L is the size of the drop (Fig. 3).

d) A curve of the type depicted in Fig. 2d corresponds to a film which is not stable in a well-defined range of thicknesses. The straight line BF which cuts off the equal areas BCD and DEF connects the points B and F with the same values of α [for identical μ; this can easily be seen from Eq. (17)]. Stable films correspond to the branches AB and FG; the range CE is completely unstable, and the ranges BC and EF are metastable.

Both limits of the region of instability (the points B and F) correspond in this case to macroscopic film thicknesses. Instability in a range from some macroscopic thickness to a molecular one would correspond to a curve of the type depicted in Fig. 2e. (This curve tends to $-\infty$ as $l \to 0$, as did the curve of Fig. 2b.) In reality, however, such a curve will most likely lead simply to a case of nonwetting. Indeed, the limit of stability would correspond to such a point on the branch BC that the horizontal intersect would cut off equal areas under the upper and above the lower parts of the curve. The latter area, however, is connected with van der Waals forces and would be small compared with the former one, which is connected with the appreciably larger forces at molecular distances. This means that the surface tension on the whole of the branch BC will be larger than the one corresponding to molecular adsorption at the surface of the substratum, and a film will thus be metastable.

The phenomenon of film instability in well-defined ranges of thickness has been observed by several authors, in particularly clear form by Frumkin, Deryagin and their co-workers.[9,10]

---

*Such behavior may occur as a high "bump" on the $\mu(l)$ curve in the molecular region of "thicknesses."

Frumkin[9] had already long ago considered different kinds of $\alpha(l)$ curves (without explicitly distinguishing between absorptive and wetting films) in order to interpret these phenomena phenomenologically. We should like to emphasize here the connection of these curves with the properties of the van der Waals forces, and through them with the spectral properties of the liquid and of the solid substratum.

We note, in particular, that the sign of the function $\mu(l)$ for sufficiently large film thicknesses is determined by the ratio of the electrostatic values ϵ_{10} and ϵ_{30}:[*] in this region $\mu > 0$ if $\epsilon_{30} > \epsilon_{10}$, and $\mu < 0$ if $\epsilon_{30} < \epsilon_{10}$. The sign of $\mu(l)$, however, in the opposite limiting case of sufficiently small l is the same as the sign of

$$\bar{\omega} = \int_0^\infty \frac{(\varepsilon_3 - 1)(\varepsilon_3 - \varepsilon_1)}{(\varepsilon_3 + 1)(\varepsilon_3 + \varepsilon_1)}\, d\xi.$$

A violation of the monotonic behavior of $\mu(l)$ in some range of l -values is, generally speaking, connected with the change in sign of the difference $\epsilon_3 - \epsilon_1$ in the wavelength region $\lambda \sim l$.

5. FORCES OF NONELECTROMAGNETIC ORIGIN

We shall estimate the contribution of forces of nonelectromagnetic origin to the chemical potential of a film.

Acoustical fluctuations (in an acoustically nondispersive medium) contribute $\mu_{ac} \sim \hbar u/l^4$ (where u is the sound velocity) to the chemical potential at the absolute zero.[†] This must be compared with the electromagnetic part $\mu_{e.m.} \sim \hbar c/l^4$ for $l \gg \bar{\lambda}_0$ or $\mu_{e.m.} \sim \hbar c/l^3\bar{\lambda}_0$ for $l \ll \bar{\lambda}_0$ ($\bar{\lambda}_0$ is a characteristic wavelength in the spectrum of the absorbing body). It is clear that $\mu_{ac} \ll \mu_{e.m.}$ for all distances large compared to atomic dimensions, and this precisely is the only region where the whole theory given here is applicable.

At nonzero temperatures the opposite limiting case, where the influence of the temperature is the dominant factor, holds, generally speaking, for μ_{ac}. The appropriate criterion is the ratio $l\kappa T/\hbar u$ (where κ is Boltzmann's constant); if this ratio is large $\mu_{ac} \sim \kappa T/l^3$ [similar to Eq. (5.5) in reference 1].[*] This quantity is compared with $\mu_{e.m.}$ only at distances $l \sim \hbar c/\kappa T$, which are so large that μ becomes very small in any case.

The same is true of the contribution of the surface oscillations. The dependence of the frequency on the wave vector for capillary oscillations on the surface of a liquid layer of thickness l is given by the well-known formula

$$\omega^2 = (\alpha k^3/\rho)\ \tanh kl,$$

where α is the surface tension (see, e.g., reference 13, Sec. 61). On a deep liquid ($l \to \infty$) we have $\omega^2 = \alpha k^3/\rho$. Evaluating the energy of the zero-point oscillations (subtracting the same energy for $l \to \infty$) we find that at the absolute zero the corresponding contribution to the chemical potential is

$$\mu_{\text{surf}} \sim \hbar\sqrt{\alpha/\rho}\, l^{-9/2}.$$

In actual fact, however, the opposite limiting case, is realized, when $(\hbar/\kappa T)\sqrt{\alpha/\rho}\ l^{-3/2} \ll 1$, i.e., the condition for classical physics is satisfied. Calculation by the general rules of statistics leads then, of course, to a contribution of the same order of magnitude, $\mu_{\text{surf}} \sim \kappa T/l^3$, as in the acoustical case.[†]

To explain the properties of helium films several authors also introduced mechanisms connected with the inhomogeneity of the density distribution of the liquid along the thickness of the film. In its roughest form, the corresponding calculation is performed by considering the helium in the film to be a perfect gas, with particles whose wave functions possess nodes at the wall and at the film surface. Such a model leads to a strongly inhomogeneous density distribution with a maximum at the center and to a contribution to the chemical potential μ proportional to l^{-2}. Such a consideration is, however, totally unacceptable (as was already stated by Mott[14]), since the interaction between the atoms will, in actual fact, smooth out the wave function of the ground state of the system, and the inhomogeneity in the density will extend (into the liquid) only over distances of the order of interatomic ones. The contribution to the chemical potential connected with this inhomogeneity decreases with the film thickness according to an exponential law.

---

[*] Provided that no important dispersion of the dielectric constant occurs at very long wavelengths (as, for instance, in water).

[†] This expression is analagous to the expression $\mu \sim \hbar c/l^4$ for the electromagnetic part (in a nondispersive medium). One can obtain it, for instance, by evaluating the energy of the acoustical zero-point vibrations in the gap (of width l) in a way similar to the one used by Casimir[11] for the electromagnetic zero-point vibrations. We note that the result of Atkins[12] who obtained for μ_{ac} a different dependence on the film thickness ($\sim l^{-2}$) is due to an incorrect way of cutting off the divergent integral.

[*] The condition $l\kappa T/\hbar u \gg 1$, like the condition $l\kappa T/\hbar c \gg 1$ in the electromagnetic case, is essentially the condition for classical physics to hold ($\hbar\omega \ll \kappa T$ with $\omega \sim l/u$ or $\omega \sim l/c$). It is thus clear a priori that the corresponding contribution to μ cannot contain $\hbar$ and the expression $\kappa T/l^3$ follows therefore from dimensional considerations.

[†] We always give estimates without numerical factors, but one must bear in mind that in reality the expressions for μ_{surf} and μ_{ac} still contain (as is shown by a more detailed analysis) small numerical coefficients, as do the expressions for the electromagnetic part $\mu_{e.m.}$. The occurrence of relatively small numerical coefficients is generally a feature of the theory given here.

The contribution connected with the specific properties (superfluidity) of helium below the λ point decreases according to the same law. Only in the immediate vicinity of the λ point, where the density of the superfluid component is very small, will the inhomogeneity in the distribution of the latter lead to an appreciable effect (see reference 15). At a distance of about 0.01° from the λ point, however, the decrement of the exponential decrease becomes comparable with interatomic distances. On the other hand, the result of Franchetti,[16] who obtained a contribution to the chemical potential proportional to l^{-2}, is due to the fact that the model he used of noninteracting elementary excitations in helium was inadequate.

6. THE LIQUID HELIUM FILM

We shall consider separately liquid helium films to which a great deal of literature has been devoted.

The general Eq. (7) can be appreciably simplified for helium films if one uses the fact that the dielectric constant of liquid helium is very nearly equal to unity, i.e., that the difference $\epsilon_3(i\xi)-1$ is small. Performing the appropriate expansion in the integrand of (7) we get

$$\mu(l) = -\frac{\hbar}{8\pi^2c^3}\int_0^\infty\int_1^\infty\left\{\frac{s_1-p}{s_1+p}+(2p^2-1)\frac{p\varepsilon_1-s_1}{p\varepsilon_1+s_1}\right\}$$

$$\times(\varepsilon_3-1)\xi^3e^{-2p\xi l/c}dp\,d\xi,$$

$$s_1=\sqrt{\varepsilon_1(i\xi)-1+p^2}. \tag{23}$$

The calculation, however, even with this simplified formula, is made difficult by the necessity to know the form of the function $\epsilon(i\xi)$ for liquid helium and for the solid wall in a wide range of frequencies, particularly in the extreme ultraviolet region. In the integral (23) the region of wavelengths $\lambdabar \sim l$ is the important one, and actual thicknesses of the helium film are of the order of 10^{-6} cm.

A reasonable approximation is a further simplification of Eq. (23), based on the fact that the main absorption region of helium lies in the extreme ultraviolet, whereas the main absorption of the solid wall (metals, quartz) is at appreciably lower frequencies. In other words, we assume that the function $\epsilon_3(i\xi)$ is practically the same as the electrostatic value ϵ_{30} in the whole range of ξ in which the difference $\epsilon_1(i\xi)-1$ [and with it the whole integrand in Eq. (23)] is not yet too small. One can then remove ϵ_3-1 from under the integral sign and proceed with the remaining integral as in the limiting case of small thicknesses l (l is small compared with the wavelengths $\lambdabar_0$ in the main absorption regions of the solid body). Thus, introducing the integration variable $x = 2p\xi l/c$ instead of p and taking into account that the values of $x \sim 1$ correspond to large values of p, we replace the curly brackets in Eq. (23) by $2p^2(\epsilon_1-1)/(\epsilon_1+1)$, and obtain as a result

$$\mu(l) = -\hbar\bar{\omega}(\varepsilon_{30}-1)/16\pi^2l^3, \tag{24}$$

where we have introduced the quantity

$$\bar{\omega} = \int_0^\infty\frac{\varepsilon_1(i\xi)-1}{\varepsilon_1(i\xi)+1}\,d\xi, \tag{25}$$

which is some average frequency that is characteristic of the given solid body.

We note that the function $[\epsilon(\omega)-1]/[\epsilon(\omega)+1]$ possesses in the upper half-plane of the complex variable ω the same analytical properties as the function $\epsilon(\omega)-1$. This is sufficient to let us apply to it the same formula for the transformation of an integral over the imaginary axis to an integral along the real axis as was valid for the function $\epsilon(\omega)-1$ (see reference 5, Sec. 62). We can thus write the integral in the form

$$\bar{\omega} = \int_0^\infty \operatorname{Im}\frac{\varepsilon_1(\omega)-1}{\varepsilon_1(\omega)+1}\,d\omega = \int_0^\infty\frac{2\varepsilon_1''(\omega)\,d\omega}{[\varepsilon_1'(\omega)+1]^2+[\varepsilon_1''(\omega)]^2}, \tag{26}$$

where $\epsilon'(\omega)$ and $\epsilon''(\omega)$ are the real and imaginary parts of the dielectric constant for real values of the frequency; i.e., they are quantities directly measured experimentally (one can transform the integral $\bar{\omega}$ in Eq. (12) in a similar way).

One must thus expect a $\mu(l) \sim 1/l^3$ dependence for the actually observed thicknesses of the helium film and hence a $l \sim z^{-1/3}$ form of the film profile. To evaluate the coefficient in this law we must, however, know the optical properties of the solid body (wall) in a wide range of frequencies. We should like to emphasize that an evaluation of this coefficient on the basis of data on the interaction of separate helium atoms with a solid body is in any case inadmissible.*

We shall also write down an expression for $\mu(l)$ for "large" film thicknesses ($l \gg \lambdabar_0$). The corresponding transition in Eq. (23) occurs by introducing the variable $x = 2p\xi l/c$ instead of ξ and replacing ϵ_1 by ϵ_{10}. The integration both over dx and over dp is performed analytically, and as a result we get

---

*We think, in particular, that the estimates given by Schiff[17] cannot be trusted at all.

$$\mu(l) = -3\hbar c(\varepsilon_{30} - 1) f(\varepsilon_{10}) / 32\pi^2 l^4,$$

$$f(\varepsilon) = \frac{1}{3} + \varepsilon + \frac{4 - \sqrt{\varepsilon}(\varepsilon + 1)}{2(\varepsilon - 1)} - \frac{\sinh^{-1}\sqrt{\varepsilon - 1}}{2(\varepsilon - 1)^{3/2}}[1 + \varepsilon + 2\varepsilon(\varepsilon - 1)^2] + \frac{\varepsilon^2}{\sqrt{\varepsilon + 1}}\left(\sinh^{-1}\sqrt{\varepsilon} - \sinh^{-1}\frac{1}{\sqrt{\varepsilon}}\right). \qquad (27)$$

For a metal $\epsilon_{10} \rightarrow \infty$ and $f(\infty) = 1$. For quartz, which has a wide band of transparency (from $\sim 0.15\,\mu$ to several μ), it is reasonable to consider the case when the thickness l falls in that range of lengths. The corresponding dependence of μ on l is then determined by the same Eq. (27) in which, however, one must understand by ϵ_{10} not the electrostatic, but the optical value ϵ_1, i.e., the square of the refractive index in the optical range of transparency (compare the note added in proof in reference 1).

Expressions (23), (24), and (27) do not contain the temperature; i.e., they refer to the absolute zero. Temperature corrections, however, must be relatively small, and there is no reason to expect any important change in the form of the film profile when the temperature is changed, in particular, below and above the λ point (outside its immediate vicinity).

The difficulties of an experimental determination of the thickness and the form of helium film profile under conditions which are sufficiently close to ideal conditions of thermal equilibrium are very great, and only in very recent times have they been overcome to a sufficient extent to permit the results obtained (in the helium II region) to be considered at all trustworthy (see the surveys by Jackson and Grimes,[18] and Atkins[19]).

As was already mentioned, there are no physical grounds whatever to expect a film profile of the form $\rho gz = a/l^3 + b/l^2$.

Anderson, Liebenberg, and Dillinger[20] state in a recent communication that data obtained by them on the thickness of a helium film on a steel surface (up to a height of 40 cm) are satisfactorily described by a law of the form $\rho gz = a/l^3$ with a constant $a \approx 3.4 \times 10^{-15}$ erg. Comparing this value with the coefficient of l^{-3} in Eq. (24) (inserting $\epsilon_{30} - 1 = 0.057$) we get $\hbar\overline{\omega} \sim 6$ ev. The data of Jackson, Ham, and Grimes[21] lead to approximately the same value ($\hbar\overline{\omega} \sim 7.5$ ev). This value is reasonable for a metal (steel).

The coefficients in Eqs. (24) and (27) (with $\epsilon_{10} \rightarrow \infty$) become equal for $l = 3c/2\overline{\omega}$, i.e., in the given case for $l \sim 5 \times 10^{-6}$ cm. This means that in the range of film thicknesses (100 – 400 A) which were experimentally observed, we are near the region where the transition from the l^{-3} to the l^{-4} law takes place.

In conclusion we express our sincere thanks to Academician L. D. Landau for a discussion of the problems considered here. We are also grateful to Professor B. V. Deryagin for informing us of his studies of films.

---

[1] E. M. Lifshitz, J. Exptl. Theoret. Phys. (U.S.S.R.) **29**, 94 (1955), Soviet Phys. JETP **2**, 73 (1956).

[2] I. E. Dzyaloshinskiĭ and L. P. Pitaevskiĭ, J. Exptl. Theoret. Phys. (U.S.S.R.) **36**, 1797 (1959), Soviet Phys. JETP **9**, 1282 (1959).

[3] Abrikosov, Gor'kov, and Dzyaloshinskiĭ, J. Exptl. Theoret. Phys. (U.S.S.R.) **36**, 900 (1959), Soviet Phys. JETP **9**, 636 (1959); E. S. Fradkin, J. Exptl. Theoret. Phys. (U.S.S.R.) **36**, 1286 (1959), Soviet Phys. JETP **9**, 912 (1959).

[4] T. Matsubara, Progr. Theor. Phys. **14**, 351 (1955).

[5] L. D. Landau and E. M. Lifshitz, Электродинамика сплошных сред (Electrodynamics of Continuous Media), Gostekhizdat, 1957.

[6] H. C. Hamaker, Physica **4**, 1058 (1937).

[7] L. D. Landau and E. M. Lifshitz, Статистическая физика (Statistical Physics), 3rd ed., Gostekhizdat, 1951 (Pergamon Press, London, 1958).

[8] B. V. Deryagin, Коллоидный ж.(Colloid Journal) **17**, 207 (1955).

[9] A. N. Frumkin, J. Phys. Chem. (U.S.S.R.) **12**, 337 (1938).

[10] B. V. Deryagin and M. M. Kusakov, Izv. Akad. Nauk SSSR, Ser. Khim. **5**, 1119 (1937); Acta Phys. Chem. U.S.S.R. 10, 25 (1939); Deryagin, Kusakov, and Lebedeva, Dokl. Akad. Nauk SSSR **23**, 671 (1939).

[11] H. B. G. Casimir, Proc. Acad. Sci. (Amsterdam) **51**, 793 (1948).

[12] K. R. Atkins, Can. J. Phys. **32**, 347 (1954).

[13] L. D. Landau and E. M. Lifshitz, Механика сплошных сред (Mechanics of Continuous Media), Gostekhizdat, 1954.

[14] N. F. Mott, Phil. Mag. **40**, 61 (1949).

[15] V. L. Ginzburg and L. P. Pitaevskiĭ, J. Exptl. Theoret. Phys. (U.S.S.R.) **34**, 1240 (1958), Soviet Phys. JETP **7**, 858 (1958).

[16] S. Franchetti, Nuovo cimento **5**, 183 (1957).

[17] L. Schiff, Phys. Rev. **59**, 839 (1941).

[18] L. C. Jackson and L. G. Grimes, Adv. in Phys. **7**, 435 (1958).

[19] K. R. Atkins, *Progress in Low Temperature Physics*, North Holland Publishing Co., Amsterdam, 1957, Vol. 2, 105.

[20] Anderson, Liebenberg, and Dillinger, Bull. Am. Phys. Soc., Ser. II, **4**, 6 (1959).

[21] A. C. Ham and L. C. Jackson, Proc. Roy. Soc. (London) **A240**, 243 (1957); L. C. Jackson, Proc. Fifth International Conference on Low Temperature Physics and Chemistry, University of Wisconsin Press, Madison, Wis., 1958, p. 59.

Translated by D. ter Haar
36

SOVIET PHYSICS JETP VOLUME 37(10), NUMBER 1 JANUARY, 1960

CONTRIBUTION TO THE THEORY OF SPIN-LATTICE RELAXATION OF NUCLEAR SPINS IN IONIC CRYSTALS

B. I. KOCHELAEV

Kazan' State University

Submitted to JETP editor February 12, 1959

J. Exptl. Theoret. Phys. (U.S.S.R.) **37**, 242-248 (July, 1959)

Relaxation of nuclear spins in ionic crystals at room temperature is examined theoretically with account of optical vibrations of the crystal lattice. Numerical calculations are made for NaCl type lattices. The agreement with experiment is satisfactory.

1. INTRODUCTION

IN the present theory of spin-lattice paramagnetic relaxation the thermal lattice vibrations are considered in the Debye approximation, i.e., only acoustic crystal vibrations are taken into account. However, the Debye method is meaningful only at low temperatures. At room temperatures there are sufficiently-excited optical vibrations at which the neighboring atoms move, on the average, in phase opposition and consequently their interaction varies more strongly than in acoustic vibrations. A disturbance causing transitions in the spin system will therefore be stronger, and this may noticeably affect the rate at which equilibrium is established between the spin system and the lattice. It is clear therefore that not only can the optical vibrations not be neglected, but in some cases the Debye model is not expected even to yield the correct order of magnitude of the spin-lattice relaxation time. This problem is best examined with the nuclear spin relaxation as an example.

Pound[1] has shown with a series of experiments that at room temperature quadrupole interactions can play a decisive role in the mechanism of nuclear spin-lattice relaxation. The first theory of nuclear spin-lattice relaxation in crystals was proposed by van Kranendonk.[2] He considered the interaction between a nucleus having a quadrupole moment and the field of point charges surrounding the ions. After calculating, in the Debye approximation, the variation of the gradient of the electric field under the influence of the thermal lattice vibrations, van Kranendonk found the probabilities of relaxation transitions in the spin system. The spin-lattice relaxation times T_1, determined with these probabilities, were found to be 10^2 to 10^5 times longer than the experimental values. Moriya and Yosida[3] have suggested that in real crystals the quadrupole interactions are much stronger than in the van Kranendonk model, owing to the partially-covalent character of the atomic bonds. The values of T_1 which they calculated differ from the experimental ones by a factor of 3 to 10. Wikner and Das,[4] assuming the bond to be purely ionic, took into account the increase in the gradient of the electric field on the nucleus due to polarization of the electron shell in the field of the ions and of the nucleus. Comparison with experiment led to results analogous to those obtained by Yosida and Moriya.[3]

In the present paper we consider theoretically the spin-lattice relaxation of nuclear spins, due to quadrupole interactions, at sufficiently high temperatures. In Sec. 2 we obtain a more convenient form for the spin-lattice interaction operator than that given by van Kranendonk.[2] In Sec. 3 we calculate the probabilities of the relaxation transitions produced by optical and acoustic vibrations of a NaCl type crystal lattice. We consider the relations between the probabilities of the transitions and quantities that are measured experimentally in the study of the relaxation effects. The comparison with experiment and the discussion of the results are treated in Sec. 4.

2. THE SPIN-LATTICE INTERACTION OPERATOR

We consider a purely ionic bond. As in reference 2, we shall assume that the relaxing nuclei are in equivalent crystal fields and that we can neglect the influence of the magnetic dipole-dipole interactions on the quadrupole relaxation. Under these assumptions, we can consider the interaction between an individual nucleus and the electric field of the surrounding ions. Since this interaction is modulated by the thermal vibrations, transitions are induced between different spin states. We place the origin at the lattice site in which the nucleus under consideration is located, and direct the z axis along the external magnetic field H. That part of the Hamiltonian which describes the quadrupole interaction of the nucleus with the crystal field is written as the scalar product of two tensors, the nuclear quadrupole moment operator and the electric field gradient operator:[1]

$$\hat{\mathscr{H}} = \sum_{\mu} (-1)^{\mu} \hat{Q}_{\mu} (\nabla E)_{-\mu}, \qquad (1)$$

where

$$Q_0 = \frac{eQ}{2I(2I-1)} [3\hat{I}_z^2 - I(I+1)],$$

$$Q_{\pm 1} = \mp \sqrt{\frac{3}{2}} \frac{eQ}{2I(2I-1)} [(\hat{I}_x \pm i\hat{I}_y)\hat{I}_z + \hat{I}_z(\hat{I}_x \pm i\hat{I}_y)], \qquad (2a)$$

$$Q_{\pm 2} = \sqrt{\frac{3}{2}} \frac{eQ}{2I(2I-1)} [(\hat{I}_x \pm i\hat{I}_y)^2], .$$

$$(\nabla E)_0 = -\frac{1}{2}\frac{\partial E_z}{\partial z}, \quad (\nabla E)_{\pm 1} = \pm \frac{1}{\sqrt{6}} \left[\frac{\partial E_x}{\partial z} \pm i \frac{\partial E_y}{\partial z}\right],$$

$$(\nabla E)_{\pm 2} = \frac{1}{\sqrt{6}} \left[\frac{\partial E_x}{\partial x} - \frac{\partial E_y}{\partial y} \pm 2i \frac{\partial E_x}{\partial y}\right]. \qquad (2b)$$

Here eQ is the quadrupole moment of the nucleus, I the nuclear spin, and $\hat{I}$ its operator.

To obtain the spin-lattice interaction operator it is necessary to find the tensor components of the gradient of the electric field that results from the displacement of the ions by the thermal vibrations. If we introduce the coefficient γ_{∞}, characterizing the degree of polarization of the electron shell of the ion under consideration, the gradient of the electric field on the nucleus can be represented as[3]

$$\nabla E = (1 - \gamma_{\infty}) \nabla E', \qquad (3)$$

where ∇E′ is the gradient of the electric field produced by the surrounding ions. The potential of this field in the vicinity of the nucleus is

$$V = \sum_t e_t / R_t,$$

where e_t is the charge of the t-th ion and R_t is the distance from its center to the nucleus under consideration. We denote the displacement of the t-th atom due to the thermal vibrations by $\mathbf{u}_t$, and the displacement of this atom relative to the central atom by $\mathbf{s}_t = \mathbf{u}_t - \mathbf{u}_0$. Considering that the relative displacements s_t are small compared with the interatomic distances, we expand V in a series of spherical functions

$$V = \sum_t \frac{e_t}{R_{0t}} \sum_{n=0}^{\infty} (-1)^n \frac{4\pi}{2n+1} \left(\frac{s_t}{R_{0t}}\right)^n$$

$$\times \sum_{m=-n}^{n} Y_n^m (\theta_s^t, \varphi_s^t) Y_n^{-m} (\theta_R^t, \varphi_R^t). \qquad (4)$$

Here R_{0t} is the equilibrium distance between the ions, θ_s^t, φ_s^t and θ_R^t, φ_R^t are respectively the angular coordinates of $\mathbf{s}_t$ and the projections on the t-th ion. Since we are interested in room temperatures, at which two-phonon processes are known to play the decisive role, the spin-lattice interaction operator should be quadratic in s_t. We need therefore consider only the term with n = 4, out of the entire sum of Eq. (4).

To find the components of the electric field gradient tensor, it is convenient to change to new coordinates

$$\xi_{\pm 1} = \mp (\mathbf{e}_x \pm i\mathbf{e}_y) / \sqrt{2}, \quad \xi_0 = \mathbf{e}_z, \qquad (5)$$

where $\mathbf{e}_q$ is a unit vector along the q axis of a Cartesian system. Using the well known expansions of the gradient in spherical functions [see, for example, reference 5, Eq. (2.57)], we obtain the following expression for the tensor components

$$\nabla_q \nabla_r V = 8\pi \sqrt{\frac{21}{5}} \sum_t \frac{e_t}{R_{0t}^5} s_t^2$$

$$\times \sum_m C(4, 1, 3; m, q) C(3, 1, 2; m+q, r)$$

$$\times Y_2^{m+q+r} (\theta_s^t, \varphi_s^t) Y_4^{-m} (\theta_R^t, \varphi_R^t).$$

Here C are the Wigner coefficients. The unknown components $(\nabla E'_{\mu})$ are

$$(\nabla E')_0 = -4\pi \sqrt{\frac{21}{5}} \sum_t \frac{e_t s_t^2}{R_{0t}^5} \sum_m C(4, 1, 3; m, 0)$$

$$\times C(3, 1, 2; m, 0)$$

$$\times Y_2^m (\theta_s^t, \varphi_s^t) Y_4^{-m} (\theta_R^t, \varphi_R^t),$$

$$(\nabla E')_{\pm 1} = \mp 8\pi \sqrt{\frac{7}{5}} \sum_t \frac{e_t s_t^2}{R_{ct}^5} \sum_m C(4, 1, 3; m, 0)$$

$$\times C(3, 1, 2; m, \pm 1) Y_2^{m\pm 1} (\theta_s^t, \varphi_s^t) Y_4^{-m} (\theta_R^t, \varphi_R^t),$$

$$(\nabla E')_{\pm 2} = -8\pi \sqrt{\frac{14}{5}} \sum_t \frac{e_t s_t^2}{R_{0t}^5} \sum_m C(4, 1, 3; m, \pm 1)$$

$$\times C(3, 1, 2; m \pm 1, \pm 1)$$

$$\times Y_2^{m\pm 2} (\theta_s^t, \varphi_s^t) Y_4^{-m} (\theta_R^t, \varphi_R^t). \qquad (6)$$

Using (1), (2a), and (6) we obtain an explicit expression for the spin-lattice interaction operator, corresponding to spin transitions from the level m to the levels m − 1 and m − 2

$$\hat{W} = \sqrt{10\pi}\,\frac{eQ\,(1-\gamma_\infty)}{I\,(2I-1)}\sum_t \frac{e_t}{R_{0t}^5}\{(\hat{I}_{+1}\hat{I}_0 + \hat{I}_0\hat{I}_{+1})$$
$$\times\Big[\sqrt{\tfrac{1}{8}}\,s_{-1}s_{-1}Y_4^1 - \sqrt{\tfrac{4}{5}}\,s_0 s_{-1}Y_4^0 + \tfrac{3}{4}\,s_0 s_0 Y_4^{-1}$$
$$-\sqrt{2}s_0 s_{+1}Y_4^{-2} - \sqrt{\tfrac{7}{8}}\,s_{+1}s_{+1}Y_4^{-3}\Big]$$
$$+\hat{I}_{+1}^2\sqrt{\tfrac{1}{10}}\,s_{-1}s_{-1}Y_4^0 - s_0 s_{-1}Y_4^{-1}$$
$$+\tfrac{3}{2}\sqrt{\tfrac{1}{2}}\,s_0 s_0 Y_4^{-2} - \sqrt{7}\,s_0 s_{+1}Y_4^{-3} + \sqrt{7}\,s_{+1}s_{+1}Y_4^{-4}\Big]\Big\}.$$

The notation of Eq. (5) is extended here to vectors and vector operators: $B_{\pm1} = \mp(B_x \pm iB_y)/\sqrt{2}$, $B_0 = B_z$. For the sake of brevity we omit the arguments of the functions $Y_4^m(\theta_R^t, \varphi_R^t)$ and the summation index t in $s_{t\mu}$.

3. SPIN-LATTICE RELAXATION TIME

We continue our calculations as applied to crystals with a NaCl type lattice. The displacement of the p-th atom in the l-th elementary cell, in the case of free oscillations, can be written as a superposition of waves

$$\mathbf{u}_p^l = \mathbf{A}_p(\sigma)\exp(-i\omega t + i\sigma\mathbf{R}_p^l/a), \qquad (7)$$

where $a\boldsymbol{\sigma}$ is the wave vector, $\mathbf{R}_p^l$ is the radius vector of the equilibrium position of the p-th atom in the l-th elementary cell, and a is the shortest distance between lattice sites.

If the Cartesian axes are aligned with the principal cubic axes of the crystal, $\boldsymbol{\sigma}$ becomes

$$\sigma = \sigma_1(\mathbf{e}_y + \mathbf{e}_z - \mathbf{e}_x) + \sigma_2(\mathbf{e}_z + \mathbf{e}_x - \mathbf{e}_y) + \sigma_3(\mathbf{e}_x + \mathbf{e}_y - \mathbf{e}_z),$$

and the solution (7) is unique if σ_1, σ_2, and σ_3 range from $-\pi/2$ to $+\pi/2$. In this case the volume of the region of variation of $\boldsymbol{\sigma}$ is $2\pi^3$. We assume that this region is a sphere having this volume. Then the maximum value of σ is $\sigma_0 = (3\pi^2/2)^{1/3}$. Let us write down the number of natural oscillations contained within an energy interval dE inside a solid angle of the wave-vector space, dΩ:

$$\rho\,dE\,d\Omega = (N/2\pi^3)\,\sigma^2\,d\sigma\,d\Omega. \qquad (8)$$

Here N is the number of elementary cells and ρ the density of the natural oscillations in the energy scale. For acoustic oscillations, dE has the simple form $dE = \hbar d\omega = \hbar v d\sigma$, where v is the velocity of sound. The density ρ is then found for acoustic oscillations directly:

$$\rho_{\text{ac}} = N\sigma^2/2\pi^3\hbar v.$$

For optical oscillations, we do not know the analytic dependence of ω on σ. We can write approximately $\omega = -\Delta\omega\cdot\sigma/\sigma_0 + \omega_0$, as can be verified by comparison with numerical computation of the natural-oscillation spectrum (cf., for example, reference 6). Here ω_0 is the frequency of the optical vibrations at $\sigma = 0$, and $\Delta\omega$ is the interval of frequency variation. Inserting ω in Eq. (8), we obtain $\rho_{\text{opt}} = N\sigma_0\sigma^2/2\pi^3\hbar\Delta\omega$.

The probability of spin transition in combination scattering of phonons is determined by the usual formula

$$P(m, m+\mu) = \sum_\alpha \frac{2\pi}{\hbar}\int \rho_\alpha(\sigma)\,\rho_\alpha(\sigma')$$
$$\times\,|\langle m+\mu, n, n'\,|\,\hat{W}\,|\,m, n+1, n'-1\rangle|^2\,d\Omega\,d\Omega'\,dE.$$

The summation indicates that all the modes of oscillations are taken into account. The energies of the emitted and absorbed phonons are connected by the relation $\hbar\omega = \hbar\omega' + |\mu|g\beta H$ by virtue of the law of conservation of energy. Here $|\mu|g\beta H$ is the energy corresponding to the transition between Zeeman sublevels, n the quantum number of the lattice oscillator, and m the magnetic quantum number.

To calculate the matrix elements that enter in Eq. (9), the displacements $\mathbf{u}_p^l$ must be expressed in terms of the normal coordinates q (σ)

$$u_{px}^l = \sum_{\alpha\sigma} q^\alpha(\sigma)\,A_{px}^\alpha\exp(i\sigma\mathbf{R}_p^l/a).$$

The matrix elements of the oscillator coordinate q (σ) are well known. Since our equations contain only the amplitudes of the relative displacements of the atoms, which depend little on σ (this follows from the work of Tolpygo[6]), we neglected this dependence. In calculating the probability of the transition due to optical oscillations, only the region directly surrounding the ions can be taken into account. The next nearest region is not of prime importance, since in that case the phase difference between the vibrations of the atoms of this region and those of the central atom is little and the change in the gradient of the electric field is small. In acoustic oscillations the contribution to the probability of transition from the next nearest region amounts to ⅓ of the contribution of the nearest neighbors. Taking this circumstance into account, and carrying out the corresponding integration over the wave-vector space, we obtain the following equation for the transition probability per unit time

$$P(m,\ m+\mu) = \pi^3 (1-\gamma_\infty)^2 (e^2/a^5 m_0^2)\, |\langle m+\mu | \hat{Q}_\mu | m \rangle|^2 L_{|\mu|},$$

$$L_2 = \frac{(f^2+1)^2 + 2}{a^5 (f+1)^2} \left[\frac{1}{\Delta\omega_\parallel \omega_\parallel^2 \sinh^2 (\hbar\omega_\parallel / 2kT)} + \frac{2}{\Delta\omega_\perp \omega_\perp^2 \sinh^2 (\hbar\omega_\perp / 2kT)} \right] + \frac{k^2T^2}{2\pi\hbar^2} \left(\frac{f}{f+1} \right)^2 \left[\frac{1}{v_\parallel^5} + \frac{2}{v_\perp^5} \right],$$

$$|\langle m+1 | Q_1 | m \rangle|^2 = \tfrac{3}{2} [eQ/2I(2I-1)]^2 (2m+1)^2 (I-m)(I+m+1),$$

$$|\langle m+2 | Q_2 | m \rangle^2 = \tfrac{3}{2} [eQ/2I(2I-1)]^2 (I-m-1)(I+m+2)(I-m) \times (I+m+1) \qquad (10)$$

L_1 differs from L_2 only in the factor 11/20. Here m_0 is the mass of the central ion, f the ratio of the mass of the central ion to that of the neighboring ion, $\omega_\parallel$ and $\omega_\perp$ are the frequencies of the longitudinal and transverse optical vibrations at $\sigma = 0$, and $v_\parallel$ and $v_\perp$ are the speeds of propagation of the longitudinal and transverse vibrations. It is assumed in the calculation that $\hbar\Delta\omega\sigma/\sigma_0 \ll 2kT$, and $\hbar v\sigma/a \ll 2kT$, which is true at room temperatures.

Knowing the probabilities of the relaxation transitions, we can determine the spin-lattice relaxation time. The relaxation of nuclear spins has been investigated heretofore mostly by the method of saturation of the nuclear magnetic resonance. One usually introduces here a time parameter $T_1(ik)$, pertaining to the two levels at which resonance is observed

$$x = (1 + g^2\beta^2 H_1^2 T_1(ik) / \hbar^2)^{-1},$$

where x is a saturation factor, equal to the ratio of the differences of the populations of the two levels in equilibrium state and in saturation, $2H_1$ is the amplitude of the radio-frequency field, and T_2 is the transverse relaxation time. In the case of a spin $I = \frac{1}{2}$, $T_1(-\frac{1}{2}, \frac{1}{2})$ has the usual meaning of longitudinal relaxation time. Using the expression given by Lloyd and Pake[7] for x in terms of the probabilities of the relaxation transitions, we obtain for $T_1(-\frac{1}{2}, \frac{1}{2})$, determined by saturation of the central peak of the nuclear-resonance spectrum, the same expressions as in reference 3:*

$$\text{for } I = {}^3/_2 \quad T_1 = 1/P({}^1/_2, {}^3/_2) + 1/P({}^3/_2, -{}^1/_2),$$

$$\text{for } I = {}^5/_2 \quad T_1 = \left\{ \frac{1}{P({}^1/_2, {}^3/_2) + [1/P({}^1/_2, {}^5/_2) + 1/P({}^5/_2, {}^3/_2)]^{-1}} + \frac{1}{P({}^3/_2, -{}^1/_2)} \right\}. \qquad (11)$$

For simplicity we have omitted here the indices that designate the spin levels.

4. COMPARISON WITH EXPERIMENT AND DISCUSSION OF THE RESULTS

The values of T_1 (in seconds) calculated from Eqs. (10) and (11) are listed in the table together with the experimental values. Columns 3 and 4 contain for comparison the results of calculations made by others.[3,4]*

Ion	Experiment	Reference 3	Reference 4	This Work
Br^{79} in KBr	0.26	19.3	0.88	0.32
I^{127} in KI	0.039	0.24	0.27	0.077
Br^{79} in LiBr	0.028	0.20	0.086	0.031

We determined the velocity of sound from the elastic constants[8] and obtained the frequencies of the optical vibrations from the dispersion frequencies.[9] For LiBr we took $\omega_\perp = 3.5 \times 10^{13}$ sec^{-1}, since the literature gives data neither for the dispersion frequency of this crystal nor for the Debye temperature Θ (in references 3 and 4, Θ was assumed to be 180°). The values of $\Delta\omega$ were estimated with the aid of the equations for the limiting frequencies of the optical vibrations of a diatomic chain, the quadrupole moments of the nuclei were taken from reference 11, while the values of γ_∞ were taken from reference 4. For the substances considered by us, the contribution of the optical vibrations to the probability of relaxation transition is of the same order of magnitude as the contribution of the acoustic vibrations, whereas in the case of Br^{79} in LiBr this contribution is determined essentially by the optical lattice vibrations. Thus, the Debye model cannot be used to explain the relaxation effects of the spin system in crystals at room temperatures. Further refinement of the theory calls for, apparently, an exact determination of the amplitudes and of the spectral density of the natural oscillations of the lattice and for an accounting of the influence of the covalence effect on the relaxation. It is seen from the table that the influence of the covalence on the relaxation is insignificant. It is a maximum for KI and probably causes a certain deviation of our results from experiment in this case.

---

*Reference 3 contains a misprint in the expression for T_1 in the case of I = 5/2: it is necessary to replace P(3/2, 1/2) in the second term by P(3/2, –1/2).

*In reference 3, the degree of covalence λ was determined from the experimental values of the chemical shift. The authors did not have experimental data for KBr and, putting λ = 0.013, they obtained T_1 = 0.77 sec. However, it follows from the measurements of Bloembergen and Sorokin[10] that λ = 0.0026, corresponding to the value of T_1 listed in the table. For I^{127} in KI, the value of T_1 is given in accordance with reference 10.

It is interesting to note that our equations give a higher value of T_1 than experiment if the given substance has other spins, which relax more rapidly. For example, in the case of Na^{23} in NaCl the value of T_1 is more than one order of magnitude greater than the experimental value.* In this case, apparently, the most effective is another relaxation mechanism, in which the energy of the excited spin is transferred rapidly to the relaxing spins, owing to magnetic dipole-dipole interactions, and is transferred from them to the lattice vibrations. This relaxation process is analogous to that discussed in references 13 — 15. Preliminary estimates confirm this assumption.

In conclusion, the author expresses deep gratitude to S. A. Al'tshuler for suggesting the topic and for interest in the investigation.

---

[1] R. V. Pound, Phys. Rev. **79**, 685 (1950).

[2] J. van Kranendonk, Physica **29**, 781 (1954).

[3] K. Yosida and T. Moriya, J. Phys. Soc. Japan **11**, 33 (1956).

[4] E. G. Wikner and T. P. Das, Phys. Rev. **109**, 360 (1958).

[5] M. E. Rose, *Multiple Fields*, Wiley, N.Y. 1955; Russ. Transl. IIL, 1957.

[6] K. B. Tolpygo, Укр. физич. журн., (Ukrainian Phys. J.) **1**, 226 1956; Труды ИФАН УССР, (Trans. Inst. Phys. Acad. Sci. Ukr. S.S.R.) **4**, 71 (1953); **6**, 102 (1955).

[7] J. P. Lloyd and G. E. Pake, Phys. Rev. **94**, 579 (1954).

[8] L. Bergmann, *Der Ultraschall und seine Anwendung in Wissenschaft und Technik*, S. Wirzel, Stuttgart, 1954; Russ. Transl. IIL, 1957.

[9] M. Born and K. Huang, *Dynamical Theory of Crystal Lattice*, Clarendon Press, Oxford, 1954; Russ. Transl. IIL, 1958.

[10] N. Bloembergen and P. P. Sorokin, Phys. Rev. **110**, 865 (1958).

[11] Kulz, Kunz, and Hartmann, Usp. Fiz. Nauk **55**, 537 (1955).

[12] W. G. Proctor and W. A. Robinson, Phys. Rev. **104**, 1344 (1956).

[13] L. Solomon and N. Bloembergen, J. Chem. Phys. **25**, 261 (1956).

[14] N. Bloembergen, J. Chem. Phys. **27**, 572 (1957).

[15] K. A. Valiev, J. Exptl. Theoret. Phys. (U.S.S.R.) **36**, 1743 (1959), Soviet Phys. JETP **9**, 1242 (1959).

---

*The experimental value $T_1 = 7$ minutes, cited in reference 4 for Na^{23} in NaCl, is incorrect. The value of T_1 is either 7.5 sec as measured by Proctor and Robinson[12] or 14.5 sec as measured by Bloembergen and Sorokin.[10] Consequently T_1 (25 minutes) calculated in reference 4 is more than 100 times greater than the experimental value.

Translated by J. G. Adashko
37

SOVIET PHYSICS JETP VOLUME 37(10), NUMBER 1 JANUARY, 1960

SUPERFLUIDITY AND THE MOMENTS OF INERTIA OF NUCLEI

A. B. MIGDAL

Submitted to JETP editor February 13, 1959

J. Exptl. Theoret. Phys. (U.S.S.R.) **37**, 249-263 (July, 1959)

A method is developed for the treatment of superfluidity of nuclei. A formula which agrees satisfactorily with experiment is obtained for the moment of inertia of a nucleus. An expression is found for the change in the energy of "pairing" in the transition from an even-even to an even-odd nucleus, and also for the change in the moment of inertia associated with this transition.

1. INTRODUCTION

SYSTEMS consisting of interacting Fermi particles can be divided into two classes, depending on the type of excited states. When forces of repulsion prevail between the particles, the resultant excitations in the system are the same as in the case of free Fermi particles, but with an effective mass that depends on the forces of interaction between the particles. In the case of attractive forces, "correlated pairs" are formed and lead to an energy gap and to superfluidity.[1-3] One should think that the second type of single particle excitations takes place in nuclei.

In particular, this follows experimentally from the fact that the energy of the first single-particle excitation in even-even nuclei is several times larger than what one should expect for systems of the first type, and is larger than in the case of even-odd nuclei. The presence of a "pairing" energy, determined from mass defects, indicates this same phenomenon.

The existence of correlated pairs and superfluidity is evidenced most clearly in nuclear moments of inertia. The moments of inertia of nuclei are two or three times smaller than those computed from the formula for the moment of inertia of a solid, and this is the most direct evidence for the superfluidity of nuclear matter. Therefore, there is fundamental interest in the calculation of moments of inertia of nuclei on the basis of the modern theory of superfluidity of Fermi-systems. The formalism of this theory has been developed for homogeneous, unbounded systems.[4] However, in the case of a nucleus, the finite dimensions of the system are found to be very important.

A method is developed below, which permits us to study superfluidity in systems of finite dimensions. The moments of inertia are calculated by this method in a quasiclassical approximation and are in satisfactory agreement with the observed values of the moments of inertia.

The computed value of the moment of inertia in the transition from even-even to even-odd nucleus, and also the gyromagnetic ratio for rotating nuclei, are found to be in agreement with experiments.

These results thus confirm the assumption of the superfluidity of nuclear matter.

We note that the superfluidity of nuclear matter can lead to interesting macroscopic phenomena if stars with neutron cores exist. Such a star would be in a superfluid state with a transition temperature corresponding to 1 Mev.

2. METHOD OF ANALYZING A SYSTEM OF FINITE DIMENSIONS

1. For a study of superfluidity in a system of finite dimensions, it is convenient to make use of a method advanced by Gor'kov.[5]

In addition to the usual Green's function of a single particle

$$G(1,2) = -i(\Phi_N^0, T\Psi(1)\Psi^+(2)\Phi_N^0), \tag{1}$$

we introduce a function $F(1,2)$, defined by the formula

$$F(1,2) = (\Phi_N^0, T\Psi^+(1)\Psi^+(2)\Phi_{N-2}^0)e^{-2i\varepsilon_0 t}. \tag{2}$$

Here Φ_N^0 and Φ_{N-2}^0 are the eigenfunctions of the ground state of systems of N and $N-2$ interacting particles, T is the chronological operator, and $\Psi(\mathbf{r}, t)$, $\Psi^+(\mathbf{r}, t)$ are the operators of annihilation and creation of particles in the Heisenberg representation.

Gor'kov obtained a system of equations which relate G and F for weak δ-type interaction between the particles.

With the aid of methods of field theory, a similar set of equations can be obtained for an arbitrary interaction between the particles.

Another way of obtaining the system of equations for an arbitrary interaction is to apply the method of Gor'kov to a system of interacting quasiparticles.

The following system of equations is obtained for G and F:

$$[\varepsilon - H(\mathbf{r})]\, G(\mathbf{r}, \mathbf{r}', \varepsilon) = \delta(\mathbf{r} - \mathbf{r}') + i\Delta(\mathbf{r})\, F(\mathbf{r}, \mathbf{r}', \varepsilon),$$
$$[\varepsilon + H^*_*(\mathbf{r}) - 2\varepsilon_0]\, F(\mathbf{r}, \mathbf{r}', \varepsilon) = -i\Delta^*(\mathbf{r})\, G(\mathbf{r}, \mathbf{r}', \varepsilon),$$
$$\Delta(\mathbf{r}) = \gamma(\mathbf{r}) \int\limits_G F^*(\mathbf{r}, \mathbf{r}', \varepsilon)\, d\varepsilon/2\pi. \qquad (3)$$

Here the functions $G(\mathbf{r}, \mathbf{r}', \epsilon)$ and $F(\mathbf{r}, \mathbf{r}', \epsilon)$ represent the Fourier transform of the functions $G(\mathbf{r}, \mathbf{r}', t - t')$ and $F(\mathbf{r}, \mathbf{r}', t - t')$, determined by Eqs. (1) and (2), with respect to the last variable. The value of ϵ_0 is given by the expression $\epsilon_0 = (E_N^0 - E_{N-2}^0)$, where E_N^0 is the ground-state energy of a system of N particles. The value of ϵ_0 determined in this way differs from the chemical potential $\epsilon_0' = E_{N+1}^0 - E_N^0$ by the "pairing" energy. The value of $\gamma(\mathbf{r})$ is determined by a function describing the interaction between the quasiparticles.

The boundary conditions for the functions G and F in $\mathbf{r}$, $\mathbf{r}'$ are determined by the boundary conditions for the eigenfunctions of the operator $H = p^2/2M_{\text{eff}} + U(\mathbf{r})$.

2. We assume that a solution of the set (3) satisfying the boundary conditions has been found. Knowing the value of $G(\mathbf{r}, \mathbf{r}', \epsilon)$, it is easy to find the single-particle density matrix

$$\rho(\mathbf{r}, \mathbf{r}') = (\Phi_N^0, \Psi^+(\mathbf{r})\, \Psi(\mathbf{r}')\, \Phi_N^0), \qquad (4)$$

with the help of which we can determine the average value over the ground state of an arbitrary quantity A given in the form of a sum over the particles, $A = \sum\limits_j A(\mathbf{r}_j, p_j)$.

The mean value of A is equal to

$$\langle A \rangle = (\Phi_N^0, \int \Psi^+ A(\mathbf{r}, p)\, \Psi\, d\mathbf{r} \Phi_N^0) = \operatorname{Sp} A\rho.$$

Comparing (4) with the definition (1) of the function G, we find

$$\rho(\mathbf{r}, \mathbf{r}') = -iG(\mathbf{r}, \mathbf{r}', \tau)\,|_{\tau \to -0} = \int\limits_C G(\mathbf{r}, \mathbf{r}', \varepsilon)\, d\varepsilon/2\pi i, \qquad (5)$$

where the contour C consists of the real axis and an infinite semicircle in the upper half plane.

3. The last equation of (3) contains the function $\gamma(\mathbf{r})$, which cannot be found without a detailed knowledge of the forces of interaction between the quasiparticles. The effective interaction between quasiparticles can be computed only in the form of a series in terms of some small parameter (for example, in the form of the series of perturbation theory, if the interaction between the particles is small). In the case of a nucleus, there is no small parameter to permit the use of approximate methods. Therefore the function $\gamma(\mathbf{r})$ in a nucleus cannot be calculated by analytic methods.

4. The system of equations (3) is materially simplified if the self-consistent potential entering into H does not depend upon the coordinates of the particle, i.e., in the case of a square potential well. Then the density of particles is constant over the volume and the function $\gamma(\mathbf{r})$, which depends upon the coordinates only through the medium of the density of the particles, is also a constant. It can be established that the function $F(\mathbf{r}, \mathbf{r}', \epsilon)$ is also independent of $\mathbf{r}$, and therefore the quantity $\Delta(\mathbf{r})$ is constant over the volume of the system.

Solutions of Eq. (3) for constant Δ are easily obtained if we expand the functions G and F in the eigenfunctions of the Hamiltonian H, which satisfy the boundary conditions for G and F:

$$G(\mathbf{r}, \mathbf{r}', \varepsilon) = \sum_{\lambda\lambda'} G_{\lambda\lambda'}(\varepsilon)\, \varphi_\lambda(\mathbf{r})\, \varphi^*_{\lambda'}(\mathbf{r}'),$$
$$F(\mathbf{r}, \mathbf{r}', \varepsilon) = \sum_{\lambda\lambda'} F_{\lambda\lambda'}(\varepsilon)\, \varphi_\lambda(\mathbf{r})\, \varphi^*_{\lambda'}(\mathbf{r}'), \qquad H\varphi_\lambda = \varepsilon_\lambda \varphi_\lambda. \qquad (6)$$

Denoting

$$\varepsilon - \varepsilon_0 \to \varepsilon, \qquad H - \varepsilon_0 \to H, \qquad \varepsilon_\lambda - \varepsilon_0 \to \varepsilon_\lambda, \qquad (7)$$

we obtain from (3)

$$(\varepsilon - H)\, G = \delta + i\Delta F, \qquad (\varepsilon + H^*)\, F = -i\Delta^* G,$$
$$\Delta = \gamma \int\limits_C F^*\, d\varepsilon/2\pi. \qquad (8)$$

Substitution of (6) into (8) gives,* for constant Δ,

$$G_{\lambda\lambda'} = \frac{\varepsilon + \varepsilon_\lambda}{\varepsilon^2 - \varepsilon_\lambda^2 - \Delta^2}\, \delta_{\lambda\lambda'}, \qquad F_{\lambda\lambda'} = -\frac{i\Delta}{\varepsilon^2 - \varepsilon_\lambda^2 - \Delta^2}\, \delta_{\lambda\lambda'}. \qquad (9)$$

The poles of $G_{\lambda\lambda'}$ determine the energy levels of the single-particle excitations

$$\varepsilon = E_\lambda = \sqrt{\Delta^2 + \varepsilon_\lambda^2}. \qquad (10)$$

5. To find the density matrix, it is necessary to know the singularities of G in the complex ϵ plane. In the denominator of $G_{\lambda\lambda'}$ we must substitute $\epsilon_\lambda - i\delta\epsilon_\lambda$, $\delta \to +0$ in place of ϵ_λ, which means the introduction of an infinitely small damping of the states that describe the particle and the hole. Then

$$E_\lambda = \sqrt{\Delta^2 + \varepsilon_\lambda^2} \to \sqrt{\Delta^2 + \varepsilon_\lambda^2 - 2i\delta\varepsilon_\lambda^2} = E_\lambda - i\delta_1, \qquad \delta_1 \to +0.$$

Thus, in the expression $\epsilon^2 - E_\lambda^2 = (\epsilon - E_\lambda)(\epsilon + E_\lambda)$, the first factor vanishes in the lower and the second in the upper half plane of ϵ.

---

*The constant phase of Δ in Eq. (8) can be chosen arbitrarily; therefore, for Δ = const we can set $\operatorname{Im}\Delta = 0$.

According to (5), the density matrix is equal to

$$\rho_{\lambda\lambda'} = \int_C G_{\lambda\lambda'}\, d\varepsilon/2\pi i = (E_\lambda - \varepsilon_\lambda)\,\delta_{\lambda\lambda'}/2E_\lambda = \nu_\lambda \delta_{\lambda\lambda'}. \quad (11)$$

Similarly, we find

$$F_{\lambda\lambda'}(\tau = 0) = \int F_{\lambda\lambda'}(\varepsilon)\, d\varepsilon/2\pi = -\Delta/2E_\lambda.$$

Substituting this result in the last equation of (8), we find the link between γ and Δ:

$$1 = -\gamma \sum_\lambda \varphi^*_\lambda(\mathbf{r})\,\varphi_\lambda(\mathbf{r})/2E_\lambda. \quad (12)$$

6. We find the solution of the system (8) for a weak perturbation $H \rightarrow H + V$. The equations for terms of first order in V will be

$$(\varepsilon - H)\,G' - VG = i\Delta' F + i\Delta F',$$
$$(\varepsilon + H)\,F' + V^* F = -i\Delta'^* G - i\Delta G',$$
$$\Delta'^*(\mathbf{r}) = \gamma \int F'(\mathbf{r}, \mathbf{r}, \varepsilon)\, d\varepsilon/2\pi. \quad (13)$$

We find

$$G' = GVG + FV^*F + iG\Delta' F + iF\Delta'^* G,$$
$$F' = -DV^*F + FVG + iF\Delta' F - iD\Delta'^* G, \quad (14)$$

where

$$D = \frac{\varepsilon - H}{\varepsilon^2 - H^2 - \Delta^2}, \qquad G = \frac{\varepsilon + H}{\varepsilon^2 - H^2 - \Delta^2},$$
$$F = -\frac{i\Delta}{\varepsilon^2 - H^2 - \Delta^2}.$$

Integrating the first equation of (14) with respect to ϵ, according to (5), we find the first-order correction to the density matrix. After simple algebraic manipulations, we obtain

$$\rho'_{\lambda\lambda'} = \int_C G'_{\lambda\lambda'} \frac{d\varepsilon}{2\pi i}$$
$$= \frac{(\varepsilon_\lambda \varepsilon_{\lambda'} - E_\lambda E_{\lambda'})\, V_{\lambda\lambda'} - \Delta^2 V^*_{\lambda\lambda'} + \Delta\,(\varepsilon_\lambda \Delta'_{\lambda\lambda'} + \varepsilon_{\lambda'} \Delta'^*_{\lambda\lambda'})}{2E_\lambda E_{\lambda'}(E_\lambda + E_{\lambda'})}. \quad (15)$$

In similar fashion we compute the quantity

$$\int F'_{\lambda\lambda'} \frac{d\varepsilon}{2\pi} = \frac{\Delta\,(\varepsilon_\lambda V^*_{\lambda\lambda'} + \varepsilon_{\lambda'} V_{\lambda\lambda'}) + \Delta^2 \Delta'_{\lambda\lambda'} - (E_\lambda E_{\lambda'} + \varepsilon_\lambda \varepsilon_{\lambda'})\, \Delta'^*_{\lambda\lambda'}}{2E_\lambda E_{\lambda'}(E_\lambda + E_{\lambda'})}. \quad (16)$$

The last equation of (13) can be written

$$\Delta'^*(\mathbf{r}) = \gamma \sum_{\lambda\lambda'} \varphi_\lambda(\mathbf{r})\,\varphi^*_{\lambda'}(\mathbf{r}) \int F'_{\lambda\lambda'}(\varepsilon)\, d\varepsilon/2\pi.$$

Here we have neglected changes in γ under the action of the perturbation V. The left side of this equation can be represented in the form

$$\Delta'^*(\mathbf{r}) = -\gamma \sum_{\lambda\lambda'} \Delta'^*_{\lambda\lambda'}\, \varphi_\lambda(\mathbf{r})\,\varphi^*_{\lambda'}(\mathbf{r})/2E_\lambda$$
$$= -\gamma \sum_{\lambda\lambda'} \Delta'^*_{\lambda\lambda'}\, \varphi_\lambda(\mathbf{r})\,\varphi^*_{\lambda'}(\mathbf{r})/2E_{\lambda'}.$$

with the help of (12). We obtain an integral equation for $\Delta'(\mathbf{r})$:

$$\sum_{\lambda\lambda'} \left[\int F'_{\lambda\lambda'}\, d\varepsilon/2\pi + \Delta'^*_{\lambda\lambda'}/4E_\lambda + \Delta'^*_{\lambda\lambda'}/4E_{\lambda'}\right] \varphi_\lambda \varphi^*_{\lambda'} = 0.$$

Making use of (16), we find

$$\sum_{\lambda\lambda'} \frac{2\Delta\,(\varepsilon_\lambda V^*_{\lambda\lambda'} + \varepsilon_{\lambda'} V_{\lambda\lambda'}) + 2\,\Delta^2 \Delta'_{\lambda\lambda'} + [2\Delta^2 + (\varepsilon_\lambda - \varepsilon_{\lambda'})^2]\, \Delta'^*_{\lambda\lambda'}}{E_\lambda E_{\lambda'}(E_\lambda + E_{\lambda'})}$$
$$\times \varphi_\lambda \varphi^*_{\lambda'} = 0. \quad (17)$$

3. METHOD OF CALCULATING THE MOMENT OF INERTIA

1. For the calculation of the moment of inertia, it is necessary to find the change in the Hamiltonian resulting from a transformation to a rotating set of coordinates.

Let $H = \mathscr{E}(\mathbf{p}) + U$, where $\mathbf{p}$ the momentum operator. To find the change in H upon transformation to the rotating system of coordinates, one must replace $\mathbf{p}$ by $\mathbf{p} - M\mathbf{r} \times \boldsymbol{\Omega}$, where M is the mass of the nucleon and Ω is the angular velocity of the system of coordinates. We obtain

$$V = -\frac{\partial\varepsilon}{\partial \mathrm{p}} M\,[\mathbf{r} \times \boldsymbol{\Omega}] = -\frac{M}{M_{eff}} \mathfrak{M}\Omega = -\frac{M}{M_{eff}} \mathfrak{M}_x\, \Omega, \quad (18)$$

where $M_{\text{eff}} = p/(\partial\epsilon/\partial p)$ is the effective mass of the quasiparticles; $\mathfrak{M} = \mathbf{r} \times \mathbf{p}$, and the x axis is chosen along $\boldsymbol{\Omega}$. Noting that $V^* = -V$, and denoting $\Delta'(\mathbf{r}) = if(\mathbf{r})\,\Omega M/M_{\text{eff}}$, we obtain from (15)

$$\frac{1}{\Omega}\rho'_{\lambda\lambda'} = \frac{(E_\lambda E_{\lambda'} - \varepsilon_\lambda \varepsilon_{\lambda'} - \Delta^2)\,\mathfrak{M}^x_{\lambda\lambda'} + i\Delta(\varepsilon_\lambda - \varepsilon_{\lambda'})\, f_{\lambda\lambda'}}{2E_\lambda E_{\lambda'}(E_\lambda + E_{\lambda'})} \frac{M}{M_{eff}}, \quad (19)$$

where

$$f_{\lambda\lambda'} = \int \varphi^*_\lambda(\mathbf{r})\, f(\mathbf{r})\, \varphi_{\lambda'}(\mathbf{r})\, d\mathbf{r}.$$

Multiplying (17) by i, we find

$$\sum_{\lambda\lambda'} \frac{2\Delta\mathfrak{M}^x_{\lambda\lambda'} + (\varepsilon_\lambda - \varepsilon_{\lambda'})\, f_{\lambda\lambda'}}{E_\lambda E_{\lambda'}(E_\lambda + E_{\lambda'})} \varphi_\lambda(\mathbf{r})\,\varphi^*_{\lambda'}(\mathbf{r}) = 0. \quad (20)$$

We find the mean value of the momentum

$$\langle \mathfrak{M}^x \rangle = \mathrm{Sp}\,\rho\,\mathfrak{M}^x = \sum_{\lambda\lambda'} \mathfrak{M}^x_{\lambda\lambda'}\, \rho_{\lambda'\lambda}.$$

The moment of inertia is obtained from the expression

$$J = \frac{\langle \mathfrak{M}^x \rangle}{\Omega} = \sum_{\lambda\lambda'} \frac{(E_\lambda E_{\lambda'} - \varepsilon_\lambda \varepsilon_{\lambda'} - \Delta^2)\,|\mathfrak{M}^x_{\lambda\lambda'}|^2 - \Delta f_{\lambda\lambda'} \dot{\mathfrak{M}}^x_{\lambda\lambda'}}{2E_\lambda E_{\lambda'}(E_\lambda + E_{\lambda'})} \frac{M}{M_{eff}}, \tag{21}$$

where f must be determined from the integral equation (20).

2. We note that the integral equation (20) for f can be obtained in another way. With the help of ρ we set up the mean value of the current density $\langle \mathbf{j}(\mathbf{r}) \rangle = \mathrm{Sp}\,(\rho' \mathbf{j} - \rho_0 \mathbf{r} \times \boldsymbol{\Omega})$; then Eq. (20) is obtained from the condition $\operatorname{div} \langle \mathbf{j}(\mathbf{r}) \rangle = 0$ without use of the third equation of (8).

This circumstance permits us to solve the first two equations of (8) with $\Delta = \mathrm{const}$ for an arbitrary initial Hamiltonian without danger of running into a contradiction, in spite of the fact that the last equation of (8) leads to $\Delta = \mathrm{const}$ only for a square potential well.

Let us consider the expression

$$J_1 = \sum_{\lambda\lambda'} \frac{E_\lambda E_{\lambda'} - \varepsilon_\lambda \varepsilon_{\lambda'} - \Delta^2}{2E_\lambda E_{\lambda'}(E_\lambda + E_{\lambda'})} |\mathfrak{M}^x_{\lambda\lambda'}|^2 \frac{M}{M_{eff}}. \tag{22}$$

It is not difficult to see that the quantity

$$\mathcal{L}(\varepsilon_\lambda, \varepsilon_{\lambda'}) = (E_\lambda E_{\lambda'} - \varepsilon_\lambda \varepsilon_{\lambda'} - \Delta^2)/2E_\lambda E_{\lambda'}(E_\lambda + E_{\lambda'}) \tag{23}$$

as a function of ϵ_λ, for a fixed difference $d = \epsilon_\lambda - \epsilon_{\lambda'}$, has a sharp maximum of width $\sim\Delta$ at the point $\epsilon_\lambda + \epsilon_{\lambda'} = 0$. We denote

$$\int \mathcal{L}(\varepsilon_\lambda, \varepsilon_\lambda + d)\, d\varepsilon_\lambda = U(d/2\Delta).$$

It is easy to establish the fact that

$$U(x) = 1 - \ln(x + \sqrt{1 + x^2})/x\sqrt{1 + x^2}. \tag{24}$$

When a sufficient number of levels are contained in the width Δ, we may replace the function $\mathcal{L}$ in (22) by

$$\mathcal{L}(\varepsilon_\lambda, \varepsilon_{\lambda'}) \to U((\varepsilon_\lambda - \varepsilon_{\lambda'})/2\Delta)\,\delta(\varepsilon_\lambda). \tag{25}$$

Making use of (24) and (25), we get in place of (22)

$$J_1 = \sum_{\lambda\lambda'} \left\{1 - g\left(\frac{\varepsilon_\lambda - \varepsilon_{\lambda'}}{2\Delta}\right)\right\} |\mathfrak{M}^x_{\lambda\lambda'}|^2\, \delta(\varepsilon_\lambda) \frac{M}{M_{eff}}, \tag{26}$$

where

$$g(x) = (\sinh^{-1} x)/x(1 + x^2)^{1/2}. \tag{27}$$

4. We now show that the expression

$$J_0 = \sum_{\lambda\lambda'} |\mathfrak{M}^x_{\lambda\lambda'}|^2\, \delta(\varepsilon_\lambda)\, M/M_{eff} \tag{28}$$

differs only by a factor from the value of the moment of inertia for a solid. We carry out a summation over λ' in (28), and denote

$$\rho(\varepsilon_0, \mathbf{r}) = \sum_\lambda \varphi^*_\lambda(\mathbf{r})\, \varphi_\lambda(\mathbf{r})\, \delta(\varepsilon_\lambda), \tag{29}$$

where $\rho(\epsilon_0, \mathbf{r})$ is the density of particles with energy ϵ_0. We obtain

$$J_0 = \int d\mathbf{r}\, \rho(\varepsilon_0, \mathbf{r}) \langle (\mathfrak{M}^x)^2 \rangle M/M_{eff}.$$

Here $(\mathfrak{M}^x)^2$ is replaced by the value of $\langle (\mathfrak{M}^x)^2 \rangle$ averaged over the angles of the momentum $\mathbf{p}$. Since all the directions of $\mathbf{p}$ are equally probable, then by averaging the operator $(\mathfrak{M}^x)^2 = y^2 p_z^2 + z^2 p_y^2 - y p_z z p_y - z p_y y p_z$ over the angles of $\mathbf{p}$, we obtain

$$\langle (\mathfrak{M}^x)^2 \rangle = {}^1/_3\, p_0^2(\mathbf{r})\,(y^2 + z^2).$$

We denote

$$n'(\mathbf{r}) = \rho(\varepsilon_0, \mathbf{r})\, p_0^2/3M_{eff},$$

Then

$$J_0 = M \int n'(\mathbf{r})\,(y^2 + z^2)\, d\mathbf{r}.$$

In the quasiclassical approximation, the density of particles is

$$n(\mathbf{r}) = C p_0^3(\mathbf{r}), \qquad p_0(\mathbf{r}) = \sqrt{2M_{eff}(\varepsilon_0 - U(\mathbf{r}))},$$
$$\rho(\varepsilon_0, \mathbf{r}) = \partial n(\mathbf{r})/\partial\varepsilon_0 = 3M_{eff}\, n(\mathbf{r})/p_0^2(\mathbf{r}), \tag{30}$$

i.e., $n'(\mathbf{r}) = n(\mathbf{r})$, and consequently J_0 coincides with the value of the moment of inertia for a solid:

$$J_{\mathrm{sol}} = \int M n(\mathbf{r})\,(y^2 + z^2)\, d\mathbf{r}.$$

However, because of the existence of shells, the density of levels on the Fermi surface $\rho_0 = \int \rho(\epsilon_0, \mathbf{r})\, d\mathbf{r}$ can differ from the classical value $\rho_0^{\mathrm{cl}} = \int (\partial n/\partial\epsilon)\, d\mathbf{r}$; therefore,

$$J_0 = (\rho_0/\rho_0^{\mathrm{cl}})\, J_{\mathrm{sol}} \tag{31}$$

We note that the effective mass does not enter into J_0, as expected.

For a sufficiently deformed nucleus ($\beta \gtrsim A^{-1/3}$) we have $\rho_0/\rho_0^{\mathrm{cl}} \approx 1$ and $J_0 = J_{\mathrm{sol}}$. For small deformations ($\beta \ll A^{-1/3}$), when the shell structure substantially affects the density of levels, $\rho_0/\rho_{\mathrm{cl}} > 1$.

5. Let us now consider the second component in the moment of inertia

$$J_2 = -\Delta \sum_{\lambda\lambda'} \frac{f_{\lambda\lambda'} \dot{\mathfrak{M}}^x_{\lambda\lambda'}}{2E_\lambda E_{\lambda'}(E_\lambda + E_{\lambda'})} \frac{M}{M_{eff}}.$$

Multiplying Eq. (20) by $f(\mathbf{r})$ and integrating over $\mathbf{r}$ we obtain

$$-\Delta \sum_{\lambda\lambda'} \frac{\dot{\mathfrak{M}}^x_{\lambda\lambda'} f_{\lambda'\lambda}}{2E_\lambda E_{\lambda'}(E_\lambda + E_{\lambda'})} = -\Delta \sum_{\lambda\lambda'} \frac{f_{\lambda\lambda'} \dot{\mathfrak{M}}^x_{\lambda'\lambda}}{2E_\lambda E_{\lambda'}(E_\lambda + E_{\lambda'})}$$
$$= \sum_{\lambda\lambda'} \frac{(\varepsilon_\lambda - \varepsilon_{\lambda'})^2 |f_{\lambda\lambda'}|^2}{4E_\lambda E_{\lambda'}(E_\lambda + E_{\lambda'})}.$$

Consequently,

$$J_2 = \sum_{\lambda\lambda'} \frac{(\varepsilon_\lambda - \varepsilon_{\lambda'})^2 \, |f_{\lambda\lambda'}|^2}{4E_\lambda E_{\lambda'} (E_\lambda + E_{\lambda'})} \frac{M}{M_{eff}}.$$

Making use of the sharp maximum of $1/E_\lambda E_{\lambda'}(E_\lambda + E_{\lambda'})$ with respect to ϵ_λ, similarly to what was done in the calculation of J_1, we obtain

$$J_2 = -\frac{1}{2\Delta} \sum_{\lambda\lambda'} f_{\lambda\lambda'} \dot{\mathfrak{M}}^x_{\lambda'\lambda} g \delta(\varepsilon_\lambda) M/M_{eff}$$

$$= \sum_{\lambda\lambda'} |f_{\lambda\lambda'}|^2 g \left(\frac{\varepsilon_\lambda - \varepsilon_{\lambda'}}{2\Delta}\right) \frac{(\varepsilon_\lambda - \varepsilon_{\lambda'})^2}{4\Delta^2} \delta(\varepsilon_\lambda) \frac{M}{M_{eff}}, \tag{32}$$

where $g(x)$ is given by (27).

6. Using the sharp maximum of $1/E_\lambda E_{\lambda'}(E_\lambda + E_{\lambda'})$ we obtain, in place of (20),

$$\sum_{\lambda\lambda'} \left[\dot{\mathfrak{M}}^x_{\lambda\lambda'}/2\Delta + f_{\lambda\lambda'}(\varepsilon_\lambda - \varepsilon_{\lambda'})^2/4\Delta^2\right]$$

$$\times g((\varepsilon_\lambda - \varepsilon_{\lambda'})/2\Delta) \varphi_\lambda(\mathbf{r}) \varphi^*_{\lambda'}(\mathbf{r}) \delta(\varepsilon_\lambda) = 0. \tag{33}$$

Thus the moment of inertia is calculated according to the formula

$$J = J_0 - \frac{M}{M_{eff}} \sum_{\lambda\lambda'} g \left(\frac{\varepsilon_\lambda - \varepsilon_{\lambda'}}{2\Delta}\right) \left|\mathfrak{M}^x_{\lambda\lambda'}\right|^2 \delta(\varepsilon_\lambda)$$

$$+ \frac{M}{M_{eff}} \sum_{\lambda\lambda'} g \left(\frac{\varepsilon_\lambda - \varepsilon_{\lambda'}}{2\Delta}\right) \left(\frac{\varepsilon_\lambda - \varepsilon_{\lambda'}}{2\Delta}\right)^2 |f_{\lambda\lambda'}|^2 \delta(\varepsilon_\lambda), \tag{34}$$

in which one must insert $f(\mathbf{r})$, found from the integral equation (33).

We introduce the quantity

$$\varkappa = \varepsilon_0 \beta / \Delta p_0 R_0, \tag{35}$$

where $\beta = 2(a-b)/(a+b)$ is a parameter of the deformation of the nucleus, a and b are the semi-axes of the spheroid, $R_0 = (a+b)/2$, and $\hbar = 1$.

It is not difficult to show that for $\kappa \gg 1$

$$J \to J_0. \tag{36}$$

In the other limiting case, when $\kappa/\beta \ll 1$, assuming that the potential U has the form $U(z^2/a^2 + (x^2 + y^2)/b^2)$, we can obtain

$$J = J_0 \left(\frac{a^2 - b^2}{a^2 + b^2}\right)^2 + C_1 J_0 \varkappa^2, \tag{37}$$

where $C_1 \sim 1$.

Thus, for $\kappa/\beta \ll 1$, the moment of inertia of the system approaches the moment of inertia of an ideal liquid. This result is quite natural. The quantity κ/β is of the order of a_0/R, where $a_0 = p_0/M\Delta$ is the correlation radius of the paired particles. When the correlation radius is much smaller than the radius of the nucleus, the equations of the hydrodynamics of an ideal liquid should be applicable.

For $\beta \to 0$ and fixed Δ, $J \sim \beta^2$.

4. COMPUTATION OF THE MOMENT OF INERTIA FOR AN OSCILLATORY POTENTIAL

Let us write the potential $U(\mathbf{r})$ in the form

$$U(\mathbf{r}) = \tfrac{1}{2} M_{eff} [\omega_z^2 z^2 + \omega_y^2 (x^2 + y^2)]. \tag{38}$$

We have the operator relation

$$\dot{\mathfrak{M}}^x = z\partial U/\partial y - y \partial U/\partial z = (\omega_y^2 - \omega_z^2) yz M_{eff}.$$

Therefore,

$$\dot{\mathfrak{M}}^x_{\lambda\lambda'} = (\omega_y^2 - \omega_z^2) y_{mm'} z_{nn'} M_{eff}.$$

Thus the matrix element $\dot{\mathfrak{M}}^x_{\lambda\lambda'}$ is different from 0 only for $m' = m \pm 1$, $n' = n \pm 1$. With quasiclassical accuracy ($n \gg 1$, $m \gg 1$), all four possible values of $\dot{\mathfrak{M}}^x_{\lambda\lambda'}$ are identical.

Moreover, noting that $\epsilon_\lambda - \epsilon_{\lambda'} = \pm(\omega_z \pm \omega_y)$, we find from (26)

$$J_1 = J_0 - \sum_{\lambda\lambda'} g \left(\frac{\varepsilon_\lambda - \varepsilon_{\lambda'}}{2\Delta}\right) \left|\dot{\mathfrak{M}}^x_{\lambda\lambda'}\right|^2 \frac{1}{(\varepsilon_\lambda - \varepsilon_{\lambda'})^2} \delta(\varepsilon_\lambda) \frac{M}{M_{eff}}$$

$$= J_0 - \frac{1}{2} \left(\frac{g_1}{\nu_1^2} + \frac{g_2}{\nu_2^2}\right) \sum_{\lambda\lambda'} |\dot{\mathfrak{M}}^x_{\lambda\lambda'}|^2 \frac{1}{4\Delta^2} \frac{M}{M_{eff}}, \tag{39}$$

where

$$\nu_1 = (\omega_z - \omega_y)/2\Delta, \qquad \nu_2 = (\omega_z + \omega_y)/2\Delta,$$

$$g_1 = g(\nu_1), \qquad g_2 = g(\nu_2).$$

Similarly, we obtain

$$J_0 = \sum_{\lambda\lambda'} |\mathfrak{M}^x_{\lambda\lambda'}|^2 \delta(\varepsilon_\lambda) \frac{M}{M_{eff}}$$

$$= \frac{1}{2} \frac{\nu_1^2 + \nu_2^2}{\nu_1^2 \nu_2^2} \frac{1}{4\Delta^2} \sum_{\lambda\lambda'} |\mathfrak{M}^x_{\lambda\lambda'}|^2 \delta(\varepsilon_\lambda) \frac{M}{M_{eff}}.$$

Substituting this result in (39), we obtain

$$J_1 = J_0 \left(1 - \frac{g_1 \nu_2^2 + g_2 \nu_1^2}{\nu_1^2 + \nu_2^2}\right). \tag{40}$$

2. We shall show that Eq. (33) is satisfied for $f = \alpha yz$. As above, we make use of the independence of the matrix elements $\dot{\mathfrak{M}}^x_{\lambda\lambda'}$, $f_{\lambda\lambda'}$, and $\varphi_\lambda \varphi^*_{\lambda'}$ of the values of λ' for a given value of λ.

From Eq. (33) we obtain

$$\Delta (g_1 + g_2) \sum_{\lambda\lambda'} \dot{\mathfrak{M}}^x_{\lambda\lambda'} \varphi_\lambda \varphi^*_{\lambda'} \delta(\varepsilon_\lambda)$$

$$= -2\Delta^2 (g_1 \nu_1^2 + g_2 \nu_2^2) \sum_{\lambda\lambda'} f_{\lambda\lambda'} \varphi_\lambda \varphi^*_{\lambda'} \delta(\varepsilon_\lambda). \tag{40a}$$

Summing over λ', we obtain

$$f(\mathbf{r}) = -\frac{g_1 + g_2}{2\Delta (g_1 \nu_1^2 + g_2 \nu_2^2)} \dot{\mathfrak{M}}^x = -\frac{(g_1 + g_2)(\omega_y^2 - \omega_z^2) yz}{2\Delta (g_1 \nu_1^2 + g_2 \nu_2^2)} M_{eff}. \tag{41}$$

Substituting (41) in (32), we find

$$J_2 = J_0 (g_1 + g_2) \nu_1^2 \nu_2^2 / (\nu_1^2 + \nu_2^2)(\nu_1^2 g_1 + \nu_2^2 g_2). \tag{42}$$

It is easy to see that the expression (40) goes over into J_0 when $\nu_1, \nu_2 \gg 1$, while J_2, determined from (42), approaches 0 so that the asymptotic formula (36) is satisfied.

For $\nu_1, \nu_2 \ll 1$, the relation (37) is satisfied, i.e., the moment of inertia approaches the moment of inertia of an ideal liquid.

3. Substitution of numerical values of ν_1 and ν_2 for the nuclei gives $\nu_2 \sim 10$, $\nu_1 \sim 1$, which permits us to write down an expression for J in the form

$$J \approx J_0 \left\{ 1 - g_1 + \frac{g_1^2 \nu_1^2}{\nu_1^2 g_1 + \ln 2\nu_2} \right\} = J_0 \Phi_1(\nu_1). \qquad (43)$$

The values of the function $\Phi_1(x)$ are given in Table I (for $\nu_2 = 10$).

5. COMPUTATION OF THE MOMENT OF INERTIA FOR A RECTANGULAR POTENTIAL WELL

1. From Eqs. (26) and (28), we have

$$J_0 - J_1 = \sum_{\lambda\lambda'} g\left(\frac{\varepsilon_\lambda - \varepsilon_{\lambda'}}{2\Delta}\right) |\mathfrak{M}^x_{\lambda\lambda'}|^2 \delta(\varepsilon_\lambda) \frac{M}{M_{eff}}. \qquad (44)$$

We shall show that only such values of λ' are to be kept in this sum for which $m' = m \pm 1$ and $\nu' = \nu$, where m is the eigenvalue of the projection of the angular momentum on the axis of symmetry and ν is the set of remaining quantum numbers.

The relation $m' = m \pm 1$ is the exact selection rule for the matrix elements of the operator $\mathfrak{M}^x$. We shall show that the components with $\nu' \neq \nu$ contribute little to the sum (44).

The index ν is determined by three quantum numbers; for example, in the case of a nucleus that is close to spherical, by the radial quantum number n, the orbital number L, and the value of the total momentum $j = l \pm \frac{1}{2}$. If one of these quantum numbers is changed, then the order of the energy change is $|\epsilon_\lambda - \epsilon_{\lambda'}| \sim \epsilon_0/p_0R \sim \epsilon_0/A^{1/3} \gg \Delta$, and the corresponding value of the function g is $\sim (\Delta p_0 R/\epsilon_0) \ll 1$. Therefore such components make a negligibly small contribution to the sum (44).

Small differences $|\epsilon_\lambda - \epsilon_{\lambda'}| \sim \epsilon_0 A^{-2/3}$ can be obtained upon an increase of one quantum number by several units simultaneous with a decrease of another. In this case, $g \sim 1$, but the matrix element $M^X_{\lambda\lambda'}$ will be small because of the difference in the number of nodes of the functions φ_λ and $\varphi_{\lambda'}$ and, moreover, will contain the factor β, inasmuch as $M^X_{\lambda\lambda'} = 0$ for a spherical well at $\nu' \neq \nu$. Therefore, only components with $\nu = \nu'$ and $m' = m \pm 1$ should remain in the sum (44):

$$J_0 - J_1 \approx \sum_{\nu, m} g\left(\frac{\varepsilon_{\nu, m+1} - \varepsilon_{\nu, m}}{2\Delta}\right) [|\mathfrak{M}^x_{\nu, m; \nu, m+1}|^2 + |\mathfrak{M}^x_{\nu, m; \nu, m-1}|^2] \delta(\varepsilon_{\nu m}) \frac{M}{M_{eff}}. \qquad (45)$$

2. Further calculations are carried out for a spherical well with effective diameter R_0. The quantity J/J_0 is a symmetric function of the semiaxes a and b, as can be seen, in particular, in the example of the calculations for an oscillatory potential. Therefore, choosing in the final result a radius equal to any mean symmetric in a and b, we determine J/J_0 with a small error of the order of β^2.

For the functions of the spherical well we have

$$|\mathfrak{M}^x_{\nu, m; \nu, m+1}|^2 + |\mathfrak{M}^x_{\nu, m; \nu, m-1}|^2 = {}^1/_2 (j^2 - m^2) + {}^1/_4 j \approx {}^1/_2 (l^2 - m^2), \qquad (46)$$

since the large values of j are important in the sum (45) and one can replace $j = l \pm \frac{1}{2}$ by l. The dependence of the energy of the particle on m is given by the equality

$$\varepsilon_{\nu m} = \varepsilon_\nu + \beta (m^2 / l^2 - {}^1/_3)(\varepsilon_0 + \varepsilon_\nu), \qquad (47)$$

where ϵ_ν is the energy of a particle in a spherical well, reckoned from ϵ_0.

Equation (47) can easily be obtained with the help of perturbation theory. Carrying out a coordinate transformation that converts the ellipsoid into a sphere, we obtain (in first order in β) the perturbation operator

$$Q = {}^1/_3 \beta (p^2 - 3p_z^2)/M_{eff}.$$

Computing the energy by the formula

$$\varepsilon_{\nu m} = \varepsilon_\nu + \int \varphi_\lambda^* Q \varphi_\lambda \, dr,$$

where φ_λ are the eigenfunctions in a spherical well, we arrive at Eq. (47).

Substituting (46) and (47) in (45), we get

$$J_0 - J_1 = \sum_{\nu, m} g\left(\frac{\beta m}{\Delta l^2} \varepsilon_0\right) \frac{l^2 - m^2}{2} \delta(\varepsilon_\nu) \frac{M}{M_{eff}} = \sum_{lm} g\left(\frac{\beta m}{\Delta l^2} \varepsilon_0\right) \frac{l^2 - m^2}{2} \rho_{lm}(\varepsilon_0) \frac{M}{M_{eff}}, \qquad (48)$$

where $\rho_{lm}(\epsilon_0)$ is the energy density of the level with specified values of l and m. Computing the volume of the phase space corresponding to the given values of l and m, we readily obtain

$$\rho_{lm}(\varepsilon_0) = {}^3/_2 \, l_0^{-3} \rho_0 \sqrt{l_0^2 - l^2}, \qquad (49)$$

in a way similar to what was done in the Thomas-Fermi theory; here $l_0 = p_0 R_0$. Making use of (30) and (31), we obtain

TABLE I. Values of the functions Φ_1 and Φ_2, determined from Eqs. (43) and (51)

x	$\Phi_1(x)$	$\Phi_2(x)$	x	$\Phi_1(x)$	$\Phi_2(x)$	x	$\Phi_1(x)$	$\Phi_2(x)$	x	$\Phi_1(x)$	$\Phi_2(x)$
0	0	0	0.7	0.32	0.13	1.3	0.64	0.24	2.0	0.80	0.37
0.1	0.01	0.005	0.8	0.38	0.15	1.4	0.67	0.26	2.2	0.81	0.40
0.2	0.03	0.02	0.9	0.43	0.17	1.5	0.71	0.28	2.4	0.83	0.43
0.3	0.07	0.03	1.0	0.49	0.19	1.6	0.74	0.30	2.6	0.85	0.45
0.4	0.13	0.06	1.1	0.53	0.21	1.7	0.75	0.32	2.7	0.86	0.48
0.5	0.19	0.08	1.2	0.60	0.23	1.8	0.77	0.34	3.0	0.87	0.50
0.6	0.26	0.10				1.9	0.79	0.36			

$$J_0 = \frac{2}{5} NMR_0^2 = \frac{2}{15} = \frac{M}{M_{eff}} \rho_0 R_0^2. \tag{50}$$

Substituting (49), (50) in (48), and introducing the variables $\eta = m/l$, $\xi = l/l_0$, we obtain

$$J_1 = J_0 \left\{ 1 - \frac{45}{4} \int_0^1 d\xi \xi^3 \sqrt{1-\xi^2} \right.$$

$$\left. \times \int_0^1 d\eta (1-\eta^2) g\left(\varkappa \frac{\eta}{\xi}\right) \right\} = J_0 \Phi_2(\varkappa), \tag{51}$$

where κ is determined by Eq. (35).

The values of the function $\Phi_2(\kappa)$ are given in Table I.

3. In the case of a rectangular potential well, the solution of Eq. (33) is found in analytic form only for the limiting cases $\kappa \ll 1$ and $\kappa \gg 1$.

The value of J_2 is shown to be much smaller than that of J_1; therefore, such a solution of Eq. (33) is not of practical interest.

We shall write down without derivation an expression for J_2 in the cases $\kappa \ll 1$ and $\kappa \gg 1$;

$$\varkappa \to 0: J_2 = J_0 \varkappa^2 / 6 \ln (5\varepsilon_0 / \Delta p_0 R_0),$$

$$\varkappa \to \infty: J_2 = J_0 5 \ln^3 (a_1 \varkappa) / 21 \varkappa^2 \ln (a_2 \varepsilon_0 / \Delta p_0 R_0), \tag{52}$$

where a_1 and a_2 are numbers of the order of unity.

The equations (52) allow us to conclude that $J_2/J_0 \lesssim 5\%$ and consequently $J_1 \approx J$.

6. NEUTRON AND PROTON MOMENTS OF INERTIA. GYROMAGNETIC RATIO

1. The calculations carried out above were performed for particles of a single kind. For comparison with experiment it is necessary to consider both types of nuclear particles.

When $Z > 20$, the Fermi surfaces for neutrons and protons move apart and the coupling of neutrons with protons is made impossible. Thus for $Z > 20$, there are two liquids — neutron and proton — which cannot exchange angular momentum since the excitations in each of them have gaps.

Therefore, the moment of inertia of the nucleus is equal to the sum of the moments of inertia of the neutrons and protons. Denoting by $\Phi(\kappa)$ the ratio $J/J_0 = \Phi(\kappa)$ computed above, we obtain the following expression for the moment of inertia

$$\frac{J}{J_0} = \frac{N}{A} \Phi(\varkappa_n) + \frac{Z}{A} \Phi(\varkappa_p), \tag{53}$$

where κ_n and κ_p are the values of κ for neutrons and protons.

2. The quantities Δ_n and Δ_p entering into κ_n and κ_p cannot be computed theoretically and must be taken from experiment.

As will be shown below, Δ_n is smaller than Δ_p; therefore, Δ_n is determined from the first single-particle levels. The value of Δ_p can be found from the experimental gyromagnetic ratio for rotating nuclei. The gyromagnetic ratio is shown to be much smaller than Z/A.*

The gyromagnetic ratio for rotating nuclei is evidently equal to

$$g_r = \frac{\int [\mathbf{r} \times \mathbf{j}_p]\, d\mathbf{r}}{\int [\mathbf{r} \times (\mathbf{j}_n + \mathbf{j}_p)]\, d\mathbf{r}} = \frac{J_p}{J_n + J_p} = \frac{Z\Phi(\varkappa_p)}{N\Phi(\varkappa_n) + Z\Phi(\varkappa_p)}. \tag{54}$$

The measured[6] value of g_r for Sm^{152}, Sm^{154}, Nd^{150} is $g_r \approx 0.21 \pm 0.04$ when $J_n/J_p = N\Phi(\kappa_n)/Z\Phi(\kappa_p) \approx 3.5 \pm 1$.

The function $\Phi_1(\kappa)$ is represented in the interval $\kappa = 1 - 2$ by $\Phi_1 = C\kappa$ with good accuracy, whence we obtain

$$J_n / J_p = (N/Z)^{4/3} \Delta_p / \Delta_n \approx 3.5 \pm 1,$$

which gives $\Delta_p/\Delta_n = 1.5$ to 2.5 [$\Phi_2(\kappa)$ gives a somewhat larger value]; such a value of Δ_p/Δ_n agrees within the limits of error with the value of Δ_p/Δ_n found from mass defects in this region of the table ($\Delta_p/\Delta_n = 1.5 \pm 0.3$).

7. MOMENTS OF INERTIA OF ODD NUCLEI. MOMENTS OF INERTIA IN EXCITED STATES.

1. Integrating Eq. (12) over the volume and denoting $\gamma/V = \gamma_1$, we obtain

---

*The attention of the author was directed to this fact by D. F. Zaretskiĭ.

$$1 = -\gamma_1 \sum_\lambda (1/2E_\lambda). \qquad (12')$$

The value of γ_1 is determined by the density of nuclear matter and by the nuclear forces, and should not change appreciably from nucleus to nucleus.

We shall show that the Δ determined from (12′) experiences significant fluctuations. We rewrite (12′) in the form

$$1 = -\gamma_1 \int_{-\varepsilon_0}^{\varepsilon_1} \rho(\varepsilon) d\varepsilon / 2\sqrt{\Delta^2 + \varepsilon^2}, \qquad (12'')$$

where $\epsilon_1 \sim \epsilon_0$, $\rho(\epsilon)$ is the energy level density.

If in the transition from one nucleus to another a change $\delta\rho$ takes place in the density of levels close to the Fermi surface, then it follows from (12″) that the corresponding change in Δ is given by the relation

$$\int_{-\varepsilon_0}^{\varepsilon_1} \delta\rho \, d\varepsilon / 2\sqrt{\Delta^2 + \varepsilon^2} - \int_{\varepsilon_0}^{\varepsilon_1} \rho(\varepsilon)\, \Delta \delta\Delta \, d\varepsilon / 2(\Delta^2 + \varepsilon^2)^{3/2} = 0.$$

Since

$$\int \Delta^2 d\varepsilon / 2\, (\Delta^2 + \varepsilon^2)^{3/2} = 1,$$

then

$$\frac{\delta\Delta}{\Delta} = \frac{1}{2\rho_0} \int \delta\rho \frac{d\varepsilon}{\sqrt{\Delta^2 + \varepsilon^2}}. \qquad (55)$$

It is natural to expect the fluctuations in ρ to be such that $\int \delta\rho \, d\epsilon \sim 1$; therefore, $\delta\Delta/\Delta \sim 1/3\rho_0\Delta \sim 10\%$ if we take $\rho_0 = 3N/2\epsilon_0 \approx 4$ (in the region of the rare earths) and $\Delta = 0.8$ Mev. This estimate agrees well with the fluctuating values of Δ found from mass defects or from the primary levels.

The fluctuations in the quantity Δ, together with the fluctuations of the sum (34) which determines J/J_0, lead to appreciable fluctuations in the moment of inertia, $\delta J/J \sim 20\%$.

2. Along with the fluctuations that lead to a random change in the moment of inertia, there is a systematic effect of decreasing Δ, and consequently of increasing moment of inertia, in the transition to an odd element.

We shall consider the excited state of the system. It can be shown that the equation for Δ changes in the following fashion:[5]

$$1 = -\gamma_1 \sum \frac{1}{2E_\lambda}(1 - 2n_\lambda), \qquad (56)$$

where n_λ is the number of quasiparticles.

The transition to an odd nucleus must be considered as the appearance of a single quasiparticle with an energy closest to ϵ_0, i.e., $n_\lambda^- = 0$, $n_\lambda^+ = \delta_{\lambda\lambda_1}$, $E_{\lambda_1} \approx \Delta$. From (56) we get, by analogy to (55),

$$(\Delta' - \Delta'')/\Delta = 1/2\rho_0\Delta'', \qquad (57)$$

where Δ' and Δ'' are the corresponding values for even and odd nuclei, $\Delta = (\Delta' + \Delta'')/2$.

The change in the moment of inertia for a change in N is given by the expression

$$\frac{J'' - J'}{J'} = \frac{J_n'' - J_n'}{J'} = \frac{J_n'}{J'} \varkappa_n \frac{d \ln \Phi(\varkappa_n)}{d\varkappa_n} \frac{\Delta_n' - \Delta_n''}{\Delta_n}$$
$$= 0.9 \frac{\Delta_n}{\Delta_n''} \frac{J_n'}{J'} \frac{1}{2\rho_0 \Delta_n''}, \qquad (58)$$

The latter equation is obtained with the help of (57) and the approximate formula $\dfrac{\kappa_n d \ln \Phi_{1,2}(\kappa_n)}{d\kappa_n} \approx 0.9$.

Similarly, we obtain the change of moment of inertia in transition to odd Z:

$$\frac{J'' - J'}{J'} = \frac{J_p'' - J_p'}{J'} = \frac{J_p'}{J'} 0.9 \frac{\Delta_p}{\rho_0^p \Delta_p''^2}. \qquad (59)$$

As will be shown below, Eqs. (58) and (59) agree well with with the experimental data.

3. An appreciable increase in the moment of inertia should occur in single-particle excitations of the nucleus. Thus in excitation with formation of a single hole and a single quasiparticle we get from (56) a relative decrease in Δ that is twice as large as in the transition from even-even to even-odd nuclei, and consequently a twofold relative change in the moment of inertia.

8. DETERMINATION OF Δ FROM THE MASSES OF THE NUCLEI

From the definition of Green's function, it is not difficult to obtain

$$G_\lambda = \sum_s \frac{|(\Phi_{N+1}^s, a_\lambda^+ \Phi_N^0)|^2}{\varepsilon - E_s(N+1) + E_0(N) + i\delta}$$
$$+ \sum_s \frac{|(\Phi_{N-1}^s, a_\lambda \Phi_N^s)|^2}{\varepsilon + E_s(N-1) - E_0(N) - i\delta}, \qquad (60)$$

a_λ, a_λ^+ are the operators of annihilation and creation of particles in the state λ.

Comparing (60) with (9) we obtain

$$E_0(N+1) - E_0(N) = \Delta + \varepsilon_0, \qquad (62)$$
$$E_0(N) - E_0(N-1) = -\Delta + \varepsilon_0. \qquad (61)$$

Equations (61) and (62) permit us to find Δ from the binding energy of the nuclei. A much more exact expression can be obtained if we eliminate from E(N) the dependence on N that is not connected with pairing. For this purpose we set up an expression in which the components with first and second derivatives in N′ = N are eliminated. The relation

TABLE II. Values of Δ_n and Δ_p computed from mass defects for certain elements according to Eqs. (57) and (63)

Element	Δ_n, Mev	Δ_p, Mev	Element	Δ_n, Mev	Δ_p, Mev	Element	Δ_n, Mev	Δ_p, Mev	Element	Δ_n, Mev	Δ_p, Mev
Sm^{150}	1.32	1.64	Gd^{157}	0.72	—	Hf^{178}	0.62	—	Th^{231}	0.56	0.81
Gd^{154}	1.15	—	Dy^{162}	0.82	—	Hf^{179}	0.42	—	Th^{232}	0.55	0.78
Gd^{156}	0.92	—	Dy^{163}	0.62	—	Th^{230}	0.76	1.05	U^{238}	0.64	0.85

TABLE III. Values of the moments of intertia, the parameters of deformation β, the quantities κ_n and κ_p determined from (64)*

Element	β^7	$\varkappa_p$	$\varkappa_n$	$(J/J_0)_{rect}$	$(J/J_0)_{osc}$	$(J/J_0)_{exp^7}$
Nd^{150}	0.26	0.54	0.94	0.15	0.38	0.35
Sm^{152}	0.24	0.65	1.02	0.17	0.43	0.38
Gd^{154}	0.26	0.52	0.88	0.13	0.35	0.36
Gd^{156}	0.33	0.87	1.37	0.22	0.57	0.48
Gd^{157}	0.29	0.93	1.60	0.22	0.64	0.60
Dy^{162}	0.30	0.84	1.43	0.23	0.57	0.50
Hf^{179}	0.20	0.99	1.75	0.27	0.66	0.52
Os^{186}	0.18	0.44	0.69	0.09	0.26	0.28
Th^{230}	0.22	0.63	0.95	0.15	0.40	0.43
Th^{232}	0.22	0.84	1.42	0.24	0.60	0.44
U^{238}	0.24	0.83	1.29	0.22	0.54	0.43

*To calculate κ_p when Δ_p is not known from mass defects, we assume $\Delta_p/\Delta_m = 1.5$. $(J/J_0)_{osc}$ is the computed value of the moment of inertia for an oscillatory potential. $(J/J_0)_{rect}$ is the same for a rectangular potential well.

$$^1/_4\,[3E(N+1)-3E(N)$$
$$+E(N-1)-E(N+2)]=\Delta. \qquad (63)$$

satisfies this condition. The values of $\Delta'_{n,p}$ and $\Delta''_{n,p}$ found from (57) and (63) are given in Table II.

9. COMPARISON WITH EXPERIMENT

1. To compare Eqs. (43) and (51) with the experimental moments of inertia, we express κ and ν_1 in terms of observed quantities. As was pointed out above, one should use for R_0 in (35) a mean radius, for example, $R_0 = (a+b)/2$. We obtain $R_0 = R(1+\beta/3)$ where $R^3 = ab^2$. Taking $R = 1.2 \times 10^{-13} A^{1/3}$ cm, we find

$$\varepsilon_0^n = 52\,(M/M_{eff})\,(N/A)^{2/3}, \quad p_0^n R = 1.9 \cdot N^{1/3},$$

$$\varkappa_n = \frac{3}{1+\beta/3}\,\frac{27}{\Delta_n A^{1/3}}\left(\frac{N}{A}\right)^{1/3}\frac{M}{M_{eff}}. \qquad (64)$$

here Δ_n is in Mev. We have similar expressions for protons.

We select $\omega_0 = (\omega_y + \omega_z)/2$ from the requirement of coincidence of the mean square $\langle r^2 \rangle$ for rectangular and oscillatory potentials. We find $\langle y^2 \rangle = \epsilon_0/4\omega_0^2 = R_0^2/5$. It is easy to obtain expressions similar to (64):

$$\varepsilon_0^n = 76\,(M/M_{eff})\,(N/A)^{2/3}, \qquad p_0^n R = 2.3\,N^{1/3},$$

$$\nu_1^n = \beta\omega_0/2\Delta_n = 0.95\,\varkappa_n \approx \varkappa_n. \qquad (65)$$

There are reasons for thinking* that the effective mass M_{eff} differs slightly from the mass of the nucleon M.

In Table III and in the drawing are shown the values of κ for $M_{eff}/M = 1$. As is seen from the drawing, all the experimental values of J/J_0 lie between the two theoretical curves.

2. To compare Eqs. (58) and (59) with experimental data, we compute the mean value of the observed moment of inertia for a group of nuclei with neighboring values of N and Z. The value averaged over five elements in rare-earth group is equal to: for Z, N even — $(J/J_0) = 0.42$; for Z even N odd — $(J/J_0) = 0.53$, $(J'' - J')/J' = 0.26$. From Eq. (58) we obtain $(J'' - J')/J' = 0.32$. For the transition to even N and odd Z we obtain from (58) and (59)

$$(J'' - J')_{\text{even}\,Z} / (J'' - J')_{\text{even}\,N} \approx J_n\Delta_p / J_p\Delta_n \approx 4$$

---

*The effective mass also enters into the expression for the orbital magnetic moment of the nucleon. For a significant difference between M_{eff} and M, the magnetic moments of the nuclei would not fit between the Schmidt curves.

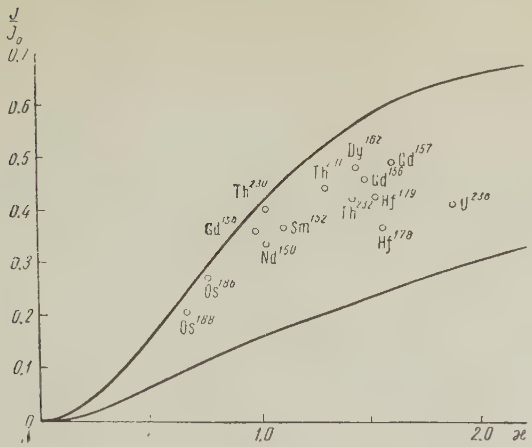

Experimental values of J/J_0 as functions of κ_n. Theoretical curves of J/J_0 for an oscillating potential (upper curve) and a rectangular potential well for $J_n/J_p = 2.5$.

in agreement with the fact that the transition to an odd proton changes the moment of inertia much less than the transition to an odd neutron.

The author expresses his gratitude to L. D. Landau, D. F. Zaretskiĭ and A. I. Larkin for interesting discussions, and also to I. M. Pavlichenkov and M. G. Urin for compiling the tables.

---

[1] L. Cooper, Phys. Rev. **104**, 1189 (1956).

[2] J. Bardeen, L. Cooper, and J. Schrieffer, Phys. Rev. **108**, 1175 (1957).

[3] N. N. Bogolyubov, J. Exptl. Theoret. Phys. (U.S.S.R.) **34**, 58, 73 (1958); Soviet Phys. **7**, 41, 51 (1958).

[4] N. N. Bogolyubov, V. V. Tolmachev, and D. V. Shirkov, Новый метод в теории сверхпроводимости (A New Method in the Theory of Superconductivity) U.S.S.R. Acad. of Sci. Press, Moscow, 1958.

[5] L. P. Gor'kov, J. Exptl. Theoret. Phys. (U.S.S.R.) **34**, 735 (1958); Soviet Phys. **7**, 305 (1958).

[6] G. G. Goldring and R. P. Scharenberg, Phys. Rev. **110**, 701 (1958).

[7] K. Alder, A. Bohr, T. Huss, B. Mottelson, and A. Winther, Revs. Modern Phys. **28**, 432 (1956).

Translated by R. T. Beyer
38

SOVIET PHYSICS JETP VOLUME 37(10), NUMBER 1 JANUARY, 1960

PASSAGE OF PARTICLES THROUGH A PLASMA

A. I. LARKIN

Submitted to JETP editor February 13, 1959

J. Exptl. Theoret. Phys. (U.S.S.R.) **37**, 264-272 (July, 1959)

The Green's function method and the diagram technique are used to calculate the energy loss per unit time by a particle passing through a plasma. Numerical values of the factors in the argument of the logarithm have been obtained for limiting cases.

1. INTRODUCTION

CALCULATION of the decelerating ability of a plasma by the method of paired collisions leads to a logarithmic divergence connected with the long-range action of the Coulomb forces. The screening effect of the medium can be neglected only when the distance between the particles is less than the Debye radius. To calculate the contribution due to close-range collisions, the Coulomb field is cut off at the Debye radius. Akhiezer and Sitenko[1] used the kinetic equation with a self-consistent field to calculate the long-range collisions, at which the momentum transferred is much less than the reciprocal of the Debye radius. These methods do not lead to a correct description of the interaction of particles separated by a distance on the order of the Debye radius, and the results have therefore only logarithmic accuracy. In the present paper we express the decelerating ability in terms of a correlation function, which is a particular case of a two-particle Green's function. To calculate the latter we use the diagram technique, the convenience of which lies in the fact that it permits us to sum an infinite number of essential terms. Furthermore, by estimating the discarded graphs, we can readily determine the accuracy of the obtained results.

2. TRANSITION PROBABILITY

We consider a system of interacting particles which are in thermal equilibrium. The Hamiltonian of the system is

$$H = H_0 + H_1, \qquad H_0 = \sum \varepsilon_{\mathbf{p}} a_{\mathbf{p}}^+ a_{\mathbf{p}},$$
$$H_1 = \tfrac{1}{2}\sum V_{\mathbf{q}} a_{\mathbf{p}}^+ a_{\mathbf{p}'}^+ a_{\mathbf{p}'-\mathbf{q}} a_{\mathbf{p}+\mathbf{q}} \tag{1}$$

(we use a system of units in which $m = \hbar = e^2 = 1$), where $a_{\mathbf{p}}^+$ and $a_{\mathbf{p}}$ are the operators of production and annihilation of particles with momentum $\mathbf{p}$, $\epsilon_{\mathbf{p}} = \mathbf{p}^2/2$, and $V_{\mathbf{q}}$ is the Fourier component of the interaction potential. For particles interacting in accordance with Coulomb's law, we have $V_{\mathbf{q}} = 4\pi/\mathbf{q}^2$. The particle passing through the medium has a mass M and a velocity v. The Hamiltonian of the interaction between the particle and the medium has the form

$$H_i = \sum V_{\mathbf{q}} a_{\mathbf{p}}^+ \alpha_{\mathbf{p}_1-\mathbf{q}}^+ \alpha_{\mathbf{p}_1} a_{\mathbf{p}_1-\mathbf{q}}, \tag{2}$$

where $\alpha_{\mathbf{p}}^+$ and $\alpha_{\mathbf{p}}$ are the operators of production and annihilation of the passing particle.

We consider the particle to be sufficiently fast, $e^2/\hbar v \ll 1$, so that its interaction with the particles of the medium can be treated by perturbation theory. The probability of a transition in which the particle goes from a state with momentum $\mathbf{p}_1 = M\mathbf{v}$ into a state with momentum $\mathbf{p}_1 - \mathbf{q}$, and the medium goes from state n into state m, is given by the known equation

$$w_{\mathbf{q}} = 2\pi \left|\langle m, \mathbf{p}_1 - \mathbf{q} \,|\, H_i \,|\, n, \mathbf{p}_1\rangle\right|^2 \times \delta(E_m - E_n - \varepsilon_{\mathbf{p}_1} + \varepsilon_{\mathbf{p}_1-\mathbf{q}}), \tag{3}$$

$$\langle m, \mathbf{p}_1 - \mathbf{q} \,|\, H_i \,|\, n, \mathbf{p}_1\rangle = V_{\mathbf{q}} \Big(\sum_{\mathbf{p}} a_{\mathbf{p}}^+ a_{\mathbf{p}-\mathbf{q}}\Big)_{mn}. \tag{4}$$

To obtain the total probability of a transition of the particle from a state with momentum $\mathbf{p}_1$ into a state with momentum $\mathbf{p}_1 - \mathbf{q}$ it is necessary to sum expression (3) over all final states of the system and to average over the initial ones with a density matrix

$$\rho = \exp\beta(\Omega + \mu N - H), \qquad \beta = 1/kT. \tag{5}$$

Using (4), we get

$$W_{\mathbf{q}} = 2\pi V_{\mathbf{q}}^2 \Phi_{\mathbf{q}}(\varepsilon_{\mathbf{p}_1} - \varepsilon_{\mathbf{p}_1-\mathbf{q}}), \tag{6}$$

where

$$\Phi_{\mathbf{q}}(\omega) = \sum_{mn} \Big|\Big(\sum_{\mathbf{p}} a_{\mathbf{p}}^+ a_{\mathbf{p}-\mathbf{q}}\Big)_{mn}\Big|^2 e^{\beta(\Omega + \mu N_n - E_n)} \times \delta(E_m - E_n - \omega). \tag{7}$$

3. TWO-PARTICLE GREEN'S FUNCTION

To find $\Phi_{\mathbf{q}}(\omega)$ let us determine its connection with the two-particle Green's function

$$K(\mathbf{r}_1, t_1, \mathbf{r}_2, t_2) = -i\,\mathrm{Sp}\exp[\beta(\Omega+\mu N - H)]$$

$$\times T\{\psi^+(\mathbf{r}_1, t_1)\psi(\mathbf{r}_1, t_1)\psi^+(\mathbf{r}_2, t_2)\psi(\mathbf{r}_2, t_2)\}, \qquad (8)$$

where

$$\psi(\mathbf{r}, t) = e^{-iHt}\sum_{\mathbf{p}} a_{\mathbf{p}} e^{i\mathbf{pr}} e^{iHt}, \qquad \psi^+(\mathbf{r}, t) = e^{-iHt}\sum_{\mathbf{p}} a_{\mathbf{p}}^+ e^{-i\mathbf{pr}} e^{iHt}.$$

We are interested only in such a two-particle function, in which the coordinates and the times of the operators ψ and ψ^+ are pairwise equal. We can obtain for such a function dispersion relations analogous to those obtained by Landau[2] for single-particle Green's functions. It is easy to verify that K depends only on the differences $\mathbf{r} = \mathbf{r}_1 - \mathbf{r}_2$ and $t = t_1 - t_2$. Let us make a Fourier transformation with respect to the variable $\mathbf{r}$

$$K_{\mathbf{q}}(t) = \int d\mathbf{r} e^{-i\mathbf{qr}} K(\mathbf{r}, t)$$

$$= \begin{cases} -i\sum\limits_{mn} e^{\beta(\Omega+\mu N_n - E_n)} \left|\left(\sum\limits_{\mathbf{p}} a_{\mathbf{p}}^+ a_{\mathbf{p}-\mathbf{q}}\right)_{mn}\right|^2 e^{i(E_n - E_m)t}, \\ \hfill t > 0, \\ -i\sum\limits_{mn} e^{\beta(\Omega+\mu N_n - E_n)} \left|\left(\sum\limits_{\mathbf{p}} a_{\mathbf{p}}^+ a_{\mathbf{p}-\mathbf{q}}\right)_{nm}\right|^2 e^{i(E_m - E_n)t}, \\ \hfill t < 0. \end{cases}$$

We interchange the summation indices in the lower sum. Then, using the definition (7) of the function $\Phi_{\mathbf{q}}(\omega)$, we get

$$K_{\mathbf{q}}(t) = \begin{cases} -i\int\limits_{-\infty}^{\infty} d\omega\Phi_{\mathbf{q}}(\omega)\, e^{-i\omega t}, & t > 0, \\ -i\int\limits_{-\infty}^{\infty} d\omega\Phi_{\mathbf{q}}(\omega)\, e^{-\beta\omega}\, e^{-i\omega t}, & t < 0. \end{cases}$$

We now go over to Fourier components in terms of the variable t

$$K(\mathbf{q}, \omega) = \int\limits_{-\infty}^{\infty} dt e^{i\omega t} K_{\mathbf{q}}(t)$$

$$= \int\limits_{-\infty}^{\infty} d\omega'\Phi_{\mathbf{q}}(\omega')\left\{(1 - e^{-\beta\omega'})\,\mathrm{P}\frac{1}{\omega' - \omega}\right.$$

$$\left. + i\pi(1 + e^{-\beta\omega'})\,\delta(\omega' - \omega)\right\}. \qquad (9)$$

The symbol P denotes that the integral is taken in the sense of its principal value. Instead of $K(\mathbf{q}, \omega)$ it is more convenient to consider the function $\widetilde{K}(\mathbf{q}, \omega)$, which is analytic in the upper half plane of the variable ω:

$$\widetilde{K}(\mathbf{q}, \omega) = \int\limits_{-\infty}^{\infty} d\omega'\Phi_{\mathbf{q}}(\omega')\,\frac{1 - e^{-\beta\omega'}}{\omega' - \omega - i\delta}. \qquad (10)$$

Equations (9) and (10) can be used to calculate $\Phi_{\mathbf{q}}(\omega)$:

$$\Phi_{\mathbf{q}}(\omega) = \frac{\mathrm{Im}\,K(\mathbf{q}, \omega)}{\pi[1 + \exp(-\beta\omega)]} = \frac{\mathrm{Im}\,\widetilde{K}(q, \omega)}{\pi[1 - \exp(-\beta\omega)]}. \qquad (11)$$

To calculate $\widetilde{K}$ we use the technique employed by Abrikosov, Gor'kov, and Dzyaloshinskiĭ[3] to find single-particle functions. For this purpose we consider the function

$$\mathscr{K}(\mathbf{r}_1, \tau_1, \mathbf{r}_2, \tau_2) = \mathrm{Sp}\, e^{\beta(\Omega+\mu N - H)}\, T$$

$$\times\{\overline{\psi}(\mathbf{r}_1, \tau_1)\psi(\mathbf{r}_1, \tau_1)\overline{\psi}(\mathbf{r}_2, \tau_2)\psi(\mathbf{r}_2, \tau_2)\}, \qquad (12)$$

$$\psi(\mathbf{r}, \tau) = e^{-(\mu N - H)\tau}\sum_{\mathbf{p}} a_{\mathbf{p}} e^{i\mathbf{pr}} e^{(\mu N - H)\tau},$$

$$\overline{\psi}(\mathbf{r}, \tau) = e^{-(\mu N - H)\tau}\sum_{\mathbf{p}} a_{\mathbf{p}}^+ e^{i\mathbf{pr}} e^{(\mu N - H)\tau}.$$

The value of $\mathscr{K}$, like that of K, depends only on the differences $\mathbf{r} = \mathbf{r}_1 - \mathbf{r}_2$ and $\tau = \tau_1 - \tau_2$; therefore, after transformations analogous to those made with the function $K(t)$, we get

$$\mathscr{K}(\mathbf{q}, \tau) = \begin{cases} \int\limits_{-\infty}^{\infty} d\omega\Phi_{\mathbf{q}}(\omega)\, e^{-\omega\tau}, \; \tau > 0, \\ \int\limits_{-\infty}^{\infty} d\omega\Phi_{\mathbf{q}}(\omega)\, e^{-\omega(\beta+\tau)}, \; \tau < 0. \end{cases} \qquad (13)$$

We shall detail below a method of calculating the function $\mathscr{K}$ in the interval $-\beta < \tau < \beta$. We shall show how, knowing $\mathscr{K}$ in this region, we can find the function $\Phi_{\mathbf{q}}(\omega)$. We shall assume that $\mathscr{K}(\tau)$ is given by (13) in the intervals $0 < \tau < \beta$, and is continued periodically outside this interval. Then the coefficients of its Fourier expansion are determined from

$$\mathscr{K}_n = \int\limits_0^{\beta}\mathscr{K}(\mathbf{q}, \tau)\exp(2\pi i n\tau/\beta)\, d\tau.$$

Inserting the value of $\mathscr{K}(\mathbf{q}, \tau)$ from (13) and integrating with respect to τ we obtain

$$\mathscr{K}_n(\mathbf{q}) = \int\limits_{-\infty}^{\infty} d\omega\Phi_{\mathbf{q}}(\omega)\,\frac{1 - e^{-\beta\omega}}{\omega - 2\pi i n/\beta}. \qquad (14)$$

A direct comparison of (10) and (14) shows that

$$\mathscr{K}_n(\mathbf{q}) = \widetilde{K}(\mathbf{q}, 2\pi i n/\beta). \qquad (15)$$

Equation (15) yields the function $\widetilde{K}(\mathbf{q}, \omega)$ for several values of the argument $\omega = 2\pi i n/\beta$. In addition, it is known that the function $\widetilde{K}(\mathbf{q}, \omega)$ is analytic in the upper half plane, and is therefore uniquely determined from its values at the indicated infinite set of points. Knowing the function $\widetilde{K}(\mathbf{q}, \omega)$ on the real axis, it is possible to find $\Phi_{\mathbf{q}}(\omega)$ from Eq. (11).

We can also calculate $K(\mathbf{q}, \tau)$ by the diagram technique. We introduce the following operators in the interaction representation

$$a_{\mathbf{p}}(\tau) = a_{\mathbf{p}} e^{-(\varepsilon_{\mathbf{p}}-\mu)\tau}, \quad \overset{+}{a}_{\mathbf{p}}(\tau) = \overset{+}{a}_{\mathbf{p}} e^{(\varepsilon_{\mathbf{p}}-\mu)\tau},$$

$$H_1(\tau) = e^{H_0\tau} H_1 e^{-H_0\tau}.$$

In Eq. (12) we go in the usual manner from the operators in the Heisenberg representation to operators in the interaction representation. In the region $0 < \tau_1 < \beta$, $0 < \tau_2 < \beta$ we obtain

$$\mathscr{K}(\mathbf{q}, \tau_1 - \tau_2) = \mathrm{Sp}\, e^{\beta(\Omega+\mu N - H_0)}$$

$$\times T\Big\{ \sum_{\mathbf{p}_1, \mathbf{p}_2} \overset{+}{a}_{\mathbf{p}_1}(\tau_1)\, a_{\mathbf{p}_1-\mathbf{q}}(\tau_1)\, \overset{+}{a}_{\mathbf{p}_2}(\tau_2)\, a_{\mathbf{p}_2+\mathbf{q}}(\tau_2)$$

$$\times \exp\Big[-\int_0^\beta H_1(\tau)\, d\tau\Big]\Big\}. \tag{16}$$

The factor $\exp\left[-\int_0^\beta H_1(\tau)\, d\tau\right]$ can be expanded in powers of H_1. Inserting this expansion into (16), we obtain an expansion of $\mathscr{K}(\mathbf{q}, \tau)$ in powers of the interaction. Each term of the expansion can be represented by a diagram. Corresponding to each dotted line on the diagram is a factor $V_{\mathbf{q}}$, and to each solid line there corresponds a null Green's function of the particle

$$G(\mathbf{p}, \tau) = \begin{cases} (1 \mp n_{\mathbf{p}})\, e^{-(\varepsilon_{\mathbf{p}}-\mu)\tau}, & \tau > 0, \\ \mp n_{\mathbf{p}}\, e^{-(\varepsilon_{\mathbf{p}}-\mu)\tau}, & \tau < 0, \end{cases} \tag{17}$$

$$n_{\mathbf{p}} = [e^{(\varepsilon_{\mathbf{p}}-\mu)\beta} \pm 1]^{-1}.$$

The upper sign pertains to Fermi particles and the lower one to Bose particles. The function $\mathscr{K}(\mathbf{q}, \tau)$ is represented by the sum of all the connected graphs that have two outer vertices. Two solid lines with momenta that differ by $\mathbf{q}$ meet at each of these vertices. Several first-order diagrams are shown in the figure.

Calculation of the probability of a transition by considering the interaction of the particle with the medium as paired collisions between the passing particle and the particles of the medium is equivalent to taking into account only the simplest diagram a in calculating the function $\mathscr{K}$. In the case of a plasma, such a method gives for the decelerating ability an expression that diverges logarithmically at small $\mathbf{q}$. To eliminate this divergence it is necessary to take into account the screening action of the medium, i.e., more complicated graphs. Terms expressed by the graphs b or d contain factors $V_{\mathbf{q}} = 4\pi/\mathbf{q}^2$ and therefore become comparable at small $\mathbf{q}$ with the term represented by graph a. Let us segregate all the graphs that contain $V_{\mathbf{q}}$; for this purpose we denote by $\Pi(\mathbf{q}, \tau)$ the set of the compact parts of the function $\mathscr{K}$, i.e., those containing no parts that are connected only by one dotted line. Examples of such graphs are a, c, f, and g. The function $\mathscr{K}(\mathbf{q}, \tau)$ is related to $\Pi(\mathbf{q}, \tau)$ by the integral equation

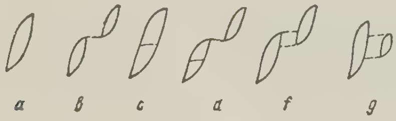

$$\mathscr{K}(\mathbf{q}, \tau) = \Pi(\mathbf{q}, \tau) + \int_0^\beta d\tau'\, \Pi(\mathbf{q}, \tau - \tau')\, V_{\mathbf{q}}\, \mathscr{K}(\mathbf{q}, \tau'). \tag{18}$$

Expanding in a Fourier series in τ and solving the resultant algebraic equation, we find

$$\mathscr{K}_n(\mathbf{q}) = \frac{\Pi_n(\mathbf{q})}{1 - V_{\mathbf{q}}\Pi_n(\mathbf{q})},$$

$$\text{where } \Pi_n(\mathbf{q}) = \int_0^\beta \Pi(\mathbf{q}, \tau) \exp\left(\frac{2\pi i n \tau}{\beta}\right) d\tau.$$

Inserting the expression obtained for $K_n(\mathbf{q})$ in (15) we get

$$\widetilde{K}(\mathbf{q}, \omega) = \Pi(\mathbf{q}, \omega) / [1 - V_{\mathbf{q}}\Pi(\mathbf{q}, \omega)], \tag{19}$$

where $\Pi(\mathbf{q}, \omega)$ is a function analytic in the upper half plane of the variable ω, which coincides with $\Pi_n(\mathbf{q})$ at the points $\omega = 2\pi i n/\beta$.

For the transition probability we obtain from Eqs. (6), (11), and (19)

$$W_{\mathbf{q}} = \frac{2V_{\mathbf{q}}^2}{1 - \exp(-\beta\omega)} \operatorname{Im} \frac{\Pi(\mathbf{q}, \omega)}{1 - V_{\mathbf{q}}\Pi(\mathbf{q}, \omega)}, \tag{20}$$

where $\omega = \epsilon_{\mathbf{p}_1} - \epsilon_{\mathbf{p}_1 - \mathbf{q}}$.

In the derivation of (20) we made no use of the properties of the medium, but the function $\Pi(\mathbf{q}, \omega)$ can be calculated only in limiting cases. For a sufficiently rarefied plasma and for a low-temperature electron gas of high density, it is possible to restrict the calculations to the term shown in graph a. From Eq. (17) we obtain in these cases by simple calculation

$$\Pi(\mathbf{q}, \omega) = -\int \frac{d^3p}{(2\pi)^3} \frac{n_{\mathbf{p}+\mathbf{q}/2} - n_{\mathbf{p}-\mathbf{q}/2}}{(\mathbf{pq}) - \omega - i\delta}. \tag{21}$$

For a rarefied plasma, the most important additions to Eq. (21) are represented by graphs of type f or g; their ratio to the principal term is on the order of $\sqrt{\beta^3 e^3 n}$. Thus, formula (21) is valid every time that the Debye theory is valid. At low temperatures the greatest correction is determined by the graph c; in this case the expansion parameter is the usual parameter of perturbation theory, $e^2 m/\hbar p_0$, where p_0 is the limiting momentum of the limiting momentum of the Fermi surface, connected with the particle density n by

$$n = p_0^3 / 3\pi\hbar^3. \qquad (22)$$

4. PLASMA OSCILLATIONS

The spectrum and the damping of collective excitations that represent the density oscillations are determined by the poles of the function $\widetilde{K}(\mathbf{q}, \omega)$ in the lower half plane. From (19) we obtain an equation for the spectrum

$$1 = V_{\mathbf{q}} \Pi(\mathbf{q}, \omega). \qquad (23)$$

Equation (23), with account of (21), is the same equation that Klimontovich and Silin[4] obtained with the aid of the quantum-kinetic equation. At small $\mathbf{q}$ we have

$$\Pi(\mathbf{q}, \omega) = n\mathbf{q}^2 / \omega^2. \qquad (24)$$

Inserting this expression into (23), we obtain the Langmuir spectrum

$$\omega = \omega_0, \qquad \omega_0^2 = 4\pi n e^2 / m, \qquad (25)$$

where the electron density is

$$n = (2\pi)^{-3} \int n_p d^3 p.$$

The damping of the excitations is determined by the imaginary part of ω, which can be found by calculating the imaginary part of $\Pi(\mathbf{q}, \omega)$. Calculation of $\operatorname{Im}\Pi(\mathbf{q}, \omega)$ from Eq. (21) leads to zero damping at zero temperature, and yields at high temperatures

$$\operatorname{Im}\omega = -\frac{(2\pi\beta)^{3/2}}{8\pi} \frac{\omega_0^4}{q^3} \exp\left(-\frac{\beta\omega_0^2}{2q^2}\right), \qquad (26)$$

which agrees with the expression derived by Landau.[5] Taking account of higher-order terms in $\Pi(\mathbf{q}, \omega)$ which are represented by graphs of type f or g, it is possible to determine the damping due to the viscosity of the electron gas. It is present at zero temperature and drops more slowly with diminishing q at high temperature, although at $q^2 \sim \beta\omega_0^2$ this damping is much less than that calculated from Eq. (26).

5. DECELERATING ABILITY OF PLASMA

The energy lost by a passing particle per unit time is given by

$$dE / dt = (2\pi)^{-3} \int (\varepsilon_{p_1} - \varepsilon_{p_1 - \mathbf{q}}) W_{\mathbf{q}} d^3 q.$$

Inserting into this equation the value of $W_{\mathbf{q}}$ from (20) and $V_{\mathbf{q}} = 4\pi/q^2$ we get

$$-\frac{dE}{dt} = 8 \int_0^\infty dq \int_{-1}^{1} dx \frac{\omega}{1 - \exp(-\beta\omega)} \operatorname{Im} \frac{\Pi(q, \omega)}{q^2 - 4\pi\Pi(q, \omega)}, \qquad (27)$$

where

$$x = \mathbf{vq} / vq, \qquad \omega = \varepsilon_{p_1} - \varepsilon_{p_1 - q} = vqx - q^2 / 2M,$$

v is the velocity and M the mass of the passing particle.

We consider the case when the particle moves with a velocity much greater than the mean thermal velocity of the electrons. The integral in (27) is broken up into two regions, $q > q_1$ and $q < q_1$, with q_1 chosen such that $1/\beta \gg q_1^2 \gg \kappa^2$, where

$$\kappa^2 = -4\pi\Pi(q, 0) = 4\pi\beta n e^2 \qquad (28)$$

(κ is the reciprocal of the Debye radius). In the first region we can neglect $4\pi\Pi(\mathbf{q}, \omega)$ compared with q^2, since Π is always of the order of κ^2. We calculate $\operatorname{Im}\Pi$ from Eq. (21)

$$\operatorname{Im}\Pi = n \frac{(2\pi\beta)^{1/2}}{2q} [1 - e^{-\beta\omega}] \exp\left\{-\frac{\beta}{2}\left(\frac{\omega}{q} - \frac{q}{2}\right)^2\right\}. \qquad (29)$$

Inserting this expression into (27) we get

$$-\frac{dE}{dt}\bigg|_1 = 4n(2\pi\beta)^{1/2} \int_{q_1}^\infty dq \int_{-1}^{1} dx \frac{vx - q/2M}{q^2} \cdot$$
$$\times \exp\left\{-\frac{\beta}{2}\left(vx - \frac{q}{2}\frac{M+1}{M}\right)\right\}. \qquad (30)$$

Neglecting terms on the order $(v_e/v)^2$ (v_e is the mean thermal velocity of the electron), we have

$$-\frac{dE}{dt}\bigg|_1 = \frac{4\pi n}{v} \ln \frac{2Mv}{q_1(M+1)}.$$

In the integral in the second region, $q < q_1$, we can put $\omega = vqx$ and go from integration with respect to x to integration with respect to ω:

$$-\frac{dE}{dt}\bigg|_2 = 8 \int_0^{q_1} \frac{dq}{vq} \operatorname{Im} \int_{-vq}^{vq} \frac{\omega d\omega}{1 - \exp(-\beta\omega)} \frac{\Pi(q, \omega)}{q^2 - 4\pi\Pi(q, \omega)}. \qquad (31)$$

In calculating the integral with respect to ω we make use of the fact that the integrand function differs from the function $\widetilde{K}(q, \omega)$ only by a multiplicative factor and is therefore analytic in the upper half-plane of the variable ω. We modify the contour integration in the upper half plane in such a way that the points $-vq$ and vq are joined not by the real axis but by a semicircle of radius vq with its center at the origin. On this contour $|\omega| = vq \gg v_e q$ and therefore, again neglecting terms of the order $(v_e/v)^2$, we use Eq. (24) for $\Pi(q, \omega)$. The integral with respect to ω in (31) becomes

$$\int \frac{d\omega}{1-\exp(-\beta\omega)} \frac{n\omega}{\omega^2-\omega_0^2}$$

The integrand is analytic in the upper half-plane, and we can therefore shift the contour back to the real axis, going around the poles $\omega = \pm\omega_0$ on the real axis from above. The imaginary part of this integral, which is of interest to us, is due to the detouring of these poles. When $vq < \omega_0$ it vanishes since the ends of the contour lie between the poles, and when $vq > \omega_0$ the imaginary part equals $\pi/2$. Inserting this into (31) we get

$$-(dE/dt)|_2 = 4\pi n \ln(vq_1/\omega_0).$$

Adding this expression to that obtained earlier for $(dE/dt)|_1$, we obtain an expression for the total losses:

$$-\frac{dE}{dt} = \frac{4\pi ne^4}{mv} \ln \frac{2Mm^{3/2}v^2}{\hbar(M+m)\sqrt{4\pi ne^2}} \tag{32}$$

This equation was obtained by Akhiezer and Sitenko[1] accurate to within a logarithmic factor. The numerical factor given in Eq. (25) of that reference, however, contains an incorrect multiplier, 1.23, under the logarithm sign.

In this expression for the total losses, the component due to paired collisions can be separated from the component due to radiation of plasma waves only with logarithmic accuracy. Collisions in which the momentum transferred is much greater than the reciprocal Debye radius can be considered paired and their contribution is

$$-dE/dt = (4\pi ne^4/mv)\ln(mv/\hbar\varkappa).$$

When $\operatorname{Im}\Pi$ is small, the contribution to dE/dt produces in the integrand of Eq. (27) a pole located in the lower half plane near the real axis. These losses are due to radiation of long-lived plasma waves, the spectrum of which is determined by the pole of the integrand, i.e., by Eq. (23). Such waves can be considered excited as long as their damping, given by Eq. (26), is small compared with their frequency, i.e., when $q \ll \kappa$. Thus, the losses connected with their emission are

$$-dE/dt = (4\pi ne^4/mv)\ln(v/v_e).$$

Equation (32) shows that the total losses of a fast particle in a plasma are independent of the temperature. It can be verified that Eq. (32) is correct for any electron velocity distribution, provided the electrons can be considered free and their mean velocity is much less than the velocity of the passing particle. In particular, Eq. (32) is valid for energy losses in a high-density electron gas at zero temperature. It is interesting to note that since, in the first order of magnitude relative to $e^2/\hbar v_e$, there is no damping of the plasma waves in this case, it is possible to determine the losses connected with the radiation of the plasma waves not with logarithmic accuracy, but accurate to terms of order $e^2/\hbar v_e$. These losses are determined by the contribution of the pole, located on the real axis, of the integrand of Eq. (27). We must go around this pole from above, and therefore

$$-\frac{dE}{dt}\bigg|_{\mathrm{pl}} = 8\pi\int_0^\infty dq \frac{\omega dx}{1-\exp(-\beta\omega)} \Pi(q,\omega)\,\delta(q^2-4\pi\Pi(q,\omega)).$$

A substantial contribution to this integral is made by the region of small $q \sim \sqrt{p_0} \ll p_0$. It is therefore possible to assume $\omega = vqx$ and to replace the difference in the numerator of Eq. (21) for $\Pi(\mathbf{q}, vqx)$ by the derivative, $n_{\mathbf{p}+\mathbf{q}/2} - n_{\mathbf{p}-\mathbf{q}/2} = (\partial n_{\mathbf{p}}/\partial p)\mathbf{pq}/p$. In this case Π is independent of q and is a function of x:

$$\Pi = \frac{p_0}{\pi^2}\left(1-\frac{vx}{p_0}\ln\frac{vx+p_0}{vx-p_0}\right).$$

It is necessary to integrate with respect to x in the limits from p_0/v to 1, for when $x < p_0/v$ the imaginary part of Π differs from zero. The integration is elementary and when $v \gg v_e$ we get

$$-\frac{dE}{dt}\bigg|_{\mathrm{pl}} = \frac{4\pi ne^4}{mv}\left(\ln\frac{mv}{2p_0}+\frac{4}{3}\right). \tag{33}$$

If the decelerating particle is an electron, the numerical factor in the argument of the logarithm in (32) should be modified because of the influence of the exchange effect. Formally, this effect manifests itself in the fact that now the interaction Hamiltonian (2) becomes

$$H_i = \frac{1}{2}\sum_{\mathbf{p}\mathbf{p}_1\mathbf{q}} V_{\mathbf{q}} a_{\mathbf{p}}^{+} a_{\mathbf{p}_1-\mathbf{q}}^{+} a_{\mathbf{p}_1} a_{\mathbf{p}-\mathbf{q}}$$

and an additional term $\Sigma_{\mathbf{p}} V_{\mathbf{p}-\mathbf{p}'} a_{\mathbf{p}}^{+} a_{\mathbf{p}-\mathbf{q}}$ appears in the matrix element (4). In addition, an electron that has a large energy after collision should be considered as primary. As is known, allowance for the exchange effect leads to an additional factor $\sqrt{e/8}$ in the argument of the logarithm. Instead of Eq. (32) we obtain the following equation for the slowing down of the electron

$$-\frac{dE}{dt}=\frac{4\pi ne^4}{mv}\left\{\ln\frac{m^{3/2}v^2}{4\hbar\sqrt{2\pi ne^2}}+1\right\}. \qquad (34)$$

Equation (32) can be obtained in the usual manner, by considering collisions with large momentum transfer as paired collisions of particles, and expressing the contribution of transitions with small momentum transfer to the decelerating ability in terms of the dielectric constant of the plasma $\epsilon(\omega) = 1 - (\omega_0/\omega)^2$.

Equation (27) can be used to find the energy lost by particles that do not have too high a velocity. It is easy to obtain a correction of order $(v_e/v)^2$ for Eq. (31). For this purpose it is necessary to calculate the integral in Eq. (30) with accuracy to terms of order $(v_e/v)^2$. We can no longer use the limiting value (24) for $\Pi(q, \omega)$ in Eq. (31), but must put

$$\Pi(q,\omega)=(nq^2/\omega^2)(1+3q^2/\beta\omega^2). \qquad (35)$$

The integrand of (31), with the value of $\Pi(q, \omega)$ from Eq. (35), has a pole in the upper half-plane, and this must be taken into account in evaluating the integral. The final formula for the losses has the form

$$-\frac{dE}{dt}=\frac{4\pi ne^4}{mv}\left\{\ln\frac{2Mmv^2}{(M+m)\hbar\omega_0}-\frac{2M+3m}{Mm\beta v^2}\right\}. \qquad (36)$$

It is also interesting to examine another limiting case, when a heavy particle moves with a velocity much lower than the thermal velocity of the electrons, $v \ll v_e$, but greater than the mean velocity of the ions, $v \gg v_i$, and sufficiently large to satisfy the perturbation-theory criterion $e^2/\hbar v \ll 1$. In this case it is more convenient to rewrite Eq. (27) as

$$-\frac{dE}{dt}=8\int_0^\infty dq\int_{-1}^{1}dx\,\frac{\omega}{1-\exp(-\beta\omega)}\,\frac{q^2\,\mathrm{Im}\,\Pi}{|q^2-4\pi\Pi|^2}. \qquad (37)$$

We express $\mathrm{Im}\,\Pi$ in terms of (29), allowing for contributions from both electrons and ions. The expression for $\Pi(q, \omega)$ contained in the denominator can be replaced, neglecting terms of order $(v/v_e)^2$, by $\Pi(q, 0)$, which is expressed in terms of the Debye radius with the aid of Eq. (28). It is necessary to account here only for the electron loops. Allowance for the ion loop leads to a correction on the order of $(v_i/v)^2$. Equation (37) becomes

$$-\frac{dE}{dt}=4(2\pi\beta)^{1/2}\int_0^\infty dq\,\frac{q^2}{(q^2+\varkappa^2)^2}\int_{-1}^{1}dx\left(vx-\frac{q}{2M}\right)$$
$$\times\left\{n_e\left[-\frac{\beta}{2m}\left(vx-\frac{q}{2m}\right)^2\right]\right.$$
$$\left.+n_i\exp\left[-\frac{\beta}{2M_i}\left(vx-q\,\frac{M+M_i}{2MM_i}\right)^2\right]\right\}. \qquad (38)$$

Equation (38) can be obtained by considering paired collisions of particles, interacting as $\exp(-\kappa r)/r$. This equality holds because the fast electrons have a chance to screen the field of the slower particle. The mean field of the particle moves together with the particle, without slowing down, and therefore in this limiting case the radiation of the plasma waves does not contribute to the energy loss.

Neglecting terms of order of $(v_i/v)^2$, we obtain for the losses in collisions with ions

$$-\frac{dE}{dt}\bigg|_i=\frac{4\pi n_ie^4}{M_iv}\left\{\ln\frac{MM_iv}{(M+M_i)\hbar\varkappa}-\frac{1}{2}\right\}. \qquad (39)$$

We calculate the losses due to collisions with electrons, neglecting terms of order $(v/v_e)^2$ and $(m/M)(v_e/v)^2$

$$-\frac{dE}{dt}\bigg|_e=\frac{2}{3}(2\pi\beta)^{1/2}\beta v^2n_ee^4\{\ln(8m/\beta\hbar^2\varkappa)-C-1\}, \qquad (40)$$

where $C = 0.58$ is Euler's constant. Equations (39) and (40) contain the reciprocal Debye radius κ, which is determined from Eq. (28) and differs from the corresponding value used in thermodynamic functions in that it is expressed only in terms of the electron density, rather than the density of all charged particles.

In conclusion I thank V. M. Galitskiĭ and A. B. Migdal for valuable advice.

---

[1] A. I. Akhiezer and A. G. Sitenko, J. Exptl. Theoret. Phys. (U.S.S.R.) **23**, 161 (1952).

[2] L. D. Landau, J. Exptl. Theoret. Phys. (U.S.S.R.) **34**, 262 (1958), Soviet Phys. JETP **7**, 182 (1958).

[3] Abrikosov, Gor'kov, and Dzyaloshinskiĭ, J. Exptl. Theoret. Phys. (U.S.S.R.) **36**, 900 (1959), Soviet Phys. JETP **9**, 636 (1959).

[4] Yu. L. Klimontovich and V. P. Silin, J. Exptl. Theoret. Phys. (U.S.S.R.) **23**, 151 (1952).

[5] L. D. Landau, J. Exptl. Theoret. Phys. (U.S.S.R.) **16**, 574 (1946).

Translated by J. G. Adashko
39

SOVIET PHYSICS JETP VOLUME 37(10), NUMBER 1 JANUARY, 1960

COLLECTIVE LOSSES OF FAST ELECTRONS IN PASSAGE THROUGH MATTER

V. P. SILIN

P. N. Lebedev Physics Institute, Academy of Sciences, U.S.S.R.

Submitted to JETP editor February 23, 1959

J. Exptl. Theoret. Phys. (U.S.S.R.) **37**, 273-282 (July, 1959)

The energy losses of fast electrons passing through thin films are considered from the viewpoint of the theory developed by Frank, Tamm, and Fermi,[1] taking into account spatial dispersion of the dielectric constant.[2] An expression is derived for the longitudinal dielectric constant which takes account of exchange effects in a high density electron gas. The phenomenological theory developed by Landau[3] is used to determine the longitudinal and transverse dielectric constants of a degenerate electron fluid. It is shown that these quantities have singularities corresponding to the propagation of zero sound. The fast-electron losses associated with the excitation of both transverse and longitudinal zero sound are discussed. The dependence of the discrete losses on the scattering angle of fast particles in passage through optically anisotropic bodies is considered.

1. The passage of fast electrons through thin films is characterized by so-called characteristic or discrete energy losses.[4] The electrons lose energy in discrete amounts or quanta; in certain cases this effect results in clearly defined spectral loss lines. The connection pointed out by Bohm and Pines between the characteristic losses and the collective oscillations of electrons in a solid body[5] is important for an understanding of the nature of these losses. The excitation of these collective oscillations corresponds to the radiation of electromagnetic waves in the medium by the charged particle. In absorbing media these waves decay rapidly and there is a transfer of energy from the fast particle to the medium via the collective oscillations. In general, longitudinal electromagnetic fields can be set up in addition to the transverse fields. It is these longitudinal oscillations which are responsible for the collective polarization losses of fast electrons.

A theory for the energy losses of fast particles, based on the excitation of electromagnetic fields in a medium has been developed by Frank and Tamm in connection with the theory of Cerenkov radiation and by Fermi in connection with polarization losses (cf. reference 1). This theory was extended by Fröhlich and Pelzer[6] in order to analyze discrete losses. In this analysis the position of the loss lines is determined by the zeros of the dielectric constant $\epsilon(\omega)$ corresponding to longitudinal oscillations of the electromagnetic field. A more precise formula for the loss line is

$$\operatorname{Im}\frac{1}{\varepsilon(\omega)} = \frac{2n\varkappa}{(n^2+\varkappa^2)^2},$$

where n is the refractive index and κ is the absorption constant.[*]

A theory for the energy losses of fast charged particles which takes account of spatial dispersion, which is a generalization of the theory developed by Frank, Tamm, and Fermi, has been developed by a number of authors.[2][†]

Spatial dispersion means that in an isotropic medium the dielectric constant becomes a tensor, assuming the form

---

[*] The macroscopic theory developed by Frank and Tamm, and Fermi for fast charged particles applies only when the impact parameters for the collisions between the fast electrons in the medium are much greater than the interatomic distances. However, this condition no longer holds when the fast-electron scattering angle becomes large compared with the velocity ratio v_0/v (v_0 is the velocity of the electrons in the medium and v is the velocity of the fast electrons).

It has been found experimentally that in scattering at such angles the energy associated with the discrete losses becomes a function of the scattering angle.[7] According to the microscopic theory[8,9] for longitudinal oscillations of the electromagnetic field (i.e., plasma oscillations) this angular dependence is natural since it indicates the dependence of the frequency of the longitudinal oscillations on wavelength. In the language of the macroscopic electrodynamic equations for a medium this corresponds to spatial dispersion of the dielectric permittivity (cf., for example, reference 10).

[†] This work is very similar to that in which various concrete models are used to represent the medium; however, no connection has been established between particle energy losses and the dielectric constant.[8,11]

$$\varepsilon_{ij}(\omega, \mathbf{k}) = \varepsilon^{tr}(\omega, k)\left\{\delta_{ij} - \frac{k_i k_j}{k^2}\right\} + \frac{k_i k_j}{k^2}\varepsilon^l(\omega, k), \qquad (2)$$

where ϵ^{tr} and ϵ^l are the transverse and longitudinal dielectric constants. Using Eq. (2), we obtain the following expression for the energy losses of a fast charged particle in passage through a medium (per unit path length)

$$W = \frac{ie^2Z^2}{\pi v^2}\int_{-\infty}^{+\infty}\omega d\omega\int_0^{\infty} q dq\, \frac{1}{q^2+\omega^2/v^2}\left\{\frac{1}{\varepsilon^l(\omega, \sqrt{q^2+\omega^2/v^2})}\right.$$

$$\left. - \frac{v^2}{c^2}\frac{q^2}{q^2+\omega^2[v^{-2} - c^{-2}\varepsilon^{tr}(\omega, \sqrt{q^2+\omega^2/v^2})]}\right\}, \qquad (3)$$

where Ze is the charge of the particle and v is its velocity. The first term in the curly brackets is responsible for the radiation of longitudinal waves while the second is responsible for the transverse Cerenkov radiation. Since the usual collective losses for fast electrons are associated with the excitation of longitudinal waves, in what follows we will concentrate our attention on the first term in Eq. (3).

From Eq. (2) we obtain the following expression for the scattering probability of a fast particle through an angle $d\theta$ with the emission of a longitudinal photon (plasmon) in the frequency interval $d\omega$ (per unit path length):

$$\frac{dW^l}{\hbar\omega\, d\Omega\, d\omega} = \frac{2e^2Z^2}{\pi\hbar v^2}\frac{1}{\theta^2+(\hbar\omega/vp)^2}\,\mathrm{Im}\,\frac{1}{\varepsilon^l(\omega, \sqrt{(p\theta/h)^2+(\omega/v)^2})}, \qquad (4)$$

where p is the momentum of the particle and it is assumed that $\theta \ll 1$.*

Since the experimentally measured quantity is $\mathrm{Im}\{1/\epsilon^l(\omega, k)\}$, it is this quantity which must be predicted by a collective-loss theory that uses a model to describe the behavior of the electrons in the medium. Below we obtain expressions for ϵ^l for a high-density electron gas and for an electron liquid and also discuss certain features of the energy losses of fast particles due to the excitation of zero sound.

2. The most detailed studies of the longitudinal dielectric constant of a degenerate electron gas have been carried out in the self-consistent Hartree approximation.[2,8,9,12] In this analysis, in the long wavelength region, where spatial dispersion may be neglected, we have

$$\varepsilon^l(\omega, k) = 1 - \omega_0^2/\omega^2 - 3p_0^2k^2/5m^2\omega^2, \qquad (5)$$

where p_0 is the momentum at the Fermi surface.

However, the self-consistent field approximation is valid only for a degenerate electron gas of high density.[12,13] Because real electron densities in solid bodies are not very great, it is convenient to determine the corrections to the work in reference 5 by means of an expansion in inverse powers of the density. The exchange correction can be obtained if we use the Hartree-Fock approximation instead of the Hartree self-consistent field.[8,9] In this case the electron distribution function is given by the equation[13,14]

$$\frac{\partial\delta f}{\partial t} + \frac{\mathbf{p}}{m}\frac{\partial\delta f}{\partial\mathbf{r}} + \frac{1}{2}\int d\mathbf{p}'\frac{4\pi e^2\hbar^2}{|\mathbf{p}-\mathbf{p}'|^2}\left[\frac{\partial f_0}{\partial\mathbf{p}}\frac{\partial}{\partial\mathbf{r}}\delta f(\mathbf{p}', \mathbf{r}) - \frac{\partial f_0}{\partial\mathbf{p}'}\frac{\partial}{\partial\mathbf{r}}\delta f(\mathbf{p}, \mathbf{r})\right]$$

$$+ e\mathbf{E}\frac{\partial f_0}{\partial\mathbf{p}} = 0, \qquad (6)$$

where δf is the non-equilibrium correction to the distribution function, f_0 is the equilibrium distribution function for an ideal Fermi gas, and E is the electric field, which is given by the equation

$$\operatorname{div}\mathbf{E} = 4\pi e\int d\mathbf{p}\,\delta f. \qquad (7)$$

We assume that the wavelengths are large compared with the distances between particles.

In order to determine the longitudinal dielectric constant by means of Eq. (6), it is necessary to express δf in terms of the electric field (the dependence of the field on coordinates and time is of the form $e^{-i\omega t + i\mathbf{kr}}$); then, from Eq. (7) we have

$$4\pi e\int d\mathbf{p}\,\delta f = \{1 - \varepsilon^l(\omega, k)\}\, i\mathbf{k}\mathbf{E}, \qquad (8)$$

whence ϵ^l can be found. In the long-wavelength region the quantity being sought can be given as an expansion in powers of k. It is not difficult to show that Eqs. (7) and (8) yield:

$$\varepsilon^l(\omega, k) \approx 1 - \frac{\omega_0^2[1 + {}^3/_5(v_0k/\omega^2)]}{\omega^2 + (e^2/3\pi\hbar v_0)v_0^2k^2}$$

$$\approx 1 - \frac{\omega_0^2}{\omega^2}\left\{1 + \frac{3p_0^2k^2}{5m^2\omega^2}\left[1 - \frac{1}{16}\left(\frac{\hbar\omega_0}{p_0^2/2m}\right)^2\right]\right\}. \qquad (9)$$

Here $v_0 = p_0/m$ is the velocity of the electron at the Fermi surface. The small numerical coefficient means that the correction which is found for

---

*We note that taking account of spatial dispersion makes the usual distinction between remote and near losses unnecessary. Thus, for high momentum transfer (near losses) $\hbar k$ is much greater than the characteristic electron momenta and the latter can be considered free electrons; for ε^l we use the expression

$$\varepsilon^l(\omega, k) = 1 - \omega_0^2/[\omega^2 - (\hbar k^2/2m)^2], \qquad (2')$$

where $\omega_0^2 = 4\pi e^2 N/m$ and N is the number of electrons per unit volume. Correspondingly, for large scattering angles (high ratio of the velocity of the electrons in the medium to the velocity of the fast particle, but much smaller than unity) Eq. (4) yields

$$dW^l/\hbar\omega d\Omega d\omega = \delta(\omega - p^2\theta^2/2m\hbar)\, N d\sigma_{\mathrm{Ruth}}/d\Omega, \qquad (4')$$

where $d\sigma_{\mathrm{Ruth}} = (2e^2Z/vp\theta^2)^2 d\Omega$. In other words, the dispersion in the dielectric constant takes account of the usual Rutherford scattering, i.e., near collisions.

the term proportional to k^2 [cf. Eq. (5)] is small even at the densities of valence electrons in real metals; in a favorable case it is 20 – 30%.

The condition for excitation of plasma oscillations corresponds to the vanishing of the quantity ϵ^l. This condition yields the following spectrum for the plasma oscillations:

$$\omega^2 = \omega_0^2 + \frac{3p_0^2k^2}{5m^2} - \omega_0^2 \frac{3}{20}\left(\frac{\hbar k}{p_0}\right)^2. \tag{10}$$

The last relation has been obtained by the author,[13] and later by Nozieres and Pines.[15]

3. We now determine the longitudinal dielectric constant of a degenerate electron liquid, using the theory of a Fermi liquid given by Landau.[3] In accordance with reference 14, we use in place of Eq. (6) the following equation for the non-equilibrium correction to the electron distribution function

$$\frac{\partial}{\partial t}\delta f + \mathbf{v}\frac{\partial}{\partial \mathbf{r}}\left\{\delta f - \frac{\partial f_0}{\partial p}\delta\varepsilon_1\right\} + e\mathbf{E}\mathbf{v}\frac{\partial f_0}{\partial \varepsilon} = 0. \tag{11}$$

Here f_0 is the equilibrium distribution function; it differs from the corresponding distribution function for an ideal gas only in that it is a function of the energy of the quasi-particles $\epsilon(\mathbf{p})$ and not the energy of the free electron;

$$\delta\varepsilon_1(\mathbf{p}, \mathbf{r}) = \int \varphi(\mathbf{p}, \mathbf{p}')\,\delta f(\mathbf{p}', \mathbf{r})\,d\mathbf{p}', \tag{12}$$

where $\varphi(\mathbf{p}, \mathbf{p}')$ is in general an unknown function which reflects the correlation between particles. In obtaining a simple qualitative picture we need not take account of the periodic ion fields. Under these conditions the electron velocity is given by the relation

$$\mathbf{v} \equiv \frac{\partial\varepsilon}{\partial \mathbf{p}} = \frac{\mathbf{p}}{m} + \int d\mathbf{p}'\varphi(\mathbf{p}, \mathbf{p}')\frac{\partial f_0}{\partial \mathbf{p}'}. \tag{13}$$

In principle, using Eq. (8) and the relations given above it is possible to determine $\epsilon^l(\omega, k)$. Without making any assumptions as to the form of the function $\varphi(\mathbf{p}, \mathbf{p}')$, however, we can only determine the longitudinal dielectric constant in the long wavelength region (small k):

$$\varepsilon^l(\omega, k) = 1 - \frac{\omega_0^2}{\omega^2}\left[1 + \frac{3}{5}\frac{v_0p_0}{m\omega^2}k^2\left(1 + \frac{5}{9}A_0 + \frac{4}{45}A_2\right)\right],$$
$$v_0 = (p_0/m)(1 + A_1/3)^{-1}, \qquad p_0 = (3\pi^2)^{1/3}N^{1/3}\hbar. \tag{14}$$

Here p_0 is the electron momentum at the Fermi surface while the coefficients A_l are defined by the expression

$$\frac{2}{(2\pi\hbar)^3}\frac{4\pi p_0^2}{v_0}\varphi(\mathbf{p}_0, \mathbf{p}_0') = \sum_l A_l P_l(\cos\chi), \tag{15}$$

where χ is the angle between the vectors $\mathbf{p}_0$ and $\mathbf{p}_0'$.

Equation (14) for ϵ^l differs from the corresponding expression for an electron gas in the Hartree approximation (5) or the Hartree-Fock approximation (9) by the coefficient for the k^2 term. In the case of an electron liquid the coefficients in the expansion of φ can also be greater than unity. We expect that the region in which the term in Eq. (14) proportional to k^2 may be assumed small will be narrower than the corresponding region for Eqs. (5) and (9). Hence we now consider the longitudinal dielectric constant in the region in which the expansion in powers of k cannot be used.

We assume further that in the expansion in (15) only the first two coefficients A_0 and A_1 are different from zero. In this case Eq. (11) becomes an integral equation with a degenerate kernel and can be solved easily. We obtain

$$\varepsilon^l(\omega, k) = 1 - \frac{3\omega_0^2}{k^2v_0^2}\,\frac{\eta(s)}{(1 + {}^1/_3A_1)[1 - A_0\eta(s)] - A_1s^2\eta(s)}, \tag{16}$$

where

$$\eta(s) = \frac{s}{2}\ln\frac{s+1}{s-1} - 1, \quad s = \frac{\omega}{kv_0}. \tag{17}$$

An important property of the expression which has been obtained for the longitudinal dielectric constant is the singularity which occurs when the denominator in Eq. (16) vanishes

$$(1 + {}^1/_3A_1)[1 - A_0\eta(s)] - A_1s^2\eta(s) = 0. \tag{18}$$

Equation (18) is the dispersion relation for zero sound.[16] Hence the existence of a singularity in (16) is completely understandable: for the value of ω/kv_0 which satisfies Eq. (18) the electromagnetic field can excite zero sound in this case.

The solution of Eq. (18) becomes especially simple in the case in which A_0 is positive and large compared with unity and A_1. In particular, in this case

$$s = \sqrt{A_0/3} \gg 1, \tag{19}$$

while the expression for ϵ^l can be written in the form

$$\varepsilon^l(\omega, k) = 1 - \omega_0^2/(\omega^2 - A_0v_0^2k^2/3). \tag{20}$$

It is interesting to note the similarity between the denominators in (20) and (9) when we do not carry out the expansion in powers of k^2 in the latter. In Eq. (9) the coefficient in front of $v_0^2k^2$ is positive and small compared with unity; the absence of a singularity in Eq. (9) indicates that it is impossible to have zero sound in this case.

The spectrum of plasma oscillations in a degenerate electron liquid has been considered by us earlier.[17,18] Using the results obtained in reference 18 we can obtain an expression for the transverse dielectric constant of the electron liquid. Assuming, as was done in deriving Eq. (16), that all the A_l with $l > 1$ are equal to zero, we have

$$\varepsilon^{tr}(\omega, k) = 1 - \frac{3\omega_0^2}{2\omega^2}\frac{1-(s^2-1)\eta(s)}{1-{}^1/_2 A_1\{({}^1/_3)-(s^2-1)\eta(s)\}}. \qquad (21)$$

The singularity in ϵ^{tr} at

$$1-\frac{1}{2}A_1\left\{\frac{1}{3}-(s^2-1)\eta(s)\right\}=0 \qquad (22)$$

is similar to the corresponding singularity in ϵ^l and provides the possibility of exciting zero sound. The sole difference is that in Eq. (16) we are considering the excitation of longitudinal zero sound while in Eq. (21) we are considering transverse sound (cf. below).

4. For small spatial dispersion the longitudinal dielectric constant assumes the form:

$$\varepsilon^l(\omega, k) = \varepsilon(\omega) - \alpha(k^2/\omega^2). \qquad (23)$$

Equation (23) allows us to write the following expression for the scattering probability of a fast electron with the emission of a longitudinal quantum (per unit path length):

$$\frac{dW^l}{\hbar\omega d\Omega d\omega} = \frac{2e^2}{\pi\hbar v^2}\frac{1}{\theta^2+(\hbar\omega/vp)^2}\operatorname{Im}\frac{1}{\varepsilon(\omega)-\alpha[(p\theta/\hbar\omega)^2+1/v^2]} \qquad (24)$$

The case of small absorption is of special interest; in this case ϵ^l may be considered real. Essentially the same situation arises in the case of Eqs. (5), (9), and (14) for frequencies much larger than the electron collision frequency. Assuming that $\alpha = a(p_0/m)^2$ (a is a numerical factor) we can write Eq. (24) in the form*

$$\frac{dW^l}{\hbar\omega d\Omega d\omega} = \frac{2e^2}{\hbar v^2}\frac{1}{\theta^2+(\hbar\omega/vp^2)}\delta\left[\varepsilon^l\left(\omega, \sqrt{\left(\frac{p\theta}{\hbar}\right)^2+\left(\frac{\omega}{v}\right)^2}\right)\right]$$
$$= \frac{2e^2}{\hbar v^2}\frac{1}{\theta^2+(\hbar\omega/vp)^2}\delta\left[\varepsilon(\omega)-a\left\{\left(\frac{p_0}{p}\right)^2+\left(\frac{p_0 v}{\hbar\omega}\right)^2\theta^2\right\}\right]. \qquad (25)$$

The dependence of the discrete energy lines on the scattering angle given by Eqs. (25) — (26) assumes the following form for an electron gas or an electron liquid:

$$\Delta E(\theta) = \hbar\omega \approx \hbar\omega_0 + (av^2p_0^2/2\hbar\omega_0)\theta^2, \qquad (26)$$

This dependence is apparently observed experimentally.[7] It is clear that the study of this dependence and the precise experimental determination of the coefficient for θ^2 is extremely important in choosing a model to describe electrons in a metal.

We now consider certain of the results obtained above and their consequences for Fermi liquids when the spatial dispersion is not weak. We may note first that ϵ^l as given by Eq. (16) becomes complex $\omega < kv_0$. In other words, one can speak of discrete loss lines and use Eq. (25) only for scattering angles which satisfy the inequality

$$\theta < \hbar\omega/v_0 p. \qquad (27)$$

For large angles a discrete loss line is impossible.*

The dielectric constant in (16) indicates a relatively complicated dependence for the loss line scattering angle in the angular region $\hbar\omega_0/vp_0$. The picture is simplified considerably for large A_0, in which case Eq. (20) holds. The differential scattering probability becomes

$$\frac{dW^l}{\hbar\omega d\Omega d\omega} = \frac{2e^2}{\hbar v^2}\frac{1}{\theta^2+(\hbar\omega/vp)^2}\frac{\omega_0^2\delta\left(\omega-\sqrt{\omega_0^2+(A_0/3)(v_0p\theta/\hbar)^2}\right)}{\sqrt{\omega_0^2+(A_0/3)(v_0p\theta/\hbar)^2}}. \qquad (28)$$

In the angular region

$$\theta \ll \theta_1 = (\hbar\omega_0/v_0p)\sqrt{A_0/3} < \hbar\omega_0/vp_0$$

the results of Eq. (28) are similar to those of Eq. (25). On the other hand, at large values of θ_1 there is an important difference. In this region the energy loss is proportional to the scattering angle $\hbar\omega \approx \sqrt{A_0/3}\, v_0 p\theta$, corresponding to the excitation of zero sound photons (19). This means that in the region $\theta > \theta_1$ the angular distribution for scattering (28) also differs considerably from the corresponding distribution for weak spatial dispersion. In particular, whereas in the region $\theta \ll \theta_1$ [as in the case of Eq. (25)] Eq. (28) gives a distribution proportional to $[\theta^2 + (\hbar\omega/vp)^2]^{-1}$, in the region $\theta \gg \theta_1$, Eq. (28) gives a distribution

$$1/\theta[\theta^2+(\hbar\omega/vp)^2].$$

The strong angular dependence of the discrete losses of the scattered electrons means that the lines for the total losses (integrated over the angle) are relatively wide. Hence attempts to observe the zero sound associated with the radiation losses of fast electrons must be directed toward a study of the angular dependence of the wide lines associated with total energy loss. This does not mean that zero sound is not also associ-

---

*In this we make use of the fact that

$$\lim \operatorname{Im}(\varepsilon^l/|\varepsilon^l|^2) = \pi\delta[\operatorname{Re}\varepsilon^l] \text{ for } \operatorname{Im}\varepsilon^l \to 0.$$

*If the condition $\omega < kv_0$ is satisfied the electrons in the liquid can radiate and absorb quanta of zero sound. This condition is analagous to the condition for Cerenkov radiation. For fast-electron scattering angles which satisfy the relation $\theta > \hbar\omega/v_0p$ the "Cerenkov" mechanism becomes important in the energy dissipation of electrons in the medium; this leads to smearing of the loss line even if the usual dissipation characterized by the imaginary part of $\mathcal{E}(\omega)$ is small.

ated with narrow lines. However, the zero sound effects should be most pronounced for wide lines.

When $A_0 \ll 1$ effects connected with zero sound do not give noticeable broadening of the total-loss lines. For positive A_0 the expression for the zero sound spectrum assumes the form

$$\omega/kv_0 = s = 1 - \exp\{-2/A_0\}. \tag{29}$$

At small A_0 the excitation of zero sound is possible only in a narrow region close to the angle $\theta = \hbar\omega/pv_0$.

5. We now consider one other possibility which leads to a dependence of the discrete losses on the scattering angle, and which is not a result of spatial dispersion. This possibility arises in optically anisotropic bodies. For example, in the motion of a fast nonrelativistic electron along the axis of symmetry a uniaxial crystal the differential scattering probability per unit path length is*

$$\frac{dW(\theta, \omega)}{\hbar\omega\, d\omega\, d\Omega} = \frac{2e^2}{\pi\hbar v} \frac{\mathrm{Im}\,\varepsilon_\perp(\omega)\,\theta^2 + \mathrm{Im}\,\varepsilon_\parallel(\omega)\,(\hbar\omega/vp)^2}{[\mathrm{Re}\,\varepsilon_\perp(\omega)\,\theta^2 + \mathrm{Re}\,\varepsilon_\parallel(\omega)\,(\hbar\omega/vp)]^2 + [\mathrm{Im}\,\varepsilon_\perp(\omega)\theta^2 + \mathrm{Im}\,\varepsilon_\parallel(\omega)(\hbar\omega/vp)]^2}. \tag{30}$$

It is clear that in the case of small absorption, for which we can neglect the imaginary part of ϵ, the discrete loss line is determined by the zeros of the expression

$$\varepsilon_\perp(\omega)\,\theta^2 + \varepsilon_\parallel(\omega)\,(\hbar\omega/vp)^2. \tag{31}$$

For an optically anisotropic medium the quantities $\epsilon_\perp$ and $\epsilon_\parallel$ vanish simultaneously only by coincidence. Hence the zeros of the expression in Eq. (31) are generally functions of the scattering angle θ. Under these conditions, in the small-angle region $\theta \ll \hbar\omega/vp$ the position of the loss line is determined by the frequency at which $\epsilon_\parallel(\omega)$ vanvanishes. On the other hand, for angles $\theta \gg \hbar\omega/vp$ the loss line is determined by the point at which $\epsilon_\perp(\omega)$ vanishes. In the general case of motion of an electron in an optically anisotropic crystal characterized by the tensor ϵ_{ij}, for arbitrary orientation of the direction of motion with respect to the crystallographic axes, in the denominator of Eq. (30), in place of Eq. (31) we have (cf. references 1 and 2) $\epsilon_{ij}k_ik_j$ [where $k_z = \omega/v$, $k_x = (p\theta/\hbar)\cos\varphi$, $k_y = (p\theta/\hbar)\sin\varphi$]. Hence, in addition to the dependence of energy loss on angle there is an azimuthal dependence on the angle φ. The dependence of the energy loss on scattering angle can lead to a broadening of the total (integrated over scattering angle) loss line.† We consider this problem in somewhat greater detail.

According to Eqs. (30) and (31) the total energy loss in the scattering angle region $\theta < \theta_{max}$ can be written as follows for small absorption:

$$\int\limits_{\theta<\theta_{max}} d\Omega(dW/\hbar\omega d\omega d\Omega) = 2\pi e^2/(\hbar v^2|\varepsilon_\perp(\omega)|), \tag{32}$$

for the condition

$$0 < -\varepsilon_\parallel(\omega)/\varepsilon_\perp(\omega) < (vp\theta_{max}/\hbar\omega)^2. \tag{33}$$

This quantity vanishes if this condition is not satisfied. Here $\theta_{max} \sim \hbar\omega/p\bar{v}$, where $\bar{v}$ is the characteristic velocity of electrons in the medium. We assume that $\epsilon_\perp$ and $\epsilon_\parallel$ do not vanish simultaneously.

Thus the line shape is determined by $\epsilon_\perp$ while the line width is given by (33). It is important, as is seen from this condition, that the frequency at which $\epsilon_\perp(\omega) = 0$ lie outside the loss line. If this frequency is far from the edge of the line, the line will be relatively smooth. On the other hand, at high velocities the edge of the loss line may be close to the point at which $\epsilon_\perp(\omega)$ vanishes. In this case the edge of the line will exhibit a sharp narrow peak which will practically obliterate the line. The latter is due to the fact that for angles $\theta \gg \hbar\omega/vp$ the loss line is determined by the point at which $\epsilon_\perp(\omega)$ vanishes. A similar picture holds for the arbitrary orientation of the direction of motion of the fast particle.

6. In considering the losses of relativistic electrons it is necessary to consider the role of transverse quanta, in particular, Cerenkov radiation. In the case of an electron gas the Cerenkov radiation is impossible since the dielectric constant (real part) is less than unity. However the situation is different in an electron liquid. According to Eq. (21) the transverse dielectric constant becomes positive in the region of frequencies and wave vectors which satisfy the condition for the propagation of transverse zero sound (22). In this connection we now consider the discrete transverse losses of relativistic electrons.

Limiting ourselves to small angles ($\theta \ll 1$), from Eq. (2) we have the following expression for the scattering probability of a fast particle per unit length into an angle $d\theta$ with the emission of a transverse quantum in the frequency range $d\omega$:

---

*Strictly speaking, for optically anisotropic bodies the radiation of plasmons is nothing more than the Cerenkov radiation.[10]

†The possibility of broadening of this kind has already been indicated in references 10 and 18.

$$\frac{dW^{tr}}{\hbar\omega d\omega d\Omega} = \frac{2e^2Z^2}{\pi\hbar c^2}\frac{1}{\theta^2 + (\hbar\omega / vp)^2}$$

$$\times \operatorname{Im}\left\{\left[\frac{v^2}{c^2}\varepsilon^{tr}\left(\omega, \sqrt{\left(\frac{p\theta}{\hbar}\right)^2 + \left(\frac{\omega}{v}\right)^2}\right) - 1\right]\left(\frac{\hbar\omega}{pv}\right)^2 - \theta^2\right\}^{-1}. \quad (34)$$

Neglecting absorption we have

$$\frac{dW^{tr}}{\hbar\omega d\omega d\Omega} = \frac{2e^2Z^2}{\hbar c^2}\frac{1}{\theta^2 + (\hbar\omega / vp)^2}$$

$$\times \delta\left\{\left[\frac{v^2}{c^2}\varepsilon^{tr}\left(\omega, \sqrt{\left(\frac{p\theta}{\hbar}\right)^2 + \left(\frac{\omega}{v}\right)^2}\right) - 1\right]\left(\frac{\hbar\omega}{vp}\right)^2 - \theta^2\right\}. \quad (35)$$

The zeros of the argument of the δ-function determine the discrete energy of the Cerenkov photon lost by a fast particle in being scattered through an angle θ.

In the region of the singularity determined by Eq. (22), the transverse dielectric constant (21) assumes the form

$$\varepsilon^{tr}(\omega, k) \approx 1 + \frac{\omega_0^2}{\omega^2}\frac{\gamma}{s - s_0}, \quad (36)$$

where $s = \omega/kv_0$, s_0 is the solution of Eq. (22), and the factor γ is

$$\gamma = \left(1 + \frac{3}{A_1}\right)\frac{s_0(s_0^2 - 1)}{3s_0^2 - 1 - A_1/3}.$$

The argument of the δ-function in Eq. (35) vanishes if we substitute ϵ^{tr} as given by Eq. (36) when

$$\hbar\omega = v_0 p\,[s_0\theta + \gamma(\hbar\omega_0 / cp)^2 / \theta]. \quad (37)$$

Here is assumed that $v \sim c$. In order for the formula to apply the condition $\theta \gg (\hbar\omega_0/cp)$ must be satisfied. Hence the frequency determined by Eq. (37) is only slightly different from the frequency of transverse zero sound. It should be noted that in order to neglect the imaginary part of ϵ^{tr} it is necessary that ω be considerably greater than the collision frequency which determines the dissipation in the electron liquid. The latter condition can be satisfied for scattering angles which are not too small.

Finally we may note that in real solid bodies in addition to the effects of electron correlation an important role is played by the lattice field which can complicate the interpretation of the problems considered above. Hence, from our point of view, most interest attaches to attempts to find experimentally qualitative features connected with zero sound and those derived from the theory of a Fermi liquid.

7. In conclusion we may make general remarks relating to the excitation of zero sound and the more general problem of interpretation of discrete losses. To what degree can one speak of the excitation of a freedom in a solid body — in our case, zero sound, and in the more widely discussed case,[4-7] the levels of individual electrons? In the latter case one considers the transitions of electrons from one level to another and the lines which are thus determined, in the opinion of a number of authors, are in fair agreement with this interpretation. For an answer to this problem we consider as an example the dielectric constant corresponding to one level ω_r:

$$\varepsilon = 1 - \omega_0^2/(\omega^2 - \omega_r^2).$$

The frequency of the longitudinal oscillation determined from the condition $\epsilon = 0$ is $\omega^2 = \omega_0^2 + \omega_r^2$. It is clear that for the level $\omega_r \ll \omega_0$ the existence of the level is unimportant for the determination of the frequency of the longitudinal photon. On the other hand, in the case $\omega_r \gg \omega_0$ the frequency of the longitudinal photon (plasmon) is essentially equal to the frequency of the level. Hence the energy of discrete losses may be close to the corresponding energy of the one-electron transitions.

Similarly, in our case it is possible to speak of the excitation of the longitudinal zero sound only under conditions in which the frequency of the zero sound is considerably greater than the frequency $\omega_0 = \sqrt{4\pi e^2 N/m}$. If this is not the case the frequency of the longitudinal oscillations excited in the medium is considerably different from the frequency of zero sound.

In conclusion I wish to express my gratitude to V. L. Ginzburg and L. D. Landau for a number of useful discussions of the problems considered in the present paper.

---

[1] I. E. Tamm and I. M. Frank, Dokl. Akad. Nauk SSSR, **14**, 107 (1937); E. Fermi, Phys. Rev., **57**, 485 (1940); L. D. Landau and E. M. Lifshitz, Электродинамика сплошных сред (Electrodynamics of Continuous Media), Gostekhizdat, 1957; B. M. Bolotovskiĭ, Usp. Fiz. Nauk **62**, 201 (1957).

[2] J. Lindhard, Det Kong. Dan. Vid. Salsk, Dan. Mat.-Fys. Medd. **28**, 8 (1954); J. Hubbard, Proc. Phys. Soc. **A68**, 441, 977 (1955); J. Neufeld and R. H. Ritchie, Phys. Rev. **98**, 1632 (1955); R. H. Ritchie, Phys. Rev. **106**, 874 (1957); V. M. Agranovich and A. A. Rukhadze, J. Exptl. Theoret. Phys. (U.S.S.R.) **35**, 982 (1958), Soviet Phys. JETP **8**, 685 (1959). P. Nozieres and D. Pines, Nuovo cimento **9**, 470 (1958).

[3] L. D. Landau, J. Exptl. Theoret. Phys. (U.S.S.R.) **30**, 1058 (1956), Soviet Phys. JETP **3**, 920 (1956).

[4] Marton, Leder, and Mendlowitz, Advances in Electronics and Electron Physics 7, N.Y. Academic Press, Inc., 1955; G. Fridman, Usp. Fiz. Nauk **62**, 427 (1957); Fortsch. Physik **5**, 51 (1957).

[5] D. Pines and D. Bohm, Phys. Rev. **85**, 338 (1952); D. Pines, Revs. Modern Phys. **28**, 184 (1956); Usp. Fiz. Nauk **62**, 399 (1957).

[6] H. Fröhlich and H. Pelzer, Proc. Phys. Soc. **A68**, 525 (1955).

[7] H. Watanabe, J. Phys. Soc. Japan **11**, 112 (1956); C. Fert and F. Pradal, Compt. rend. **248**, 666 (1959).

[8] A. A. Vlasov, J. Exptl. Theoret. Phys. (U.S.S.R.) 8, 291 (1938); Уч. зап. МГУ (Sci. Notes, Moscow State University) No. 75, Vol. 2, #1 (1945).

[9] I. I. Gol’dman, J. Exptl. Theoret. Phys. (U.S.S.R.) **17**, 681 (1947); Yu. L. Klimontovich, and V. P. Silin, Dokl. Akad. Nauk SSSR **82**, 361 (1952); J. Exptl. Theoret. Phys. (U.S.S.R.) **23**, 151 (1952); D. Bohm and D. Pines, Phys. Rev. **92**, 609 (1953); P. S. Zyryanov and V. M. Eleonskiĭ, J. Exptl. Theoret. Phys. (U.S.S.R.) **30**, 592 (1956), Soviet Phys. JETP **3**, 620 (1956); R. A. Ferrell, Phys. Rev. **107**, 450 (1957).

[10] V. L. Ginzburg, J. Exptl. Theoret. Phys. (U.S.S.R.) **34**, 1593 (1958), Soviet Phys. JETP **7**, 1096 (1958).

[11] R. Kronig and K. Korringa, Physica, **10**, 406, 800 (1943); A. I. Akhiezer and A. G. Sitenko, J. Exptl. Theoret. Phys. (U.S.S.R.) **23**, 161 (1952); E. L. Feĭnberg, J. Exptl. Theoret. Phys. (U.S.S.R.) **34**, 1125 (1958), Soviet Phys. JETP **7**, 780 (1958); A. Ya. Vyatskin, J. Tech. Phys. (U.S.S.R.) **28**, 2217, 2455 (1958), Soviet Phys. “Tech. Physics” **3**, 2038, 2252 (1959).

[12] Sawada, Brueckner, Fukuda, and Brout, Phys. Rev. **108**, 507 (1958); R. Brout, Phys. Rev. **108**, 515 (1958).

[13] V. P. Silin, Физика металлов и металловедение (Physics of Metals and Metallography) **3**, 193 (1956).

[14] V. P. Silin, J. Exptl. Theoret. Phys. (U.S.S.R.) **33**, 495 (1957), Soviet Phys. JETP **6**, 387 (1958).

[15] P. Nozieres and D. Pines, Phys. Rev. **111**, 442 (1958).

[16] L. D. Landau, J. Exptl. Theoret. Phys. (U.S.S.R.) **32**, 59 (1957), Soviet Phys. JETP **5**, 101 (1957); I. M. Khalatnikov and A. A. Abrikosov, J. Exptl. Theoret. Phys. (U.S.S.R.) **33**, 110 (1957), Soviet Phys. JETP **6**, 84 (1958).

[17] V. P. Silin, J. Exptl. Theoret. Phys. (U.S.S.R.) **34**, 781 (1958), Soviet Phys. JETP **7**, 538 (1958).

[18] V. P. Silin, J. Exptl. Theoret. Phys. (U.S.S.R.) **35**, 1243 (1958), Soviet Phys. JETP **8**, 870 (1959).

Translated by H. Lashinsky
40

SOVIET PHYSICS JETP VOLUME 37 (10), NUMBER 1 JANUARY, 1960

ON THE PROBLEM OF INVESTIGATING THE INTERACTION BETWEEN π MESONS AND HYPERONS

L. I. LAPIDUS and CHOU KUANG-CHAO

Joint Institute of Nuclear Studies

Submitted to JETP editor February 27, 1959

J. Exptl. Theoret. Phys. (U.S.S.R.) **37**, 283-288 (1959)

It is shown that use of the unitary property of the S matrix makes it possible to obtain some information about the scattering of π mesons by Λ and Σ hyperons from an analysis of the data on the interaction of K mesons with nucleons. The possibility of studying the π-Λ and π-Σ interactions by examining peripheral collisions of hyperons with nucleons is discussed.

THE study of the interactions of π mesons with hyperons is of special interest in connection with the determination of the symmetry properties of the interactions of π mesons with various baryons.

1. Let us consider the reactions

$$\widetilde{K}+N\rightarrow\widetilde{K}+N, \qquad (1a)$$
$$\widetilde{K}+N\rightarrow\Sigma(\Lambda)+\pi, \qquad (1b)$$
$$\Sigma(\Lambda)+\pi\rightarrow\Sigma(\Lambda)+\pi \qquad (1c)$$

in a range of K-meson energies in which one can neglect channels in which two pions are produced. Since the elements of the S matrix for the reactions (1) are connected with each other by the condition of unitarity, the question arises as to what information about the scattering amplitudes $\Sigma(\Lambda)+\pi\rightarrow\Sigma(\Lambda)+\pi$ can be obtained by studying the cross sections and polarizations in processes (1a) and (1b). The first part of the present paper contains an attempt to answer this question.

In what follows we assume that the spin of the K meson is zero and that the hyperon spin is $\frac{1}{2}$. We further assume that the interactions are invariant under space inversion, time reversal, and rotations in isotopic space.

The reactions (1) are described by elements of the T matrix ($iT = S-1$) diagonal in the isotopic-spin quantum number,

$$T^0=\begin{pmatrix} a_K^0 & a_{K\Sigma}^0 \\ a_{\Sigma K}^0 & a_\Sigma^0 \end{pmatrix}, \quad T^1=\begin{pmatrix} a_K^1 & a_{K\Sigma}^1 & a_{K\Lambda} \\ a_{\Sigma K}^1 & a_\Sigma^1 & a_{\Sigma\Lambda} \\ a_{\Lambda K} & a_{\Lambda\Sigma} & a_\Lambda \end{pmatrix}, \qquad (2)$$

where $a_K^0(a_K^1)$ is the amplitude for scattering $\widetilde{K}+N\rightarrow\widetilde{K}+N$ in the state with the indicated value of the isotopic spin, 0 (1); $a_{K\Sigma}^0(a_{K\Sigma}^1)$ is the amplitude for the reaction $\widetilde{K}+N\rightarrow\Sigma+\pi$ in the state with the isotopic spin 0 (1), and so on.

The spin structure of the scattering amplitude a_α can be represented in the form

$$a_\alpha = A_\alpha + iB_\alpha(\sigma[\mathbf{n}\times\mathbf{n}']), \qquad (3)$$

where $\mathbf{n}\,(\mathbf{n}')$ is the unit vector parallel to the momentum of the particles in the initial (final) state, in the center-of-mass system; A_α and B_α are two complex functions of the energy and of $\mathbf{n}\cdot\mathbf{n}'$.

The reaction amplitude $a_{\alpha\beta}$ has the form

$$a_{\alpha\beta} = A_{\alpha\beta} + iB_{\alpha\beta}(\sigma[\mathbf{n}\times\mathbf{n}']), \qquad (4)$$

when the product of the intrinsic parities of all four particles in the initial (final) states is $\Pi = +1$, and the form

$$a_{\alpha\beta} = A_{\alpha\beta}(\sigma\mathbf{n}) + B_{\alpha\beta}(\sigma\mathbf{n}'), \qquad (5)$$

when $\Pi = -1$. Here $A_{\alpha\beta}$ and $B_{\alpha\beta}$ are two complex functions of the energy and of $\mathbf{n}\cdot\mathbf{n}'$.

Let us turn to the analysis of the conditions for determining the T matrix from the experimental data. It can be seen from Eqs. (2), (3), and (4) that the number of real scalar functions involved in the matrixes T^0 and T^1 is $13\times4=52$. The invariance of the interaction under time reversal means that the S matrix is symmetric, and this reduces the number of functions determining the T matrix from 52 to 36. It can be shown further that when the conditions for the S matrix to be unitary are taken into account, the number of independent real functions is decreased by a factor of two and becomes 18.

The same result is obtained if we use the general formulas obtained in reference 1.

Let us now consider what information can be obtained by studying only processes (1a) and (1b). The number of real functions characterizing these processes is $5\times4=20$. They satisfy four relations of unitarity. Therefore only 16 of them are independent.

Reaction	Amplitude
(a) $K^- + p \to K^- + p$	$^1/_2\,(a_K^1 + a_K^0)$
(b) $K^- + p \to K^0 + n$	$^1/_2\,(a_K^1 - a_K^0)$
(c) $K_2^0 + p \to K_1^0 + p$	$^1/_2\,(a_K^1 - \widetilde{a}_K^0)$
(d) $K_2^0 + p \to K_2^0 + p$	$^1/_2\,(a_K^1 + \widetilde{a}_K^0)$
(e) $K^- + p \to \Lambda + \pi^0$	$a_{K\Lambda}$
(f) $K^- + p \to \Sigma^- + \pi^+$	$-(a_{K\Sigma}^0/\sqrt{6} + a_{K\Sigma}^1/2)$
(g) $K^- + p \to \Sigma^0 + \pi^0$	$a_{K\Sigma}^0/\sqrt{6}$
(h) $K^- + p \to \Sigma^+ + \pi^-$	$-(a_{K\Sigma}^0/\sqrt{6} - a_{K\Sigma}^1/2)$

The table shows 8 reactions of types (1a) and (1b) and their amplitudes. The symbol K_2^0 (K_1^0) denotes the long-lived (short-lived) K^0 meson; a_K^0 is the scattering amplitude of the K^0 mesons, which is determined in the analysis of the scattering of K^+ mesons by nucleons. In what follows we assume that the amplitude a_K^0 is already known.

In reality the reactions (c) and (d) in the table are the same process. By studying the time dependences of the scattering cross section and of the polarization after scattering (i.e., the dependences on the distance to the target), one can determine the amplitudes of reactions (c) and (d) separately.

By measuring the differential cross sections and the polarization of the nucleons in reactions (a) — (d) as shown in the table, we can completely fix the scattering amplitudes a_K^0 and a_K^1. The experimental data on the cross sections and polarizations of the hyperons in reactions (e) — (h), together with the four relations of unitarity, enable us to determine the reaction amplitudes $a_{K\Sigma}^0$, $a_{K\Sigma}^1$, and $a_{K\Lambda}$, apart from a common phase factor.

Since the expressions for the cross sections and polarizations, and also the unitarity relations for reactions (1a) and (1b) are invariant under the replacement

$$a_{K\Sigma}^0 \to e^{i\delta_0(E)} a_{K\Sigma}^0, \quad a_{K\Sigma}^1 \to e^{i\delta_0(E)} a_{K\Sigma}^1,$$
$$a_{K\Lambda} \to e^{i\delta_1(E)} a_{K\Lambda}, \tag{6}$$

we cannot determine two phase factors $e^{i\delta_0}$ and $e^{i\delta_1}$, which are functions of the energy alone. This last follows from the relations that the amplitudes (4) and (5) satisfy by virtue of the unitary property of the S matrix.

Since the number of independent real functions involved in T^0 and T^1 is 18, and 16 of them are determined apart from two phase factors through the study of processes (1a) and (1b), for the complete reconstruction of the scattering amplitudes of pions by Λ and Σ hyperons in the states with isotopic spins 0 and 1, we need to determine in addition two more real functions of the energy and $\mathbf{n}\cdot\mathbf{n}'$, and two phase factors.

For each state with total angular momentum j and orbital angular momentum $l = j \pm \frac{1}{2}$, the T^0 matrix can be written in the form

$$-i\begin{pmatrix} \rho_K^0 \exp(2i\delta_K^0) - 1 & i\rho_{K\Sigma}^0 \exp(i\delta_{K\Sigma}^0) \\ i\rho_{K\Sigma}^0 \exp(i\delta_{K\Sigma}^0) & \rho_\Sigma^0 \exp(2i\delta_\Sigma^0) - 1 \end{pmatrix}, \tag{7}$$

where the ρ_α are certain positive functions of the energy, and the δ_α are the phases of the corresponding processes.

From the conditions for unitarity of the S matrix it follows that

$$\delta_{K\Sigma}^0 = \delta_K^0 + \delta_\Sigma^0, \qquad \rho_\Sigma^0 = \rho_K^0 = \{1 - (\rho_{K\Sigma}^0)^2\}^{1/2}. \tag{8}$$

The quantities ρ_K^0, δ_K^0, $\delta_{K\Sigma}^0$ can be determined apart from a common phase factor by studying processes (1a) and (1b). The quantities ρ_Σ^0 and δ_Σ^0 are then determined to the same accuracy from the relations (8).

Thus for π-Σ scattering the difference of the phases in the various states with zero isotopic spin is completely determined by the study of the reactions with K particles.*

For the states with isotopic spin (1) we have instead of the matrix (7)

$$-i\begin{pmatrix} \rho_K e^{2i\delta_K} - 1 & \rho_{K\Sigma} e^{i\delta_{K\Sigma}} & \rho_{K\Lambda} e^{i\delta_{K\Lambda}} \\ \rho_{K\Sigma} e^{i\delta_{K\Sigma}} & \rho_\Sigma e^{2i\delta_\Sigma} - 1 & \rho_{\Sigma\Lambda} e^{i\delta_{\Sigma\Lambda}} \\ \rho_{K\Lambda} e^{i\delta_{K\Lambda}} & \rho_{\Sigma\Lambda} e^{i\delta_{\Sigma\Lambda}} & \rho_\Lambda e^{2i\delta_\Lambda} - 1 \end{pmatrix}. \tag{9}$$

Here and in what follows, we shall write instead of $\rho_\alpha^1(\delta_\alpha^1)$ simply $\rho_\alpha(\delta_\alpha)$.

From the unitarity conditions we get

$$\rho_{K\Sigma}^2 + \rho_\Sigma^2 + \rho_{\Sigma\Lambda}^2 = 1, \qquad \rho_{K\Lambda}^2 + \rho_{\Sigma\Lambda}^2 + \rho_\Lambda^2 = 1, \tag{10}$$

$$\cos(2\delta_\Sigma + 2\delta_K - 2\delta_{K\Sigma}) = \frac{(\rho_K\rho_{K\Sigma})^2 + (\rho_{K\Sigma}\rho_\Sigma)^2 - (\rho_{K\Lambda}\rho_{\Sigma\Lambda})^2}{2\rho_\Sigma\rho_K(\rho_{K\Sigma})^2}, \tag{11}$$

$$\cos(\delta_{\Sigma\Lambda} + 2\delta_K - \delta_{K\Lambda} - \delta_{K\Sigma}) = \frac{(\rho_{K\Lambda}\rho_{\Sigma\Lambda})^2 + (\rho_K\rho_{K\Sigma})^2 - (\rho_{K\Sigma}\rho_\Sigma)^2}{2\rho_{K\Lambda}\rho_{\Sigma\Lambda}\rho_K\rho_{K\Sigma}}, \tag{12}$$

$$\cos(2\delta_\Lambda + 2\delta_K - 2\delta_{K\Lambda}) = \frac{(\rho_K\rho_{K\Lambda})^2 + (\rho_{K\Lambda}\rho_\Lambda)^2 - (\rho_{K\Sigma}\rho_{\Sigma\Lambda})^2}{2\rho_\Lambda\rho_K(\rho_{K\Lambda})^2}. \tag{13}$$

---

*It may turn out that in carrying out an unambiguous analysis it will be helpful to take into account Coulomb effects and the energy dependence of the S matrix at low energies.

We note that the Minami ambiguity exists for the reactions in question.

Some possibilities for determining the parity of the K meson relative to the hyperons through the analysis of the reactions (1) have recently been discussed by Amati and Vitale.[2]

It is easy to convince oneself that even when ρ_K, $\rho_{K\Sigma}$, $\rho_{K\Lambda}$, δ_K, $\delta_{K\Sigma}$, and $\delta_{K\Lambda}$ are known, the unitarity relations (10) — (13) are insufficient for the reconstruction of the matrix T^1. For this we need to know one more parameter in each state (for example, ρ_Σ).

We note that the relations (10) — (13) lead to some interesting inequalities. Noting that $\rho_\alpha > 0$ and $|\cos\theta| < 1$, we get from Eqs. (10) and (11)

$$0 < \rho_\Sigma^2 = 1 - \rho_{K\Sigma}^2 - \rho_{\Sigma\Lambda}^2 < 1 - \rho_{K\Sigma}^2, \tag{14}$$

$$|(\rho_K\rho_{K\Sigma})^2 + (\rho_{K\Sigma}\rho_\Sigma)^2 - \rho_{K\Lambda}^2(1 - \rho_{K\Sigma}^2 - \rho_\Sigma^2)| < 2\rho_\Sigma\rho_K(\rho_{K\Sigma})^2. \tag{15}$$

Let us introduce the new notations

$$\rho_{K\Sigma}^2 + \rho_{K\Lambda}^2 = a, \quad \rho_K\rho_{K\Sigma}^2 = b, \quad (\rho_K\rho_{K\Sigma})^2 - \rho_{K\Lambda}^2(1 - \rho_{K\Sigma}^2) = c.$$

Then Eq. (15) can be rewritten in the form

$$|a\rho_\Sigma^2 + c| < 2b\rho_\Sigma. \tag{15'}$$

From Eq. (15′) together with Eq. (14) we get

$$\max\left\{0;\ \frac{b}{a} - \frac{1}{a}\sqrt{b^2 - ac}\right\} < \rho_\Sigma < \min\left\{\sqrt{1 - \rho_{K\Sigma}^2};\ \frac{b}{a} + \frac{1}{a}\sqrt{b^2 - ac}\right\}. \tag{16}$$

The inequality (15′) holds only for $b^2 - ac \geq 0$. Consequently, the observable quantities ρ_K, $\rho_{K\Lambda}$, and $\rho_{K\Sigma}$ must satisfy this inequality. Similarly we have

$$\max\left\{0;\ \frac{b_1}{a_1} - \frac{1}{a_1}\sqrt{b_1^2 - a_1c_1}\right\} < \rho_{\Sigma\Lambda} < \min\left\{\sqrt{1 - \rho_{K\Sigma}^2};\ \sqrt{1 - \rho_{K\Lambda}^2};\ \frac{b_1}{a_1} + \frac{1}{a_1}\sqrt{b_1^2 - a_1c_1}\right\}, \tag{17}$$

$$\max\left\{0;\ \frac{b_2}{a_2} - \frac{1}{a_2}\sqrt{b_2^2 - a_2c_2}\right\} < \rho_\Lambda < \min\left\{\sqrt{1 - \rho_{K\Lambda}^2};\ \frac{b_2}{a_2} + \frac{1}{a_2}\sqrt{b_2^2 - a_2c_2}\right\}, \tag{18}$$

where

$$a_1 \equiv \rho_{K\Lambda}^2 + \rho_{K\Sigma}^2 = a, \qquad b_1 \equiv \rho_{K\Lambda}\rho_K\rho_{K\Sigma},$$
$$a_2 \equiv \rho_{K\Lambda}^2 + \rho_{K\Sigma}^2 = a, \qquad b_2 \equiv \rho_K(\rho_{K\Lambda})^2,$$
$$c_1 \equiv (\rho_K\rho_{K\Sigma})^2 - \rho_{K\Sigma}^2(1 - \rho_{K\Sigma}^2),$$
$$c_2 \equiv (\rho_\Lambda\rho_{K\Lambda})^2 - \rho_{K\Sigma}^2(1 - \rho_{K\Lambda}^2).$$

2. Recently Chew and Low, and Okun' and Pomeranchuk,[3] have suggested that peripheral collisions be studied as a method for determining interactions between unstable particles. We shall assume that this method can be used for the determination of the scattering amplitude for $\Sigma(\Lambda) + \pi \rightarrow \Sigma(\Lambda) + \pi$ through studies of the processes $\Sigma + N \rightarrow \Sigma(\Lambda) + N + \pi$ and $\Lambda + N \rightarrow \Sigma + N + \pi$. The key point of the method is that the amplitude for the reaction $\Sigma + N \rightarrow \Sigma(\Lambda) + N + \pi$, regarded as a function of $(p'_N - p_N)^2$, where p_N (p'_N) is the four-vector momentum of the nucleon in the initial (final) state, has a pole in the nonphysical region, $(p'_N - p_N)^2 = \mu^2$ (μ is the mass of the π meson). It is shown that the virtual process

$$N \rightarrow N + \pi, \qquad \Sigma(\Lambda) + \pi \rightarrow \Sigma(\Lambda) + \pi \tag{19}$$

corresponds to the pole term, whose residue is proportional to the amplitude for $\pi - \Lambda(\Sigma)$ scattering. Assuming that in the physical region near the pole the reaction $\Sigma + N \rightarrow \Sigma(\Lambda) + N + \pi$ is determined by the process (19), one can extrapolate its amplitude into the nonphysical region and separate out the residue of the pole term.

To estimate the effect of other terms in the physical region near the pole, we shall formulate certain rules that must be fulfilled if the contribution of the pole term in actually predominant in this region.

a) In the region near the pole the amplitude of the reaction $\Sigma^+ + p \rightarrow \Sigma^+ + p + \pi^0$ is equal to that of the reaction $\Sigma^- + p \rightarrow \Sigma^- + p + \pi^0$. This rule follows from the invariance of the virtual process

$$\pi^0 + \Sigma^\pm \rightarrow \pi^0 + \Sigma^\pm \tag{20}$$

under rotations in the isotopic space. Similarly it can be shown that the amplitudes for the following pairs of processes are equal:

$\Sigma^+ + p \rightarrow \Sigma^0 + p + \pi^+$ and $\Sigma^- + p \rightarrow \Sigma^0 + p + \pi^-$,
$\Lambda + p \rightarrow \Sigma^+ + n + \pi^0$ and $\Lambda + p \rightarrow \Sigma^0 + n + \pi^+$,
$\pi^+ + p \rightarrow \pi^+ + \pi^0 + p$ and $\pi^- + p \rightarrow \pi^- + \pi^0 + p$ etc.

b) Near the pole the amplitudes for the reactions

$$\Sigma^\pm(\Lambda) + p \rightarrow \Sigma^\pm(\Lambda) + p + \pi^0$$
and $$\tilde{\Sigma}^\pm(\tilde{\Lambda}) + p \rightarrow \tilde{\Sigma}^\pm(\tilde{\Lambda}) + p + \pi^0$$

are equal to each other. This rule follows from the invariance of the virtual process (20) under charge conjugation. In our case it is not of any great practical importance, but it can be of interest in other cases. For example, it can be shown that the amplitudes for the reactions $K^\pm + N \rightarrow K^\pm + N + \pi^0$ are equal. This equality is useful for the determination of the interaction of K mesons with π mesons, and has been noted by Okun' and Pomeranchuk.

c) If the nucleons are unpolarized in the initial state, then they remain unpolarized in the final state also.

Let us consider a reaction of the type

$$\Sigma^+ + p \rightarrow \Lambda + p + \pi^+ \tag{21}$$

in the region near the pole $(p_\Sigma - p_\Lambda)^2 = \mu^2$. We assume that the dominant process in this region is

$$\Sigma^+ \to \Lambda + \pi^+, \qquad \pi^+ + p \to \pi^+ + p, \tag{22}$$

the amplitude for which is proportional to

$$\frac{\bar{u}(p_\Lambda)\Gamma u(p_\Sigma)}{(p_\Lambda - p_\Sigma)^2 - \mu^2} a_{\pi p}, \tag{23}$$

where $\Gamma = 1$ if the relative parity Π of the Σ and Λ particles is -1, and $\Gamma = \gamma_5$ if $\Pi = +1$; $a_{\pi p}$ is the amplitude for the scattering $\pi^+ + p \to \pi^+ + p$. The amplitude for the process (22) does not contain any dependence on the spin operators of the hyperons for $\Pi = -1$ (more exactly, it contains a term proportional to σ_Y, but with a small coefficient); on the other hand, if $\Pi = +1$, the amplitude is proportional to $\sigma_Y \cdot \mathbf{k}$, where $\mathbf{k}$ is the unit vector parallel to the difference

$$\mathbf{P}_\Sigma / (E_\Sigma + M_\Sigma) - \mathbf{P}_\Lambda / (E_\Lambda + M_\Lambda).$$

If in the initial state the Σ^+ is polarized (polarization vector $\mathbf{P}$), then it can be shown from Eq. (23) that in the final state the polarization vector $\mathbf{P}'$ of the Λ particle is given by

$$\mathbf{P}' = \mathbf{P} \text{ for } \Pi = -1,$$
$$\mathbf{P}' = 2(\mathbf{P}\mathbf{k})\mathbf{k} - \mathbf{P} \text{ for } \Pi = +1. \tag{24}$$

Thus if in the region where the pole term predominates one could measure the polarization of the Λ particles produced in the reaction (21) with polarized Σ, then it would be possible not only to evaluate the effect of the non-pole terms, but also to get information about the relative parity of the Λ and Σ hyperons.

In a number of cases the study of the polarization of the products from peripheral collisions can be a source of information about the parities of unstable particles.*

The writers express their deep gratitude to Professor M. A. Markov for helpful discussions.

---

[1] Bilen'kiĭ, Lapidus, Puzikov, and Ryndin, J. Exptl. Theoret. Phys. (U.S.S.R.) **35**, 959 (1958), Soviet Phys. JETP **8**, 669 (1959); Nucl. Phys. **7**, 646 (1958).

[2] D. Amati and B. Vitale, Nuovo cimento **9**, 895 (1958).

[3] G. F. Chew, Proc. CERN Annual Conference, 1958, Geneva, page 97; preprint, 1958. L. B. Okun' and I. Ya. Pomeranchuk, J. Exptl. Theoret. Phys. (U.S.S.R.) **36**, 300 (1959), Soviet Phys. JETP **9**, 207 (1959). G. F. Chew and F. E. Low, preprint, 1958.

[4] J. G. Taylor, Nucl. Phys. **9**, 357 (1959); preprint, 1959.

Translated by W. H. Furry
41

---

*The possibility of determining the parities of particles by the study of peripheral collisions without considering the polarization has been discussed recently by Taylor.[4]

SOVIET PHYSICS JETP VOLUME 37(10), NUMBER 1 JANUARY, 1960

ON THE MECHANISM OF CAPTURE OF STOPPED K⁻ MESONS

D. K. KOPYLOVA, Yu. B. KOROLEVICH, N. I. PETUKHOVA, and M. I. PODGORETSKIĬ

Joint Institute of Nuclear Studies

Submitted to JETP editor February 27, 1959

J. Exptl. Theoret. Phys. (U.S.S.R.) **37**, 289-291 (July, 1959)

The problem considered is that of the mechanism of capture of stopped K^- mesons by the nuclei of a photographic emulsion. On the assumption of a surface model of one-nucleon capture it is found that the fraction of two-nucleon captures is close to 30 percent.

It is well-known that the capture of K^- mesons by nuclei occurs through one-nucleon (reactions of the type $K^- + N \rightarrow Y + \pi$) and two-nucleon (reactions of type $K^- + 2N \rightarrow Y + N$) interactions of the K^- mesons. A direct indication of the existence of reactions of the second type is found in cases of the emission of fast hyperons ($E_\Sigma > 60$ Mev) in σ_K stars, and cases of the simultaneous emission of a fast hyperon and a fast proton. It is usually assumed that the two-nucleon captures of K^- mesons make up not more than 10 to 12 percent of the total number of interactions of stopped K^- mesons.[1-4*]

In the present paper we make an estimate of the fraction of two-nucleon captures on the basis of an analysis of the observed number of π mesons emitted in σ_K stars.

Let x be the unknown fraction of two-nucleon interactions, α the expected percentage of emerging π mesons (calculated from the known mean free path against interactions of π mesons in nuclear matter on the assumption of a definite model for the capture of K^- mesons), and β the experimentally observed fraction of the interactions of stopped K^- mesons in which π mesons are emitted. Then we have the relation: $(1 - x)\alpha = \beta$.

According to the data given in reference 2, charged π mesons are emitted in 34 ± 2 percent of all nuclear captures of stopped K^- mesons. If we take account of neutral π mesons, the fraction of π mesons is increased to 51 ± 3 percent ($\beta = 0.51$).*

One of the immediate consequences of this fact is that the number of two-nucleon captures cannot exceed 49 ± 3 percent of the total number of interactions. The expected fraction α of emerging π mesons is calculated in reference 7 for π mesons accompanying Σ and Λ^0 hyperons, on the assumptions of surface and volume models for the capture of K^- mesons.†

The fraction of π mesons that have not undergone any interaction can be obtained if one knows the mean free path of π mesons in nuclear matter. It is harder to calculate what part of the π mesons that have been inelastically scattered in the first collision will still get out of the nucleus without being absorbed.

It was decided to estimate upper and lower limits on α (and correspondingly, upper and lower limits on x) by assuming that all the π mesons that undergo inelastic scattering get out of the nucleus (upper limit), or that they are all absorbed in the nucleus (lower limit). It must be noted that the absorption coefficient of π mesons that have undergone inelastic scattering is rather small, and consequently a large fraction of them actually get out of the nucleus. Therefore the upper limit found as described differs only a little from the true value of α.

---

*There are indications that two-nucleon interactions play a much more important part (30 to 50 percent).[5,6] Unfortunately the estimates given in the preprint of Eisenberg et al. are evidently not final results, and the brief indication contained in the report of Kaplon[6] is not accompanied by supporting evidence.

*It can easily be shown, from general considerations of isotopic invariance, that in the interaction of K^- mesons with nuclei of zero isotopic spin, the number of charged π mesons (Σ hyperons) produced is twice the number of neutral π mesons (Λ hyperons), independent of the type of interaction. It is natural to assume that the nuclei of a photographic emulsion satisfy this condition, since for them $[(N - Z)/A] \ll 1$.

†This same question has been discussed in a paper by K. Lanius, whom the writers thank for sending them a preprint.

For the calculation of α it was necessary to choose a definite ratio between the number of reactions of the type $K^- + N \rightarrow \Lambda^0 + \pi$, and the number of the type $K^- + N \rightarrow \Sigma + \pi$. In accordance with reference 7, we assume that $\Lambda^0/\Sigma^{\pm,0} = 0.21$ for the surface model and $\Lambda^0/\Sigma^{\pm,0} = 0.50$ for the volume model.

To find the sensitivity of the results to small changes of the surface-absorption model, a special examination was made of the case in which the K^- mesons are absorbed at a depth of one-nucleon radius inside the surface of the nucleus.[4]

The results of the calculations are as follows:

Surface absorption:	$0.64 < \alpha < 0.75$	$0.20 < x < 0.32$
Absorption of the K-mesons at a depth of one-nucleon radius:	$0.62 < \alpha < 0.72$	$0.18 < x < 0.29$
Volume absorption:	$0.32 < \alpha < 0.52$	—

It can be seen from this that the first two models do not differ much from each other. It can also be seen that the volume model leaves no room for two-nucleon capture. Since, according to direct estimates (fast hyperons), the quantity x is at least 10 to 12 percent, the result obtained here can be regarded as an indication that the volume model actually has no relevance for one-nucleon capture of stopped K^- mesons. This is in complete agreement with the idea that has come to be accepted in the literature, that one-nucleon capture of stopped K^- mesons occurs mainly at the surface of the nucleus (see, in particular, references 5 and 6). In this case, the fraction of two-nucleon capture is evidently close to 30 percent, but does not exceed that amount.

In connection with this estimate of the fraction of two-nucleon captures, the question of direct production of Λ^0 particles in one-nucleon capture reactions of surface absorption is of interest. According to references 2, 4, 7, and 8, reactions of the type $K^- + N \rightarrow \Lambda^0 + \pi$ make up 15 to 35 percent of all one-nucleon capture reactions.

Charged Σ hyperons of energy $E_\Sigma < 60$ Mev are emitted in 14 percent of all cases of interactions of K^- mesons with nuclei.[6]* Taking account of the neutral hyperons we find, on the assumption of a surface model, that slow Σ hyperons are produced in less than 42 percent of all interactions.* Consequently, Λ^0 would have to occur in more than 58 percent of all interactions, which contradicts the results of the papers cited here. The assumption of about 30 percent of two-nucleon captures removes this contradiction. It reappears if we assume that slow Σ hyperons ($E_\Sigma < 60$ Mev) are weakly absorbed in nuclei. In fact, in this case it is necessary to assume that direct production of Λ^0 particles occurs in the great majority of captures.

Thus if we work with the surface model of one-nucleon capture, we must accept the idea that two-nucleon capture occurs in about 30 percent of all cases and that Σ hyperons with $E_\Sigma < 60$ Mev are strongly absorbed inside the nucleus.

A direct indication that Σ hyperons with $E_\Sigma < 60$ Mev are absorbed more strongly than the accompanying π mesons comes from a comparison of the experimental data on the yields of π mesons and Σ hyperons from the capture of K^- mesons. As has already been said, charged π mesons are emitted in 34 percent, and charged Σ hyperons with energies $E_\Sigma < 60$ Mev in 14 percent, of all interactions of stopped K^- mesons. It follows from this that the absorption of Σ hyperons with $E_\Sigma < 60$ Mev is stronger than that of the accompanying π mesons by a factor of 1.5 to 2.[†]

According to the data of Kaplon,[6] the number of fast Σ hyperons with $E_\Sigma > 60$ Mev (charged and neutral) is about 3.5 percent of the total number of captures of K^- mesons. A comparison of this number with the estimate given here of the fraction of two-nucleon captures (~30 percent) shows that either the overwhelming majority of two-nucleon captures leads to direct production of Λ^0 particles, or else the fast Σ hyperons that are formed have a high probability of going over into Λ^0 particles in their subsequent passage through the nucleus, or that they lose energy and become slow particles. In other words, in the second case we have to assume a large cross-section for interaction of fast Σ hyperons with nucleons. Furthermore we must also conclude that two-nucleon capture does not occur at the surfaces of nuclei, since not over half of the fast Σ hyperons could be absorbed in the case of surface capture.

The writers thank M. Ya. Danysh for participating in discussions and for making it possible for us to learn of the critical comments of E. Markit.

---

[*] The number of Σ hyperons produced in one-nucleon capture reactions is smaller than 14 percent, since some of the hyperons with $E_\Sigma < 60$ Mev have come from the slowing down of fast Σ hyperons ($E_\Sigma > 60$ Mev) produced in two-nucleon captures.

[*] For surface absorption of K^- mesons, the fraction of emerging hyperons (or π mesons) must be $\geqslant 0.5$.

[†] Here it is assumed that $\Lambda^0/\Sigma^{\pm 0} = 0.25$ and $0.20 < x < 0.32$.

---

[1] C. Dilworth, Proc. of Seventh Annual Rochester Conference, 1957, p. VI-19.

[2] K$^-$-stack Collaboration, Intl. Conf. on Mesons and Newly Discovered Particles, Padova-Venezia, 1957, p. II-15.

[3] S. Goldhaber, Proc. of Sixth Annual Rochester Conference, 1956, p. V-26.

[4] J. Hornbostel and G. T. Zorn, Phys. Rev. **109**, 165 (1958).

[5] Eisenberg, Roch, Nicolic, Schneeberger, and Winzeler, preprint, 1958.

[6] M. F. Kaplon, CERN Annual Intl. Conf. on High Energy Physics, 1958, p. 171.

[7] Webb, Iloff, Featherston, Chupp, Goldhaber, and Goldhaber, Int. Conf. on Mesons and Newly Discovered Particles, Padova-Venezia, 1957, p. II-69; same authors, Nuovo cimento **8**, 899 (1958).

[8] Fry, Schneps, Snow, Swami, and Wold, Phys. Rev. **107**, 257 (1957).

Translated by W. H. Furry
42

Letters to the Editor

ON AN ESTIMATE OF ENERGY CHARACTERISTICS OF SHOWER PRODUCING PARTICLES

É. G. BOOS and Zh. S. TAKIBAEV

Nuclear Physics Institute, Academy of Sciences, Kazakh S.S.R.

Submitted to JETP editor January 15, 1959

J. Exptl. Theoret. Phys. (U.S.S.R.) **37**, 292-293 (July, 1959)

It has been shown that the values of the transverse momenta of particles $p_\perp$ (in units of μc, where μ is the particle mass) produced in cosmic ray showers are distributed in such a way that $p_\perp \sim 1$,[1-3] while separate values do not differ greatly from the average. This experimental fact, together with the assumption about the symmetrical emission of shower particles in the c.m.s., makes it possible to determine the parameter $\gamma_c = 1/\sqrt{1-\beta_c^2}$, where β_c is the velocity of the center of mass with respect to the laboratory system of coordinates. Correspondingly, we shall consider two variants of the symmetrical emission in c.m.s.: (a) exact angular symmetry (to each particle with emission angle θ_i' with respect to the axis there corresponds another with angle $\theta_j' = \pi - \theta_i'$); (b) an equal number of particles is contained on the two sides of the plane perpendicular to the motion of the center of mass.

Making use of the relation between the angles of emission of particles in c.m.s. and in the laboratory system

$$\cot\theta_i = \gamma_c \cot\theta_i - \sqrt{\gamma_i^2 - 1}\,\sqrt{z_i^2 + \cot^2\theta_i},\qquad z_i^2 = (p_{\perp i}^2 + 1)/p_{\perp i}^2, \tag{1}$$

we can obtain for case (a)

$$\gamma_c = \varphi_1/\sqrt{\varphi_1^2 - \varphi_2^2},\qquad \varphi_1 = \sum_{i=1}^{n_s}\sqrt{z_i^2 + \cot^2\theta_i},\qquad \varphi_2 = \sum_{i=1}^{n_s}\cot\theta_i; \tag{2}$$

In case (b), for the medium value (Y_m) of the value $Y_i = \sqrt{z_i^2 + \cot^2\theta_i}/\cot\theta_i$, the following relation is true:

$$\gamma_c = Y_m/\sqrt{Y_m^2 - 1}. \tag{3}$$

The fraction of the energy transferred to mesons can be estimated from the relation

$$K \approx 1.5 \sum_{i=1}^{n_s} \varepsilon_i'/E';\quad \varepsilon_i' = \mu_i c^2 p_{\perp i} \times \{\gamma_c\sqrt{z_i^2 + \cot^2\theta_i} - \sqrt{\gamma_c^2 - 1}\cot\theta_i\}, \tag{4}$$

where, for a nucleon-nucleon collision, $E' = 2Mc^2(\gamma_c - 1)$.

Making use of Eqs. (1) — (4) for "narrow" showers ($\cot^2\theta_i \gg z_i^2 \approx 1$; $\gamma_c^2 \gg 1$), we can obtain the simplified relations

$$\text{a)}\quad \gamma_c = \left[\sum_{i=1}^{n_s}\cot\theta_i \Big/ \sum_{i=1}^{n_s} z_i^2 \tan\theta_i\right]^{1/2};$$

$$\text{b)}\quad \gamma_c = \left(\frac{\cot\theta_i}{z_i}\right)_m,\qquad \varepsilon_i' \approx \frac{\mu_i c^2}{2} p_{\perp i}\left\{\frac{\gamma_c z_i^2}{\cot\theta_i} + \frac{\cot\theta_i}{\gamma_c}\right\}. \tag{5}$$

For the sake of comparison, the table lists showers in which it was found to be possible to measure the energy of secondary particles.[4-8] This made it possible to use formulae (4) and (5) directly for an estimate of γ_c and K (columns 3 — 7) under the assumption that all shower particles are π mesons. In formulae (2) to (5), all information which can be obtained from the measurements of the angles and momenta of secondary particles in the laboratory system is used.

Allowance for the distribution of transverse momenta of the particles leads to lower values of

Type of Shower	γ_c	a) γ_c	b) γ_c	a) K	b) K	$p_{\perp i}$	$p_\perp = 1$; $z = 1.5$; a) γ_c	b) γ_c	a) K	b) K
1	2	3	4	5	6	7	8	9	10	11
2+15 (p) [4]	204	>60	220	⩽0.4	0.1	⩾1	160	200	0.1	0.1
3+39 (p) [5]*	44	33	27	0.8	1.2	2.3	38	25	0.5	0.8
2+16 (p) [6]†	52	35	34	0.2	0.2	1.2	32	42	0.2	0.2
2+14 (p) [7]	78	64	53	0.1	0.2	1.2	59	44	0.1	0.1
0+ 7 (p) [8]	29	10	20	0.2	0.1	1.3	13	15	0.1	0.1

*A more detailed analysis shows that, evidently, a collision of the primary nucleon with a group of nucleons in the nucleus has occurred in this case.

†In a subsequent study it was found that one of the particles (number 15) was not a π meson. In the estimate of γ_c (column 3 and 4), this particle was not taken into account.

γ_c as compared with the values obtained by the method of the Rome group[1] (column 2).

With the exception of one shower,[5] the inelasticity factor is substantially smaller than 1. The error in the determination of γ_c and K, arising out of the fluctuation of the angular distribution of particles can be taken into account analogously to the procedure in reference 9.

The average value of the transverse momentum (column 7) lies within the limits of 1 to 2. To explain how the assumption of constant transverse momentum influences the estimated values of γ_c and K, the latter were calculated from Eqs. (4) and (5) for the value $p_{\perp i} \approx 1$. The assumption of constant transverse momentum ($p_\perp \approx 1$) does not lead to substantial changes of the estimated values (columns 8 to 11). This makes it possible to generalize the described method for an estimate of the energy characteristics (γ_c and K) in showers in which only the angular distribution of secondary shower particles is known. It should be noted that the estimated values of γ_c found by such a method are in good agreement with the values obtained by Takibaev under the assumption of a power-law energy spectrum of produced mesons.

---

[1] Edwards, Losty, Perkins, Pinkau, and Reynolds, Phil. Mag. **3**, 237 (1958).

[2] Co-operative Emulsion Group in Japan, Suppl. Nuovo cimento **8**, Ser. 10, 761 (1958).

[3] G. B. Zhdanov, J. Exptl. Theoret. Phys. (U.S.S.R.) **34**, 856 (1958), Soviet Phys. JETP **7**, 592 (1958).

[4] Schein, Glasser, and Haskin, Nuovo cimento **2**, 647 (1955).

[5] Debenedetti, Garelli, Tallone, and Vigone, Nuovo cimento **4**, 1142 (1956).

[6] Boos, Vinitskiĭ, Takibaev, and Chasnikov, J. Exptl. Theoret. Phys. (U.S.S.R.) **34**, 622 (1958), Soviet Phys. JETP **7**, 430 (1958).

[7] Zh. S. Takibaev, Тр. Ин-та ядерной физики АН КазССР (Proceedings, Nuclear Physics Institute, Academy of Sciences, Kazakh S.S.R.) Vol. 1, p. 129, Alma-Ata, Press of the Academy of Sciences, Kazakh S.S.R., 1958.

[8] Hopper, Biswas, and Darby, Phys. Rev. **84**, 457 (1951).

[9] San'ko, Takibaev, and Shakhova, J. Exptl. Theoret. Phys. (U.S.S.R.) **35**, 574 (1958), Soviet Phys. JETP **8**, 827 (1959).

Translated by H. Kasha
43

ON THE METHODS OF BORN AND PAIS FOR FINDING PHASE SHIFTS

T. TITTS

University of the City of Lodz, Poland

Submitted to JETP editor February 2, 1959

J. Exptl. Theoret. Phys. (U.S.S.R.) **37**, 294-295 (July, 1959)

As is well known, in cases in which the Born approximation for finding the phase shifts is not applicable, we must use some other more accurate method, for example the method of Pais. The purpose of this note is to give a brief derivation of the approximations of Born[1] and Pais[2] and also a numerical comparison of the phase shifts obtained by these two methods.

Let us write the Schrödinger equation in the following form:

$$y'' + [k^2 - U - l(l+1)/r^2]\, y = 0, \tag{1a}$$

$$u'' + [k^2 - l(l+1)/r^2]\, u = 0, \tag{1b}$$

$$v'' + [k^2 - (l(l+1) - a^2)/r^2]\, v = 0, \tag{1c}$$

$k = mv/\hbar$, and a^2 is a certain constant. The interaction potential is connected with U by the relation $U = (2m/\hbar^2)V$. The exact solutions of Eqs. (1b) and (1c) are well-known:

$$u = \sqrt{\pi kr/2}\, J_{l+1/2}(kr), \qquad v = \sqrt{\pi kr/2}\, J_{\sqrt{(l+1/2)^2 - a^2}}(kr). \tag{2}$$

They satisfy the following boundary conditions:

$$u(0) = 0, \qquad u(\infty) \to \sin(kr - l\pi/2),$$
$$v(0) = 0, \qquad v(\infty) \to \sin\left(kr - \frac{\pi}{2}\sqrt{(l + 1/2)^2 - a^2} + \frac{\pi}{4}\right). \tag{3}$$

The exact solution of Eq. (1a) satisfies the boundary conditions

$$y(0) = 0, \qquad y(\infty) \to \sin(kr - l\pi/2 + \eta_l). \tag{4}$$

If we now require that the solution v of Eq. (1c) satisfy the same boundary conditions (4) as the exact solution of Eq. (1a), then the constant a^2 must be

$$a^2 = 4\pi^{-2}[-\eta_l^2 + \pi(l + \tfrac{1}{2})\,\eta_l]. \tag{5}$$

Then

$$v = \sqrt{\pi kr/2}\, J_{(l+1/2) - 2\eta_l/\pi}(kr). \tag{6}$$

Let us multiply Eq. (1a) by u and Eq. (1b) by y, subtract one equation from the other, and integrate from zero to ∞, taking account of the boundary conditions (3) and (4) for u and y. Furthermore, in the integral that contains the interaction potential V, the solution u is inserted instead of the exact solution y. This procedure gives the well-known Born approximation:

$$\eta_l = -\frac{\pi m}{\hbar^2}\int_0^\infty V(r) J^2_{l+1/2}(kr)\, r\, dr. \tag{7}$$

Applying this same procedure to Eqs. (1b) and (1c), we get the well-known Kapteyn integral[3]

$$\int_0^\infty J_\mu(\alpha t) J_\nu(\alpha t)\frac{dt}{t} = \begin{cases} \dfrac{2}{\pi}\dfrac{\sin[\pi(\nu-\mu)/2]}{\nu^2-\mu^2}, & \mu \neq \nu \\ \dfrac{1}{2\mu}, & \mu = \nu. \end{cases} \tag{8}$$

Finally, applying this procedure to Eqs. (1a) and (1c), where the solution for v is given by Eq. (6), and using Eq. (8), we get the Pais approximation for the phase shifts:

$$\frac{2l+1-2\eta_l/\pi}{2l+1-4\eta_l/\pi}\eta_l = -\frac{\pi m}{\hbar^2}\int_0^\infty V(r) J^2{}_{l+1/2-2\eta_l/\pi}(kr)\, r\, dr. \tag{9}$$

Pais obtained this formula by means of a variational principle. We see that one can obtain the approximate formulas of Born and Pais for the phase shifts by using a single kind of procedure.

The examples considered below show the accuracies of the Born and Pais approximations (it must be emphasized that the Pais formula (9) is incorrect for the zeroth-order phase shift). For the Gauss potential $V(r) = -V_0 \exp(-\alpha^2 r^2)$, Eqs. (7) and (9) give

$$\eta_{l\,\mathrm{Born}} = \eta_l^{(1)} = \frac{\pi M V_0}{4\hbar^2\alpha^2}\exp\left(-\frac{k^2}{2\alpha^2}\right) J_{l+1/2}\left(\frac{k^2}{2\alpha^2}\right),$$

$$\frac{2l+1-2\eta_l/\pi}{2l+1-4\eta_l/\pi}\eta_l = \frac{\pi M V_0}{4\hbar^2\alpha^2}\exp\left(-\frac{k^2}{2\alpha^2}\right) J_{l+1/2-2\eta_l/\pi}\left(\frac{k^2}{2\alpha^2}\right). \tag{10}$$

Considering the scattering of a neutron by a proton (M is the mass of the proton) at 100 Mev, and choosing for the constants the values $V_0 = 45$ Mev and $\alpha^2 = 0.266 \times 10^{26}$ cm^{-2}, we get the following values of the phase shifts by the Pais method: $\eta_1 = 0.534$, $\eta_2 = 0.221$, whereas the Born method gives $\eta_1 = 0.487$ and $\eta_2 = 0.197$. Since the second Born approximation gives better results than the first, we shall compare the values obtained above for the phase shifts with the results of the second Born approximation,[4] $\eta_1 = 0.552$ and $\eta_2 = 0.213$. We see that the Pais method gives considerably better results than the first Born approximation.

For large values of l the phase shifts η_l calculated by the Born and Pais methods approach each other, as can be seen from Eqs. (7) and (9).

---

[1] N. F. Mott and H. S. W. Massey, The Theory of Atomic Collisions, Oxford, 1949, Russ. Transl., IIL, 1951.

[2] A. Pais, Proc. Cambridge Phil. Soc. **42**, 45 (1946).

[3] N. Watson, A Treatise on the Theory of Bessel Functions, Cambridge Univ. Press, 1944.

[4] Ta-You Wu, Phys. Rev. **73**, 934 (1948).

Translated by W. H. Furry
44

THE RADIATIVE CORRECTION TO THE MASS OF THE ELECTRON IN NONLINEAR ELECTRODYNAMICS

V. Yu. URBAKH

Institute of Biophysics, Academy of Sciences, U.S.S.R.

Submitted to JETP editor February 11, 1959

J. Exptl. Theoret. Phys. (U.S.S.R.) **37**, 295-296 (July, 1959)

IT has been shown in a previous paper[1] that if in analogy with Einstein's theory of the gravitational field one describes the electromagnetic (vector) field as the curvature of an auxiliary "space" with the metric $ds = \gamma_i dx^i$, then one can obtain a nonlinear Lagrangian of the electromagnetic field, which in the case of a static spherically symmetrical field leads to the potential

$$\varphi = (e/r_0\sqrt{2})\sinh(r_0\sqrt{2}/r), \qquad r_0 = e^2/m_0c^2. \tag{1}$$

This gives for the classical (unquantized) field mass of a stationary electron $m_{cl} \approx m_0/5$, where m_0 is the experimental rest mass of the electron (the value $m_{cl} \approx m_0/3$ is erroneously given in reference 1).

To calculate the radiative (quantum) correction Δm_q to the mass of the electron, caused by the interaction of the stationary electron with the photon and electron-positron backgrounds, we must first of all find the wave solution of the field equations corresponding to the nonlinear Lagrangian in question. Since this is practically unfeasible because of the great mathematical difficulties, it is not without interest to try to give at least a preliminary and approximate estimate of the size of Δm_q. The idea of the calculation is as follows.

In the nonlinear theory under consideration, one gets in accordance with Eq. (1) for the energy of a stationary charge e situated in the field of another charge e, not the value $E_1 = e\varphi_1 = e^2/r$, but instead

$$E = e\varphi = \frac{c^2}{r_0\sqrt{2}} \sinh \frac{r_0\sqrt{2}}{r} = \frac{m_0c^2}{\sqrt{2}} \sinh\left(\frac{\sqrt{2}}{m_0c^2} E_1\right).$$

If now we assume that this relation between the energies in the linear and nonlinear theories holds not only for the energy of the field of a stationary point charge, but in general for every electromagnetic energy, and apply it to the energy of electromagnetic quanta, then

$$\omega = (\omega_0/\sqrt{2}) \sinh(\sqrt{2}\,\omega_1/\omega_0), \tag{2}$$

where ω_1 is the frequency in the linear theory, and $\omega_0 = m_0c^2/\hbar$ is the critical frequency at which the quantum energy equals the rest energy of the particle with which the quantized field interacts.

In view of the obviously preliminary nature of the present calculation, there is no point in carrying out exact computations of Δm_q; for an approximate quantitative estimate, it suffices to use the simplified formula from the first papers of Weisskopf,[2] according to which

$$\Delta m_{\mathbf{q}} = \frac{\pi e^2 h}{m_0c^2}\left(\int_0^{\omega_0} \frac{1}{\omega}\, dN + \omega_0^2 \int_{\omega_0}^{\infty} \frac{1}{\omega^3}\, dN\right), \qquad dN = \frac{8\pi\omega^2 d\omega}{(2\pi c)^3}.$$

Making here the change indicated in Eq. (2) (it is clear that the change is to be made only in the matrix elements and not in dN), we also change the intermediate limit of the integrations: instead of ω_0, we write $\eta\omega_0$, choosing the factor $\eta \sim 1$ in such a way that the integrands have the same value at the place where they are joined. The substitution leads to the expression

$$\Delta m_{\mathbf{q}} = \frac{\alpha}{2\pi} m_0 2\sqrt{2}\left(\int_0^{\eta} \frac{\xi^2 d\xi}{\sinh\sqrt{2}\,\xi} + 2\int_{\eta}^{\infty} \frac{\xi^2 d\xi}{\sinh^3\sqrt{2}\,\xi}\right), \quad \alpha = \frac{e^2}{hc},$$

where $\eta \approx 0.81$. Numerical integration gives a value ≈ 0.374 for the quantity in brackets, so that we have $2 \times 2^{1/2} \times 0.374 \approx 1.06$; therefore we get finally

$$\Delta m_{\mathbf{q}} \approx (\alpha/2\pi)\, m_0.$$

We note that the final value of Δm_q is gotten just from the strong singularity of φ at the origin. This result cannot be given by nonlinear theories with a finite potential at the origin (the Born-Infeld type of theory).

---

[1] V. Yu. Urbakh, J. Exptl. Theoret. Phys. (U.S.S.R.) **35**, 208 (1958), Soviet Phys. JETP **8**, 143 (1959).

[2] V. F. Weisskopf, Phys. Rev. **56**, 72 (1939); Usp. Fiz. Nauk **41**, 165 (1950), Russ. Transl. of Revs. Modern Phys. **21**, 305 (1949).

Translated by W. H. Furry
45

PARAMAGNETIC ABSORPTION AND ROTATION OF PLANE OF POLARIZATION FOR CERTAIN SALTS IN THE MICROWAVE BAND

A. I. KURUSHIN

Perm State University

Submitted to JETP editor February 21, 1959

J. Exptl. Theoret. Phys. (U.S.S.R.) **37**, 297-298 (July, 1959)

SEVERAL recently-reported experimental investigations[1-4] are devoted to a study of paramagnetic rotation of the plane of polarization in the microwave band, for the case when the preferred direction in the medium (the gyration direction) is perpendicular to the direction of the propagation of the incident wave. For several substances, critical relations were obtained for the angle of rotation of the plane of polarization, β, as a function of the constant field H_0. Curves of this type can be obtained also by other means without directly measuring the angle β. In fact (see references 1 and 6), starting with general considerations, we can obtain the following expression for the angle of rotation of the plane of polarization per unit length of the paramagnet

$$\beta = -(\pi\omega\sqrt{\varepsilon}/c)\,(\chi''_{\perp} - \chi''_{\parallel}) \sin 2\alpha, \tag{1}$$

where α is the angle between the constant $(\mathbf{H}_0)$ and high frequency fields; $\chi''_{\perp}$ and $\chi''_{\parallel}$ are the imaginary parts of the magnetic susceptibility of the paramagnet for perpendicular and parallel fields. To explain the dependence of β on H_0 it is necessary to know the corresponding dependences of the imaginary parts of the magnetic susceptibility, $\chi''_{\perp}$ and $\chi''_{\parallel}$, on the field, and these are readily obtained by experiment. Certain results of such experiments are listed below.

The apparatus used in the present investigation, with which we could obtain the dependence of χ'' on H_0 for all angles α, was analogous to the apparatus described by us earlier.[5] The only difference was, first, that in addition to being able to use a cylindrical cavity in the H_{011} mode we could also use a rectangular cavity in the H_{102} mode, and could thus reduce considerably the electromagnet gap, and second, that the generator portion of the apparatus was rigidly coupled to the measuring portion. This eliminated completely the possibility of contact error inherent in the rotating flange of the previous version of the apparatus. To vary the angle α, the entire apparatus was rotated as a unit.

The experiments were performed at room temperature and at 9150 Mcs, using powdered paramagnetic salts placed in polystyrol containers in the antinode of the magnetic field of the cavity. By suitably locating the cavity in the constant magnetic field it was possible to make the high frequency and constant fields either parallel or perpendicular to each other. Keeping the cavity position fixed, we plotted point by point the absorption vs. magnitude of the constant magnetic field, first with perpendicular fields and then with parallel fields. This was followed by control experiments: the constant field was left unchanged and the apparatus was rotated many times so as to make the fields alternately parallel and perpendicular, and the values of absorption $\chi''_{\perp}$ and $\chi''_{\parallel}$ corresponding to these positions were measured. Such experiments were carried out at various values of the constant field and, particularly, at fields considerably greater than the resonant values, at which the values of $\chi''_{\perp}$ and $\chi''_{\parallel}$ are close to each other. The experiments were performed with powdered salts $MnSO_4 \cdot H_2O$, $MnCl_2 \cdot 4H_2O$, $GdSO_4 \cdot 8H_2O$, GdF_3, $GdCl_3 \cdot 6H_2O$, $GdBr_3 \cdot 6H_2O$, $GdI_3 \cdot 6H_2O$.

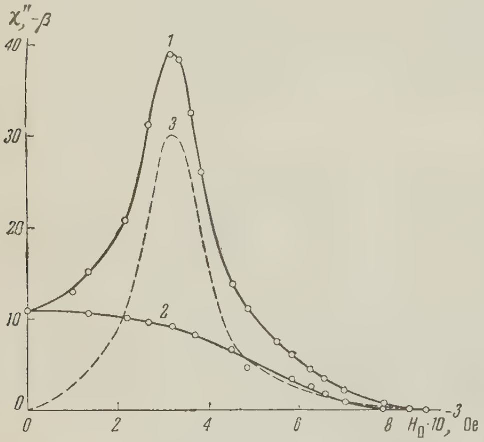

It was established by these experiments that, for all the foregoing salts, at fields ranging from 0 to 6000 oersteds, the absorption curves in perpendicular fields lie always above the corresponding curves in parallel fields. We observed no intersecting curves. The diagram shows the absorption curves in perpendicular (curve 1) and parallel (curve 2) fields (the ordinate units are arbitrary) for $MnCl_2 \cdot 4H_2O$. The absorption curves for all other substances listed above are analogous to those shown in the diagram. The only difference is in the widths of the resonance curves, in the position of the maximum, and in the value of the initial absorption $\chi''(0)$. Thus, for $MnSO_4 \cdot H_2O$ and $GdI_3 \cdot 6H_2O$, the values of initial absorption are quite small and the permanent fields hardly influence the absorption in parallel fields, while the paramagnetic resonance is sharply pronounced in perpendicular fields. Many other paramagnetic salts exhibit absorption in parallel and perpendicular fields analogous to that we obtained for $MnCl_2 \cdot 4H_2O$. This follows from the work of Hadders, Locher, and Gorter.[7]

The diagram shows also the dependence of the angle $(-\beta)$ of rotation of the plane of polarization (in arbitrary units) on the value of the permanent field (curve 3), determined as a difference of ordinates of curves 1 and 2, in accordance with Eq. (1). It is seen from the diagram that the rotation curve does not reverse sign over a large interval of fields. (For other substances listed above, the curves of rotation will obviously be analogous.) Imamutdinov, Neprimerov, and Shekun[1] obtained for $MnCl_2 \cdot 4H_2O$ a polarization-plane rotation curve of different shape, one that reverses sign at fields of approximately 4×10^3 oersteds. Obviously this difference in the shapes of the curves calls for further study and it appears to us that it would be interesting to determine the effect of the type of wave propagating in the substance on the rotating ability.

In view of the weak dependence of absorption in parallel fields on the permanent field, the shape of the rotation curve for the salt $MnSO_4 \cdot H_2O$ is close to the shape of the paramagnetic resonance curve, in good agreement with the data of Gozzini.[3]

---

[1] Imamutdinov, Neprimerov, and Shekun, J. Exptl. Theoret. Phys. (U.S.S.R.) **34**, 1019 (1958), Soviet Phys. JETP **7**, 704 (1958).

[2] Battaglia, Gozzini, and Polacco, Nuovo cimento **10**, 1205 (1953).

[3] A. Gozzini, Cahiers Phys. **79**, 123 (1957).

[4] P. Hedvig, Acta Phys. Acad. Sci. Hung. **6**, 489 (1957).

[5] A. I. Kurushin, Izv. Akad. Nauk SSSR, Ser. Fiz. **20**, 1232 (1956), Columbia Tech. Transl. p. 1122.

[6] L. M. Tsirul'nikova, J. Exptl. Theoret. Phys. (U.S.S.R.) **36**, 1428 (1959), Soviet Phys. JETP **9**, 1015 (1959).

[7] Hadders, Locher, and Gorter, Physica **24**, 839 (1958).

Translated by J. G. Adashko
46

EFFECT OF INTERACTION ON THE PHASE MOTION OF ELECTRONS IN A SYNCHROTRON

L. V. IOGANSEN

Moscow State Pedagogical Institute

Submitted to JETP editor March 4, 1959

J. Exptl. Theoret. Phys. (U.S.S.R.) 37, 299-300 (July, 1959)

MANY laboratories have recently built electronic accumulating systems for energies of hundreds of millions of electron volts, with the number of bunched electrons reaching $N \sim 10^{14}$. In the calculations, the forces of electromagnetic interaction of the electrons in the bunches are disregarded. In the present note we calculate approximately the effect of these forces on the phase motion of the electrons and obtain an estimate of the equilibrium angular dimensions of the bunch, determined by the interaction forces. We use in our calculations Eq. (3) below for the tangential forces of interaction in the bunch; this equation is correct if the angular dimensions of the bunch are $\vartheta_0 \ll 1$ (reference 1). We do not take into account the screening of the electron interaction by the walls of the chamber and by the magnet. This estimate is therefore valid only for sufficiently small bunches. For bunches whose dimensions are on the order of the transverse diameter of the chamber, the specific nature of the construction of the accelerator must be taken into account. The problem of the influence of the interaction forces on the motion of electrons in a synchrotron was first raised and examined by I. E. Tamm for a specific case (Report of the Physics Institute, U.S.S.R. Academy of Sciences, 1948).

For a circular orbit, limiting ourselves to the ultrarelativistic case $\gamma = E/mc^2 \gg 1$, we obtain, by using the usual derivation, a linearized phase equation in the form

$$\ddot{\psi} + \eta\dot{\psi} + \Omega^2\psi + \frac{c}{(1-n)\,aE_s}\,]W_{s\,\mathrm{coh}} + c\bar{f}_\tau(\psi)] = 0, \qquad (1)$$

where ψ is the phase of the electron, measured from the phasing point ψ_s, a is the radius of the stable orbit, and n is the decrement index of the magnetic field. The phasing point is determined from the condition

$$\frac{c}{2\pi a}\,eV_0\sin\psi_s = \dot{E}_s + W_{\gamma s} + W_{s\,\mathrm{coh}},$$

where V_0 is the amplitude of the resonator voltage, E_s the energy of the stable electron, $W_{\gamma s} = (2e^2c/3a^2)\gamma^4$ is the energy lost by a single electron to radiation,

$$W_{s\,\mathrm{coh}} = -c\int\limits_{-\infty}^{+\infty}\bar{f}_\tau(\psi)\,\varphi(\psi)\,d\psi \sim Ne^2c/a^2\vartheta_0^{4/3} \qquad (2)$$

is the mean energy lost by a single electron to coherent radiation, and

$$\eta = \left\{\left(\frac{3-4n}{1-n}\right)\frac{W_{\gamma s}}{E_s} + \frac{\dot{E}_s}{E_s} + \frac{1}{(1-n)}\,\frac{W_{s\,\mathrm{coh}}}{E_s}\right\},$$

$$\Omega^2 = \frac{c^2eV}{2\pi(1-n)\,a^2E_s}, \qquad V = V_0\cos\psi_s,$$

$$\bar{f}_\tau(\psi) = -\frac{d}{d\psi}\Phi(\psi) = -\frac{d}{d\psi}\left\{\frac{2}{3^{1/3}}\,\frac{Ne^2}{a^2}\int\limits_0^\infty\varphi(\psi-\xi)\,\frac{d\xi}{\xi^{1/3}}\right\}. \qquad (3)$$

The distribution of particles by phases, $\varphi(\psi)$, depends on the character of the phase motion and on the distribution of particles by parameters of this motion. As the phase motion proceeds, $\varphi(\psi)$ will in general change. As a result, $\bar{f}_\tau(\psi)$ will also change, making it difficult to obtain an exact solution of Eq. (1). We shall give below a qualitative estimate of the solutions of (1), assuming $\varphi(\psi)$ to be specified and constant. In this case Eq. (1) describes dissipative motion in a well with a potential

$$U(\psi) = \frac{\Omega^2}{2}\psi^2 + \frac{c}{(1-n)\,aE_s}\,[W_{s\,\mathrm{coh}}\psi - c\Phi(\psi)]. \qquad (4)$$

We obtain from (2), by the mean-value theorem, $W_{s\,\mathrm{coh}} = -c\bar{f}_\tau(\psi_1)$, where ψ_1 is not an extremal point. Consequently the sum $W_{s\,\mathrm{coh}} + c\bar{f}_\tau(\psi)$ vanishes in the region $|\psi| \lesssim \vartheta_0$ at least at two points, and is negative between these two points. The second term in (4) is therefore essentially a straight line with a positive slope, but must have a well in the region $|\psi| \lesssim \vartheta_0$. The edge of the well lies near $\psi = -\vartheta_0$, and the ends of the bunch always project outside this well. The shape of the potential (4) depends on the ratio of the first and second terms near the point $\psi = -\vartheta_0$. This ratio is best characterized by the dimensionless parameter

$$p = \frac{\Omega^2\vartheta_0}{cW_{s\,\mathrm{coh}}/(1-n)\,aE_s} \sim \left(\frac{aV}{2\pi Ne}\right)\vartheta_0^{7/3}. \qquad (5)$$

If $p \gg 1$, the first term in (4) predominates and the potential differs little from an ordinary parabola. To the contrary, when $p \ll 1$, the second term predominates. In this case the potential has two minima, one in the front, in the region $\psi \leq \vartheta_0$ and one in the rear, in the region $\psi < -\vartheta_0$; these are separated by a hump near the point $\psi = -\vartheta_0$. The bunch is located essentially in the forward well, but its ends always project beyond its limits. In the intermediate case $p \sim 1$ we get a point of inflection instead of the rear well and the hump.

It is easy to visualize qualitatively the variation of the dimensions of the bunch in the accumulating system. First, as long as the bunch is large, $p \gg 1$ and the particles perform the ordinary damped oscillations in an almost-parabolic potential. The bunch becomes compressed, the potential (4) is deformed, and the oscillations become distorted. If it becomes possible to compress the bunch in some manner so that $p \ll 1$, the potential will already have two minima. Thanks to the fact that the ends of the bunch project beyond the forward potential wall, the bunch begins to overflow backwards and increases in size. Consequently, there should exist an equilibrium bunch, with angular dimensions of an order of magnitude determined by the condition $p \sim 1$ or

$$\vartheta_0 \sim (2\pi Ne/aV)^{3/7}, \qquad \gamma \gg 1; \qquad \vartheta_0 \ll 1. \tag{6}$$

In one of the installations now being designed, $N \sim 10^{14}$, $V_0 \sim 10^5$ v, and $a \sim 10^2$ cm (reference 2). It is assumed that the equilibrium angular dimensions of the bunch are determined by the swing of the phase oscillations due to quantum fluctuations of the radiation, and are small at these parameters. Inserting the numerical values in (6) we get $\vartheta_0 \sim 2$. This means that the interaction forces cannot be neglected. However, the estimate (6) itself can no longer be applied. To determine the dimensions of the bunch under these conditions and to answer the question whether the phase stability is disturbed, it is necessary to perform the calculation with allowance for the forces of interaction between the electrons without assuming the bunch to be small, and to take into account the interaction between the bunch and the walls of the chamber and the magnet.

In conclusion, I express my sincere gratitude to Prof. M. S. Rabinovich for valuable advice.

---

[1] L. V. Iogansen and M. S. Rabinovich, J. Exptl. Theoret. Phys. (U.S.S.R.) **37**, 118 (1959), Soviet Phys. JETP this issue, p. 83.

[2] G. K. O'Neill, Stanford University Report, 1958.

Translated by J. G. Adashko
47

DETERMINATION OF THE p-p SCATTERING MATRIX AT 90°

S. B. NURUSHEV

Joint Institute for Nuclear Research

Submitted to JETP editor March 4, 1959

J. Exptl. Theoret. Phys. (U.S.S.R.) **37**, 301-302 (July, 1959)

To determine the p-p scattering matrix at 90° it is necessary to perform five experiments. If we measure at this angle of the value of the cross section I, the coefficient of spin correlation C_{nn}, and the Wolfenstein parameters[1] D, R, and A, then the amplitudes and phases of the components of the p-p scattering matrix can be determined from the relations

$$b^2 = |B|^2/4I = {}^1/_2(1 - C_{nn}),$$

$$c^2 = 2|C|^2/I = {}^1/_4(1 + C_{nn} + 2D),$$

$$h^2 = |H|^2/2I = {}^1/_4(1 + C_{nn} - 2D),$$

$$\sin\delta_C = -(R + A)/2bC, \quad \cos\delta_H = (A - R)/2bh,$$

where B, C, and H are given by

$$B = |B|e^{i\varphi_B}, \quad C = |C|e^{i(\delta_C+\varphi_B)}, \quad H = |H|e^{i(\delta_H+\varphi_B)}.$$

The symbols used are the same as in Wolfenstein's paper.[1]

Since the experimental data are incomplete, we can only estimate the region of possible values of the amplitudes. If we assume $D(90°) = -0.75 \pm 0.15$ for an energy of 140 Mev, which follows from an extrapolation of the data of Taylor,[2] then $0 \leq b^2 \leq 40\%$, $0 \leq c^2 \leq 20\%$, and $75 \leq h^2 \leq 95\%$. For 315 Mev, an estimate was made by Wolfenstein.[3] Combining the experimental data at energies of 382 Mev[4] and 415 Mev[5] and referring them to 400 Mev, we obtain $b^2 = (30 \pm 4)\%$, $c^2 = (56 \pm 5)\%$, and $h^2 = (14 \pm 5)\%$. Using the value of the correlation tensor $C_{kp} = 0.63 \pm 0.10$, measured at 90° and 382 Mev,[6] we can determine the phase difference $\delta_C - \delta_H$, which equals 90°. For 635 Mev, as follows from reference 7, $0 \leq b^2 \leq 24\%$, $76 \leq c^2 \leq 100\%$, and $0 \leq h^2 \leq 12\%$. From this we can determine the possible values of the correlation tensor C_{nn} and of the parameters R and A at 635 Mev, namely $52 \leq C_{nn} \leq 100\%$, $|R| \leq 27\%$, and $|A| \leq 21\%$.

It follows from this estimate that in the energy range under consideration the principal contribution to the cross section is made by the triplet interaction. Furthermore, the tensor-like triplet term h^2 predominates in the lower interval, while the spin-orbit triplet term c^2 predominates in the upper interval.

To determine the phases and to make a numerical estimate of the amplitudes, we obtain the lacking data from the calculations performed for 140 Mev (see reference 8) and for 315 Mev (see reference 9, solution No. 4).

We then obtain the following values for the amplitudes and phases:

E, Mev	b^2, %	c^2, %	h^2, %	δ_C	δ_H
140	5	13	82	0°	60°
315	25	62	13	—90°	143°
400	30	56	14	$\delta_C - \delta_H = 90°$	
635	24	76	12		

If we assume that at energies on the order of several Bev the nucleon is a black sphere, which apparently does not contradict the available experimental data, then only the amplitude B differs from zero, and $b^2 = 100\%$. Consequently, as the energy increases, the contribution of the triplet interaction, due to the terms h^2 and c^2, should decrease.

Similar results are obtained for p-p scattering at 90° from the following type of nucleon interaction. Let the phases of all waves (the number of which is arbitrary) be imaginary and large. Then at 90° only the amplitude B differs from 0, as in the case of a black sphere. But unlike the latter, such a model leads to an angular dependence of the Wolfenstein parameters and of the correlation tensor:

$$D(\theta) = 2\cos\theta\,\frac{1+\cos^2\theta}{1+3\cos^2\theta}, \qquad R(\theta) = 4\cos\theta\,\frac{\cos^3(\theta/2)}{1+3\cos^2\theta},$$

$$A(\theta) = -\sin 2\theta\,\frac{\cos(\theta/2)}{1+3\cos^2\theta}, \qquad C_{nn}(\theta) = \frac{-1+\cos^2\theta}{1+3\cos^2\theta}.$$

In this model there is no polarization at all.

Note added in proof (May 28, 1959). A recent communication on triple scattering at 143 Mev (C. F. Hwang et al., Phys. Rev. Lett. **2**, 210, 1959) reports a different result than in reference 2: $D(90°) = 0.3 \pm 0.15$ at 90° in the c.m.s., hence $30 \le c^2 \le 70\%$ and $0 \le h^2 \le 35\%$.

---

[1] L. Wolfenstein, Phys. Rev. **96**, 1654 (1958).

[2] A. E. Taylor, Annual International Conference on High Energy Physics, CERN, 1958.

[3] L. Wolfenstein, Bull. Am. Phys. Soc. **1**, 36 (1956).

[4] Kane, Stallwood, Sutton, and Fox, Bull. Am. Phys. Soc. **1**, 9 (1956).

[5] Ashmore, Diddens, Huxtable, and Suarsvag, Proc. Phys. Soc. **72**, 289 (1958).

[6] Kumekin, Meshcheryakov, Nurushev, and Stoletov, J. Exptl. Theoret. Phys. (U.S.S.R.) **35**, 1398 (1958), Soviet Phys. JETP **8**, 977 (1959).

[7] P. S. Signell and R. E. Marshak, Phys. Rev. **109**, 1229 (1958).

[8] Stapp, Ypsilantis, and Metropolis, Phys. Rev. **105**, 313 (1957).

[9] Ashmore, Diddens, and Huxtable (preprint, 1959).

Translated by J. G. Adashko
48

PARAMAGNETIC RESONANCE IN POTASSIUM OZONIDE

A. K. PISKUNOV, A. A. MANENKOV, and Z. A. BAGDASAR' YAN

L. Ya. Karpov Physico-Chemical Institute

Submitted to JETP editor March 4, 1959

J. Exptl. Theoret. Phys. (U.S.S.R.) **37**, 302-304 (July, 1959)

KAZARNOVSKIĬ, Nikol'skiĭ, and Abletsov[1] have proposed that the magnetism of potassium ozonide, KO_3, is due to the molecular ozone ion O_3^- and that the latter has the character of a free radical with one unsaturated valence. It is of interest to investigate potassium ozonide by the method of electronic paramagnetic resonance (EPR), in order to investigate in greater detail the nature of its paramagnetism.

We have investigated paramagnetic resonance in polycrystalline specimens, containing approximately 90% KO_3, at frequencies of 2580, 9375, 12,000 and 37,000 Mcs at room temperature and at temperature of liquid nitrogen. At 2580, 9375, and 12,000 Mcs we observed one symmetric absorption line, the width of which was 31 ± 3, 39 ± 2, and 45 ± 3 gausses respectively. At 37,000 Mcs the observed line is noticeably asymmetric and has a width of approximately 77 gausses at the level of half the intensity of the principal peak. For illustration, the diagram shows an oscillogram of the absorption line, observed at 37,000 Mcs at room temperature. The dependence of the width of the EPR line on the frequency, and particularly the asymmetry of the line at 37,000 Mcs, are direct evidence of anisotropy of the g-factor. It is seen from the diagram that this anisotropy is due to the actual symmetry of the electric field of the crystal. Since the investigated specimens were polycrystalline, the relative contribution of the crystals with axis perpen-

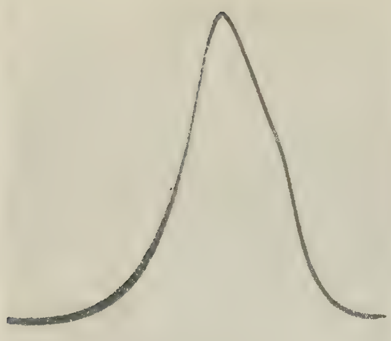

dicular to the external magnetic field is greater than the contribution of the crystals with parallel orientation. Measurements of the g-factor for the perpendicular and parallel orientations yielded respectively

$$g_{\perp} = 2.012 \pm 0.002, \qquad g_{\parallel} = 2.005 \pm 0.003.$$

The line width may be due to spin-lattice, magnetic-dipole, and exchange spin-spin interactions. For a given frequency, the width of the KO_3 line did not change at room temperature and at liquid-nitrogen temperature, within the experimental error, indicating the absence of noticeable influence of spin-lattice interaction on the line width at these temperatures. It is known that in the case of magnetically-concentrated systems with spin $S = \frac{1}{2}$, dipole spin-spin interactions should lead to a line width of approximately 100 gausses. From the value obtained for the line width at 2580 Mcs (at which the anisotropic broadening is small) it follows that in KO_3 there are considerable exchange interactions, which reduce the effectiveness of the dipole interactions and thus cause narrowing of the line.

The fact that the value obtained for the g-factor is close to 2 and the presence of considerable exchange interactions confirm the previously advanced suggestion[1,2] that the magnetism of the molecular ion of ozone, O_3^-, to which the observed paramagnetic resonance in KO_3 is due, has the character of a free radical. The deviation of the value of the g-factor from that of a free electron and the observed anisotropy indicate the presence of a considerable orbital contribution to the paramagnetism of KO_3.

The values obtained by Neĭding[3] for the static magnetic susceptibility of potassium ozonide, are different from the pure-spin value, in agreement with our results.

Bennett, Ingram, and Schonland[4] report an investigation of EPR of sodium ozonide, in which the absorption line at a wavelength of 1.25 cm has a weak asymmetry towards the higher fields, analogous to that observed in KO_3. Within the experimental accuracy, the values of the g-factor coincide with those we obtained for potassium ozonide. This may serve as a confirmation that in ozonides the bond between the metal and the molecular group O_3 is ionic.

We have also investigated the kinetics of the spontaneous decomposition of KO_3 at 295° K. Such investigations were previously made by chemical methods.[2] The comparison standard used was the time-stable free radical of diphenylpicrylhydrazyl (DPPH). A specimen of diphenylpicrylhydrazyl, covered with a film of polystyrol glue to prevent its oxidation, was placed together with the investigated specimen of KO_3 in the cavity of the radio spectroscope. The intensity of the paramagnetic-resonance line of KO_3 was measured relative to the intensity of the diphenylpicrylhydrazyl line at definite time intervals. These measurements show that the decomposition of KO_3 in a time interval of 47 to 168 hours after the preparation of the compound follows approximately an exponential law with a time constant of 0.02 hr^{-1}. A detailed analysis of the results of the investigation of the kinetics of the decay of potassium ozonide will be published elsewhere.

We thank D. N. Shigorin and S. D. Kaĭtmazov for help in the measurements and for an evaluation of the results of the work.

---

[1] Kazarnovskiĭ, Nikol'skiĭ, and Abletsova, Dokl. Akad. Nauk SSSR **64**, 69 (1949).

[2] Kazarnovskiĭ, Raĭkhshteĭn, and Bykova, Dokl. Akad. Nauk SSSR **108**, 641 (1956).

[3] A. B. Neĭding, Dissertation, L. Ya. Karpov Physico-Chemical Institute, 1950.

[4] Bennett, Ingram, and Schonland, Proc. Phys. Soc. **A69**, 556 (1956).

Translated by J. G. Adashko
49

THE INFLUENCE OF COLLISIONS BETWEEN ELECTRONS ON THEIR VELOCITY DISTRIBUTION IN GASES AND IN SEMICONDUCTORS IN AN ELECTRIC FIELD

A. V. GUREVICH

P. N. Lebedev Physics Institute, Academy of Sciences, U.S.S.R.

Submitted to JETP editor March 4, 1959

J. Exptl. Theoret. Phys. (U.S.S.R.) **37**, 304-306 (July, 1959)

IT is well known[1] that in a plasma located in an electric field the velocity distribution function of the electrons will be on the whole symmetrical, i.e., will depend only upon the absolute magnitude of the velocity. Its form is determined for very small degrees of ionization of the plasma by the collisions of the electrons with the heavy particles (atoms, molecules). For higher degrees of ionization an important and even a basic role is played by the collisions between the electrons themselves which must, of course, lead to the approach of the distribution function to the Maxwellian. It is the aim of the present paper* to study the influence of the interelectronic collisions on the symmetric part of the distribution function $f_0(v, t)$.

Following Landau,[4] and also taking the symmetry of the main part of the distribution function into account, we can write the integral for interelectronic collisions S_{ee} in the following form (compare references 5 and 6):

$$S_{ee}(f_0, f_0) = -\frac{1}{v^2}\frac{\partial}{\partial v}\left\{v^2\nu_{ee}\left[A_1(f_0)\frac{\partial f_0}{\partial v} + A_2(f_0)vf_0\right]\right\}. \quad (1)$$

Here $\nu_{ee}(v)$ is the frequency of collisions between electrons, and A_1 and A_2 coefficients defined by the relations:

$$A_1 = \frac{4\pi}{3N_e}\left\{\int_0^v v_1^4 f_0(v_1)\,dv_1 + v^3\int_v^\infty v_1 f_0(v_1)\,dv_1\right\},$$

$$A_2 = \frac{4\pi}{N_e}\int_0^v v_1^2 f_0(v_1)\,dv_1,$$

$$\nu_{ee} = (4\pi e^4 N_e/m^2v^3)\ln\left[k^{3/2}T_eT^{1/2}/e^3N_e^{1/2}\right], \quad (1')$$

where e, m are the charge and mass of an electron, N_e and T_e the density and temperature of the electrons, and T the temperature of the heavy particles.

Taking collisions between the electrons into

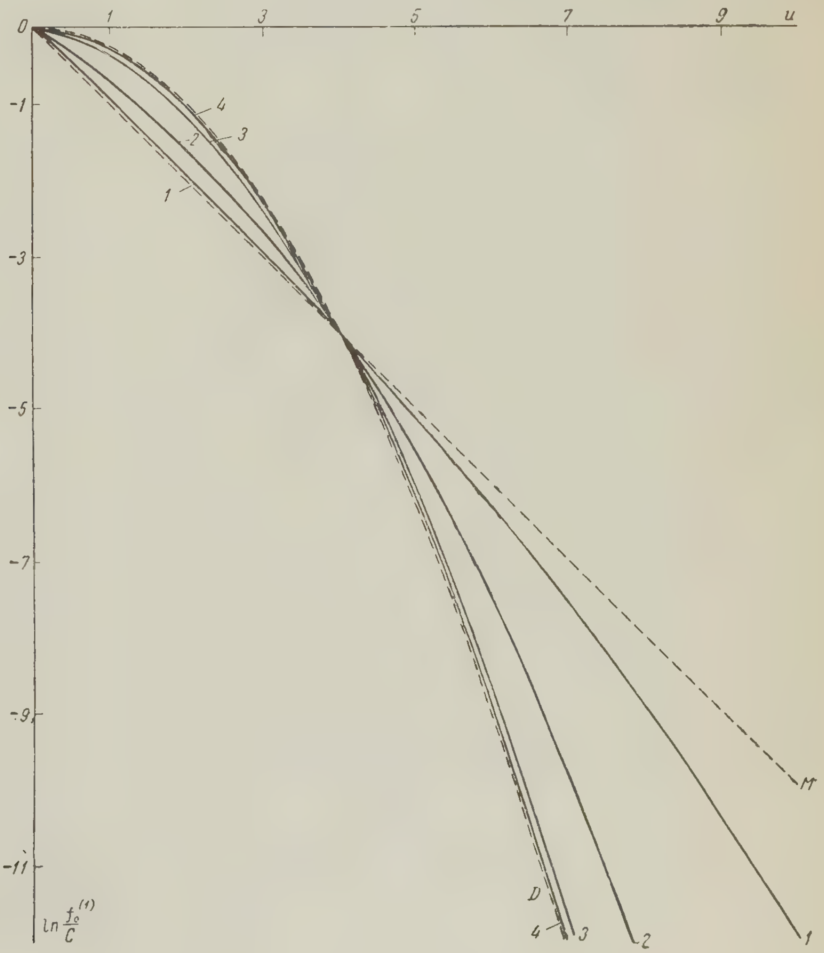

The dependence of $\ln(f_0^{(1)}/C)$ on $u = mv^2/2kT_e$ for different values of the parameter p: curve 1) p = 100; curve 2) p = 10; curve 3) p = 1; curve 4) p = 0.1. The dotted curves are the Maxwellian distribution (M) and the Druyvestein distribution (D).

account, the equation for the function f_0 (see references 1 and 7) becomes an integro-differential and nonlinear equation. Its solution can be obtained by an iteration method. Choosing as the zeroth approximation, $f_0^{(0)}$, the Maxwellian distribution function with an electron temperature defined in the usual way (see, for instance, reference 3), we find that in that approximation the coefficients $A_1^{(0)}$ and $A_2^{(0)}$ are given by the following expressions:

$$A_1^{(0)} = \frac{kT_e}{m} A_2^{(0)} = \frac{kT_e}{m} A(\sqrt{u}), \text{ where } u = \frac{mv^2}{2kT_e},$$

$$A(x) = \Phi(x) - \frac{2}{\sqrt{\pi}} x \cdot e^{-x^2} \tag{2}$$

[$\Phi(x)$ is the error integral]. Substituting now (1) and (2) into the equation for the function f_0, we find easily its solution and thus obtain the first iteration $f_0^{(1)}$. In the case of a strong constant electric field, for instance ($E \gg kT\sqrt{\delta}/el$):†

$$f_0^{(1)} = C \exp\left\{-\int_0^{mv^2/2kT_e} \frac{u^2 + pA(\sqrt{u})}{2u + pA(\sqrt{u})} du\right\}. \tag{3}$$

Here $T_e = eEl/\sqrt{6\delta}$ is the temperature of the electrons, l the mean free path of the electrons which is independent of the velocities, δ the average fraction of energy lost by an electron in one collision (in the case of elastic collisions $\delta = 2m/M$). Finally,

$$p = \frac{2\nu_{ee}(\sqrt{2kT_e/m})l}{\delta\sqrt{2kT_e/m}} = \frac{12\pi e^2 N_e}{lE^2} \ln\left(\frac{k^{3/2} T_e T^{1/2}}{e^3 N_e^{1/2}}\right).$$

The parameter p characterizes the influence of the interelectronic collisions on the distribution function. For small values of p the function $f_0^{(1)}$ is the same as the one given by Druyvestein,[8] and for large p the same as the Maxwellian one, as should be the case. From the graphs given in the figure it is clear that in the region of large u (i.e., in the "tail" of the distribution function) the deviations from the Maxwellian distribution are appreciable even for $p = 100$.

Calculations show that the next iterations lead only to an unimportant change in the distribution function: the difference between $f_0^{(1)}$ and $f_0^{(2)}$ is a maximum for $p \sim 10$, but in that case $0.9 \leq f_0^{(1)}/f_0^{(2)} \leq 1.0$ (while $0.5 \leq f_0^{(0)}/f_0^{(1)} \lesssim \infty$). We note also that for large values of u the functions $f_0^{(1)}$ and $f_0^{(2)}$ practically coincide; in that case the function f_0 is given approximately by the following expression:

$$f_0 = C \exp\left\{-\frac{u^2}{4} + \frac{pu}{4} - \frac{p(p+4)}{8} \ln\left(1 + \frac{2u}{p}\right)\right\}. \tag{4}$$

The influence of the interelectronic collisions on the distribution function of electrons in semiconductors can be taken into account in a similar way. In a strong electric field, in particular, the same expression (3) is valid for $f_0^{(1)}$ (one needs only bear in mind that in semiconductors $\delta = 2mv_s^2/kT$, where v_s is the sound velocity[1]).

The author is grateful to V. L. Ginzburg, L. V. Keldysh, L. M. Kovrizhnykh for a fruitful discussion and to L. V. Pariĭskaya for performing the calculations.

---

*The influence of the collisions between the electrons on the directed (current) part of the distribution function in a strongly ionized plasma was considered by Landshoff[2] and the author.[3] It is inappreciable in the case of a weakly ionized plasma.

†A similar expression for the function $f_0^{(1)}$ is also obtained in a variable electric field and also when there is a constant magnetic field present (see reference 7).

---

[1] B. I. Davydov, J. Exptl. Theoret. Phys. (U.S.S.R.) 7, 1069 (1937).

[2] R. Landshoff, Phys. Rev. **76**, 904 (1949).

[3] A. V. Gurevich, J. Exptl. Theoret. Phys. (U.S.S.R.) **35**, 392 (1958), Soviet Phys. JETP **8**, 271 (1959).

[4] L. D. Landau, J. Exptl. Theoret. Phys. (U.S.S.R.) 7, 203 (1937).

[5] S. Chandrasekhar, Revs. Modern Phys. **15**, 1 (1943).

[6] Rosenbluth, MacDonald, and Judd, Phys. Rev. **107**, 1 (1957).

[7] A. V. Gurevich, J. Exptl. Theoret. Phys. (U.S.S.R.) **32**, 1237 (1957) and **30**, 1112 (1956), Soviet Phys. JETP **5**, 1006 (1957) and **3**, 895 (1957).

[8] M. Druyvestein, Physica (old series) **10**, 69 (1930).

Translated by D. ter Haar
50

ANGULAR CORRELATION IN INTERNAL CONVERSION, INCLUDING EFFECTS OF SCREENING AND OF THE FINITE SIZE OF THE NUCLEUS

A. K. USTINOVA

Submitted to JETP editor March 12, 1959

J. Exptl. Theoret. Phys. (U.S.S.R.) **37**, 307-308 (July, 1959)

As has been shown in papers by Rose et al.[1] and by Dolginov,[2] the angular correlation of a conversion electron with any subsequent radiation x can be expressed in the following way:

$$W_{e-x}(\vartheta) = \sum_{\nu=0}^{\nu_m} b_\nu A_\nu(\gamma - x) P_\nu(\cos\vartheta)$$

using the notation of Rose. Here b_ν are the angular correlation coefficients. If $b_\nu = 1$, we get the well-known expansion of the angular correlation function between the γ-ray quantum and the radiation x in terms of Legendre polynomials $P_\nu(\cos\vartheta)$. The formulas for the calculation of the b_ν in the case of the K shell are:

$$b_\nu^{(L)}(e) = 1 + \frac{\nu(\nu+1)}{2L(L+1) - \nu(\nu+1)} \frac{L}{2L+1} \frac{|L+1+T_e|^2}{L(L+1) + |T_e|^2},$$

$$T_e = \frac{\exp(i\delta_L)}{\exp(i\delta_{-L-1})} \frac{[L(R_1+R_2) - (2L+1)R_3 - R_4]_{\varkappa=L}}{[R_1+R_2+2R_4]_{\varkappa=-L-1}};$$

$$b_\nu^{(L)}(m) = 1 + \frac{\nu(\nu+1)}{2L(L+1) - \nu(\nu+1)} \frac{L(L+1)}{2L+1}$$

$$\times \frac{|1-T_m|^2}{L+1+L|T_m|^2},$$

$$T_m = \frac{\exp(i\delta_{L+1})}{\exp(i\delta_{-L})} \frac{(R_3'+R_4')_{\varkappa=L+1}}{(R_3'+R_4')_{\varkappa=-L}},$$

$L = 1, 2, 3, 4, 5;\ \nu = 0, 2, 4.$

Here $b_\nu^{(L)}(e)$ are the coefficients for electric transitions, $b_\nu^{(L)}(m)$ are those for magnetic transitions, L is the degree of the multipole, δ_L and δ_{-L} are phase shifts, and R_i and R_i' are radial integrals.

All of the coefficients b_ν $(\nu > 2)$ can be obtained from b_2 by the formula

$$b_\nu(\pi) - 1 = \frac{\nu(\nu+1)[L(L+1)-3]}{3[2L(L+1) - \nu(\nu+1)]}[b_2(\pi) - 1],$$

where $\pi = e$ or m.

The paper by Rose et al.[1] presents curves of $b_2(\pi)$ for 12 elements, $10 \le Z \le 96$, obtained on the assumption of the Coulomb field of a point nucleus. We have obtained curves of $b_2(\pi)$ for $Z = 81, 84, 88, 92$, using the phase shifts[3] and radial integrals calculated with allowance for effects of screening and of the finite size of the nucleus, as in the work of Sliv and Band[4] on internal conversion coefficients. Let us compare these curves over the range of variation of the energy k from 0.5 to 2.0 mc^2.

All of our curves are displaced toward smaller Z as compared with those of Rose (for example, our curves for $Z = 92$ are displaced relative to those of Rose toward the curves for $Z = 88$). For most of the cases the maximum shift is insignificant [for $b_2^{(1)}(e)$, $b_2^{(3)}(e)$, $b_2^{(4)}(e)$, $b_2^{(2)}(m)$, $b_2^{(3)}(m)$, $b_2^{(4)}(m)$ it is 1 percent, for $b_2^{(5)}(e)$, 0.2 percent, and for $b_2^{(5)}(m)$, 0.1 percent], and occurs at energy $k = 2.0\ mc^2$. The exceptions are $b_2^{(2)}(e)$ and $b_2^{(1)}(m)$. The maximum shift of $b_2^{(2)}(e)$ reaches 7 percent at $k = 0.5$; that of $b_2^{(1)}(m)$ at $k = 2.0$ for $Z = 88$ is 60 percent, and for $Z = 92$ it is 100 percent. (See Figs. 1 and 2; the curves of Rose are shown as dashed lines.)

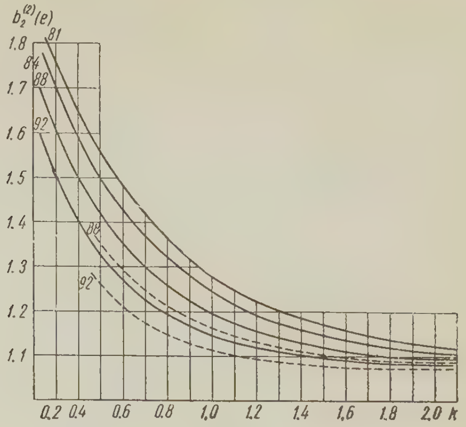

FIG. 1

These deviations agree with previously obtained results,[4] since the tables of internal conversion coefficients (ICC) and our curves for $b_2^{(L)}$ have been obtained with the same radial integrals. The largest deviations of the ICC from the Coulomb values were found in the case of magnetic dipole transitions (L = 1) for heavy elements.

At present, analogous calculations of the coefficients b_2 are being made for the L shell.

In conclusion the writer expresses her deep gratitude to A. Z. Dolginov and L. A. Sliv for valuable advice and suggestions that have been used in the preparation of this paper.

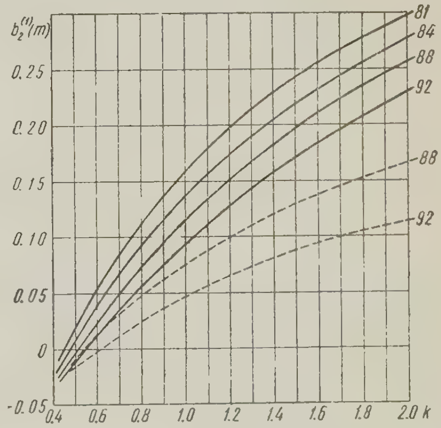

FIG. 2

---

[1] Rose, Biedenharn, and Arfken, Phys. Rev. **85**, 5 (1952).

[2] A. Z. Dolginov, Izv. Akad. Nauk SSSR, Ser. Fiz. **16**, 322 (1952).

[3] Band, Guman, and Sogomonova, Таблицы

волновых функций и фаз электронов (Tables of Electron Wave Functions and Phase Shifts), U.S.S.R. Acad. Sci. Press, 1959.

[4] L. A. Sliv and I. M. Band, Таблицы коэффициентов внутренней конверсии γ-излучения (Tables of Internal Conversion Coefficients for γ Radiation). Part I, 1956.

Translated by W. H. Furry
51

MEASUREMENTS OF THE TRANSVERSE PROTON RELAXATION TIME IN AQUEOUS SOLUTIONS OF PARAMAGNETIC SALTS BY THE SPIN-ECHO METHOD

V. D. KOREPANOV, R. A. DAUTOV, and V. M. FADEEV

Kazan' State University

Submitted to JETP editor March 25, 1959

J. Exptl. Theoret. Phys. (U.S.S.R.) **37**, 308-309 (July, 1959)

THE spin-echo effect[1,2] makes it possible to determine experimentally the absolute values of the longitudinal and transverse nuclear relaxation times T_1 and T_2. The advantage of the spin-echo method over other methods is particularly evident in measurements of nuclear relaxation times in low-viscosity liquids.[2]

To obtain the spin-echo effect, we constructed apparatus for the quantitative measurement of the transverse relaxation time T_2 of protons in water, in the presence of paramagnetic ions. The measurement was carried out at 12.2 Mcs in the field of a permanent magnet. A radio-frequency magnetic field with an amplitude of ~3.7 oersteds was applied to the sample in the form of two successive short rectangular pulses, with approximate durations of 16 and 32 microseconds, insuring 90° and 180° nutations respectively in the magnetic polarization of the water protons. The interval between the pulses could be varied from 0.3 to 2 milliseconds.

The solution to be studied, contained in a glass tube, was placed in a radio-frequency induction head of the "through-flow" type,[3] whose receiving coil picked up the induced nuclear echo signal, which was then amplified by a receiver with a 120 kcs bandwidth. The amplified output voltage from the receiver was applied to an oscillograph, and the echo signal on its screen was photographed. The non-uniformity of the permanent magnet field was estimated from the width of the echo signal. It proved to be equal to 1.2 oersted in the region where the sample (1 cm^3 in volume) was located.

In a field of the above non-uniformity, the effect of the self-diffusion of water molecules during the experimentally-determined time T_2 (about 10^{-3} sec) was negligible.

As a check on the operation of the apparatus, experiments were carried out on the hydrolysis of iron in nitric acid solution. In all the experiments the concentrations of Fe^{+++} and nitrate ions were constant and equal to 0.02 M and 0.6 M respectively. The results of the T_2 measurements for water protons in $Fe(NO_3)_3$ solutions are shown in the figure as a function of the acidity (pH). It is well known[4] that the proton relaxation effect in solutions of paramagnetic salts depends on the degree to which the ions are bound into a complex. The values of T_2 at higher pH are considerably larger than at high acidity. The gradual reduction in T_2 with increasing acidity indicates an increase in the effectiveness of the paramagnetic iron ions in shortening the transverse relaxation time of protons. This can be explained by the fact that when the pH is reduced the concentration of hydroxyl ions in the solution is decreased, leading to the dissociation of the iron hydro-complex. With increasing relative amounts of free iron ions in the solution, which are more effective in causing relaxation, the time T_2 must become shorter, as is well confirmed by the trend of the data shown in the figure.

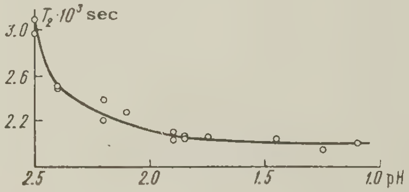

For discussions of the results and continued interest in the work, the authors are grateful to A. A. Popel' and A. I. Rivkind.

---

[1] E. L. Hahn, Phys. Rev. **80**, 580 (1950).

[2] H. Y. Carr and E. M. Purcell, Phys. Rev. **94**, 630 (1954).

[3] J. Arnold, Phys. Rev. **102**, 136 (1956).

[4] A. I. Rivkind, Dokl. Akad. Nauk SSSR **100**, 93° (1955).

Translated by D. C. West
52

OSCILLATIONS IN THE ABSORPTION COEFFICIENT OF SOUND IN TIN AT LOW TEMPERATURES

A. A. GALKIN and A. P. KOROLYUK

Institute for Radiophysics and Electronics, Academy of Sciences, Ukrainian S.S.R.

Submitted to JETP editor March 25, 1959

J. Exptl. Theoret. Phys. (U.S.S.R.) 37, 310-312 (July, 1959)

IT has been shown by several authors[1-3] that the ultrasound absorption coefficient in metals does not vary monotonically with the magnetic field and shows a sharp anisotropy.[1] In the present work we give the results of a more detailed study of the anisotropy in absorption at 70 Mcs, made by a pulse method, using a specially constructed two-dimensional automatic plotter.

The measurements were made on a 15-mm diameter single crystal sphere of tin, which had planes cut on it for fixing the quartz. The normals to these planes were parallel to the binary and fourfold axes. The planes were cut by an electric spark, which spoils a single crystal only to a depth of about 10 μ.

The absorption coefficient was determined using longitudinal sound waves with wave vectors **k**, parallel to the binary or fourfold axes. The specimen was rotated in the magnetic field **H**, and the vector **k** was perpendicular to **H**.

The amplitude of the transmitted pulse for fields between 45 and 1000 oe ($T = 4.2°K$) is shown in Fig. 1 for the sound propagated along the binary axis, with the fourfold axis kept parallel to **H**. There are many maxima and minima on the curve, with a constant inverse field period of oscillation. This is in agreement with Gurevich's theory.[4]

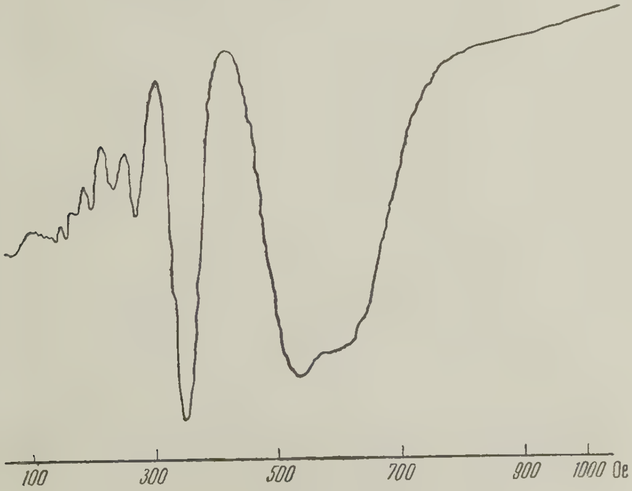

FIG. 1

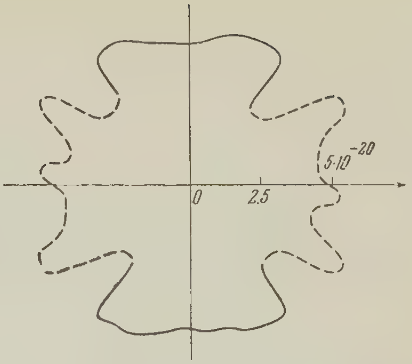

FIG. 2

The limiting electron momentum was deduced from the period of oscillation to be $p = 5 \times 10^{-20}$ g-cm/sec, and its projection on the (001) plane is shown in Fig. 2 as a function of the angles between the binary and fourfold axes. The full curve corresponds to angles for which many oscillations were found and sufficient accuracy could be achieved whereas the dashed part corresponds to momenta which could only be obtained roughly because of the few maxima observed.

The oscillation curves for sound propagated along the fourfold axis have fewer maxima, and these are not periodic in the inverse field, due presumably to the smaller electron mean free path along the fourfold axis.

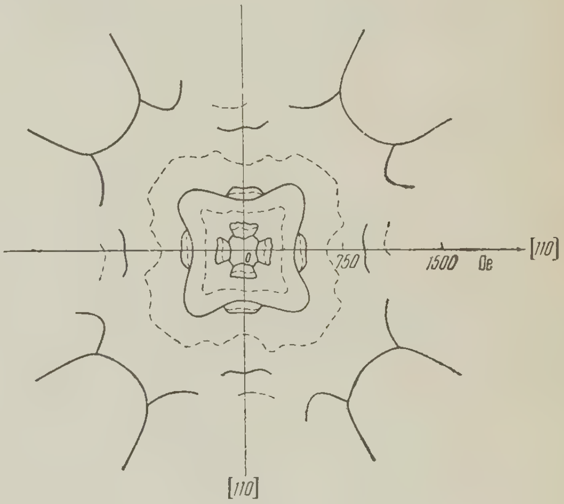

FIG. 3

Some results for the absorption coefficient as a function of magnetic field intensity and angle of rotation in the (001) plane are plotted in Fig. 3. The angle $\varphi = 0$ corresponds to the direction of the binary axis. The full curves give the magnetic field for maximum absorption as a function of angle, and the dashed curves are for the minima. Figure 4 shows the angular dependence of the

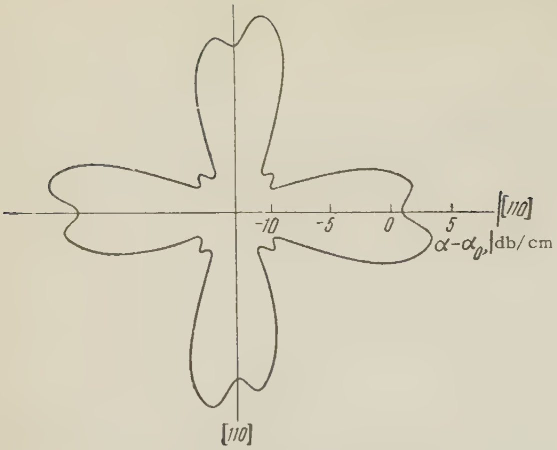

FIG. 4

absorption coefficient at a field of 7×10^3 oe for the field rotated in the (001) plane.

The absorption measured with the field $\mathbf{H} \parallel \mathbf{k}$ has singular points in the $\alpha(H)$ curve. In agreement with Gurevich's theory, the magnetic field at these points satisfies the relation $H_i = \text{const}/n$, where n is an integer.

---

[1] A. A. Galkin and A. P. Korolyuk, J. Exptl. Theoret. Phys. (U.S.S.R.) **37**, 310 (1959), Soviet Phys. JETP **10**, 219, this issue.

[2] H. E. Bömmel, Phys. Rev. **100**, 758 (1955).

[3] Morse, Bohm, and Gavenda, Phys. Rev. **109**, 1394 (1955).

[4] V. L. Gurevich, J. Exptl. Theoret. Phys. (U.S.S.R.) **37**, 71 (1959), Soviet Phys. JETP **10**, 51, this issue.

Translated by R. Berman
53

FINE STRUCTURE IN THE PARAMAGNETIC RESONANCE SPECTRUM OF NATURAL SAPPHIRE

V. M. VINOKUROV, M. M. ZARIPOV, and N. R. YAFAEV

Kazan' State University

Submitted to JETP editor March 28, 1959

J. Exptl. Theoret. Phys. (U.S.S.R.) **37**, 312-313 (July, 1959)

WE have investigated the paramagnetic resonance spectrum of several natural sapphire single crystals at room temperature, in the range 9600 to 9200 Mcs.

The grey-blue color of sapphire is due to the Fe^{3+} and Ti^{3+} ions replacing Al^{3+} isomorphically in the corundum lattice.[1] The Ti^{3+} ions do not produce any effect because of the short spin-lattice relaxation time at room temperature. One can, therefore, assume that the effect is produced by the Fe^{3+} ions, and the analysis of the spectrum is made on this assumption.

Kornienko and Prokhorov[2] have recently examined the fine structure of the electron paramagnetic resonance spectrum of Fe^{3+} ions artificially introduced into the Al_2O_3 lattice. The interpretation of the spectrum observed was carried out using the following Hamiltonian:*

$$\mathcal{H} = g\beta\,\mathbf{HS} + DS_z^2 + \frac{F}{180}\left[35\,S_z^4 - 30S(S+1)\,S_z^2 + 25S_z^2\right] + \frac{a}{6}\left[S_\xi^4 + S_\eta^4 + S_\zeta^4\right], \qquad (1)$$

where g is the spectroscopic splitting factor, β the Bohr magneton, S the spin operator, H the magnetic field strength, a the cubic field constant, and D and F the trigonal field constants. The coordinate system ξ, η, ζ is constructed on the cubic crystal field axes, and the z axis, directed along the trigonal axis, is also the (111) axis of the ξ, η, ζ system. The approximate energy levels were calculated by Kornienko and Prokhorov on the assumption that the last two terms in Eq. (1) can be treated as perturbations. This is not suitable for explaining the spectrum at a wavelength $\lambda \sim 3.2$ cm, as the second-order corrections can then be larger than the unperturbed values, and each term in Eq. (1) must be evaluated.

The required solution of Eq. (1) can be written in explicit form only for the case of a constant magnetic field directed along the trigonal symmetry axis of the electric field. The problem then becomes one of finding the roots of a sixth-order secular equation. Computations yield the follow-

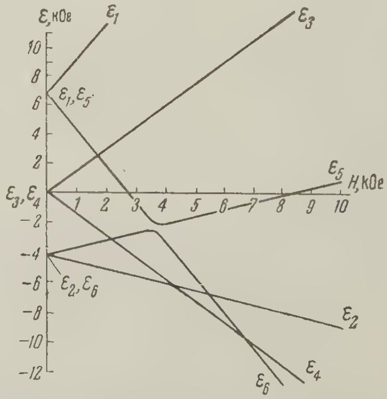

FIG. 1. Dependence of spin energy levels ε_i of Fe^{3+} atoms in sapphire on the magnetic field H, for $\mathbf{H} \parallel z$.

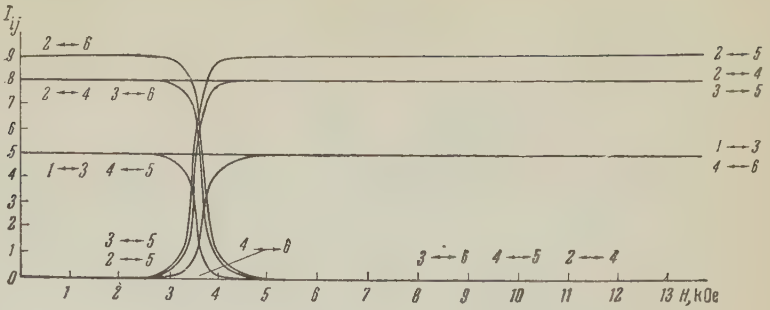

FIG. 2. Dependence of transition probabilities I_{ij} of magnetic dipole transitions on the magnetic field ($H \parallel z$).

ing expressions for the energy levels:

$$\varepsilon_{1,2} = H - {}^3/_2(a-F) + D \pm {}^1/_6\sqrt{[9H + (a-F) + 18D]^2 + 40a^2},$$

$$\varepsilon_{3,4} = \pm {}^3/_2 H, \qquad \varepsilon_{5,6} = -H - {}^3/_2(a-F) + D \pm {}^1/_6\sqrt{[-9H + (a-F) + 18D]^2 + 40a^2}. \qquad (2)$$

The values of ϵ_i ($i = 1, \ldots, 6$) are expressed in units of $g\beta$. The dependence of ϵ_i on H is shown graphically in Fig. 1.

We have calculated the relative transition probabilities I_{ij}, for magnetic dipole transitions between energy levels ϵ_i. The results are shown in Fig. 2. Transitions between other pairs of energy levels are forbidden.

A comparison of the spectrum observed with that calculated shows that the values of the constants in the Hamiltonian Eq. (1) for natural sapphire are, within the limits of experimental error, the same as those for Fe^{3+} ions artificially introduced into Al_2O_3, i.e.,

$$g = 2.003 \pm 0.001, \quad |D| = (1801 \pm 3)\ \text{Oe},$$
$$|a-F| = (357 \pm 2)\ \text{Oe}, \quad |a| = (280 \pm 20)\ \text{Oe}.$$

Finally we may note that Kornienko and Prokhorov[2] found a splitting of the atomic Fe^3 lines in Al_2O_3 for directions of the magnetic field other than parallel and perpendicular to the trigonal axis of the electric field. We found the same effect in natural sapphire crystals.

---

*Small constants, dependent on the spin quantum number S, are omitted.

---

[1] S. V. Grum-Grzhimaĭlo, Записки Всесоюзн. минерал. об-ва, (Notes, All-Union Mineral. Soc.) Ser. 2 **37**, 129 (1958).

[2] L. S. Kornienko and A. M. Prokhorov, J. Exptl. Theoret. Phys. (U.S.S.R.) 33, 805 (1957); Soviet Phys. JETP **6**, 620 (1958).

Translated by R. Berman
54

DECAY OF Te^{131} ($T_{1/2}$ = 30 HOURS)

A. BEDESCU, K. P. MITROFANOV, A. A. SOROKIN, and V. S. SHPINEL'

Institute of Nuclear Physics, Moscow State University

Submitted to JETP editor April 8, 1959

J. Exptl. Theoret. Phys. (U.S.S.R.) **37**, 314-315 (July, 1959)

INVESTIGATIONS of the decay of Te^{131} were reported in many papers.[1-3] The only decay scheme proposed in one of these papers[3] is based practically only on the energy balance of the observed beta and gamma transitions. In the present investigation we obtained a more accurate scheme for the lower levels of I^{131} excited in the decay of the 30-hour isomer Te^{131}, and obtained several new data on gamma transitions in this nucleus.

The investigation was carried out with a magnetic lens spectrometer and a scintillation coincidence spectrometer. The Te^{131} was obtained by irradiating metallic tellurium of high chemical purity with slow neutrons. After irradiation, the I^{131} that accumulated during the irradiation process was removed. Measurements of the gamma spectrum with a single-crystal scintillation spectrometer and with a beta spectrometer (using the secondary electrons) have shown that whereas the soft portion of the spectrum contains gamma radiation due to other isotopes of Te and to I^{131}, the gamma rays produced in the region $E_\gamma > 720$ kev belong only to Te^{131}.

We determined the relative intensities of the gamma transitions in this region. These are listed in Table I.

TABLE I

E, kev	I,%	E, kev	I,%
780	100	1220*	25
850	40	1600	~5
925	15	1850*	~2
1140	35	2200*	~0.5

The transitions marked with an asterisk in the table were observed first. Among the gamma transitions observed in the soft region, those at 80, 100, 147, 240, 330, 440, and 590 kev, which were seen both in single spectra and in spectra of β-γ and γ-γ coincidences, were ascribed to Te^{131}. Measurements of the coincidences have shown that the first excited level of I^{131} is the 147-kev level, and that the 780-kev transition goes into the ground state of I^{131}. In addition, we confirmed the 780 — 1150 and 780 — 850 kev γ-γ cascades reported by Hebb,[3] and observed in addition also the following cascades: 780 — 80, 780 — 100, 780 — 330, and 850 — 330 kev.

The K-shell conversion coefficient for the 780 and 850 kev transitions were determined with the magnetic spectrometer from the ratio of the areas of the peaks of the external and internal conversions; for the 147-kev transition the determination was from the ratio of the peaks of the gamma rays and the accompanying K radiation of iodine in the spectrum of coincidences with the hard beta rays of Te^{131}. The results are listed in Table II.

The delayed-coincidence setup was also used to measure the lifetime of the 147 kev level. The result obtained, $T_{1/2} = (8 \pm 1) \times 10^{-10}$ sec, is in good agreement with the results of de Waard and Gerholm[5] and indicates that the M1 component is l-forbidden.

The diagram shows the decay scheme for Te^{131}, containing only the most reliable of the established facts; the characteristics of the levels are based on the multiplicities of the gamma transitions and on the well known value of spin and parity of the ground state of I^{131} (reference 6). The energies of the beta transitions, indicated by solid lines, are taken from Hebb's paper.[3]

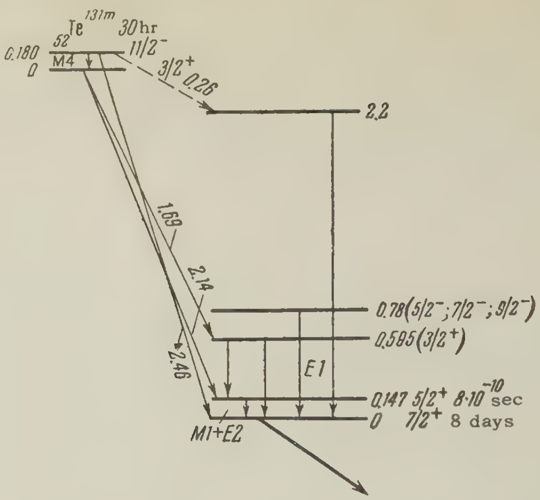

TABLE II

E_γ, kev	$\alpha_K^{exp} \cdot 10^3$	$\alpha_K^{theoret} \cdot 10^3$			Identification
		E1	E2	M1	
780	0.8±0.2	0.84	2.3	3.0	E1
850	1.6±0.6	0.71	1.9	2.5	E2 (+ M1)
147	260±50	—	330	220	M1 + E2

---

[1] K. Geiger, Z. Naturforsch. **7(a)**, 579 (1952).

[2] Mallmann, Aten, Bes, and McMillan, Phys. Rev. **99**, 7 (1955).

[3] E. Hebb, Phys. Rev. **97**, 987 (1955).

[4] L. A. Sliv and I. M. Band, Таблицы коэффициентов внутренней конверсии на *K*-оболочке (Tables of Coefficients of Internal Conversion on the K Shell), 1956.

[5] H. deWaard and T. R. Gerholm, Nucl. Phys. **1**, 281 (1956).

[6] E. Lipworth and H. L. Garvin, Bull. Am. Phys. Soc. Ser. II, **2**, 316 (1957).

Translated by J. G. Adashko
55

POSSIBLE METHOD OF IDENTIFYING NEW TRANSURANIC ELEMENTS

V. I. GOL'DANSKIĬ and M. I. PODGORETSKIĬ

P. N. Lebedev Physics Institute and Joint Institute for Nuclear Research

Submitted to JETP editor April 10, 1959

J. Exptl. Theoret. Phys. (U.S.S.R.) **37**, 315-317 (July, 1959)

As the atomic number of the presently synthesized and investigated far-transuranic elements increases, it becomes more and more important to "tie-in" the investigated new isotope to the previously identified daughter product of its decay: since the daughter isotope and the type of decay of the parent isotope are known, an investigation of a genetic connection between the two makes it possible to identify the parent isotope.

We propose here a new method for establishing a genetic connection between the parent isotope A and a longer-lived daughter isotope B, based on the measurement of the duration of the intervals (τ_{BB}) between two neighboring decays (B and B) and the intervals τ_{AB} between the decays A and the neighboring decays B. If the decays of A and B are independent of each other, then the mean duration $\bar{\tau}_{AB}$ (of the interval between the neighboring decays A and B should be the equal to the mean duration $\bar{\tau}_{BB}$ (of the interval between two neighboring decays of A). However, if some part of the observed decays of B is due to preceding decays of A, then $\bar{\tau}_{AB}$ should be less than $\bar{\tau}_{BB}$. This is the basis of the proposed method.

It is assumed that the decays of A and B are always distinguishable (for example, they are registered in different channels of a multi-channel α-particle analyzer), and that in the general case the nuclei B can appear both as the result of the decay of A, and as the primary product of target bombardment. For the sake of simplicity, the intensity of the continuous or pulsed flux of bombarding particles is assumed to be constant over the entire experiment. The decays of A and B are registered either continuously (for example, in the intervals between pulses of the accelerator of the bombarding particles), or during counting-time intervals alternating with the intervals of irradiation time. Many other variants of the experiment are possible. It is clear that when working with very short-lived daughter isotopes A, the first method is more effective but is fraught with greater experimental difficulties. As long as the lifetime of A can be measured at least in seconds, the realization of the second method is more feasible.

It is easy to derive equations that establish the existence of a connection between the decays of A and B. Let n be the mean frequency of the decays of B, λ the radioactive decay constant of B, and g the efficiency of registration of the decays of B. Let, furthermore, (M + 1) decays of B be observed during the entire experiment (i.e., M intervals BB) and let the number of observed decays of A be N (i.e., N intervals AB). Then, for the case of continuous observation of decays A and B we obtain

$$\varkappa = (\bar{\tau}_{BB} - \bar{\tau}_{AB})/\bar{\tau}_{AB} = g\lambda/[gn + (1-g)\lambda], \qquad (1)$$

where the quantity κ characterizes the mutual relation between the A and B decays and can be called a correlation coefficient; if the A and B decays are completely independent (i.e., when $\lambda/n \to 0$), then $\kappa = 0$; if $g = 1$, we have $\kappa = \lambda/n$.

For an experiment in which M intervals BB and N intervals AB are observed (we assume for simplicity $M \gg N$) we obtain the following expression for the absolute error in the determination of κ:

$$\Delta\varkappa \approx \frac{gn+\lambda}{gn+(1-g)\lambda}\left[\frac{1}{M}+\frac{1}{N}\left\{1-\frac{g\lambda\,(g\lambda+2gn)}{(gn+\lambda)^2}\right\}\right]^{1/2}. \qquad (2)$$

When $g = 1$, Eq. (2) becomes

$$\Delta\varkappa \approx [(1+\varkappa)^2/M + 1/N]^{1/2}. \qquad (3)$$

Going now to the case where the irradiation and the observation of the A and B decays alternate we assume for simplicity that the duration of the alternating intervals of irradiation and registration of A and B decays has a constant value T, with $nT \ll 1$. Thus, irradiation continues during one-half of the experiment, while registration of the decays continues during the second half. Then the only difference from the version where the observation is continuous lies in the fact that to observe a given number of intervals BB and AB it is necessary to double the overall length of the experiment.

We give a simple numerical example for the version where the irradiation and count alternate. Assume that 100 BB intervals (i.e., 101 decays of B nuclei) and 10 AB intervals (i.e., 10 decays of A nuclei) are observed in a series of experiments which lasts a total of 10^4 minutes. Then at $g = 1$, we get $n = 0.02\ \text{min}^{-1}$. Assume $\lambda \approx n$, which corresponds to a mean lifetime of the B nuclei of $\tau_B = 1/\lambda = 50$ min. In this case $\kappa = 1$, and $\Delta\kappa = 0.37$, which is quite satisfactory for such poor statistics. It is expected that different versions of the proposed method will find use in the investigation of new transuranic elements.

Translated by J. G. Adashko
56

TOTAL CROSS SECTION OF PHOTOPRODUCTION OF π^0 MESONS ON PROTONS AT LOW ENERGIES

R. G. VASIL' KOV and B. B. GOVORKOV

P. N. Lebedev Physics Institute, Academy of Sciences, U.S.S.R.

Submitted to JETP editor April 17, 1959

J. Exptl. Theoret. Phys. (U.S.S.R.) 37, 317-318 (July, 1959)

We have measured the total cross section of photoproduction of neutral pions, from the threshold energy of the primary γ quanta to 245 Mev. The measurements were made with the synchrotron of the Physics Institute of the U.S.S.R. Academy of Sciences at 265 Mev, using a liquid-hydrogen target. Using a method described previously,[1] in which a gamma telescope is placed at 90° to the direction of the primary photon beam, we measured simultaneously the entire curve of the yield of decay γ quanta, from threshold energy of primary photons to 250 Mev (in steps of 10 Mev). The smearing in the maximum energy of the bremsstrahlung γ spectrum amounted to ±1 Mev. The yield of the decay photons was plotted with a statistical accuracy of 2 — 3%. The background produced by an empty target was 8 — 10% of the count produced by a hydrogen-filled target. A detailed description of the measurement procedure and of the absolutization of the results obtained was given previously.[1,2]

The dependence of the cross sections of production of decay γ quanta on the photon energy was calculated from the yield curve by the "photon difference" method. As shown by Koester and Mills,[3] the measured yields of the decay γ quanta per photon, at an angle close to 90° in the laboratory system, is connected with a total cross section of photoproduction of π^0 mesons. Thus, if the photoproduction cross section has the following form in the center-of-mass system

$$d\sigma/d\Omega = A + B\cos\theta + C\cos^2\theta,$$

where θ is the angle of emission of the meson, then the total cross section can be obtained from

$$\sigma_t = 4\pi J\,(90°)\,(A + {}^1\!/_3\,C)/(\alpha A + \beta B + \gamma C), \qquad (1)$$

where J (90°) is the yield of decay γ quanta (per photon) at 90°, while α, β, and γ are functions that vary smoothly with the energy of the primary photon, and are calculated from kinematic considerations and from the γ telescope efficiency curve. Both the quantity β and the coefficient B are small in the energy range considered here, and the term βB in Eq. (1) can therefore be neglected. Measurements of the angular distributions[2] show that the ratio C/A does not change greatly with energy of the primary photons and is close to − 0.6 in the investigated energy range.

The calculated experimental values of σ_t, as functions of the primary-photon energies, are compared in the diagram with the theoretical curve, calculated for the photoproduction amplitudes obtained by solving the dispersion relations of Chew et al.[4] The calculations were carried out for $f^2 = 0.08$ and $\omega_r = 2.1$. We neglected in these calculations the contributions made to the total cross section by the amplitudes of the electric-dipole E1 and electric-quadrupole E2 transitions. As can be seen, good agreement is observed between the theoretical curve (which is estimated by the authors of reference 4 to be accurate to ~ 10%) and the obtained results; this agreement is due in final analysis to the fact that the principal contribution to

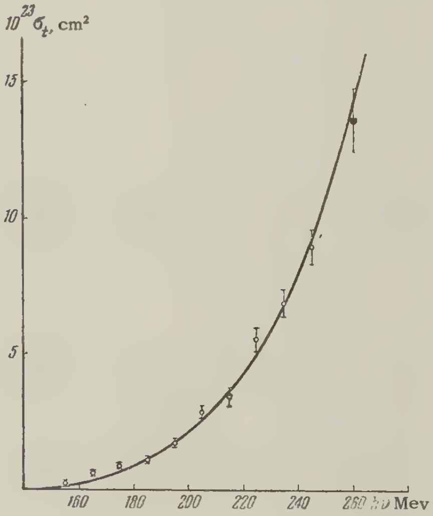

The total cross section σ_t of π^0-meson photoproduction in hydrogen; ○ — data of this paper, □ — data from reference 5.

σ_t is made by the scattering length a_{33}, for which the solution obtained for the dispersion relations of Chew et al. is apparently satisfactory. Deviations of the experimental points from the theoretical curve in the region close to the threshold (up to 180 Mev) indicate that E1 does make a definite contribution to the total cross section.

The variation of σ_t with the energy, obtained in the present work, is in good agreement with the variation of the cross section as obtained by Koester and Mills,[3] but the absolute values given by the latter for σ_t are 30% less.

In conclusion we thank I. A. Erofeev for help in the measurements and for the processing of the experimental data, and to V. I. Gol'danskiĭ and A. M. Baldin for valuable advice.

[1] Vasil'kov, Govorkov, and Kutsenko, Приборы и техника эксперимента (Instruments and Measurement Engg.) in press.

[2] Vasil'kov, Govorkov, and Gol'danskiĭ, J. Exptl. Theoret. Phys. (U.S.S.R.) **37**, 11 (1959), Soviet Phys. JETP, this issue, p. 7.

[3] L. J. Koester and F. E. Mills, Phys. Rev. **105**, 1900 (1957).

[4] Chew, Goldberger, Low, and Nambu, Phys. Rev. **106**, 1345 (1957).

[5] McDonald, Peterson, and Corson, Phys. Rev. **107**, 577 (1957).

Translated by J. G. Adashko
57

THREE-ELECTRON DECAY OF THE MUON

I. I. GUREVICH, B. A. NIKOL' SKIĬ, and L. V. SURKOVA

Submitted to JETP editor April 17, 1959

J. Exptl. Theoret. Phys. (U.S.S.R.) **37**, 318-319 (July, 1959)

IN measuring the asymmetry of the angular distribution of the electrons from $\pi \to \mu \to e$ decay, we observed an event in which three relativistic electrons escaped from a stopped muon. A microprojection of this event is shown in Fig. 1. All three electrons from the muon decay have a large dip angle, and therefore accurate measurements of grain density are not significant. Nevertheless the grain density was close to that of relativistic particles, and consequently they have in each case an energy above 1 Mev. The muon was stopped in the last pellicle of an emulsion stack, and all decay electrons escaped from the emulsion stack.

The recorded part of the electron tracks consisted of $L_{e_1} = 455\,\mu$, $L_{e_2} = 562\,\mu$, and $L_{e_3} = 455\,\mu$.

An additional argument for the energy of all the electrons being sufficiently large is the rectilinearity of their trajectories in the recorded part of the track. The muon track was 598-μ long, while the average track length for muons from $\pi \to \mu$ decay is $602\,\mu$ in R-NIKFI emulsion. The angles between the electrons are $\theta_{12} = 8.6°$, $\theta_{13} = 10.6°$, and $\theta_{23} = 10.5°$. From the microprojection it is evident that the event is not a three-particle decay of the muon ($\mu \to 3e$), since in that case the electrons would have to be coplanar with zero total momentum. It is not possible to interpret the observed event as the decay of a muon into an electron and a photon with a subsequent conversion of the latter at the point of decay into an electron-positron pair (Dalitz effect). In such a process the photon and consequently also the components of the pair must escape to the side opposite from the decay electron.

The present event can be interpreted as a decay $\mu^+ \to e^+ + e^+ + e^- + \nu + \tilde{\nu}$. In this interpreta-

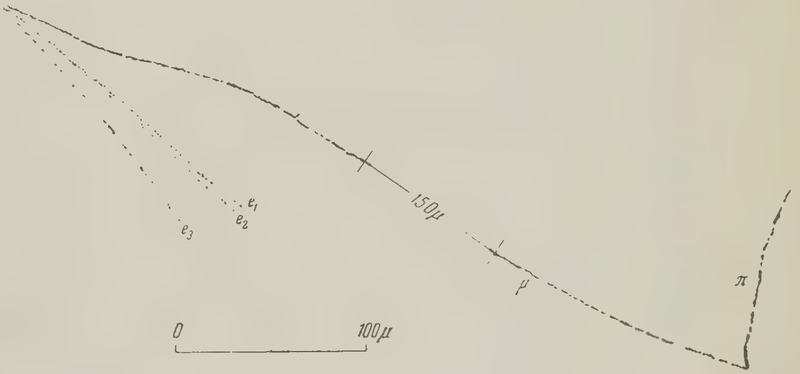

FIG. 1. Microprojection of the three-electron decay of a muon.

tion the question remains open whether we are dealing with the conversion of a virtual or a real photon into an electron-positron pair. One of the possible explanations is the decay $\mu^+ \rightarrow e^+ + \nu + \widetilde{\nu} + \gamma$ with subsequent conversion of the photon into a pair.

The present event was observed in scanning about 50,000 muon decays. Thus the relative probability of a “three-electron” decay of a muon may be estimated as $p(3e)/p(e) \leq 2 \times 10^{-5}$. If the data of other authors, who have observed a large number of μ-e decays and have not discovered the “three-electron” decay, are considered, then the estimated probability of such a process must be reduced to a few times 10^{-6}. The reliability of this number is not great, since only one case of “three-electron” decay has been observed, and therefore it is impossible to absolutely exclude the possibility of an accidental superposition of tracks.

The probability $p(3e)/p(e)$ of the order of 10^{-6} can be obtained by assuming a second-order radiative process: emission of a virtual photon during the escape of the electron with its subsequent conversion into an electron-positron pair. The energy of such an electron-positron pair may be estimated from the angle formed by the tracks of the pair, which is about 8°, approximately the same for all three possible pairs of electron tracks, and is equal to 15 Mev.

The authors are pleased to thank I. S. Shapiro for interesting discussions.

Translated by J. Heberle
58

HYDRODYNAMICS OF SOLUTIONS OF STRANGE PARTICLES IN HELIUM II NEAR THE λ POINT

D. G. SANIKIDZE

Institute of Physics, Academy of Sciences, Georgian S.S.R.

Submitted to JETP editor April 21, 1959

J. Exptl. Theoret. Phys. (U.S.S.R.) 37, 320-321 (July, 1959)

We have derived the equations for the hydrodynamics of solutions of strange particles in helium II in the immediate vicinity of the λ-transition point. In contradistinction to the usual set of equations, from the point of view considered here (compare reference 1) ρ_s is not a given function of p, T, and the concentration c, but is determined from these equations themselves which also describe the process by which ρ_s approaches its equilibrium value. As in the paper by Ginzburg and Pitaevskiĭ[1] the superfluid part of the liquid is described by a complex function $\psi(x, y, z, t) = \eta e^{i\varphi}$ defined in such a way that

$$\rho_s = m|\psi|^2, \qquad \mathbf{v}_s = (\hbar/m)\nabla\varphi$$

(m is the mass of a He^4 atom).

The derivation is analogous to the one used by Pitaevskiĭ[2] in deriving the equations for the hydrodynamics of pure helium II near the λ point. We shall, therefore, not give the calculations but write down the final result:

$$i\hbar\frac{\partial\psi}{\partial t} = -\frac{\hbar^2}{2m}\Delta\psi + \left[\left(\frac{\partial\varepsilon}{\partial\rho}\right)_{\rho_s, S, c} + \left(\frac{\partial\varepsilon}{\partial\rho_s}\right)_{\rho, S, c} - \frac{Z}{\rho}c\right]m\psi$$
$$- i\Lambda\left[\frac{1}{2}\left(-\frac{i\hbar}{m}\nabla - \mathbf{v}_n\right)^2 + \left(\frac{\partial\varepsilon}{\partial\rho_s}\right)_{\rho, S, c}\right]m\psi; \qquad (1)$$

$$\partial\rho/\partial t + \operatorname{div}(\rho - m|\psi|^2)\mathbf{v}_n + (i\hbar/2)(\psi\Delta\psi^* - \psi^*\Delta\psi) = 0; \qquad (2)$$

$$\partial(\rho c)/\partial t + \operatorname{div}(\rho c\mathbf{v}_n + \mathbf{g}) = 0; \qquad (3)$$

$$\frac{\partial}{\partial t}\left\{(\rho - m|\psi|^2)v_{ni} + \frac{i\hbar}{2}\left(\psi\frac{\partial\psi^*}{\partial x_i} - \psi^*\frac{\partial\psi}{\partial x_i}\right)\right\}$$
$$= -\frac{\partial}{\partial x_k}\left\{(\rho - m|\psi|^2)v_{ni}v_{nk}\right.$$
$$+ \frac{\hbar^2}{2m}\left(\frac{\partial\psi}{\partial x_i}\frac{\partial\psi^*}{\partial x_k} - \psi\frac{\partial^2\psi^*}{\partial x_i\partial x_k} + \text{c.c.}\right)$$
$$\left. + p\delta_{ik} - \eta\left(\frac{\partial v_{ni}}{\partial x_k} + \frac{\partial v_{nk}}{\partial x_i} - \frac{2}{3}\delta_{ik}\operatorname{div}\mathbf{v}_n\right)\right\}; \qquad (4)$$

$$\frac{\partial S}{\partial t} + \operatorname{div}\left[S\mathbf{v}_n + \frac{1}{T}\left(\mathbf{q} - \frac{\mathbf{g}Z}{\rho}\right)\right] = \frac{R}{T}. \qquad (5)$$

The dissipative function of the liquid is

$$R = \frac{2\Lambda}{\hbar}\left|\left[\frac{1}{2}\left(-\frac{i\hbar}{m}\nabla - \mathbf{v}_n\right)^2 + \left(\frac{\partial\varepsilon}{\partial\rho_1}\right)_{\rho, S, c}\right]m\psi\right|^2$$
$$+ \frac{1}{2}\eta\left(\frac{\partial v_{ni}}{\partial x_k} + \frac{\partial v_{nk}}{\partial x_i} - \frac{2}{3}\delta_{ik}\frac{\partial v_{nl}}{\partial x_l}\right)^2$$
$$- \mathbf{q}\frac{\nabla T}{T} - \mathbf{g}T\nabla\frac{Z}{\rho T}.$$

The impurity current $\mathbf{g}$ and heat current $\mathbf{q}$ are expressed by the usual equations.[3]

In the case of small gradients of ρ_s Eqs. (1) to (5) go over into the following ones:

$$\mathbf{v}_s + \nabla\left\{\frac{v_s^2}{2} + \left(\frac{\partial\varepsilon}{\partial\rho}\right)_{\rho_s, S, c} + \left(\frac{\partial\varepsilon}{\partial\rho_s}\right)_{\rho, S, c}\right.$$
$$\left. - \frac{Z}{\rho}c - \frac{\hbar\Lambda}{2m\rho_s}\operatorname{div}\rho_s(\mathbf{v}_s - \mathbf{v}_n)\right\} = 0, \qquad (6)$$

$$\partial\rho/\partial t + \operatorname{div}(\rho_s\mathbf{v}_s + \rho_n\mathbf{v}_n) = 0, \qquad (7)$$

$$\partial(\rho c)/\partial t + \operatorname{div}(\rho c\mathbf{v}_n + \mathbf{g}) = 0, \qquad (8)$$

$$\frac{\partial}{\partial t}(\rho_n v_{ni} + \rho_s v_{si}) + \frac{\partial}{\partial x_k}\Big\{\rho_n v_{ni} v_{nk} + \rho_s v_{si} v_{sk} + p\delta_{ik} - \eta\left(\frac{\partial v_{ni}}{\partial x_k} + \frac{\partial v_{nk}}{\partial x_i} - \frac{2}{3}\delta_{ik}\operatorname{div}\mathbf{v}_n\right)\Big\} = 0, \qquad (9)$$

$$\frac{\partial S}{\partial t} + \operatorname{div}\left[S\mathbf{v}_n + \frac{1}{T}\left(\mathbf{q} - \frac{\mathbf{g}Z}{\rho}\right)\right] = \frac{R}{T}, \qquad (10)$$

$$\frac{\partial \rho_s}{\partial t} + \operatorname{div}\rho_s\mathbf{v}_s = -\frac{\Lambda m}{2\hbar}\left\{\frac{(\mathbf{v}_n - \mathbf{v}_s)^2}{2} + \left(\frac{\partial \varepsilon}{\partial \rho_s}\right)_{\rho, S, c}\right\}\rho_s. \qquad (11)$$

The dissipative function of the liquid is

$$R = \frac{\hbar\Lambda}{2m\rho_s}[\operatorname{div}\rho_s(\mathbf{v}_s - \mathbf{v}_n)]^2 + \frac{2\Lambda m}{\hbar}\left[\frac{1}{2}(\mathbf{v}_s - \mathbf{v}_n)^2 + \left(\frac{\partial \varepsilon}{\partial \rho_s}\right)_{\rho, S, c}\right]^2\rho_s + \frac{1}{2}\eta\left(\frac{\partial v_{ni}}{\partial x_k} + \frac{\partial v_{nk}}{\partial x_i} - \frac{2}{3}\delta_{ik}\frac{\partial v_{kl}}{\partial x_l}\right)^2 - \mathbf{q}\frac{\nabla T}{T} - \mathbf{g}T\nabla\frac{Z}{\rho T}.$$

Formally Eqs. (6) to (10) are the same as the usual set of equations for the hydrodynamics of solutions of extraneous particles in helium II except, however, that ρ_s is not given in them but is an independent quantity for which the approach to its equilibrium value is described by the additional Eq. (11). In the given equations the quantity

$$(\partial\varepsilon/\partial\rho_s)_{\rho_s, S, c} + (\partial\varepsilon/\partial\rho)_{\rho, S, c} - Zc/\rho,$$

where $Z = (\partial\epsilon/\partial c)_{\rho, S, \rho_s}$, plays the role of the chemical potential of He^4 in the solution.

The parameter Λ entering into the equations could be estimated from a comparison of the absorption coefficient for first sound evaluated from Eqs. (6) to (11) with the measured value of the absorption coefficient in He^3-He^4 solutions near the λ point. There are not, however, at the present time any such experimental data. An estimate made by Pitaevskiĭ[2] for pure helium II gives $\Lambda \approx 15$.

For definite applications of the theory it is necessary to know the function $\epsilon(\rho, S, \rho_S, c)$, which can be determined from experimental data on the dependence of the superfluid component of He^3-He^4 solutions near the λ point on p, T, c, and on its density.

In conclusion the author expresses his sincere gratitude to I. M. Khalatnikov and L. P. Pitaevskiĭ for suggesting this topic and for valuable discussions.

---

[1] V. L. Ginzburg and L. P. Pitaevskiĭ, J. Exptl. Theoret. Phys. (U.S.S.R.) **34**, 1240 (1958), Soviet Phys. JETP **7**, 858 (1958).

[2] L. P. Pitaevskiĭ, J. Exptl. Theoret. Phys. (U.S.S.R.) **35**, 408 (1958), Soviet Phys. JETP **8**, 282 (1959).

[3] I. M. Khalatnikov, Usp. Fiz. Nauk **60**, 69 (1956), Fortschr. Phys. **5**, 287 (1957).

Translated by D. ter Haar
59

---

*THE PROPAGATION OF OSCILLATIONS ALONG VORTEX LINES IN ROTATING HELIUM II**

É. L. ANDRONIKASHVILI and D. S. TSAKADZE

Tbilisi State University

Submitted to JETP editor April 28, 1959

J. Exptl. Theoret. Phys. (U.S.S.R.) **37**, 322-323 (July, 1959)

ACCORDING to the theory developed by Feynman[1] on the basis of Onsager's hypothesis, there should appear in rotating helium II vortex lines parallel to the axis of rotation and running through the whole of the liquid. Experiments performed by us to confirm this hypothesis[2] showed that rotating helium II possesses, when twirled around, a quite appreciable elasticity. The presence of such an elasticity is also confirmed by the experiments of Hall.[3]

In the interpretation of these experiments we assumed that transverse elastic waves were propagated along the vortex lines. This point of view was confirmed by Hall (private communication), who observed a periodic change in the frequency of the oscillation of a light disc suspended in rotating helium II under such conditions that the liquid level above it was changing continuously. At the same time the length of the vortices, which on the one side were fastened to the surface of the disc and on the other side to the free surface of the liquid, was also changing, as assumed by Hall. The periodic changes in the frequency of the oscillations were within a range of one per cent.

In contradistinction to Hall, we measured the magnitude of the logarithmic decrement of the damping δ of the oscillations of an elastically suspended disc, which were performed at the same time as the rotation together with the helium II. The damping decrement was measured by a method described earlier.[4] The time dependence of the distance between the disc and the liquid surface was studied by a periscope system of mirrors and a cathetometer.

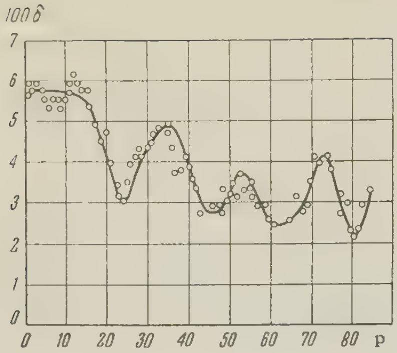

FIG. 1

We show in Fig. 1 the results of our measurement performed using one disc covered on both sides with grains of linear dimensions $l \approx 50\mu$ (the number of periods is along the abscissa). The measurement took place at 1.38° K and the rotational frequency was $\omega = 55 \times 10^{-3}\ \text{sec}^{-1}$. The level of the helium above the surface of the disc changed rapidly thanks to intensive illumination (rate of evaporation 3.6×10^{-2} mm/min). The initial part of the curve corresponds to the induced swinging of the oscillating system. In Fig. 2 we show the results of an experiment performed under the same conditions as the previous one, except for the fact that the rate of change of the liquid level above the disc was much slower in this case (0.5 mm/sec) because the illumination was switched off.

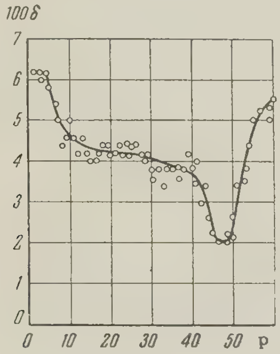

FIG. 2

From the curves obtained it is clear that when the rate of evaporation of the helium above the disc is changed the character of the periodicity of the damping is also changed. This result may be explained by assuming that a standing transverse wave appears in the vortex lines when the disc oscillates. The distance between two adjacent resonances corresponded to a lowering of the level by ~ 0.065 cm.

The authors express their thanks to Yu. G. Mamaladze for his active participation in the discussion of the experimental results in all stages of their development, and to T. M. Shul'ts, K. B. Mesoed, and I. M. Chkheidze for their help in performing the experiment.

---

*Reported at the Fifth All-Union Conference on Low Temperature Physics at Tbilisi, October 1958.

---

[1] R. P. Feynman, Progress in Low Temperature Physics, North Holland Publishing Company, Amsterdam, 1955, Vol. 1, p. 17.

[2] D. S. Tsakadze and E. L. Andronikashvili, Сообщения АН ГрузССР, (Reports, Acad. Sci. Georgian S.S.R.) 20, 667 (1958).

[3] H. É. Hall, Proc. Roy. Soc. (London) **A245**, 546 (1958).

[4] Andronikashvili, Mamaladze, and Tsakadze, Тр. Ин-та Физики АН ГрузССР (Trans. Phys. Inst. Acad. Sci. Georgian S.S.R.) 7, No. 1 (1959).

Translated by D. ter Haar
60

THE USE OF A SUPERCONDUCTING RING FOR REGISTERING THE PHASE TRANSITION IN LIQUID HELIUM

B. N. ESEL' SON and A. D. SHVETS

Physico-Technical Institute, Academy of Sciences, Ukrainian S.S.R.

Submitted to JETP editor May 13, 1959

J. Exptl. Theoret. Phys. (U.S.S.R.) **37**, 323-324 (July, 1959)

It is often desirable, when investigating the properties of He^3-He^4 mixtures, especially the properties of rotating helium, to have a thermometer which does not need external leads, is sufficiently sensitive, and dissipates a negligible amount of heat. These requirements are satisfied by a superconducting ring,* in which a current is induced by switching on and off an external magnetic field higher than the critical value.

When the temperature dependence of the current in the ring is known, the determination of the temperature of the liquid helium reduces to a measurement of the magnetic field of the ring by some instrument located outside the apparatus.

In experiments where there is a steady increase in temperature and, consequently, a continuous decrease of current in the ring, a stationary induction coil connected to a galvanometer can be used, and an emf will be induced by the decreasing magnetic field of the ring. The magnitude of the emf depends on the rate of change of current in the ring, i.e., on the rate of temperature rise which, for a constant heat input, is determined by the heat capacity of the system. This makes the use of a superconducting ring especially convenient for registering phase transitions.

We have used this system under conditions of a slow transition from He II to He I. In this experiment the current was induced in a tin ring fixed in a plexiglass vessel containing liquid helium[2] at 1.5° K, after which pumping of the helium vapor was stopped and the vessel was illuminated with a beam of light.

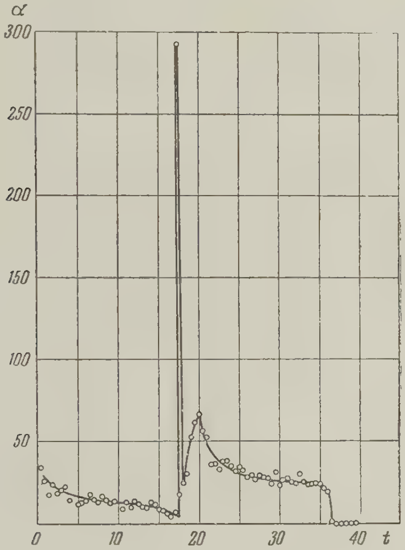

The results are shown in the figure, where the deflection (α) of the mirror of the galvanometer connected to the stationary coil is plotted as a function of the time (t) of warming of the helium (t = 0 corresponds to 1.5° K). Insofar as the heat influx to the system remained practically constant during the course of the experiment, the variation of α(t) determines the temperature dependence of the heat capacity of liquid helium. This explains the decrease in α with increasing temperature from 1.5° K to the λ point (from t = 0 to t = 17.5 min), the sharp increase in α at the λ point corresponding to the specific heat jump at this temperature, and the slow decrease in α in the He I region. At the transition temperature for tin the deflection must, of course, become zero (T = 3.73° K, t = 36.5 min).

We should point out that during the transition through the λ point there is a large and sharp peak superimposed on the variation of α(t) described, probably connected with the appearance of a small temperature difference between the ring and the helium under the conditions described. Such a temperature difference can perhaps be explained by a change in the mechanism of heat transfer in He II and He I. When the helium was heated electrically by a heater in the liquid, instead of by light, the change in α corresponded to the temperature dependence of the heat capacity of helium and the peak was absent. The sharp change in α makes it possible to record the transition through the λ point with great accuracy.

This method will be used to investigate the He II-He I transition in rotating helium and to determine the λ temperature of isotopic mixtures.

In conclusion we would like to thank Professor B. G. Lazarev for discussion of the results.

---

*A ring of tin was used by Galkin, Kan and Lazarev to study the properties of the superconducting transition[1] and to measure the thermal conductivity of copper.

---

[1] Galkin, Kan and Lazarev, J. Exptl. Theoret. Phys. (U.S.S.R.) **32**, 1582 (1957), Soviet Phys. JETP **5**, 1292 (1957).

[2] Esel'son, Lazarev, Sinel'nikov, and Shvets, J. Exptl. Theoret. Phys. (U.S.S.R.) **31**, 912 (1956), Soviet Phys. JETP **4**, 774 (1957).

Translated by R. Berman
61

NUCLEAR REACTIONS INDUCED BY HEAVY IONS

J. H. FREMLIN and J. S. LILLE

Birmingham, England

Submitted to JETP editor April 27, 1959

J. Exptl. Theoret. Phys. (U.S.S.R.) **37**, 324-326 (July, 1959)

PARFANOVICH, Rabin, and Semchinova[1] have studied stars produced in nuclear emulsions by accelerated nitrogen and oxygen ions. Two interesting and unexpected effects were observed, one of which is a strong forward directional effect of protons and α particles in the stars. Secondly, the proton to α particle ratio is much smaller than would be expected according to Le Couteur's theory of evaporation of a compound nucleus. Both effects have been confirmed by qualitative observations in our laboratory at Birmingham.

We are now conducting a detailed investigation of secondary particles emitted during collisions between nitrogen and silver nuclei and wish to report some preliminary results.

We directed an incompletely collimated beam of nitrogen ions accelerated by the Birmingham 150-cm cyclotron through a silver foil, and registered the secondary α particles and protons in a C-2 nuclear emulsion in the angular range 45° to 170° with respect to the beam. Details of the apparatus will be published elsewhere. The incident beam energy covered a broad range from 10 to 120 Mev, but because of the high potential barrier of silver only the fastest particles could participate in the reactions. Therefore the actual mean effective energy of the beam was 65 Mev and the effective halfwidth of the distribution was 12 Mev. The motion of the center of mass was easily taken into account.

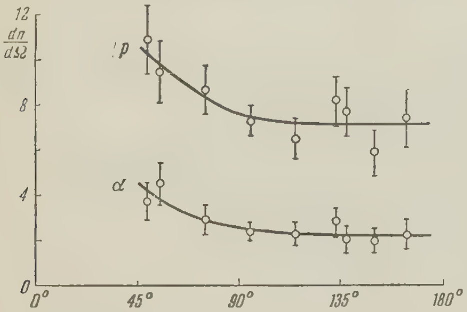

FIG. 1. Angular distribution of protons and α particles in c.m. system.

Figure 1 shows our preliminary results for the angular distribution, which confirm the strong forward peak of α particles and protons that was found by Parfanovich et al. On the other hand, we found that protons were more numerous than α particles, rather than the contrary. However, our results may not conflict entirely with those obtained in Moscow, since our observations did not extend to angles smaller than 45°, whereas Parfanovich et al. covered all angles. We also obtained qualitative indications that at angles below 45° the number of α particles increases much more rapidly than the number of protons.

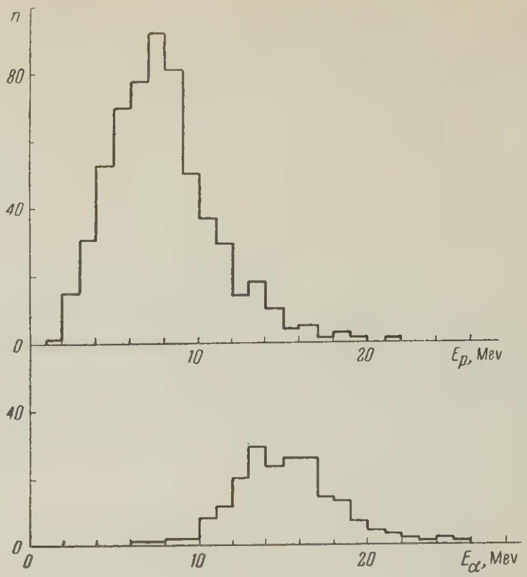

FIG. 2. Energy distribution of protons and α particles in c.m. system.

Figure 2 shows the energy distribution of the particles, using mean values derived from observations at each of six given angles. A small increase of the mean energy was observed with increasing angle, but this can be entirely accounted for by translational motion of the center of mass, which was taken into account in calculating the mean values. The results therefore represent the distribution in the c.m. system or in the laboratory system at 90° with respect to the N^{14} beam. We note that the majority of both protons and α particles emerge with energy less than the potential barrier of a compound nucleus (Xe^{121} or Xe^{123}). This is in agreement with the conclusions of Parfanovich et al.,but the advantage of our work lies in the assurance that all reactions involved only silver. In work with nuclear emulsions it is impossible to separate reactions with silver from reactions with bromine.

We are continuing to obtain similar measurements for interactions of nitrogen with gold and with aluminum and expect to include reactions with C^{13} ions.

---

[1] Parfanovich, Rabin, and Semchinova, J. Exptl. Theoret. Phys. (U.S.S.R.) 31, 188 (1956), Soviet Phys. JETP 4, 99 (1957).

Translated by I. Emin
62

ENERGY DEPENDENCE OF THE SPATIAL ASYMMETRY OF POSITRONS IN $\pi^+ \to \mu^+ \to e^+$ DECAY

A. O. VAĬSENBERG, V. A. SMIRNIT-SKIĬ, É. D. KOLGANOVA, and N. V. RABIN

Submitted to JETP editor May 7, 1959

J. Exptl. Theoret. Phys. (U.S.S.R.) **37**, 326-328 (July, 1959)

We have obtained previously[1] a value of 0.077 ± 0.012 for the asymmetry coefficient a, averaged over the entire spectrum, in the formula $dN = (1 + a\cos\vartheta)\,d\Omega$ for the angular distribution of positrons from the $\pi \to \mu \to e$ decay (ϑ is the angle between the directions of emission of the μ meson and the electron, $d\Omega$ is the element of solid angle). This value, found for a NIKFI-R emulsion, increases to 0.28 ± 0.02 when the emulsion is placed in a 17,000-gauss magnetic field. Such an increase makes it possible to obtain exact data on the energy dependence of the asymmetry coefficient, since even if the number of particles in the spectrum is the same, the statistical reliability of the measurement increases by almost four times over measurements made without the field. For the purpose of improving our measurements of the energy dependence of the coefficient of asymmetry and of obtaining a differential spectrum of this dependence, we have placed stacks of NIKFI-R photo emulsions, consisting of pellicles measuring 10 × 10 × 0.04 cm, in a 17,000-gauss vertical magnetic field parallel to the plane of the emulsion, and exposed these emulsions in the synchrocyclotron of the Joint Institute for Nuclear Research to a beam of positive pions sufficiently slowed down by filters to make them stop in the emulsion.

The positron energies were measured by the method of multiple scattering using the Koritska MS-2 and MBI-9 microscopes. Some of the measurements were performed with a machine for semi-automatic measurement of the scattering. A total of 565 tracks was measured, selected in accordance with the following criteria: 1) the entire sequence of $\pi^+ \to \mu^+ \to e^+$ decays lies in one emulsion layer, 2) the vertex of the $\mu^+ \to e^+$ decay is not farther than 100 μ from the surface of the emulsion, 3) the lengths of the positron tracks are not less than 1 μ, and 4) the projections of the μ-meson and positron tracks on the plane of the emulsion are inclined to the direction of the magnetic field at angles between 0 and ±45° (first quadrant of the ocular scale) and 180 ± 45° (opposite third quadrant of the scale).

It is easy to show that under these conditions the asymmetry coefficient is

$$a(\varepsilon) = 1.27\,\frac{N_f - N_b}{N_f + N_b} \pm \frac{(1.27^2 - a^2(\varepsilon))}{\sqrt{N_f + N_b}} \qquad (1)$$

Here N_f is the number of decays "forward," at which the mu meson and positron are emitted in the same direction (i.e., the projections of the angle of emission on the emulsion plane, measured from the direction of the magnetic field, lie in the same quadrant of the scale), and N_b (number of "backward" decays) pertains to the opposite direction (angles of emissions of the μ meson and electron are in opposite quadrants of the scale). The positron energy was determined from the second differences at a signal-to-noise ratio equal to 4 or 5. Analysis of the data by third differences has shown that the effect of distortion on the measurements of the energy can be neglected. The relative statistical error was determined from the formula $\sigma = 0.8/\sqrt{n}$, where n is the number of cells. The distribution of tracks over σ was as follows:

σ, % =	8—15	15—20	20—25	25
N, % =	41	41	14	4

The results of the measurements are listed in the table, where the energy intervals and the corresponding values of N_f and N_b are given. The

Energy Interval	0—0.3	0.3—0.4	0.4—0.5	0.5—0.6	0.6—0.7	0.7—0.8	0.8—0.9	0.9—1.0	1.0—1.1	1.1
N_f	19	26	16	42	32	33	25	10	8	6
N_b	23	24	32	36	56	48	53	28	23	25

energy dependence of the asymmetry coefficient is shown in the diagram, where the abscissas represent the positron energy ϵ, expressed in fractions of the maximum positron energy in the μ-e decay, while the ordinates represent the asymmetry coefficient calculated from Eq. (1). The solid curve gives the value of the asymmetry coefficient from the theory of the two-component neutrino: $a(\epsilon) = 3 \times 0.28\,(1 - 2\epsilon)/(2\epsilon - 3)$ (here 0.28 ± 0.02 is the value of the asymmetry coefficient for a 17-kilogauss field). The dotted lines show the energy dependence of the asymmetry coefficient as smeared out by the statistical errors in the measurement of the energy and by the bremsstrahlung under the conditions of our measurements: the upper curve corresponds to 10% dispersion and to tracks 4 mm long, while the lower curve to 20%

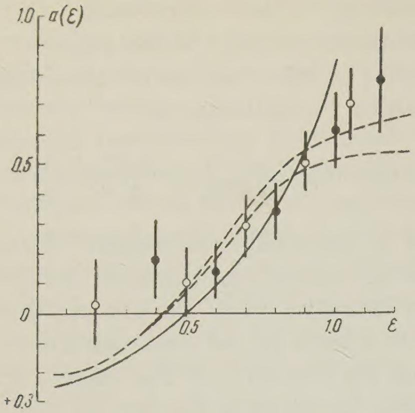

dispersion and tracks 1 mm long. More than 85% of all the particles contained in the spectrum lie between these two extreme cases. The values of the asymmetry coefficient, shown as empty circles, correspond to energy intervals 0 — 0.4, 0.4 — 0.6, 0.6 — 0.8, 0.8 — 1.0, and 1.0. The filled circles are the values of the asymmetry coefficient for the shifted energy intervals 0.5 — 0.7, 0.7 — 0.9, 0.9 — 1.1, and > 1.1. These values are therefore not independent statistically, but do indicate the absence of an effect due to grouping of the data by intervals. The resultant differential spectrum of the values a (ϵ) increases rapidly with energy and agrees with the two-component neutrino theory. These measurements show no positive asymmetry at low energies. In our previous work,[2] performed with NIKFI-R photoemulsions (a = − 0.077 ± 0.012), an average asymmetry coefficient a = + 0.14 ± 0.10 was obtained in the energy region 0 — 0.3, whereas the value expected from the two-component theory was approximately + 0.04. Were such high a value of the asymmetry coefficient real, a pronounced positive excess would appear in the present series of measurements. This, however, did not happen.

The authors thank Z. V. Minervina and E. A. Pesotskaya for participating in the measurements; D. M. Samoĭlovich in whose laboratory the emulsions were developed without noticeable distortion, and B. A. Nikol'skiĭ for helping with irradiations in his electromagnet.

---

[1] Vaĭsenberg, Rabin, and Smirnit-skiĭ, J. Exptl. Theoret. Phys. (U.S.S.R.) **36**, 1680 (1959), Soviet Phys. **9**, 1197 (1959).

[2] A. O. Vaĭsenberg and V. A. Smirnit-skiĭ, J. Exptl. Theoret. Phys. (U.S.S.R.) **33**, 621 (1957), Soviet Phys. JETP **6**, 477 (1958).

[3] Vaĭsenberg, Smirnit-skiĭ, Kolganova, Minervina, Pesotskaya, and Rabin, J. Exptl. Theoret. Phys. (U.S.S.R.) **35**, 645 (1958), Soviet Phys. JETP **8**, 448 (1959).

Translated by J. G. Adashko
63

ON A SYMMETRY IN τ^0 DECAY

M. I. SHIROKOV

J. Exptl. Theoret. Phys. (U.S.S.R.) **37**, 328-329 (July, 1959)

SUPPOSE the decay process $K_2^0 \rightarrow \pi^+ + \pi^- + \pi^0$ is invariant under charge conjugation. We shall show that then the angular distribution of the π^+ and π^- has the following symmetry:

$$F(-\mathbf{p}, \mathbf{p}') = F(\mathbf{p}, \mathbf{p}'), \qquad (1)$$

where **p** is proportional to the difference of the momenta of the π^+ and π^- in the center-of-mass system of the reaction (c.m.s.), and **p′** is the sum of these momenta.

Let us denote by $\langle \mathbf{pp}' | S | JM \rangle$ the transition amplitude from the initial state (the spin of the K meson is J, the spin projection M) to a state with definite values of **p** and **p′**. It can also be called the wave function of the decay products, written in the momentum representation. As a function of the spherical angles ϑ, φ and ϑ', φ' of the momenta **p** and **p′**, it can be put in the form of an expansion

$$\langle \mathbf{pp}' | S | JM \rangle = \sum_{l,\,\mu,\,l',\,\mu'} Y_{l\mu}(\vartheta, \varphi)\, Y_{l'\mu'}(\vartheta', \varphi')\, \langle l\mu p, l'\mu' p' | S \mid JM \rangle.$$

Assuming that if $J \neq 0$ the decaying K mesons are unpolarized, we have for the angular distribution in the c.m.s.:

$$F(\mathbf{p}, \mathbf{p}') \equiv \sum_M | \langle \mathbf{pp}' | S | JM \rangle |^2$$

$$= \sum Y_{l_1\mu_1}(\mathbf{n})\, Y^*_{l_2\mu_2}(\mathbf{n})\, Y_{l'_1,\, \mu'_1}(\mathbf{n}')\, Y^*_{l'_2,\, \mu'_2}(\mathbf{n}')$$

$$\times \langle l_1\mu_1 p,\ l'_1\mu'_1 p' | S | JM \rangle \langle l_2\mu_2 p,\ l'_2\mu'_2 p' | S | JM \rangle^*, \qquad (2)$$

where the summation is taken over M, l_1, μ_1, l_2, μ_2, l'_1, μ'_1, l'_2, μ'_2.

If charge parity is conserved, then $-1 = (-1)^l \cdot (+1)$, where $(+1)$ is the charge parity of the system of the π^0 meson, and $(-1)^l$ is the charge parity of the system (π^+, π^-). Therefore $(-1)^{l_1} =$

$(-1)^{l_2} = -1$; i.e., the parities of l_1 and l_2 in Eq. (2) are the same and $(-1)^{l_1 + l_2} = +1$. From Eq. (2) and the equation $Y_{l\mu}(-\mathbf{n}) = (-1)^l Y_{l\mu}(\mathbf{n})$ we get Eq. (1).

If, in addition, the spatial parity is also conserved, then the spatial parity of the K meson must be $(-1)^{l' + l}(-1)(-1)(-1)$. Together with $(-1)^l = -1$, this gives the result that l_1' and l_2' then also have the same parity, from which it follows that $F(\mathbf{p}, -\mathbf{p}') = F(\mathbf{p}, \mathbf{p}')$. This property exists also if only the combined parity is conserved [the symmetry (1) does not exist in this case].

The property (1) means symmetry relative to the origin from which the momenta are reckoned, and does not depend on the choice of the coordinate axes. If as the z axis we choose the direction of $\mathbf{p}'$, then in view of the fact that $Y_{l'\mu'}(0, \varphi') \sim \delta_{\mu' 0}$, we shall have $\mu_1 = \mu_2 = M$ in Eq. (2), and instead of Eq. (1) we get

$$F(\theta) = F(\pi - \theta), \tag{3}$$

where θ is the unoriented angle (i.e., $0 \leq \theta \leq \pi$) between $\mathbf{p}$ and $\mathbf{p}'$.

The symmetry (1) or (3) can be proved for any decay of the type $a \rightarrow b^+ + b^- + c$, where a and c have definite charge parities, and b^+ and b^- are each other's charge conjugates (a, $b^\pm$, c can have arbitrary spins).

But for $K_{1,2}^0$ mesons, decays of this type other than the one we have discussed,

$$K^0 \rightarrow \pi^+ + \pi^- + \gamma, \qquad K^0 \rightarrow \mu^+ + \mu^- + \pi^0(\gamma),$$
$$K^0 \rightarrow e^+ + e^- + \pi^0(\gamma).$$

are not observed.

It would seem that a check of Eq. (1) or Eq. (3) for the reaction $\pi^0 \rightarrow e^+ + e^- + \gamma$ could serve as a check of invariance under charge conjugation,* or of the presence of a charge-odd part in π^0. But for this purpose, only a search for the decay $\pi^0 \rightarrow 3\gamma$ is useful from a practical point of view† (for such a search, a xenon bubble chamber is particularly suitable, as M. A. Markov has pointed out).

I express my gratitude to Professor M. A. Markov and Chou Kuang-Chao for discussions.

*The Feynman diagrams of this decay can contain vertices of the types (πYY), (KYN), etc. The possibility of nonconservation of charge parity in such decays is so far not excluded.

†Chou Kuang-Chao has remarked that since virtual photons have definite charge parity, only an admixture of a virtual decay channel $\pi^0 \rightarrow 3\gamma \rightarrow e^+ + e^- + \gamma$ to the ordinary channel $\pi^0 \rightarrow 2\gamma \rightarrow e^+ + e^- + \gamma$ can lead to violation of Eqs. (1) and (3). It must be expected, however, that this admixture will be small, simply because the diagrams for the channel $\pi^0 \rightarrow 3\gamma \rightarrow e^+ + e^- + \gamma$ contain two additional electromagnetic vertices as compared with the diagrams for the ordinary channel.

Translated by W. H. Furry
64

SOVIET PHYSICS JOURNALS

Published in English by the American Institute of Physics

Soviet Physics – JETP

A translation, beginning with 1955 issues of "Journal of Experimental and Theoretical Physics" of the USSR Academy of Sciences. Leading physics journal of Soviet Union. Similar to "The Physical Review" in quality and range of topics. Outstanding new work is most likely to appear in this journal.

Twelve issues, approximately 3,500 pages. $75 domestic, $79 foreign. Libraries $35 domestic, $39 foreign. Single copies, $8.*

Soviet Physics – SOLID STATE

A translation, beginning with 1959 issues of "Fizika Tverdogo Tela" of the USSR Academy of Sciences. Offering results of theoretical and experimental investigations in the physics of semiconductors, dielectrics, and on applied physics associated with these problems. Also publishes papers on electronic processes taking place in the interior and on the surface of solids.

Twelve issues, approximately 2,000 pages. $55 domestic, $59 foreign. Libraries $25 domestic, $29 foreign. Single copies, $8.*

Soviet Physics – TECHNICAL PHYSICS

A translation, beginning with the 1956 issues of the "Journal of Technical Physics" of the USSR Academy of Sciences. Contains work on plasma physics and magnetohydrodynamics, aerodynamics, ion and electron optics and radio physics. Also publishes articles in mathematical physics, the physics of accelerators and molecular physics.

Twelve issues, approximately 2,000 pages, $55 domestic, $59 foreign. Libraries $25 domestic, $29 foreign. Single copies, $8.*

Soviet Physics– ACOUSTICS

A translation, beginning with 1955 issues of "Journal of Acoustics" of USSR Academy of Sciences. Devoted principally to physical acoustics but includes electro, bio, and psycho acoustics. Mathematical and experimental work with emphasis on pure research.

Four issues, approximately 400 pages. $12 domestic, $14 foreign. (No library discounts) Single copies, $4.

Soviet Physics – DOKLADY

A translation, beginning with 1956 issues of "Physics Sections" of Proceedings of USSR Academy of Sciences. All-science journal offering four-page reports of recent research in physics and borderline subjects.

Six issues, approximately 1,500 pages. $35 domestic, $38 foreign. Libraries $15 domestic, $18 foreign. Single copies Vols. 1 and 2, $5; Vol. 3 and later issues, $7.*

Soviet Physics – CRYSTALLOGRAPHY

A translation, beginning with 1957 issues of the journal "Crystallography" of USSR Academy of Sciences. Experimental and theoretical papers on crystal structure, lattice theory, diffraction studies, and other topics of interest to crystallographers, mineralogists, and metallurgists.

Six issues, approximately 1,000 pages. $25 domestic, $27 foreign. Libraries $10 domestic, $12 foreign. Single copies, $5.*

SOVIET ASTRONOMY – AJ

A translation, beginning with 1957 issues of "Astronomical Journal" of USSR Academy of Sciences. Covers various problems of interest to astronomers and astrophysicists including solar activity, stellar studies, spectroscopic investigations of radio astronomy.

Six issues, approximately 1,100 pages. $25 domestic, $27 foreign. Libraries $10 domestic, $12 foreign. Single copies, $5.*

Soviet Physics – USPEKHI

A translation, beginning with September, 1958 issue of "Uspekhi Fizicheskikh Nauk" of USSR Academy of Sciences. Offers reviews of recent developments comparable in scope and treatment to those carried in "Reviews of Modern Physics." Also contains reports on scientific meetings within the Soviet Union, book reviews, and personalia.

Six issues, approximately 1,700 pages. (Contents limited to material from Soviet sources.) $45 domestic, $48 foreign. Libraries $20 domestic, $23 foreign. Single copies, $9.*

*For libraries of non-profit degree-granting academic institutions.

Subscription prices subject to annual variation depending on size of Russian originals.

Please send orders and inquiries to

American Institute of Physics

335 East 45 Street, New York 17, N. Y.